

**Understanding the molecular basis for MMP-13
repression by IL-4**

Rachel Duncan

**A thesis submitted to the Faculty of Medicine, University of Newcastle,
in partial fulfilment of the requirements for the degree of Doctor of
Philosophy**

**Institute of Cellular Medicine
Newcastle University**

January 2011

Abstract

Cartilage destruction in arthritic disease is characterised by irreversible collagenolysis, resulting in loss of efficient joint function. Of the enzymes capable of hydrolysing native collagen fibrils, matrix metalloproteinase-13 (MMP-13) is the major collagenolytic MMP in osteoarthritis (OA), making this MMP an important disease-modifying target. Addition of interleukin-1 (IL-1) and oncostatin M (OSM) to bovine nasal cartilage in explant culture results in a synergistic loss of the collagen matrix, accompanied by a dramatic increase in the expression of collagenase enzymes. Interleukin-4 (IL-4) is able to ameliorate this collagen degradation by the strong repression of IL-1+OSM-induced MMP-13 expression. The aim of this work was to determine the mechanism by which IL-4 abolishes IL-1+OSM-induced MMP-13 expression.

Work examining the effect of IL-4 on the methylation status of CpG residues within the MMP-13 promoter failed to identify a role for epigenetic modification in the mechanism of action of IL-4. Subsequent cell signalling studies demonstrated Akt activation by IL-4. Therefore, genome-wide microarray analyses of cytokine stimulated cartilage and chondrocytes was used to identify candidate Akt-interacting proteins involved in the repressive effects of IL-4 on MMP-13. Trb1 was identified as a novel gene potentially involved in the repression of MMP-13 by IL-4 via Akt. Gene silencing experiments in chondrocytes confirmed that transfection with Trb1 specific siRNA resulted in the rescue of IL-4 mediated repression of IL-1+OSM-induced MMP-13 expression, indicating an anti-inflammatory role for Trb1. Trb1 belongs to family of three tribbles proteins and additional studies to investigate the roles of other tribbles family members in MMP regulation identified Trb3 as having a potentially pro-inflammatory role in MMP regulation in chondrocytes. Silencing of Trb3 was reproducibly shown to abolish IL-1+OSM-induced MMP-13 expression. The novel data presented in this thesis indicate that tribbles proteins act as key regulators of catabolic and anabolic responses in chondrocytes. From these findings it could be hypothesised that alterations in functional levels of specific tribbles proteins may protect against aberrant MMP gene expression in chondrocytes. The identification of this potentially important regulatory mechanism of signalling pathways important in MMP-13 gene expression in chondrocytes could be translated into a tractable therapy for arthritis once the mechanism has been unravelled.

Acknowledgements

Firstly, I would like to thank my supervisors, Professor Drew Rowan and Dr Gary Litherland, for their advice and encouragement over the past three years. I also thank Dr David Young for advice and discussion towards successful completion of this thesis. Thanks also to all the members of the Musculoskeletal Research Group. I thank the trustees of the FARNE fund at the Community Foundation serving Tyne & Wear and Northumberland for funding this Ph.D.

Declaration

This thesis is based on research performed in the Musculoskeletal Research Group (Rheumatology), Institute of Cellular Medicine, University of Newcastle, Newcastle upon Tyne, UK. Except for commonly held concepts, and where specific reference is made to other work, the content of the thesis is original. No part of this thesis has been submitted for the award of any other degree.

Table of contents

Table of contents	i
List of Figures	vii
List of Tables.	xi
Abbreviations	xii
Chapter 1: Introduction	1
1.1 Articular cartilage.....	1
1.1.1 Structure and function.....	1
1.1.2 Chondrocytes	2
1.1.3 Extracellular matrix.....	3
1.1.3.1 Collagen	3
1.1.3.2 Proteoglycans	5
1.2 Arthritis	6
1.2.1 Rheumatoid arthritis.....	7
1.2.2 Osteoarthritis	9
1.2.3 Arthritis treatment	10
1.3 Proteinases	10
1.3.1 Matrix metalloproteinases.....	11
1.3.2 Structure of matrix metalloproteinases	14
1.3.2.1 The collagenases	15
1.3.2.2 The stromelysins	17
1.3.2.3 The gelatinases	17
1.3.2.4 The matrilysins.....	18
1.3.2.5 The membrane-type MMPs	18
1.3.3 Regulation of matrix metalloproteinases	18
1.3.3.1 Synthesis	19
1.3.3.2 Activation of proenzymes	19
1.3.3.3 Inhibition.....	20
1.3.3.3.1 Natural inhibitors of MMPs	20
1.3.3.3.2 Synthetic inhibitors of MMPs	22

1.4 Pro-inflammatory cytokines in arthritis	23
1.4.1 Interleukin-1	24
1.4.1.1 Interleukin-1 and arthritis.....	25
1.4.2 Oncostatin M.....	27
1.4.2.1 OSM and arthritis.....	27
1.4.3 Other pro-inflammatory cytokines.....	29
1.5 Anti-inflammatory cytokines in arthritis.....	30
1.5.1 Interleukin-4.....	30
1.5.2 IL-4 in arthritis	30
1.5.3 Regulation of MMPs by IL-4.....	32
1.5.3.1 Epigenetic regulation	33
1.5.4 IL-4 in other diseases	33
1.5.5 IL-4 signalling.....	34
1.5.5.1 STAT6.....	36
1.5.5.2 IRS1/-2	39
1.5.6 Other anti-inflammatory cytokines	40
1.6 Summary and aims of this study	40
Chapter 2: Materials and Methods.....	42
2.1 Materials.....	42
2.1.1 Antibodies	42
2.1.2 Cell lines	42
2.1.3 Cell culture reagents.....	42
2.1.4 Commercially available kits.....	43
2.1.5 Biochemical Biology Reagents	43
2.1.6 Molecular Biology Reagents.....	43
2.1.7 Immunoblotting reagents	44
2.1.8 Inhibitors	44
2.1.9 Cytokines	44
2.2 Methods.....	45
2.2.1 Cartilage Sample Collection	45
2.2.2 Chondrocyte Extraction and Culture.....	45
2.2.2.1 Bovine nasal chondrocyte extraction	45

2.2.2.2 HAC extraction	46
2.2.3 Cell culture	46
2.2.4 Bovine nasal cartilage explant culture	47
2.2.4.1 Bovine nasal cartilage degradation assay.....	47
2.2.4.2 Hydroxyproline assay.....	48
2.2.4.3 Collagenase assay.....	49
2.2.5 RNA isolation and real-time polymerase chain reaction	51
2.2.5.1 Extraction of RNA from bovine nasal cartilage.....	51
2.2.5.2 Reverse Transcription	52
2.2.5.3.1 Taqman® Probe-Based Real-Time RT-PCR.....	53
2.2.5.3.2 SYBR® Green Real-Time PCR.....	54
2.2.6 Preparation of total cell lysates	55
2.2.7 Subcellular protein fractionation.....	55
2.2.8 SDS-Polyacrylamide gel electrophoresis (SDS-PAGE)	57
2.2.9 Western blotting.....	59
2.2.10 Gelatin zymography.....	60
2.2.11 RNAi and over-expression plasmid assays	61
2.2.11.1 RNAi assays.....	62
2.2.11.2 Over-expression plasmid assays	63
2.2.11.3 GFP-based protein fragment complementation assay.....	64
2.2.11.4 shRNA assays	65
2.2.12 Genome-wide Arrays	66
2.2.12.1 Affymetrix Bovine GeneChip Array.....	66
2.2.12.2 Sentrix Human-6 Expression BeadChip	67
2.2.13 DNA methylation analysis	68
2.2.13.1 Isolation of DNA from Primary Cells.....	68
2.2.13.2 Primer design and optimisation.....	69
2.2.13.3 Amplification and purification of PCR products	70
2.2.13.4 Cloning of PCR products	71
2.2.13.5 Analysis of DNA methylation.....	72
2.2.13.6 Agarose Gel Electrophoresis.....	72
2.2.13.7 Pyrosequencing	73

2.2.13.7.1 Assay design and optimisation.....	73
2.2.13.7.2 Amplification and purification of PCR products	74
2.2.13.7.3 Pyrosequencing	74
2.2.14 Statistical analysis	76
Chapter 3: Investigations into the effects of IL-4 on IL-1+OSM-induced cartilage collagen release and collagenase expression in chondrocytes and cartilage.....	77
3.1 Introduction	77
3.2 Results	79
3.2.1 The effect of IL-4 on the release of collagen from bovine cartilage treated with IL-1±OSM.....	79
3.2.2 The effect of delayed addition of IL-4 on IL-1+OSM-induced collagen and active collagenase levels in bovine nasal cartilage.	79
3.2.3 The effect of IL-4 on IL-1+OSM–induced gene expression of MMP-1 and MMP-13 in bovine chondrocytes.....	81
3.2.4 The effect of IL-4 on IL-1+OSM–induced gene expression of MMP-1 and MMP-13 in human articular chondrocytes and SW1353 cells.	84
3.2.5 The effect of different concentrations of IL-4 on MMP-1 and MMP-13 mRNA expression in bovine chondrocytes.	84
3.2.6 Profiling the effect of IL-4 on collagenase gene expression and collagenolysis in resorbing cartilage.....	87
3.2.7 Profiling the effect of IL-4 on gelatinolytic activity in resorbing cartilage.	89
3.2.8 Profiling the effect of IL-4 on IL-1+OSM-induced non-collagenolytic MMP expression in resorbing cartilage.....	89
3.3 Discussion	92
3.4 Summary	96
Chapter 4: Assessment of epigenetic regulation of MMP-13 by DNA methylation in bovine nasal chondrocytes.....	98
4.1 Introduction	98
4.2 Results	102
4.2.1 MMP-13 promoter methylation in bovine nasal chondrocytes.....	102
4.2.1.1 Optimisation of Primers for Bisulphite PCR	102
4.2.1.2 Bisulphite sequencing of MMP-13 promoter in treated DNA.....	103

4.2.2 Analysis of DNA methylation by pyrosequencing	105
4.3 Discussion	110
4.4 Summary	114
Chapter 5: The effect of IL-4 on PI3K-dependent signalling in chondrocytes	115
5.1 Introduction	115
5.2 Results	118
5.2.1 The effect of different concentrations of IL-4 on STAT6 and Akt phosphorylation in bovine chondrocytes	118
5.2.2 Timecourse to investigate the effect of IL-4 on STAT6 activation in primary bovine and human articular chondrocytes.....	118
5.2.3 The effect of IL-4 on OSM-stimulated Akt and GSK-3 phosphorylation in bovine chondrocytes.....	121
5.2.4 Stimulation of Akt and GSK-3 by IL-4 is PI3K-dependent in bovine chondrocytes	121
5.2.5 The effect of selective PI3K 110 β inhibition on IL-4- and OSM-induced Akt and phosphorylation in bovine chondrocytes	124
5.2.6 The effect of PI3K p110 α inhibition on IL-4- and OSM-induced Akt phosphorylation in bovine chondrocytes	124
5.2.7 The effect of PI3K p110 α , β and δ silencing on OSM- and IL-4-induced Akt phosphorylation in SW1353 cells	127
5.2.8 The effect of PI3K p110 isoform silencing on IL-1+OSM \pm IL-4-induced MMP-13 expression in SW1353 cells	129
5.3 Discussion	131
5.4 Summary	135
Chapter 6: Assessment of altered gene expression following IL-4 stimulation of cartilage and chondrocytes by genome-wide microarray analysis	136
6.1 Introduction	136
6.2 Results	137
6.2.1 Preliminary data	137
6.2.2 Analysis of genome-wide microarray results.....	143
6.2.3 Candidate genes selected for further study	149
6.3 Discussion	156

6.4 Summary	160
Chapter 7: The role of the Tribbles family of proteins in MMP-13 expression in chondrocytes..	161
7.1 Introduction	161
7.2 Results	166
7.2.1 The effect of various gene silencing on IL-1+OSM-induced MMP-13 expression in SW1353 cells.	166
7.2.2 The effect of Trb1 and STAT6 gene silencing on MMP-13 expression in SW1353 cells and human articular chondrocytes	168
7.2.3 IL-4-induced Trb1 expression is STAT6-dependent	168
7.2.4 The effect of STAT6 and Trb1 gene silencing on STAT6 and phospho-STAT6 abundance.....	168
7.2.5 The effect of STAT6 and Trb1 gene silencing on MMP-1 mRNA expression in SW1353 cells	171
7.2.6 The effect of tribbles protein family gene silencing on IL-1+OSM-induced collagenase gene expression in SW1353 cells	171
7.2.7 Transfection timecourse to determine the efficiency of Trb1 and Trb3 gene silencing in SW1353 cells.....	172
7.2.8 Investigations into the efficiency of Trb1 gene silencing	177
7.2.9 The effect of over-expression of Trb1, 2 or 3 on MMP-13 expression in SW1353 cells	182
7.2.10 The effect of IL-1+OSM and IL-1+OSM+IL-4 on the subcellular localisation of Trb1 and Trb3	182
7.2.11 MKK-Trb1 and -Trb3 interactions in SW1353 cells.....	184
7.3 Discussion	188
7.4 Summary	192
Chapter 8: General discussion.....	194
References.....	204
Appendix A.....	224
Appendix B.....	225
Appendix C.....	247
Appendix D.....	265

List of Figures

Chapter 1

Figure 1.1 The zones of articular cartilage	2
Figure 1.2 Structure and organisation of collagen	4
Figure 1.3 Structure of aggrecan	5
Figure 1.4 Schematic representation of the joint inflammatory events in rheumatoid arthritis (RA)	8
Figure 1.5 The five main classes of proteinases	11
Figure 1.6 Domain structure of MMPs	15
Figure 1.7 The regulation of MMPs occurs at three distinct levels: synthesis and secretion, activation and inhibition	19
Figure 1.8 IL-1 signalling pathways	26
Figure 1.9 OSM signalling pathways	28
Figure 1.10 IL-4 signalling pathways	37

Chapter 3

Figure 3.1 The effect of IL-4 on the release of collagen from the bovine nasal cartilage model treated with IL-1±OSM	80
Figure 3.2 The effect of delayed addition of IL-4 on IL-1+OSM-induced collagen and active collagenase levels in bovine nasal cartilage	82
Figure 3.3 The effect of IL-4 on IL-1+OSM-induced gene expression of MMP-1 and MMP-13 in bovine nasal chondrocytes	83
Figure 3.4 The effect of IL-4 on IL-1+OSM-induced gene expression of MMP-1 and MMP-13 in human articular chondrocytes and SW1353 cells	85
Figure 3.5 The effect of different concentrations of IL-4 on MMP-1 and MMP-13 mRNA expression in bovine nasal chondrocytes	86
Figure 3.6 Profiling the effect of IL-4 on collagenase gene expression and collagenolysis in resorbing cartilage	88
Figure 3.7 Profiling the effect of IL-4 on gelatinolytic activity in resorbing cartilage	90

Figure 3.8 Profiling the effect of IL-4 on IL-1+OSM-induced non-collagenolytic MMP expression in resorbing cartilage	91
--	----

Chapter 4

Figure 4.1 The formation of 5-methylcytosine	99
Figure 4.2 Bisulphite treatment of DNA	100
Figure 4.3 MethPrimer result	104
Figure 4.4 Optimisation of primers designed to amplify a 369 bp region of the MMP-13 promoter in bisulphite treated bovine DNA	106
Figure 4.5 The effect of IL-1, IL-1+OSM and IL-1+OSM+IL-4 on bovine MMP-13 promoter methylation	107
Figure 4.6 The bovine MMP-13 promoter	108
Figure 4.7 The effect of IL-1, IL-1+OSM and IL-1+OSM+IL-4 on bovine MMP-13 promoter methylation	109

Chapter 5

Figure 5.1 The effect of different concentrations of IL-4 on STAT6 and Akt phosphorylation in bovine nasal chondrocytes, as determined by Western blot	119
Figure 5.2 Timecourse to investigate the effect of IL-4 on STAT6 activation in primary bovine nasal and human articular chondrocytes, as determined by Western blot	120
Figure 5.3 The effect of IL-4 on OSM-stimulated Akt and GSK-3 phosphorylation in bovine nasal chondrocytes, as determined by Western blot	122
Figure 5.4 Stimulation of Akt and GSK-3 by IL-4 is PI3K-dependent in bovine nasal chondrocytes, as determined by Western blot	123
Figure 5.5 The effect of TGX-221, a selective PI3K p110 β inhibitor, on IL-4- and OSM-induced Akt phosphorylation in bovine chondrocytes, as determined by Western blot	125
Figure 5.6 The effect of compound 15e, a PI3K p110 α specific inhibitor, on IL-4- and OSM-induced Akt phosphorylation in bovine chondrocytes, as determined by Western blot	126

Figure 5.7 The effect of PI3K p110 α , β and δ silencing on OSM- and IL-4-induced Akt phosphorylation in SW1353 cells	128
Figure 5.8 The effect of PI3K p110 isoform silencing on IL-1+OSM \pm IL-4-induced MMP-13 expression in SW1353 cells	130
Chapter 6	
Figure 6.1 Preliminary data from the bovine nasal cartilage model used to generate RNA for use on the GeneChip® Bovine Genome Array	140
Figure 6.2 Preliminary data from human articular chondrocytes used to generate RNA for the Sentrix Human-6 Expression BeadChip	141
Figure 6.3 Preliminary data from SW1353 cells used to generate RNA for the Sentrix Human-6 Expression BeadChip	142
Figure 6.4 Gene tree: GeneChip® Bovine Genome Array	144
Figure 6.5 Gene tree: Human articular chondrocyte Sentrix Human-6 Expression BeadChip	145
Figure 6.6 Gene tree: SW1353 cells Sentrix Human-6 Expression BeadChip	146
Figure 6.7 Venn diagrams showing the overlap of genes up- or down-regulated ≥ 2 fold in IL-1+OSM+IL-4-stimulated bovine cartilage, human articular cartilage and SW1353 cells compared to IL-1+OSM-stimulated bovine cartilage, human articular chondrocytes and SW1353 cells	147
Figure 6.8 Venn diagrams showing the overlap of genes up- or down-regulated ≥ 1.5 fold in IL-1+OSM+IL-4-stimulated human articular cartilage and SW1353 cells compared to IL-1+OSM-stimulated human articular chondrocytes and SW1353 cells	148
Figure 6.9 Scatter plot showing genes up- or down-regulated >2 fold (IL-1+OSM+IL-4 versus IL-1+OSM) on the GeneChip® Bovine Genome Array	153
Figure 6.10 Scatter plot showing genes up- or down-regulated >1.5 fold (IL-1+OSM+IL-4 versus IL-1+OSM) on the Sentrix Human-6 Expression BeadChip (human articular chondrocytes)	154
Figure 6.11 Scatter plot showing genes up- or down-regulated >1.5 fold (IL-1+OSM+IL-4 versus IL-1+OSM) on the Sentrix Human-6 Expression BeadChip (SW1353 cells)	155

Chapter 7

Figure 7.1 The effect of various gene silencing on IL-1+OSM-induced MMP-13 expression in SW1353 cells	167
Figure 7.2 The effect of Trb1 and STAT6 gene silencing on MMP-13 expression in SW1353 cells (a) and human articular chondrocytes (b)	169
Figure 7.3 The effect of STAT6 gene silencing on Trb1 expression in SW1353 cells (a) and human articular chondrocytes (b)	170
Figure 7.4 The effect of STAT6 and Trb1 gene silencing on STAT6 and phospho-STAT6 abundance	173
Figure 7.5 The effect of STAT6 and Trb1 gene silencing on MMP-1 mRNA expression in SW1353 cells	174
Figure 7.6 The effect of Trb protein family gene silencing on IL-1+OSM-induced collagenase gene expression in SW1353 cells	175
Figure 7.7 The effect of Trb protein family gene silencing on TNF α +OSM-induced collagenase gene expression in SW1353 cells	176
Figure 7.8 Transfection timecourse to determine the efficiency of Trb1 and Trb3 gene silencing in SW1353 cells, as determined by Western blot	178
Figure 7.9 The effect of Trb1 gene silencing on MMP-13 expression in SW1353 cells	180
Figure 7.10 The effect of shRNA Trb1 gene silencing on MMP-13 expression in SW1353 cells	181
Figure 7.11 The effect of over-expression of Trb1, 2 or 3 on MMP-13 expression in SW1353 cells	183
Figure 7.12 The effect of IL-1+OSM and IL-1+OSM+IL-4 on the subcellular localisation of Akt, Trb1 and Trb3, as determined by Western blot	185
Figure 7.13 MEK1- and MKK-Trb1 interactions in SW1353 cells	186
Figure 7.14 MEK1- and MKK-Trb3 interactions in SW1353 cells	187
 Chapter 8	
Figure 8.1 Diagram summarising the possible involvement of Trb proteins in MMP-13 expression and repression	200

List of Tables

Chapter 1

Table 1.1 Matrix Metalloproteinases	13
Table 1.2 Potential activators of MMPs	20
Table 1.3 Properties of TIMPs	21

Chapter 2

Table 2.1 Human Taqman® probe-based real-time PCR primers and probes	53
Table 2.2 SYBR® Green primers for real-time RT-PCR	54
Table 2.3 Subcellular protein fractionation reagent volumes for different packed cell volumes	56
Table 2.4 Preparation of SDS-PAGE gels (volumes for 2 gels)	58
Table 2.5 DNA methylation analysis primers	70

Chapter 4

Table 4.1 The effect of IL-1, IL-1+OSM and IL-4 on the percentage of unmethylated CpG sites	107
---	-----

Chapter 6

Table 6.1 List of genes selected for further study from microarray data	152
---	-----

Abbreviations

°C	degree Celsius
µg	microgram
µl	microlitre
ADAM	a disintegrin and a metalloproteinase
ADAMTS	a disintegrin and a metalloproteinase with thrombospondin motifs
AP-1	activator protein-1
APMA	<i>p</i> -amino phenyl-mercuric acetate
APS	ammonium peroxodisulphate
bp	base pairs
BSA	bovine serum albumin
cDNA	complementary DNA
CIA	collagen-induced arthritis
DAB	<i>p</i> -diaminobenzadine tetrahydrochloride
dH ₂ O	distilled H ₂ O
DMB	1,9-dimethylmethylene blue
DMEM	Dulbecco's modification of Eagle's medium
DMSO	dimethylsulphoxide
DNA	deoxyribonucleic acid
DNase	deoxyribonuclease
ECM	extracellular matrix
EDTA	ethylenediaminetetraacetic acid
ERK	extracellular regulated kinase
FCS	foetal calf serum
g	relative centrifugal force
GAG	glycosaminoglycan
GAPDH	glyceraldehyde-3-phosphate dehydrogenase
HRP	horse-radish peroxidase
Ig	immunoglobulin
IGD	interglobular domain
IGF	insulin-like growth factor
IL	interleukin
IL-1Ra	interleukin-1 receptor antagonist
IL-4R	interleukin-4 receptor
IRS	insulin receptor substrate
JAK	janus kinase
JNK	c-Jun N-terminal kinase
kb	kilobase
kDa	kilodalton
MAPK	mitogen-activated protein kinase
mg	microgram
MMP	matrix metalloproteinase
<i>M_r</i>	relative molecular mass
mRNA	messenger RNA
MT-MMP	membrane type MMP

MW	molecular weight
NFκB	nuclear factor κB
OA	osteoarthritis
OSM	oncostatin M
PAGE	polyacrylamide gel electrophoresis
PBS	phosphate buffered saline
PCR	polymerase chain reaction
PI3K	phosphatidylinositol 3-kinase
RA	rheumatoid arthritis
RNA	ribonucleic acid
RNase	ribonuclease
RT-PCR	reverse transcriptase PCR
SDS	sodium dodecyl sulphate
Sh	src homology
SOCS	silencers of cytokine signalling
STAT	signal transducer and activator of transcription
TEMED	N,N,N',N'-tetramethylethylene-diamine
TGF-β	transforming growth factor-β
TIMP	tissue inhibitor of metalloproteinases
TNF	tumour necrosis factor
Tris	tris(hydroxymethyl)aminomethane
Triton X-100	t-Octylphenoxypolyethoxyethanol
Tween 20	polyoxyethylene sorbitan monolaurate
v/v	volume/volume
w/v	weight/volume

Chapter 1: Introduction

1.1 Articular cartilage

1.1.1 Structure and function

Articular cartilage covers the articulating surfaces of bones, providing a friction-free surface to facilitate joint motion. This unique tissue is both avascular and aneural and populated by only one cell type, the chondrocyte. The absence of blood vessels and lymphatics means that delivery of nutrients and removal of waste products must occur by diffusion through the extracellular matrix (ECM) (Kuettner 1992). Like other connective tissues, articular cartilage derives its form and mechanical properties from its ECM (Buckwalter and Mankin 1997). Articular cartilage must be able to absorb and distribute high compressive forces. Two major macromolecules enable cartilage to provide this function: proteoglycan and type II collagen. Aggrecan is the predominant proteoglycan found in articular cartilage. It has a high sulphated glycosaminoglycan (GAG) content that, by nature of its negative charge, draws water into the tissue enabling it to resist compression. The proteoglycan is held within the cartilage by a cross-linked network of triple-helical type II collagen fibrils, which provide cartilage with its tensile strength (Muir 1995; Temenoff and Mikos 2000). Other molecules such as decorin, biglycan, laminin, tenascin, fibromodulin and minor collagens (types VI, IX, X and XI) assist in maintaining the tissue through the spatial organisation of the ECM (Temenoff and Mikos 2000).

Articular cartilage can be divided into four zones (superficial, transitional, middle and calcified) based on differences in matrix morphology and biochemical composition. The superficial zone (zone 1) is the thinnest zone and is located adjacent to the joint cavity. Within this zone there are two distinct layers. An acellular sheet of predominantly collagen fibers (the lamina splendens) covers the joint and underneath this is a second layer, composed of flattened chondrocytes and containing a high concentration of water, more collagen and less proteoglycan than the other zones. This combination of molecules in the

superficial zone imparts more tensile strength to this area of the matrix, enabling it to resist shearing forces from the articulating surfaces. Zone 2, known as the transitional zone, contains chondrocytes that are spherical and synthesise an ECM that has larger collagen fibrils, more proteoglycan and less collagen and water than in the previous zone. The third zone (middle or radial zone) contains rounded chondrocytes that are stacked in columns perpendicular to the articulating surface. These cells show high synthetic activity, ten times that of superficial zone chondrocytes (Wong et al. 1996). A tidemark separates the third zone from the fourth zone. Zone 4 (calcified zone) lies closest to the subchondral bone and consists of a thin layer of calcified cartilage (Figure 1.1).

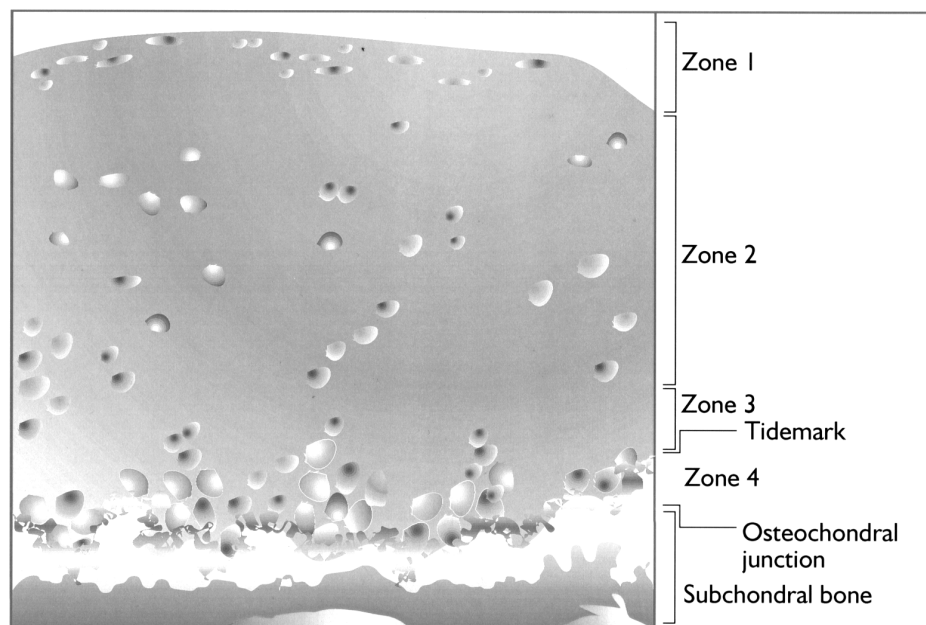


Figure 1.1 The zones of articular cartilage. See section 1.1.1 for details (taken from Elliott and Cawston 2001).

1.1.2 Chondrocytes

Chondrocytes represent only a small percentage (approximately 1%) of the total volume of articular cartilage, but are vital for the synthesis and maintenance of the cartilaginous matrix. These cells originate from mesenchymal stem cells (MSCs) found in the bone marrow in mature individuals. During embryogenesis, MSCs differentiate into chondrocytes and secrete the cartilage ECM. In the absence of a vascular supply, chondrocytes receive nutrients from the synovial fluid, which is synthesised by fibroblasts

in the synovial membrane. Maintenance of the articular cartilage requires replacement of matrix components. Not only can chondrocytes synthesise all the components of the ECM, they then must assemble and organise these components into a highly ordered framework (Buckwalter and Mankin 1997).

Under normal circumstances, proliferation of chondrocytes is limited and it is thought they maintain the ECM through low-turnover replacement of certain matrix proteins. If the equilibrium between synthesis and degradation is disrupted, as in ageing and joint disease, the rate of loss of collagens and proteoglycans from the matrix exceeds the rate of deposition of newly synthesized molecules. Originally thought of as an inert tissue, cartilage is now thought to respond to extrinsic factors that regulate gene expression and protein synthesis in chondrocytes. Many studies over the last two decades have confirmed that chondrocytes are able to respond to mechanical stress and stimuli such as cytokines and growth factors that ultimately contribute to structural changes in the surrounding cartilage matrix (Goldring and Goldring 2007).

1.1.3 Extracellular matrix

The articular cartilage matrix consists of two components: the tissue fluid, which accounts for as much as 80% of the wet weight of the tissue, and the macromolecular framework that gives the tissue its form and stability and accounts for the remaining ~20% of the wet weight (Buckwalter et al. 1997).

1.1.3.1 Collagen

Articular cartilage contains various genetically distinct collagen types, specifically types II, VI, IX, X and XI. Together, types II, IX and XI form the cross-banded fibrils seen with electron microscopy of articular cartilage. It is the formation of these fibrils into a tight meshwork that endows articular cartilage with its tensile strength, in addition to entrapping the larger proteoglycans thus contributing to the cohesiveness of the cartilage (Buckwalter et al. 1997). Each collagen molecule is composed of three α -chains, characterised by a Gly-Xaa-Yaa sequence, where Xaa is often proline and Yaa is hydroxyproline. Due to the high content of imino amino acids, the α -chains of collagen all form a left-handed α -helix. Furthermore, the presence of a glycine residue at every third residue allows the α -chains to

twist around one another to form a superhelix. The triple-helical structure is such that the peptide bonds linking the adjacent amino acids are buried within the molecule, making it highly resistant to proteolytic degradation (Cremer et al. 1998). Type II collagen is almost exclusively found in articular cartilage, with type I collagen predominating in other connective tissues such as bone, skin and tendon. In adult articular cartilage, type II collagen accounts for 90-95% of the collagen. The type II collagen molecule is composed of three identical polypeptide chains $[\alpha 1(\text{II})]_3$, each consisting of a single 300 nm-long triple helix with short telopeptides at each end (Figure 1.2). Although the functions of the other types of collagen present in articular cartilage are not fully understood, it is thought that type IX and XI are needed to stabilise the fibrillar network (Kuettnner 1992). Type X collagen has been immunolocalised to the zone of calcified cartilage and is synthesised only by hypertrophic cells within this zone. Type VI collagen is thought to be localised in the capsular matrix around chondrocytes and chondrons (Kuettnner 1992).

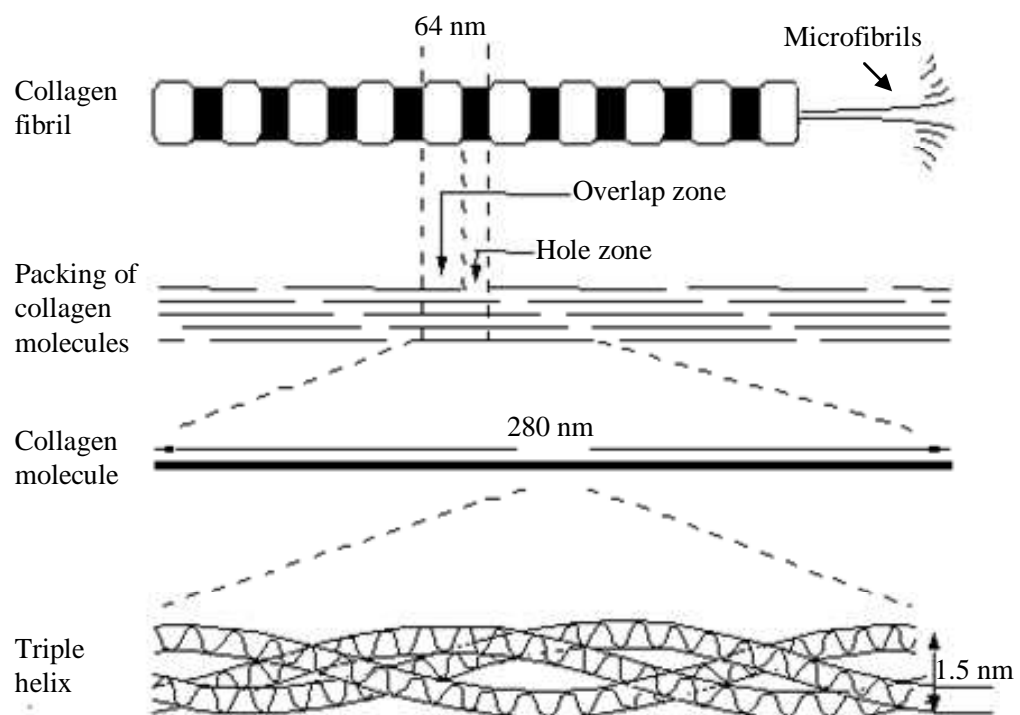


Figure 1.2 Structure and organisation of collagen. Three polypeptide α -chains assemble to form a triple helical precursor molecule, procollagen. After secretion, the globular regions are cleaved from each end of the procollagen molecule to form collagen. Collagen molecules assemble in a precise staggered arrangement, overlapping to give a 64 nm periodicity seen under the electron microscope (taken from Cleaver 2000).

1.1.3.2 Proteoglycans

A proteoglycan is a protein which has one or more attached GAG chains. A variety of proteoglycans are found in articular cartilage that are essential for its normal function, including aggrecan, decorin, biglycan, fibromodulin and lumican. Articular cartilage is characterised by its high aggrecan content, which forms proteoglycan aggregates in association with hyaluronan (HA) and link proteins (LP) (small non-collagenous proteins). It is these aggregates that are crucial in distributing load in weight-bearing joints and providing the osmotic properties needed to resist compressive loads as well as anchoring the proteoglycans within the matrix. These hydrophilic proteoglycan aggregates draw water into the tissue, enabling it to undergo reversible deformation. Aggrecan accounts for 90% of the proteoglycan mass in articular cartilage. It has multiple functional domains and its core protein consists of three globular regions, known as G1, G2 and G3 (Figure 1.3).

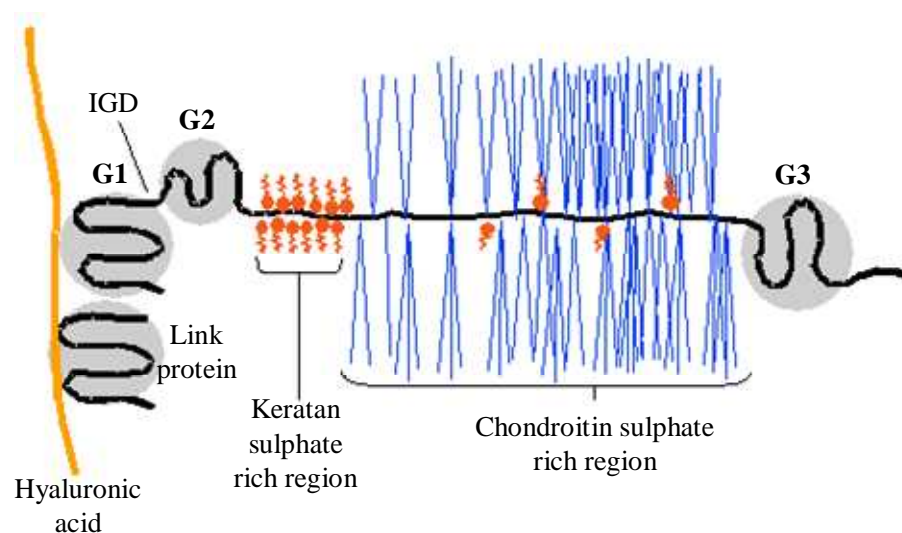


Figure 1.3 Structure of aggrecan. Aggrecan consists of three globular domains (G1, G2 and G3) separated by linear portions of polypeptide. The aggrecan interglobular domain (IGD) between G1 and G2 is particularly susceptible to proteolytic cleavage. The region between G2 and G3 binds highly sulphated GAGs. Aggrecan molecules bind to hyaluronic acid via the G1 domain and this binding is enhanced by link protein (taken from Pyle 2003).

The interglobular domain (IGD) that links the G1 and G2 domains is a target for proteolytic attack and is a key site for cleavage as it separates the major GAG bearing region of aggrecan from the G1 domain that anchors it in the matrix. Almost 90% of the aggrecan mass is carbohydrate, which consists mostly of chondroitin sulphate chains, but also

includes keratan sulphate chains and O- and N-linked oligosaccharides (Hardingham and Fosang 1992; Hardingham and Fosang 1995; Roughley 2006).

In addition to aggrecan, other non-aggregating proteoglycans have been identified in articular cartilage. These proteoglycans have shorter protein cores, fewer GAG chains and instead of directly contributing to the mechanical behaviour of the tissue are thought to be involved in the organisation of collagen molecules. Decorin, biglycan, fibromodulin and lumican are all small leucine-rich repeat proteoglycans (SLRPs) and are characterised by multiple adjacent domains possessing a common leucine-rich motif (Hocking et al. 1998). Decorin, fibromodulin and lumican are known to interact with type II collagen and so may play a role in the stabilisation of the collagen meshwork (Hedbom and Heinegard 1993). The interactions of biglycan are less well understood. In addition to a stabilisation role, SLRPs appear to help limit access of collagenases to their unique cleavage site, therefore they may also be important in preventing proteolytic damage (Hocking et al. 1998; Roughley 2006).

1.2 Arthritis

Despite its durability and ability to maintain itself, articular cartilage is susceptible to injuries and disease resulting in irreparable tissue damage. One in five adults have long-term health problems due to arthritis (Arthritis Research Campaign 2002). Whilst many types of arthritis exist, the most common examples of arthritic disease are rheumatoid arthritis (RA) and osteoarthritis (OA).

The arthritides are characterised by a progressive loss of articular cartilage and this loss of cartilage is associated with degradation of major ECM components. As described earlier (section 1.1.1), the ECM consists mainly of aggrecan and Type II collagen. Collagen provides cartilage with its tensile strength and aggrecan (due to its negative charge) draws water into the cartilage, thus enabling it to resist compression (Moore and Dalley 1999). The loss of aggrecan during cartilage degradation is rapid but reversible. Collagen is much less readily released, however when collagen degradation does occur, the tissue is irreversibly damaged. Collagen breakdown is therefore considered to be the key step in

controlling cartilage turnover (Jubb and Fell 1980). Human articular cartilage undergoes remodelling as a consequence of anabolic and catabolic processes. Formation and progression of cartilage lesions is widely accepted to be, at least partly, a consequence of secretion of inflammatory mediators that disrupt cartilage-matrix homeostasis, thus altering chondrocyte metabolism (Pelletier et al. 1993). Healthy cartilage ECM is maintained in a state of dynamic equilibrium, with a balance between synthetic and degradative pathways. However, in both RA and OA this balance is disrupted, with degradation exceeding synthesis. This results in breakdown of cartilage tissue and subsequent loss of joint function (Shingleton et al. 1996).

1.2.1 Rheumatoid arthritis

RA affects approximately 1% of adults in developed countries and is characterised by chronic inflammation of multiple joints and subsequent destruction of cartilage and bone (Figure 1.4). Genetic, environmental, infectious and hormonal factors are all thought to be involved in the development of RA. Although the precise pathogenesis of RA remains unclear, T cells, B cells, macrophages, neutrophils and synovial fibroblasts are known to be central to the mechanisms of joint inflammation and disease progression. The initiating trigger in RA is unclear, however the disease is generally considered to have an autoimmune basis. A number of potential antigens have been proposed to play a role including collagen type II, heat shock proteins and gp39. However, only rheumatoid factor, antibodies to citrullinated antigens, and antibodies to immunoglobulin binding protein have shown sufficient sensitivity and specificity to be considered clinically. The controversy of whether autoantibodies contribute to, or are secondary to, the pathogenesis of RA is still a matter of debate (Andersson et al. 2008).

Genetic predisposition to RA is polygenic and complex. The concordance of monozygotic twins of 12–15% in comparison with the concordance of dizygotic twins of 2–4% provides evidence of a genetic contribution to the disease (Jirholt et al. 2001). In recent years there has been a huge increase in the number of confirmed susceptibility loci identified for RA, although the largest contribution to RA susceptibility remains on the HLA-DRB1 gene. A strong association between possession of HLA-DR haplotypes (DRB1*0101, 0401, 0405

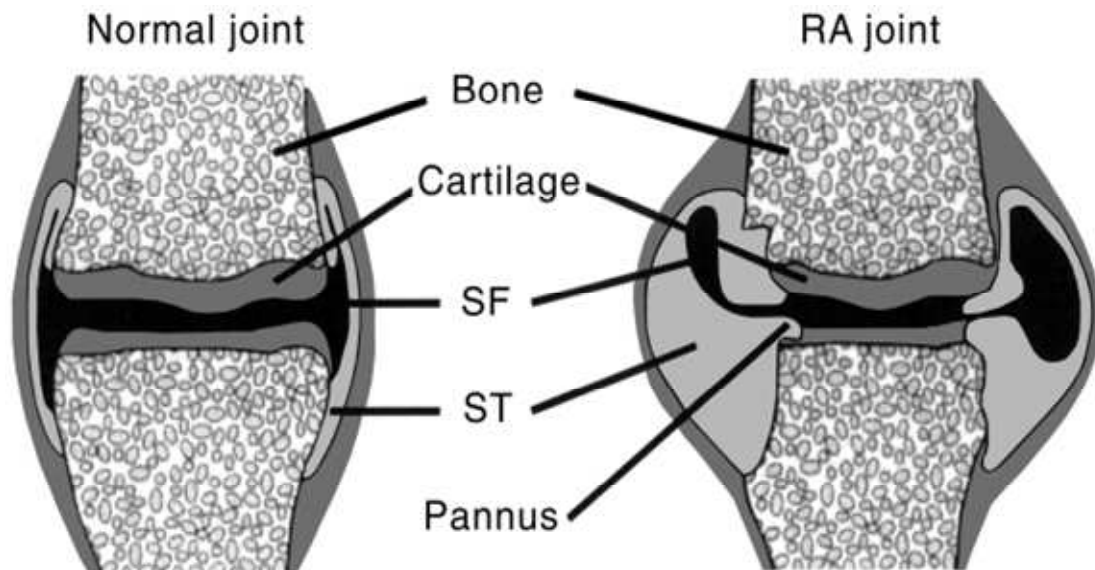


Figure 1.4 Schematic representation of the joint inflammatory events in rheumatoid arthritis (RA). The inflammatory response in the RA joint is characterized by marked swelling and inflammation. Immune cell infiltration into both the synovial fluid (SF) and synovial tissue (ST) accompanies this inflammation, in addition to the proliferation of resident ST cells and angiogenesis. Formation of the destructive tissue front or pannus occurs as the ST extends over cartilage and bone. The majority of the cartilage destruction and bone erosion occurs at the junction with pannus (taken from Pettit and Thomas 1999).

and 1402) and an increased risk of developing RA has been demonstrated. These subtypes were found to possess a 'shared' epitope (Gregerson 1997).

As mentioned previously the initiating trigger in RA is unknown, however it has been proposed that the initiating event in RA involves an infectious agent or other environmental exposure. The initiating trigger is followed by the induction of an immune response that results in inflammation in the synovial membrane. The synovium lines the joint cavity and is the site of production of synovial fluid. The normal synovium is comprised of macrophage- and fibroblast-like cells known as synoviocytes. In RA, the lining becomes hyperplastic due to an increase in macrophages and fibroblasts. In addition, increased vascularisation is also observed. The synovial lining gradually proliferates leading to formation of the pannus, which extends over the articular cartilage. Although there is an

association between inflammation and joint damage, it is now thought that these two processes may not in fact be coupled. There is increasing clinical and experimental evidence to show that inflammation and destruction can be uncoupled and that different cells and mediators are important in these processes. The sustained degradation of the ECM may be a later consequence of the inflammatory process via stimulation of the resident chondrocytes (van den Berg and van Riel 2005). Cartilage destruction is mediated through the increased expression of degradative enzymes, resulting in breakdown of cartilage and erosion of the subchondral bone leading to disruption of normal joint function (Sweeney and Firestein 2004; Otero and Goldring 2007).

1.2.2 Osteoarthritis

OA is the most common of the arthritides, with the majority of individuals over the age of 65 showing radiographic and/or clinical evidence of OA. The most commonly affected sites include the hands, knees, hips and spine (Felson 2006). OA is characterised by the progressive loss of articular cartilage, thickening of the subchondral plate, formation of new bone at the joint margins and the formation of subchondral bone cysts resulting in symptoms such as pain, stiffness and loss of mobility (Goldring and Goldring 2006). A variety of risk factors are associated with susceptibility to OA, such as increasing age, obesity, joint injury and genetic predisposition (Felson et al. 2000). OA can be subdivided into two categories; primary OA occurs in middle-aged to elderly patients and was considered to be a consequence of ‘wear and tear’ (although this is now known to be an over-simplified explanation), and secondary OA that can occur at any age as a result of trauma or disease.

Historically, OA has been considered a process involving a disturbance of the normal balance between degradation and repair in the articular cartilage and subchondral bone. OA was therefore thought of as a primarily non-inflammatory condition as opposed to RA where both local and systemic inflammation is a central feature. However, this theory is now being reconsidered. Low-grade synovitis, increased vascularity and inflammatory-cell infiltration have been reported in patients with all grades of OA (Smith et al. 1997). More recently, magnetic resonance imaging (MRI) has reinforced the idea that synovitis is a frequent feature of OA (Loeuille et al. 2005). Inflammatory cytokines and mediators

produced by joint tissues are increasingly being shown to play a role in the pathogenesis of OA, perpetuating disease progression and therefore representing potential therapeutic targets (Abramson and Attur 2009).

1.2.3 Arthritis treatment

Treatment for OA has changed little over the last fifty years and is limited to pain relief and in severe cases, joint replacement. However, articular cartilage is able to provide stable movement with less friction than any prosthetic replacement, and can also alter its properties in response to differences in loading. There is no available treatment that can prevent or slow disease progression. RA, however, has many more treatment options including disease modifying anti-rheumatoid drugs (DMARDs) and the more recently developed anti-TNF α (Etanercept and Infliximab) and targeted B-cell (Rituximab) therapies (Kumar and Clark 2005). Although anti-TNF α therapy can offer significant disease remission in some, it is by no means effective in all patients and can cause potentially life-threatening side effects (British Medical Association and Royal Pharmaceutical Society of Great Britain 2005). Hence, research into new treatments is ongoing.

1.3 Proteinases

The primary cause of the cartilage and bone destruction associated with the arthritides is an elevation of the levels of active proteinases. Proteinases are responsible for enzymatic cleavage of peptide bonds, a process that is an essential requirement of many biological processes (Rengel et al. 2007). These enzymes are secreted by various cells within the joint and degrade the ECM. The expression of these proteinases is regulated by various cytokines and growth factors acting on the cells found within the joint.

Exopeptidases specifically cleave substrates at the N-terminal or C-terminal positions of polypeptides, whilst endopeptidases (also called proteinases) cleave internal peptide bonds. Proteinases can be subclassified into five main classes of proteinases. This subclassification is based on their mechanism of catalysis, which is related to the chemical group involved in the process of hydrolysis. Therefore, proteinases are described as aspartate, cysteine and

threonine types, which act intracellularly in an acid pH, or as serine and metallo catalytic types, which act extracellularly in a neutral pH (Figure 1.5) (Barrett 1980; Rengel et al. 2007).

A subdivision of the metalloproteinase superfamily is the metzincins, a structurally related group of zinc-dependent endoproteinases that include the serralsins, the astacins, ADAMs (a disintegrin and metalloproteinase), MMPs (matrix metalloproteinases) and pappalysins (Barrett 1980; Overgaard et al. 2001). It is now thought that the enzymes mainly responsible for the degradation of cartilage are the MMPs.

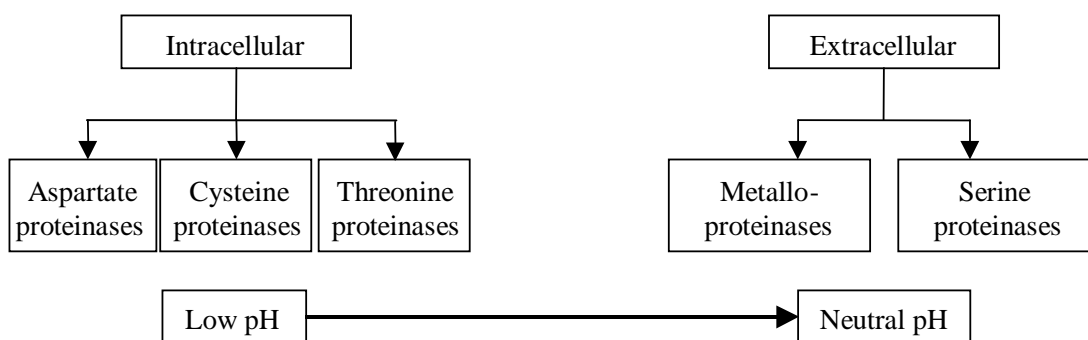


Figure 1.5 The five main classes of proteinases. Adapted from Rengel et al. (2007).

1.3.1 Matrix metalloproteinases

The MMPs are a large family of endopeptidases, which collectively are capable of degrading all components of the ECM and therefore have been extensively studied in relation to the modulation of matrix function (Nagase and Woessner 1999; Cawston and Young 2010). They play key roles in normal biological processes such as morphogenesis, wound healing, tissue repair and remodelling in response to injury. However, they are also central in the progression of diseases such as atheroma, arthritis, cancer and chronic tissue ulcers (Nagase et al. 2006). MMPs are known to be involved in the turnover and breakdown of the ECM, both in healthy and arthritic cartilage. MMPs are extracellular proteins, but recent studies have suggested that MMP-1 (Limb et al. 2005), MMP-2 (Kwan et al. 2004) and MMP-11 (Luo et al. 2002) are also found intracellularly and could act on intracellular proteins. Traditionally, MMPs have been classified according to primary

structure, substrate specificity and cellular location resulting in five groups; the collagenases, stromelysins, gelatinases, matrilysins and membrane-type (MT) MMPs, although several recently discovered enzymes do not fit this classification, including MMP-12 (metalloelastase), MMP-19, MMP-20 (enamelysin), and MMP-23 (Clark and Parker 2003) (Table 1.1).

MMP subfamily	MMP	Alternative name(s)	MW (kDa)	Known matrix substrates
Collagenases	MMP-1	Interstitial collagenase Fibroblast collagenase Collagenase-1	55/45	Collagens I, II, III, VII, VIII, X; gelatin; aggrecan; proteoglycan link protein; tenascin; entactin; α 1-PI; α 2-M
	MMP-8	Neutrophil collagenase Collagenase-2	75/58	<i>Collagen types I, IV, V, VII, X, XI, XIV; gelatin</i> ; aggrecan; α 1-PI; α 2-antiplasmin; fibronectin
	MMP-13	Collagenase-3	60/48	Collagens I, II, III, IV, VII, X; gelatin; plasminogen activator inhibitor 2; aggrecan; tenascin
	MMP-18	Xenopus collagenase Collagenase-4	55/42	Collagen I, gelatin
Gelatinases	MMP-2	Gelatinase-A 72 kDa gelatinase Type IV collagenase	72/66	Collagens I, IV, V, VII, X, XI, XIV; gelatin; elastin; fibronectin; vitronectin; aggrecan; link protein; α 1-PI; activates MMP-9 and MMP-13
	MMP-9	Gelatinase-B 92 kDa gelatinase Type V collagenase	92/86	Collagens I, IV, V, VII, X, XI, XIV; gelatin; elastin; fibronectin; aggrecan; link protein; α 1-PI
Stromelysins	MMP-3	Stromelysin-1 Transin Proteoglycanase	57/45	Collagens I, II, III, IV, V, VIII, IX, X, XI; gelatin; aggrecan; link protein; fibronectin; α 1-PI; laminin; α 2-M; activates MMP-1, -7, -8, -9 and -13.
	MMP-10	Stromelysin-2 Transin-2	57/44	Collagens III, IV, V; gelatin; aggrecan; elastin; link protein; fibronectin; activates MMP-1 and MMP-8
	MMP-11	Stromelysin-3	51/44	α 1-PI
Membrane-type MMPs	MMP-14	MT1-MMP	66/56	Collagens I, II, III, IV; gelatin; elastin; aggrecan; proteoglycan; fibronectin; vitronectin; activates MMP-2 and MMP-13
	MMP-15	MT2-MMP	72/60	Collagens I, II; gelatin; fibronectin; tenascin; laminin; proteoglycan; activates MMP-2
	MMP-16	MT3-MMP	64/52	Activates MMP-2
	MMP-17	MT4-MMP	57/53	Gelatin
	MMP-24	MT5-MMP	63/45	Gelatin; fibronectin; proteoglycan; activates MMP-2
	MMP-25	MT6-MMP Leukolysin	63/?	Activates MMP-2
Others	MMP-7	Matrilysin	28/19	Collagens IV, X; gelatin; aggrecan; link protein; tenascin; fibronectin; laminin; elastin; entactin; α 1-PI; activates MMP-1, -2 and -9
	MMP-12	Macrophage elastase	54/45/22	Collagen IV; gelatin; elastin; α 1-PI; fibronectin; vitronectin; laminin
	MMP-19	<i>RAS1-1</i>	54/45	Aggrecan
	MMP-20	Enamelysin	54/22	Amelogenin
	MMP-21	X MMP	70/53	Not known
	MMP-22	CMMP	52/43	Gelatin
	MMP-23		??/?	Not known
	MMP-26	Endometase Matrilysin-2	28/?	Gelatin; α 1-PI

Table 1.1 Matrix Metalloproteinases. MMPs can be sub-grouped according to similarities in domain structure and function. Molecular weight (MW) of the latent (bold) and active forms are shown. Adapted from Bigg and Rowan (2001).

1.3.2 Structure of matrix metalloproteinases

The MMPs possess a multidomain structure (Figure 1.6):

Pre-domain encodes a short hydrophobic signal peptide of 18-30 residues, which is required for enzyme maturation and its secretion from the cell into the extracellular space.

Propeptide domain is approximately 80 residues in length and contains the highly conserved PRCG(V/N)PD sequence motif. The cysteine residue within this motif is known as the 'cysteine switch' and ligates with the catalytic zinc to maintain the enzymes in their latent state (Van Wart and Birkedal-Hansen 1990).

Catalytic domain is approximately 170 amino acids in length. This domain characteristically contains a zinc atom and is responsible for enzyme activity (Rengel et al. 2007).

Hinge domain separates the N- and C-terminal domains and is of variable length.

Haemopexin domain is about 200 amino acids in length. The haemopexin domain is required for hydrolysis of triple helical collagens. Removal of the MMP-1, MMP-8, MMP-13, or MMP-14 haemopexin domain results in a loss of collagenolytic activity (Lauer-Fields et al. 2009).

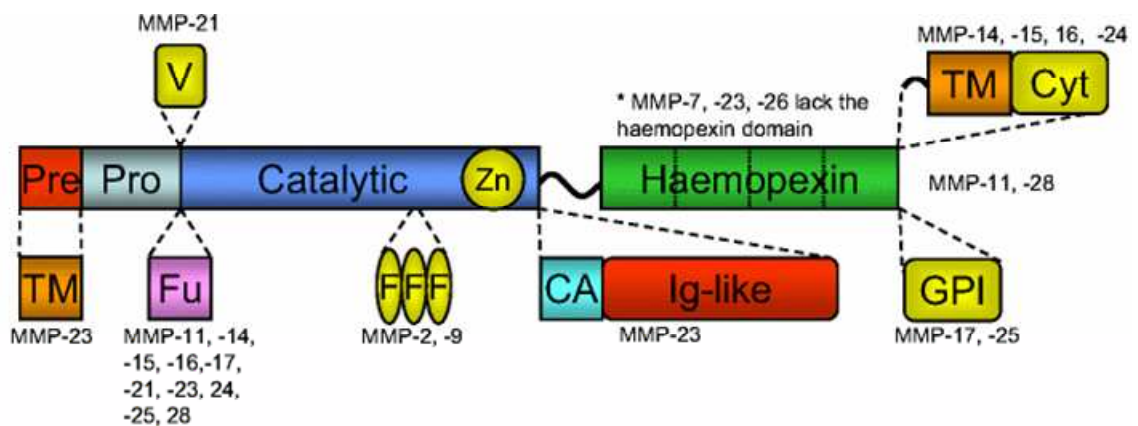


Figure 1.6 Domain structure of MMPs. All MMPs have a catalytic domain containing the active site zinc (Zn). In addition, several MMPs contain a furin recognition motif (Fu), which enables intracellular activation by furin-like proteinases. All MMPs (with the exception of MMP-7, -23 and -26) possess a haemopexin domain. Several other domains are present in certain MMPs including fibronectin-like domains (F) in MMP-2 and -9 and a vitronectin-like domain (V) in MMP-21. Some MMPs are anchored to the cell surface via a glycosylphosphatidyl inositol (GPI) anchor and others by a transmembrane domain (TM) with cytoplasmic tail (Cyt). Unlike all other MMPs, MMP-23 possesses an N-terminal TM domain, a cysteine array (CA) and an immunoglobulin (Ig-like) domain. Taken from Cawston and Young (2010).

1.3.2.1 The collagenases

Type II collagen is extremely resistant to most proteinases because of its triple helical structure. Thus, the only enzymes that are capable of degrading type II collagen are the collagenases. The three human collagenases, MMP-1, MMP-8 and MMP-13, are known to cleave the three α chains of types I, II and III collagen at a single site to give 3/4 and 1/4 length products (Miller et al. 1976). MMP-2 (a gelatinase) and MMP-14 (a MT-MMP) have also been shown to degrade collagen (Bigg and Rowan 2001). However, the specific activity of MMP-14 for type II collagen is extremely weak (Ohuchi et al. 1997). The catalytic domains of collagenases are also capable of cleaving non-collagenous substrates, but they are unable to cleave native fibrillar collagens without their haemopexin domain. It is the cooperation between the catalytic and haemopexin domains that is thought to be necessary for their collagenolytic activity (Chung et al. 2004). After the collagen molecules have been cleaved by the collagenases, these fragments are no longer stable at body temperature and the helical structure is lost. The fragments then become susceptible to proteolytic degradation by other MMPs.

Collagen is not readily released from articular cartilage, however when collagen degradation does occur, the tissue is irreversibly damaged (Jubb and Fell 1980). MMP-1 and MMP-13 have predominant roles in RA and OA because they are rate limiting in the process of collagen degradation, making these collagenase enzymes potential targets for therapy in arthritis.

Although all the collagenases cleave collagen, it is probable that the relative importance of individual collagenases differs in different forms of arthritis. Current dogma suggests MMP-1 is the key collagenase in RA, whereas MMP-13 is thought to be the important collagenase in OA. MMP-8 is only a minor gene product of human articular chondrocytes (Stremme et al. 2003), so it is likely that MMP-8 is not involved in the cartilage destruction seen in OA and RA. Instead, MMP-8 is thought to be a key enzyme in septic arthritis due its production by neutrophils (Rajasekhar et al. 2004).

MMP-1 is also known as interstitial collagenase, fibroblast collagenase and collagenase-1. Type III collagen is cleaved most efficiently by MMP-1, followed by type I collagen and then type II collagen (Welgus et al. 1981). MMP-1 is known to be expressed in many cell types including stromal fibroblasts, macrophages, endothelial cells, epithelial cells and chondrocytes (Brinckerhoff et al. 2000; Mengshol et al. 2000). Under normal physiological conditions the expression of MMP-1 is low, however it is readily induced under pathological and inflammatory conditions (Brinckerhoff et al. 2000).

MMP-8, also referred to as collagenase-2 or neutrophil collagenase, was originally thought to be expressed solely by maturing neutrophils, and functionally restricted to ECM breakdown. However, in recent years it has been discovered that this protease can be expressed by a wide variety of cell types and plays an important regulatory role in acute and chronic inflammation (Van Lint and Libert 2006). Whilst MMP-8 is active against type II collagen, type I collagen appears to be the preferential substrate of MMP-8 (Hasty et al. 1987).

MMP-13, also known as collagenase 3, was previously thought to be associated exclusively with malignancy due to its discovery in breast carcinomas (Freije et al. 1994).

However, it has since been associated with a variety of non-malignant conditions, in particular arthritis (Mitchell et al. 1996). It is expressed by both chondrocytes and synovial cells in human OA and RA and is thought to play a critical role in cartilage destruction. MMP-13 preferentially degrades type II collagen (Knauper et al. 1996a) and is able to cleave type II collagen approximately five times faster than MMP-1 (Reboul et al. 1996). MMP-13 knock-out mice exhibit a normal lifespan and do not show any major phenotypic abnormalities. However, microscopic analysis does demonstrate defects in the growth plate cartilage with an increase in the hypertrophic chondrocyte zone and a delay in primary ossification (Takaishi et al. 2008). To date there have been no published studies examining OA-like pathology in the MMP-13 knockout mouse.

1.3.2.2 The stromelysins

There are three stromelysins; MMP-3 (stromelysin 1), MMP-10 (stromelysin 2) and MMP-11 (stromelysin 3). MMP-3 and MMP-10 are highly homologous, with similar structures and substrate specificity. MMP-3 is not constitutively expressed but can be induced by IL-1 and TNF- α in chondrocytes and fibroblasts (MacNaul et al. 1990). MMP-3 is able to activate other MMPs, including the collagenases (Murphy et al. 1987). MMP-10 is also able to activate various MMPs, including MMP-1 and -8 (Knauper et al. 1996b). Homology between MMP-11 and the other stromelysins is reduced because of the presence of a 10-amino acid insert between the pro- and catalytic domains that enables recognition of furin. In addition, both MMP-3 and -10 are secreted from cells as inactive pro-MMPs, whereas MMP-11 is activated intracellularly by furin and so is secreted from the cell as an active enzyme (Pei and Weiss 1995).

1.3.2.3 The gelatinases

This sub-group consists of MMP-2 (gelatinase A) and MMP-9 (gelatinase B). The gelatinases differ from the other MMPs in that they possess three repeats of a fibronectin type II motif inserted into their catalytic domain, which enable efficient binding to gelatin (Steffensen et al. 1995). These enzymes possess similar catalytic activity and are important in the cleavage of denatured collagen (gelatin). Their substrates also include type IV and type V collagen and laminin (Murphy and Nagase 2008). MMP-2 is the most widespread of all the MMPs and it is able to activate proMMP-9 (Fridman et al. 1995) and -13 (Knauper et al. 1996c). It has been suggested that MMP-2 digests native collagen in a similar manner

to the 'classical' collagenases (Patterson et al. 2001), however the collagenolytic activity of MMP-2 is much weaker than the other collagenases. MMP-9 is expressed in many transformed and tumour-derived cells as well as in chondrocytes, neutrophils, monocytes and alveolar macrophages (Matrisian 1992).

1.3.2.4 The matrilysins

This group consists of MMP-7 and MMP-26. Their structure differs from that of other MMPs because they lack the haemopexin domain. MMP-7 is synthesised by epithelial cells and MMP-26 is expressed in many cells such as those of the endometrium, but also in some carcinomas (Murphy and Nagase 2008).

1.3.2.5 The membrane-type MMPs

The membrane-type MMPs (MT-MMPs) can be further subdivided into two groups. The first contains four MMPs that are type I transmembrane proteins (MMP-14, -15, -16 and -24) and the second consists of two glycosylphosphatidylinositol-anchored proteins (MMP-17 and -25). All MT-MMPs possess a furin-like pro-protein convertase recognition sequence and so are activated intracellularly. With the exception of MMP-17, all MT-MMPs can activate proMMP2 (English et al. 2001). MMP-14 is able to activate MMP-13 on the cell surface and therefore is of particular relevance to cartilage degradation (Knauper et al. 1996c). The latent form of MMP-14 is activated by furin and plasmin (Okumura et al. 1997) and once activated, is capable of degrading components of the ECM (including interstitial collagens) (Ohuchi et al. 1997).

1.3.3 Regulation of matrix metalloproteinases

MMPs regulate many biological processes and the production and activation of MMPs is strictly regulated *in vivo* at various critical steps (Burrage et al. 2006). Constitutive expression is minimal and cells within intact tissues do not usually store MMPs (with the exception of neutrophils) (Reunanen and Kähäri 2005). The potent proteolytic activity of MMPs is tightly controlled at 3 stages; synthesis, proenzyme activation and inhibition (Figure 1.7).

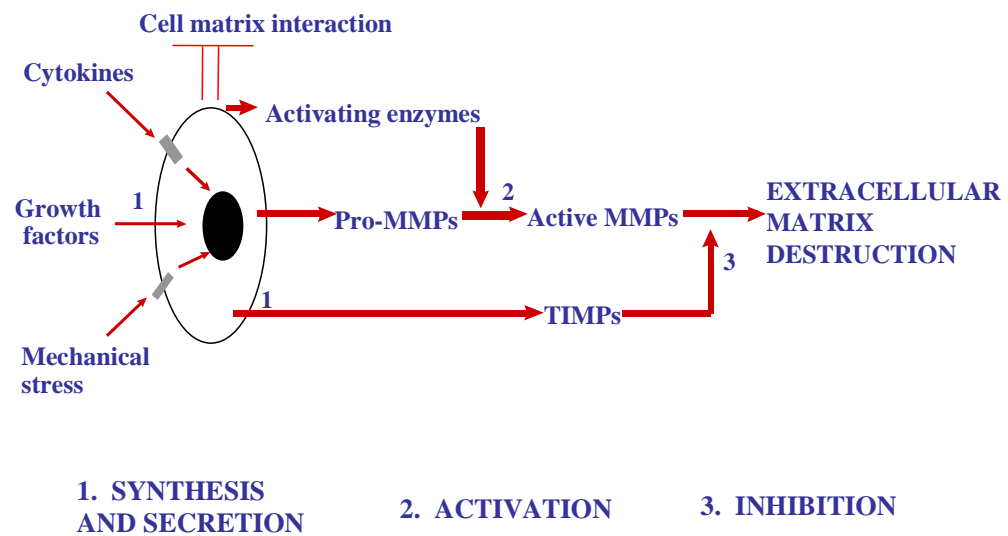


Figure 1.7 The regulation of MMPs occurs at three distinct levels: synthesis and secretion, activation and inhibition. Taken from Hochberg et al. (2003).

1.3.3.1 Synthesis

Within the rheumatoid joint are large numbers of inflammatory cells, T cells, macrophages and neutrophils. These cells interact with synovial cells, resulting in the production of cytokines such as IL-1 and TNF- α , which in turn stimulate many cell types to produce MMPs. Furthermore, certain cytokines (for example IL-1 or TNF- α in combination with OSM (Cawston et al. 1998) act synergistically to increase the production of MMPs by cells. Genetic variations can influence basal and inducible levels of MMP expression, in turn influencing the development of diseases such as coronary heart disease and cancers. Naturally occurring single-nucleotide polymorphisms (SNPs) have been detected in the promoter of a number of MMP genes and these sequence alterations have been shown to have allele-specific effects on the transcriptional activities of MMP gene promoters (Ye 2000; Decock et al. 2008).

1.3.3.2 Activation of proenzymes

All MMPs are synthesised in a proenzyme form. Activation of the proenzyme requires proteolytic removal of the 10 kDa pro-peptide region. This process removes the conserved cysteine residue, which in the proenzyme, blocks the active-site zinc atom (Springman et al. 1990). The activation of proMMPs by other active MMPs is well documented and suggests that carefully controlled activation cascades exist *in vivo*. Some MMPs, including MMP-

14, possess a conserved sequence of 10-12 amino acids between the propeptide and N-terminal domain that is recognised by the furin family of serine proteinases (Pei and Weiss 1995). This enables activation of these MMPs within the Golgi. These enzymes are then able to arrive at the cell surface in an active form that is thought to be responsible for the activation of other MMPs (Cawston 1998). For those MMPs without this furin site, proteolytic removal of the propeptide is thought to occur close to the cell surface. Plasmin and other serine proteinases (such as trypsin, chymotrypsin, elastase and kallikreins) are able to activate certain pro-MMPs. The activators of the MMPs of particular relevance to the arthritides are summarized in Table 1.2.

Pro-MMP	Activators
ProMMP-1	MMP-3, MMP-10, plasmin, kallikreins, chymase
ProMMP-13	MMP-2, MMP-3, MMP-14, plasmin
ProMMP-2	MMP-14, MMP-15 MMP-16 MMP-24, MMP-25
ProMMP-9	MMP-1, MMP-2, MMP-3, MMP-7, MMP-10, MMP-13, kallikreins, elastase, plasmin
ProMMP-3	Plasmin, tryptase, chymotrypsin, neutrophil elastase, cathepsin G, kallikreins, thermolysin, chymase
ProMMP-14	Proprotein convertases (e.g. furin), plasmin, urokinase

Table 1.2 Potential activators of MMPs. Adapted from Murphy et al. (2000).

1.3.3.3 Inhibition

1.3.3.3.1 Natural inhibitors of MMPs

Any disruption in the balance of active MMPs and their inhibitors can result in diseases associated with uncontrolled ECM turnover, such as arthritis. Tissue inhibitors of metalloproteinases (TIMPs) are endogenous inhibitors of MMPs and so are important regulators of ECM turnover (Brew and Nagase 2010). They are not only important in the inhibition of active enzymes, but also play a role in proMMP activation, matrix binding and cell growth (Brew et al. 2000). To date, four homologous TIMPs have been identified:

TIMP-1 (Welgus et al. 1979), TIMP-2 (Stetler-Stevenson et al. 1989), TIMP-3 (Pavloff et al. 1992) and TIMP-4 (Greene et al. 1996). TIMPs -1, -2, -3 and -4 inhibit MMP activity through noncovalent binding to the zinc-binding sites of MMPs (Reunanen and Kähäri 2005). They bind with a 1:1 stoichiometry and this binding is essentially irreversible. Whilst all four TIMPs can be described as broad spectrum MMP inhibitors, their specificity for individual MMPs does differ (Table 1.3). TIMP-3 is thought to have the widest range of inhibition as it not only inhibits MMPs, but also several members of the ADAM (a protein with a metalloprotease and disintegrin domain) (-10, -12, -17, -28 and -33) and ADAMTS (an ADAM with a thrombospondin-like motif) (-1, -2, -4 and -5) families (Brew and Nagase 2010). The overall shape of TIMPs has been elucidated based on crystal structures of TIMP-MMP complexes and appears to be “wedge-like” (Nagase et al. 2006). The N-terminal region of TIMPs is important for the inhibitory activity of the molecule and the C-terminal is necessary for enzyme binding (Cawston 1998). TIMP-1 and TIMP-2 have been shown to prevent the release of collagen from bovine nasal cartilage in culture (Ellis et al. 1994). Whilst TIMP-1 has been detected in the RA synovium (Hembry et al. 1995), the balance of MMPs to TIMPs appears to be altered in favour of the catabolic enzymes (MacNaul et al. 1990).

	TIMP-1	TIMP-2	TIMP-3	TIMP-4
Inhibition	All MMPs except most MT-MMPs	All	All	MMP-1, -2, - 3, -7 and -9
Molecular mass (kDa)	20.6	21.5	21.6	22.3
Soluble	Yes	Yes	No	Yes
Expression	Inducible	Constitutive	Inducible	?
Expression in cartilage	Yes	Yes	Yes	?
Binding to pro- MMPs	MMP-9	MMP-2	MMP-2,-9	MMP-2

Table 1.3 Properties of TIMPs. Adapted from Bigg and Rowan (2001).

All active MMPs can also be inhibited by α_2 -macroglobulin, a plasma glycoprotein that inhibits proteinases by trapping the enzyme within the macroglobin. The complex is then cleared by receptor-mediated endocytosis (Strickland et al. 1990).

1.3.3.3.2 Synthetic inhibitors of MMPs

Broad spectrum MMP inhibitors have long been considered to be a possible therapeutic option for treatment of RA and OA. However, the use of such MMP inhibitors has been restricted by a toxicity known as musculoskeletal syndrome (MSS) (Clark and Parker 2003). In an attempt to avoid MSS, low dose administration of broad spectrum MMP inhibitors was tried; however this resulted in a lack of efficacy. It is thought that MSS is probably due to the nonselective inhibition of multiple MMPs, however the exact molecular mechanism is unknown. As current dogma suggests MMP-13 to be the key collagenase in OA, the design of a highly selective MMP-13 inhibitor appears to be a good strategy for developing a treatment for arthritis. In recent years, Johnson et al. (2007) reported the generation of an orally active MMP-13 inhibitor that effectively reduced cartilage damage *in vivo* and did not induce joint fibroplasia in a rat model of MSS. A 2010 study has shown that fully selective MMP-13 inhibitors are able to reduce collagen degradation in human OA cartilage explants (Piecha et al. 2010). A reduction of 41-49% in collagen degradation was observed with selective MMP-13 inhibitors, compared with a reduction of 81% by the broad spectrum MMP inhibitor GM6001. The authors suggest that MMP-13 is therefore likely to be responsible for 50-60% of the increased collagenase activity in OA. The same study demonstrated that selective MMP-13 inhibitors were able to completely block IL-1+OSM-induced collagen degradation in a bovine articular cartilage model. The significant level of inhibition by selective MMP-13 inhibitors in both the human and bovine systems demonstrates the integral role played by MMP-13 in cartilage degradation but highlights the need for further study to understand the seemingly more complex situation in human OA cartilage.

Selective MMP-13 inhibitors have also been shown to reduce cartilage erosion in the SCID (severe combined immunodeficiency) mouse co-implantation model of RA and the collagen-induced arthritis (CIA) model in mice, but not in the antigen-induced arthritis

model (AIA) in rabbits (Jungel et al. 2010). The results of these studies taken together strongly support the development of this class of drugs to reduce cartilage destruction in arthritis patients.

1.4 Pro-inflammatory cytokines in arthritis

Cytokines are cell surface or soluble molecules that are important in mediating cell-cell interactions. Originally, they were classified according to their principal biological activity and cellular location. However, it now seems that the biological activity of particular cytokines can change in different situations (Goldring and Goldring 2004). Unlike hormones, the expression of cytokines is usually transient. The rheumatoid synovium contains a variety of cytokine-producing cells including macrophages, neutrophils and T cells. OA was traditionally thought of as non-inflammatory disease, an opinion that was historically based on the low numbers of leucocytes in the synovial fluid of OA patients. However the role of inflammatory cytokines in the pathogenesis of OA is attracting increased attention as inflammatory mediators are now thought to be involved in disease progression (Abramson and Attur 2009).

Pro-inflammatory cytokines produced by the synovium and chondrocytes play a central role in cartilage destruction. Chronic arthritis is characterised by persistent joint inflammation, with IL-1 and TNF- α considered to be the key mediators in perpetuating cartilage and bone destruction. Both have been found to be produced in increased quantities by RA synovium and can be detected in the synovial fluid of RA patients (Lubberts et al. 2000). OA is also characterised by an increased production of IL-1 and TNF- α by articular chondrocytes (Pelletier et al. 2001). Although joint swelling due to inflammation is a severe clinical problem, bone and cartilage destruction can occur uncoupled from inflammation (van den Berg 1998). Studies in experimental models have revealed that whilst TNF- α is an important cytokine in joint swelling, IL-1 is the dominant cytokine in cartilage destruction (van den Berg 1998). Cytokines are capable of acting in synergy, whereby the combined effects of two or more cytokines far exceeds the effects of either cytokine alone. For example, IL-1, when in combination with oncostatin M (OSM), induces a marked catabolic effect. The combination of IL-1 and OSM synergistically

induces the synthesis and activation of procollagenases, resulting in almost complete resorption of bovine nasal cartilage within a 14-day assay (Cawston et al. 1995; Cawston et al. 1998). Both IL-1 and OSM are relevant to the joint destruction observed in the arthritides as increased levels of both cytokines can be detected in the arthritic joint (Cawston et al. 1998). In addition, adenoviral gene transfer of IL-1 in combination with OSM has been shown to induce MMP production and joint damage in murine joints, similar to that seen in RA patients (Rowan et al. 2003).

1.4.1 Interleukin-1

IL-1 is involved in the mediation of a wide variety of biological events and has been implicated in the pathogenesis of several diseases, including RA. IL-1 activates important cell signalling pathways and is a mediator in the pathogenesis of many immunologically and inflammatory mediated diseases (Stylianou and Saklatvala 1998). Prior to its molecular identification in the 1980s, IL-1 had been studied for many years under various names (such as leukocyte endogenous mediator, haematopoietin 1, endogenous pyrogen, catabolin and osteoclast activating factor). To date, The IL-1 family comprises eleven members: IL-1 α , IL-1 β , IL-1 receptor antagonist (IL-1Ra), IL-18, IL-33 and IL-1F5–IL-1F10. It is likely that they arose from the duplication of a common ancestral gene, as all eleven members possess a highly conserved gene structure (Sims and Smith 2010). IL-1 α and IL-1 β have identical biological activities because they signal through the same receptor complex. However, IL-1 α and IL-1 β differ in other respects. Both are synthesised as cytosolic precursors with molecular weights of 31 kDa that are cleaved to produce 17 kDa mature forms. However, whilst both pro- and mature forms of IL-1 α are biologically active, IL-1 β is only active after precursor cleavage by the cysteine proteinase IL-1 β converting enzyme (ICE) (Black et al. 1988). Secondly, IL-1 β is secreted and acts systemically; IL-1 α is normally associated with the cell membrane and therefore acts locally. Thirdly, IL-1 β is mainly produced by monocytes and macrophages, whereas IL-1 α expression is more widespread. Lastly, the pro-domain of IL-1 α has a nuclear localisation sequence. Nuclear IL-1 α is a transcriptional transactivator and this activity is enhanced by interaction with histone acetyltransferases and can influence gene expression and cell survival (Sims and Smith 2010).

To date, two distinct forms of IL-1 receptor have been reported; the 80 kDa biologically active type I receptor (IL-1RI) and the 68 kDa biologically inert type II receptor (IL-1RII). The IL-1RII is thought to function as a decoy receptor, by binding IL-1 and preventing it from interacting with the functional IL-1RI (Colotta et al. 1994). The IL-1RI is widely expressed and preferentially binds IL-1 α , whereas the IL-1RII preferentially binds IL-1 β and is found mainly on B cells, neutrophils and monocytes (Stylianou and Saklatvala 1998). The IL-1RI is able to bind the mature form of IL-1 β and both forms of IL-1 α . After binding of IL-1 α or IL-1 β to the single chain IL-1RI, a second subunit, called the IL-1 receptor accessory protein (IL-1R AcP), is brought into the complex (Greenfeder et al. 1995). The IL-1R AcP is required for internalisation of the activated IL-1R complex and for intracellular signalling. Signal transduction pathways activated by IL-1RI and the IL-1R AcP include the NF- κ B, JNK/AP-1, and p38 MAP kinase pathways (Figure 1.8).

A third ligand in the IL-1 family is IL-1 receptor antagonist (IL-1Ra), a structural variant of IL-1 that binds to both IL-1R but fails to activate cells (Arend et al. 1994). The IL-1Ra is a naturally occurring inhibitor of IL-1. Despite the high affinity of IL-1Ra for the IL-1RI, it is thought that a 10- to a 100- fold excess of the inhibitor is required to block the effect of IL-1 due to the ability of IL-1 to activate cells at very low receptor occupancy (Arend and Dayer 1990). In fact, IL-1 is able to induce a biological response when less than 5% of the receptors are engaged.

1.4.1.1 Interleukin-1 and arthritis

A role for IL-1 in arthritis was first elucidated by Jubb and Fell (1980) when they identified a soluble factor produced by porcine synovial fragments that was able to stimulate chondrocytes to produce various enzymes that degraded the ECM. This soluble factor was shown to be IL-1. IL-1 is synthesised by articular chondrocytes and joint synovial tissue and can also be detected in the synovial fluid of arthritis patients (Fontana et al. 1982). It is able to cause cartilage degradation by stimulating the release of degradative enzymes such as MMPs. Inter-articular injection of IL-1 into rabbit knees led to leukocyte influx and loss of proteoglycans from articular cartilage (Pettipher et al. 1986) and injection of IL-1 into mouse knees led to similar effects with enhanced proteoglycan degradation and inhibition of proteoglycan synthesis (van de Loo and van den Berg 1990). Blocking IL-1 with anti-IL-1 monoclonal antibodies or endogenous IL-1Ra has been shown to protect against cartilage

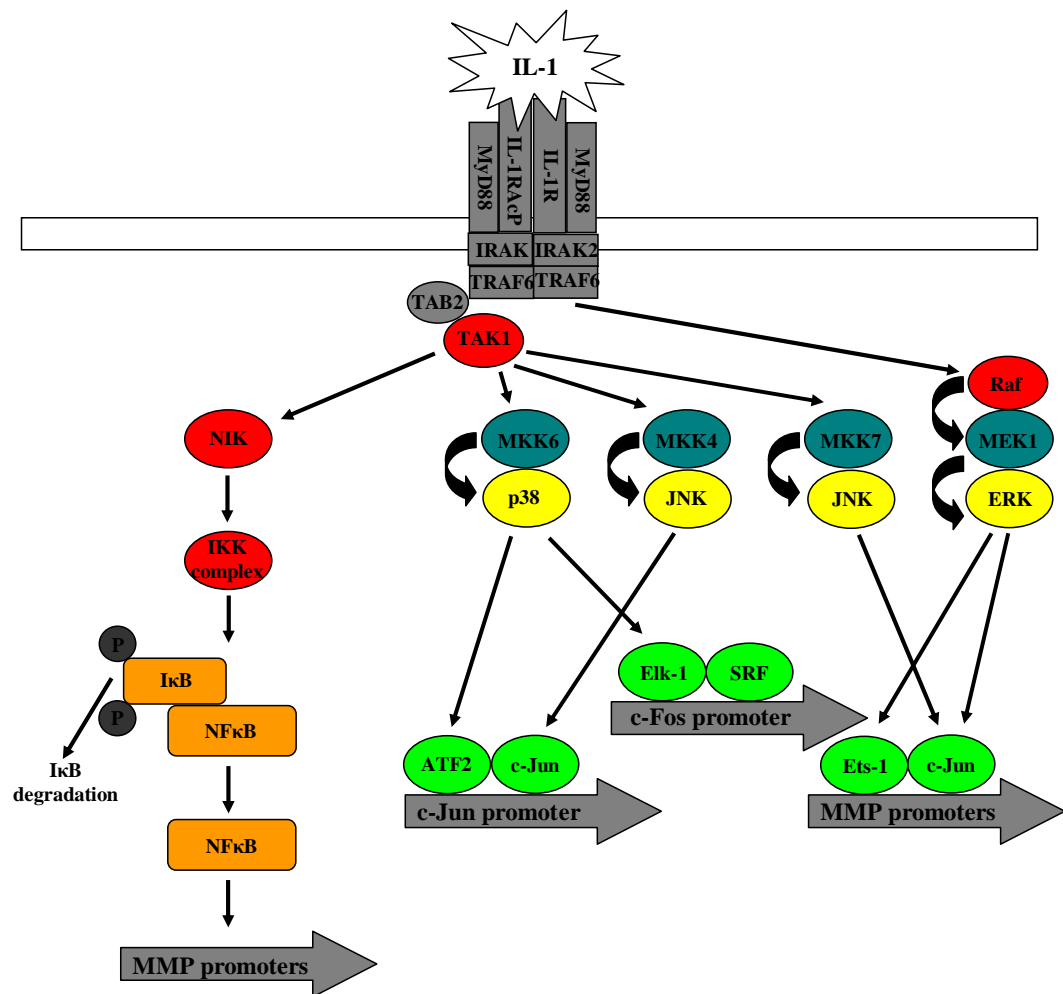


Figure 1.8 IL-1 signalling pathways. Of particular relevance to MMP expression are the NFκB and MAPK signalling pathways activated by IL-1. IL-1 binds to its receptor (IL-1R1) and receptor-associated protein (IL-1RAcP), causing conformational changes in multiple receptor-bound proteins (MyD88, IRAK (IL-1R activated kinase), TRAF6 (TNF receptor-associated factor), TAB2 (Tak-binding protein)). This results in recruitment and activation of transforming-growth-factor-κ-activated kinase-1 (TAK1), which phosphorylates and activates NFκB-inducing kinase (NIK). Subsequently, NIK activates the inhibitor of κB kinase (IKK) complex, which is responsible for the phosphorylation of inhibitor of NFκB (IκB). Following phosphorylation, IκB becomes polyubiquitinated, targeting it for degradation, which allows translocation of NFκB subunits to the nucleus where they can bind and activate the promoters of target genes, including MMPs. Stimulation by IL-1 also activates the MAPKKKs, transforming-growth-factor-β-activated kinase-1 (TAK1) and Raf, which are then able to phosphorylate and activate several MAPKKs (MKK6, MKK4, MKK7 and MEK1). These MAPKKs then phosphorylate and activate the MAPKs (p38, JNK and ERK), which translocate to the nucleus where they phosphorylate and activate various transcription factors (activating transcription factor 2 (ATF2), c-Jun, ETS-like gene 1 (Elk-1) and erythroblastosis twenty six (Ets-1)) that contribute to MMP transcription. SRF (serum response factor) is a protein that regulates the activity of many immediate-early genes such as c-Fos. Adapted from Vincenti and Brinckerhoff (2002).

and bone destruction (Abramson and Amin 2002). Although elevated levels of IL-1Ra have been detected in RA patients, it appears these levels are not sufficiently high to inhibit IL-1-induced inflammatory responses.

1.4.2 Oncostatin M

OSM is a member of the IL-6 family of cytokines and is produced by activated T cells and macrophages. IL-6 type cytokines are known to bind to plasma membrane receptor complexes containing the common signal transducing receptor chain glycoprotein 130 (gp130). As the IL-6 family of receptors do not possess intrinsic kinase activity, subsequent signal transduction involves the activation of Janus kinases (JAK) tyrosine kinase family members. Following this interaction, the activated JAKs tyrosine phosphorylate both themselves and the cytoplasmic tail of gp130. These phosphorylated tyrosine residues act as docking sites for signalling molecules containing SH2 (src homology 2) domains, including members of the signal transducers and activators of transcription (STAT) family of transcription factors. Once bound, STATs also undergo tyrosine phosphorylation causing them to dimerise and translocate to the nucleus where they are able to bind DNA and regulate the transcription of target genes. In addition to the JAK/STAT signalling pathway, OSM can also stimulate the activation of the MAPK (mitogen-activated protein kinases) cascade (Gomez-Lechon 1999; Heinrich et al. 2003). MAPKs are serine-threonine kinases and the MAPK family includes extracellular signal-regulated kinase (ERK), p38, and c-Jun NH(2)-terminal kinase (JNK). Each MAPK signalling pathway consists of at least three components, a MAPK kinase kinase (MAP3K), a MAPK kinase (MAP2K), and a MAPK; MAP3Ks phosphorylate and activate MAP2Ks, which subsequently phosphorylate and activate MAPKs. Activated MAPKs are then able to phosphorylate numerous substrate proteins including transcription factors such as c-Jun (Kim and Choi 2010) (Figure 1.9).

1.4.2.1 OSM and arthritis

As with IL-1, elevated levels of OSM are seen in human rheumatoid synovial fluids (Cawston et al. 1998). Several cytokines have been shown to synergise with OSM, to profoundly affect MMP and TIMP levels. For example, OSM greatly exacerbates IL-1- and TNF α -mediated effects on cartilage (Hui et al. 2003). OSM alone is able to stimulate aggrecan catabolism in porcine cartilage explants (Hui et al. 1996). Although OSM levels

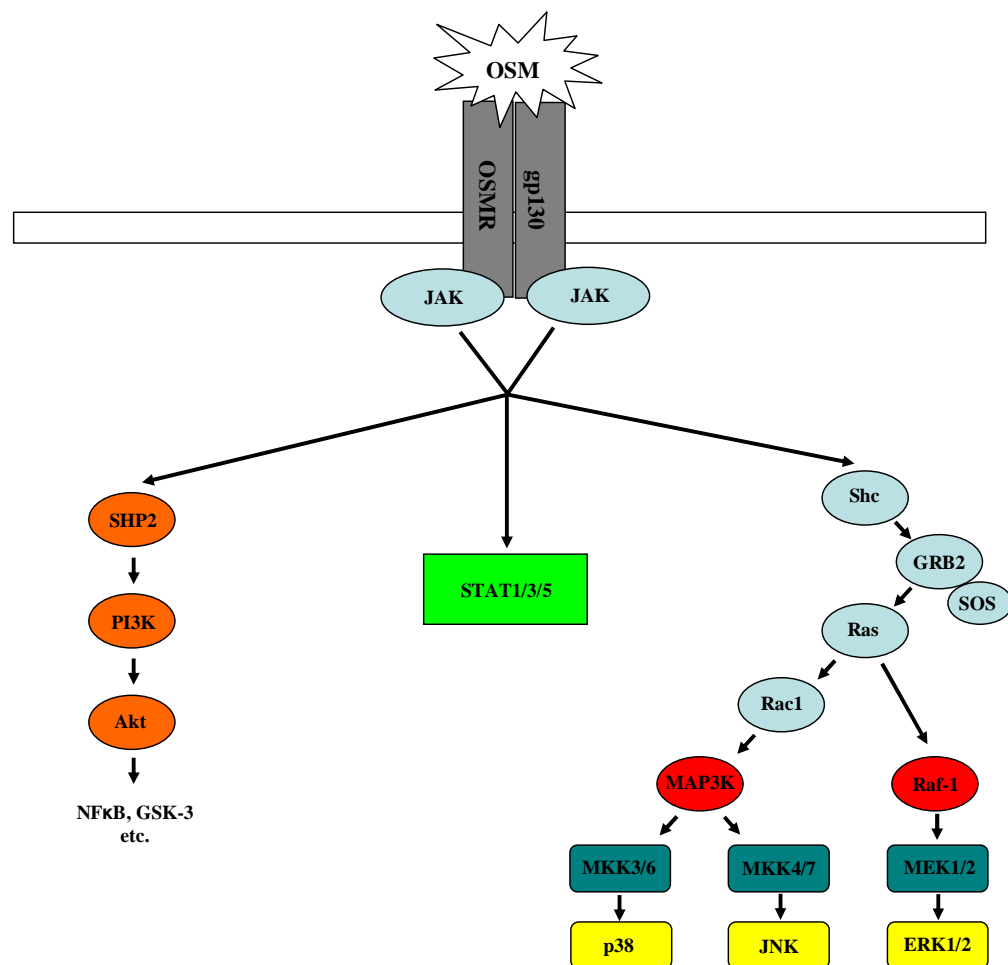


Figure 1.9 OSM signalling pathways. Binding of OSM to its receptor subunits, OSM receptor (OSMR) and gp130, activates several signalling pathways including the PI3K/Akt pathway, the JAK/STAT pathway and the MAPK pathway. As the IL-6 family of receptors do not possess intrinsic kinase activity, subsequent signal transduction involves the activation of JAKs. The phosphorylation and activation of SHP2 (SH2 domain-containing tyrosine phosphatase) by JAKs is thought to play a role in the PI3K signalling pathway, resulting in Akt activation and phosphorylation of downstream molecules. Binding of OSM to its receptor subunits also induces the JAK/STAT signaling pathway. Activated JAKs recruit and activate STAT proteins. Phosphorylated STATs then dimerise, translocate to the nucleus, bind to regulatory elements in the promoter of OSM-responsive genes and induce gene expression. OSM predominantly activates STAT1, STAT3 and STAT5. The OSMR is also known to recruit Shc as a downstream signaling molecule, initiating MAPK signalling cascades via GRB2 (growth factor receptor-bound protein 2). Activated GRB2 is bound with the GTP-exchange factor SOS (Son of sevenless homolog). SOS interacts with Ras, which recruits Rac1 (Ras-related C3 botulinum toxin substrate 1) and Raf-1 (a MAP3K). Activated Rac1 results in the activation of p38 and JNK via MAP3K/MKK cascades. Activated Raf-1 transmits its signal via the MEK/ERK1/2 cascade, leading to alterations in gene expression. Adapted from www.genego.com (Oncostatin M signaling via JAK/STAT in human cells and Oncostatin M signaling via MAPK in human cells).

present in RA synovial fluid are thought to be too low to stimulate cartilage degradation if acting in isolation, this does not rule out a role for OSM alongside IL-1 in the progressive destruction of joint tissues (Manicourt et al. 2000). A key role for endogenously produced OSM as a potent mediator of joint pathology was demonstrated by a study in which mice with CIA treated with anti-OSM antibody showed significant amelioration of clinical severity and the number of affected paws compared with control animals (Plater-Zyberk et al. 2001).

1.4.3 Other pro-inflammatory cytokines

TNF- α is another potent pro-inflammatory cytokine implicated in the arthritides. TNF- α has been shown to be present at high concentrations in the synovial fluids (Tetta et al. 1990) and cartilage-pannus junction (Chu et al. 1991) of RA patients. TNF- α is known to act synergistically with IL-1 to promote cartilage damage (Henderson and Pettipher 1989). Alone, TNF- α has been shown to exhibit similar biological properties to IL-1, enhancing the resorption and inhibiting the synthesis of cartilage proteoglycan (Saklatvala 1986) and stimulating the release of collagenases (Dayer et al. 1985). Clinical trials of biologic anti-TNF- α drugs performed in the late 1990s confirmed the importance of TNF- α in the pathogenesis of RA and these trials yielded positive results. Millions of patients worldwide have now received the first marketed anti-TNF- α drugs; the monoclonal anti-TNF- α antibodies infliximab and adalimumab and the soluble TNF- α receptor antagonist etanercept. However, only 60% of those patients who do not benefit from standard nonbiologic treatments for arthritis respond to TNF- α antagonists and so there is still a need for the development of new arthritis treatments (Sfikakis 2010).

IL-17 has been implicated as a mediator of cartilage collagen breakdown in inflammatory joint disease. Animal studies have suggested a role for IL-17 in several models of arthritis (Bush et al. 2001; Lubberts et al. 2001; Lubberts et al. 2002). Similarly to OSM, IL-17 has also been shown to act in synergy with other pro-inflammatory cytokines such as IL-1 to promote type II collagen release from bovine nasal cartilage in an MMP-dependent manner (Koshy et al. 2002).

1.5 Anti-inflammatory cytokines in arthritis

1.5.1 Interleukin-4

Several cytokines have been shown to antagonise the effects of pro-inflammatory cytokines. These include IL-4 (Cawston et al. 1996), IL-10 (van Roon et al. 1996) and IL-13 (Cleaver et al. 2001). IL-4 is a cytokine that is able to exert either stimulatory or suppressive effects on different cell types (Joosten et al. 1999). It was originally identified as a B cell growth factor (BCGF), but was subsequently revealed to be a multifunctional cytokine that interacts with cells of multiple lineages, including T-cells, monocytes, macrophages and fibroblasts. Consequently, BCGF was re-named B cell stimulatory factor, and later IL-4. IL-4 is produced principally by CD4⁺ T cells, but also by basophils, B cells, macrophages, monocytes, fibroblasts and endothelial cells (Paul 1991). The IL-4 gene resides on the long arm of chromosome 5 at q23-31 and is a 20 kDa glycosylated protein. Several binding sites for transcription factors have been identified in the IL-4 promoter, including STAT6. IL-4 stimulates the proliferation, differentiation and activation of multiple cell types but is known for its role as a potent anti-inflammatory cytokine, inhibiting the synthesis of pro-inflammatory cytokines such as TNF- α , IL-1 and IL-6 (Hart et al. 1989; te Velde et al. 1990; DeKruyff et al. 1995). In addition, IL-4 stimulates the synthesis of a number of cytokine inhibitors including IL-1R α , IL-1-receptor type II and TNF receptors (Vannier et al. 1992; Colotta et al. 1993; Cope et al. 1993). IL-4 suppresses metalloproteinase production, whilst increasing TIMP-1 production in cartilage explants, suggesting that IL-4 functions to protect the ECM (Cawston 1998).

1.5.2 IL-4 in arthritis

It has been well documented that the destructive process mediated by pro-inflammatory cytokines can be limited by anti-inflammatory mediators such as IL-4. Whilst upregulation of anti-inflammatory cytokines and inhibitory mediators does occur in chronic inflammatory conditions such as RA, it occurs at levels insufficient to prevent cartilage degradation. This imbalance between pro- and anti-inflammatory cytokines is reflected by an abundance of pro-inflammatory cytokines, but a virtual absence of anti-inflammatory cytokines such as IL-4 in RA synovium. This is despite the presence of high levels of IL-4 in peripheral blood mononuclear cells of RA patients (Miossec et al. 1990). Typically,

anti-inflammatory cytokines counteract the effects of pro-inflammatory cytokines, therefore promoting the synthesis of ECM components. It is thought that IL-4 fulfils its role as an anti-inflammatory cytokine, partly, by promoting the differentiation of T cells into Th2 cells rather than pro-inflammatory Th1 cells. In addition to suppressing Th1 cells and upregulating IL-1Ra in synovial cells and chondrocytes, IL-4 also potently reduces inducible NO (nitric oxide) synthase (iNOS) expression (Bogdan et al. 1994). This results in a suppression of NO production, which is a secondary mediator in IL-1-mediated inhibition of proteoglycan synthesis by chondrocytes (van den Berg 1998).

IL-4 is characteristically absent from the RA joint, suggesting the disease is driven exclusively via a Th1 response, or is not driven by T cells at all. This absence of IL-4 makes IL-4 administration or local enrichment of IL-4 producing cells a possible therapeutic option (van den Berg 1998). A study by Joosten et al. (1999) demonstrated that systemic IL-4 treatment ameliorates disease progression of established murine CIA, a widely used model of arthritis that displays several features of human RA. In the same year, the first demonstration of the cartilage-protective effects of local IL-4 gene therapy in experimental arthritis were seen. Despite having only a moderate effect on inflammation, 1 µg/day IL-4 strongly protected against cartilage and bone destruction (Joosten et al. 1999). A later study by van Lent et al. (2002) showed that over-expression of IL-4 in an immune complex (IC)-mediated arthritic knee joint protected the cartilage ECM from MMP-mediated destruction, by preventing subsequent matrix erosion. The same study suggested that IL-4 does not inhibit MMP-mediated cartilage destruction by preventing MMP release into the cartilage, but possibly by inhibiting synovial factors involved in the activation of pro-MMPs.

Various cytokine-based therapies are being considered to block the catabolic pathways thought to be responsible for the cartilage damage seen in human OA. A large amount of research has indicated the potential of IL-4 as a future therapeutic agent. However, it is important to note the pro-inflammatory role of IL-4 before considering its therapeutic use. Inhibition of IL-4 in diseases where IL-4 has a pro-inflammatory effect, such as asthma, has shown promise. However, administration of IL-4 to treat arthritis could cause potentially disastrous side-effects due to its pro-inflammatory effects on target cells in other parts of

the body. It is also possible that any beneficial effects of IL-4 may be inhibited by other agents. Aspirin, the most widely used non-steroidal anti-inflammatory drug, is known to inhibit IL-4-induced STAT6 activation (Perez et al. 2002). It is very likely that administration of IL-4 itself will prove too dangerous for use *in vivo*. Despite this, work currently being carried out to elucidate the protective mechanism of action of IL-4 has the potential to identify a vast array of targets involved in the anti-inflammatory effect of IL-4, leading to alternative therapeutic agents.

1.5.3 Regulation of MMPs by IL-4

It is widely accepted that production of MMPs by chondrocytes and synovial fibroblasts is regulated by various cytokines and growth factors. It is therefore of no surprise that IL-4 has been implicated in the suppression of MMPs, in addition to its role in the suppression of pro-inflammatory mediators. IL-4 has been shown to down-regulate MMP activity in a number of cell types involved in arthritis. In 1996, Cawston et al. demonstrated the chondroprotective ability of IL-4, by showing that IL-4 specifically blocked bovine cartilage collagen resorption. Inhibition of collagen release was accompanied by a decrease in collagenase activity and an increase in TIMP levels (Cawston et al. 1996). Previously, it was demonstrated that IL-4 suppressed IL-1-stimulated MMP-3 protein and enzyme activity and was able to suppress IL-1-induced MMP-3 mRNA in human articular chondrocytes. In contrast, IL-4 did not alter the level of TIMP-1 protein and mRNA (Nemoto et al. 1997). The chondroprotective mechanism of action of IL-4 has been further elucidated by work carried out by the Salter group on the effect of mechanical stimulation on human articular chondrocytes. They have developed a technique that enables the application of controlled forces to cultured cells and so are able to demonstrate that mechanical signals can be transmitted across ECM-cell contacts. This technique was used to demonstrate that mechanical stimulation of human chondrocytes induced the release of IL-4 by human chondrocytes (Millward-Sadler et al. 1999). In 2000 it was shown that chondrocytes from normal and osteoarthritic human articular cartilage show differential responses to mechanical stimulation. Mechanical stimulation of normal human articular chondrocytes *in vitro* resulted in an increase in levels of aggrecan mRNA and a decrease in levels of MMP-3 mRNA. This response was shown to be dependent on IL-4. No changes in aggrecan or MMP-3 mRNA expression were found in OA chondrocytes, suggesting a

failure in the IL-4-dependent chondroprotective response (Millward-Sadler et al. 2000). A later study went on to show that autocrine and paracrine activity of IL-4 plays a critical role in the increased levels of aggrecan mRNA and decreased levels of MMP-3 mRNA seen after mechanical stimulation of normal human articular chondrocytes. This further adds to the evidence that abnormalities in mechanical signalling may contribute to disease progression in OA (Salter et al. 2001).

As mentioned previously, collagen release is considered the key point in cartilage degradation. Of the three known collagenases, MMP-1 and MMP-13 are considered to be the most important in terms of the collagenolysis seen in the arthritides. MMP-13 is thought to be of greater importance in OA due to the fact that it preferentially degrades type II collagen (Knauper et al. 1996a) and because its expression is increased in OA (Tetlow et al. 2001). Previous data have consistently shown IL-4 to completely inhibit MMP-13 mRNA expression (Cleaver 2000; Cleaver et al. 2001; Pyle 2003), but to slightly increase MMP-1 mRNA expression (Cleaver 2000; Cleaver et al. 2001).

1.5.3.1 Epigenetic regulation

Epigenetics, literally meaning “beyond genetics”, can be defined as stable and heritable (or potentially heritable) changes in gene expression that do not entail a change in DNA sequence (Jiang et al. 2004). There are two key epigenetic modifications; DNA methylation and histone modifications (such as acetylation, methylation and phosphorylation). The methylated base 5-methylcytosine was first discovered in the calf thymus 60 years ago (Hotchkiss 1948). Generally, only cytosines that precede guanines can be methylated i.e. cytosines within CpG dinucleotides. The CpG notation (where ‘p’ represents the phosphate connecting the two nucleotides) is used to distinguish between a cytosine followed by a guanine in the DNA sequence and a cytosine base-paired to a guanine (Dahl and Guldberg 2003).

Recent studies have examined the methylation status of four degradative enzymes (MMP-3, MMP-9, MMP-13 and ADAMTS-4) and have shown that changes in the expression of these enzymes in OA correlated with demethylation of specific CpG sites within their promoters (Roach et al. 2005). In addition, it has been shown that one of the genes

upregulated in OA cartilage is leptin, a cytokine-like peptide hormone thought to act as a regulator of bone growth. A study by Iliopoulos et al. (2007) has shown that leptin can be regulated by epigenetic mechanisms in OA. Leptin was found to be methylated in normal chondrocytes and unmethylated in both mildly and severely affected OA chondrocytes. Epigenetic regulation of leptin using siRNA was found to affect MMP-13, with MMP-13 expression down-regulated.

Methylation of genomic DNA is clearly an important mechanism in the regulation of gene expression. DNA methylation is heritable and so any changes in methylation status are transmitted to daughter cells. When aberrant changes in DNA methylation occur, these changes are also heritable because cells have no way of “remembering” what their correct methylation status should be. Initial experimental evidence indicates that aberrant DNA methylation patterns could be responsible for at least some of the changed MMP gene expression patterns seen in OA.

1.5.4 IL-4 in other diseases

As mentioned previously, the effect of certain cytokines, in particular IL-4, depends greatly on the target cell. Recent work has provided compelling evidence that IL-4 produces a pro-inflammatory environment via oxidative stress-mediated up-regulation of inflammatory mediators in vascular endothelium. In addition, IL-4 has been demonstrated to induce the apoptosis of human vascular endothelial cells via the caspase-3-dependent pathway. Vascular endothelial cell injury has been implicated in the onset and progression of cardiovascular diseases such as atherosclerosis (Lee and Hirani 2006). IL-4 has been well documented for its pro-inflammatory role in asthma, possibly being involved in the airway remodelling response seen in asthmatics by inducing ECM production by fibroblasts (Hashimoto et al. 2001).

To further complicate matters, IL-4 appears to have both positive and negative effects on the control of tumour growth. A number of studies have assessed the impact of IL-4 on tumour clearance by recombinantly expressing IL-4 in tumour cell lines. Using these models, investigators found that IL-4 enabled the clearance of numerous tumour types (melanoma, renal carcinoma, colon carcinoma, plasmacytoma) in mice that had been

otherwise unable to clear the tumour (Tepper et al. 1989; Tepper et al. 1992; Noffz et al. 1998). Other reports indicate that IL-4 impairs tumour clearance. Vaccination with IL-4-expressing mesothelioma cells resulted in accelerated growth of tumour cells (Olver et al. 2007). The same study suggests that the effect of IL-4 on tumour growth is dependent on the type of tumour model and the type of effector cells mediating tumour clearance.

The growth of bone is a highly regulated process, involving bone-forming cells (osteoblasts) and bone-resorbing cells (osteoclasts). IL-4 has been shown to be an inhibitor of bone resorption (Watanabe et al. 1990) and so could be of therapeutic benefit in bone-resorbing diseases such as osteoporosis and arthritis. In addition to cartilage loss, bone destruction is a major complication in arthritic disease. The first report demonstrating the bone protective effects of local IL-4 gene therapy came in 2000 (Lubberts et al. 2000). Local over-expression of IL-4 reduced tartrate-resistant acid phosphatase (TRAP) activity, suggesting that IL-4 inhibits formation of osteoclast-like cells. IL-6 and IL-12 protein production was also suppressed, as were mRNA levels of IL-17, IL-12 and cathepsin K. *In vitro* studies using bone samples from arthritis patients revealed suppression of type I collagen breakdown by IL-4, but also enhanced synthesis of type I procollagen, indicating that IL-4 is able to promote tissue repair. More recent work has further elucidated the molecular mechanism of IL-4 action on osteoclasts. It is known that IL-4 dose-dependently inhibits receptor activator of NF κ B ligand (RANKL)-induced bone resorption by mature osteoclasts (Mangashetti et al. 2005). There is also evidence demonstrating how constitutively active STAT6 can inhibit bone erosion through blockade of JNK and NF κ B activation (Hirayama et al. 2005). Modulation of these systems could present a novel approach to the alleviation of bone destruction in arthritis.

1.5.5 IL-4 signalling

IL-4 induces cellular responses by binding to a multimeric receptor. IL-4 receptors consist of two transmembrane proteins. IL-4 binds to the IL-4R α chain, leading to dimerisation with one of two other proteins, to form either a type I or type II receptor. In haematopoietic cells, type I receptors are formed by the recruitment of a common gamma chain (γ C). In cells of nonhaematopoietic lineage, the type II receptor is formed by interaction of the IL-4R α with IL-13R α 1 (Kelly-Welch et al. 2003). The IL-4 signalling pathway downstream of

the receptor involves the phosphorylation of two distinct proteins; STAT6 (Hou et al. 1994) and insulin receptor substrate-1/-2 (IRS1/2) (Kelly-Welch et al. 2003) (Figure 1.10). However, a number of other cytoplasmic signalling proteins have been demonstrated to be phosphorylated in response to IL-4R stimulation, including FRIP (IL-4 receptor interacting protein), SHIP (SH2 domain-containing inositol-5'-phosphatase) and Shp (small heterodimer partner) (Hou et al. 1994; Sun et al. 1995; Imani et al. 1997; Nelms et al. 1998; Zamorano and Keegan 1998). Type I cytokine receptors, in contrast to other receptor classes, do not have intrinsic kinase activity. Their initial signalling steps rely on JAKs. The binding of IL-4 to its receptor leads to the phosphorylation, and hence activation, of JAK1 and JAK3. The phosphorylation of JAKs is followed by phosphorylation of the IL-4 receptor components and cytoplasmic signalling proteins (Hebenstreit et al. 2006). IL-4 stimulation results in activation of JAK 1 and 3, in turn leading to phosphorylation of tyrosine residues in the cytoplasmic domain of the IL-4R α chain. Once phosphorylated, these tyrosine residues act as docking sites for signalling molecules (Kelly-Welch et al. 2003).

1.5.5.1 STAT6

STAT6 signalling is classically associated with IL-4 and IL-13 and the examination of STAT6-deficient mice has shown that STAT6 is essential for IL-4-dependent gene induction (Kuhn et al. 1991). STAT6 is one of seven members of the STAT protein family, which consists of STAT1, STAT2, STAT3, STAT4, STAT5a, STAT5b and STAT6. STAT6 is recruited to the activated IL-4R α through its SH2 domain and becomes tyrosine phosphorylated leading to its dimerisation and translocation to the nucleus, where the homodimer activates transcription of IL-4 responsive genes, in what is commonly referred to as the JAK-STAT pathway of signal transduction (Leonard and O'Shea 1998). A number of studies have demonstrated the importance of the three central tyrosine residues (Y575, Y603 and Y631) in the IL-4R α chain for the activation of STAT6 (Pernis et al. 1995; Wang et al. 1996; Ryan et al. 1998). These three residues become phosphorylated following stimulation of the IL-4 receptor, thus providing docking sites for STAT6 monomers. Furthermore, phosphorylation of any one of these three tyrosines is sufficient for STAT6 activation (Ryan et al. 1998).

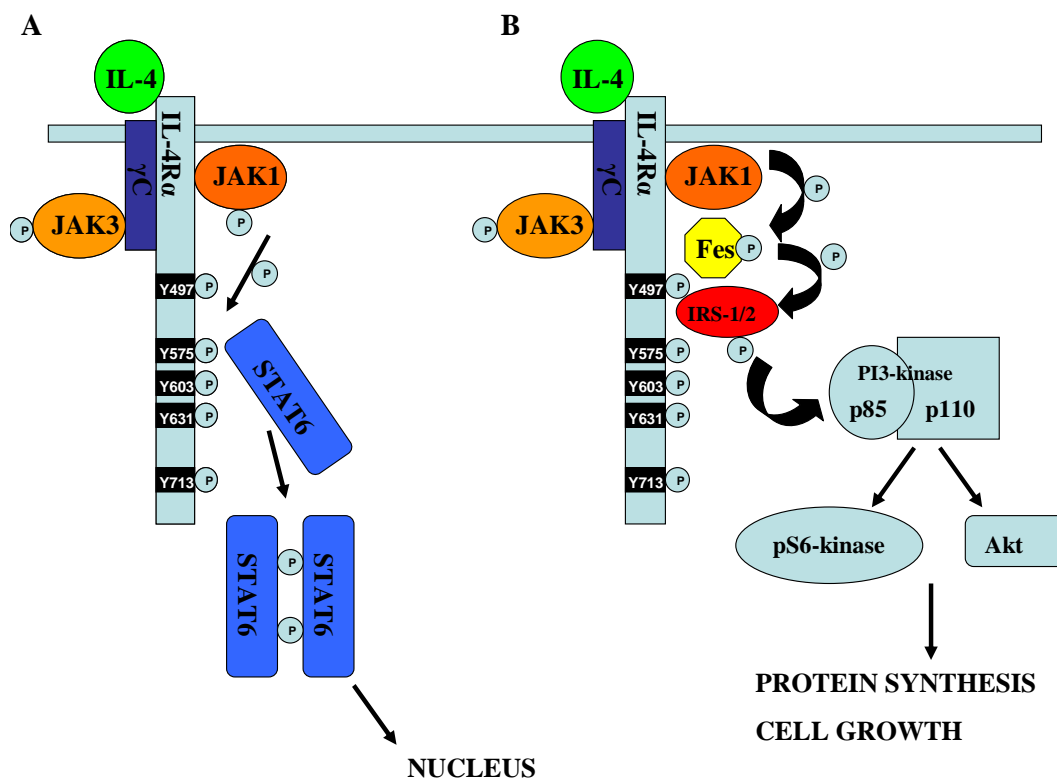


Figure 1.10 IL-4 signalling pathways. **A**, STAT6 is the only STAT protein activated and recruited to the IL4Rα chain. Binding of IL-4 to the receptor complex promotes the activation of JAK1 and JAK3. Activated JAKs initiate intracellular signalling events by phosphorylating specific tyrosine residues in the cytoplasmic domain of IL-4Rα. Once phosphorylated, these tyrosine residues act as docking sites for signalling molecules. STAT6 is recruited to activated IL-4Rα through its SH2 domain and becomes tyrosine phosphorylated leading to its dimerisation and translocation to the nucleus, where the homodimer activates transcription of IL-4 responsive genes. **B**, IL-4 binding induces activation of JAKs and Fes kinases. Fes in turn is responsible for phosphorylation of IRS-1/2. Phosphorylation of IRS-1/2 activates the PI3 kinase (PI3K) pathway by interacting with p85 catalytic subunit. Activated PI3K appears to regulate the pS6K pathway, resulting in promotion of translational process required for cell growth. Adapted from Jiang et al. (2000).

Although STAT6 activation in response to IL-4 has been well documented, the mechanisms responsible for the regulation of STAT6 signalling are less well understood. Several negative regulators of the JAK-STAT signalling pathway have been described. Suppressors of cytokine signalling (SOCS) proteins form a negative feedback loop whereby cytokine stimulation induces SOCS genes, which subsequently inhibit cytokine signalling. SOCS-1 has been shown to potently inhibit the activation of JAK1 kinase and STAT6 in response to IL-4 (Losman et al. 1999). Protein inhibitors of activated STAT (PIAS) are thought to bind specifically to phosphorylated STAT dimers and prevent them from binding DNA (Liu et al. 1998). Chen et al. (2004) examined the effect of methylation on STAT6. It was discovered that in the presence of methylation inhibitors, STAT6 methylation was reduced, as was phosphorylation of STAT6 and STAT6 DNA binding activity. It therefore seems that methylation is necessary for maximal STAT6 phosphorylation, nuclear translocation and DNA-binding activity (Chen et al. 2004).

STAT6 binding to DNA alone is normally not sufficient to stimulate activation of transcription. In order to initiate transcription, STAT6 must interact with the basal transcription machinery via various transcriptional co-regulatory proteins. The molecular mechanisms by which transcription is selectively activated by STAT6 represents a key issue in the understanding of IL-4-mediated cellular responses. STAT6 has been shown to interact with NF κ B (Stutz and Woisetschlager 1999), PU.1 (Pesu et al. 2003), IRF-4 (Gupta et al. 1999), BSAP (Thienes et al. 1997; Mikita et al. 1998) and C/EBP β (Mikita et al. 1998) transcription factors. The trans-activation potential of a transcription factor is dependent on the co-factors that it recruits; this is a key mechanism by which transcription factors mediate specificity for the promoters they activate. Various transcriptional co-regulators for STAT6 have been identified, including CREB-binding protein (CBP), p300 and NcoA1 (a member of the p160 family of coactivators). CBP/p300 stimulates the transcription of target genes by the regulation of chromatin remodelling through intrinsic histone acetyltransferase activity (Ogryzko et al. 1996; Yang et al. 1996) and by associating with p/CAF, another histone acetyltransferase (Yang et al. 1996). Work by Silvennoinen and colleagues have identified several STAT6 transcriptional activation domain (TAD) interacting nuclear proteins. The first of these to be discovered was coactivator protein p100, which regulates IL-4-induced transcription by connecting STAT6 with RNA

polymerase II (Yang et al. 2002). A subsequent study suggested that p100 has an important role in the assembly of the STAT6 transcriptosome, and that p100 stimulates IL-4-dependent transcription by mediating interaction between STAT6 and CBP and recruiting chromatin modifying activities to STAT6-responsive promoters (Valineva et al. 2005). It is now thought that p100 could also participate in mRNA splicing (Shaw et al. 2007; Yang et al. 2007). mRNA splicing and transcription are the two key nuclear processes in eukaryotic gene expression. RNA helicase A (RHA) has now also been described as a novel component of the STAT6 transcriptosome. Whilst RHA was found to not directly interact with STAT6, p100 protein was found to mediate the assembly of the ternary complex of STAT6-p100-RHA. RHA was found to enhance IL-4-induced transcription and the participation of RHA in IL-4-regulated transcription was supported by RNAi experiments (Valineva et al. 2006). Goenka et al (2007) have recently identified an additional novel co-factor of STAT6. Collaborator of STAT6 (CoaSt6) was found to associate with STAT6 and enhance its transcriptional activity. Sequence homologies have placed CoaSt6 within the poly(ADP-ribosyl)polymerase (PARP)-like protein superfamily. This study also went on to demonstrate that PARP enzymatic activity is associated with CoaSt6 (Goenka et al. 2007).

1.5.5.2 IRS1/-2

The IRS proteins are cytoplasmic docking proteins that function downstream of activated cell surface receptors. They do not possess intrinsic kinase activity, instead functioning as adaptors; organising signalling complexes to initiate intracellular signalling cascades (White 2006). Three IRS family members are expressed in humans; IRS1, IRS2 and IRS-4. IRS1 and IRS2 are expressed ubiquitously and share considerable homology. The expression of IRS-4 is much more restricted. The importance of the activation of IRS1/IRS2 in IL-4 signalling was first demonstrated in the 32D myeloid progenitor cell line, which does not express endogenous IRS1 or IRS2. Reconstitution of these cells with IRS1 allowed them to proliferate in response to IL-4 (Wang et al. 1993). Following IL-4 stimulation, IRS1 and IRS2 are recruited to the IL-4R complex by the phosphorylated tyrosine residue Y497 in the IL-4R α and undergo tyrosine phosphorylation by JAK 1 (Chen et al. 1997) (Figure 1.10). The tyrosine-phosphorylated IRS proteins subsequently act as docking sites for SH2 domain-containing signalling proteins such as the p85 subunit of PI3K (Backer et al. 1992) and growth factor receptor-bound protein 2 (Grb-2) (Skolnik et al. 1993). PI3K has consistently been shown to play an important role in IL-4-mediated cell

proliferation (Kelly-Welch et al. 2003). The downstream effectors of activated PI3K include Akt/protein kinase B (PKB), PKC and p70 ribosomal protein S6 kinase (p70S6-K) (Pesu et al. 2000).

1.5.6 Other anti-inflammatory cytokines

IL-10 is found at increased levels in both RA synovial fluid and serum (Cush et al. 1995) and a strong negative correlation has been found between IL-10 production and joint damage in RA patients (Verhoef et al. 2001). The synthesis of pro-inflammatory cytokines such as IL-1, IL-8, IL-12, IL-6 and TNF- α can be inhibited by IL-10 in monocytes (de Waal Malefyt et al. 1991). It also is able to synergise with IL-4 to inhibit cartilage degradation induced by antigen-stimulated mononuclear cells of RA patients *in vitro* (van Roon et al. 1996). IL-10 is able to suppress established CIA through the inhibition of pro-inflammatory cytokine production (Walmsley et al. 1996). In summary, IL-10 appears to be the key in the regulation of inflammation however its inhibitory effect appears to be increased when in combination with IL-4 (Joosten et al. 1997).

IL-13 strongly resembles IL-4, exhibiting many of the same biological activities and sharing approximately 30% homology at the protein level (Minty et al. 1993). IL-13 has been demonstrated to inhibit the production of a range of other pro-inflammatory cytokines including TNF α , IL-6 and IL-8. In a similar manner to IL-4, IL-13 has been shown to act in a chondroprotective manner by blocking collagen release from bovine nasal cartilage stimulated to resorb by IL-1 and OSM (Cleaver et al. 2001).

1.6 Summary and aims of this study

The degradation of articular cartilage and subsequent erosion of subchondral bone in the arthritides results in loss of joint function. Articular cartilage is composed primarily of collagens, proteoglycans and chondrocytes, however it is the loss of collagen from articular cartilage that is considered the key step in cartilage degradation. The imbalance of collagen synthesis and degradation has been shown in humans to correlate with disease progression. Pro-inflammatory cytokines, such as IL-1 and OSM, are upregulated in arthritis and

contribute to cartilage damage through the induction of MMPs. MMP-13, the major type II collagenase, is highly upregulated in arthritic diseases and therefore strongly implicated in the pathogenesis of OA.

Studies have shown that the synergistic collagen degradation in cartilage explants by IL-1 and OSM (Cawston et al 1995, 1998) can be ameliorated by the addition of IL-4. Further studies demonstrated that IL-4 is able to completely inhibit MMP-13 mRNA expression in both cartilage and cell culture models. The aim of this PhD was to elucidate the mechanism of action by which IL-4 suppresses MMP-13 expression, thereby inhibiting cartilage collagen breakdown.

The aims of this work were to:

- Determine the effect of IL-4 on IL-1+OSM-induced collagenase gene expression in chondrocytes.
- Determine the time dependence of IL-4 addition on IL-1+OSM-induced collagenase gene expression in the bovine nasal cartilage model.
- Examine IL-4 signalling in chondrocytes and their effect on MMP-13 expression.
- Perform genome-wide arrays to examine global gene expression following IL-1+OSM±IL-4 addition.
- Attempt to recover IL-1+OSM+IL-4-induced MMP-13 expression through gene silencing experiments.

Chapter 2: Materials and Methods

2.1 Materials

2.1.1 Antibodies

All antibodies are rabbit polyclonal, unless otherwise stated. Phospho-Akt (Ser473) (#4060), phospho-Akt (Thr308) (#4056), phospho-STAT6 (Tyr641) (#9361), phospho-GSK-3-beta (Ser9) (#9336), Histone H3 (#9717B), Lamin A/C (#2032) and Caveolin 1 (#3267B) were purchased from Cell Signaling Technology (Danvers, MA, USA). Trb1 polyclonal antibody (#09-126) was purchased from Millipore (MA, USA). Trb3 (#2488-1) and MEK2 (#04-377) monoclonal antibodies and β -tubulin polyclonal antibody (#1799-1) were purchased from Epitomics (Insight Biotech, Wembley). STAT6 (#sc-981) polyclonal antibody, mouse monoclonal Trb2 antibody (#sc-100878) and mouse monoclonal c-Myc antibody (#sc-40) were purchased from Santa Cruz (California, USA).

2.1.2 Cell lines

The human chondrosarcoma cell line, SW1353, was purchased from the American Type Culture Collection (ATCC). Cells were cultured in Dulbecco's Modified Eagle's Medium (DMEM) in a 1:1 ratio with Ham's F-12 medium (DMEM:F12) as described in section 2.2.3.

2.1.3 Cell culture reagents

DMEM, DMEM-F12, and foetal bovine serum (FBS) were obtained from Invitrogen (Paisley, UK). Phosphate buffered saline (PBS) was from Lonza (Wokingham, UK). Penicillin-streptomycin solution (10 000 U/ml and 10 mg/ml, respectively), L-glutamine solution (200 mM), Nystatin suspension (10,000 U/ml), trypsin-EDTA (ethylenediaminetetraacetic acid) solution (0.5 g porcine trypsin and 0.2 g/L EDTA), hyaluronidase (from bovine testes, 439 U/mg), trypsin (from porcine pancreas, 1020 U/mg) and collagenase (from *Clostridium histolyticum* type I) were obtained from Sigma-Aldrich (Poole, UK). Tryptone, yeast extract and bacto-agar were purchased from Difco

Laboratories (Detroit, MI, USA). Syringe filters (0.2 µm) were purchased from Pall Life Sciences (Portsmouth, UK). Cell strainers (100 micron) were from Scientific Laboratory Supplies (Hessle, UK).

2.1.4 Commercially available kits

RNeasy[®] Mini Kit, Qiaprep Spin Midi/Maxi Kit and Epitect[®] Bisulphite Kit were purchased from Qiagen (Crawley, UK). PureLink[™] Genomic DNA MiniPrep Kit and the TOPO TA Cloning[®] Kit with Dual Promoter pCR[®]II-TOPO[®] vector were purchased from Invitrogen. Subcellular Protein Fractionation Kit was purchased from ThermoScientific (Loughborough, UK).

2.1.5 Biochemical Biology Reagents

Bovine serum albumin (BSA), chondroitin sulphate A (from bovine trachea), collagenase (type I from *Clostridium histolyticum*), L-cysteine hydrochloride, *p*-dimethylaminobenzaldehyde (DAB), 4-aminophenylmercuric acetate (APMA) and ethylenediamine tetraacetic acid (EDTA) were obtained from Sigma-Aldrich. Chloramine T and papain were purchased from BDH (Poole, UK).

2.1.6 Molecular Biology Reagents

Dharmafect[™] 1 lipid reagent and SMARTpool[®] small interfering RNA (siRNA) were from Dharmacon (Cramlington, UK). Trb-1 MISSION[®] Lentiviral Transduction Particles and hexadimethrine bromide were from Sigma-Aldrich. FuGene HD Transfection Reagent was purchased from Roche (Burgess Hill, UK) and Lipofectamine 2000 Reagent from Invitrogen (Paisley, UK). Trb1, Trb2 and Trb3 over-expression plasmids (see appendix A for plasmid maps) and GFP constructs were a kind gift from Dr Endre Kiss-Toth (Sheffield University, UK). Sidestep[™] Lysis and Stabilization Buffer was purchased from Agilent Technologies, Stratagene Product Division (CA, USA). Real-time reverse transcriptase polymerase chain reaction (RT-PCR) primers and probes were purchased from Sigma-Genosys (Poole, UK). Superscript[™] II reverse transcriptase, Moloney Murine Leukemia Virus (M-MLV) reverse transcriptase and RNaseOut Recombinant Ribonuclease Inhibitor were purchased from Invitrogen. SYBR Green and Titanium[™] Taq DNA Polymerase were purchased from TaKaRa Bio Inc (Shiga, Japan). Jumpstart Taq Ready Mix was purchased from Sigma. *Eco*R1 was purchased from Fermentas Life Sciences (York, UK). Agarose

(electrophoretic grade) and TRIzol® Reagent were purchased from Invitrogen. VECTASHIELD mounting medium with DAPI was purchased from Vector Labs. RNase- and DNase-free H₂O was from Sigma-Aldrich.

2.1.7 Immunoblotting reagents

Ammonium peroxodisulphate (APS) and gelatin were obtained from BDH. β-mercaptoethanol, N,N,N',N'-tetramethylethylenediamine (TEMED), 1,10-phenanthroline and polyoxyethylenesorbitan monolaurate (Tween 20) were obtained from Sigma-Aldrich. 40% (w/v) acrylamide/bis-acrylamide (37.5:1) solution was obtained from Amresco (Solon, OH, USA). PageRuler™ prestained protein ladder and GeneRuler™ 1 kb DNA ladder were purchased from Fermentas Life Sciences. Enhanced chemiluminescence (ECL) western blot detection reagents were obtained from Amersham Biosciences (Little Chalfont, UK).

2.1.8 Inhibitors

LY294002 (selective PI3K inhibitor), TGX-221 (selective PI3K p110β inhibitor) and compound 15e (selective PI3K p110α inhibitor) were purchased from Calbiochem (Nottingham, UK). All inhibitors were reconstituted in sterile filtered DMSO. All inhibitors were screened for cytotoxicity using the ToxiLight™ Bioassay Kit according to the manufacturer's instructions (Lonza). Briefly, the assay quantitatively measured the release of adenylate cyclase (AK) from damaged cells. Cell supernatant (20 μl) was transferred to a luminescence compatible 96-well plate. AK Detection Reagent (100 μl) was added to each well. After 5 minutes, a 1 second integrated reading was taken using a MicroLumatPlus LB 96V (Berthold Technologies UK Ltd, Hertfordshire).

2.1.9 Cytokines

Recombinant human IL-1α was a kind gift from GlaxoSmithKline (Stevenage, UK) and was stored at -20°C prior to formulation at the appropriate concentration in the relevant culture medium. Recombinant OSM was prepared in-house and stored at a stock concentration of 85 μg/ml at -80°C prior to formulation at the appropriate concentration in the relevant culture medium. Recombinant human IL-4 was purchased from R&D Systems (Abington, UK) and diluted from powder form in sterile PBS containing 1% BSA (Sigma Aldrich) to a stock concentration of 50 μg/ml, aliquoted and stored at -80°C prior to formulation at the appropriate concentration in the relevant culture medium.

All other standard laboratory chemicals and reagents, unless otherwise indicated, were commercially available from Sigma-Aldrich, Invitrogen or BDH Chemicals.

2.2 Methods

2.2.1 Cartilage Sample Collection

Human articular cartilage samples were obtained from patients undergoing whole joint replacement surgery due to end-stage OA in accordance with university ethical guidelines (All subjects gave informed consent and the study performed with Newcastle and North Tyneside Research Ethics Committee 1 approval (Reference 09/H0906/72), as well as Newcastle upon Tyne Hospitals NHS Trust Research and Development approval (Reference 5044)). Cartilage was processed to extract chondrocytes. Bovine cartilage was obtained from a local abattoir.

2.2.2 Chondrocyte Extraction and Culture

Bovine nasal septum cartilage was used as a source of primary chondrocytes. Human articular cartilage obtained from patients undergoing joint replacement was also used as a source of chondrocytes. A three-step enzymatic digest of cartilage was used to isolate chondrocytes.

2.2.2.1 Bovine nasal chondrocyte extraction

Reagents:

- PBS containing 200 IU/ml penicillin, 200 ug/ml streptomycin and 40 IU/ml Nystatin.
- DMEM culture medium containing 10% (w/v) FBS, 2 mM L-glutamine, 200 IU/ml penicillin, 200 ug/ml streptomycin and 40 IU/ml Nystatin.
- Hyaluronidase (1 mg/mL in PBS, 5 ml/g cartilage)
- Trypsin (2.5 mg/mL in PBS, 5 ml/g cartilage)
- Collagenase (2.5 mg/mL in DMEM containing 10% FBS, 3 ml/g cartilage)

Method:

Cartilage was removed from bovine nasal septum, either on the day of slaughter or the following day after storage at 4°C, and cut into small pieces. Pieces were washed 3 x 15 minutes in PBS containing antibiotics. Samples were placed in a pre-weighed 50 ml Falcon tube. Cartilage was then incubated for 15 minutes with hyaluronidase at 37°C with rotation. Supernatant was removed and cartilage washed 3 times with PBS (+ antibiotics). Cartilage was then incubated with trypsin for 30 minutes at 37°C with rotation. The supernatant was removed and the cartilage was washed twice with DMEM+FBS. Cartilage was then incubated with collagenase for 15-20 hours at 37°C with rotation. Falcon tubes were left upright for 15 minutes to allow undigested cartilage to settle at the bottom of the Falcon tube. The supernatant (containing chondrocytes) was removed and passed through a cell strainer (0.2 µm) and centrifuged at 112 x g for 10 minutes in sterile Falcon tubes to obtain the cell pellet. Pellets were combined and washed with PBS, spun at 112 x g for 10 minutes and the final pellet resuspended in 20 ml DMEM+FBS.

2.2.2.2 Human articular chondrocyte extraction

Residual, macroscopically normal cartilage was removed from the subchondral bone and washed in PBS. Cartilage was cut into small pieces and sequentially digested as described in section 2.2.2.1.

2.2.3 Cell culture**Reagents:**

- For bovine nasal chondrocyte and human articular chondrocyte culture: DMEM culture medium containing 10% (w/v) FBS, 2 mM L-glutamine, 200 IU/ml penicillin, 200 µg/ml streptomycin and 40 IU/ml Nystatin.
- For SW1353 culture: DMEM:F12 culture medium containing 10% (w/v) FBS, 2 mM L-glutamine, 200 IU/ml penicillin and 200 µg/ml streptomycin.

Method:

Cells were counted and seeded at a density of 40 000 cells/cm² into 96-well plates, 6-well plates or T75 cm² flasks. Cells were grown to 70-80% confluence at 37°C in 5% (v/v) CO₂/humidified air. SW1353 monolayers were washed with PBS before incubation with

trypsin-EDTA solution to release cells. Cells were then split into appropriate culture vessels for experimentation or into further T75 cm² flasks to continue the cell line.

2.2.4 Bovine nasal cartilage explant culture

As a model of cartilage degradation, bovine nasal cartilage in explant culture was stimulated to resorb with the pro-inflammatory cytokines IL-1 and OSM. Serum was excluded from cartilage explants as it has been shown to increase cartilage metabolism in the absence of exogenous cytokine(s) (Sah et al. 1994). The absence of serum has been shown not to affect the viability of the tissue and previous studies have shown that cartilage in serum-free culture for 8-9 days can still respond to serum and other growth factors (Hascall et al. 1983).

Reagents:

- For bovine nasal cartilage culture: DMEM culture medium containing 2 mM L-glutamine 200 IU/ml penicillin, 200 µg/ml streptomycin, 40 IU/ml Nystatin and 100 µg/ml gentamicin.

2.2.4.1 Bovine nasal cartilage degradation assay

Bovine nasal cartilage in explant culture was stimulated to resorb with the cytokines IL-1 ± OSM. Bovine nasal septum was obtained from a local abattoir after slaughter and stored at 4°C overnight. The cartilage from four separate cartilage samples was cut into 2 mm thick slices. One slice was taken from each cartilage sample and the four slices were cut into 2 mm x 2 mm pieces. These pieces of cartilage were then mixed and divided between 4 wells of a 6-well tissue culture plate. This process was repeated until all wells were filled. To each well, 6 ml of bovine nasal cartilage culture medium were added and the plates were incubated overnight at 37°C. Media were removed from each well and replaced with 6 ml fresh culture medium containing the appropriate cytokine(s) (day 0). For RNA extraction, cartilage and culture supernatants were harvested at specific days, according to the experiment. Harvested cartilage was placed in RNAlater (Ambion), stored at 4°C overnight and stored at -80°C until RNA extraction. At day 7, media were removed and replenished with identical cytokine(s) to day 0. At day 14, the remaining cartilage was digested with papain to release any remaining proteoglycan and collagen. Cartilage was placed in capped

bijoux tubes with 5.5 ml phosphate buffer (137 ml 0.1M NaH₂PO₄ and 63 ml 0.1 M NaHPO₄, pH 6.5) containing papain (4.5 mg/ml), cysteine-HCl (5 mM) and EDTA (5 mM). Following overnight (20 hours) digestion at 65°C, cartilage digests were frozen at -20°C until assayed.

2.2.4.2 Hydroxyproline assay

The amino acid sequence glycine-proline-hydroxyproline occurs frequently in collagen and hydroxyproline is found in very few other proteins. Therefore, hydroxyproline was assayed as a measure of collagen. Protein was hydrolysed to its constituent amino acids. The assay is based on the oxidation of hydroxyproline by chloramine T to a compound related to pyrrole, and the subsequent condensation of this intermediate with DAB to produce a red colour, which is measured at A₅₆₀ nm. Hydroxyproline present in samples was assayed using a microtitre modification of the assay described by Bergman and Loxley (1963).

Reagents:

- Acetate-citrate buffer: 420 mM sodium acetate, 130 mM tri-sodium citrate, 26 mM citric acid and 38.5% (v/v) propan-2-ol, pH 6.
- DAB: 4.5 M stock in 70% (v/v) perchloric acid, stored 4°C.
- Chloramine T: 250 mM in dH₂O, made fresh.

Method:

The media or cartilage digests (200 µl) to be assayed were mixed with 200 µl of 12 M HCl in 2 ml capped Sarstedt tubes. Samples were then hydrolysed in a hot-block overnight at 105°C. The hydrolysates were dried in a centrifugal evaporator using an acid-resistant integrated Savant Speed Vac (Life Sciences International, Basingstoke, UK) for 1-2 hours. The residue was resuspended in 200 µl dH₂O and stored at room temperature until assayed. Standards (0-30 µg/ml) were produced by diluting hydroxyproline (1 mg/ml) in dH₂O. On the day of use, chloramine T (250 mM) was diluted 1:4 in acetate-citrate buffer and DAB was diluted 1:3 in propan-2-ol. To a 96-well microtitre plate, 40 µl of sample or standard was added in duplicate (neat or diluted in dH₂O). Using a stopwatch, 25 µl of 62.5 mM chloramine T was added at time 0 minutes. After 4 minutes, 150 µl of 1.5 M DAB was added in the same order. The plate was then incubated for 35 minutes at 65°C, allowed to

cool and the absorbance measured at 560 nm (Sunrise multilabel counter, TECAN, Reading, UK). The standard curve was used to calculate the hydroxyproline content of the samples. The release of hydroxyproline from the cartilage was then calculated using the following equation:

$$\% \text{ hydroxyproline release} = \frac{\text{[hydroxyproline in supernatants (}\mu\text{g/ml)]}}{\text{[total hydroxyproline (}\mu\text{g/ml)]}} \times 100$$

Where total hydroxyproline is the amount of hydroxyproline in supernatants and cartilage digests. The % release of hydroxyproline was considered to be representative of the % release of collagen.

2.2.4.3 Collagenase assay

Collagenolytic activity present in supernatants from bovine nasal cartilage explant cultures was determined using a 96-well plate modification (Koshy et al. 1999) of the diffuse fibril assay (Cawston and Barrett, 1979). Collagen at neutral pH and at temperatures above 25°C forms into fibrils where the individual collagen molecules associate to form a viscous gel. In this assay, collagen, which has been acetylated with [³H]-acetic anhydride, is allowed to form fibrils. At the end of the assay, undigested collagen fibrils are spun down in the centrifuge and the amount of [³H] in the supernatant gives a measure of the amount of collagen digested. As well as measuring active collagenase activity, a measure of total collagenase activity can be obtained by adding APMA (0.67 mM) to the assay, which activates latent proMMPs.

Reagents:

- Tris assay buffer: 100 mM TrisHCl, pH 7.6, 15 mM CaCl₂ and 0.02% (w/v) NaN₃.
- 10 mM stock solution APMA: 35.2 mg APMA was dissolved in 200 μl DMSO and diluted to 10 ml with 100 mM TrisHCl, pH 8.5. This was stored at 4°C in a foil-wrapped container for up to 3 months.
- Tris-APMA assay buffer: At the time of assay, APMA was diluted to 2 mM in Tris assay buffer.

- Cacodylate buffer: 25 mM sodium cacodylate, pH 7.6, 0.05% (w/v) Brij-35 and 0.02% (w/v) NaN₃.
- [³H]-acetylated collagen: Acid-soluble type I collagen was extracted and purified from calf skin using the method previously described (Cawston and Barrett, 1979). The purified collagen was freeze-dried and stored at -20°C. When required the collagen was thawed and redissolved in 0.2 M acetic acid at 4°C. Collagen was radiolabelled with [³H]-acetic anhydride (925 MBq; Amersham Pharmacia Biotech Ltd. (Buckinghamshire, UK)) to a high specificity as described (Cawston et al. 2001). For the assay, a 1 mg/ml solution (50 mM TrisHCl pH 7.6, containing 200 mM NaCl and 0.02% (w/v) NaN₃) with a specific activity of approximately 1 x 10⁵ dpm/mg was used.
- Trypsin: 100 µg/ml trypsin in 1 mM HCl. Stored -20°C.
- Bacterial collagenase: 100 µg/ml bacterial collagenase in cacodylate buffer. Stored -20°C.

Controls:

Total lysis of collagen was obtained by the addition of bacterial collagenase.

Negative control (cacodylate buffer) was used to determine the background counts.

Trypsin control was used to determine maximum susceptibility of the labelled non-helical telopeptides to non-specific proteolytic cleavage and to identify if denaturation of the triple helix had occurred before the assay. Trypsin activity of between 10-20% lysis of total collagen was acceptable. The linear range of the assay was between 10-80% lysis of total collagen.

Method:

A measure of total collagenase activity was obtained by adding APMA (0.67 mM) to the assay. APMA activates the pro-form of MMPs by destabilising the propeptide, making it accessible to autolytic cleavage (Koshy et al. 1999). 50 µl of Tris assay buffer (100 mM Tris/HCl and 15 mM CaCl₂, pH 7.6 at room temperature) ± APMA was added to each well of a V-bottomed 96-well plate. At the time of assay, APMA was diluted to 2 mM in Tris assay buffer. This was followed by 40 µl cacodylate buffer (CCA) (25 mM sodium cacodylate, 0.05% (w/v) Brij 35 and 0.02% (w/v) azide; pH 7.5) + 10 µl sample or standard

in duplicate (neat or diluted in cacodylate buffer). Three sets of controls (in duplicate) were also included 1) CCA (50 μ l) (negative control to determine the background counts obtained in the assay); 2) 10 μ l trypsin (100 μ g/ml in 1 mM HCl) + 40 μ l CCA (used to ensure the collagen has not been denatured and thus become susceptible to non-specific, non-collagenolytic proteolytic cleavage); 3) 50 μ l bacterial collagenase (100 μ g/ml in CCA) (the total lysis control is used to determine the counts obtained if all the collagen is cleaved). This was followed by the addition of 50 μ l of [3 H]-acetylated collagen (1 mg/ml) (50 mM TrisHCl, pH 7.6, 200 mM NaCl, 0.02% (w/v) NaN₃). The 96-well plate was incubated at 37°C (16-20 hours) then centrifuged at 1056 x g, 4°C for 30 minutes in a Sorvall RC5C Plus centrifuge. Supernatant (50 μ l) was removed and placed in a flexible 96-well sample plate with 200 μ l of Optiphase “Supermix” scintillation fluid. Counts were read in a 1450 Micro-Beta Trilux liquid scintillation and luminescence counter (Wallac). Collagenase activity was measured in units/ml, where one unit can degrade 1 μ g of collagen per minute at 37°C.

Equation for calculating collagenase activity (units/ml):

$$= 50/(\text{total lysis-blank}) \times 1000/(\text{sample volume } (\mu\text{l})) \times 1/(\text{time (minute)}) \times (\text{sample} - \text{blank})$$

2.2.5 RNA isolation and real-time polymerase chain reaction

2.2.5.1 Extraction of RNA from bovine nasal cartilage

During cartilage experiments, RNA was extracted from powdered cartilage using TRIzol[®] Reagent. This extraction procedure is a modification of the single-step acid-phenol guanidinium extraction method developed by (Chomczynski and Sacchi 2006). Cartilage stored in RNAlater at -80°C was thawed and RNAlater removed. Cartilage was snap-frozen in liquid nitrogen and immediately ground (10 minutes pre-cool, 5 cycles of 2 minutes of grinding and 2 minutes of cooling, impact frequency of 10 Hz) in a SPEX CertiPrep 6750 freezer mill (Glen Creston, Stanmore, UK). 3 ml TRIzol[®] Reagent was added to the powdered cartilage, shaken vigorously, incubated at room temperature for 10 minutes and centrifuged at maximum speed for 10 minutes at 4°C to remove insoluble material. Chloroform (450 μ l chloroform per 750 μ l TRIzol) was added to the supernatant, the samples were vortexed and incubated at room temperature for 10 minutes. Samples were

then centrifuged at maximum speed for 15 minutes at 4°C. The aqueous phase was allowed to separate for up to 3 days at 4°C. The aqueous phase was removed and mixed with a half volume of 100% ethanol. Total cellular RNA was extracted and purified using the RNeasy kit. This included an on-column DNase step, as per the manufacturer's instructions. Total RNA (1 µg) was reverse transcribed in a 20 µl reaction using superscript II reverse transcriptase (Invitrogen) according to the manufacturer's instructions. cDNA was stored at -20°C until use in downstream real-time RT-PCR.

2.2.5.2 Reverse Transcription

RNA extracted using RNeasy® Mini Kit: RNA was quantified by spectrophotometry (Nanodrop ND 1000 spectrophotometer) and complementary DNA (cDNA) was synthesised from 1 µg of total RNA. RNA was combined with 2 µg of random hexamers (1 µg/ml) (GE Healthcare, Little Chalfont, UK) in a final volume of 12.5 µl and heated at 70°C for 10 minutes. Samples were chilled immediately on ice and the following was added to each well: 4 µl 5x First Strand Synthesis Buffer, 2 µl DTT (0.1 M), 0.5 µl Superscript II (200 U/µl), 0.5 µl RNaseOut (40 U/µl) and 0.5 µl dNTPs (10 mM). Samples were then incubated at 42°C for 1 hour. cDNA diluted 1:100 in dH₂O for target gene quantification or 1:500 for housekeeping gene quantification and stored at -20°C until required.

RNA extracted using SideStep™ Kit: Cells were seeded into 96-well plates at a density of 10,000 cells per well and grown until 70-80% confluent. After the desired period of cytokine incubation, culture medium was removed and cells were washed once with ice-cold PBS. 10 µl SideStep™ Lysis and Stabilization Buffer was added to each well and the plate was then vortexed for 2 minutes to ensure complete cell lysis. 5 µl cell lysate was transferred to a new 96-well plate and diluted with 15 µl dH₂O. 4 µl of the diluted cell lysate was transferred to a new 96-well plate for reverse transcription. To each well of the 96-well plate 1 µl random hexamers (0.2 µg/ml) and 3 µl dNTPs (2.5 mM) were added and the plate heated at 70°C for 5 minutes. The plate was immediately placed on ice where 4 µl 5x First Strand Synthesis Buffer, 2 µl DTT (0.1 M), 0.125 µl RNaseOut (40 U/µl) and 0.5 µl MMLV (200 U/µl) were added to each well. The plate was incubated at 37°C for 50 minutes, followed by 70°C for 15 minutes. Bovine cDNA was diluted 1:100 and human

cDNA was diluted 1:20 for housekeeping gene quantification. All cDNA was stored at -20°C until required.

2.2.5.3 Taqman® Probe-Based Real-Time RT-PCR

Oligonucleotide primers and probes were designed using Primer Express 1.0 (Applied Biosystems, Warrington, UK) (Table 2.1) and were used to measure mRNA expression in human articular chondrocytes and SW1353. Relative quantification of genes was performed using the ABI prism 7900HT sequence detection system (Applied Biosystems, Foster City, Ca, USA). To a 96-well microtitre plate 5 µl of real-time RT-PCR mix containing the following was added: 3.3 µl Jumpstart Taq Readymix, 0.8 µl MgCl₂ at a final concentration of 2 mM, 0.3 µl each of forward and reverse primer (final concentration 300 nM), 0.1 µl probe (final concentration 150 nM) and 0.2 µl ROX reference dye. 5 µl of cDNA was then added to each well, to make a final volume of 10 µl per well. Conditions for real-time RT-PCR were as follows: for 18S, MMP-1, MMP-13, Trb2 and Trb3, 2 minutes at 50°C, 10 minutes at 95°C, then 40 cycles of 15 seconds at 95°C and 1 minute at 60°C. To normalise for different amounts of total RNA present in each sample, 18S rRNA was used as an endogenous control.

Gene	Sequence (5'-3')	Length (bp)
18S	CGAATGGCTCATTAATCAGTTATGG	26
	TATTAGCTCTAGAATTACCACAGTTATCC	29
	FAM-CAGAGAGTACAACCTTACATCGTGTTGCGGCTC-TAMRA	32
MMP-1	AAGATGAAAGGTGGACCAACAATT	24
	CCAAGAGAATGGCCGAGTTC	20
	FAM-CAGAGAGTACAACCTTACATCGTGTTGCGGCTC-TAMRA	32
MMP-13	AAATTATGGAGGAGATGCCCAT	23
	TCCTTGGAGTGGTCAAGACCTAA	23
	FAM-CTACAACCTGTTTCTTGTTGCTGCGCATGA-TAMRA	30
Trb2	CATACACAGGTCTACCCCC	19
	TCCGCGGACCTTATAGAC	18
	FAM-CTTCGAAATCCTGGGTTTT-TAMRA	19
Trb3	CTGCCCGCTGTCTGGTTC	18
	GGGCATCGGGTCCTGTTCG	18
	FAM-TGCCTCCTTCGTGCGGAG-TAMRA	18

Table 2.1 Human Taqman® probe-based real-time PCR primers and probes.

2.2.5.4 SYBR[®] Green Real-Time PCR

Oligonucleotide primers were designed using DNASTar (DNASTAR, Inc, Madison, WI, USA) (Table 2.2). Relative quantification of genes was performed using the ABI prism 7900HT sequence detection system (Applied Biosystems, Foster City, Ca, USA). Bovine MMP gene expression was determined using SYBR Green. Takara SYBR Green mixtures contained 50% SYBR Green PCR mix (Takara) and 1 pmole of each primer in a total volume of 10 μ l. Conditions for real-time RT-PCR were as follows: for MMP-1 and 18S, 10 seconds at 95°C, then 40 cycles consisting of 5 seconds at 95°C and 30 seconds at 60°C, followed by a dissociation plot; for MMP-13, 10 seconds at 95°C, then 40 cycles consisting of 5 seconds at 95°C, 15 seconds at 55°C and 20 seconds at 72°C, followed by a dissociation plot; and for Trb1 and STAT6 10 seconds at 95°C, then 40 cycles consisting of 15 seconds at 95°C and 1 minute at 60°C, followed by a dissociation plot. To normalise for different amounts of total RNA present in each sample, 18S rRNA was used as an endogenous control.

Gene	Sequence (5'-3')	Length (bp)
Bovine	GATGCCGCTGTTTCTGAGGA	20
MMP-1	GACTGAGCGACTAACACGACACAT	24
Bovine	TTAGAGAACATGGGGACTTTTTG	23
MMP-3	CGGGTTCGGGAGGCACAG	18
Bovine	CCCTCTGGTCTGTTGGCTCAC	21
MMP-13	CTGGCGTTTTGGGATGTTTAGA	22
Bovine	AGGCCGACATCATGATCTTCTTTG	24
MMP-14	CTGGGTTGAGGGGCATCTTAGTG	24
Human	TTCTCTGCCAGCTTCACACTT	21
STAT6	CACCAGGGGCAGAGACAG	18
Human	CCCCAAAGCCAGGTGCCT	18
Trb1	TACCCGGGTTCCAAGACG	18

Table 2.2 SYBR[®] Green primers for real-time RT-PCR.

2.2.6 Preparation of total cell lysates

Reagents:

- Lysis buffer (50 mM Tris, pH 7.4, 10% (v/v) glycerol, 1 mM EDTA, 1 mM EGTA, 1 mM Na_3VO_4 , 5 mM NaF, 10 mM β glycerol phosphate, 5 mM $\text{Na}_4\text{P}_2\text{O}_7$, 1% (v/v) Triton X-100, 1 μM microcystin-LF and 1 Complete protease inhibitor Mini tablet from (Roche Diagnostics, Burgess Hill, UK) for 50 ml buffer).

Method:

Cells were plated in 6-well plates or 25 cm² flasks at a density of 25 000 cells/cm². After the desired period of cytokine incubation, culture medium was removed and cells rinsed with ice-cold PBS. The PBS was then removed and replaced with ice-cold Lysis buffer at the following volumes: 150 μl /well of a 6-well plate and 200 μl /75 cm² flask. The cells were scraped into the lysis buffer then transferred to an Eppendorf tube on ice. Samples were vortexed for 10 seconds and incubated on ice for 20 minutes, followed by centrifugation at 10,000 x g at 4°C for 3 minutes. The supernatant was then removed, snap frozen on dry ice and stored immediately at -80°C.

2.2.7 Subcellular protein fractionation

The Subcellular Protein Fractionation Kit from ThermoScientific was used to separate the cytoplasmic, membrane, soluble nuclear, chromatin-bound nuclear and cytoskeletal fractions. The first reagent added to the cell pellet causes selective membrane permeabilisation, releasing soluble cytoplasmic contents. The second reagent dissolves plasma, mitochondria and ER/golgi membranes but does not solubilise the nuclear membranes. After recovering intact nuclei by centrifugation, a third reagent yields the soluble nuclear extract. An additional nuclear extraction with micrococcal nuclease is performed to release chromatin-bound nuclear proteins. The recovered insoluble pellet is then extracted with the final reagent to isolate cytoskeletal proteins.

Reagents:

- Ice-cold PBS
- Subcellular Protein Fractionation Kit containing:
 - Cytoplasmic Extraction Buffer (CEB), stored at -20°C

- Membrane Extraction Buffer (MEB)), stored at 4°C
- Nuclear Extraction Buffer (NEB)), stored at 4°C
- Pellet Extraction Buffer (PEB)), stored at room temperature
- Micrococcal Nuclease ≥ 100 units/ μ l), stored at -20°C
- CaCl₂ (100 mM), stored at 4°C
- Halt™ Protease Inhibitor Cocktail (100X), stored at 4°C

Method:

SW1353 cells were cultured as described in section 2.2.3. Following cytokine stimulation, cells were washed once with ice-cold PBS. Cells were scraped into 1 ml ice-cold PBS and centrifuged at 500 x g for 3 minutes to pellet. The supernatant was discarded. Protease inhibitors were added to required volume of reagents as per Table 2.3.

Packed cell volume (μ l)	CEB (μ l)	MEB (μ l)	NEB (μ l)	NEB (μ l) + CaCl ₂ , MNase*	PEB (μ l)
10	100	100	50	50	50
20	200	200	100	100	100
50	500	500	250	250	250

* MNase = Micrococcal nuclease

Table 2.3 Subcellular protein fractionation reagent volumes for different packed cell volumes.

Ice-cold CEB buffer containing protease inhibitors was added to the cell volume (Table 2.3) and the tube incubated at 4°C for 10 minutes with gentle mixing. The tube was centrifuged at 500 x g for 5 minutes at 4°C and the supernatant (cytoplasmic extract) transferred to a clean pre-chilled tube on ice. Ice-cold MEB buffer containing protease inhibitors was added to the pellet and vortexed for 5 seconds on highest setting. The tube was then incubated at 4°C for 10 minutes with gentle mixing and centrifuged at 3000 x g for 5 minutes at 4°C. The supernatant (membrane extract) was transferred to a clean pre-chilled tube on ice. Ice-cold NEB containing protease inhibitors was added to the pellet and vortexed for 15 seconds on the highest setting, then incubated at 4°C for 30 minutes with gentle mixing. The tube was centrifuged at 5000 x g for 5 minutes at 4°C and the supernatant (soluble nuclear extract) transferred to a clean pre-chilled tube on ice. The

chromatin-bound extraction buffer was prepared by adding 5 μ l 100 mM CaCl_2 and 3 μ l of Micrococcal Nuclease (300 units) per 100 μ l of room temperature NEB and added to the pellet. The tube was vortexed for 15 seconds on the highest setting, incubated at room temperature for 15 minutes and centrifuged at 16000 x g for 5 minutes at 4°C. The supernatant (chromatin-bound nuclear extract) was transferred to a clean pre-chilled tube on ice. Room temperature PEB containing protease inhibitors was added to the pellet, vortexed at the highest setting for 15 seconds and incubated at room temperature for 10 minutes. The tube was centrifuged at 16000 x g for 5 minutes at 4°C and the supernatant (cytoskeletal extract) transferred to clean tube. Fractions were snap frozen and stored at –80°C until required.

2.2.8 SDS-Polyacrylamide gel electrophoresis (SDS-PAGE)

Proteins were separated based on size by SDS-PAGE performed under reducing conditions (Laemmli 1970). The polymerisation of acrylamide is initiated by the addition of APS and TEMED. TEMED catalyses the decomposition of the persulphate ion to give a free radical which initiates the polymerisation reaction. Samples were prepared by boiling in β -mercaptoethanol and SDS. β -mercaptoethanol reduces any disulphide bridges and the SDS, an anionic detergent, denatures proteins. The bound SDS masks the charge of the proteins, forming anionic complexes with constant net negative charge per unit mass. The purpose of the stacking gel is to concentrate the protein sample into a sharp band before it enters the main separating gel. This is achieved by utilising differences in ionic strength and pH between the electrophoresis buffer and the stacking gel. The stacking gel has a large pore size, allowing the proteins to move freely and stack under the effect of the electric field. The band-sharpening effect relies on the fact that negatively charged glycinate ions (in the electrophoresis buffer) have a lower electrophoretic mobility than the protein-SDS complexes, which, in turn, have lower mobility than the chloride ions of the loading buffer and the stacking gel. Proteins are separated by their size, with smaller proteins moving more easily through the pores of the gel and larger proteins moving more slowly. After the tracking dye (bromophenol blue) reaches the bottom of the gel, electrophoresis is stopped.

Reagents:

- 4 x Lower gel buffer (LGB): 1.5 M TrisHCl pH 8.8, 0.4% (w/v) SDS.
- 4 x Upper gel buffer (UGB): 0.5 M Tris HCl pH 6.8, 0.4% (w/v) SDS.
- Stacking gel: 40% bis/acrylamide diluted to 4.5% with water and 4 x UGB.
- 5 x Final sample buffer (FSB): 0.625 mM Tris HCl pH 6.8, 40% (v/v) glycerol, 10% (w/v) SDS, 0.5% (w/v) bromophenol blue, 5% (v/v) β -mercaptoethanol.
- 10 x Running Buffer: 250 mM Tris, 2 M glycine, 10% (w/v) SDS.

Method:

Electrophoresis was performed in a Bio-Rad Mini-Protean II apparatus with 1.0 mm spacers and combs. Polyacrylamide-bis-acrylamide was purchased as a 40% (w/v) (37.5:1 acrylamide:bis) solution, diluted with water and 3 ml of 4 x LGB to the required percentage (Table 2.4). Gel mixture (12 ml) was polymerised by the addition of 20 μ l TEMED and 60 μ l APS (0.2% w/v) immediately before pouring the gel. The lower gel was overlaid with propan-2-ol to exclude oxygen and allowed to polymerise. Once set, propan-2-ol was washed off the gel and a 4.5% bis/acrylamide stacking gel laid on top, combs inserted and the stacker allowed to set. Upper gel (5 ml) was set with 10 μ l TEMED and 30 μ l 0.2% (w/v) APS. The gel kit was assembled and filled with 1 x Running Buffer. Cell lysate samples were prepared as follows: 1 ml of 5 x sample buffer was mixed with 250 μ l β -mercaptoethanol. Sample buffer (4 μ l) was added to 20 μ l of each cell lysate sample and heated to 105°C for 5 minutes. Molecular weight markers were PageRuler pre-stained protein standards (Fermentas). Proteins were electrophoresed at a constant 80 V in Running Buffer for approximately 1 hour 30 minutes, until the dye front had run to the end of the separating gel.

Percentage gel (%)	40% (w/v) acryl/bis solution (37.5:1) (ml)	dH ₂ O (ml)	4x LGB (ml)
12.5	3.75	5.25	3.0
10	3.0	6.0	3.0
7.5	2.25	6.75	3.0

Table 2.4 Preparation of SDS-PAGE gels (volumes for 2 gels).

2.2.9 Western blotting

Reagents:

- Transfer Buffer: 39 mM glycine, 48 mM Tris, 0.0375% (w/v) SDS and 20% (v/v) methanol.
- Tris Buffered Saline (TBS): 10 mM TrisHCl pH 7.4, 0.15 M NaCl.

Method:

Proteins were separated by SDS-PAGE (section 2.2.8) and semi-dry blotted onto PVDF membrane essentially according to the method of (Towbin et al. 1979). Proteins were transferred from SDS gels to PVDF membrane (0.2 μ m pore size) (Millipore) using a semi-dry transfer unit (Bio-Rad). The gel, PVDF membrane and 4 sheets of filter paper were soaked in transfer buffer. A sandwich was made on the anode plate consisting of 2 sheets of filter paper followed by the PVDF membrane, the gel and the remaining 2 sheets of filter paper. The sandwich was rolled gently to remove any air bubbles and the cathode plate lowered on top. Transfer was allowed to proceed for 1 hour 30 minutes at a current of 80 mA per gel (35 V, 200 W). Following transfer, the blot was blocked with TBS containing 0.2% Tween 20 (TBS-T) containing 5% (w/v) non-fat dried milk in blocking buffer for 1 hour at room temperature. The blot was incubated overnight at room temperature with primary antibody diluted in TBS-T (containing 5% BSA). The blot was then washed three times in 20 ml TBS/0.05% Tween for 5 minutes in a small dish on a rocking table. The blot was incubated for 1-2 hours with a secondary antibody conjugated with HRP. The blot was then washed three times in TBS-T for 5 minutes.

Towards the end of this PhD, the above method was replaced by the iBlot® Dry Blotting System (Invitrogen), carried out according to manufacturer's instructions. The iBlot® Dry Blotting System blots proteins from polyacrylamide gels in 7 minutes, without the need for additional buffers or an external power supply. Briefly, the iBlot™ Gel Transfer Device is a self-contained blotting unit with an integrated power supply that allows for fast, dry blotting of proteins. The iBlot™ Gel Transfer Stacks are disposable stacks with an integrated nitrocellulose transfer membrane to perform dry blotting of proteins. Each iBlot™ Gel Transfer Stack contains a copper electrode and appropriate cathode and anode

buffers in the gel matrix to allow fast dry blotting of proteins without the need to prepare buffers.

Protein detection by enhanced chemiluminescent (ECL) was carried out according to the manufacturer's instructions.

2.2.10 Gelatin zymography

Proteins were separated on an SDS-PAGE gel, co-polymerised with 0.1% w/v gelatine. SDS was then washed from the gel to allow proteins to refold and become active. Gels were incubated overnight in Tris/Triton/Ca²⁺/Zn²⁺ buffer to allow gelatin digestion to occur. The gels were stained with Coomassie blue and destained. Clear bands on a blue background indicated the presence of gelatin activity.

Reagents:

- 5 x sample buffer: 10 ml 10 x Upper Gel Buffer (UGB), 2 g SDS, 8 ml glycerol, 2 ml bromophenol blue (0.1% (w/v) in ethanol).
- 10 x zymography buffer: 200 mM Tris pH 7.8.
- Tris/Triton buffer: 20 mM Tris pH 7.8, 2.5% (w/v) Triton-X100.
- Tris/Triton/Ca²⁺/Zn²⁺ buffer: 20 mM Tris pH 7.8, 10 mM CaCl₂, 5 μM ZnCl₂, 1% Triton-X100.
- Coomassie stain: 2.5 g Coomassie G250, 400 ml methanol, 100 ml acetic acid, 500 ml H₂O.
- Destain: 800 ml methanol, 100 ml acetic acid, 1100 ml H₂O.

Method:

Gelatin zymography was used to assay gelatinase activity in the culture supernatants. Samples were electrophoresed under non-reducing conditions by SDS-PAGE in 7.5% polyacrylamide gels copolymerised with 0.1% (w/v) gelatin. To remove SDS, gels were washed twice for 1 hour in Tris/Triton buffer, then incubated overnight (16 hours) in Tris/Triton/Ca²⁺/Zn²⁺ buffer at 37°C. Coomassie Brilliant Blue was used to stain gels.

2.2.11 RNAi and over-expression plasmid assays

2.2.11.1 RNAi assays

Reagents:

- Dharmacon siGENOME™ SMARTpools®
- siCONTROL (non-targeting siRNA #2, Cat: 001210-02)
- Dharmafect™ 1 lipid reagent

Method:

Primary human chondrocytes or SW1353 cells were prepared and cultured as described in sections 2.2.2.2 and 2.1.2, respectively. For siRNA transfections, cells were trypsinized and re-seeded at approximately 50% confluency. Dharmacon siGENOME™ SMARTpools® of 4 specific siRNA duplexes (total of 100 nM siRNA) were used to transfect SW1353 cells using Dharmafect™ 1 lipid reagent. siRNA pools were used to target Trb1 (NM_025195, Cat: 003633); Trb2 (NM_021643, Cat: 005391); Trb3 (NM_021158, Cat: 003754), STAT6 (NM_003153, Cat: 006690); S100A8 (NM_002964, Cat: 011770); S100A9 (NM_002965, Cat: 011384); SNFT (NM_018664, Cat: 003633); IRS1 (NM_005544, Cat: 003015) and IRS2 (NM_003749, Cat: 003554).

96-well plate format: Several hours prior to transfection, all medium was removed from the human articular chondrocytes or SW1353 cells and replaced with 50 µl of FBS-containing DMEM or DMEM-F12, respectively. For each well, 100 nM siRNA in a total volume of 15 µl FBS-free DMEM or DMEM-F12 and 0.26 µl Dharmafect™ 1 lipid reagent in a total volume of 15 µl of FBS-free DMEM or DMEM:F12 was prepared. These two mixes were combined and incubated at room temperature for 20 minutes before addition to cells, to allow complex formation. Cells were transfected for 28 hours and serum starved for 20 hours prior to the addition of cytokines for a further 24 hours. Total RNA was isolated and reverse-transcribed as described in section 2.2.5.2. Expression of genes of interest was measured by real-time PCR as described in section 2.2.5.3.1. Changes in gene-specific mRNA levels were calculated by comparison of expression levels with cells transfected with 100 nM siCONTROL.

6-well plate format: Several hours prior to transfection, all media was removed from the SW1353 cells and replaced with 500 μ l of serum-containing DMEM-F12. For each well, 100 nM siRNA in a total volume of 250 μ l serum-free DMEM-F12 and 3.25 μ l DharmafectTM 1 lipid reagent in a total volume of 250 μ l of DMEM:F12 was prepared. These two mixes were combined and incubated at room temperature for 20 minutes before addition to cells, to allow complex formation. Cells were transfected for 28 hours and serum starved for 20 hours prior to the addition of cytokines for a further 24 hours. Total cell lysates were prepared as described in section 2.2.6 and proteins were separated by SDS-PAGE as described in section 2.2.8. Protein fractions were transferred to PVDF membranes (as described in section 2.2.9) and blots were probed with the relevant antibody to confirm successful knock-down of genes by siRNA at the protein level.

2.2.11.2 Over-expression plasmid assays

Preparation of plasmid DNA:

Reagents:

- Luria broth (LB) containing 10 g NaCl, 10 g tryptone and 5 g yeast extract per litre dH₂O.
- LB Agar containing 10 g NaCl, 10 g tryptone, 5 g yeast extract and 15 g agar per litre dH₂O.
- Qiaprep Spin Midi/Maxi Kit.

Reagents were autoclaved prior to use and ampicillin added at a final concentration of 100 μ g/ml in filter-sterilised water for selection. Standard aseptic technique was used throughout the cloning procedure.

Mach1TM-T1[®] chemically competent E.coli (30 μ l) and 0.5 μ l plasmid (see appendix A for plasmid maps) was added to a 1.5 ml Eppendorf tube and swirled to mix. The tube was then incubated on ice for 30 minutes and heat shocked at 42°C for 30 seconds. The tube was incubated on ice for 2 minutes before the addition of 500 μ l pre-warmed LB (37°C). Tubes were incubated for 1 hour in a 37°C water bath. On pre-warmed agar plates containing ampicillin (100 μ g/ml), 20 μ l and 50 μ l volumes were streaked out. Plates were allowed to dry for 5 minutes before incubation at 37°C overnight. One colony for each plasmid was

picked and placed in a universal with 2 ml LB containing 100 µg/ml ampicillin. This was shaken at 37°C for 8 hours at 250 rpm before transferring the 2 ml culture to a conical flask containing 250 ml LB (plus 100 µg/ml ampicillin). The conical flasks were shaken at 37°C overnight (16 hours) at 250 rpm. Overnight cultures were centrifuged at 6000 x g for 15 minutes at 4°C to pellet cells. The supernatant was discarded and the bacterial pellet resuspended in 10 ml Buffer P1 (Qiagen) and vortexed until the pellet was fully resuspended. Buffer P2 (Qiagen) (10 ml) was added and inverted 6 times to mix and incubated for 5 minutes at room temperature. Buffer P3 (Qiagen) (10 ml) was added and incubated on ice for 20 minutes before centrifuging at 20000 x g for 30 minutes at 4°C. The supernatant was transferred to a clean bottle and centrifuged again at 20000 x g for 30 minutes at 4°C. Qiagen MaxiPrep columns were equilibrated by applying 10 ml Buffer QBT. The supernatant was applied to the column. Columns were then washed with 2 x 30 ml Buffer QC and the plasmid DNA was eluted with 15 ml Buffer QF. Plasmid DNA was precipitated by adding 10.5 ml propan-2-ol and centrifuging at 15000 x g for 30 minutes at 4°C. The supernatant was discarded and 350 µl dH₂O was added to resuspend pellet. This was transferred to a 2 ml screw-cap tube. dH₂O (150 µl) was added to the original tube to resuspend any remaining DNA and then transferred to the same 2 ml tube. Ethanol (100%, 1125 µl) was added to the 2 ml tube and centrifuged at maximum speed for 10 minutes. The supernatant was discarded and the pellets air-dried. Pellets were resuspended in 300 µl dH₂O and plasmid DNA was quantified by spectrophotometry (Nanodrop ND 1000 spectrophotometer) and stored at -20°C until required.

Over-expression plasmid assay:

Reagents:

- FuGene HD Transfection Reagent
- Lipofectamine 2000 Reagent

Method:

SW1353 cells were prepared and cultured as described in section 2.1.2. For over-expression plasmid transfections, cells were trypsinized and re-seeded at approximately 50% confluency. Trb1 (c-Myc tagged), Trb3 (c-Myc tagged) and STAT6 over-expression

plasmids were used to transfect SW1353 cells using FuGene HD Transfection Reagent or Lipofectamine 2000 Reagent (see individual experiments).

96-well plate format: Several hours prior to transfection, all media was removed from the SW1353 cells and this was replaced with 100 μ l serum-containing DMEM:F12. Cells were then transfected with 0.1 μ g of plasmid DNA and 0.3 μ l of transfection reagent in a total volume of 3 μ l serum-free DMEM:F12. This mix was incubated for 20 minutes at room temperature before addition to cells to allow for complex formation. Cells were transfected for 28 hours and serum starved for 20 hours prior to the addition of cytokines for a further 24 hours. Total RNA was isolated and reverse-transcribed as described in section 2.2.5.2. Expression of genes of interest was measured by real-time RT-PCR as described in section 2.2.5.3.1. Changes in gene-specific mRNA levels were calculated by comparison of expression levels with cells transfected with the empty vector, pcDNA3.1.

6-well plate format: Several hours prior to transfection, all media was removed from the SW1353 cells and this was replaced with 1 ml serum-containing DMEM:F12. Cells were then transfected with 1 μ g of plasmid DNA and 3 μ l of transfection reagent in a total volume of 20 μ l serum-free DMEM:F12. This mix was incubated for 20 minutes at room temperature before addition to cells to allow for complex formation. Cells were transfected for 28 hours before preparation of total cell lysates (as described in section 2.2.6) and separation of proteins by SDS-PAGE (as described in section 2.2.8). Protein fractions were transferred to PVDF membranes (as described in section 2.2.9) and blots were probed with c-Myc or STAT6 antibody to confirm protein over-expression.

2.2.11.3 GFP-based protein fragment complementation assay

To assess any physical interactions between the tribbles and MAPKKs, a green fluorescent protein (GFP)-based protein fragment complementation assay was used. The venus variant of GFP was used in this assay. MEK1, MKK4, MKK6 and MKK7 were fused to the N-terminal fragment of Venus GFP (V1) and Trb1 and Trb3 were fused to the C-terminal fragment of Venus GFP (V2). Various combinations of expression constructs were co-transfected and the GFP signal was visualised by fluorescent microscopy. Plasmids for the

GFP-based protein fragment complementation assay were a kind gift of Endre Kiss-Toth (Sheffield University).

Reagents:

- FuGene HD Transfection Reagent

Method:

SW1353 cells were prepared and cultured as described in section 2.1.2. Cells were trypsinized and re-seeded in 8-well chamber slides at approximately 50% confluency. Several hours prior to transfection, all media was removed and replaced with 250 μ l serum-containing DMEM:F12. Cells were then transfected with 0.1 μ g of plasmid DNA and 0.3 μ l of FuGene HD Transfection Reagent in a total volume of 3 μ l serum-free DMEM:F12. This mix was incubated for 20 minutes at room temperature before addition to cells to allow for complex formation. After 28 hours incubation, cells were washed twice with PBS and fixed in 4% paraformaldehyde for 10 minutes. Cells were washed a further 2 times in PBS and slides mounted in VECTASHIELD with DAPI. All fluorescent images of cells were taken using a Leica DM LB microscope (Leica Microsystems, Milton Keynes, UK). Images were captured using a RT_{KE} SPOT™ camera and SPOT™ Advanced imaging software from Diagnostic Instruments Inc. (Sterling Heights, MI, USA). Cell fixing was performed by Beth Gibson and microscopy was performed with the assistance of Christos Gabrielides.

2.2.11.4 shRNA assays

Reagents:

- MISSION® Lentiviral Transduction Particles
- Hexadimethrine bromide

Method:

SW1353 cells were prepared and cultured in 96-well plates as described in section 2.1.2. For shRNA transfections, cells were trypsinized and re-seeded at approximately 50% confluency. MISSION® Lentiviral Transduction Particles for *trb1* (Clone IDs TRCN0000001535, TRCN0000001536, TRCN0000001537, TRCN0000001538, TRCN0000001539) were used to transduce SW1353 cells. Several hours prior to transduction, all media was removed from the SW1353 cells and this was replaced with 100

µl serum-containing DMEM:F12. Immediately prior to transduction, hexadimethrine bromide was added to the cells at a final concentration of 8 µg/ml. The appropriate amount of viral particles was then added at a suitable multiplicity of infection (MOI) (10 or 25), where the MOI is the number of lentiviral transducing particles per cell. The volume of lentiviral particles required for the desired MOI depends on the number of transducing units (TU) in the provided solution and is determined using the calculation ((No. of cells x M.O.I) / TU per mL reported). The cell-viral particle mix was then incubated at 37°C for 28 hours. The cells were serum starved for 20 hours prior to the addition of cytokines for a further 24 hours. Total RNA was isolated and reverse-transcribed as described in section 2.2.5.2. Expression of genes of interest was measured by real-time RT-PCR as described in section 2.2.5.3.1. Changes in gene-specific mRNA levels were calculated by comparison of expression levels with untransduced cells.

2.2.12 Genome-wide Arrays

2.2.12.1 Affymetrix Bovine GeneChip Array

The GeneChip[®] Bovine Genome Array allows the gene expression of over 23,000 bovine transcripts to be analysed.

Preparation of RNA:

A 14-day bovine nasal cartilage degradation assay was performed to generate RNA for the GeneChip[®] Bovine Genome Array. Bovine nasal cartilage was stimulated with control media ± IL-1 ± OSM ± IL-4 (added at day 7 of timecourse only) for 14 days as described in section 2.2.4.1. RNA was extracted from the bovine cartilage as described in section 2.2.5.1.

Data normalisation:

Data normalisation was performed by Dr Daniel Swan (Newcastle University). Affymetrix Bovine GeneChip CEL files were imported into GeneSpring 10 (Agilent). An experiment was created where the chips were normalised with MAS5 expression algorithm to produce Present, Marginal or Absent flag data. A list was derived where a probeset had to have a present or marginal signal in 3/4 samples in order to be included, reducing the probeset list to 15367 entities (reduced from 24128 entities). Data were then renormalised in an

independent experiment using GCRMA. A list of Affymetrix control probes (denoted by an AFFX_ prefix) was generated. From the MAS5 generated list, the Affymetrix control probesets were subtracted, leaving a final quality controlled list of probesets with 14928 entities for further analysis. Chips were then compared on a pairwise basis to generate lists of probesets for each comparison which had a fold change greater than 2.

2.2.12.2 Sentrix Human-6 Expression BeadChip

The Sentrix Human-6 Expression BeadChip contains 6 arrays on a single BeadChip, each with >46,000 probes derived from human genes in the National Center for Biotechnology Information (NCBI) Reference Sequence (RefSeq) and UniGene databases.

Preparation of RNA:

Human articular chondrocytes and SW1353 cells were cultured as described in 2.2.3. Following 24 hour cytokine stimulation, RNA was extracted as described in section 2.2.5.2.

Data normalisation:

Data normalisation was carried out by the Centre for Microarray Resources (Cambridge, UK). The selection of the data removed non-expressed genes or data that were too close to the background to be distinguished. Not removing these genes would add noise to the data.

The selection was done using the following criteria:

- Threshold for selection: detection p-value inferior to 0.01 for a measurement to be selected.
- The selection is applied so that a gene must be present on all the samples used.
- The set is then use to generate the raw data plot present in the archive.

Once the raw data plot has been generated, the data are re-selected using a less stringent parameter:

- the genes must be present on at least one of the array/samples analysed.

The data were then transformed using a variance stabilisation algorithm (Lin et al. 2008) and then normalised using quantile normalisation. All of this was performed using the lumi package (Du et al. 2008).

Analysis results:

Number of genes selected after normalisation: 15184 of the 48804, which represents 31% of the total genes.

2.2.13 DNA methylation analysis

Methylation is the most widely studied type of epigenetic modifications of DNA. The development of bisulphite sequencing PCR (BSP) by Frommer et al. (1992) greatly advanced the study of DNA methylation and is now one of the most frequently used techniques in the field. This method begins with the bisulphite treatment of genomic DNA (to convert unmethylated cytosine bases to uracil), followed by PCR amplification of the region of interest within the modified DNA. Conventional sequencing of the amplified product can then be carried out to specifically evaluate DNA methylation within a particular DNA sequence (Reed et al. 2009).

2.2.13.1 Isolation of DNA from Primary Cells

Method: DNA was isolated from primary cells using the PureLink™ Genomic DNA Kit according to the manufacturer's instructions. Briefly, cells were harvested in PBS and centrifuged at 250 x g for 5 minutes to pellet the cells. PBS was removed and the cells resuspended in 200 µl PBS. Proteinase K (20 µl) (>600 mAU/ml) was added, followed by 20 µl RNaseA and the sample was mixed well by vortexing and incubated at room temperature for 2 minutes. PureLink™ Genomic Lysis/Binding Buffer (200 µl) was added and the sample mixed by vortexing to obtain a homogenous solution and incubated at 55°C for 10 minutes to promote protein digestion. Ethanol (100%, 200 µl) was added to the lysate and vortexed for 5 seconds. The lysate was then added to a PureLink™ Spin Column and centrifuged at 10,000 x g for 1 minute at room temperature. The collection tube was discarded and the spin column placed into a clean PureLink™ collection tube. Wash Buffer 1 (500 µl) prepared with ethanol was added to the column and the column was centrifuged at room temperature at 10,000 x g for 1 minute. The column was placed into a clean PureLink™ collection tube and 500 µl Wash Buffer 2 prepared with ethanol was added.

The column was centrifuged at maximum speed for 3 minutes at room temperature. The column was then placed in a sterile 1.5 ml Eppendorf tube and 100 µl PureLink™ Genomic Elution Buffer was added to the column, which was then incubated at room temperature for 1 minute. To recover the genomic DNA, the column was centrifuged at maximum speed for 1.5 minutes at room temperature. The purified DNA was stored at -20°C until bisulphite conversion.

2.2.13.2 Primer design and optimisation

Bisulphite conversion of bovine nasal chondrocyte DNA: Total DNA was isolated as described in section 2.2.12.1. To provide DNA for primer optimisation, 1 µg aliquots of bovine nasal chondrocyte DNA were subject to bisulphite conversion using the Epiect® Bisulphite Kit according to manufacturer's instructions. Bisulphite reactions were prepared by combining 1 µg bovine nasal chondrocyte DNA, 85 µg bisulphite mix and 35 µg DNA protect buffer in a final volume of 140 µl. Bisulphite conversion was carried out using a PTC-200 DNA Engine Thermal Cycler (Bio-Rad). Cycling conditions were 99°C for 5 minutes, 60°C for 25 minutes, 99°C for 5 minutes, 60°C for 85 minutes, 99°C for 5 minutes and 60°C for 175 minutes. Clean up of bisulphite converted DNA was performed using Epiect® spin columns according to manufacturers instructions. Purified DNA was eluted in 20 µl dH₂O and stored at -20°C prior to analysis by PCR.

Primer design: Primers were designed to amplify a region of the bovine MMP-13 promoter containing 7 CpG sites. Primers were designed using the MethPrimer software (available at www.urogene.org/methprimer), which identifies suitable regions of DNA in a bisulphite converted sequence against which primers can be designed. All primer sequences are shown in Table 2.5.

Primer name	Sequence
Bovine MMP-13 Forward	TAGTTGTTTTTTTTGTAAAGGGGAAA
Bovine MMP-13 Reverse	AAACCAACCAAAAACCCTTAAAC
Pyrosequencing PCR bovine MMP-13 Forward	GAGGTTGTTATTTTGTAAAGA
Pyrosequencing PCR bovine MMP-13 Reverse	AACCAACCAAAAACCCTTA
Pyrosequencing sequencing primer 1	GTTGAAAGGAGAGAAGTTT
Pyrosequencing sequencing primer 2	TTGTTTGGGAAAAGATAG

Table 2.5 DNA methylation analysis primers.

Optimisation of cycling conditions: 6 identical 20 µl reactions were prepared by combining 2 µl TitaniumTM Taq buffer, 0.4 µl forward primer, 0.4 µl reverse primer, 0.4 µl Taq, 0.4 µl dNTPs (2.5 mM) and 1 µl bisulphite treated genomic DNA in a final reaction volume of 20 µl in dH₂O. Optimal annealing temperatures were determined using a TaKaRa PCR Thermal Cycler Dice (SANYO E&E Europe Ltd., Loughborough, UK). Cycling conditions were: 95°C for 1 minute, 40 cycles of [95°C for 15 seconds, 50-65°C gradient for 30 seconds, 68°C for 1 minute], 68°C for 7 minutes. A 5 µl aliquot of each reaction was run out on a 1.2% agarose gel to determine the optimal annealing temperature required to amplify the desired PCR product.

Once primer optimisation had been carried out, bovine nasal chondrocytes were grown to 80-90% confluency as described in section 2.2.3, serum-starved overnight and stimulated with DMEM ± IL-1 (1 ng/µl) ± OSM (10 ng/µl) ± IL-4 (20 ng/µl). Total DNA was isolated as in section 2.2.12.1 and bisulphite conversion of this DNA was carried out as in section 2.2.13.2.

2.2.13.3 Amplification and purification of PCR products

Bisulphite treatment of DNA from bovine DNA: DNA was obtained from and extracted as described in section 2.2.2.1. Approximately 1 µl DNA was subject to bisulphite conversion as described in section 2.2.13.2.

PCR analysis: PCR was performed using bovine MMP-13 primers (Table 2.5) to amplify a 369 base pair (bp) region of the MMP-13 promoter. The PCR was carried as described in section 2.2.13.2. Optimised PCR cycling conditions for bovine MMP-13 primers were: 95°C for 1 minute, 40 cycles of [95°C for 15 seconds, 65°C for 30 seconds, 68°C for 1 minute], 68°C for 7 minutes.

2.2.13.4 Cloning of PCR products

Reagents:

- Luria broth (LB) containing 10 g NaCl, 10 g tryptone and 5 g yeast extract per litre dH₂O.
- LB Agar containing 10 g NaCl, 10 g tryptone, 5 g yeast extract and 15 g agar per litre dH₂O.

Reagents were autoclaved prior to use and ampicillin added at a final concentration of 100 µg/ml in filter-sterilised water for selection. Standard aseptic technique was used throughout the cloning procedure.

Method:

Ligation and transformation: Purified PCR products were cloned using the TOPO TA cloning[®] kit and Dual Promoter pCR[®]II-TOPO[®] vector according to manufacturer's instructions. Briefly, ligation reactions were prepared by combining 4 µl PCR product, 1 µl salt solution and 0.5 µl pCR[®]II-TOPO[®] in a final volume of 6 µl in dH₂O. Ligations were incubated at room temp for 20 minutes then placed on ice and 2 µl of the reaction added to 25 µl Mach1TM-T1[®] chemically competent *E.coli*. Reactions were incubated on ice for 10 minutes prior to transformation by heat shock at 42°C for 30 seconds followed by immediate removal to ice. A 250 µl aliquot of SOC medium (Invitrogen) was added to each vial and cultures were shaken (200 rpm) at 37°C for 1 hour. A 100 µl aliquot of each transformation was spread onto a pre-warmed agar plate containing 40 µg/ml 5-bromo-4-chloro-3-indolyl-b-D-galactopyranoside (X-GAL) in dimethylformamide (DMF) and 100 µg/ml ampicillin to allow blue/white screening. Plates were incubated at 37°C for 16 hours for colonies to develop.

Preparation of overnight cultures: White colonies were selected and added to 5 ml LB containing 100 µg/ml ampicillin. Cultures were shaken at 200 rpm at 37°C for 16 hours in an orbital shaker.

Quick MiniPreps of plasmid DNA: A 1.5 ml aliquot of culture was transferred to a 1.5 ml Eppendorf tube and centrifuged at 20 seconds at 9500 x g. The supernatant was discarded and cells resuspended in 100 µl Buffer P1 (Qiagen) by vortexing. Subsequently, 200 µl Buffer P2 (Qiagen) was added to cells and mixed thoroughly by inverting 10 times. A 150 µl aliquot of Buffer P3 (Qiagen) was then added and mixed immediately by inverting 10 times. Lysates were centrifuged for 3 minutes at 9500 x g and the supernatant removed to a new Eppendorf tube containing 1 ml 100% ethanol. Samples were vortexed for 10 seconds to mix thoroughly and centrifuged for 10 minutes at 9500 x g. All ethanol was removed and pellets were air-dried before resuspension in 50 µl dH₂O.

Restriction digests: A 2 µl aliquot of each miniprep was digested using the restriction enzyme *EcoR*1. Plasmid DNA was combined with 5 U *EcoR*1 (0.5 µl), 1.5 µl 10x *EcoR*1 buffer and dH₂O in a final volume of 15 µl and incubated at 37°C for 1 hour. A 10 µl aliquot of each digest was electrophoresed on a 1.2% agarose gel, as described in section 2.2.13.6 to determine if it contained an insert of the correct size.

2.2.13.5 Analysis of DNA methylation

The inserts of numerous colonies were sequenced via the AP6 promoter until 20 unique clones from each treatment group were obtained. DNA methylation analysis was performed using BiQ analyzer software (available at <http://biq-analyzer.bioinf.mpiinf.mpg.de/>). Sequences were required to be 80% identical to the original sequence and have >90% C-T conversion (excluding CpG). Any potential sequence clones identified by the software were also removed to ensure only unique sequences were analysed.

2.2.13.6 Agarose Gel Electrophoresis

Reagents:

- 1 x Tris-acetate-ethylenediamine tetraacetic acid (TAE) containing 0.04 M Tris (pH 8), 5.7% (v/v) glacial acetic acid and 0.1 mM EDTA.

- Loading buffer containing Tris 0.125 M (pH 6.8), 2% (w/v) SDS, 10% (v/v) glycerol and 0.001% (w/v) bromophenol blue.

Method:

Agarose gels were prepared at 1.2% (w/v) by dissolving the required amount of agarose in 1 x TAE buffer through boiling. Ethidium bromide (3,8-Diamino-5-ethyl-6-phenylphenanthridinium bromide) solution was added to cooled agarose at a final concentration of 0.2 µg/ml. Gels were poured, allowed to set and the required amount of DNA loaded in loading buffer. Bands were separated at 100 V for approximately 40 minutes and visualised on a ChemiGenius II Biolumager (Syngene, Cambridge, UK) using GeneRuler™ 1 kb DNA ladder to assess product size.

2.2.13.7 Pyrosequencing

Pyrosequencing was recently adapted to study DNA methylation and is now an alternative to conventional bisulphite-sequencing PCR (BSP). This technique also requires the bisulphite treatment of genomic DNA and PCR amplification of the target sequence, but this is followed by pyrosequencing rather than conventional sequencing methods (Reed et al 2009). Pyrosequencing is a sequencing-by-synthesis method that quantitatively monitors the real-time incorporation of nucleotides through the enzymatic conversion of released pyrophosphate into a proportional light signal (Tost and Gut 2007). Incorporation of a cytosine is indicative of a methylated residue, whereas the incorporation of a thymine indicates an originally unmethylated cytosine. Therefore, the methylation status of a CpG site can be determined from the ratio of T and C.

Method:

2.2.13.7.1 Assay design and optimisation

Bisulphite conversion of bovine nasal chondrocyte DNA: Bovine nasal chondrocytes were grown to 80-90% confluency as described in section 2.2.3, serum-starved overnight and stimulated with DMEM ± IL-1 (1 ng/µl) ± OSM (10 ng/µl) ± IL-4 (20 ng/µl). Total DNA was isolated as in section 2.2.12.1 and bisulphite conversion of this DNA was carried out as in section 2.2.13.2.

Primer design: PCR primers and sequencing primers were designed using Pyrosequencing™ Assay Design Software, which automatically designed both pyrosequencing PCR primers and pyrosequencing sequencing primers. All primer sequences are shown in table 2.4. The PCR primers were designed to amplify the region of the bovine MMP-13 promoter containing 6 of the 7 CpG sites analysed in section 2.2.13.5. The reverse primer was biotinylated to facilitate immobilization onto streptavidin-coated beads and to render the PCR product single stranded.

Positive and negative controls: Positive and negative controls were picked from clones generated in section 2.2.13.4. The positive control was a clone in which all 7 CpG sites were methylated and the negative control was a clone in which all 7 CpG sites were unmethylated.

Optimisation of cycling conditions: Primer cycling condition optimisation was carried out as in section 2.2.13.2. Control bisulphite-treated bovine DNA was used for primer optimisation. Optimised PCR cycling conditions for pyrosequencing PCR bovine MMP-13 primers were: 95°C for 1 minute, 40 cycles of [95°C for 15 seconds, 65°C for 30 seconds, 68°C for 1 minute], 68°C for 7 minutes. A 5 µl aliquot of each reaction was run out on a 1.2% agarose gel to determine the optimal annealing temperature required to amplify the desired PCR product.

2.2.12.7.2 Amplification and purification of PCR products

PCR analysis: PCR was performed using pyrosequencing PCR bovine MMP-13 primers to amplify a 240 bp region of the bovine MMP-13 promoter. The PCR was carried as described in section 2.2.13.2. Optimised PCR cycling conditions for MMP-13 primers were: 95°C for 1 minute, 40 cycles of [95°C for 15 seconds, 65°C for 30 seconds, 68°C for 1 minute], 68°C for 7 minutes.

2.2.13.7.3 Pyrosequencing

Reagents:

- Binding buffer: 10 mM Tris, 2 M NaCl, 1 mM EDTA, 0.1% (v/v) Tween 20, pH 7.6
- Denaturing Solution: 0.2 M NaOH

- Wash buffer: 10 mM Tris, pH 7.6
- Annealing buffer: 20 mM Tris, 2 mM Mg-acetate, pH 7.6
- Streptavidin-coated sepharose beads

Preparation of single-stranded DNA template: The single stranded DNA template was prepared using immobilisation on streptavidin-coated sepharose beads. The following was added to individual wells of a 96-well PCR plate (binding mix): 10 μ l PCR product, 2 μ l streptavidin-coated sepharose beads, and 38 μ l binding buffer made up to a total volume of 80 μ l with dH₂O. The plate was sealed and vortexed for 5 minutes.

Next, 0.5 μ l sequencing primer (10 μ M) and 11.5 μ l annealing buffer was added to each well of a 96-well pyrosequencing plate (annealing mix).

A PyroMark Vacuum Prep Workstation (Qiagen) is a sample preparation terminal designed to batch process up to 96 DNA samples in parallel. The Vacuum Prep Workstation consists of a hand-held Vacuum Prep Tool and a Vacuum Prep Worktable, connected to a vacuum source, containing four solution troughs. The Vacuum Prep Tool consists of a hand-grip with 96 replaceable filter probes, which is connected to a vacuum source. The binding mix was aspirated from the wells of the PCR plate by placing the hand-grip block into the PCR plate resulting in the capture of the beads on the filter probes. The hand-grip filter tips were then immersed in three successive baths for 5 seconds each as follows: 70% (v/v) ethanol, denaturing buffer and wash buffer. At this point the vacuum was switched off and the hand-grip block immersed in the annealing mix of the pyrosequencing plate and gently agitated to release the beads. The pyrosequencing plate was then heated at 80°C for 2 minutes. The plate was then cooled to room temperature to allow annealing of the primers to the PCR product.

Pyrosequencing: The sequencing run was programmed into the pyrosequencer (PyroMark Q96 MD, Qiagen) using the Pyro Q-CpGTM software. The reagents (nucleotides, substrate and enzyme mix (Qiagen)) were dispensed into the appropriate wells of the cartridge according to the volume calculation of the software. The pyrosequencing plate and the reagent cartridges were placed in the pyrosequencer and the software run.

Analysis of methylation: Analysis of methylation status was performed by the Pyro Q-CpG™ software.

2.2.14 Statistical analysis

The difference between sample group means was tested for statistical significance using ANOVA (analysis of variance) with a posthoc Bonferroni multiple comparison test. For hydroxyproline and collagenase assay data, values are given as mean and standard deviation (S.D.), where * $p \leq 0.05$, ** $p \leq 0.01$ and *** $p \leq 0.001$. Real-time RT-PCR data were normalised against 18S rRNA, then plotted as the fold induction of the target gene expression over control levels. Levels of statistical significance are shown as * $p \leq 0.05$, ** $p \leq 0.01$ and *** $p \leq 0.001$. For clarity, only selected comparisons are presented in some figures.

Chapter 3: Investigations into the effects of IL-4 on IL-1+OSM-induced cartilage collagen release and collagenase expression in chondrocytes and cartilage

3.1 Introduction

Arthritic disease is characterised by the irreversible loss of the cartilage matrix resulting in the loss of normal joint function and disability. Degradation of proteoglycan is rapid yet reversible (Dingle et al. 1987); collagen loss occurs more slowly but this loss irreversibly compromises the structural integrity of the tissue (Jubb and Fell 1980). Cartilage collagen loss is therefore regarded as being the key control point in cartilage breakdown.

The bovine nasal cartilage explant culture model has provided a valuable system for studying collagen loss and identifying factors that contribute to the breakdown of the tissue (Cawston et al. 1995). It has also facilitated the investigation of chondroprotective agents such as IL-4 and IL-13 (Cawston et al. 1996; Cleaver et al. 2001). Addition of the pro-inflammatory cytokine combination of IL-1 and OSM to bovine nasal cartilage induces collagen release through the increase in synthesis of collagenases. In 1996, Cawston et al. reported that IL-4 acted as a protective factor by specifically blocking the release of collagen from bovine nasal cartilage stimulated to resorb with IL-1+OSM, preventing pro-inflammatory cytokine-induced cartilage breakdown. Subsequent data from the department have indicated that IL-4 mediates its protective effect by reducing the levels of active collagenase and that this was most likely due to a reduction in MMP-13 expression (Pyle 2003). Furthermore, these studies demonstrated that MMP-1 expression was seemingly unaffected by IL-4 in stimulated cartilage. These key observations, firstly that IL-4 was able to block pro-inflammatory cytokine-induced collagen release and secondly that IL-4 differentially regulated MMP-1 and MMP-13, formed the basis of this PhD project.

The bovine nasal cartilage model has been used to investigate the chondroprotective effect of IL-4 on cartilage as opposed to a human cartilage model because bovine tissue is conveniently available in large quantities. Human articular cartilage is very difficult to obtain in amounts large enough for such experiments. Resorption of human articular cartilage in explant culture treated with IL-1 and OSM is variable with only approximately 50% of samples responding with the release of collagen and even in those samples the levels of collagen release are low (Cawston et al. 1998). The reasons for this low response are currently unclear. However, the lack of response in terms of collagen release may be explained by the fact that the majority of human articular cartilage samples are from elderly patients, which are suspected to have low numbers of chondrocytes. Whilst the levels of collagen release from the bovine nasal cartilage model can also be variable, the majority of samples release typically $\geq 60\%$ of their collagen.

Pro-inflammatory cytokines are well understood to stimulate the production of MMPs, including the collagenases. IL-1 is a potent inducer of MMP-13 expression in chondrocytes (Borden et al. 1996). The combination of IL-1 and OSM has been shown to synergistically promote the expression of MMP-1 mRNA in human articular chondrocytes (Cawston et al. 1998). It is also known that IL-1+OSM-induced collagen degradation in bovine nasal cartilage is MMP-dependent (Cawston et al. 1995). Given that IL-4 acts as a protective factor in the bovine nasal cartilage model by preventing IL-1+OSM-induced collagen breakdown, this chapter aims to elucidate the effect of IL-4 on collagenase expression at the transcriptional level. Previous studies (Cleaver 2000, Pyle 2003) addressed the effect of IL-4 on IL-1+OSM-induced MMP-1 and MMP-13 mRNA expression by Northern blot. IL-4 was shown to increase IL-1+OSM-induced MMP-1 expression in bovine nasal chondrocytes, human articular chondrocytes and SW1353 cells and decrease MMP-13 expression in human articular chondrocytes and SW1353 cells. Data regarding the effect of IL-4 on IL-1+OSM-induced MMP-13 expression in bovine nasal chondrocytes was inconclusive (Pyle 2003). This chapter will address the effect of IL-4 on IL-1+OSM-induced MMP-1 and MMP-13 mRNA expression using the more sensitive technique of real-time RT-PCR.

The aims of this chapter were to:

- Confirm the original findings of Cawston et al. (1996) demonstrating that IL-4 was able to block IL-1+OSM-induced collagen release in the bovine nasal cartilage model.
- Determine the effect of delayed IL-4 addition to bovine nasal cartilage stimulated to resorb with IL-1+OSM.
- Investigate the effect of IL-4 on IL-1+OSM-induced collagenase gene expression in bovine nasal chondrocytes, human articular chondrocytes and SW1353 cells.
- Profile collagenase expression in resorbing bovine nasal cartilage.

3.2 Results

3.2.1 The effect of IL-4 on the release of collagen from bovine cartilage treated with IL-1±OSM.

Experiments were performed using bovine nasal cartilage in culture to recapitulate the findings of Cawston et al. (1996) that originally showed IL-4 specifically blocked collagen release in this model. Cartilage stimulated with IL-1 alone resulted in 14.8% total collagen release over 14 days (Figure 3.1). In response to the pro-inflammatory combination of IL-1+OSM, 78.3% of the collagen was released. The addition of IL-4 to IL-1+OSM significantly inhibited collagen release, reducing the total collagen release to 3.7 %. These data demonstrate that the previous results of Cawston et al. (1996) are indeed reproducible.

3.2.2 The effect of delayed addition of IL-4 on IL-1+OSM-induced collagen and active collagenase levels in bovine nasal cartilage.

Previous work in the department (Pyle 2003) has shown that IL-4 does not need to be present for the full 14 days of culture in order to protect against IL-1+OSM-induced cartilage degradation. Experiments demonstrated that addition of IL-4 as late as day 8 of culture still significantly inhibited IL-1+OSM (0.2 and 2 ng/ml respectively)-induced cartilage degradation. The concentrations of IL-1 and OSM were reduced from the normal 1 and 10 ng/ml, respectively, to allow resorption to proceed at a slower rate. This

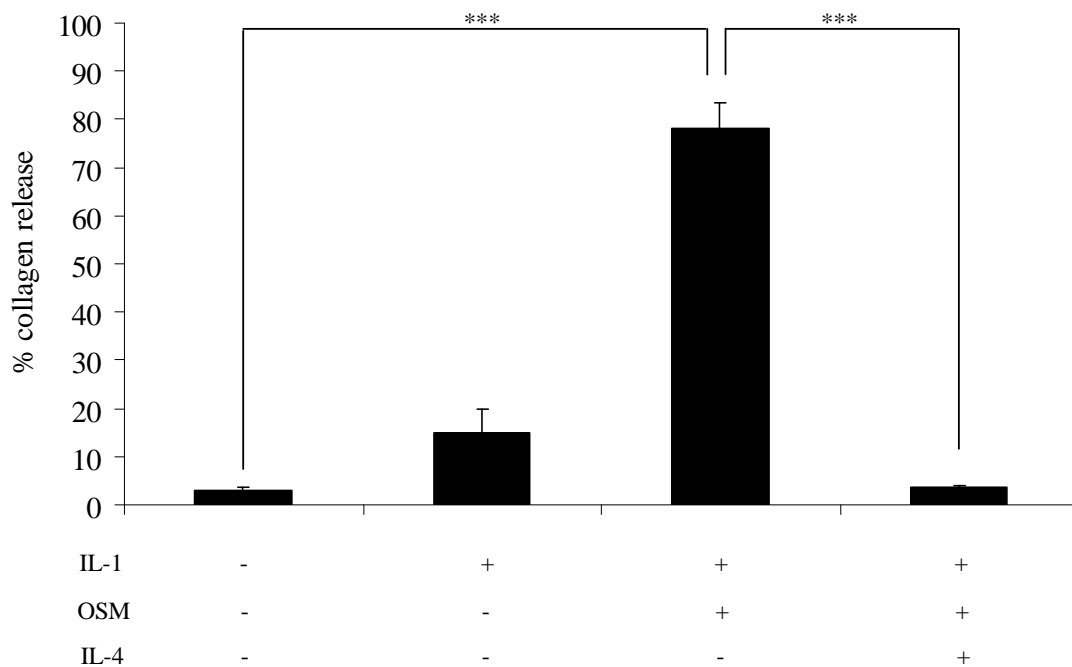


Figure 3.1 The effect of IL-4 on the release of collagen from the bovine nasal cartilage model treated with IL-1±OSM. Bovine nasal cartilage chips were cultured in medium + IL-1 (1 ng/ml) ± OSM (10 ng/ml) ± IL-4 (20 ng/ml) for 14 days. At day 7, medium was removed and replenished with identical cytokines. Media were harvested at days 7 and 14 and cartilage was harvested at day 14. As a measure of collagen release, the levels of hydroxyproline released into the media were assayed as described in section 2.2.4.4. The cumulative levels (day 7 + day 14) of hydroxyproline released in the medium were expressed as a % of the total collagen. Values are the mean ± standard deviation (n=4). *** = $p \leq 0.001$. This experiment is representative of three separate cartilages.

experiment aimed to confirm the findings that delayed IL-4 addition could still protect against collagen release, but with IL-1 and OSM used at the standard concentrations of 1 and 10 ng/ml, respectively, in order to enable greater overall % collagen release and to standardise experiments. In this experiment, IL-1+OSM (1 and 10 ng/ml respectively) stimulated a 53% collagen release (Figure 3.2a). The levels of collagen release induced by IL-1+OSM is known to vary between experiments. Tests to determine if this is due to a loss of cytokine activity have shown that this is not the reason behind reduced levels of collagen release in certain experiments (data not shown). It is thought that these differences can be explained by the cartilage explant model being a variable biological system and susceptibility to resorption is bound to vary between different cartilage samples, just as susceptibility to OA differs between different humans. The addition of IL-4 to IL-1+OSM from day 0 of the timecourse reduced the collagen release to 1%. Delayed addition of IL-4 to IL-1+OSM until day 7 still dramatically reduced collagen release (2%) (Figure 3.2a). Active collagenase (Figure 3.2b) was reduced to levels that were undetectable by the collagenase assay following addition of IL-4 at both day 0 and day 7 of the timecourse.

3.2.3 The effect of IL-4 on IL-1+OSM-induced gene expression of MMP-1 and MMP-13 in bovine chondrocytes.

This was the first opportunity to look at gene expression in bovine chondrocytes using the sensitive technique of real-time RT-PCR. Whilst previous studies have looked at MMP mRNA expression in bovine chondrocytes, gene expression in these studies was analysed using Northern blots (Pyle 2003). Both MMP-1 and MMP-13 mRNA were synergistically induced by IL-1+OSM when compared with IL-1 alone (Figure 3.3). Addition of IL-4 to the pro-inflammatory combination of IL-1+OSM was able to substantially block the induction of MMP-13 mRNA (Figure 3.3b), whilst this addition of IL-4 to IL-1+OSM had no significant effect on MMP-1 mRNA levels (Figure 3.3a).

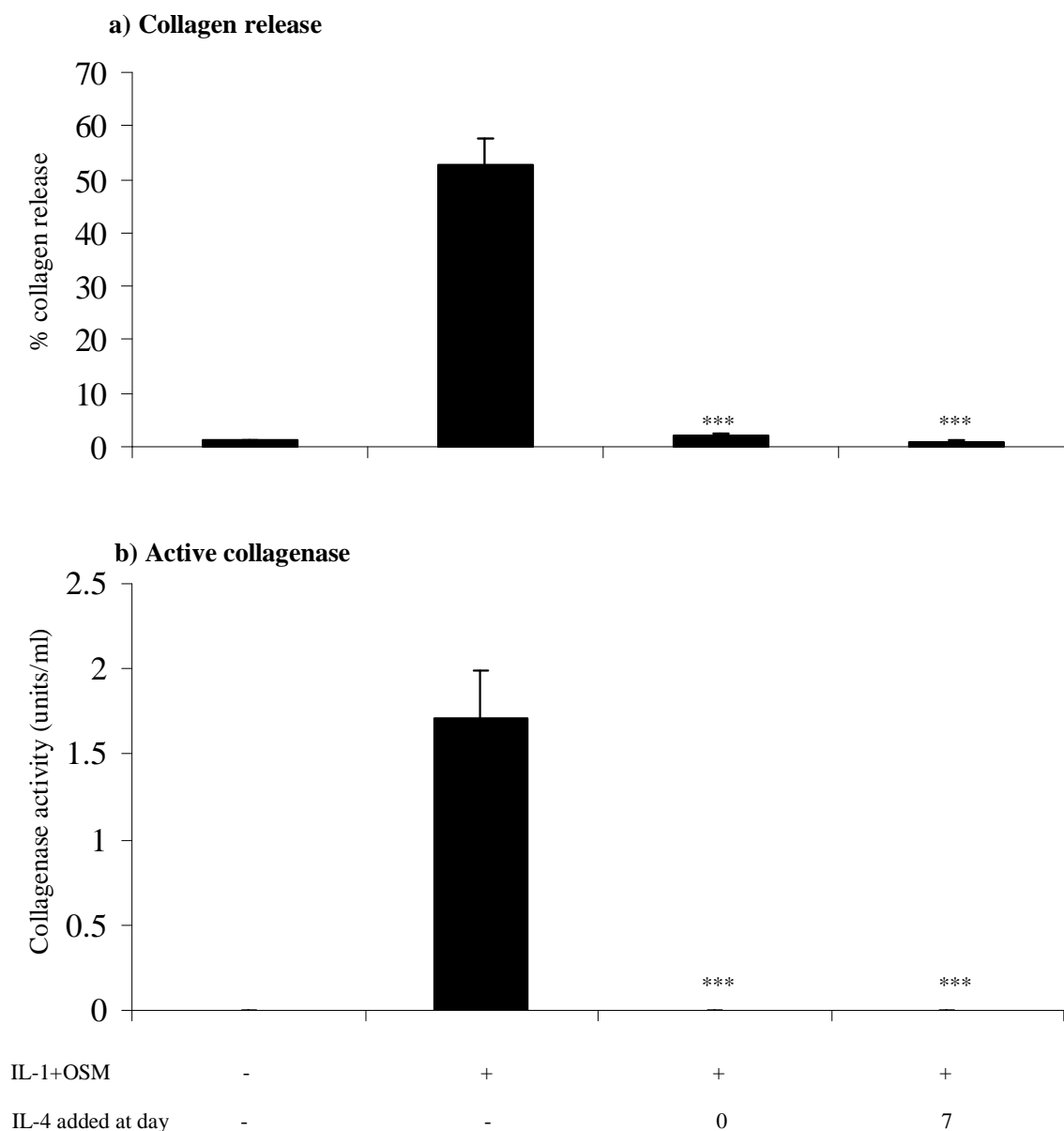


Figure 3.2 The effect of delayed addition of IL-4 on IL-1+OSM-induced collagen and active collagenase levels in bovine nasal cartilage. Bovine nasal cartilage chips were cultured in medium + IL-1 (1 ng/ml) + OSM (10 ng/ml) ± IL-4 (20 ng/ml, added at day 0 or day 7) for 14 days. At day 7, medium was removed and replenished. Media were harvested at days 7 and 14 and cartilage was harvested at day 14. As a measure of collagen release, the levels of hydroxyproline released into the media were assayed as described in section 2.2.4.4. The cumulative levels (day 7 + day 14) of hydroxyproline released in the medium were expressed as a % of the total collagen. Day 14 medium was assayed for active collagenase activity as described in section 2.2.4.5. Values are the mean ± standard deviation (n=4). *** = $p \leq 0.001$ compared to IL-1+OSM in the absence of IL-4. This experiment was performed three times with tissue from three different animals. The results shown are representative of all three experiments.

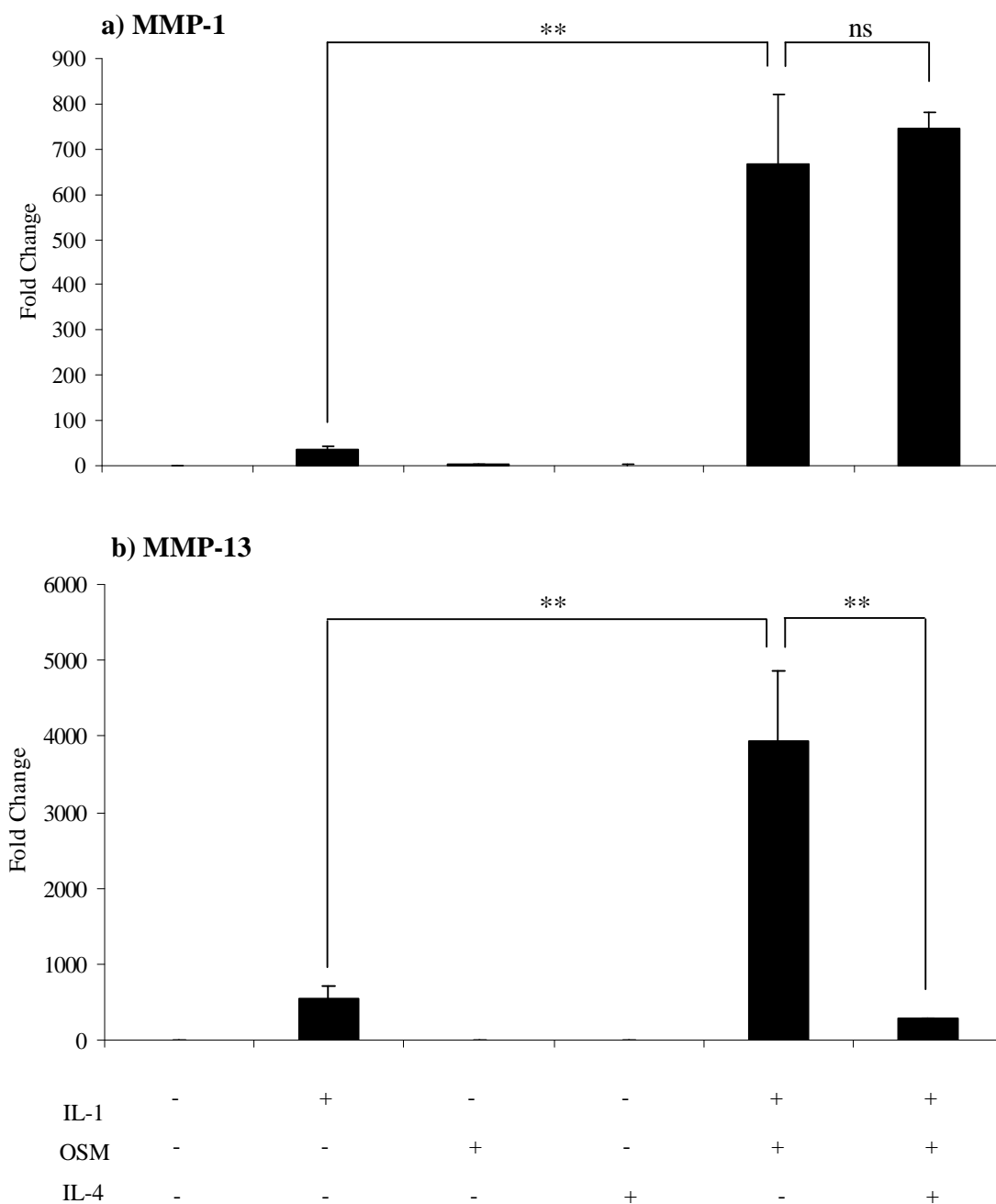


Figure 3.3 The effect of IL-4 on IL-1+OSM-induced gene expression of MMP-1 and MMP-13 in bovine nasal chondrocytes. Bovine nasal chondrocytes were stimulated for 24 hours with medium \pm IL-1 (1 ng/ml) \pm OSM (10 ng/ml) \pm IL-4 (20 ng/ml). Following treatment, total RNA was isolated from cells, reverse transcribed and the cDNA was used in real-time RT-PCR reaction assays, as described in section 2.2.5, to examine MMP-1 and MMP-13 gene expression. Data are presented as fold induction relative to the basal expression and represent mean \pm SEM (n=4), and are representative of four independent experiments. ** = $p \leq 0.01$; ns = not significant.

3.2.4 The effect of IL-4 on IL-1+OSM-induced gene expression of MMP-1 and MMP-13 in human articular chondrocytes and SW1353 cells.

The induction of MMP-1 and MMP-13 mRNA in both human articular chondrocytes and SW1353 by IL-1+OSM (Figure 3.4) and particularly the synergy observed, was not as strong as that observed in bovine chondrocytes (Figures 3.2 and 3.3). Consequently, the inhibition of MMP-13 by IL-4 in both human cell types (Figure 3.4) was not as complete as that observed in bovine nasal chondrocytes (Figure 3.3). Whilst the inhibition of MMP-13 in SW1353 cells was not significant when compared with IL-1+OSM-treated cells due to the large standard error, the inhibition of MMP-13 by IL-4 in human articular chondrocytes was significant. The effect of IL-4 on IL-1+OSM-induced MMP-1 expression in human articular chondrocytes and SW1353 cells was consistent with the results observed in bovine chondrocytes, where the addition of IL-4 to IL-1+OSM had no significant effect on MMP-1 mRNA expression.

3.2.5 The effect of different concentrations of IL-4 on MMP-1 and MMP-13 mRNA expression in bovine chondrocytes.

A titration of IL-4 between 20 and 0.02 ng/ml was performed in bovine chondrocytes to determine the concentration dependence for the effects of IL-4 on MMP-13 repression. The data show that the repression of MMP-13 by IL-4 was less complete at decreasing concentrations of IL-4 (Figure 3.5b). Concentrations below 2 ng/ml of IL-4 were unable to significantly repress IL-1+OSM-induced MMP-13 expression. As observed in previous experiments, the effect of IL-4 on IL-1+OSM-induced MMP-1 expression was generally insignificant. However, IL-4 is often seen to slightly increase IL-1+OSM-induced MMP-1 mRNA expression, although this increase is less frequently significant. Figure 3.5a shows a concentration-dependent decrease in MMP-1 expression with decreasing concentrations of IL-4, although none of these decreases were statistically significant.

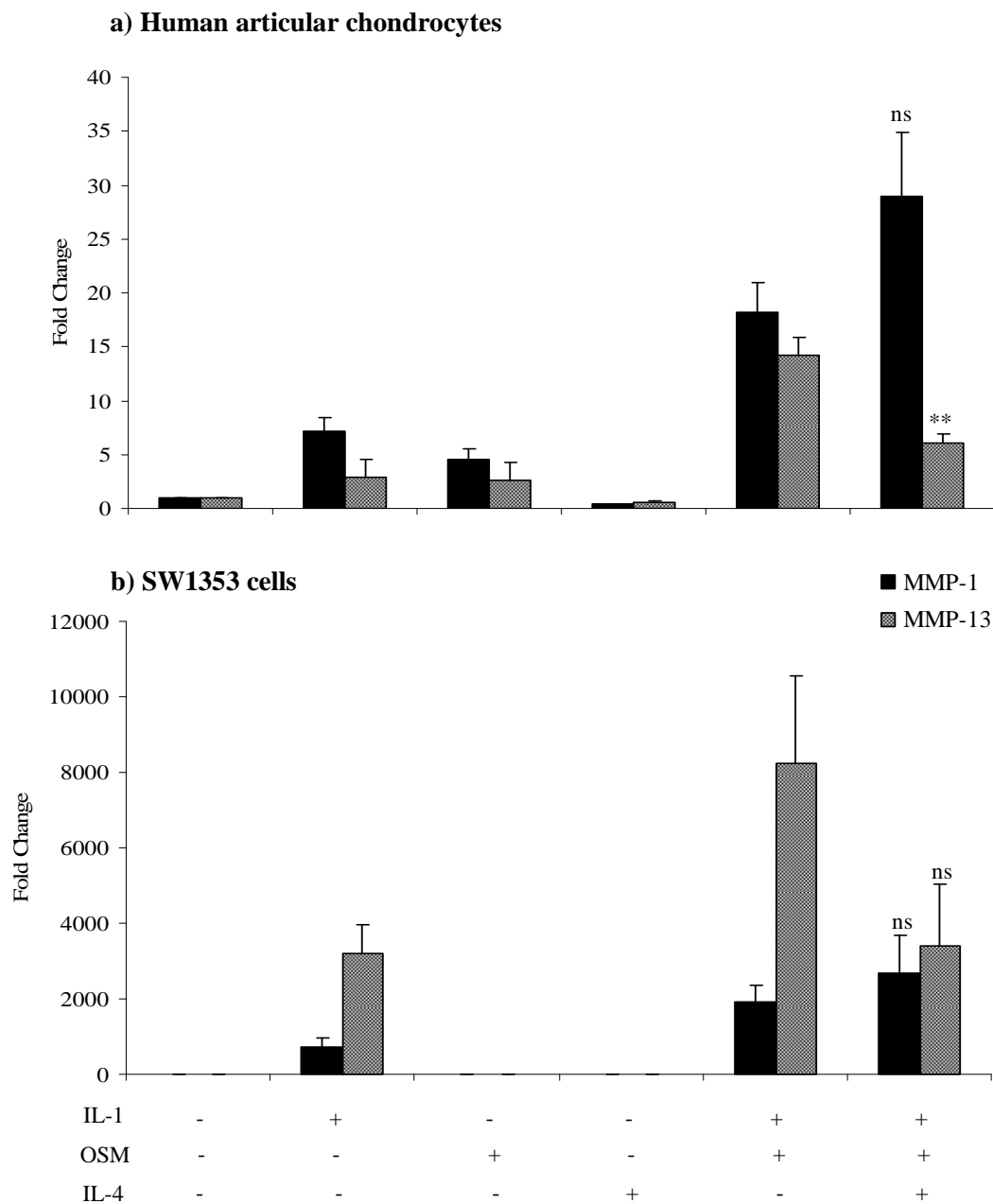


Figure 3.4 The effect of IL-4 on IL-1+OSM-induced gene expression of MMP-1 and MMP-13 in human articular chondrocytes and SW1353 cells. Human articular chondrocytes were stimulated for 24 hours with medium \pm IL-1 (0.02 ng/ml) \pm OSM (10 ng/ml) \pm IL-4 (20 ng/ml). SW1353 were stimulated for 24 hours with medium \pm IL-1 (0.5 ng/ml) \pm OSM (10 ng/ml) \pm IL-4 (20 ng/ml). Following treatment, total RNA was isolated from cells, reverse transcribed and the cDNA was used in real-time RT-PCR reaction assays, as described in section 2.2.5, to examine MMP-1 and MMP-13 gene expression. Data are presented as fold induction relative to the basal expression and represent mean \pm SEM (n=4) and are representative of two independent experiments. *** = $p \leq 0.001$; ns = not significant for IL-1+OSM vs IL-1+OSM+IL-4.

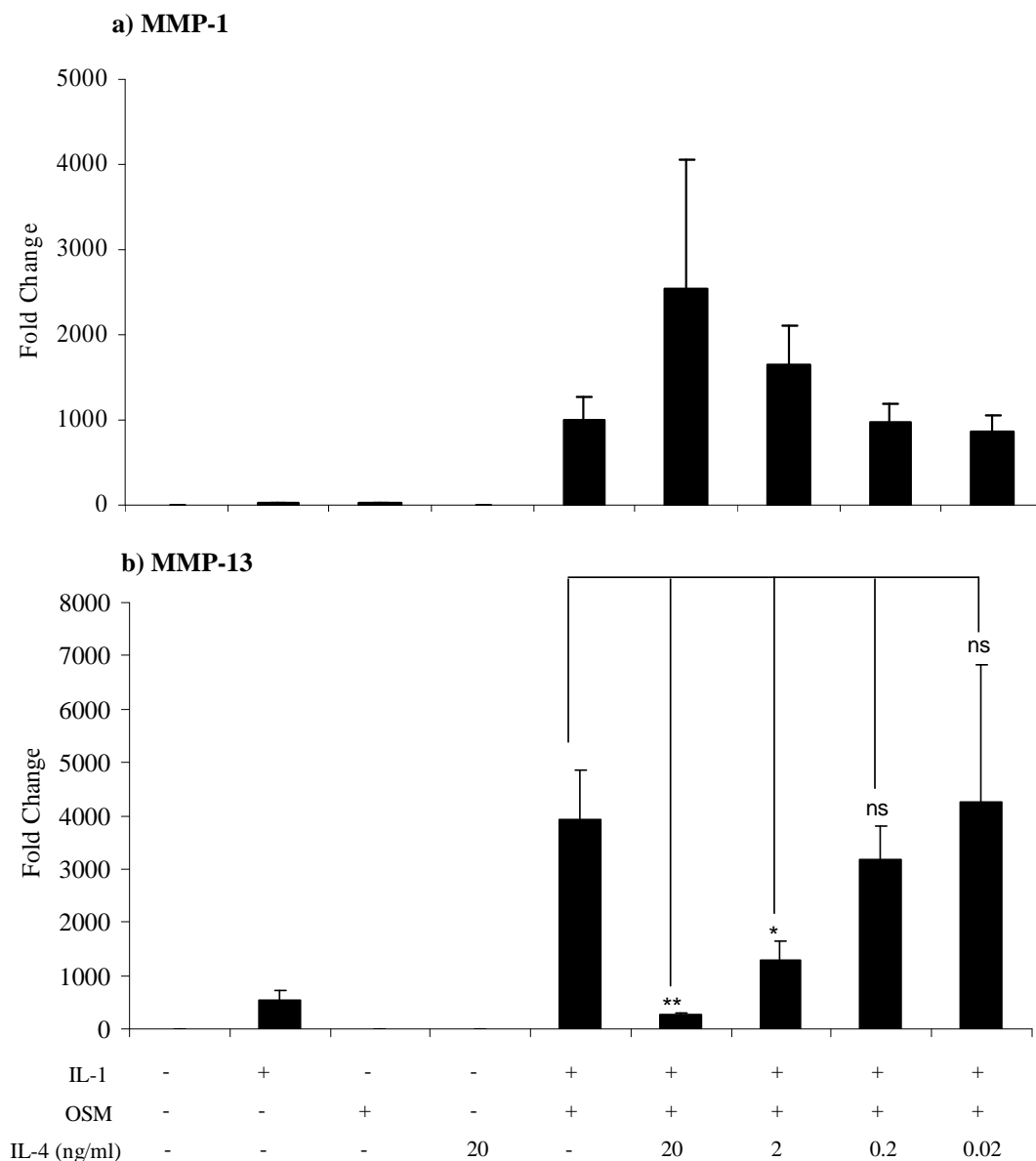


Figure 3.5 The effect of different concentrations of IL-4 on MMP-1 and MMP-13 mRNA expression in bovine nasal chondrocytes. Bovine nasal chondrocytes were stimulated for 24 hours with medium \pm IL-1 (1 ng/ml) \pm OSM (10 ng/ml) \pm IL-4 (0.02 - 20 ng/ml). Following treatment, total RNA was isolated from cells, reverse transcribed and the cDNA was used in real-time RT-PCR reaction assays, as described in section 2.2.5, to examine MMP-13 gene expression. Data are presented as fold induction relative to the basal expression and represent mean \pm SEM (n=4). ** = $p \leq 0.01$; * = $p \leq 0.05$; ns = not significant.

3.2.6 Profiling the effect of IL-4 on collagenase gene expression and collagenolysis in resorbing cartilage.

Experiments performed in monolayer bovine chondrocytes have shown that IL-4 blocks IL-1+OSM-induced MMP-13 expression, but not MMP-1 expression. To confirm this, MMP expression was examined in the bovine nasal cartilage explant culture system, a more biologically relevant model. The expression and regulation of MMPs in response to pro-inflammatory cytokines in chondrocytes have been profiled in two previous studies (Koshy et al. 2002; Barksby et al. 2006). However, both these studies were restricted to examining gene expression in isolated chondrocyte monolayers. Work by (Milner et al. 2006) has enabled the profiling of gene expression of multiple MMPs in actively resorbing cartilage by real-time RT-PCR.

Figure 3.2 demonstrated that IL-4 does not need to be present for the full 14 days of culture in order to protect against IL-1+OSM-induced cartilage degradation. Previous work has demonstrated that addition of IL-4 as late as day 8 of culture still significantly inhibited IL-1+OSM-induced cartilage degradation. Experiments were performed to confirm these findings and to examine the effect of delayed addition of IL-4 on collagenase mRNA expression. Both MMP-1 and MMP-13 were markedly and rapidly induced by IL-1+OSM, as reported previously (Milner et al. 2006) (Figures 3.6a and 3.6b). With IL-4 present in the culture from day 0, MMP-13 gene expression was completely inhibited. After day 3, the expression of MMP-1 reaches a plateau and IL-4 appears to have no overall effect during the remainder of the culture period. Following addition of IL-4 at day 7 of culture, MMP-13 gene expression was immediately down-regulated. MMP-1 gene expression remained constant after addition of IL-4, with neither a significant increase nor decrease in expression levels. Procollagenases were first detected in the culture medium at day 3 (Figure 3.6e). However, active collagenase (Figure 3.6d) was not detected until day 10 of culture and collagenolysis (Figure 3.6c) was not detected until day 12 of culture. In the presence of IL-4, procollagenases were detected in the culture medium, although at reduced levels compared to IL-1+OSM culture medium. Despite the presence of procollagenases, active collagenases and collagenolysis were both completely inhibited.

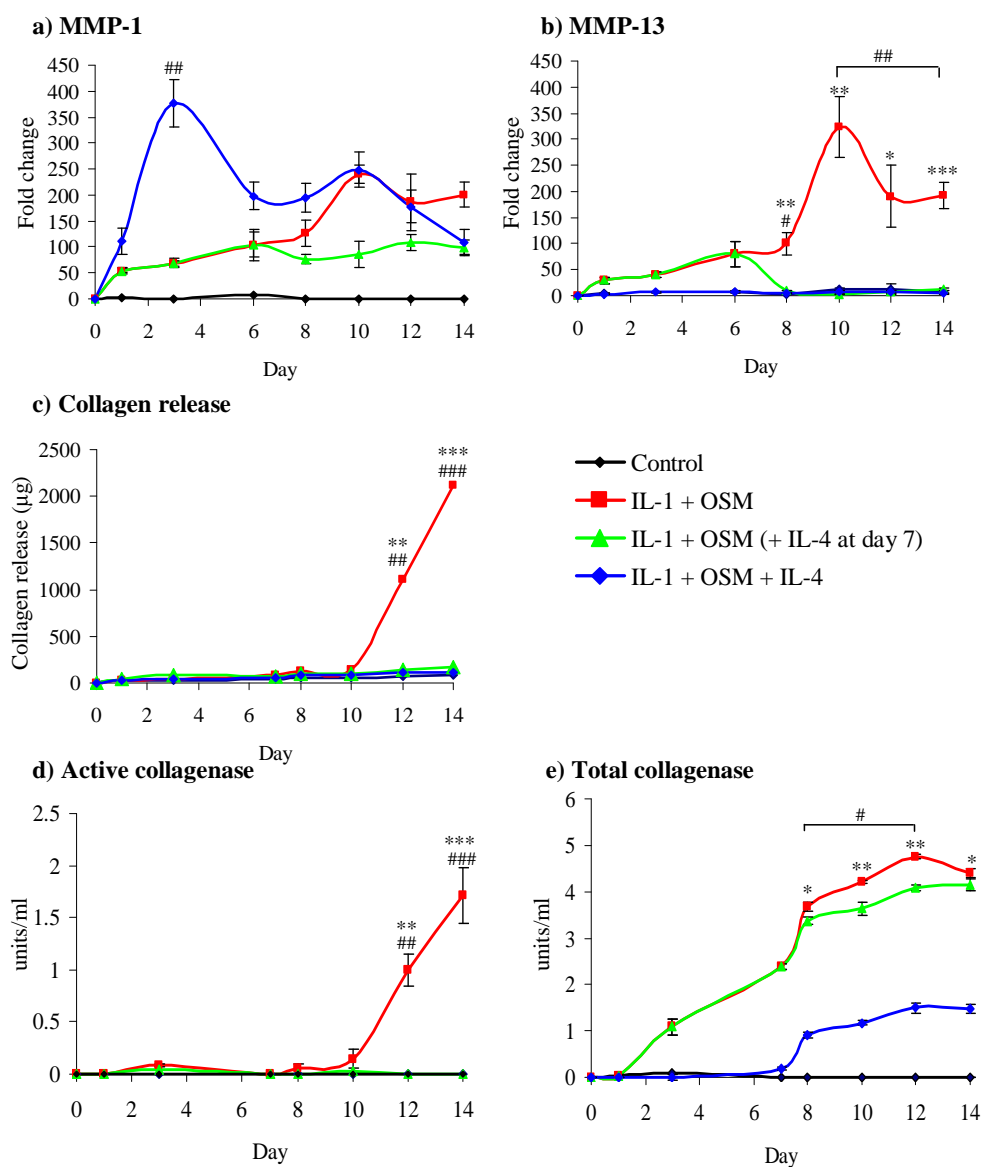


Figure 3.6 Profiling the effect of IL-4 on collagenase gene expression and collagenolysis in resorbing cartilage. Bovine nasal cartilage pieces were cultured in medium + IL-1 (1 ng/ml) + OSM (10 ng/ml) \pm IL-4 (20 ng/ml) for 14 days. At day 7, medium was removed and replenished with identical cytokines. Each time point and condition were performed in quadruplicate. RNA was extracted from the cartilage and collagenase gene expression determined by real-time RT-PCR as described in section 2.2.5. Data are presented as fold induction relative to the basal expression (a and b). As a measure of collagen release, the levels of hydroxyproline (OHPro) released into the media were assayed as described in section 2.2.4.3; cumulative OHPro release is shown (c). Levels of active collagenase were measured (d) and APMA was used to activate pro-collagenases to provide a measure of total collagenase activity (pro+active) (e) as in section 2.2.4.4. Values are the mean \pm standard error of the mean. *** = $p \leq 0.001$; ** = $p \leq 0.01$; * = $p \leq 0.05$ for IL-1+OSM vs IL-1+OSM(+IL-4 at day 7). ### = $p \leq 0.001$; ## = $p \leq 0.01$; # = $p \leq 0.05$ for IL-1+OSM vs IL-1+OSM+IL-4.

3.2.7 Profiling the effect of IL-4 on gelatinolytic activity in resorbing cartilage.

Previous work has shown IL-4 to have potent effects on the gelatinases MMP-2 and MMP-9. IL-4 did not appear to have a significant effect on either pro or active MMP-2 expression. Active MMP-9 however, was almost completely inhibited by the presence of IL-4 and proMMP-9 was barely detectable (data not shown). These observations appeared to support the findings of Milner et al. (2006) that MMP-9 is the predominant gelatinase in actively resorbing cartilage. Figure 3.7 shows the effect of delayed IL-4 addition on gelatinase activity. ProMMP-2 was expressed constitutively, regardless of cytokine treatment. In IL-1+OSM-treated cartilage, active MMP-2 was detectable from day 3 of culture and increased thereafter. Both pro and active MMP-2 were inhibited by IL-4, but this inhibition was not complete. ProMMP-9 was induced by IL-1+OSM and was detectable by day 3 of culture, however the addition of IL-4 strongly inhibited proMMP-9 (Figure 3.7b and 3.7c). Active MMP-9 was first detected at day 7 of culture in IL-1+OSM-treated cartilage (Figure 3.7a), but completely undetectable in IL-1+OSM+IL-4-treated cartilage (Figure 3.7b). The addition of IL-4 at day 7 of culture resulted in strong inhibition of active MMP-9 (Figure 3.7c), however this inhibition was slightly less complete than in cartilage in which IL-4 had been present from day 0 of culture. The data presented in Figure 3.7 support previous real-time RT-PCR data, which showed a complete inhibition of IL-1+OSM-induced MMP-9 mRNA by IL-4, but a lesser inhibition of IL-1+OSM-induced MMP-2 mRNA.

3.2.8 Profiling the effect of IL-4 on IL-1+OSM-induced non-collagenolytic MMP expression in resorbing cartilage.

MMP-3 is known to activate several proMMPs, including the collagenases proMMP-1 and 13 (Murphy et al. 1987; Knauper et al. 1996b). IL-4 downregulated IL-1+OSM-induced MMP-3 mRNA expression by day 8 of the bovine nasal cartilage timecourse, regardless of whether IL-4 was present from day 0 or day 7 (Figure 3.8). It has been suggested that MMP-14 is able to degrade type II collagen (Ohuchi et al. 1997), although to a much lesser degree than either MMP-1 or MMP-13. Figure 3.8 demonstrates that IL-4 does not significantly alter the expression of IL-1+OSM-induced MMP-14 expression at any point in the 14-day timecourse.

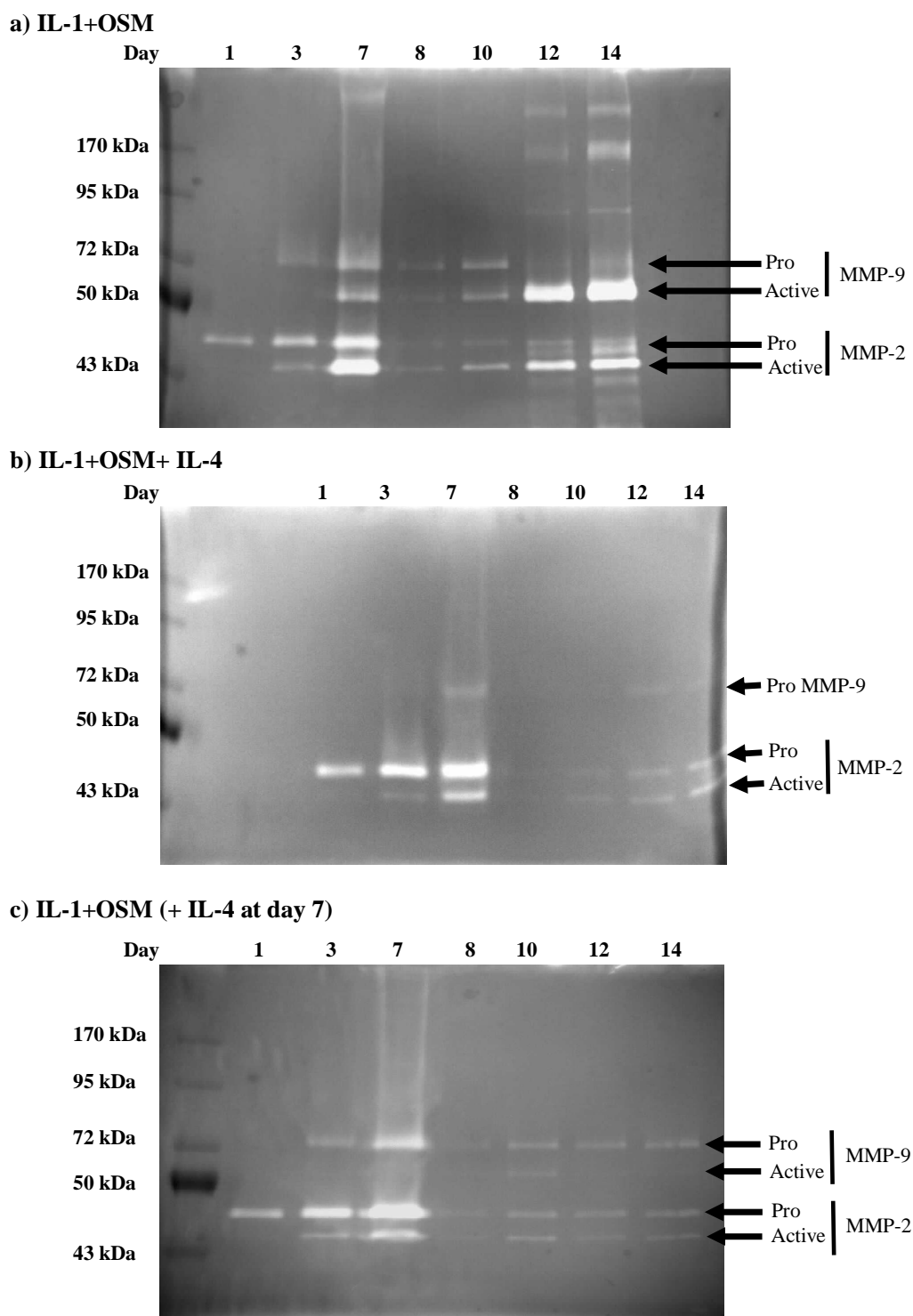
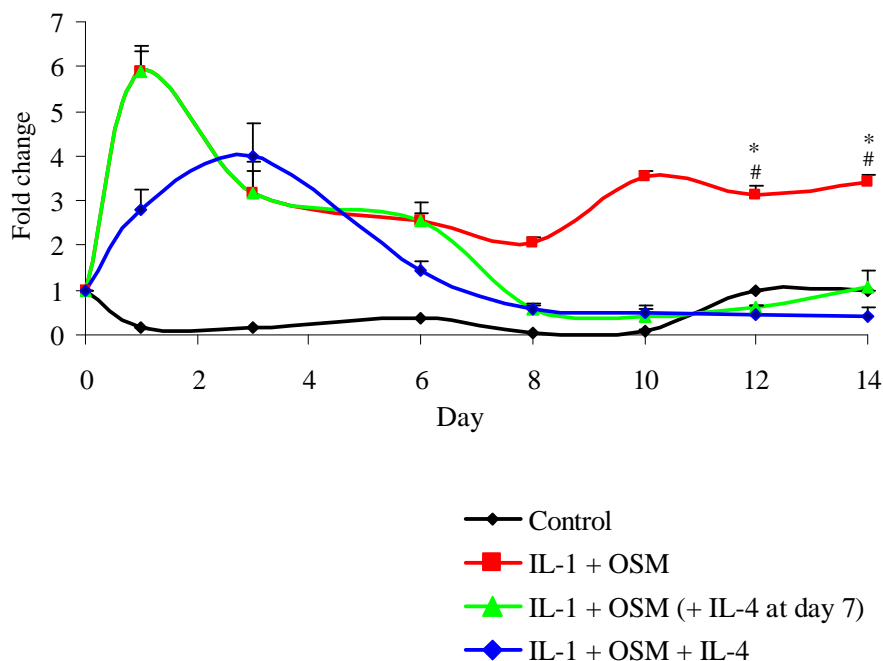


Figure 3.7 Profiling the effect of IL-4 on gelatinolytic activity in resorbing cartilage. Bovine nasal cartilage chips were cultured in medium + IL-1 (1 ng/ml) + OSM (10 ng/ml) \pm IL-4 (20 ng/ml) for 14 days. At day 7, medium was removed and replenished with identical cytokines. Cartilage and media were harvested at days 1, 3, 7, 8, 10, 12 and 14. Each time point and condition were performed in quadruplicate and representative data is shown. Gelatin zymography was performed as in section 2.2.4.2.

a) MMP-3



b) MMP-14

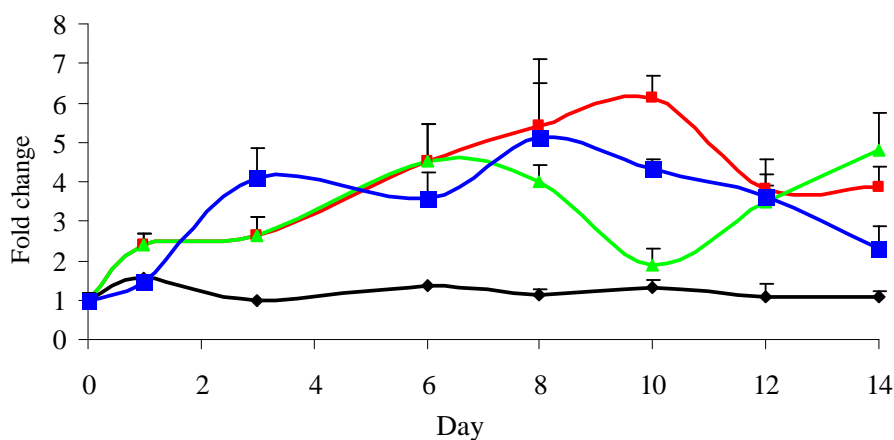


Figure 3.8 Profiling the effect of IL-4 on IL-1+OSM-induced non-collagenolytic MMP expression in resorbing cartilage. Bovine nasal cartilage pieces were cultured in medium + IL-1 (1 ng/ml) + OSM (10 ng/ml) \pm IL-4 (20 ng/ml) for 14 days. At day 7, medium was removed and replenished with identical cytokines. Each time point and condition were performed in quadruplicate. RNA was extracted from the cartilage and MMP-3 (a) and MMP-14 (b) gene expression were determined by real-time RT-PCR as described in section 2.2.5. Data are presented as fold induction relative to the basal expression and represent mean \pm SEM (n=4). ** = $p \leq 0.01$; * = $p \leq 0.05$ for IL-1+OSM vs IL-1+OSM(+IL-4 at day 7). ## = $p \leq 0.01$; # = $p \leq 0.05$ for IL-1+OSM vs IL-1+OSM+IL-4.

3.3 Discussion

Collagen breakdown is considered to be a key step in cartilage destruction. This chapter investigated the mechanism of IL-4 in the protection of bovine nasal cartilage from IL-1+OSM-induced degradation, specifically its effect on the two key collagenases, MMP-1 and MMP-13. Previous work demonstrated that bovine nasal cartilage stimulated with IL-1+OSM synergistically promoted cartilage collagen release, which was accompanied by a large increase in collagenolytic activity (Cawston et al. 1995). IL-13, a related anti-inflammatory cytokine, has likewise been shown to inhibit IL-1+OSM-induced collagen release from bovine nasal cartilage (Cleaver et al. 2001).

The first results in this chapter confirmed the findings of Cawston et al. (1996), demonstrating that IL-4 was able to act in a chondroprotective manner by blocking the release of collagen from bovine nasal cartilage stimulated with the pro-inflammatory combination of IL-1+OSM. IL-4 was shown to be equally chondroprotective when addition was delayed until day 7 of the 14 day timecourse. IL-1+OSM-induced active collagenase was completely inhibited by the addition of IL-4, both at day 0 and day 7. This demonstrates that the protective mechanism of action of IL-4 is extremely effective.

MMPs have been extensively studied in relation to the modulation of matrix function; between them they are able to degrade all ECM components. It is widely accepted that production of MMPs by chondrocytes and synovial fibroblasts is regulated by various cytokines and growth factors. It is therefore of no surprise that IL-4 has been implicated in the suppression of MMPs. IL-4 has been shown to downregulate MMP activity in a number of cell types involved in arthritis. Nemoto et al. (1997) demonstrated that IL-4 suppressed IL-1 stimulated MMP-3 protein and enzyme activity and was able to suppress IL-1-induced MMP-3 mRNA in human articular chondrocytes. As mentioned previously, collagen release is considered a key point in cartilage degradation. Of the three known collagenases, MMP-1 and MMP-13 are considered to be the most important in terms of the collagenolysis seen in the arthritides. MMP-13 is thought to be of greater importance in OA due to the fact that it preferentially degrades type II collagen (Knauper et al. 1996a) and because its expression is increased in OA (Tetlow et al. 2001). A key aim of this chapter

was to assess the effect of IL-4 on the regulation of MMP-1 and MMP-13 in both human and bovine chondrocytes. Due to the difficulties in obtaining sufficient quantities of human articular cartilage, it was necessary to use a human chondrocyte cell line in addition to primary human articular chondrocytes. The human chondrosarcoma SW1353 cell line is frequently used as a model for primary OA chondrocytes (Borden et al. 1996, Mengshol et al. 2000). IL-4 was found to inhibit IL-1+OSM-induced MMP-13 in bovine nasal chondrocytes and, albeit to a slightly lesser extent, in human articular chondrocytes and SW1353 cells (although this did not reach significance in the latter cell line). In contrast, IL-4 appeared to have no significant effect on IL-1+OSM-induced MMP-1 expression in any of the three cell types. If anything, a pattern of increasing MMP-1 expression in the presence of IL-4 was observed in all three cell types, although these increases were not always statistically significant. The apparent lack of effect of IL-4 on IL-1+OSM-induced MMP-1 expression compared with the potent inhibitory effect on IL-1+OSM-induced MMP-13 expression demonstrates differential regulation of the collagenases by IL-4. Indeed, this observation also further supports the observations of differential regulation of MMP-1 and -13 by IL-1+OSM (Litherland et al. 2008, 2010).

The inhibitory effect of IL-4 on MMP-13 has been documented by other groups. El Mabrouk et al. (2008) reported a strong inhibition of OSM-induced MMP-13 gene expression by IL-4 in chondrocytes. Doi et al. (2008) found that IL-4 was able to downregulate mechanical stress-induced MMP-13 in chondrocytes. There have been differing reports in the literature regarding the effect of IL-4 on MMP-1 expression. A study by Chizzolini et al. (2000) found that IL-4 specifically enhanced MMP-1 production by mononuclear phagocytes at various stages of differentiation with the exception of freshly isolated PBMC (peripheral blood mononuclear cells), in which IL-4 was found to inhibit MMP-1 activity. The type I IL-4 receptor consists of IL-4R α and γ c chain. Bonder et al. (1998) have already demonstrated that the culturing of monocytes in GM-CSF (granulocyte macrophage colony-stimulating factor) results in the loss of the γ c chain and that this loss is accompanied by decreased STAT6 activity. Therefore, Chizzolini et al. (2000) hypothesised that the ability of IL-4 to inhibit MMP-1 production is dependent on γ c expression and γ c-dependent intracellular signalling. When γ c is no longer expressed, IL-4 enhances rather than suppresses MMP-1 production.

Importantly, the data presented in this chapter demonstrates that IL-4 has similar effects on MMP expression in the SW1353 cell line as it does in primary human chondrocytes, supporting the use of SW1353 cells when large amounts of material are required. Additionally, the effects of IL-4 on MMP expression in primary bovine chondrocytes are very similar to those observed in human chondrocytes. As human articular cartilage is unavailable in quantities large enough to perform explant culture experiments for RNA extraction, these data suggest that the use of bovine nasal cartilage in such experiments is a biologically relevant alternative.

Experiments utilising the 14 day bovine nasal explant culture model have demonstrated that strong down-regulation of MMP-13 mRNA by IL-4 is rapid, occurring within 24 hours of IL-4 addition. As collagen release does not occur until at least day 10 of culture in this model, IL-4 is able to completely block cartilage collagen degradation when addition is delayed until day 7 of culture. IL-1+OSM stimulate the production of active collagenases in bovine nasal cartilage; previous data and results in this chapter demonstrate that this activity can be inhibited by IL-4. Activation of any latent proenzymes with APMA allows total (pro + active) collagenolytic activity to be measured. The presence of IL-4 throughout all 14 days of culture significantly inhibits IL-1+OSM-induced levels of total collagenase, however the levels of total collagenase are not significantly inhibited if addition of IL-4 is delayed until day 7 of culture. Despite this, levels of active collagenase are virtually undetectable throughout the 14 day culture regardless of whether addition of IL-4 is delayed until day 7. Despite the presence of procollagenases in IL-1+OSM+IL-4 conditioned media, active collagenases and collagenolysis were both completely inhibited. These data give further support to the hypothesis Milner et al. (2001) that activation of procollagenases is a key control point in cartilage collagen degradation. It is possible that IL-4 could function by inhibiting the activation of procollagenases. Further evidence supporting this hypothesis is provided in a study by Cleaver et al. (2001), which showed that addition of MMP-3, a known activator of proMMPs, resulted in the recovery of collagen release in the presence of IL-1+OSM+IL-4, demonstrating that sufficient levels of procollagenases are present to promote extensive collagen loss if activated.

Previous work in the department (Pyle 2003) led to the hypothesis that IL-4 acts by inhibiting the activation of procollagenases in the bovine nasal cartilage system, in particular, by blocking serine proteinase activity. It has previously been shown that serine proteinase inhibitors can block IL-1+OSM-induced cartilage collagenolysis, implicating serine proteinases in the activation cascades that lead to the generation of active collagenases (Milner et al. 2003). These findings have yet to be pursued further. Thus, IL-4 appears to be chondroprotective by two distinct, but possibly inter-related mechanisms; MMP-13 repression and blockade of serine proteinase activity. It could be that the downregulation of MMP-13 mRNA by IL-4 is incidental and it is the inhibition of proMMP-1 activation by IL-4 that explains the chondroprotective effects of IL-4. However, data presented in this chapter and by other groups suggest this is probably not the case. Previous data (Pyle 2003) had indicated that IL-4 can be added as late as day 8 or 9 of culture in the bovine nasal cartilage model and still protect against cartilage degradation. This could have been due to rapid repression of MMP-13 or via the hypothesised ability of IL-4 to prevent procollagenase activation. A key experiment in this chapter demonstrated the effect of delayed addition of IL-4 on IL-1+OSM-induced MMP-13 mRNA expression. By day 7 of culture in the bovine nasal cartilage model, MMP-13 expression had been strongly induced. Addition of IL-4 at day 7 resulted in rapid repression of MMP-13, providing a strong indicator of the protective mechanism of action of IL-4. Studies involving selective MMP-13 inhibitors (Johnson et al. 2007, Jungel et al. 2010, Piecha et al. 2010) have demonstrated a reduction in collagen degradation with these inhibitors. These studies, along with the data presented in this chapter and the fact that MMP-13 is known to cleave type II collagen five times faster than MMP-1, strongly suggest that MMP-13 plays an integral role in collagen degradation and supports the development of selective MMP-13 inhibitors to reduce cartilage destruction in arthritis patients.

Analysis of the effect of IL-4 on non-collagenolytic MMPs provided further evidence that MMP-13 is central to the collagen degradation observed in the bovine nasal cartilage model. It has been suggested that both MMP-2 and MMP-14 possess collagenolytic activity (Ohuchi et al. 1997). However, data presented in this chapter demonstrated that whilst IL-4 appears to slightly inhibit both IL-1+OSM-induced MMP-2 (both pro and active) and MMP-14 mRNA expression, this inhibition is by no means complete and certainly not

comparable to the level of inhibition of MMP-13. These data would suggest that neither of these enzymes are responsible for the collagen degradation in this model as active MMP-2 and MMP-14 mRNA have been shown to be present in the assay at timepoints where collagenolysis was completed inhibited. Of more relevance is the inhibition of IL-1+OSM-induced MMP-3 by IL-4. MMP-3 is a known activator of numerous MMPs, including the collagenases (Murphy et al. 1987). IL-4 was shown to significantly inhibit IL-1+OSM-induced MMP-3 mRNA expression when present from day 0 or day 7 of the timecourse. These findings support those of Nemoto et al. (1997), who found that IL-4 was able to suppress IL-1-induced MMP-3 expression in human articular chondrocytes. The inhibition of MMP-3 mRNA by IL-4 could explain why MMP-1 mRNA is present throughout the timecourse and yet does not result in any collagenolysis.

Despite the established chondroprotective effects of IL-4, the use of IL-4 as a therapeutic agent would not be recommended. IL-4 is known to have strong pro-inflammatory effects in other diseases, in particular asthma. Therefore, the direct administration of IL-4 would undoubtedly result in unwanted side effects. Therefore it is vitally important to establish the exact protective mechanism of action of IL-4 so that this protective pathway may be targeted at a more specific level. The most significant finding of this chapter is that IL-4 is able to strongly and reproducibly downregulate IL-1+OSM-induced MMP-13 expression in both primary chondrocytes and bovine cartilage. This suggests that MMP-13 could be the key collagenase in IL-1+OSM-induced cartilage collagen breakdown and therefore an important therapeutic target. The aim of the following studies is to further elucidate the mechanism by which IL-4 so effectively inhibits MMP-13.

3.4 Summary

Studies in this chapter have shown that:

- IL-4 specifically blocked collagen release from bovine nasal cartilage stimulated to resorb with IL-1+OSM, in agreement with reports by Cawston et al. (1996).
- Delayed addition of IL-4 until day 7 of culture still completely blocked IL-1+OSM-induced cartilage collagen release.

- Prevention of collagen loss was accompanied by a concomitant reduction in active collagenase levels. The presence of IL-4 throughout the 14 days of culture significantly reduced total collagenase levels and to a lesser extent when addition of IL-4 was delayed.
- IL-4 differentially regulated IL-1+OSM-induced MMP-1 and MMP-13 mRNA expression in bovine nasal chondrocytes, human articular chondrocytes and SW1353 cells. IL-4 reproducibly down-regulated MMP-13 mRNA expression in all three cell types, whereas MMP-1 mRNA expression remained unchanged.
- Addition of IL-4 to IL-1+OSM in the bovine nasal cartilage model resulted in a rapid down-regulation of MMP-13 mRNA but no overall effect on MMP-1 mRNA, suggesting MMP-13 is the key collagenase in cartilage collagen degradation.
- Addition of IL-4 to IL-1+OSM in the bovine nasal cartilage model resulted in a strong down-regulation of active MMP-9.
- IL-1+OSM-induced MMP-2 and MMP-14 were only partially inhibited by IL-4 in the bovine nasal cartilage model, suggesting neither are responsible for cartilage degradation in this model.
- IL-1+OSM-induced MMP-3 mRNA expression was repressed by IL-4 in the bovine nasal cartilage model.

Chapter 4: Assessment of epigenetic regulation of MMP-13 by DNA methylation in bovine chondrocytes

4.1 Introduction

Data presented in Chapter 3 of this thesis demonstrated that IL-4 is able to rapidly repress IL-1+OSM-induced MMP-13 expression. One possible explanation for this rapid repression is that IL-4 induces epigenetic changes in the MMP-13 promoter, thereby leading to reduced gene expression. This hypothesis was examined in this chapter.

There is a growing awareness that individual characteristics can be determined by factors other than genetic sequences. Epigenetics, literally meaning “beyond genetics”, can be defined as stable and heritable (or potentially heritable) changes in gene expression that do not entail a change in DNA sequence (Jiang et al. 2004). Essentially, epigenetic modifications provide information as to where and when a gene should be expressed as opposed to altering the structure or function of a gene. There are two key epigenetic modifications; DNA methylation and histone modifications (such as acetylation and phosphorylation). Over recent years there has been considerable progress in the understanding of DNA methylation, the predominant epigenetic modification of DNA in mammalian genomes, and the importance of this process in both normal cellular function and disease.

The methylated base 5-methylcytosine was first discovered in the calf thymus 60 years ago (Hotchkiss 1948). It was subsequently discovered that methylcytosines are nonrandomly distributed throughout the genome (Razin and Cedar 1977). Unlike the other four bases in the genome, 5-methylcytosine does not exist as a free nucleotide in the cellular environment. Instead, methylation of cytosine residues occurs after DNA replication. With few exceptions, only cytosines that precede guanines can be methylated i.e. cytosines within CpG dinucleotides. The CpG notation (where ‘p’ represents the phosphate connecting the two nucleotides) is used to distinguish between a cytosine followed by a

guanine in the DNA sequence and a cytosine base-paired to a guanine (Dahl and Guldborg 2003). Low levels of DNA methylation correlate with active gene expression and high levels of DNA methylation result in gene silencing (Jaenisch and Bird 2003). The process of DNA methylation is mediated by the DNA methyltransferases (DNMT), which catalyse the transfer of a methyl group from the methyl-donor *S*-adenosylmethionine (SAM) to the cytosine residue (Pradhan and Esteve 2003) (Figure 4.1).

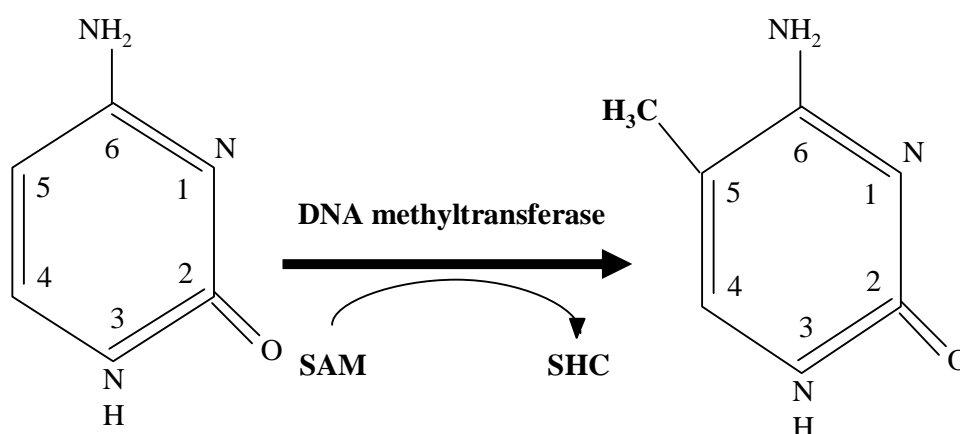


Figure 4.1 The formation of 5-methylcytosine. A DNA methyltransferase catalyses the transfer of a methyl group (CH_3) from *S*-adenosylmethionine (SAM) to cytosine producing 5-methylcytosine and *S*-adenosylhomocysteine (SHC). Adapted from Roach and Aigner (2007).

CpG sites are not evenly distributed throughout the genome and sequences containing CpG sites can be divided into two groups: those which are CpG rich and those which are CpG poor or sparse (McClelland and Ivarie 1982). The CpG-rich regions became known as CpG islands and they constitute between 1 and 2% of the genome and account for virtually all the unmethylated CpG dinucleotides. Any remaining CpG dinucleotides are found outside of CpG islands and the majority of these are methylated. CpG islands are defined as being longer than 500 bp and having a GC content of greater than 55% (Takai and Jones 2002). The promoter region of the collagenase MMP-13 is a so called ‘sparse CpG’ promoter as it contains only six CpG sites (Roach et al. 2005). In healthy cells, CpG sparse regions are generally methylated, whereas CpG islands are usually hypomethylated. During cancer development, the converse occurs, with CpG islands becoming hypermethylated and sparse CpG regions undergoing hypomethylation. This change in DNA methylation ultimately

resulting in, for example, the silencing of tumour suppressor genes (Jones and Baylin 2002). Until recently, the methylation status of ‘sparse CpG’ promoters has not been examined because it was widely believed that the methylation of many CpGs within a promoter was required to repress gene transcription. Whilst it is thought that this remains true for promoters with enhancer elements, it is now thought that silencing of genes with sparse CpG promoters by DNA methylation is feasible and that the chance of pathological demethylation is in fact increased in sparse CpG promoters (Roach and Aigner 2007).

There are two methods available for the analysis of methylation status: cleavage with specific methylation-sensitive restriction enzymes (MSREs) (Singer-Sam et al. 1990) and bisulphite modification (Frommer et al. 1992). Bacterial restriction endonucleases with varying sensitivities to 5-methylcytosine have been widely used to analyse the methylation status of cytosine at specific sites. If the cytosines of interest are methylated, then post-restriction PCR amplification produces a band equivalent to that of untreated control samples. If the cytosines are unmethylated and cleavage by the restriction enzyme induces DNA strand breaks, no band will be detected. MSRE-based analysis is limited because it can only provide information about CpGs within the cleavage sites of specific enzymes and is also prone to false positives due to incomplete digestion. Bisulphite treatment has one major advantage over the use of MSREs; it enables the methylation status of virtually all CpGs in the genome to be determined (Dahl and Guldborg 2003). Bisulphite treatment of genomic DNA results in the conversion of unmethylated cytosine residues to uracil, leaving any methylated cytosines unchanged according to the protocol originally developed by (Frommer et al. 1992). Hence, bisulphite treatment gives rise to different DNA sequences for methylated and unmethylated DNA (Figure 4.2).

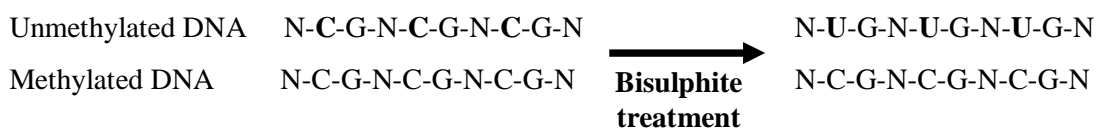


Figure 4.2 Bisulphite treatment of DNA. Incubation of target DNA with sodium bisulphite results in the conversion of unmethylated cytosines to uracil, leaving methylated cytosines unchanged, hence, giving rise to different DNA sequences for methylated and unmethylated DNA.

Whilst the CpG methylation pattern within the genome is relatively stable and clonally inherited (Leonhardt et al. 1992), pathological alterations are known to occur in cells as

they age (Richardson 2003). The examination of the DNA methylation status of chondrocytic genes has not been extensively studied, however several studies have indicated that DNA methylation may play a part in OA development. During OA, it is thought that increasing numbers of chondrocytes undergo a phenotypic modulation, producing 'degradative' chondrocytes or chondrocytes with hypertrophic characteristics. As with all adult somatic cells, the phenotype of chondrocytes is stabilised by the epigenetic status of the DNA within the cell. It is therefore likely that the destabilisation of the chondrocyte phenotype in OA is at least partly due to epigenetic changes (Aigner and Dudhia 1997; Spector and MacGregor 2004). Recent work has shown that various genes are up- or down-regulated in OA chondrocytes compared to normal chondrocytes (Burrage et al. 2006; Eleswarapu et al. 2007), indicating that OA chondrocytes have a modulated phenotype. One of the most recent studies examining the role of DNA methylation in OA demonstrated that DNA methylation had been lost at specific CpG residues in the ADAMTS-4 promoter. ADAMTS-4 is known to contribute to aggrecan degradation in human OA. The results of this study indicate that the upregulation of ADAMTS-4 in OA involves loss of DNA methylation at these specific CpG sites resulting in a permanent expression of ADAMTS-4 in OA chondrocytes (Cheung et al. 2008). OA chondrocytes that have been shown to exhibit changes in gene expression appear to be mainly confined in clusters in the superficial zone of OA cartilage. These clusters of chondrocytes are thought to result from the clonal expansion of a single chondrocyte in an attempt to repair cartilage damage (Sandell and Aigner 2001). The presence of such clusters is indicative of gene expression changes being under epigenetic control (Roach and Aigner 2007). The first, and currently only study to investigate whether abnormal gene expression seen in OA is due to epigenetic "unsilencing" was by Roach et al. (2005). This study investigated whether the abnormal expression of MMPs 3, 9 and 13 and ADAMTS-4 by human OA chondrocytes is associated with demethylation. The methylation status of the promoter regions of these genes were analysed using MSREs and it was found that the overall percentage of nonmethylated sites was increased in OA patients (48.6%) compared with controls (20.1%). It was also discovered that for each enzyme, there was one specific CpG site where the demethylation in OA patients was significantly higher than that in controls. If alterations in DNA methylation are responsible for aberrant gene expression in OA, it is possible that a random loss of methylation occurs simply with aging. In fact, binding of

transcription factors to both promoter and nonpromoter sequences is sufficient to cause passive demethylation of nearby CpG dinucleotides. However, it is also possible that active demethylation mechanisms exist, which target specific genes. Active demethylation would require a demethylase to remove the associated methyl group. However, whilst several putative demethylases have been described, none of the current candidates appear to exhibit the required characteristics to explain demethylation patterns observed *in vivo* (Ooi and Bestor 2008). DNA methylation is heritable and so any changes in methylation status are transmitted to daughter cells. When aberrant changes in DNA methylation occur, these changes are also heritable because cells have no way of “remembering” what their correct methylation status should be. Initial experimental evidence indicates that aberrant DNA methylation patterns could be responsible for at least some of the changed gene expression patterns seen in OA. Whether these DNA methylation patterns can be influenced therapeutically will undoubtedly be a major future research interest, as although heritable, DNA methylation is potentially reversible.

The aim of this chapter was to:

- Determine if IL-4 (in combination with IL-1+OSM) decreases IL-1+OSM-induced MMP-13 mRNA expression by increasing MMP-13 promoter methylation.

4.2 Results

4.2.1 MMP-13 promoter methylation in bovine nasal chondrocytes

4.2.1.1 Optimisation of Primers for Bisulphite PCR

Preliminary experiments to determine if IL-4 (in combination with IL-1+OSM) decreased MMP-13 mRNA expression by increasing MMP-13 promoter methylation were performed using bovine nasal chondrocytes. The predicted bovine MMP-13 promoter sequence was obtained by performing a BLAST search with the human MMP-13 promoter (U52692.1) against the *Bos Taurus* genome. The PCR was initially performed on control bisulphite treated bovine nasal chondrocyte DNA using primers and conditions as described

previously (section 2.2.12). Methprimer was used to design primers to amplify a 369 bp region of the MMP-13 promoter between - 325 and + 47 (Li and Dahiya 2002) (Figure 4.3). Primer pairs 4 and 5 (Figure 4.3) were tested using bisulphite-treated control bovine nasal chondrocyte DNA (as described in section 2.2.12). A band of the correct size was observed with both primer pairs (data not shown). In order to amplify the longest possible section of the MMP-13 promoter (369 bp), primer F5 (from this point referred to as bovine MMP-13 F) and R4 (from this point referred to as bovine MMP-13 R) were used (Figure 4.3). The annealing temperature was optimised using bisulphite-treated control bovine nasal chondrocyte DNA over a temperature gradient of 50 - 65°C (described in section 2.2.12.2). The optimum annealing temp for the MMP-13 primers was shown to be 65°C (Figure 4.4). The 369 bp region of the MMP-13 promoter was shown to be specifically amplified at these temperatures with no contaminating non-specific PCR products.

4.2.1.2 Bisulphite sequencing of MMP-13 promoter in treated DNA

The MMP-13 primers were used to amplify the -325 to +47 region of the bovine MMP-13 promoter in bisulphite treated DNA samples isolated from bovine nasal chondrocytes. The PCR products were then transformed into chemically competent *E.coli* and the resultant colonies sequenced until twenty non-clonal sequences were obtained for each treatment group as described in section 2.2.12. The bisulphite sequence data were then analysed to compare the methylation status of control, IL-1, IL-1+OSM and IL-1+OSM+IL-4-treated bovine nasal chondrocytes (after a 24 hour cytokine stimulation). Fisher's exact test was used to determine any significant difference in methylation pattern.

Sequencing of twenty non-clonal sequences for each treatment group showed no statistically significant difference in methylation status between different treatment groups. However, a pattern of altered methylation status was observed in five out of the seven (CpG sites 2 and 4-7) CpG sites analysed (Figure 4.5, Table 4.1). IL-1+OSM increased the level of demethylation compared with control and IL-1+OSM+IL-4 decreased the level of demethylation compared with IL-1+OSM. Despite the lack of statistical differences in this

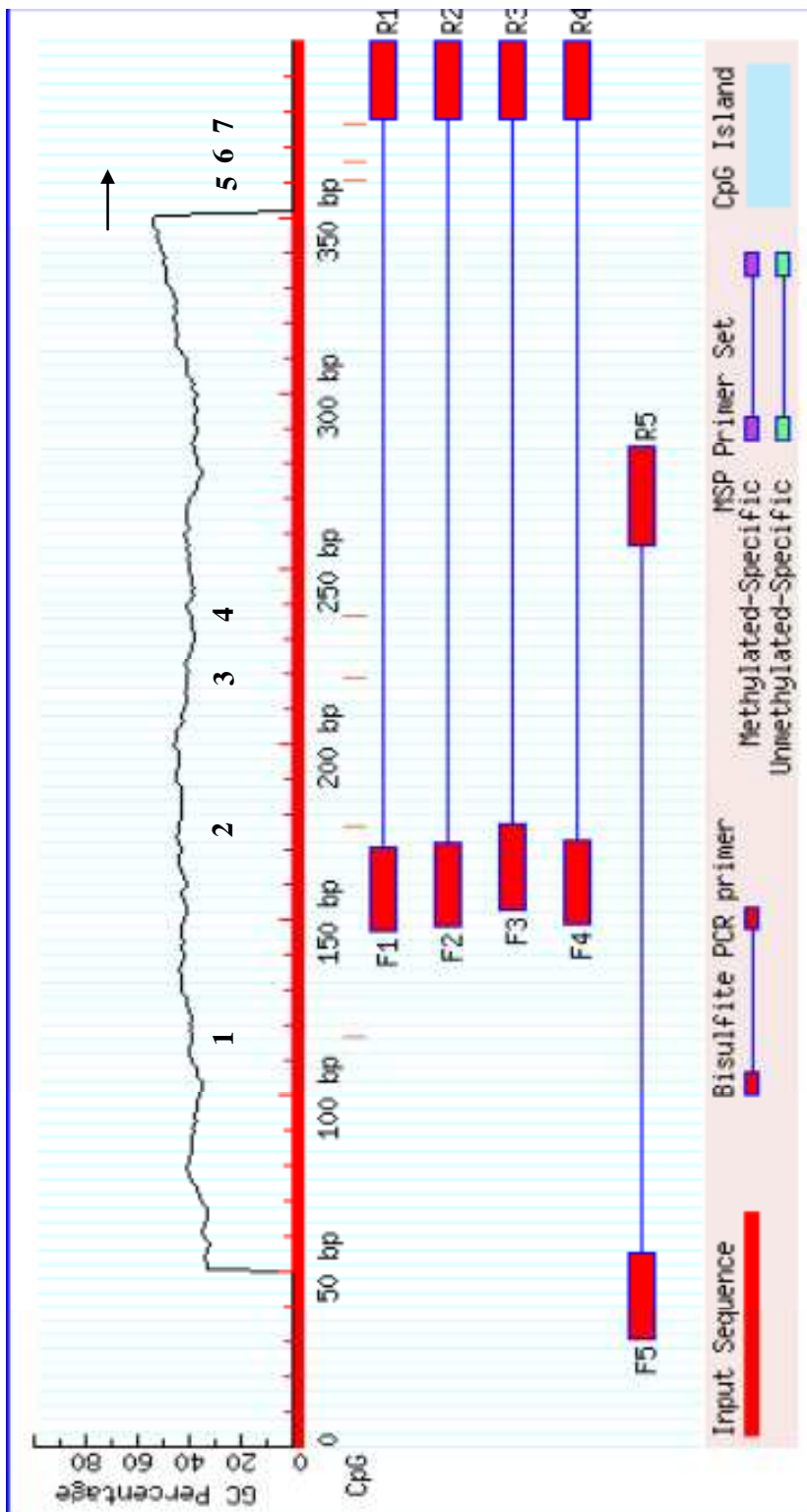


Figure 4.3 MethPrimer result. Schematic diagram of the CpG sites within the MMP-13 promoter. The diagram shows each CpG site (vertical red lines numbered sequentially) within a 369 bp region of the MMP-13 promoter and coding sequence. F1-F5 represent the positions of the forward bisulphite PCR primers and R1-R5 the position of the reverse bisulphite PCR primers. The position of the transcription start site (\rightarrow) is indicated. The regions of the MMP-13 promoter amplified by each primer pair and their position relative to the transcription start sites are indicated.

experiment, it was felt that the pattern of altered methylation observed, albeit limited, warranted further investigation.

4.2.2 Analysis of DNA methylation by pyrosequencing

As described previously, pyrosequencing is a sequencing-by-synthesis method that quantitatively monitors the real-time incorporation of nucleotides through the enzymatic conversion of released pyrophosphate into a proportional light signal (Tost and Gut 2007). After bisulphite treatment and PCR, the percentage methylation at each CpG site in a sequence is determined from the ratio of T and C. The ability of pyrosequencing to reliably detect differences in DNA methylation across cell populations without requiring the cloning of bisulphite-treated DNA into bacterial expression vectors gives pyrosequencing a major advantage over the bisulphite-treated PCR technique.

Bovine nasal chondrocytes were treated with control, IL-1, IL-1+OSM or IL-1+OSM+IL-4 for 24 hours. The DNA was then extracted and bisulphite treated (as described in section 2.2.12). The pyrosequencing bovine MMP-13 primers (see Table 2.5) were then used to amplify the -234 to +46 region of the bovine MMP-13 promoter in these samples. The reverse pyrosequencing primer was biotinylated at its 5' terminus. The biotinylated primer is required for the PCR product to be immobilised on streptavidin-coated beads, which renders the PCR product single-stranded. A sequencing primer (see Table 2.5) complementary to the single-stranded template was then hybridised to the single-stranded template. The pyrosequencing reaction was then performed as described in section 2.2.12.7.3.

The results from the pyrosequencing reaction failed to show any significant difference in methylation status between the different cytokine combinations at any of the six CpG sites analysed (Figure 4.7). Due to the greater statistical power of the pyrosequencing method, it was therefore concluded that there was no evidence of a role for alterations in MMP-13 promoter methylation in the regulation of MMP-13 gene expression by IL-1, IL-1+OSM or IL-1+OSM+IL-4.

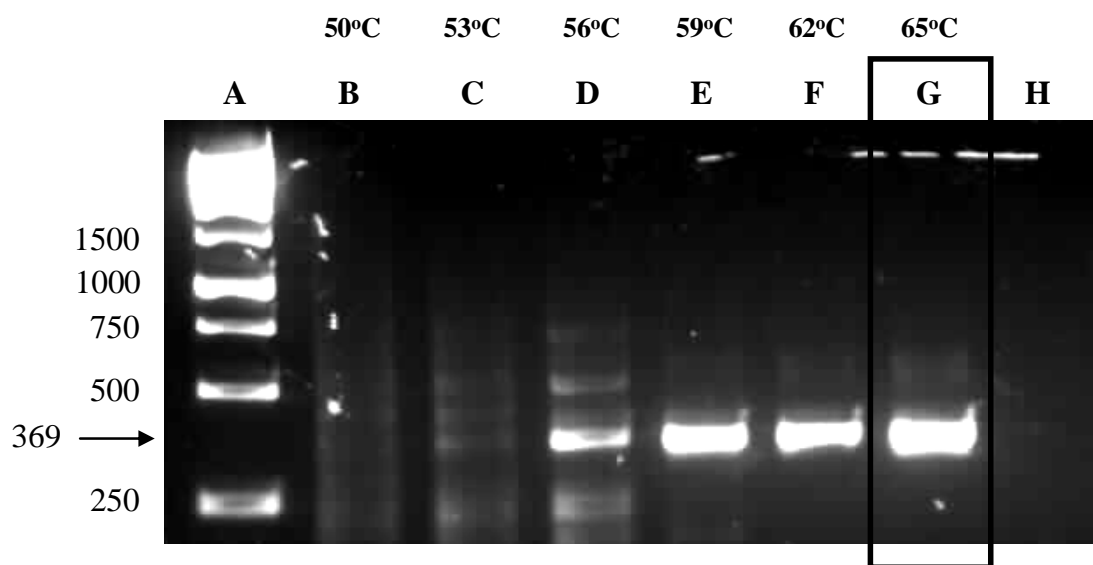


Figure 4.4 Optimisation of primers designed to amplify a 369 bp region of the MMP-13 promoter in bisulphite treated bovine DNA: agarose gel analysis of PCR products generated using bovine MMP-13 F and bovine MMP-13 R. Lane A shows the 1 kb ladder, lanes B to G show the products amplified in bisulphite treated BNC DNA over a temperature gradient of 50-65°C. The optimal annealing temperature and corresponding PCR product is indicated by a black box. Lane H shows the water control.

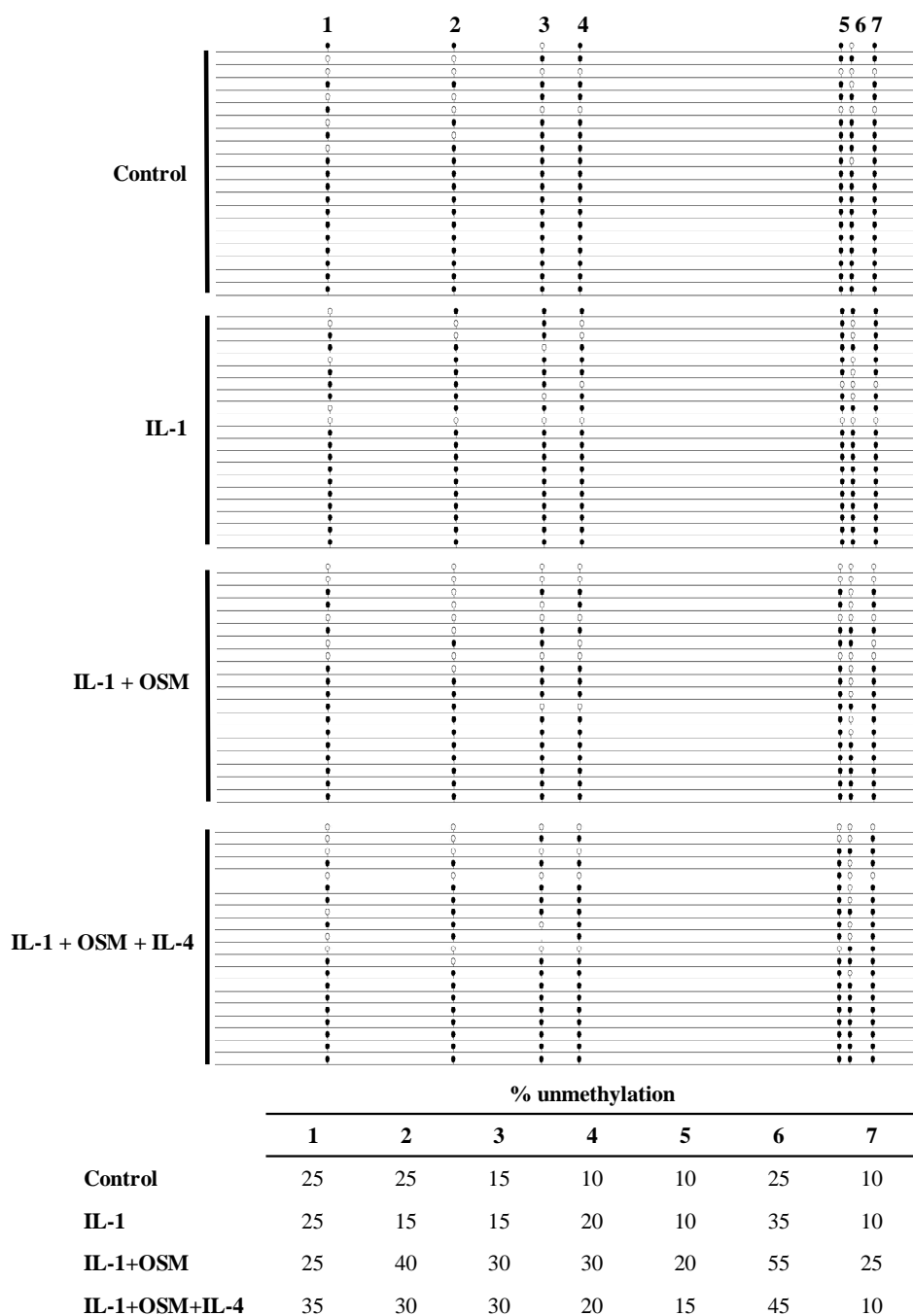


Figure 4.5 The effect of **IL-1**, **IL-1+OSM** and **IL-1+OSM+IL-4** on bovine **MMP-13** promoter methylation. DNA methylation analysis of a 369 base pair region of the bovine **MMP-13** promoter in DNA isolated from bovine nasal chondrocytes. DNA from bovine nasal chondrocytes treated with control, **IL-1**, **IL-1+OSM** or **IL-1+OSM+IL-4** was analysed to determine the methylation status of the 7 CpG sites within the sequenced section. For each treatment group, 20 non-clonal sequences were sequenced. Each dot represents a CpG site from one clone with black dots representing methylated CpG sites and white dots representing unmethylated CpG sites.

Table 4.1 The effect of **IL-1**, **IL-1+OSM** and **IL-4** on the percentage of unmethylated CpG sites.

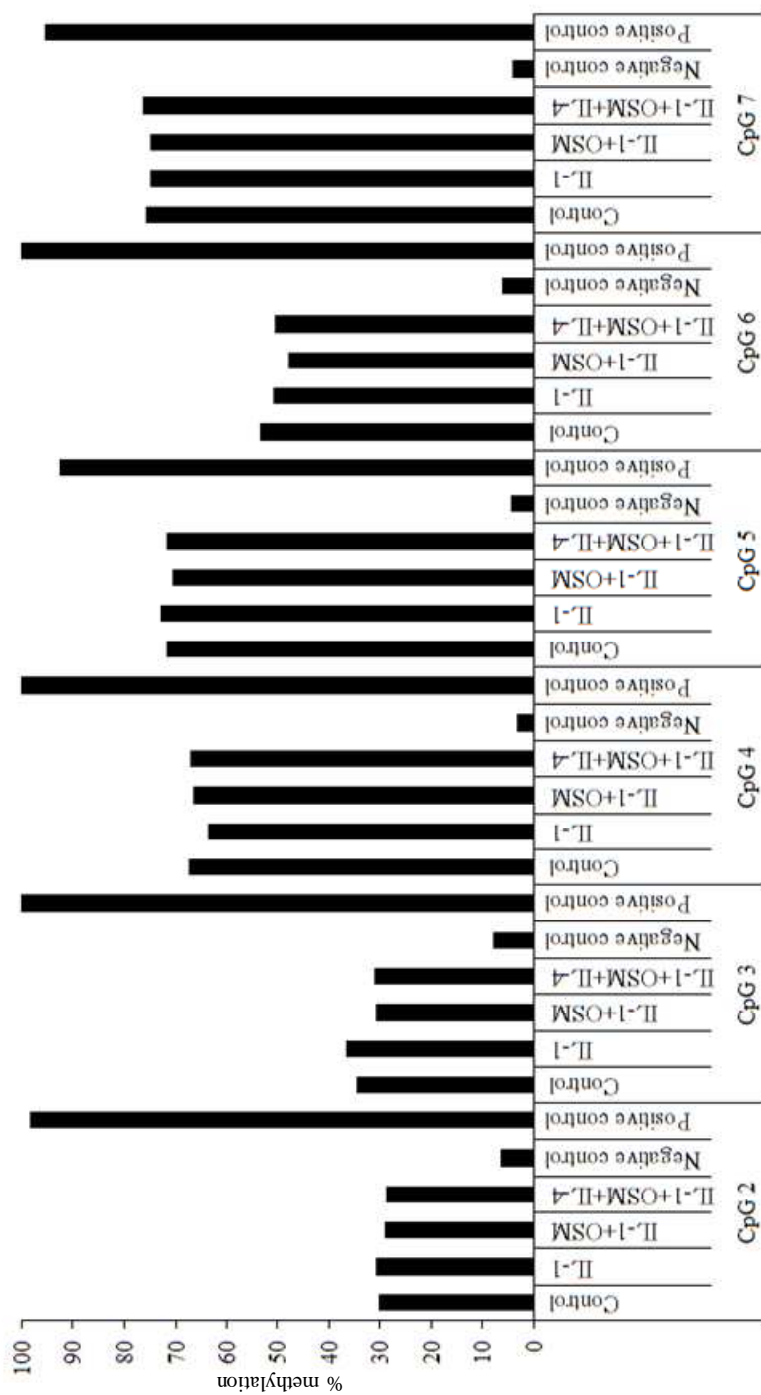


Figure 4.7 The effect of IL-1, IL-1+OSM and IL-1+OSM+IL-4 on bovine MMP-13 promoter methylation. DNA methylation analysis of a 280 base pair region of the bovine MMP-13 promoter in DNA isolated from bovine nasal chondrocytes. DNA from bovine nasal chondrocytes treated with control, IL-1, IL-1+OSM or IL-1+OSM+IL-4 was analysed to determine the methylation status of the 6 CpG sites within the sequenced section. Percentage DNA methylation was determined by pyrosequencing.

4.3 Discussion

Methylation is the most widely studied type of epigenetic modification of DNA. The development of bisulphite sequencing PCR by Frommer et al. (1992) greatly advanced the study of DNA methylation and is now one of the most frequently used techniques in the field. The aim of these experiments was to determine if IL-4 (in combination with IL-1+OSM) decreased MMP-13 mRNA expression by increasing MMP-13 promoter methylation in bovine nasal chondrocytes. Prior studies of DNA methylation within cartilage are very limited. Until recently, the methylation status of 'sparse CpG' promoters has not been examined because it was widely believed that the methylation of many CpGs was required to repress gene transcription. However, preliminary evidence has suggested that changes in DNA methylation with age not only affect transcription of genes that contain CpG islands, but also genes that are considered CpG poor (such as MMP-13) (Richardson 2002).

Recent studies have shown that changes in the expression of MMP-13 correlated with demethylation of specific CpG sites within its promoter (Roach et al. 2005). This study examined the methylation status of four degradative enzymes (MMP-3, MMP-9, MMP-13 and ADAMTS-4) in human OA chondrocytes and normal human chondrocytes. The 600 bp of the human MMP-13 promoter examined in this report was found to contain six CpG sites. Loss of methylation was detected in OA chondrocytes at sites -134 and -110. This provided the first evidence that changes in the expression of the matrix-degrading enzyme MMP-13 may occur as a result of changes in DNA methylation. The induction of MMP-13 expression by the pro-inflammatory cytokine combination of IL-1+OSM and the rapid repression (within 24 hours) of IL-1+OSM-induced MMP-13 mRNA expression by IL-4 was clearly demonstrated in this chapter. Low levels of DNA methylation correlate with active gene expression and high levels of DNA methylation result in gene silencing. It was therefore hypothesised that the pro-inflammatory cytokines IL-1+OSM could cause demethylation of the MMP-13 promoter, thereby resulting in active MMP-13 gene expression and IL-4 may act by preventing this demethylation or causing unmethylated CpG sites to be re-methylated, hence preventing expression of MMP-13. Due to the ease in obtaining bovine nasal cartilage for bovine nasal chondrocyte extraction and the difficulty

in obtaining normal human articular cartilage, these experiments were carried out in bovine nasal chondrocytes with the view to repeating any positive results in human articular chondrocytes.

Bisulphite sequencing is one of the best available methods currently available for detailed studies of DNA methylation as it allows analysis of all CpGs in a specific sequence. The bisulphite conversion generally produces a C-T conversion rate of over 95%, indicating that the results obtained in this chapter were an accurate measure of the methylation status of MMP-13. Other methods such as cleavage with MSREs are restricted to a specific number of sites within the genome. The study by Roach et al. (2005) employed the use of MSREs. In contrast to the bisulphite sequencing technique used in this chapter, the MSRE method is only able to provide information about CpGs within the cleavage sites of the restriction enzymes. In addition, false positives are common place in MSRE-based analysis due to incomplete digestion, resulting in the false conclusion that some CpGs in the target sequence were methylated (Dahl and Guldberg 2003). However, the paper by Roach et al. (2005) acknowledges the problem of false positives and addressed this by comparing the intensity of the PCR band with the no-enzyme control.

Use of the bisulphite sequencing PCR technique to sequence twenty non-clonal sequences for each treatment group (control, IL-1, IL-1+OSM and IL-1+OSM+IL-4) showed no significant difference in methylation status between different treatment groups. Unfortunately, the -110 CpG site in the human MMP-13 promoter (where a statistically significant loss of methylation was detected in OA chondrocytes when compared to normal chondrocytes (Roach et al. 2005)) is not present in the bovine MMP-13 promoter, therefore it is impossible to compare the results with the data presented in this chapter. However, the CpG located at position -134 is present in both the human and bovine MMP-13 promoters. Data presented in this chapter show a decrease in methylation at this site in the bovine MMP-13 promoter following IL-1+OSM stimulation, which is in concordance with the loss of methylation detected at this site in OA chondrocytes by the Roach study (Roach et al. 2005). As the pro-inflammatory cytokine combination of IL-1+OSM is used to mimic the degradation that would occur in an arthritic joint, this is not an unexpected result. However, treatment with IL-1+OSM+IL-4 failed to result in any re-methylation at this site, implying

that IL-4 does not repress MMP-13 gene expression by increasing MMP-13 promoter methylation.

The bisulphite sequencing method of analysing methylation status is very laborious, therefore in order to obtain statistically significant data, pyrosequencing was used to analyse methylation status on a larger scale. Pyrosequencing enables the reliable detection of differences in DNA methylation across cell populations without requiring the cloning of bisulphite-treated DNA into bacterial expression vectors. The limitation of the read-length is the main disadvantage of the pyrosequencing technology for DNA methylation analysis. This means that multiple sequencing primers must be designed and multiple reactions performed in order to analyse the whole sequence of interest (in the case of the bovine MMP-13 promoter, two sequencing primers had to be designed in order to analyse the methylation status of the desired number of CpGs). The methylation status of the CpG sites was further analysed by pyrosequencing, however this also failed to show any significant difference in methylation status between the different cytokine treatments. Both positive and negative controls were included in the pyrosequencing experiment to ensure the method was working as expected. These controls were selected from clones produced during the bisulphite sequencing experiment. The negative control consisted of a control in which, following sequencing, all seven CpG sites were known to be unmethylated. Similarly, the positive control consisted of a clone in which all seven CpG sites were known to be methylated. Due to the greater statistical power of the pyrosequencing method, it was concluded from the results that there was no evidence of a role for MMP-13 promoter methylation in the regulation of MMP-13 gene expression by IL-1, IL-1+OSM or IL-1+OSM+IL-4.

Whilst there was no literature available at the time of writing on the role of IL-4 in epigenetic modifications in the MMP-13 promoter or in arthritis generally, IL-4 has been implicated in epigenetic changes in other cell types. A 2009 study found that continuous IL-4 treatment led to decreased histone H3 lysine-27 methylation in activated macrophages (Ishii et al. 2009). In relation to the epigenetic regulation of MMP-13, it has been shown that one of the genes upregulated in OA cartilage is leptin, a cytokine-like peptide hormone thought to act as a regulator of bone growth by inducing osteoblast proliferation, collagen

synthesis and bone mineralisation. A study by Iliopoulos et al. (2007) has shown for the first time that leptin can be regulated by epigenetic mechanisms in OA. Leptin was found to be methylated in normal chondrocytes and unmethylated in both mildly and severely affected OA chondrocytes. Epigenetic regulation of leptin using siRNA was found to affect MMP-13, with MMP-13 expression down-regulated. Interestingly, this had no effect on the expression levels of other MMPs. Studies have shown that promoter methylation is important in the regulation of other MMPs. For example, the treatment of lymphoma cells with a DNA methylation inhibitor was found to decrease MMP-9 promoter methylation and increase MMP-9 messenger RNA and protein secretion (Chicoine et al. 2002). The expression of MMP-2, -7 and -9 and has been demonstrated to be associated with DNA methylations in pancreatic adenocarcinoma cells (Sato et al. 2003). DNA hypomethylation of normal synovial fibroblasts has been found to induce changes resulting in them resembling RA synovial fibroblasts (RASFs). RASFs are known to exhibit aggressive behaviour resulting in the upregulation of matrix-degrading enzymes and cytokines. This study suggests that DNA hypomethylation may play a role in the pathogenesis of RA by resulting in the activation of normally silenced genes, explaining the aggressive nature of RASFs (Karouzakis et al. 2009). Therefore, whilst the preliminary data presented in this chapter imply that changes in MMP-13 gene expression in response to IL-4 are not caused by epigenetic modifications, there is evidence to suggest that changes in genomic methylation play a role in the pathogenesis of arthritis in general.

The data presented in this chapter are by no means sufficient to completely exclude possible epigenetic regulation of IL-1+OSM-induced MMP-13 expression by IL-4. The MMP-13 promoter contains relatively few CpG sites, a property that could well favour a loss of methylation in disease and studies indicate that epigenetic mechanisms will no doubt be found to play an important role in the pathology of OA. Preliminary data would suggest that the chondroprotective nature of IL-4 is not due to it inducing any changes in the methylation status of the MMP-13 promoter. However, given more time, multiple experiments to assess the methylation status of the MMP-13 promoter would need to be performed in bovine chondrocytes, and more importantly in human chondrocytes to fully rule out the epigenetic regulation of MMP-13 as an explanation for the chondroprotective abilities of IL-4.

4.4 Summary

- Data presented in this chapter found no evidence of a role for changes in MMP-13 promoter methylation in the regulation of MMP-13 gene expression by IL-1, IL-1+OSM or IL-1+OSM+IL-4 in bovine chondrocytes.

Chapter 5: The effect of IL-4 on PI3K-dependent signalling in chondrocytes

5.1 Introduction

The chondroprotective effect of IL-4 in IL-1+OSM-induced cartilage collagen degradation is strongly thought to be due to the repression of MMP-13 mRNA expression and/or the inhibition of activation of latent MMPs. Data presented in Chapter 3 strongly suggests that it is the rapid repression of MMP-13 by IL-4 that is responsible for the protective effect of IL-4 on cartilage. Chapter 4 investigated changes in the DNA methylation status of the MMP-13 promoter by IL-4 as a possible mechanism of action for the rapid repression of MMP-13 mRNA. These data failed to show any role for epigenetic regulation by IL-4 in the regulation of MMP-13 mRNA expression, therefore, the next logical line of investigation was to examine the effect of IL-4 on cell signalling in chondrocytes.

The binding of IL-4 to its receptor leads to the phosphorylation, and hence activation, of JAK1 and JAK3. The phosphorylation of JAKs is followed by phosphorylation of the IL-4 receptor components and cytoplasmic signalling proteins (Hebenstreit et al. 2006). Once phosphorylated, these tyrosine residues act as docking sites for signalling molecules. STAT6 signalling is classically associated with IL-4 and the examination of STAT6-deficient mice has shown that STAT6 is essential for IL-4-dependent gene induction (Kuhn et al. 1991). STAT6 is recruited to the activated IL-4R α through its SH2 domain and becomes phosphorylated on tyrosine 641 by JAKs leading to its dimerization and translocation to the nucleus, where the homodimer activates transcription of IL-4 responsive genes (Leonard and O'Shea 1998). IL-4 is also known to signal through IRS2, resulting in the activation of PI3K and its downstream target Akt. However, the role of this pathway in IL-4-induced gene expression is still unclear. This chapter details investigations of the involvement of PI3K in IL-4-induced Akt activation.

Previous work in the group (Litherland et al. 2008) has demonstrated that OSM stimulates Akt phosphorylation at both Thr308 and Ser473 in human articular chondrocytes, indicating Akt activation. In addition, the same study showed that PI3K inhibition was able to block both IL-1+OSM-induced cartilage degradation and IL-1+OSM-induced collagenase expression. Stimulation with IL-1 does not result in Akt activation and so experiments in this chapter have focused on the effect of OSM alone as opposed to the usual combination of IL-1+OSM. As mentioned previously, IL-4 has been shown to signal via the PI3K/Akt pathway, in addition to the JAK/STAT pathway (Kaminski et al. 2010). However, the effect of IL-4 on the PI3K/Akt pathway in chondrocytes has yet to be examined. This is therefore one of the key aims of this chapter.

Activation of the PI3K signalling pathway is now known to be one of the central pathways by which cellular functions are controlled. The PI3Ks are a group of enzymes that catalyse the phosphorylation of the 3'-position of the inositol ring in phosphoinositides. They have been classified into three major classes on the basis of their structural and functional homologies: I, II and III (Hawkins et al. 2006). Activation of class I PI3Ks, in particular, is known to be very important in the control of various cellular processes by cytokines and growth factors. The Class I PI3Ks consist of four closely related approximately 110 kDa catalytic subunits and two distinct families of regulatory subunits, which form the basis of their further subdivisions into Class IA and IB. Class IA PI3Ks comprise heterodimers consisting of a p110 catalytic subunit (p110 α , β or δ), associated with a p50, p55 or p85 regulatory subunit. The class IB PI3Ks consist of dimers of the p110 γ catalytic subunit paired with either a p84 or p101 regulatory subunit. Akt is a serine/threonine kinase that acts downstream of PI3K and is known to be of vital importance to PI3K signalling pathway events. The Akt kinase family is comprised of three highly homologous isoforms: Akt1, Akt2 and Akt3 (Gonzalez and McGraw 2009). They are regulated by phosphoinositide-dependent kinase-1 (PDK1), a PH (plekstrin homology) domain-containing kinase downstream of PI3K, which phosphorylates all three Akt isoforms (Franke 2008). Maximum activation of Akt requires phosphorylation at two different sites, Thr308 (by phosphoinositide-dependent kinase 1 (PDK1)) and Ser473 (by PDK2) (Liang and Slingerland 2003). Many findings have pointed to functional differences between the Akt isoforms and it is widely suspected that different Akt isoforms are associated with

different disease processes (Franke 2008). Another downstream substrate of the PI3K signalling pathway is GSK-3 (glycogen synthase kinase-3), a serine/threonine kinase. GSK-3 is unusual in that it is active in unstimulated cells and its activity is reduced during cellular responses. GSK-3 is negatively regulated by PI3K-mediated activation of Akt (Doble and Woodgett 2003). Two homologous isoforms of GSK-3 exist, GSK-3 α and GSK-3 β . Whilst they both have similar functions, gene knockout studies have shown they are not functionally redundant (Rayasam et al. 2009).

The PI3K/Akt signalling pathway has been implicated in the pathogenesis of many diseases and the modulation of specific PI3K isoform activity is already a well-established therapeutic target. Many mutations in the PI3K/Akt pathway have been found to be common in human malignancies (Carnero 2010). Of particular relevance to this thesis, was the finding that blockade of PI3K γ can ameliorate joint damage in mouse models of RA (Camps et al. 2005).

This chapter aimed to further investigate the mechanism of MMP-13 repression by IL-4 by examining the role of the PI3K/Akt pathway in IL-4 signalling. Data presented in Chapter 3 of this thesis demonstrated that bovine nasal chondrocytes appear to behave very similarly to human articular chondrocytes. For this reason, bovine nasal chondrocytes were used in the majority of the experiments in this chapter due to their availability and plentiful supply.

The aims of this chapter were to:

- Determine the optimum timepoint for examination of STAT6 phosphorylation by IL-4 in bovine nasal chondrocytes.
- Assess Akt involvement in IL-4 signalling, by determining the effect of IL-4 on OSM-stimulated Akt and GSK-3 phosphorylation in bovine nasal chondrocytes.
- Determine if IL-4-mediated Akt phosphorylation is PI3K-dependent and if so, which isoform(s) of PI3K are involved in IL-4-dependent Akt phosphorylation.

5.2 Results

5.2.1 The effect of different concentrations of IL-4 on STAT6 and Akt phosphorylation in bovine chondrocytes

STAT6 signalling is classically associated with IL-4 and the examination of STAT6-deficient mice has shown that STAT6 is essential for IL-4-dependent gene induction (Kuhn et al. 1991). Previous investigations into IL-4 signalling in chondrocytes used IL-4 at a concentration of 50 ng/ml (Pyle 2003). However, Chapter 3 in this thesis demonstrated that IL-4 could be used at 20 ng/ml in chondrocytes to repress MMP-13 mRNA expression. The purpose of this experiment was to examine if this correlated with the concentration dependence of cell signalling experiments. Figure 5.1 clearly demonstrates the phosphorylation of both STAT6 and Akt (Ser473) at both 5 ng/ml and 20 ng/ml, however the phosphorylation was stronger when IL-4 was used at 20 ng/ml. Therefore, in further signalling experiments, IL-4 was used at 20 ng/ml.

5.2.2 Timecourse to investigate the effect of IL-4 on STAT6 activation in primary bovine and human articular chondrocytes

The examination of IL-4-induced STAT6 phosphorylation over a timecourse was performed twice. Previous work in the department has shown latent STAT6 to be present at all timepoints (Pyle 2003). Both bovine nasal (Figure 5.2a) and human articular chondrocytes (Figure 5.2b) demonstrated weak tyrosine phosphorylation of STAT6 after a 5 minute stimulation with IL-4. In bovine nasal chondrocytes, this increased to a maximum at 20 minutes and decreased thereafter. The maximum timepoint of STAT6 phosphorylation by IL-4 in human articular chondrocytes was more sustained, but reached a maximum around 10-20 minutes.

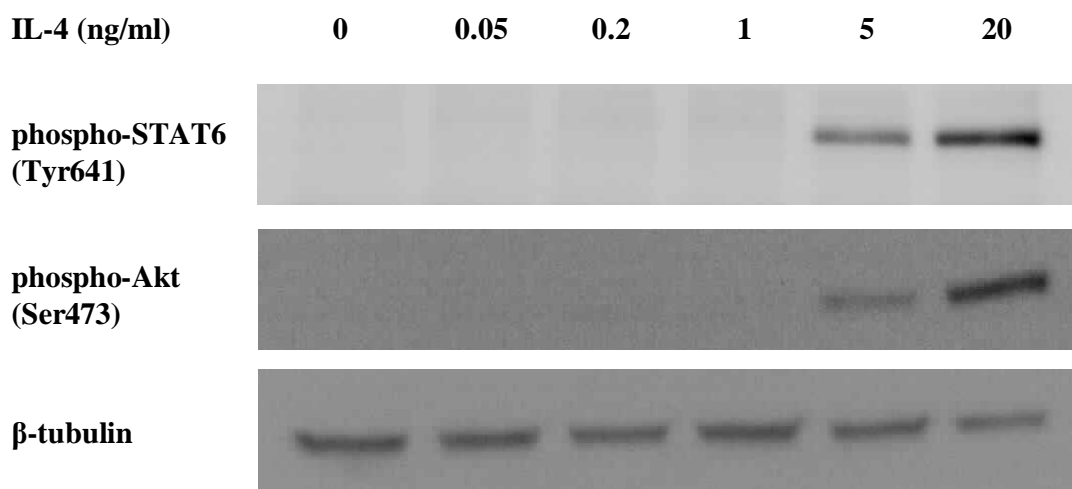


Figure 5.1 The effect of different concentrations of IL-4 on STAT6 and Akt phosphorylation in bovine nasal chondrocytes, as determined by Western blot. Primary bovine nasal chondrocytes were treated with medium containing IL-4 (0-20 ng/ml) for 20 minutes at 37°C. Total cell lysates were prepared and separated by SDS-PAGE on a 10% polyacrylamide gel with a molecular weight marker. Protein fractions were transferred to PVDF membranes. Blots were probed with phospho-STAT6 (Tyr641), phospho-Akt (Ser473) and β -tubulin followed by goat anti-rabbit HRP. The blots were visualised using ECL. Results are representative of two independent experiments.

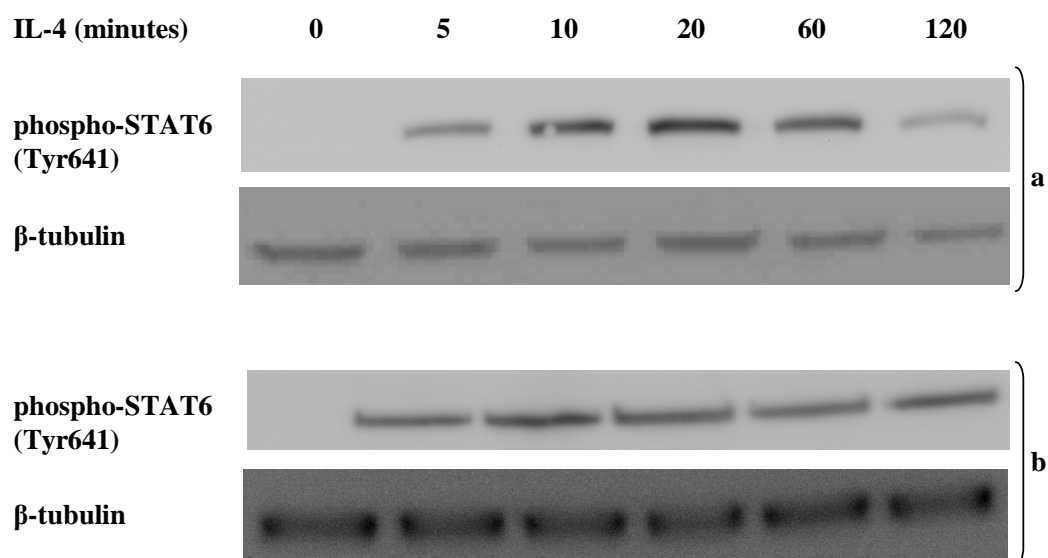


Figure 5.2 Timecourse to investigate the effect of IL-4 on STAT6 activation in primary bovine nasal and human articular chondrocytes, as determined by Western blot. Primary bovine nasal chondrocytes (a) and human articular chondrocytes (b) were treated with medium containing IL-4 (20 ng/ml) for 0-120 minutes at 37°C. Total cell lysates were prepared and separated by SDS-PAGE on a 10% polyacrylamide gel with a molecular weight marker. Protein fractions were transferred to PVDF membranes. Blots were probed with phospho-STAT6 (Tyr641) and β -tubulin followed by goat anti-rabbit HRP. The blots were visualised using ECL. Results are representative of two independent experiments.

5.2.3 The effect of IL-4 on OSM-stimulated Akt and GSK-3 phosphorylation in bovine chondrocytes

One potential mechanism to explain the effects of IL-4 in negating IL-1+OSM-dependent MMP-13 induction (which is dependent on Akt (Litherland et al. 2008)) is that IL-4 stimulation of Akt may lead to a state of resistance of Akt to further stimulation by OSM. To test this possibility, the effect of IL-4 on OSM-stimulated Akt and GSK-3 phosphorylation was examined. As already demonstrated in Figures 5.1 and 5.2, IL-4 induced tyrosine phosphorylation of STAT6. It has previously been reported that OSM stimulates Akt phosphorylation in human chondrocytes at both Thr308 and Ser473 (Litherland et al. 2008) and Figure 5.3 confirmed that the same was true in bovine nasal chondrocytes. Interestingly, the effects of IL-4 on Akt phosphorylation was much weaker than that of OSM but the combination of IL-4 and OSM was seen to enhance Akt phosphorylation. Pretreatment of bovine nasal chondrocytes with IL-4 was shown to reduce phosphorylation of Akt and GSK-3 in response to IL-4+OSM, suggesting that pre-incubation with IL-4 in some way inhibits the OSM-stimulated phosphorylation of Akt and GSK-3. This interference is a common phenomenon and has been observed for stimuli such as insulin in other systems (Litherland et al. 2007).

5.2.4 Stimulation of Akt and GSK-3 by IL-4 is PI3K-dependent in bovine chondrocytes

Previous data presented in this chapter have shown that stimulation of bovine nasal chondrocytes with IL-4 resulted in both Akt and GSK-3 phosphorylation. Therefore, the next aim was to determine if this phosphorylation was PI3K-dependent as is the case for OSM-dependent Akt phosphorylation (Litherland et al. 2008). Experiments were performed using the selective PI3K inhibitor, LY294002. Figure 5.4 clearly shows that the PI3K inhibitor inhibited IL-4-stimulated phosphorylation of both Akt and GSK-3 in a concentration-dependent manner, therefore showing that IL-4-stimulation of Akt/GSK-3 is dependent on PI3K. STAT6 phosphorylation, which is not thought to be PI3K-dependent was unaffected by LY294002.

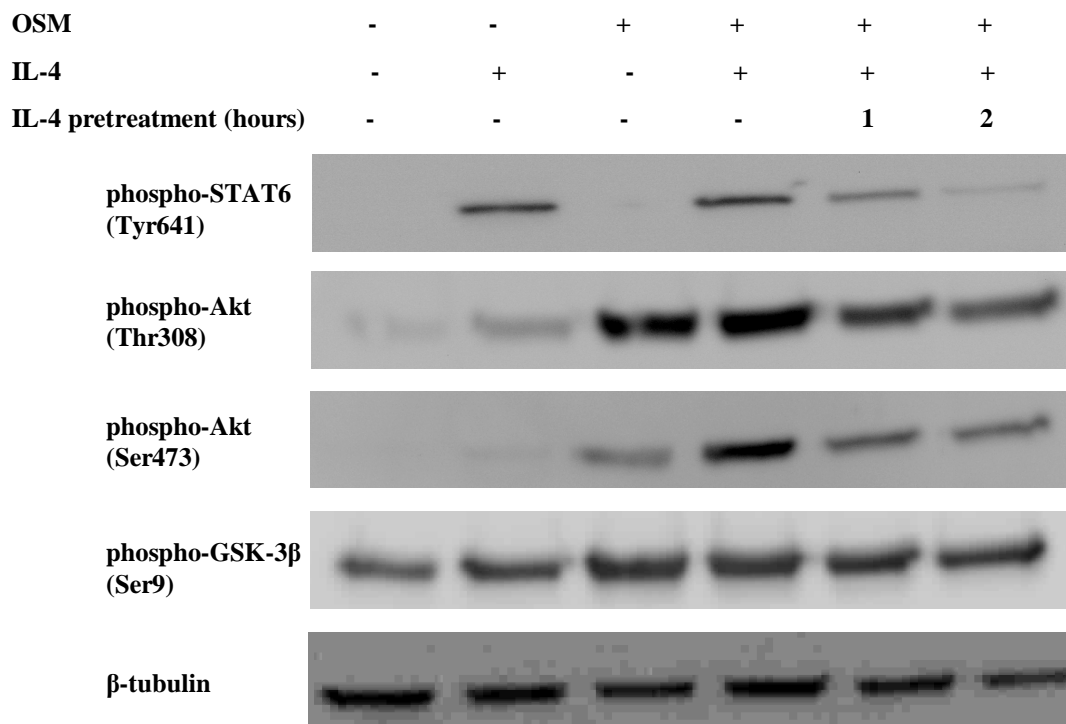


Figure 5.3 The effect of IL-4 on OSM-stimulated Akt and GSK-3 phosphorylation in bovine nasal chondrocytes, as determined by Western blot. Primary bovine nasal chondrocytes were treated with medium containing \pm OSM (10 ng/ml) \pm IL-4 (20 ng/ml) for 20 minutes at 37°C. Total cell lysates were prepared and separated by SDS-PAGE on a 10% polyacrylamide gel with a molecular weight marker. Blots were probed with phospho-STAT6 (Tyr641), phospho-Akt (Thr308), phospho-Akt (Ser473), phospho-GSK-3 β (Ser9) and β -tubulin followed by goat anti-rabbit HRP. Protein fractions were transferred to PVDF membranes. The blots were visualised using ECL. Results are representative of two independent experiments.

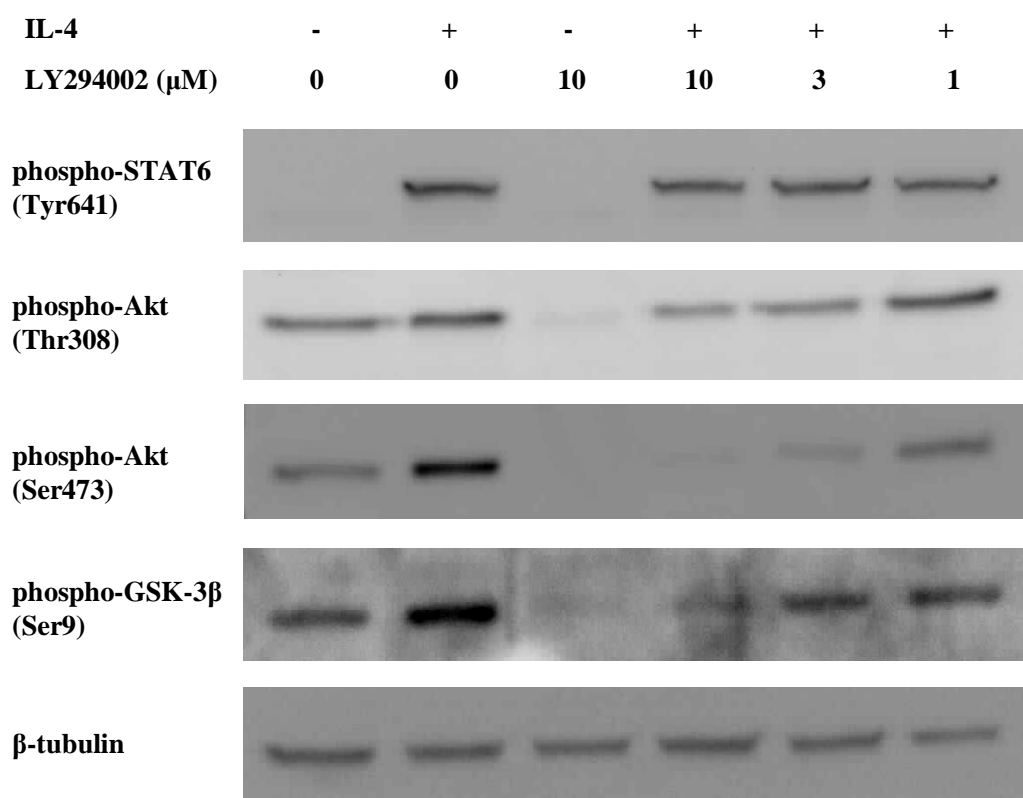


Figure 5.4 Stimulation of Akt and GSK-3 by IL-4 is PI3K-dependent in bovine nasal chondrocytes, as determined by Western blot. Primary bovine nasal chondrocytes were treated with medium containing IL-4 (20 ng/ml) \pm LY294002 (1-10 μ M) for 20 minutes, with a 30 minute pretreatment with LY294002 at 37°C. Total cell lysates were prepared and separated by SDS-PAGE on a 10% polyacrylamide gel with a molecular weight marker. Protein fractions were transferred to PVDF membranes. Blots were probed with phospho-STAT6 (Tyr641), phospho-Akt (Thr308), phospho-Akt (Ser473), phospho-GSK-3 β (Ser9) and β -tubulin followed by goat anti-rabbit HRP. The blots were visualised using ECL. Results are representative of two independent experiments.

5.2.5 The effect of selective PI3K 110 β inhibition on IL-4- and OSM-induced Akt and phosphorylation in bovine chondrocytes

Given that the phosphorylation of Akt and GSK-3 has been shown to be PI3K-dependent (Figure 5.4), the next step was to determine if this phosphorylation was dependent on a particular isoform of PI3K. Treatment with TGX-221 (3 μ M) partially blocked OSM- and IL-4-dependent Akt phosphorylation (Ser473), suggesting that phosphorylation by either stimulus is partly PI3K p110 β -dependent (Figure 5.5). The effects of PI3K p110 β inhibition on Akt308 were not reproducible and so are not shown. PI3K p110 β inhibition had no effect on IL-4-induced STAT6 phosphorylation.

5.2.6 The effect of PI3K p110 α inhibition on IL-4- and OSM-induced Akt phosphorylation in bovine chondrocytes

This experiment demonstrated a concentration-dependent, but incomplete, inhibition of IL-4-stimulated Akt (Ser473) phosphorylation by compound 15e (Figure 5.6). The p110 α is thought to be the major PI3K isoform involved in OSM-induced Akt activation in human chondrocytes (Litherland et al. 2008). The strong inhibition of OSM-stimulated Akt (Ser473) phosphorylation by compound 15e at all concentrations supports this. IL-4-dependent Akt phosphorylation can be inhibited by compound 15e, but was less sensitive to compound 15e than OSM-dependent Akt phosphorylation, which remained inhibited at lower concentrations of compound 15e. This suggests that IL-4-stimulated Akt phosphorylation is only partially dependent on the p110 α isoform in bovine chondrocytes. PI3K p110 α inhibition had no effect on IL-4-induced STAT6 phosphorylation.

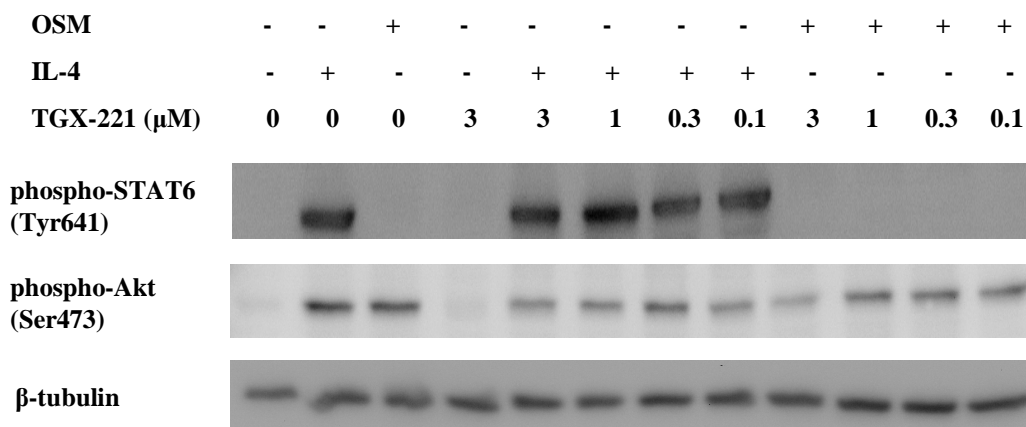


Figure 5.5 The effect of TGX-221, a selective PI3K p110 β inhibitor, on IL-4- and OSM-induced Akt phosphorylation in bovine chondrocytes, as determined by Western blot. Primary bovine nasal chondrocytes were treated with medium containing IL-4 (20 ng/ml) or OSM (10 ng/ml) for 20 minutes, with a 30 minute pretreatment with TGX-221 (0.1-3 μM) at 37°C. Total cell lysates were prepared and separated by SDS-PAGE on a 10% polyacrylamide gel with a molecular weight marker. Protein fractions were transferred to PVDF membranes. Blots were probed with phospho-STAT6 (Tyr641), phospho-Akt (Ser473) and β -tubulin followed by goat anti-rabbit HRP. The blots were visualised using ECL. Results are representative of two independent experiments.

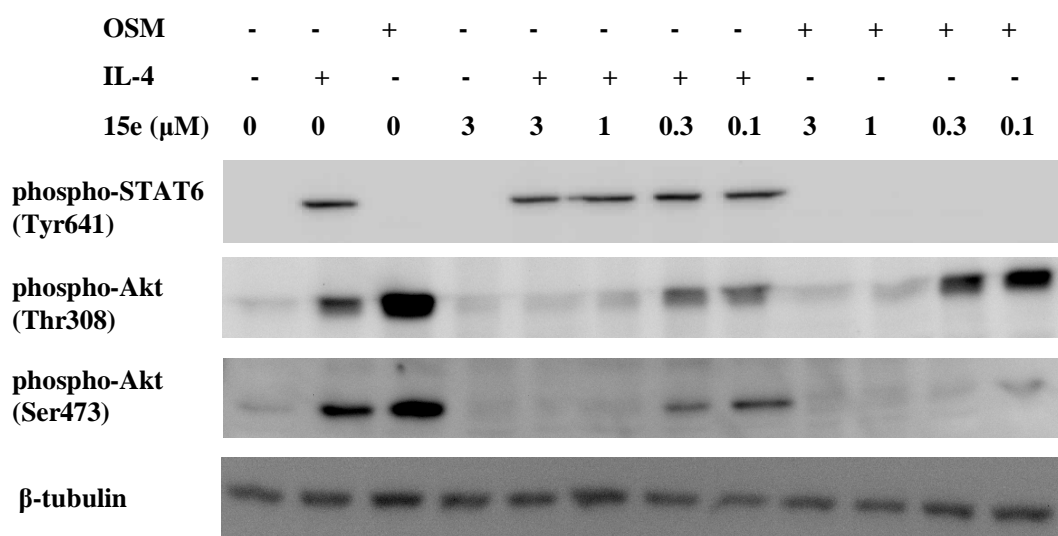


Figure 5.6 The effect of compound 15e, a PI3K p110 α specific inhibitor, on IL-4- and OSM-induced Akt phosphorylation in bovine chondrocytes, as determined by Western blot. Primary bovine nasal chondrocytes were treated with medium containing IL-4 (20 ng/ml) or OSM (10 ng/ml) for 20 minutes, with a 30 minute pretreatment with compound 15e (0.1-3 μM) at 37°C. Total cell lysates were prepared and separated by SDS-PAGE on a 10% polyacrylamide gel with a molecular weight marker. Protein fractions were transferred to PVDF membranes. Blots were probed with phospho-STAT6 (Tyr641), phospho-Akt (Thr308), phospho-Akt (Ser473) and β -tubulin followed by goat anti-rabbit HRP. The blots were visualised using ECL. Results are representative of two independent experiments.

5.2.7 The effect of PI3K p110 α , β and δ silencing on OSM- and IL-4-induced Akt phosphorylation in SW1353 cells

Following experiments into the effect of PI3K p110 inhibitors on IL-4-dependent Akt phosphorylation, siRNA was used in order to validate these results and investigate a possible role for PI3K p110 δ , for which there were no inhibitors available commercially. Previous work within the group meant that siRNAs specific for the human α , β and δ isoforms of PI3K p110 had been validated (Litherland et al. 2008) and were available. This work was performed in the chondrocyte cell line SW1353 as SW1353 cells are transfected more readily than human articular chondrocytes. Data presented in Chapter 3 demonstrated that SW1353 appeared to be an appropriate alternative to primary human chondrocytes. This experiment was performed only once and therefore cannot be interpreted robustly.

As expected, transfection with siCon had no effect on OSM- or IL-4-induced Akt phosphorylation. Both cytokines stimulated an increase in Akt phosphorylation, with the increase in phosphorylation stronger in the presence of OSM (Figure 5.7). As mentioned previously, the p110 α is thought to be the major PI3K isoform involved in OSM-induced Akt activation in human chondrocytes (Litherland et al. 2008). Figure 5.7 shows a slight reduction in OSM-induced phosphorylation following PI3K p110 α silencing. However, silencing of PI3K p110 α would have been expected to have a more pronounced effect on Akt phosphorylation and so this result could suggest some inefficiency in p110 α knockdown or differences in the involvement of particular p110 isoforms between primary chondrocytes and the SW1353 cell line. In contrast to the results shown in Figure 5.6, silencing of PI3K p110 α appears to have no apparent effect on IL-4-induced Akt phosphorylation. Unexpectedly, silencing of PI3K p110 β strongly reduced both OSM- and IL-4-induced Akt phosphorylation, which is in contrast to the results obtained in Figure 5.5, where only OSM-induced Akt phosphorylation was effected by inhibition of PI3K p110 β . Silencing of PI3K p110 δ was shown to strongly inhibit both OSM- and IL-4-induced Akt phosphorylation, suggesting that the δ isoform of PI3K p110 is important in Akt phosphorylation by both OSM and IL-4. Overall, these results do not highlight one specific PI3K isoform as being crucial for IL-4-induced Akt phosphorylation; instead the data suggest interplay between several isoforms, but caution should be exercised as this experiment was performed only once.

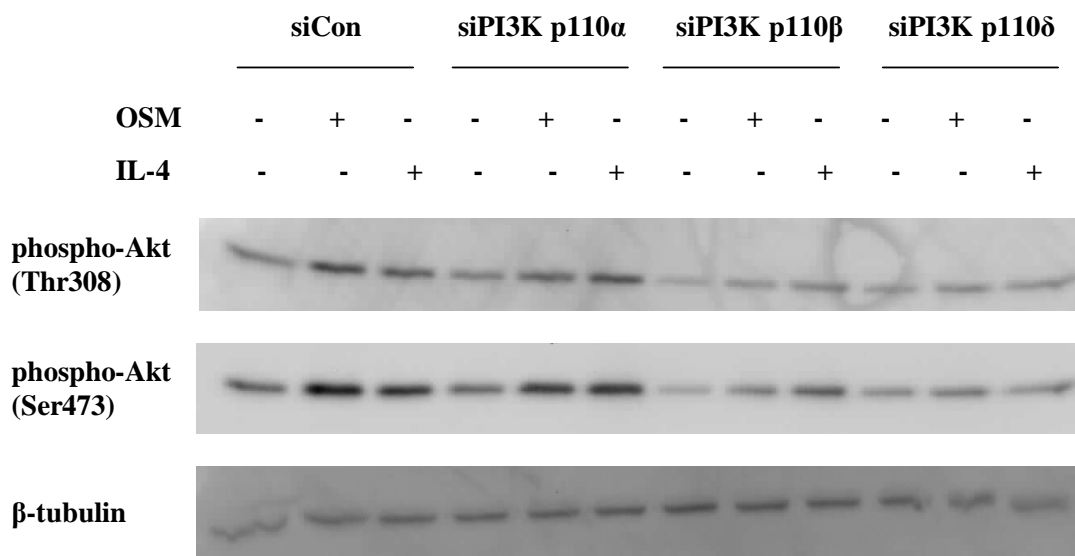


Figure 5.7 The effect of PI3K p110 α , β and δ silencing on OSM- and IL-4-induced Akt phosphorylation in SW1353 cells. SW1353 cells were stimulated with media \pm OSM (10 ng/ml) \pm IL-4 (20 ng/ml) for 20 minutes at 37°C following a 48 hour transfection with siRNA specific to PI3K p110 α , PI3K p110 β , PI3K p110 δ or siCon (100 nM). Total cell lysates were prepared and separated by SDS-PAGE on a 10% polyacrylamide gel with a molecular weight marker. Protein fractions were transferred to PVDF membranes. Blots were probed with phospho-Akt (Thr308), phospho-Akt (Ser473) and β -tubulin followed by goat anti-rabbit HRP. The blots were visualised using ECL. Data are from a single experiment only.

5.2.8 The effect of PI3K p110 isoform silencing on IL-1+OSM ± IL-4-induced MMP-13 expression in SW1353 cells

Given that siRNA specific to the PI3K isoforms was already available, a logical experiment was to assess the effect of PI3K p110 isoform silencing on IL-1+OSM ± IL-4-induced MMP-13 expression in SW1353 cells by real-time RT-PCR. Data presented in Figure 5.7 suggest that the δ isoform of PI3K p110 plays an important role in IL-4-induced Akt phosphorylation. The aim of this experiment was to determine if the repression of IL-1+OSM-induced MMP-13 expression is dependent on any particular PI3K isoform. It has already been shown that the specific PI3K inhibitor, LY294002, significantly inhibits IL-1+OSM-induced MMP-1 and MMP-13 expression in human articular chondrocytes (Litherland et al. 2008). The same study suggested that p110 α and p110 δ are involved in IL-1+OSM-stimulated collagenase induction in human chondrocytes. Figure 5.8 shows that silencing of the p110 δ isoform significantly reduces IL-1+OSM-induced MMP-13 expression. Unfortunately, as silencing of p110 δ prevented the induction of MMP-13 by IL-1+OSM, it is impossible to tell whether p110 δ is important in the repression of MMP-13 by IL-4. Silencing of the p110 α isoform did not reduce IL-1+OSM-induced MMP-13 expression, as was reported in human articular chondrocytes (Litherland et al. 2008). This could suggest a difference in signalling mechanisms between primary chondrocytes and SW1353 cells. However, silencing of p110 α did significantly reduce the ability of IL-4 to suppress IL-1+OSM-induced MMP-13 expression, suggesting a possible role for p110 α in the chondroprotective effect of IL-4. As reported previously (Litherland et al. 2008), silencing of p110 β had no significant effect on the induction of MMP-13.

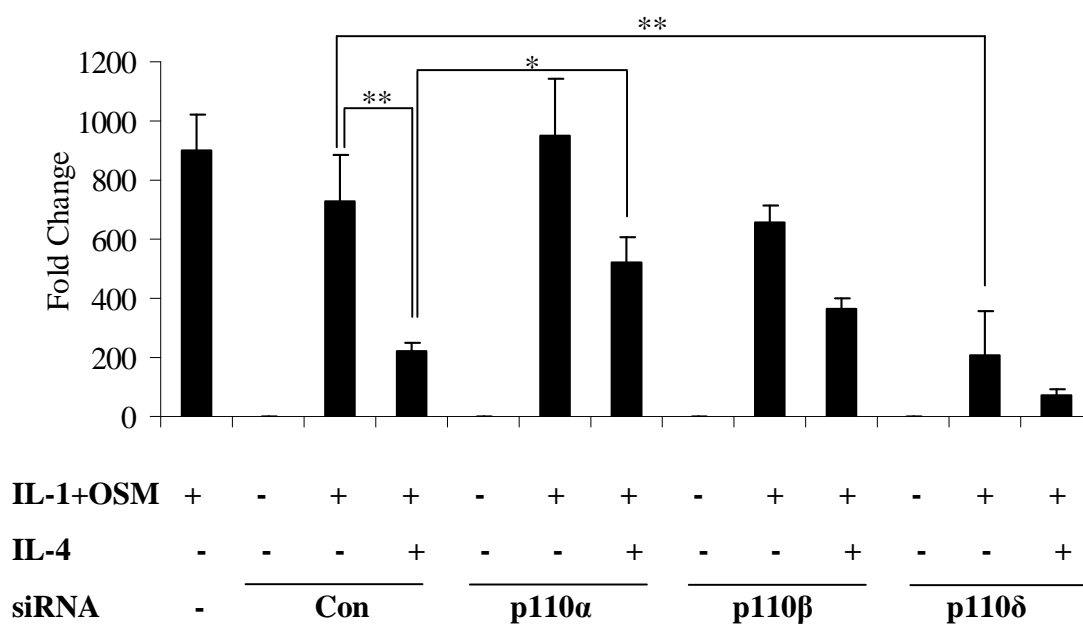


Figure 5.8 The effect of PI3K p110 isoform silencing on IL-1+OSM ± IL-4-induced MMP-13 expression in SW1353 cells. SW1353 were stimulated with control, IL-1+OSM (0.5 and 10 ng/ml, respectively) or IL-1+OSM+IL-4 (0.5, 10 and 20 ng/ml, respectively) for 24 hours following a 28 hour transfection with siRNA specific to p110α, p110β, p110δ or siCon (100 nM). Real-time RT-PCR of the isolated RNA was performed for MMP-13 72 hours after the start of transfection. Data are presented as fold induction relative to the siCon basal expression (mean ± S.E.M, $n = 6$). ** = $p \leq 0.01$; * = $p \leq 0.05$; ns = not significant. Data are from a single experiment only.

5.3 Discussion

Little is currently known about the possible function of PI3K/Akt signalling in chondrocytes and cartilage degradation in arthritis. Recent data published by this laboratory (Litherland et al. 2008) demonstrated a requirement for PI3K/Akt signalling in ECM catabolism via a role in IL-1+OSM-induced collagenase gene expression in human articular chondrocytes. This study indicated a role for p110 α and Akt1 in collagenase (MMP-1 and MMP-13) gene induction by IL-1+OSM. In addition, involvement of p110 δ and Akt3 were implicated in MMP-13 induction.

This chapter has confirmed the rapid tyrosine phosphorylation of STAT6 in response to IL-4 stimulation in chondrocytes. Maximal phosphorylation of STAT6 was shown to occur at 20 minutes in bovine nasal chondrocytes and as such this timepoint was used to examine STAT6 phosphorylation in further experiments. Previous work within the department had already established that 20 minutes was the most appropriate timepoint for examination of OSM-induced Akt phosphorylation.

The role of STAT6 in IL-4 signalling has been well documented. Whilst it has been known for some time that IL-4 can also signal through the PI3K/Akt pathway, the effect of IL-4 on Akt and GSK-3 phosphorylation had yet to be examined in chondrocytes. Data presented in this chapter demonstrate the phosphorylation, and hence activation, of Akt at both the Thr308 and Ser473 sites in response to IL-4. OSM is now strongly indicated in the pathological destruction of cartilage (Cawston et al. 1998; Hui et al. 2003; Rowan et al. 2003), in particular when in combination with other pro-inflammatory mediators such as IL-1. The report by Litherland et al. (2008) strongly suggested a role for OSM-mediated PI3K/Akt signalling in the synergistic induction of collagenase genes. OSM is known to stimulate Akt phosphorylation in human chondrocytes at both Thr308 and Ser473 (Litherland et al. 2008) and the combination of IL-4 and OSM was seen to enhance Akt phosphorylation. Pretreatment of bovine nasal chondrocytes with IL-4 was shown to reduce phosphorylation of Akt and GSK-3 in response to IL-4+OSM, suggesting that pre-incubation with IL-4 in some way inhibits the subsequent OSM-stimulated phosphorylation of Akt and GSK3. One possible explanation for this may be that IL-4 effects the

localisation of certain signalling molecules, resulting in them being unavailable for use by OSM in the phosphorylation of Akt. In many cases, the PI3K/Akt signalling pathway has been shown to be responsible for GSK-3 phosphorylation. Unusually, phosphorylation of GSK-3 by Akt results in the inactivation of GSK-3. Given that the phosphorylation of other proteins by GSK-3 often results in their inactivation, phosphorylation of GSK-3 by Akt results in the activation of many downstream pathways normally blocked by active GSK-3 (Doble and Woodgett 2003). Very few studies have investigated the cytokine-mediated phosphorylation of GSK-3 and only one other study has examined (and reported) the phosphorylation of GSK-3 by IL-4 (Vilimek and Duronio 2006). The data presented in this chapter have demonstrated that the phosphorylation, and hence inactivation, of GSK-3 by IL-4 is PI3K dependent. This would suggest that IL-4 stimulation, via the PI3K/Akt signalling pathway, results in the activation of various signalling pathways downstream of GSK-3 that would be kept inactivated by a normally constitutively active GSK-3. GSK-3 is known to participate in the insulin signalling pathway and Wnt signalling pathway, with its downstream targets including glycogen synthase and β -catenin (Rayasam et al. 2009).

At the time of writing, there was no literature available on the effect of IL-4 on the PI3K/Akt pathway in chondrocytes or in relation to arthritis. However, several reports have investigated the role of IL-4 in this signalling pathway in other cell types or in relation to other biological pathways. A recent report demonstrated an increased phosphorylation of Akt in pancreatic beta-cells following IL-4 incubation (Kaminski et al. 2010). Another study has shown that IL-4 protects the B-cell lymphoma cell line CH31 from anti-IgM-induced growth arrest and apoptosis, with the Akt pathway thought to play a major role in the suppression of the apoptotic pathway activated by IgM (Carey et al. 2007). Treatment with the Akt inhibitor, Akt1, blocked the IL-4-mediated protection of CH31 cells from anti-IgM-induced apoptosis, indicating that Akt plays a central role in the signals generated by IL-4 that protect these cells from apoptosis.

Having established that stimulation of bovine nasal chondrocytes with IL-4 results in phosphorylation of Akt and GSK-3, the next aim of this chapter was to investigate whether this phosphorylation was PI3K-dependent. Experiments performed in bovine nasal chondrocytes using the selective PI3K inhibitor, LY294002, clearly showed that the PI3K

inhibitor inhibited IL-4-stimulated phosphorylation of both Akt and GSK-3 in a concentration-dependent manner, therefore showing that IL-4-stimulation of Akt/GSK-3 is dependent on PI3K in bovine chondrocytes. Inhibition of the PI3K signalling pathway was shown to have no effect on STAT6 phosphorylation, confirming that IL-4 signals through at least two independent pathways.

Whilst LY294002 is a selective PI3K inhibitor, it does not distinguish between the four Class I PI3Ks. As discussed previously, the Class I PI3Ks consist of four closely related approximately 110 kDa catalytic subunits, namely α , β , δ and γ . To date there is little evidence that there are any significant preferences for specific catalytic subunit/regulatory subunit pairs. For that reason, the classification of a PI3K isoform in the literature generally refers only to the catalytic subunit present in the dimer. No doubt as our knowledge of PI3K signalling increases, specific functions of the regulatory subunits will be revealed (Hawkins et al. 2006). PI3K p110 α and β are known to be ubiquitously expressed in mammalian tissues whereas δ and γ expression was thought to be localised to leukocytes (Rommel et al. 2007). The study by Litherland et al. (2008) was the first to find evidence of p110 δ expression in primary human chondrocytes. Expression of all four class I PI3K isoforms has been reported in the pre-chondrogenic cell line ATDC5 (Fujita et al. 2004).

Experiments using p110 isoform-specific inhibitors were performed to investigate the roles of specific p110 isoforms in IL-4-mediated Akt phosphorylation. These experiments demonstrated that IL-4-dependent Akt activation is largely not PI3K p110 β -dependent, but may be partially dependent on p110 α . In order to investigate the role, if any, of PI3K p110 δ in IL-4-dependent Akt phosphorylation an siRNA approach was used as no p110 δ -selective inhibitors were commercially available at the time of this study. Silencing of the α , β and δ isoforms of p110 has been shown previously to be effective (≥ 75 % mRNA reduction) and selective in human chondrocytes (data not shown). Experiments utilising siRNA against the PI3K p110 isoforms in SW1353 cells demonstrated that silencing of both p110 β and p110 δ reduced both OSM- and IL-4-induced Akt phosphorylation. This was in contrast to inhibitor data presented earlier in the chapter that indicated IL-4-dependent Akt activation was not p110 β -dependent in bovine nasal chondrocytes. Data presented in Chapter 3 of this thesis demonstrated that the effect of IL-1+OSM and IL-1+OSM+IL-4 on collagenase gene

expression was very similar in bovine nasal chondrocytes, human articular chondrocytes and SW1353 cells. However, these results could indicate subtle differences in PI3K p110 isoform involvement in OSM-induced Akt phosphorylation in different types of chondrocytes.

Previous reports have indicated a role for p110 α and p110 δ in the induction of MMP-13 by IL-1+OSM (Litherland et al. 2008) in human chondrocytes. Data presented in this chapter show a significant reduction in MMP-13 induction by IL-1+OSM in SW1353 cells following p110 δ silencing, but not following p110 α silencing. Again, this could be indicative of differences in PI3K signalling in primary chondrocytes and the SW1353 cell line. Interestingly, silencing of p110 α appeared to reduce the ability of IL-4 to repress IL-1+OSM-induced MMP-13 expression. Unfortunately, due to time constraints, siRNA work was not extended to bovine chondrocytes. In addition, the siRNA experiments were only performed once. In order to confirm the results obtained in this chapter, it would be necessary to perform several repeats of these experiments. As optimisation of p110 silencing was originally performed in human chondrocytes, it would also be necessary to perform optimisation experiments in SW1353 cells to confirm the effectiveness and selectivity of gene knockdown.

The data presented in this chapter further highlight the complexity of the PI3K/Akt signalling pathway. Further work is needed to better understand the importance of specific isoforms in IL-4-induced Akt phosphorylation. Unfortunately, given that the induction of MMP-13 by IL-1+OSM has been shown to be PI3K-dependent (Litherland et al. 2008), investigating the effect of PI3K inhibition on IL-1+OSM+IL-4-mediated MMP-13 repression will clearly be problematic.

Whilst the results presented in this chapter are mostly preliminary, an important finding was that stimulation of chondrocytes with the pro-inflammatory cytokine OSM and the chondroprotective cytokine IL-4, both resulted in Akt phosphorylation, indicating Akt activation. The study by Litherland et al. (2008) also suggested that Akt activation in chondrocytes may mediate different downstream signalling events, depending on the nature of the stimulus. As mentioned previously, the three different Akt isoforms are suspected of

having different biological functions, suggesting that additional mechanisms exist to fine-tune the downstream effects following Akt phosphorylation. Numerous Akt-interacting proteins have been identified, some of which appear to lack any intrinsic kinase activity, suggesting they modulate the activity of Akt by affecting enzymatic activity or cellular localisation and distribution (Franke 2008). One of the aims of the remainder of this PhD is to investigate candidate Akt-interacting proteins that could be responsible for the dramatically different downstream effects of OSM and IL-4 following Akt activation.

5.4 Summary

- IL-4 induces the tyrosine phosphorylation of STAT6 in bovine and human chondrocytes.
- Phosphorylation of Akt and GSK-3 by IL-4 is PI3K-dependent in bovine nasal chondrocytes.
- Phosphorylation of Akt by IL-4 is partially dependent on p110 α in bovine nasal chondrocytes.
- Preliminary results suggest that silencing of both p110 β and p110 δ appears to inhibit IL-4-induced Akt phosphorylation in SW1353 cells, and silencing of p110 δ inhibits the induction of MMP-13 by IL-1+OSM in SW1353 cells.

Chapter 6: Assessment of altered gene expression following IL-4 stimulation of cartilage and chondrocytes by genome-wide microarray analysis

6.1 Introduction

IL-4 has been shown to act as a protective factor in cartilage, preventing pro-inflammatory cytokine-induced cartilage breakdown (Cawston et al. 1996). Data indicate that IL-4 mediates its effect by reducing levels of active collagenase, in particular MMP-13. In order to provide clues to the protective mechanism of action of IL-4, whole genome-wide arrays were performed to assess the effect of IL-4 and the pro-inflammatory cytokines IL-1±OSM on global gene expression in cartilage and chondrocytes.

Genome-wide microarray analysis is an extremely powerful technique that enables the examination of the gene expression of thousands of transcripts in one single experiment. Several research groups have used this technique to increase understanding regarding the molecular changes observed in OA (Aigner et al. 2006; Sato et al. 2006; Appleton et al. 2007; Fukui et al. 2008; Geyer et al. 2009; Karlsson et al. 2010). These studies compared gene expression levels in normal cartilage to OA cartilage as well as in cartilage from animals with experimentally-induced arthritis. The data presented in this chapter are the first to examine the effect of pro- and anti-inflammatory cytokine treatment in the context of arthritis on a genome-wide basis.

In this chapter, global gene expression following cytokine stimulation was examined in bovine nasal cartilage, primary human articular chondrocytes and SW1353 cells. Analysis of three independent systems was performed to assess similarity in gene expression profiles between the three different systems and to aid validation and the robustness of results.

The aim of this chapter was to:

- Perform genome-wide microarray analyses of stimulated cartilage and chondrocytes (control, IL-1, IL-1+OSM and IL-1+OSM+IL-4) in order to identify genes potentially involved in the chondroprotective action of IL-4 and hence the repression of MMP-13.

6.2 Results

6.2.1 Preliminary data

6.2.1.1 Preliminary data from the bovine nasal cartilage model used to generate RNA for use on the GeneChip® Bovine Genome Array.

The GeneChip® Bovine Genome Array allows the gene expression of over 23,000 bovine transcripts to be analysed. A 14-day bovine nasal cartilage degradation assay was performed to generate RNA for the GeneChip® Bovine Genome Array. Bovine nasal cartilage was stimulated with control medium ± IL-1 ± OSM ± IL-4 (added at day 7 of timecourse only) for 14 days. Figure 6.1 shows a variety of preliminary data from the bovine nasal cartilage experiment that was used to generate RNA for the genome-wide microarray. Due to the quantity of RNA required for the array, it was not possible to perform replicates in this experiment (the size of the experiment was limited by the size of the bovine nasal septum used) and so all the data presented in Figure 6.1 are representative of a single data set only. A hydroxyproline assay was performed to confirm that IL-4 had effectively protected the bovine nasal cartilage from IL-1+OSM-induced collagen release. Figure 6.1a shows that IL-1+OSM stimulated a 54% collagen release and the protective effect of IL-4 reduced this collagen release to 2.5%. Ordinarily in a 14-day timecourse, cartilage is harvested and RNA extracted at regular timepoints throughout the 14-days in order to provide an overall view of collagen release and gene expression during cartilage degradation. However, due to cost, it was only possible to perform genome-wide arrays on four samples. As four different cytokine treatments were included in the experiment (control, IL-1, IL-1+OSM and IL-1+OSM+IL-4), it was necessary to select only one timepoint for genome-wide analysis. Collagen release occurs during a very short timeframe and so a “snapshot” of the gene profile immediately preceding this collagen release was

judged to be the most appropriate use of the arrays. Previous experiments using the bovine nasal cartilage model have reproducibly demonstrated that collagen release occurs between day 11 and day 12 of the 14-day timecourse and as such the experiment was performed so that cartilage was harvested at days 10, 11, 12 and 14 of the timecourse. Figure 6.1b clearly shows that collagen release began between day 11 and day 12 of the timecourse and so RNA from the cartilage harvested on day 11 of the assay was selected for use in the array.

Before the RNA from day 11 of the timecourse was used on the genome-wide array, it was important to perform several other preliminary checks to act as internal controls. Active and total collagenase levels were examined to confirm that IL-4 had suppressed levels of active collagenase, as previously observed in data presented in Chapter 3 of this thesis. IL-4 was shown to completely inhibit IL-1+OSM-induced active collagenase levels (Figure 6.1c) and strongly reduce the levels of total collagenase (Figure 6.1d). Real-time RT-PCR was performed to confirm the effect of IL-4 on the collagenases was as expected i.e. to confirm that IL-1+OSM-induced MMP-13 was completely repressed by IL-4 and MMP-1 was slightly up-regulated (Figure 6.1e and f). All the preliminary experiments performed on the RNA produced the expected results and so the four samples of bovine RNA from day 11 of the assay were sent to Geneservice (Nottingham, UK) for completion of the array.

6.2.1.2 Preliminary data from human articular chondrocytes and SW1353 cells used to generate RNA for the Sentrix Human-6 Expression BeadChip.

The majority of the work presented in this thesis has involved either bovine cartilage or bovine chondrocytes, hence the decision to perform genome-wide screening in the bovine model. However, a human genome-wide array would be more relevant to human disease and so it was decided to also generate human RNA for use on an Illumina Array. The Sentrix Human-6 Expression BeadChip contains six arrays on a single BeadChip, each with >46,000 probes derived from human genes in the National Center for Biotechnology Information (NCBI) Reference Sequence (RefSeq) and UniGene databases. Again, due to cost, only six RNA samples could be selected for the array. RNA generated from a combination of both human articular chondrocytes and SW1353 cells was used. Due to the inherent variability in cultures of primary human osteoarthritic chondrocytes, if a genome-

wide array showed a similar gene expression profile between human articular chondrocytes and SW1353 cells, this would increase the confidence with which highlighted potential targets could be pursued. As only six samples could be chosen, it was necessary to eliminate one of the four cytokine treatments that had been included on the bovine array, for both human articular chondrocytes and SW1353 cells. For human articular chondrocytes, control, IL-1+OSM and IL-1+OSM+IL-4 treatments were selected. It was decided not to select a control sample for the SW1353 cells as well, but instead to select IL-1, IL-1+OSM and IL-1+OSM+IL-4 as this might provide additional data regarding the mechanism of synergy between IL-1+OSM in a model where this feature is more robust. Human articular chondrocytes and SW1353 cells were stimulated with the appropriate cytokines for 24 hours, at which point they were lysed and the RNA extracted. As with the bovine RNA, several preliminary checks were performed to assess the effect of IL-4 on the collagenase genes prior to it being sent for microarray analysis. For both human articular chondrocytes and SW1353 cells, cells were seeded in both T25 flasks (to provide sufficient RNA for the array) and 96-well plates (to enable real-time RT-PCR to be performed). Figure 6.2 confirms that in the RNA used for the array, IL-4 was able to significantly inhibit IL-1+OSM-induced MMP-13 expression in human articular chondrocytes (Figure 6.2c and d), but had no significant effect on IL-1+OSM-induced MMP-1 expression (Figure 6.2a and b). Figure 6.3 confirmed the same to be true in the RNA extracted from SW1353 cells to be used in the array. As all preliminary experiments produced the expected results, the RNA was sent to the Centre for Microarray Resources (Cambridge, UK) for completion of the Illumina array.

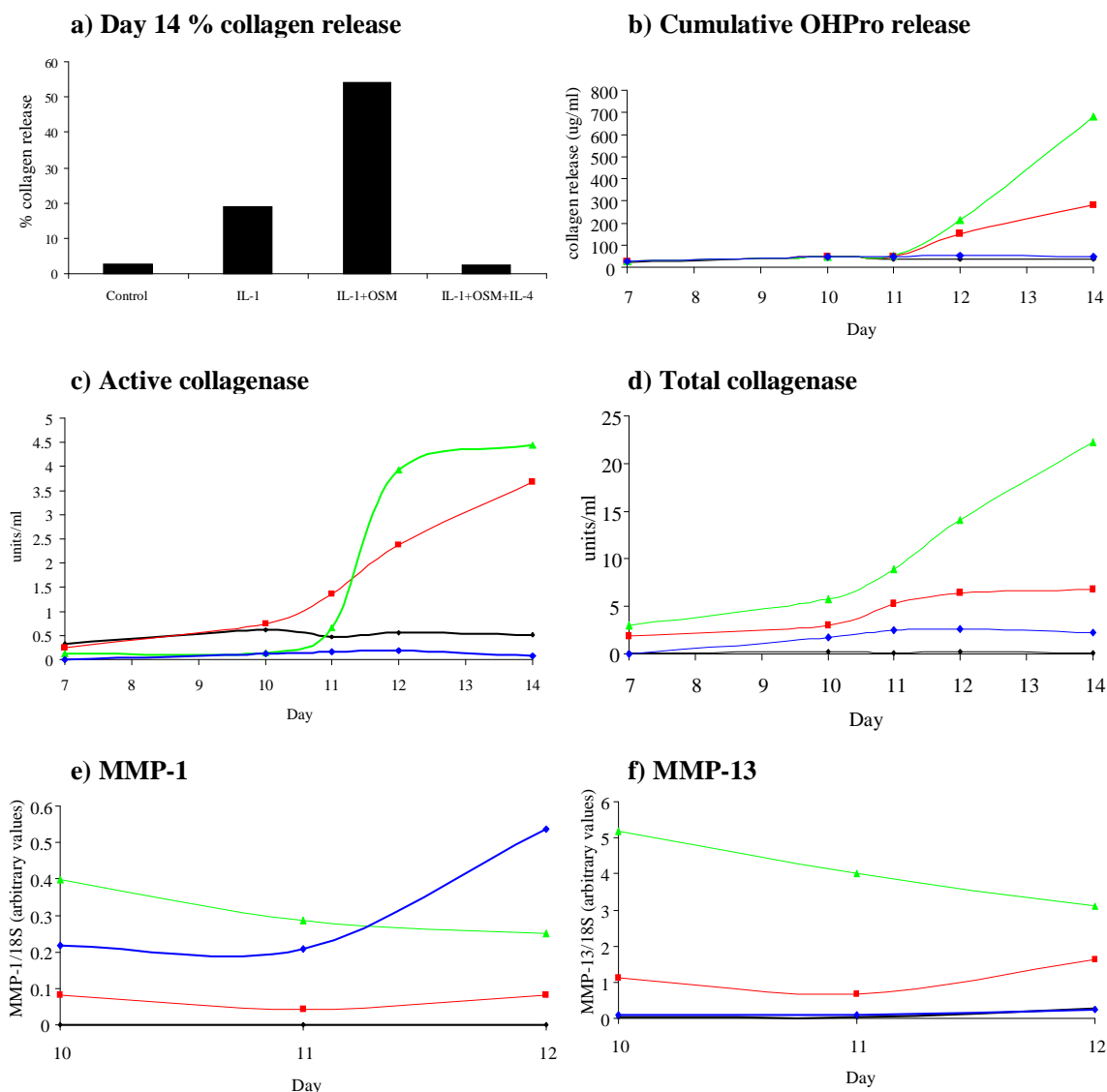


Figure 6.1 Preliminary data from the bovine nasal cartilage model used to generate RNA for use on the GeneChip® Bovine Genome Array. Bovine nasal cartilage chips (n=1) were cultured in DMEM ± IL-1 (1 ng/ml) ± OSM (10 ng/ml) ± IL-4 (20 ng/ml, added at day 7 of culture) for 14 days. At day 7, medium was removed and replenished. Cartilage and media were harvested at days 10, 11, 12 and 14. As a measure of collagen release, the levels of hydroxyproline (OHPro) released into the media were assayed; percentage collagen release at day 14 and cumulative OHPro release are shown (a and b). Levels of active collagenase were measured (c) and APMA was used to activate pro-collagenases in order to measure the total collagenase activity (pro+active) (d). RNA was extracted from the cartilage and collagenase gene expression was determined by real-time RT-PCR (e and f). The real-time RT-PCR data are presented relative to 18S rRNA. Key: ◆ = control, ■ = IL-1, ▲ = IL-1+OSM, ◆ = IL-1+OSM+IL-4.

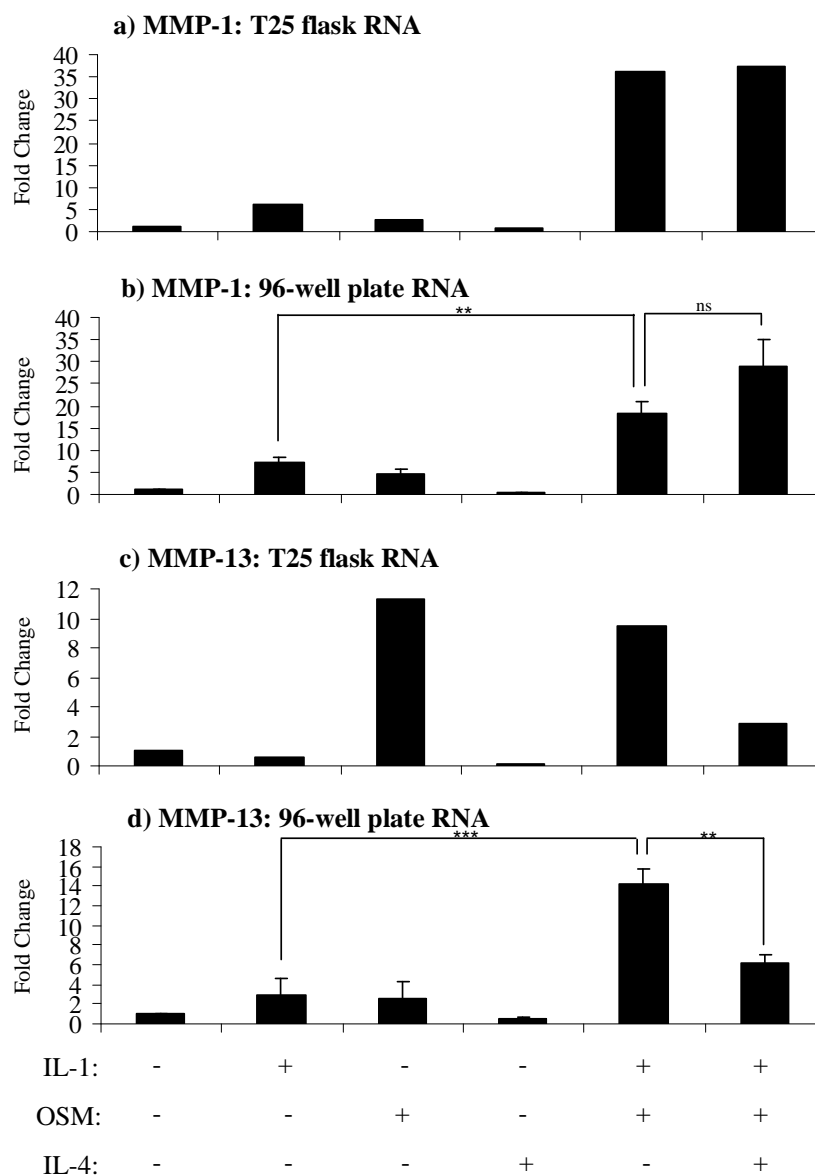


Figure 6.2 Preliminary data from human articular chondrocytes used to generate RNA for the Sentrix Human-6 Expression BeadChip. Human articular chondrocytes were seeded in 96-well plates and T25 flasks according to section 2.2.3 of Materials and Methods and stimulated for 24 hours with DMEM \pm IL-1 (0.02 ng/ml) \pm OSM (10 ng/ml) \pm IL-4 (20 ng/ml). Following treatment, total RNA was isolated from cells, reverse transcribed and the cDNA was used in real-time RT-PCR reaction assays, as described in Materials and Methods section 2.2.5, to examine MMP-1 and MMP-13 gene expression. RNA was extracted from human articular chondrocytes in 96-well plates using the SideStepTM Kit to confirm the expected MMP-1 and MMP-13 expression (n=6) and from human articular chondrocytes in T25 flasks using the RNeasy[®] Mini Kit to prepare RNA for the Sentrix Human-6 Expression BeadChip (n=1). Results from 96-well plate experiments were normalised to 18S rRNA and expressed as mean \pm SEM (n=6). *** = $p \leq 0.001$; ** = $p \leq 0.01$; ns = not significant.

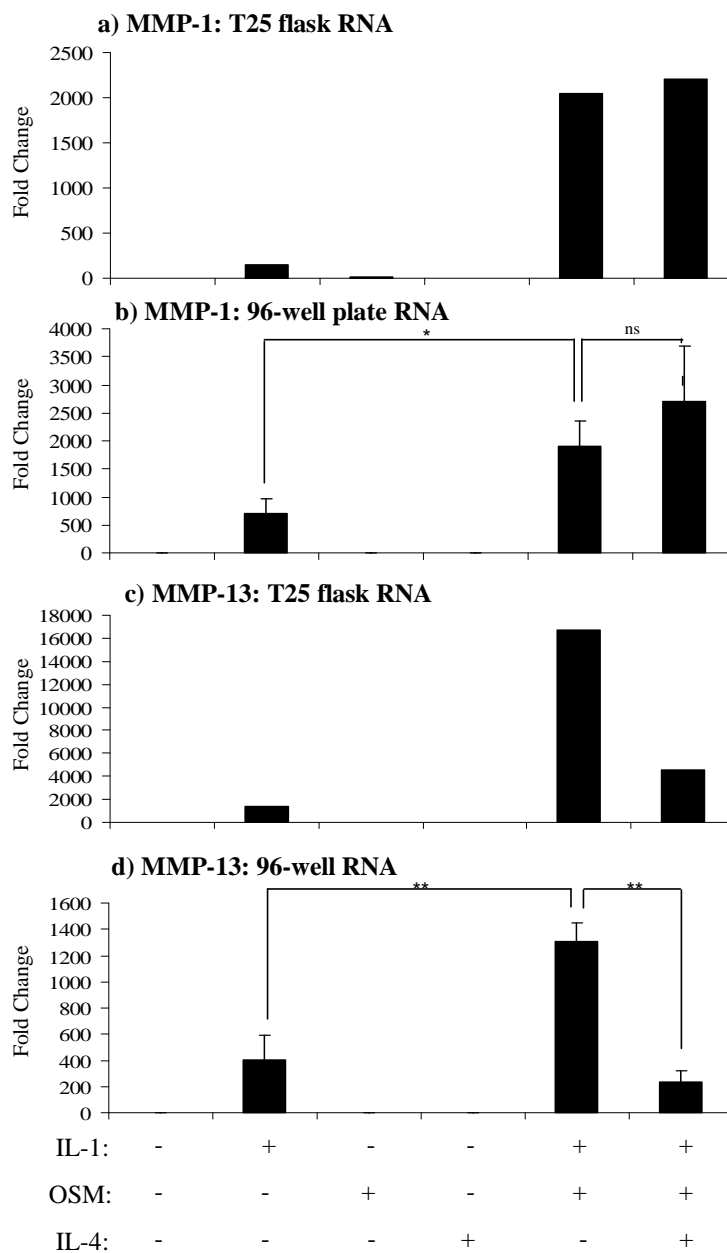


Figure 6.3 Preliminary data from SW1353 cells used to generate RNA for the Sentrix Human-6 Expression BeadChip. SW1353 cells were seeded in 96-well plates and T25 flasks according to section 2.2.3 of Materials and Methods and stimulated for 24 hours with DMEM:F12 \pm IL-1 (0.5 ng/ml) \pm OSM (10 ng/ml) \pm IL-4 (20 ng/ml). Following treatment, total RNA was isolated from cells, reverse transcribed and the cDNA was used in real-time RT-PCR reaction assays, as described in Materials and Methods section 2.2.5, to examine MMP-1 and MMP-13 gene expression. RNA was extracted from SW1353 cells in 96-well plates using the SideStepTM Kit to confirm the expected MMP-1 and MMP-13 expression (n=6) and from SW1353 cells in T25 flasks using the RNeasy[®] Mini Kit to prepare RNA for the Sentrix Human-6 Expression BeadChip (n=1). Results from 96-well plate experiments were normalised to 18S rRNA and expressed as mean \pm SEM (n=6). ** = $p \leq 0.01$; ns = not significant.

6.2.2 Analysis of genome-wide microarray results

Gene expression analysis was carried out using GeneSpring GX software. Due to the vast amount of data generated by the microarrays, thresholds of fold change were set to produce more manageable sized gene lists. For unknown reasons, Affymetrix arrays (GeneChip® Bovine Genome Array) characteristically produce higher fold changes than Illumina arrays (Sentrix Human-6 Expression BeadChip) (personal communication, Dr Daniel Swan, Newcastle University). As such only genes with ≥ 2 fold change in the bovine array were examined (see appendix B for full gene lists). This threshold was lowered to ≥ 1.5 fold change for the Illumina array data (human articular chondrocytes and SW1353 cells) (see appendices C and D for full gene lists). Figures 6.4, 6.5 and 6.6 show the gene trees generated by the GeneSpring software, with red bars indicating up-regulated genes and blue bars indicating down-regulated genes.

One of the aims of the microarray analysis was to examine the similarity in gene profiles between the three different models used in this thesis, namely, bovine nasal cartilage, human articular chondrocytes and SW1353 cells. Venn diagrams were used to show the number of overlapping up- or down-regulated genes between the different models (Figures 6.7 and 6.8) The lack of similarity between up and down-regulated genes shown in the ≥ 2 fold change Venn diagram (Figure 6.7) was not unexpected and highlights the difference between 3D tissue and cells in monolayer. When the fold change threshold was lowered to include all genes which were up or down-regulated by ≥ 1.5 fold, the number of common genes between human articular chondrocytes and SW1353 cells increased (Figure 6.8).

Following examination of the gene profiles produced by GeneSpring, a thorough literature search was performed to shortlist genes for further study.

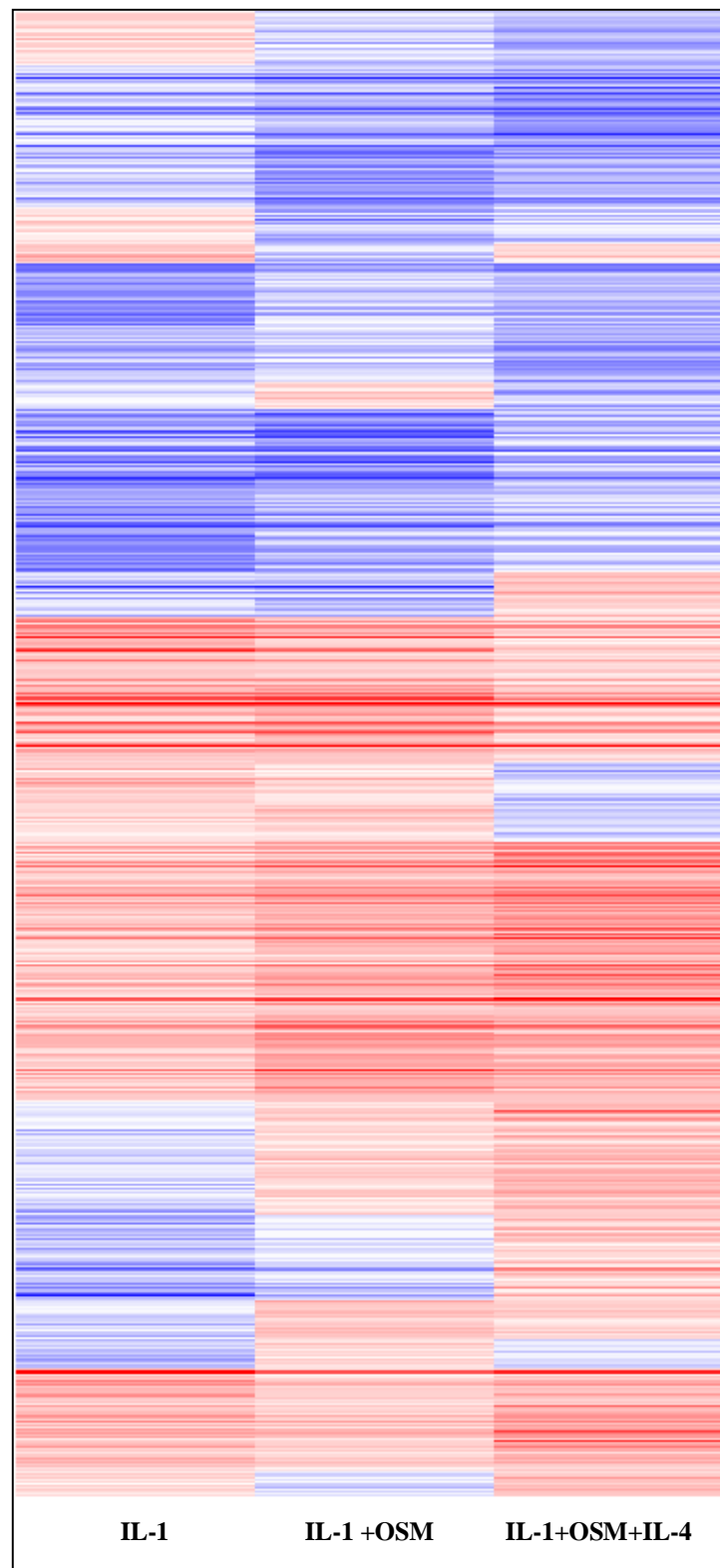


Figure 6.4 Gene tree: GeneChip® Bovine Genome Array. Coloured according to expression versus control samples, with red bars indicating up-regulated genes, blue bars indicating down-regulated genes and white bars representing genes with no change in expression versus control.

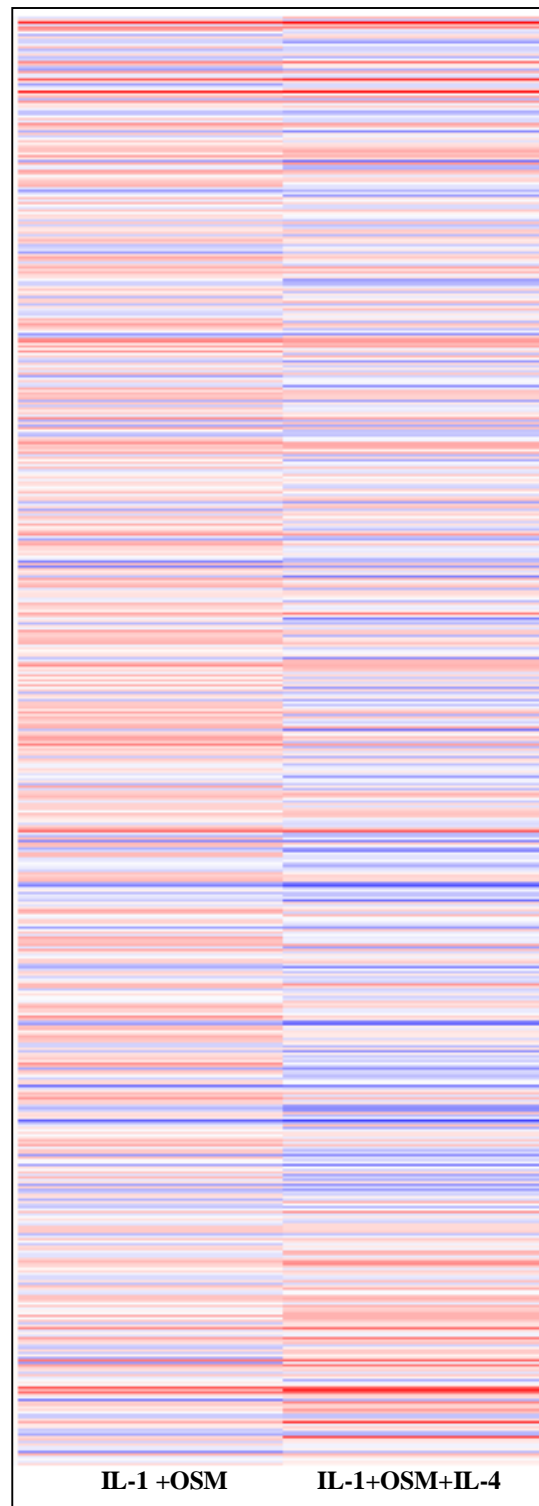


Figure 6.5 Gene tree: Human articular chondrocyte Sentrix Human-6 Expression BeadChip. Coloured according to expression versus control samples, with red bars indicating up-regulated genes, blue bars indicating down-regulated genes and white genes representing a gene with no change in expression versus control.

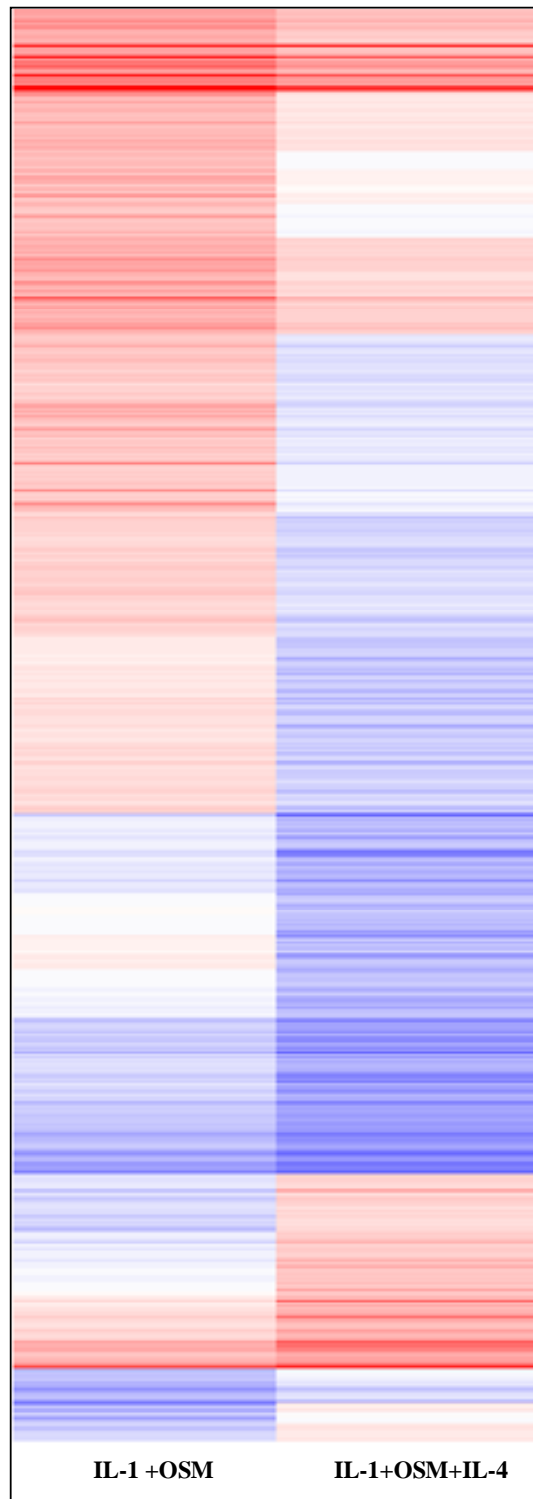


Figure 6.6 Gene tree: SW1353 cells Sentrix Human-6 Expression BeadChip. Coloured according to expression versus IL-1-treated samples, with red bars indicating up-regulated genes, blue bars indicating down-regulated genes and white bars representing genes with no change in expression versus IL-1-treated samples.

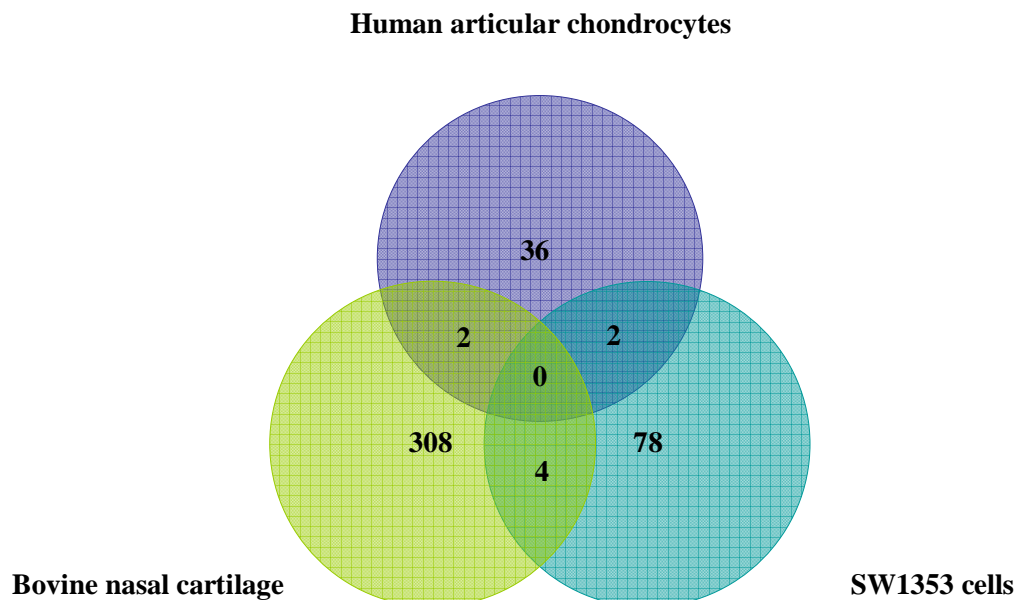
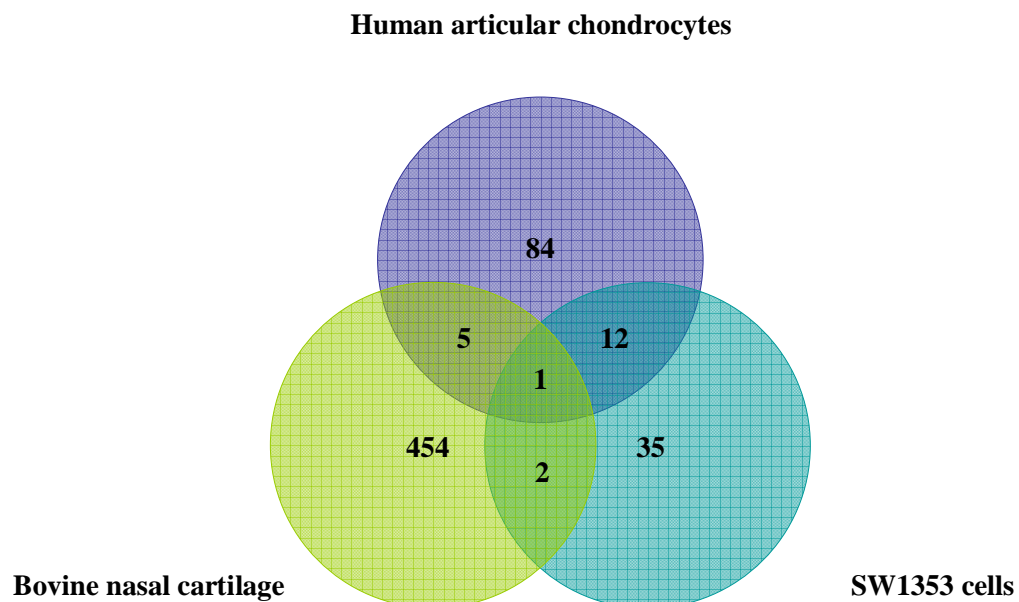
a) Up-regulated ≥ 2 foldb) Down-regulated ≥ 2 fold

Figure 6.7 Venn diagrams showing the overlap of genes up- or down-regulated ≥ 2 fold in IL-1+OSM+IL-4-stimulated bovine cartilage, human articular cartilage and SW1353 cells compared to IL-1+OSM-stimulated bovine cartilage, human articular chondrocytes and SW1353 cells.

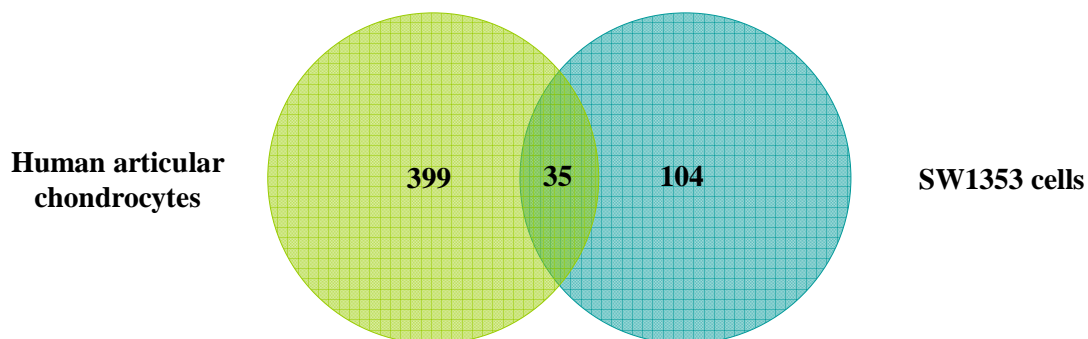
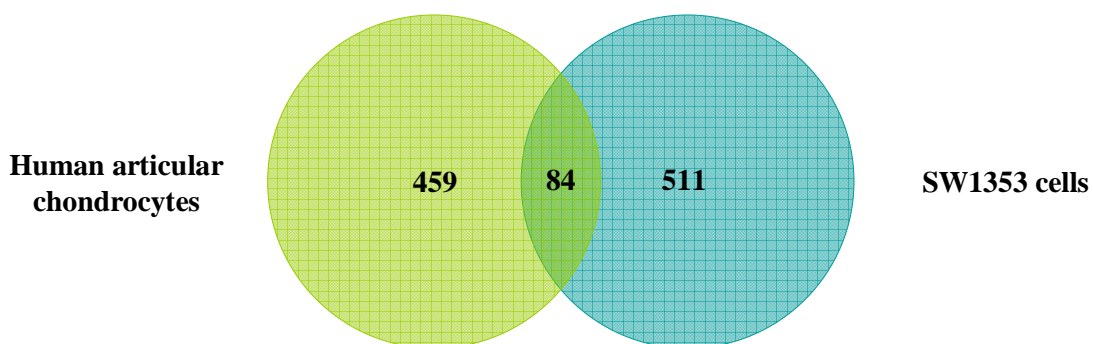
a) Up-regulated ≥ 1.5 fold**b) Down-regulated ≥ 1.5 fold**

Figure 6.8 Venn diagrams showing the overlap of genes up- or down-regulated ≥ 1.5 fold in IL-1+OSM+IL-4-stimulated human articular cartilage and SW1353 cells compared to IL-1+OSM-stimulated human articular chondrocytes and SW1353 cells.

6.2.3 Candidate genes selected for further study

The primary aim of this study was to increase the understanding of the chondroprotective mechanism of action of IL-4 and in particular, how IL-4 is able to strongly repress IL-1+OSM-induced MMP-13 expression. Therefore, this section focuses on the differences in gene expression profiles between IL-1+OSM-stimulated cartilage/cells and IL-1+OSM+IL-4-stimulated cartilage/cells. After examination of the most highly up- or down-regulated genes (IL-1+OSM+IL-4 vs IL-1+OSM) and a thorough literature search, the genes listed in section 6.2.3.1 and Table 6.1 were selected as candidate genes in the protective mechanism of action of IL-4 and therefore shortlisted for further study (Figures 6.9, 6.10 and 6.11).

6.2.3.1 Reasoning behind selection of shortlisted genes

Genes up-regulated by IL-1+OSM+IL-4 vs IL-1+OSM

A newly induced gene, and thus a gain of function, could help to explain the mechanism of MMP-13 repression following inclusion of IL-4.

Chemokine ligand 26 (CCL26)

- CCL26, also known as eotaxin-3, is a small cytokine belonging to the CC chemokine family.
- Highest up-regulated gene in both human articular chondrocytes and SW1353 cells.
- CCL26 contains two STAT6 binding sites (through which IL-4 is known to signal) (Blanchard et al. 2005).
- Polymorphisms of CCL26 may be associated with susceptibility to RA (Chae et al. 2005).

Protein kinase C zeta (PKC ζ)

- PKC ζ is a serine/threonine kinase involved in the regulation of various signalling pathways, including the NF κ B pathway.
- Indicated in previous literature (Hussain et al. 2002) and current studies in the lab to be important in collagenase expression.

Regulator of G-protein signalling 4 (RGS4)

- RGS4 belongs to the RGS family of proteins, which act as negative regulators of G-protein mediated signalling by increasing the intrinsic GTPase activity of heterotrimeric G proteins (Bansal et al. 2007).
- Up-regulated in both human articular chondrocytes and SW1353 cells.
- Involvement of G proteins such as PAR is suspected to be important in collagenase gene expression.

Basic leucine zipper transcription factor (BATF3/SNFT)

- BATF3 is a small nuclear factor originally isolated from T cells, the over-expression of which leads to the repression of transcription from several AP-1-driven promoters (Bower et al. 2004).
- Up-regulated in both human articular chondrocytes and SW1353 cells.
- Over-expression of p21SNFT had been shown to repress MMP-1 expression (Bower et al. 2004).

Tribble 1 (Trb1)

- Trb1 is one of three members of a newly identified family of proteins, thought to play a role in regulating cell signalling pathways (Hegedus et al. 2007).
- Up-regulated in human articular chondrocytes, SW1353 cells and bovine cartilage.
- Trb3 is a known regulator of Akt (Matsumoto et al. 2006), which is involved in collagenase expression and Akt is known to be activated by IL-4.

Genes down-regulated by IL-1+OSM+IL-4 vs IL-1+OSM

A newly down-regulated gene, and thus a loss of function, could also help explain the mechanism of MMP-13 repression following inclusion of IL-4.

Autotaxin (ENNP2)

- ENNP2 is a secreted glycosylated enzyme that exhibits lysophospholipase D activity, hydrolyzing lysophosphatidylcholine to lysophosphatidic acid.
- Over-expressed in RA patients (Kehlen et al. 2001).
- Important in the generation of lysophosphatidic acid (LPA), which plays a critical role in the induction of COX-2 in collaboration with inflammatory cytokines in RA synovial cells (Nochi et al. 2008).

Growth arrest-specific 1 (GAS1)

- GAS1 is an integral membrane protein.
- Down-regulated in both human articular chondrocytes and SW1353.
- Chondrocytes over-expressing GAS1 are unable to participate in cartilage formation (Lee et al. 2001) therefore down-regulation of GAS1 may be part of the protective mechanism of action of IL-4.

Phosphodiesterase 5 (PDE5)

- PDE5 belongs to a family of enzymes that degrade the phosphodiester bond in cAMP and cGMP, thereby acting as important regulators of signal transduction mediated by these molecules.
- PDE5 specific inhibitors suppress IL-1-induced nitric oxide (NO) release and inducible nitric oxide synthase (iNOS) mRNA expression (Geng et al. 1998) and NO has previously been linked to collagenase expression (Zaragoza et al. 2002; Zaragoza et al. 2006).

S100A8/S100A9

- S100A8 and S100A9 are calcium binding proteins that are important pro-inflammatory mediators in acute and chronic inflammation.
- Inflammatory cytokines such as IL-1 have been shown to upregulate S100A8/S100A9, which are both found in and around chondrocytes in experimental models of arthritis. Stimulation of chondrocytes with S100A8 has been shown to significantly upregulate various MMPs, including MMP-13 (van Lent et al. 2008).
- RAGE (receptor for advanced glycation end products)-mediated signalling cascades are known to lead to increased production of MMP-13 (Yammani et al. 2006). S100A8 and S100A9 have been shown to interact with RAGE (Boyd et al. 2008) and therefore a decrease in S100A8/S100A9 could be at least partly responsible for the repression of MMP-13 by IL-4.

Syndecan 1 (SDC1)

- SDC1 is a transmembrane heparan sulphate proteoglycan important in cell binding, cell signalling and cytoskeletal organisation.
- Down-regulated in human articular chondrocytes, SW1353 cells and bovine cartilage.

- SDC1 is up-regulated in articular cartilage during early stages of cartilage degeneration suggesting it is involved in attempted repair (Salminen-Mankonen et al. 2005).
- Expression of SDC1 is higher in chondrocytes derived from OA cartilage than in those from normal cartilage (Barre et al. 2000).

Thrombospondin 1 (THBS1)

- THBS1 is a large glycoprotein that is secreted in response to cell injury and various growth factors.
- Down-regulated in human articular chondrocytes, SW1353 cells and bovine cartilage.
- Increased plasma levels of THBS1 correlate with increased levels of pro-inflammatory cytokines in RA patients (Rico et al. 2008).

Genes up-regulated by IL-1+OSM+IL-4 vs IL-1+OSM				Genes down-regulated by IL-1+OSM+IL-4 vs IL-1+OSM			
Gene	Fold Change			Gene	Fold Change		
	HAC	SW	Bovine		HAC	SW	Bovine
CCL26	88	21	N/A	ENPP2	2.1	1.2	N/A
PKC ζ	2	N/A	N/A	GAS1	4	1.8	N/A
RGS4	8.6	4.7	N/A	PDE5	2	N/A	N/A
SNFT	15.3	4.7	N/A	S100A8	1.1	3.7	1.9
TRIB1	1.2	1.6	3.9	S100A9	1.1	4.9	3.7
				SDC1	2.6	1.5	2
				THBS1	2.2	2.5	2

Table 6.1 List of genes selected for further study from microarray data. HAC = human articular chondrocyte array results, SW = SW1353 cells array results and bovine = bovine articular cartilage array results. N/A refers to a gene either not being present on the array or to a gene failing to pass the normalisation process.

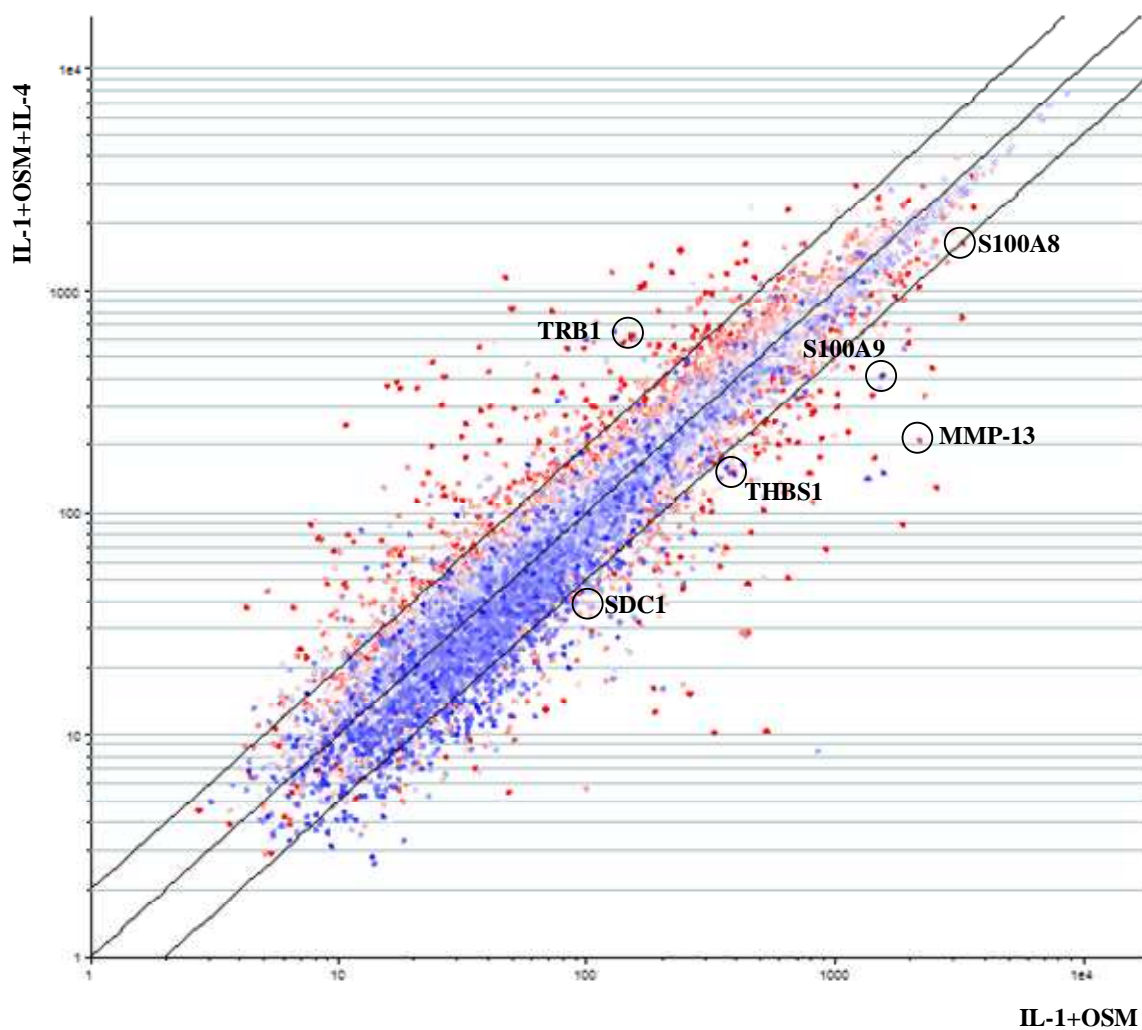


Figure 6.9 Scatter plot showing genes up- or down-regulated >2 fold (IL-1+OSM+IL-4 versus IL-1+OSM) on the GeneChip® Bovine Genome Array. Coloured according to expression versus control samples, with red dots representing up-regulated genes and blue dots representing down-regulated genes. Genes of interest have been circled.

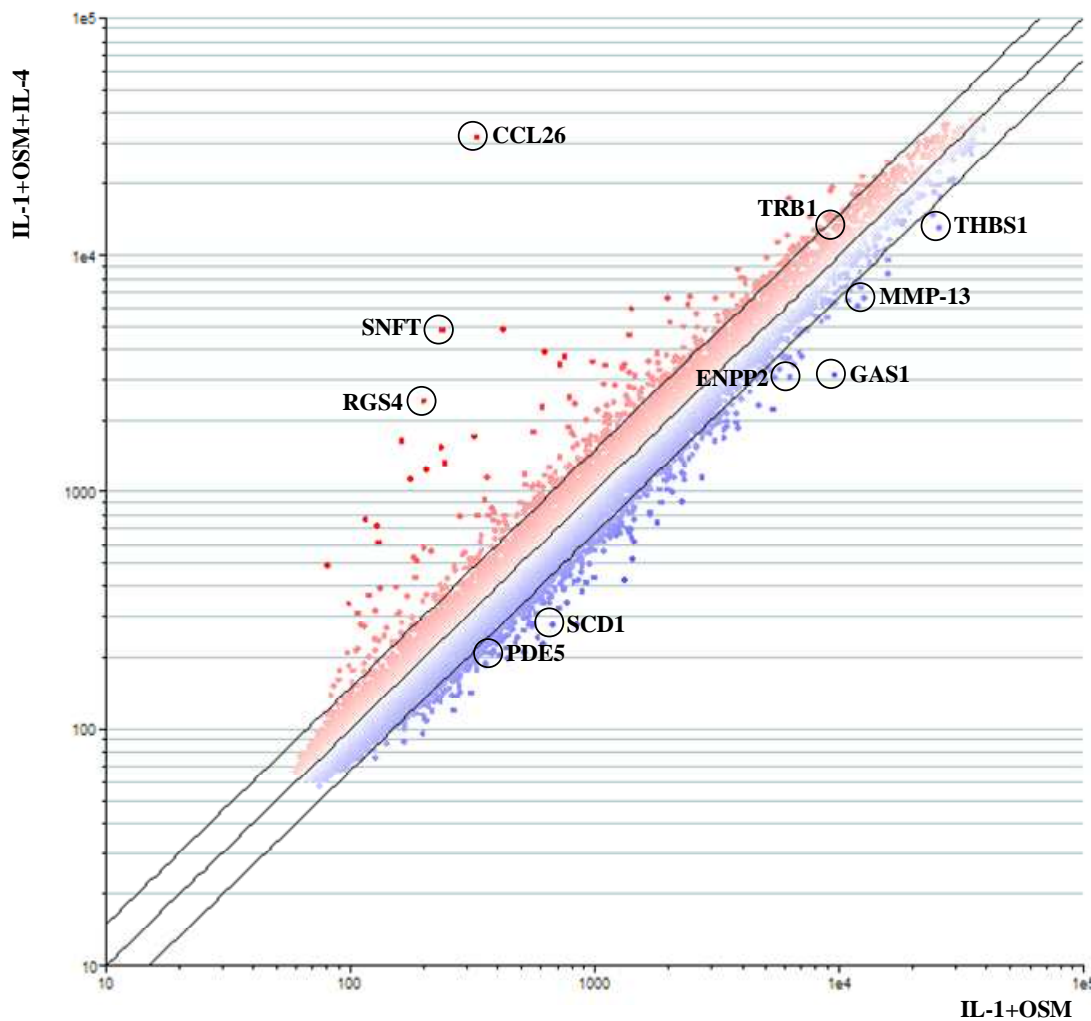


Figure 6.10 Scatter plot showing genes up- or down-regulated >1.5 fold (IL-1+OSM+IL-4 versus IL-1+OSM) on the Sentrix Human-6 Expression BeadChip (human articular chondrocytes). Coloured according to expression versus IL-1+OSM+IL-4 samples, with red dots representing up-regulated genes and blue dots representing down-regulated genes. Genes of interest have been circled.

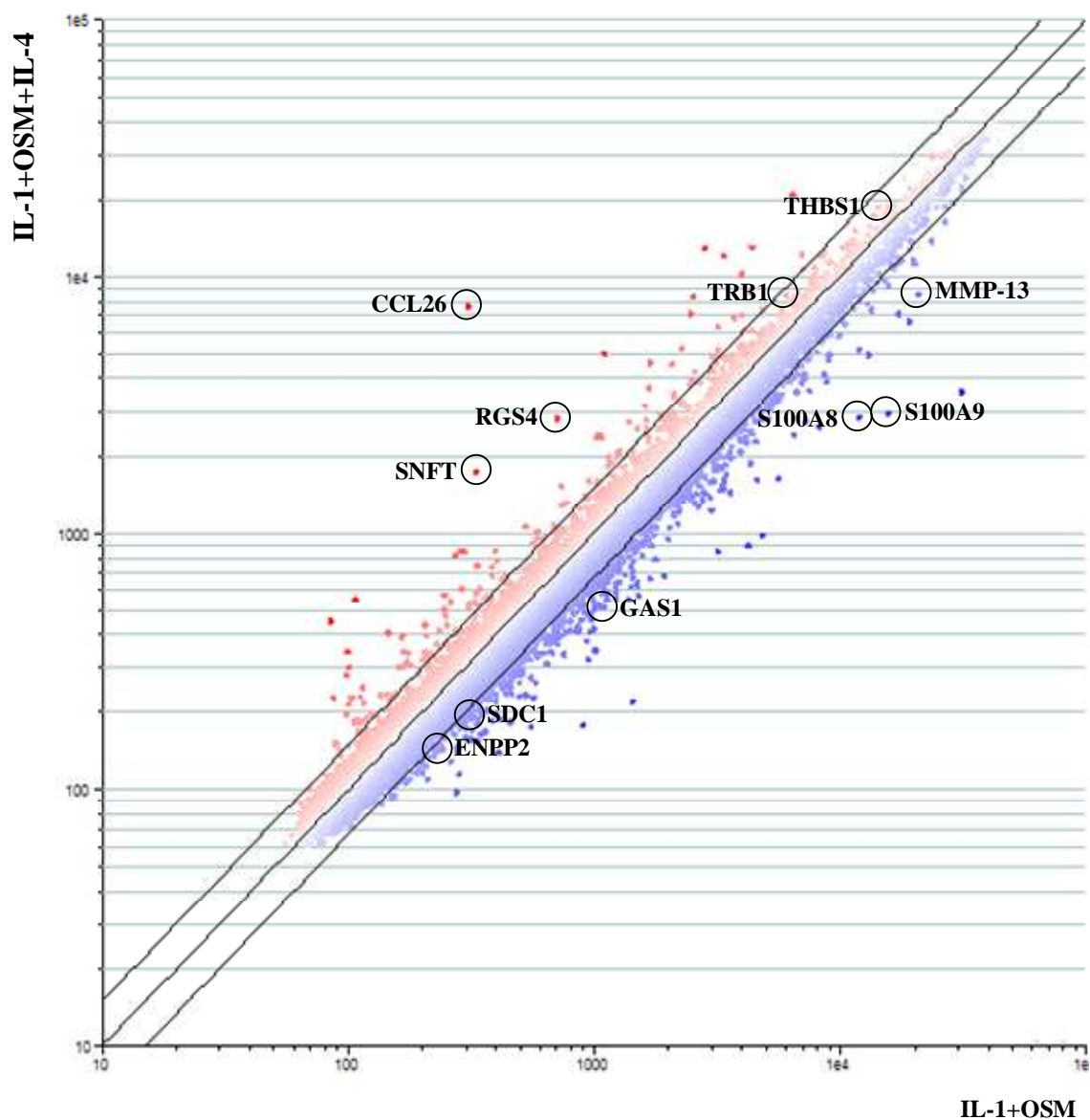


Figure 6.11 Scatter plot showing genes up- or down-regulated >1.5 fold (IL-1+OSM+IL-4 versus IL-1+OSM) on the Sentrix Human-6 Expression BeadChip (SW1353 cells). Coloured according to expression versus IL-1+OSM+IL-4 samples, with red dots representing up-regulated genes and blue dots representing down-regulated genes. Genes of interest have been circled.

6.3 Discussion

In this chapter the genome-wide effects of various cytokine combinations (control, IL-1, IL-1+OSM and IL-1+OSM+IL-4) were compared in three different systems; bovine nasal cartilage, human articular chondrocytes and SW1353 cells. In order to identify genes potentially involved in the repression of MMP-13 by IL-4, this chapter focused on the differences in gene expression profiles between IL-1+OSM-treated cells/cartilage and IL-1+OSM+IL-4-treated cells/cartilage. However, the data generated by this screen have also provided information regarding the genes involved in synergy between IL-1 and OSM.

Whilst several groups have examined differences in gene expression profiles between normal and OA cartilage, this is the first genome-wide array to examine the specific effects of certain cytokine combinations (known to be relevant to arthritic disease) on global gene expression. One problem encountered by groups examining gene profiles from both OA and normal cartilage has been the high variability of gene expression levels between different donors. This is perhaps not surprising in OA tissue; however the large difference in gene expression in normal donors indicates that a wide range of gene expression is compatible with normal joint function. Unfortunately, this also suggests that complicated networks of genes are responsible for abnormal joint changes, rather than single components (Aigner et al. 2006). As no replicates were performed in the genome-wide screens performed in this chapter, it is impossible to comment on any variation between different bovine or human cartilage donors. However, as three different systems were examined, it is acceptable to presume that any similarity in up- or down-regulation of particular genes found in all three models represents an accurate result.

Previous genome-wide analyses have identified many differentially expressed genes in OA cartilage. Many of these genes, such as those involved in matrix synthesis, were expected to be differentially expressed. Some of the newly identified differentially expressed genes include those involved in oxidative stress defence (down-regulation of superoxide dismutases (SOD) 2 and 3 and glutathione peroxidase 3), indicating that continuous oxidative stress to the cells and the matrix is one major underlying pathogenic mechanism in OA (Aigner et al. 2006). As the major feature of arthritic disease is cartilage destruction,

many proteases (DKFZP586H2123, ADAMTS6, ADAM12, and PRSS11) are known to be up-regulated in damaged vs intact cartilage (Sato et al. 2006). The same study also found the expression levels of three genes known to inhibit degradation of the ECM (TNFAIP6, SERPINE1, and TIMP3) to be increased in damaged vs intact cartilage, indicating an attempt by the body to halt cartilage destruction. Several serpin peptidase inhibitors were shown to be dramatically up-regulated in IL-1+OSM+IL-4 vs IL-1+OSM cells/cartilage in the data presented in this chapter. Appleton et al. (2007) identified dysregulation of members of the insulin-like growth factor (IGF) family, including increased levels of expression of IGF binding proteins, which sequester IGFs and prevent their anabolic influences in chondrocytes. This study also reported the modulation of oxidative defense genes (e.g. SOD2). Another study examined the differential gene expression profile of damaged vs intact cartilage areas within the same joint of patients with OA of the knee and found several genes to be up-regulated in all patients (IGF binding protein 3 (IGFBP-3), wnt-1-inducible signalling protein 1 (WISP-1), aquaporin 1 (AQP-1), delta/notch-like EGF-repeat containing (DNER), decay accelerating factor (DAF), complement factor I (IF)) (Geyer et al. 2009). In agreement with this study, IGFBP-3 was up-regulated in both bovine cartilage (5.99 fold) and SW1353 cells (2.28 fold) in the data presented in this chapter. In addition, DAF was up-regulated 2.81 fold in bovine cartilage. These similarities indicate that the cytokine treatments used in this array, do appropriately mimic the *in vivo* action of cytokines in OA.

The most recent genome-wide analysis identified several genes that had not previously been associated with OA (Karlsson et al 2010). These included an up-regulation in OA cartilage of TFPI2 (tissue factor pathway inhibitor 2), a gene previously demonstrated to reduce the ability of MMP-1 and -13 to degrade collagen and also reduce the activity of MMP-2 and -9. This finding again suggests the presence in OA cartilage of a mechanism to counteract matrix degradation. TFPI2 was up-regulated 7.69 fold in bovine cartilage (IL-1+OSM+IL-4 vs IL-1+OSM), indicating the presence of a similar mechanism. Increased expression of SGPP1 was also observed in OA cartilage compared to normal. SGPP1 regulates sphingolipid biosynthesis and is known to be involved in programmed cell death (Johnson et al. 2003).

After examination of the genome-wide array data and extensive literature searches, a number of genes that were differentially regulated between IL-1+OSM+IL-4- vs IL-1+OSM-treated cells/cartilage were selected as potential candidates for further study. The decision as to whether a gene warranted further study was based on a number of factors; (1) the fold change up or down regulation of a particular gene, (2) if existing literature had identified a particular gene as playing a role in arthritic disease or MMP regulation, and (3) whether a particular gene was up or down regulated in at least two out of the three systems examined. Unlike previous genome-wide studies (Aigner et al. 2006; Sato et al. 2006; Appleton et al. 2007; Fukui et al. 2008; Geyer et al. 2009; Karlsson et al. 2010) that were interested in genes differentially expressed in OA vs normal cartilage, the more specific aim of this chapter (to identify genes involved in the repression of MMP-13 by IL-4) made selection of genes for further study more complicated. Many of the most highly up or down-regulated genes were not selected for further study because there was no evidence that they played a role in the repression of MMP-13 by IL-4 and therefore the chondroprotective mechanism of action of IL-4. In addition, many genes involved in, for example, the general inflammatory process (such as C-reactive protein) or genes involved in matrix synthesis (such as the collagens) were discounted from further study. Instead, genes that were potentially involved in cell signalling pathways (such as Trb1) were selected as being more likely to be involved in the repression of MMP-13 by IL-4. Moreover, relatively subtle changes in cell signalling molecules could have significant effects on MMP expression (Litherland et al. 2008, Litherland et al. 2010).

All genome-wide screens in relation to arthritis to date have utilised OA cartilage or cartilage from animal models. This analysis of disease 'end-point' may not reflect gene expression patterns during the initiation of cartilage destruction. An advantage of the screen performed in this chapter is that the stimulation of cartilage with cytokines enabled a snapshot of gene expression changes immediately preceding collagen loss and cartilage degradation, and for isolated chondrocytes at a timepoint during which MMP-13 expression was marked.

One of the reasons behind performing genome-wide arrays in three different systems (bovine cartilage, human articular chondrocytes and SW1353 cells) was to assess the

similarity in gene expression profiles. A strong similarity would validate the use of bovine cartilage and the cell line SW1353 cells as an alternative to primary human chondrocytes when the latter was unavailable. At the time of writing, a large proportion of the genes included on the bovine Affymetrix array had yet to be transcribed and this explains the lack of similarity in gene profiles between the Affymetrix and Illumina array data. Illumina arrays are known to produce smaller fold changes than Affymetrix arrays so; again, this goes some way as to explaining the lack of common genes between the three models. The Venn diagrams presented in this chapter may actually underestimate the number of common genes, as they do not include genes encoding different protein isoforms (for example IGFBP-3 was up-regulated in SW1353 cells and bovine cartilage and IGFBP-5 was up-regulated in human articular chondrocytes and bovine cartilage). Therefore, these genes do not count as common genes, despite the fact that similar processes are obviously occurring in all three models, albeit by slightly different mechanisms. Despite the lack of similarity between the bovine and human gene expression data (for reasons explained previously), the data presented in this chapter suggest that human articular chondrocytes and SW1353 cells are appropriate complementary model systems as their gene expression profiles are very similar. This is in agreement with studies by another group, which also demonstrated similarity between SW1353 cells and human articular chondrocytes (following IL-1 β treatment) (Gebauer et al. 2005).

Unfortunately due to the cost of performing genome-wide arrays, it was not possible to include replicates on any of the arrays. As no statistical analysis could be performed on the resulting data, these arrays acted as a basic screen to identify genes that could be involved in the chondroprotective action of IL-4. Despite this obvious drawback to the study, the extensive preliminary experiments performed on the RNA used for the arrays does increase the confidence in the gene expression data. Additionally, the expression levels of genes that have been extensively studied previously in response to these cytokine combinations acted as positive internal controls. The gene expression profile of these internal controls was found to follow the same pattern of up- or down-regulation in the array results as in previous data (Chapter 3 of this thesis). For example, MMP-13 was down-regulated by IL-1+OSM+IL-4 compared with IL-1+OSM in bovine cartilage, human articular chondrocytes and SW1353 cells (-10.5, -2.1 and -2.63 fold, respectively). These results correlate strongly

to those presented in Chapter 3 of this thesis, whereby IL-4 repressed IL-1+OSM-induced MMP-13 expression in all systems, but to a greater extent in the bovine system. The fact that the gene expression data for MMP-13 from all three arrays corresponds so closely to data obtained from numerous previous experiments, strengthens the confidence in the results for other genes on the array, despite the lack of replicates and therefore statistical power. Furthermore, the genome wide arrays were performed in three different models. Therefore any up- or down-regulation of genes observed in two or three of the models can confidently be viewed as an accurate observation.

The remainder of this study will examine the role of candidate genes identified in this chapter, in the repression of MMP-13 by IL-4. RNA interference-mediated knockdown of up-regulated genes in IL-1+OSM+IL-4 treated cells/cartilage will be used to determine if this recovers MMP-13 expression. In down-regulated genes, siRNA will be used in IL-1+OSM treated cells/cartilage to determine if knockdown of these genes mimics the effect of IL-4 (i.e. blocks MMP-13 expression).

The data presented in this chapter provide a basis for future studies on the function of certain genes in the chondroprotective mechanism of action of IL-4. Many of the genes highlighted in this chapter have not before been implicated in arthritic disease and so any involvement will be a novel finding.

6.4 Summary

- Genome-wide microarray analysis of bovine cartilage, human articular chondrocytes and SW1353 cells provided data on the gene expression profile differences between IL-1+OSM+IL-4 vs IL-1+OSM.
- These data, along with an extensive literature search, enabled a shortlist of genes, with a possible involvement in the repression of MMP-13 by IL-4, to be selected for further study.

Chapter 7: The role of the Tribbles family of proteins in MMP-13 expression in chondrocytes

7.1 Introduction

Data presented in this thesis have demonstrated that IL-4 prevents cartilage destruction via MMP-13 repression. Transcriptome analyses of stimulated cartilage and chondrocytes to provide clues to the mechanism of action of IL-4 revealed numerous genes with potential involvement in the chondroprotective action of IL-4. An RNA interference approach was used to further investigate the involvement of genes highlighted in Chapter 6 as having a potential role in the mechanism of action of IL-4. It was hypothesised that silencing (via siRNA) of genes up-regulated by IL-4 might rescue IL-4-mediated repression of IL-1+OSM-induced MMP-13. In genes down-regulated by IL-1+OSM+IL-4, gene silencing would mimic the effect of IL-4 (i.e. block MMP-13 expression by IL-1+OSM). This approach was used against several genes and preliminary results indicated a role for Trb1 in the repression of MMP-13 by IL-4. This chapter examines the role of the tribbles (trb) family of proteins in MMP-13 expression in chondrocytes.

Regulators of cellular signalling have evolved to regulate and integrate the huge variety of extracellular signals, ultimately determining the cellular response. The recent identification of tribbles as regulators of cell signalling pathways has generated a large amount of interest in this family of proteins. An expanding literature on tribbles indicates that the proteins encoded by these genes play an important role in the regulation and modulation of numerous signalling pathways and transcription factors, perhaps affecting the balance of activation between key signalling pathways. These regulatory mechanisms usually involve enzymes with catalytic activity. However, this unusual family of signalling regulatory proteins appear to be catalytically inactive, despite resembling Ser/Thr kinases. Instead, it is thought that tribbles evolved as adaptor proteins with a scaffold-like regulatory function. It is widely believed that these proteins do have an important physiological function, despite

their apparent lack of kinase activity, however the molecular basis of tribbles function is still poorly understood (Hegedus et al. 2007).

In mammals, three tribbles proteins have been described to date. The three human tribbles share 45% sequence similarity and bear a strong resemblance to *tribbles*, a *Drosophila* protein that inhibits mitosis early in development (Mata et al. 2000; Seher and Leptin 2000).

Trb1

Trb1, originally named c8fw, was first identified as a homologue of Trb2 (first called c5fw). In a yeast two-hybrid screen, LOX-12 (an enzyme that metabolises arachidonic acid) was found to be a Trb1 interacting protein (Tang et al. 2000). Trb1 was subsequently found to regulate the activity of stress kinase pathways through interaction with MAPKKs (mitogen-activated protein kinase kinase) (Kiss-Toth et al. 2004). Activation of MAPK pathways can occur in response to a wide range of stimuli, such as stress, pro-inflammatory cytokines and growth factors. MAPKs are subdivided into 3 groups, namely Jun kinases (JNK), p38 and extracellular signal-regulated protein kinases (ERK) and are activated by upstream kinases called MAPKKs. Co-immunoprecipitation experiments in HeLa cells with over-expressed Trb1, MAPKs, MAPKKs and MAPKK kinases revealed specific interactions of Trb1 with MEK1 and MKK4/SEK1 (a Jun activator kinase) (Sung et al. 2007). This study evaluated the importance of Trb proteins in the cellular responses of vascular smooth muscle cells to inflammatory stimuli. Trb1 was found to control vascular smooth muscle cell proliferation and chemotaxis through the JNK pathway via direct interactions between Trb1 and MKK4/SEK1.

Trb2

Trb2 has been identified as a candidate autoantigen in autoimmune uveitis (Zhang et al. 2005). Several studies have investigated the binding partners of Trb2. The first reported the interaction of Trb2 with over-expressed Akt in co-immunoprecipitation assays (Du et al. 2003). The second showed that Trb2 appears to have anti-adipogenic effects (Naiki et al. 2007). Both Trb2 and Trb3 were shown to exhibit anti-adipogenic effects through inhibition of Akt activation. However, Trb2 only partially inhibited Akt phosphorylation

suggesting that Trb2 inhibits adipogenesis through an additional mechanism to Akt inhibition. Trb2 was shown to also interact with C/EBP β (CCAAT-enhancer-binding protein β , a transcription factor required for an early stage of adipogenesis) and block adipogenesis through proteasome-dependent degradation of C/EBP β . A later study demonstrated that Trb2 associated with and inhibited C/EBP α . Trb2 expression was found to be elevated in a subset of human acute myelogenous leukemia (AML) patient samples suggesting that Trb2 is an oncogene that induces AML through a mechanism involving inactivation of C/EBP α (Keeshan et al. 2006). Trb2 has been also been described as a pro-apoptotic molecule, inducing the apoptosis of cells mainly of hematopoietic origin (Lin et al. 2007). In 2009, Trb2 was identified as a highly regulated gene in vulnerable atherosclerotic lesions (Deng et al. 2009). Inhibition of macrophage IL-10 biosynthesis appeared to be a potential consequence of high Trb2 expression, which the authors suggest may contribute to plaque instability. Trb2 has been identified as a novel regulator of inflammatory activation of monocytes (Eder et al. 2008). Most recently, anti-Trb2 antibodies have been associated with narcolepsy (Toyoda et al. 2010).

Trb3

Trb3 is the most studied member of the mammalian Trb family. Two separate groups reported the identification of Trb3 in 1999. Mayumi-Matsuda et al. (1999) identified a kinase-like protein involved in neuronal cell death and designated this protein NIPK (Neuronal cell death Inducible Putative Kinase). The second study by Klingenspor et al. (1999) analysed the altered pattern of gene expression in the fatty liver of fld (fatty liver dystrophy) mice and found a novel Ser/Thr kinase, which they called *Ifld2*.

In 2003, Trb3 was reported to be a negative regulator of Akt (Du et al. 2003). In order to identify additional proteins that modulate Akt activity, a yeast two-hybrid assay was used to screen for proteins from a preadipocyte F422A cDNA library that interacted with a GAL4-Akt Δ PH construct lacking the NH₂-terminal pleckstrin homology domain of Akt1. Twenty-five independent transformants from a screen of 2×10^6 cDNAs were found to encode a protein recently identified as Trb3. Interaction between endogenous Trb3 and Akt was confirmed by co-immunoprecipitation assays using HepG2 cell extracts. To determine whether the association of Akt with Trb3 modulated the activity of Akt, Akt

phosphorylation in response to IGF-1 was monitored. IGF-1 induced phosphorylation of Akt at Thr³⁰⁸ and Ser⁴⁷³ in human embryonic kidney 293 (HEK293) cells within 15 minutes, however expression of Trb3 inhibited Akt phosphorylation at both sites without altering total amounts of Akt protein. This study therefore demonstrated that Trb3 appears to block Akt activity by disrupting its phosphorylation without reducing the abundance of the protein (Du et al. 2003). The same study investigated possible mechanisms by which Trb3 inhibits Akt phosphorylation. A phosphorylation-defective T308A mutant Akt was shown to associate more efficiently with Trb3 when compared to wild-type protein. Conversely, substitution of Thr³⁰⁸ with Asp to mimic Thr³⁰⁸ phosphorylation was shown to strongly inhibit the interaction between Trb3 and Akt, suggesting that Trb3 preferentially binds to the unphosphorylated form of Akt. Akt is a principal target of insulin signalling that inhibits hepatic glucose output when glucose is available from food and so the conclusion of this study was that Trb3 may contribute to insulin resistance by interfering with Akt activation. Trb3 has also been shown to inhibit the phosphorylation of Akt at Thr308 in FGC-4 cells, a highly differentiated rat hepatoma cell line (He et al. 2006). However, a contradictory study by Iynedjian (Iynedjian 2005) failed to find any evidence of a role for Trb3 as an inhibitor of Akt-mediated insulin signalling in primary rat hepatocytes. These opposing findings could suggest that the function of Trb3 varies depending on experimental procedures and/or cell type. A 2006 study identified Trb3 as a transcriptional target of PI3K (Schwarzer et al. 2006). Inhibition of PI3K in the prostate cancer cell line, PC-3, reduced Trb3 expression.

To date, only one study has looked at the role of tribbles in the context of OA (Cravero et al. 2009). As mentioned previously, Trb3 has been shown to inhibit IGF-1-mediated activation of Akt in HEK 293 cells (Du et al. 2003). It is known that the chondrocyte response to IGF-1 is reduced both with ageing and in OA chondrocytes. The study by Cravero et al. (2009) first confirmed the expression of Trb3 in human articular chondrocytes. It went on to demonstrate that a significantly higher level of Trb3 was found in OA chondrocytes when compared to age-matched control chondrocytes. Over-expression of Trb3 in normal chondrocytes was found to block IGF-1 stimulation of proteoglycan synthesis and reduce cell survival by almost 40%. IGF-1-mediated production of proteoglycan by chondrocytes has previously been shown to be dependent on the PI3K signalling pathway (Starkman et al. 2005). Cravero et al. (2009) suggest that an increase in

the level of Trb3 in OA chondrocytes may be partly responsible for the decreased response of OA chondrocytes to IGF-1 and the cell death and cell matrix loss that occurs during OA progression. Cravero et al. (2009) also found that an increase in endoplasmic reticulum (ER) stress resulted in increased chondrocyte Trb3 levels. Yang et al. (2007) demonstrated that ER stress in chondrocytes decreases the expression of cartilage matrix genes. Taken together, it appears Trb3 could play a role in causing the imbalance between anabolic and catabolic activity associated with the development of OA.

Tribbles structure

The kinase-like domain of tribbles proteins is located in the middle of the protein, flanked by relatively short N- and C-terminal sequences. The N-terminal segment of human tribbles proteins is approximately 60–80 residues long (Hegedus et al. 2007). A notable feature of the N-terminal portion of tribbles is a very high serine (7-24%) and proline (6-23%) content, predominantly in the section of sequence adjacent to the kinase-like domain. This is of note because a high level of these particular amino acids is an important feature of PEST regions (a polypeptide sequence that is enriched in proline (P), glutamic acid (E), serine (S) and threonine (T)). The presence of these regions is thought to result in the rapid intracellular degradation of the proteins containing them (Rogers et al. 1986; Rechsteiner and Rogers 1996). This observation corroborates the findings of a previous report that demonstrated Trb2 to be an unstable protein (Wilkin et al. 1997). It also adds weight to the growing hypothesis that tribbles are regulators of cell division and cell signalling, both of which often involve proteins with a rapid turnover. In addition, the presence of a proline-rich region is potentially associated with other functions such as the anchoring of SH3 or WW domains of other proteins (Macias et al. 2002) or as substrates for proline-dependent phosphorylation (MAP and CDK-like proteins phosphorylated a Ser/Thr residue preceding a Pro residue).

The importance of tribbles in various physiological processes is now well accepted; however the cellular and molecular basis for their action is poorly understood. The three tribbles proteins have been implicated in the control of stress response, cell viability and metabolic processes, and have been linked to medical conditions such as insulin resistance

and diabetes. Therefore, the understanding of mechanisms that regulate tribbles expression is of considerable importance.

The aims of this chapter were to:

- Determine the involvement of the tribbles protein family in IL-1+OSM- and IL-1+OSM+IL-4-induced MMP-13 expression/repression through gene silencing and over-expression experiments.
- Determine the subcellular localisation of tribbles proteins under basal conditions in chondrocytes and examine the effect of cytokine stimulation on this localisation.
- Examine the physical interactions of tribbles proteins with MAPKKs.

7.2 Results

7.2.1 The effect of various gene silencing on IL-1+OSM-induced MMP-13 expression in SW1353 cells

Of the genes selected in Chapter 6 as being potentially involved in the repression of MMP-13 by IL-4, several were selected for preliminary RNA interference experiments using siRNA (S100A8, S100A9 and Trb1). Along with these genes, three other targets were selected for RNA interference due to their known involvement in IL-4 signalling pathways; namely, STAT6, IRS1 and IRS2. Of the genes investigated in these experiments, silencing of STAT6 and Trb1 appeared to rescue IL-4-mediated repression of IL-1+OSM-induced MMP-13 (Figure 7.1). IL-1+OSM-induced S100A8 and S100A9 expression was down-regulated by IL-4 in the microarray performed in Chapter 6. Therefore, silencing of S100A8 and S100A9 would have been expected to abolish IL-1+OSM-induced MMP-13 expression if these genes were involved in the mechanism of action of IL-4. Surprisingly, silencing of S100A9 was found to rescue IL-4-mediated repression of IL-1+OSM-induced MMP-13 (Figure 7.1a). Silencing of neither IRS-1 nor IRS-2 significantly interfered with the ability of IL-4 to repress IL-1+OSM-induced MMP-13 (Figure 7.1b). As IL-4 signalling is known to involve either STAT6 or IRS-1/-2, these observations would suggest that the repression of MMP-13 by IL-4 is solely mediated through the STAT6 signalling pathway.

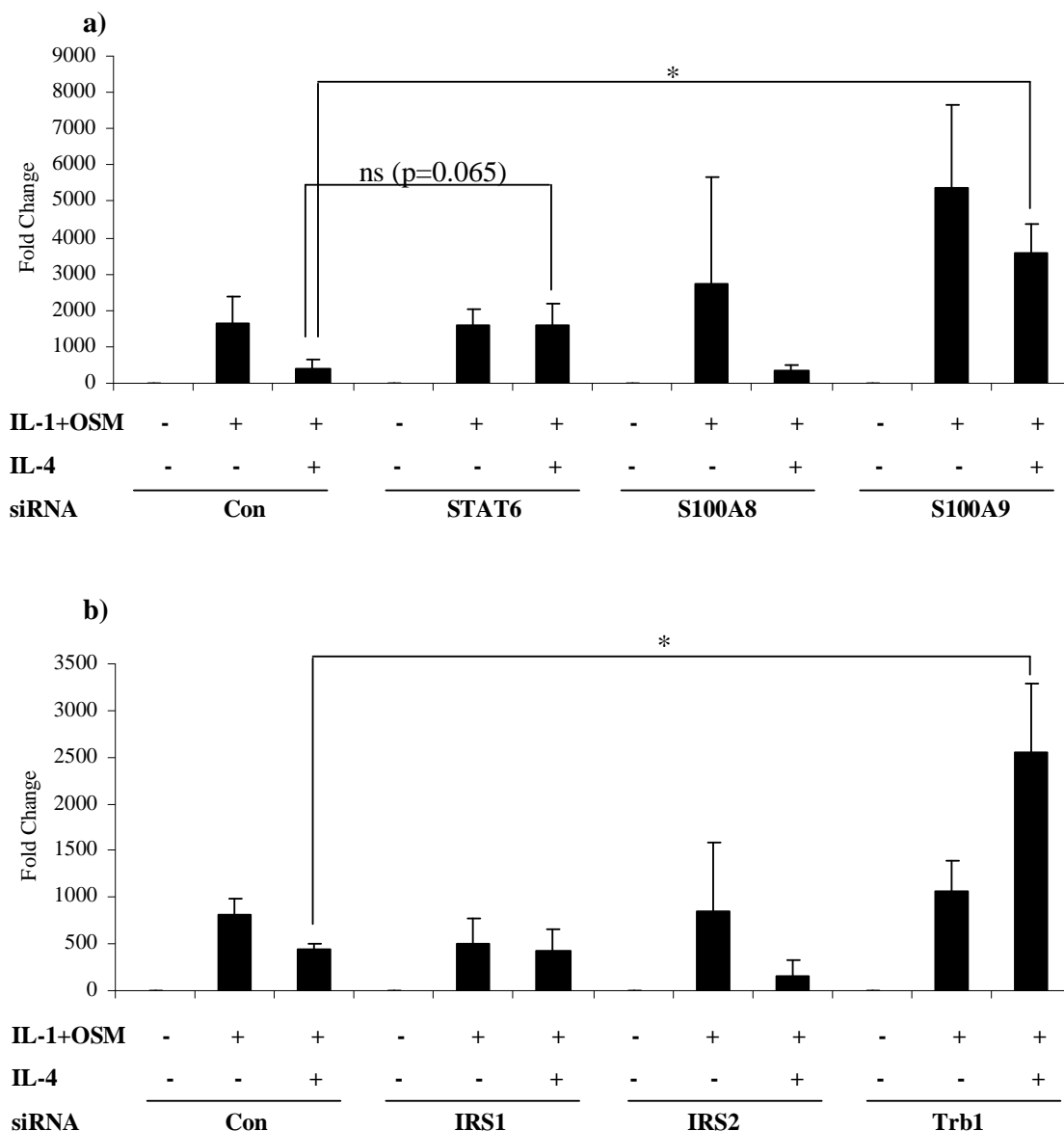


Figure 7.1 The effect of various gene silencing on IL-1+OSM-induced MMP-13 expression in SW1353 cells. SW1353 cells were stimulated with control, IL-1+OSM (0.5 and 10 ng/ml, respectively) or IL-1+OSM+IL-4 (0.5, 10 and 20 ng/ml, respectively) for 24 hours following a 28 hour transfection with siRNA specific to STAT6, S100A8, S100A9, IRS1, IRS2, Trb1 or siCon (100 nM). Real-time RT-PCR of the isolated RNA was performed for MMP-13 72 hours after the start of transfection. Data are presented as fold induction relative to the basal siCon-transfected expression (mean \pm S.E.M, $n = 8$) and are representative of two independent experiments. * = $p \leq 0.05$; ns = not significant.

7.2.2 The effect of Trb1 and STAT6 gene silencing on MMP-13 expression in SW1353 cells and human articular chondrocytes

The significant involvement of STAT6 and Trb1 in the repression of MMP-13 by IL-4 demonstrated in Figure 7.1 warranted further experiments to investigate the reproducibility of these findings. A further experiment in SW1353 cells (Figure 7.2a) and in human articular chondrocytes (Figure 7.2b), again, demonstrated that silencing of Trb1 rescued IL-4-mediated repression of IL-1+OSM-induced MMP-13. Silencing of STAT6 did not appear to rescue IL-4-mediated repression of IL-1+OSM-induced MMP-13 in these experiments. However, the repression of MMP-13 observed with the inclusion of IL-4 was no longer observed when compared to IL-1+OSM-treated cells following STAT6 siRNA treatment. Alternatively, this could be due to the fact that repression of IL-1+OSM-induced MMP-13 expression by IL-4 was not as strong as observed in previous experiments. Interestingly, in both cell types (Figure 7.2a and b) MMP-13 expression following Trb1 silencing was greater than that induced by IL-1+OSM. This suggests alterations in Trb1 levels regulate the magnitude of the resultant pro-inflammatory stimulus in terms of MMP expression.

7.2.3 IL-4-induced Trb1 expression is STAT6-dependent

Examination of Trb1 gene expression via real-time RT-PCR demonstrated that IL-4-induced Trb1 expression is STAT6-dependent in both SW1353 cells and human articular chondrocytes (Figure 7.3). STAT6 gene silencing significantly inhibits IL-1+OSM+IL-4-induced Trb1 expression in both cell types. Bioinformatic examination of the Trb1 promoter region revealed a STAT6-binding element (5'-TTC(N)₂₋₄GAA-3'). These data suggest that the Trb1-dependent MMP-13 repression by IL-4 is STAT6-dependent suggesting STAT6 is upstream of Trb1, with increased Trb1 transcription occurring via STAT6-binding to the Trb1 promoter.

7.2.4 The effect of STAT6 and Trb1 gene silencing on STAT6 and phospho-STAT6 abundance

Silencing of STAT6 via siRNA is shown to virtually eliminate STAT6 protein levels (confirming that the gene silencing is effective) (Figure 7.4). IL-4 stimulated the

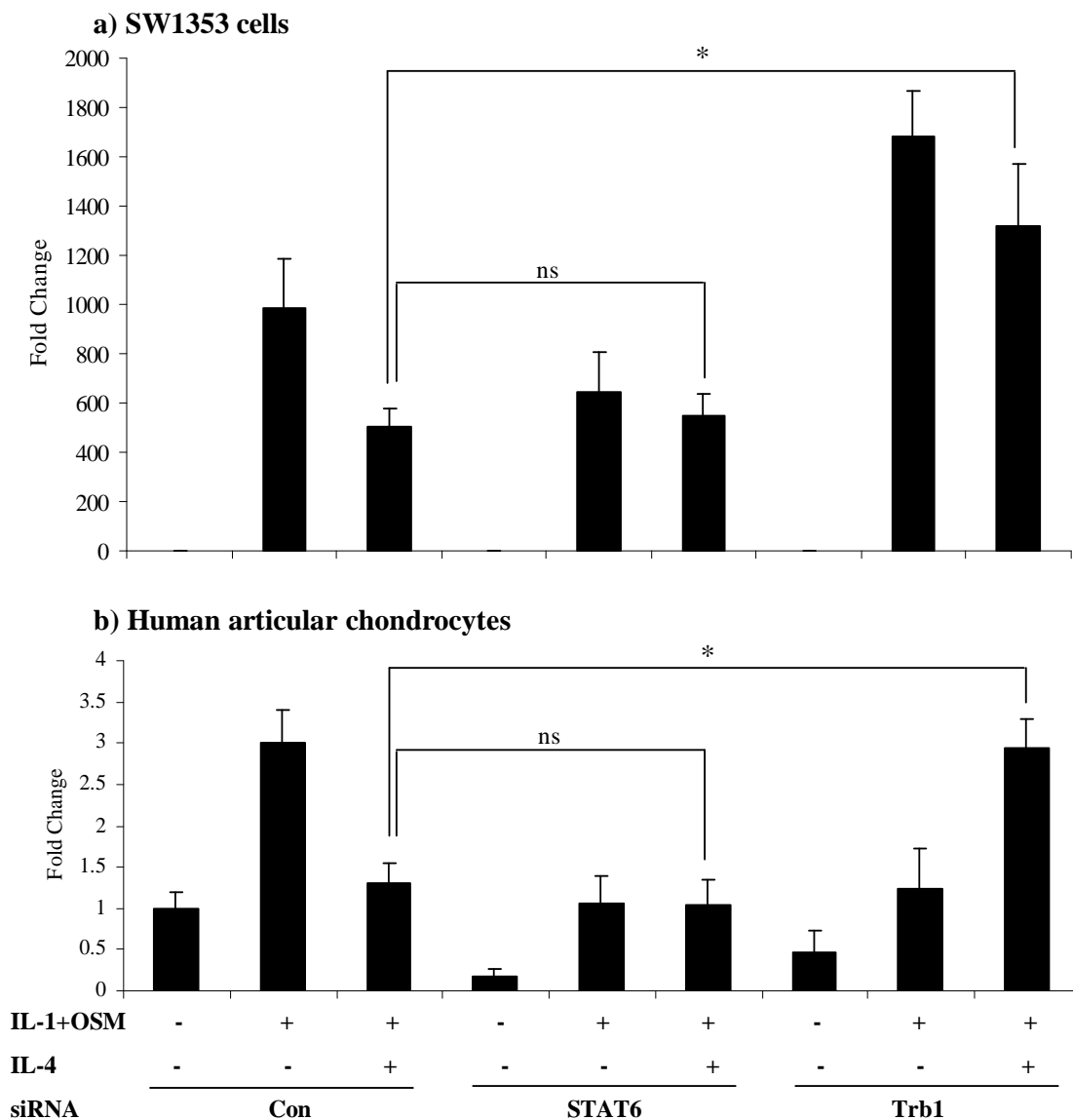


Figure 7.2 The effect of Trb1 and STAT6 gene silencing on MMP-13 expression in SW1353 cells (a) and human articular chondrocytes (b). SW1353 cells were stimulated with control, IL-1+OSM (0.5 and 10 ng/ml, respectively) or IL-1+OSM+IL-4 (0.5, 10 and 20 ng/ml, respectively) and human articular chondrocytes were stimulated with control, IL-1+OSM (0.02 and 10 ng/ml, respectively) or IL-1+OSM+IL-4 (0.02, 10 and 20 ng/ml, respectively) for 24 hours following a 28 hour transfection with siRNA specific to STAT6, Trb1 or siCon (100 nM). Real-time RT-PCR of the isolated RNA was performed for MMP-13 72 hours after the start of transfection. Data are presented as fold induction relative to the basal siCon-transfected expression (mean \pm S.E.M, $n = 8$). Data are representative of two independent experiments in SW1353 cells and human articular chondrocytes. * = $p \leq 0.05$; ns = not significant.

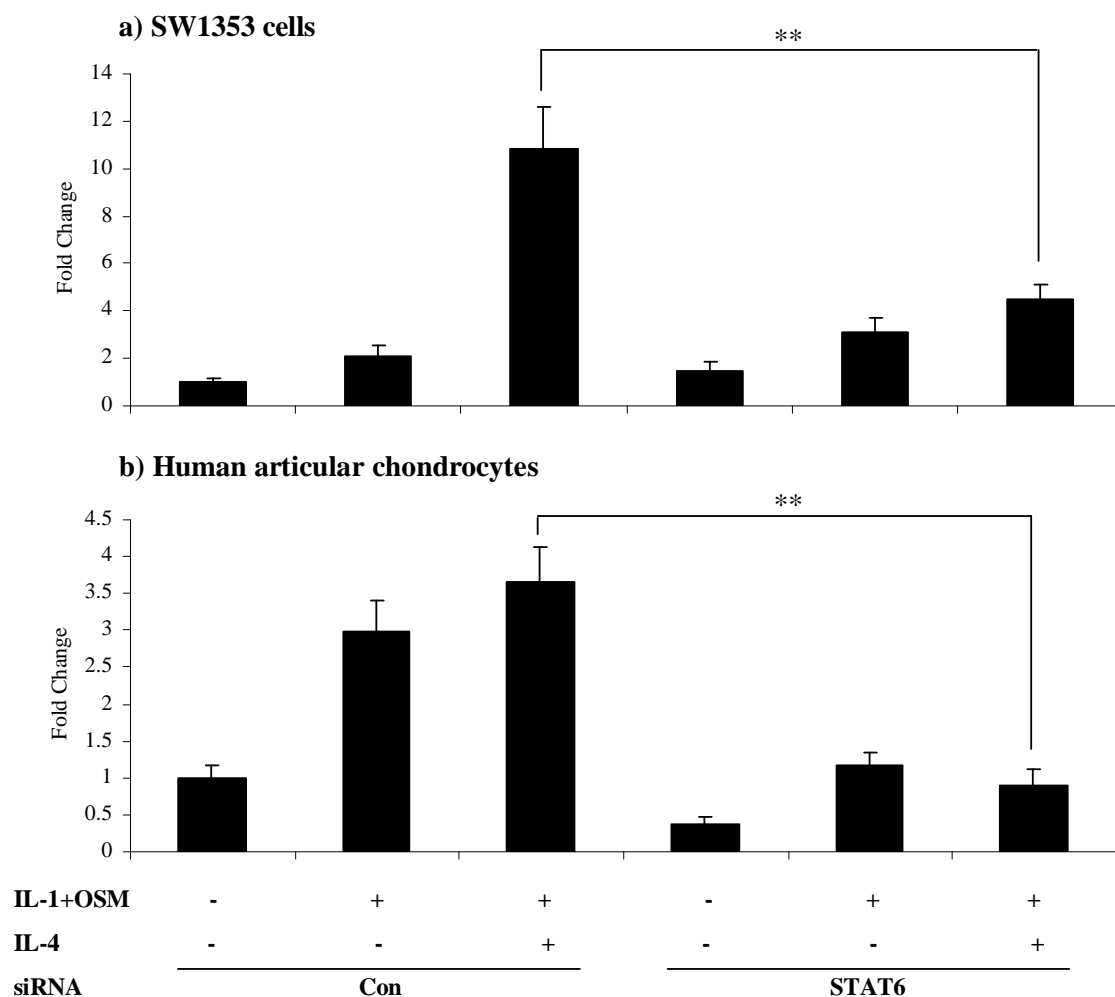


Figure 7.3 The effect of STAT6 gene silencing on Trb1 expression in SW1353 cells (a) and human articular chondrocytes (b). SW1353 cells were stimulated with control, IL-1+OSM (0.5 and 10 ng/ml, respectively) or IL-1+OSM+IL-4 (0.5, 10 and 20 ng/ml, respectively) and human articular chondrocytes were stimulated with control, IL-1+OSM (0.02 and 10 ng/ml, respectively) or IL-1+OSM+IL-4 (0.02, 10 and 20 ng/ml, respectively) for 24 hours following a 28 hour transfection with siRNA specific to STAT6 or siCon (100 nM). Real-time RT-PCR of the isolated RNA was performed for Trb1 72 hours after the start of transfection. Data are presented as fold induction relative to the basal siCon-transfected expression (mean \pm S.E.M, $n = 8$) and are taken from a single experiment. ** = $p \leq 0.01$.

phosphorylation of STAT6 as expected and silencing of STAT6 reduced phospho-STAT6 protein expression. However, silencing of Trb1 did not prevent the phosphorylation of STAT6 by IL-4. This, along with the data presented in Figure 7.3, suggests that Trb1 acts downstream of STAT6.

7.2.5 The effect of STAT6 and Trb1 gene silencing on MMP-1 mRNA expression in SW1353 cells

Data presented in this thesis have consistently demonstrated a differential regulation of MMP-13 and MMP-1 by IL-4. IL-4 appears to increase IL-1+OSM-induced MMP-1 expression in many experiments, therefore the effect of STAT6 and Trb1 gene silencing on IL-1+OSM-induced MMP-1 expression was examined. Figure 7.5 demonstrates that increased MMP-1 expression with IL-1+OSM+IL-4 appears to be STAT6-dependent. Whilst Trb1 gene silencing significantly reduces IL-1+OSM+IL-4-induced MMP-1 expression, MMP-1 expression remains greater in the presence of IL-4 than in the absence of IL-4 (as has been consistently observed before).

7.2.6 The effect of tribbles protein family gene silencing on IL-1+OSM-induced collagenase gene expression in SW1353 cells

Trb1 is one of three members of the tribbles protein family and so it was important to assess the effect of Trb2 and Trb3 (in addition to Trb1) gene silencing on MMP-13 mRNA expression. Further attempts to replicate the preliminary findings of the effect of Trb1 gene silencing on MMP-13 gene expression (Figures 7.1 and 7.2) yielded inconsistent results. For unknown reasons, Trb1 gene silencing did not consistently rescue IL-4-mediated repression of IL-1+OSM-induced MMP-13 (Figure 7.6a). Silencing of Trb2 consistently had no significant effect on IL-1+OSM or IL-1+OSM+IL-4-induced MMP-13 expression, suggesting that Trb2 is not involved in either the induction of MMP-13 by pro-inflammatory cytokines or the repression of MMP-13 by anti-inflammatory cytokines. Despite problems with the reproducibility of the rescue of IL-4-mediated repression of IL-1+OSM-induced MMP-13 following Trb1 gene silencing, tribbles-regulated MMP expression is further supported in that Trb3 silencing abolished IL-1+OSM-induced MMP-

13 expression (Figure 7.6a and b). This finding was highly reproducible (representative of four independent experiments) and suggests that individual tribbles may have opposing roles in MMP regulation. These preliminary data support a pro-inflammatory role for Trb3.

In order to extend these initial observations, Figure 7.7 confirms that other pro-inflammatory stimuli (TNF α +OSM) are also Trb3-dependent for MMP-13. Taken together, these preliminary data are suggestive of a model whereby Trb1 and Trb3 regulate MMP-13 gene expression during pro-inflammatory signalling, with a pro-inflammatory role for Trb3 and a possible anti-inflammatory role for Trb1.

7.2.7 Transfection timecourse to determine the efficiency of Trb1 and Trb3 gene silencing in SW1353 cells

After problems with the reproducibility of the rescue of IL-4-mediated repression of IL-1+OSM-induced MMP-13 following Trb1 gene silencing, a Trb1 and Trb3 siRNA transfection timecourse was performed in SW1353 cells. The purpose of this experiment was to determine, not only if the Trb1 gene silencing was effectively reducing Trb1 protein expression but also to examine the most appropriate timepoint for examination of the effect of Trb1 gene silencing on MMP-13 expression. Figure 7.8 clearly shows that whilst Trb3 gene silencing via siRNA was effective at reducing Trb3 protein expression (at all timepoints tested). Trb1 silencing was less effective, although appeared to reduce Trb1 protein expression at 48 hours by approximately 50%. This experiment suggests that the problems encountered in reproducing the preliminary findings of Trb1 gene silencing on IL-4-mediated repression of IL-1+OSM-induced MMP-13 are due to the Trb1 siRNA producing only a partial knock-down, thereby resulting in poor reproducibility.

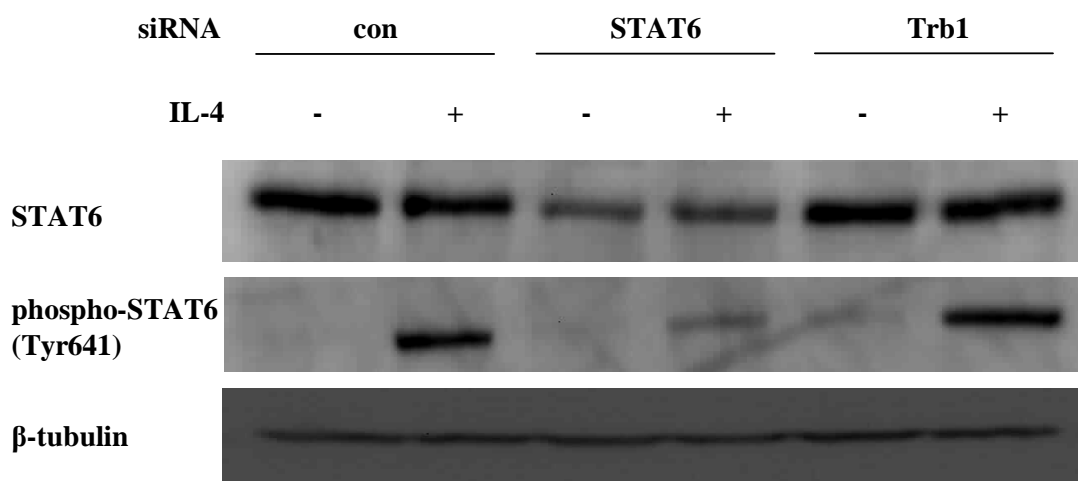


Figure 7.4 The effect of STAT6 and Trb1 gene silencing on STAT6 and phospho-STAT6 abundance. SW1353 cells were stimulated with control or IL-4 (20 ng/ml) for 20 minutes following a 48 hour transfection with siRNA specific to STAT6, Trb1 or siCon (100 nM). Total cell lysates were prepared and separated by SDS-PAGE on a 10% polyacrylamide gel with a molecular weight marker. Protein fractions were transferred to PVDF membranes. Blots were probed with STAT6, phospho-STAT6 and β -tubulin followed by goat anti-rabbit HRP. The blots were visualised using ECL and are representative of two independent experiments.

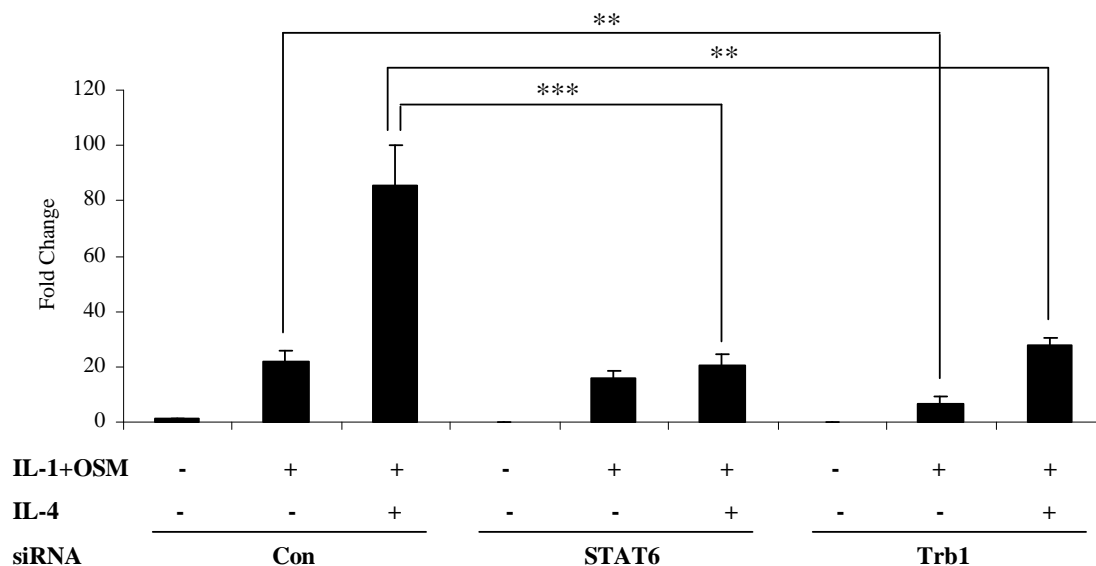


Figure 7.5 The effect of STAT6 and Trb1 gene silencing on MMP-1 mRNA expression in SW1353 cells. SW1353 cells were stimulated with control, IL-1+OSM (0.5 and 10 ng/ml, respectively) or IL-1+OSM+IL-4 (0.5, 10 and 20 ng/ml, respectively) for 24 hours following a 28 hour transfection with siRNA specific to STAT6, Trb1 or siCon (100 nM). Real-time RT-PCR of the isolated RNA was performed for MMP-1 72 hours after the start of transfection. Data are presented as fold induction relative to the basal siCon-transfected expression (mean \pm S.E.M, $n = 8$). Data are representative of two independent experiments. *** = $p \leq 0.001$; ** = $p \leq 0.01$.

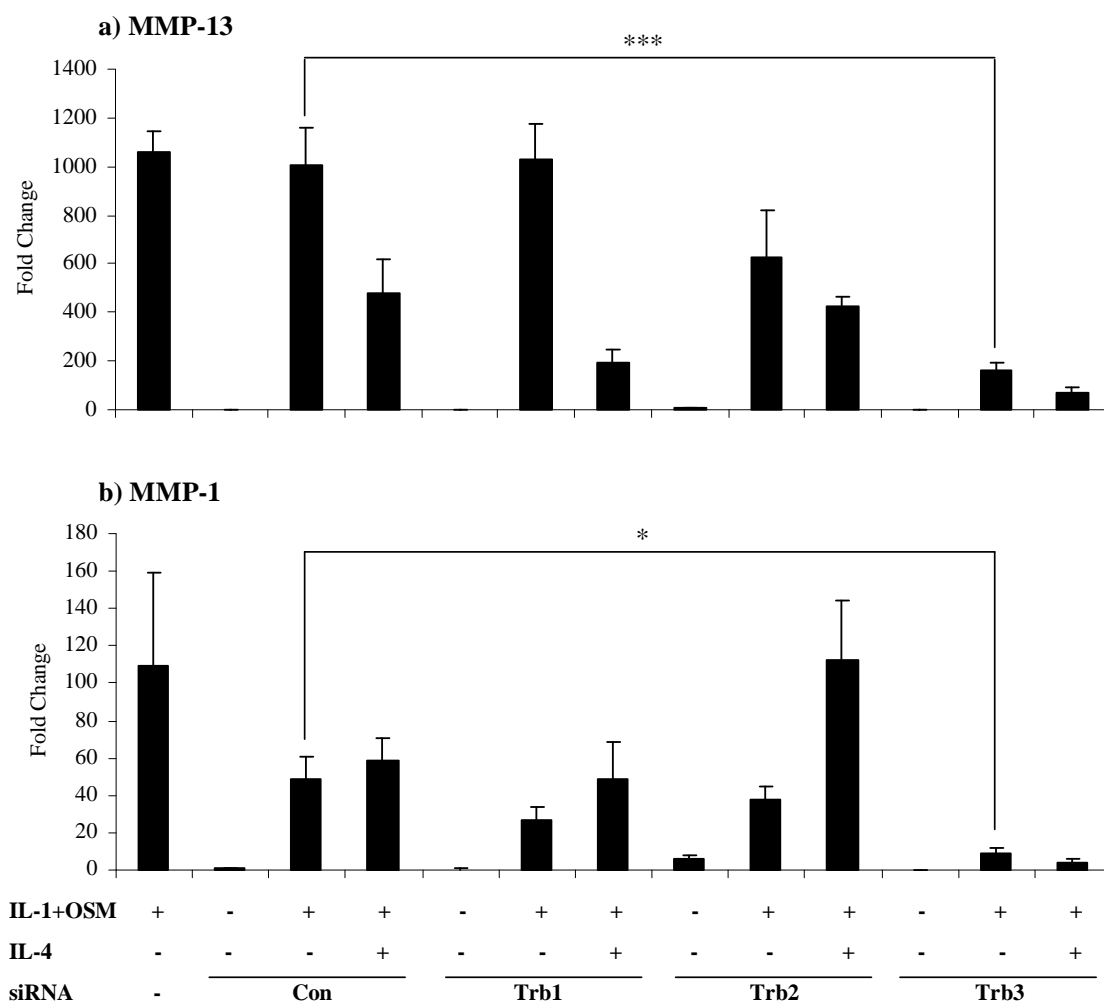


Figure 7.6 The effect of Trb protein family gene silencing on IL-1+OSM-induced collagenase gene expression in SW1353 cells. SW1353 cells were stimulated with control, IL-1+OSM (0.5 and 10 ng/ml, respectively) or IL-1+OSM+IL-4 (0.5, 10 and 20 ng/ml, respectively) for 24 hours following a 28 hour transfection \pm siRNA specific to Trb1, Trb2, Trb3 or siCon (100 nM). Real-time RT-PCR of the isolated RNA was performed for MMP-13 (a) and MMP-1 (b) 72 hours after the start of transfection. Data are presented as fold induction relative to the basal siCon-transfected expression (mean \pm S.E.M, $n = 6$) and are representative of four independent experiments. *** = $p \leq 0.001$; * = $p \leq 0.05$.

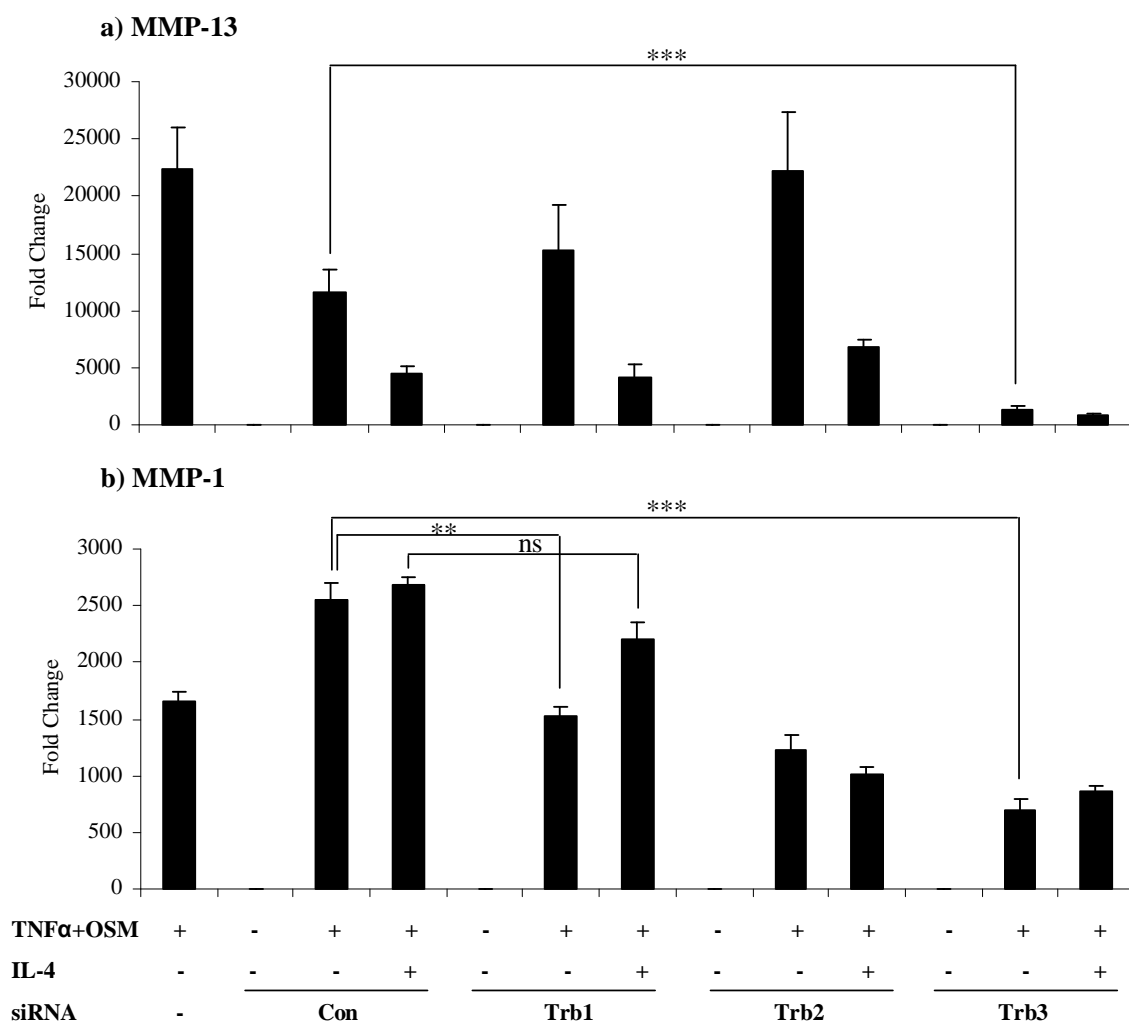


Figure 7.7 The effect of Trb protein family gene silencing on TNF α +OSM-induced collagenase gene expression in SW1353 cells. SW1353 cells were stimulated with control, TNF α +OSM (10 and 10 ng/ml, respectively), TNF α +OSM+IL-4 (10, 10 and 20 ng/ml, respectively) for 24 hours following a 28 hour transfection \pm siRNA specific to Trb1, Trb2, Trb3 or siCon (100 nM). Real-time RT-PCR of the isolated RNA was performed for MMP-13 (a) and MMP-1 (b) 72 hours after the start of transfection. Data are presented as fold induction relative to the basal siCon-transfected expression (mean \pm S.E.M, $n = 6$) and are taken from a single experiment. *** = $p \leq 0.001$; ** = $p \leq 0.01$; ns = not significant.

7.2.8 Investigations into the efficiency of Trb1 gene silencing

7.2.8.1 The effect of Trb1 gene silencing using siRNA on MMP-13 expression in SW1353 cells

The siRNA used to silence Trb1 in Figures 7.1 - 7.8 was SMARTpool[®] small interfering RNA (siRNA) from Dharmacon. This SMARTpool[®] siRNA consists of a mixture of four siRNA provided as a single reagent, so whilst the total Trb1 siRNA concentration in experiments was 100 nM, the actual concentration of each individual siRNA was only 25 nM. The first theory tested as to why Trb1 SMARTpool[®] siRNA was ineffective in reproducibly silencing Trb1 gene expression was that perhaps only one of the four siRNAs provided in the SMARTpool[®] was effectively silencing Trb1. To test this hypothesis, the four single siRNAs were purchased individually from Dharmacon and used separately in SW1353 cells at four times the concentration they had been present at in previous experiments. However, none of the four individual Trb1 siRNAs were able to rescue IL-4-mediated repression of IL-1+OSM-induced MMP-13 (Figure 7.9).

7.2.8.2 The effect of Trb1 gene silencing using shRNA on MMP-13 expression in SW1353 cells

The failure to observe consistent knockdown of Trb1 using siRNA purchased from Dharmacon led to the use of Trb1 shRNA in an attempt to produce efficient knockdown of Trb1 and reproducible rescue of IL-4-mediated repression of IL-1+OSM-induced MMP-13. MISSION shRNA clones were purchased from Sigma-Aldrich. Each clone was constructed within the lentivirus plasmid vector pLKO.1-Puro followed by transformation into *E. coli*. All five clones available from Sigma-Aldrich were purchased, each of which targeted a different region of the Trb1 gene sequence. Previous work in the department (Scott, 2009) had determined that the optimal multiplicity of infection (M.O.I.) for human articular chondrocytes was 15. As SW1353 cells are characteristically transfected more efficiently than primary chondrocytes, the initial experiment in SW1353 cells used an M.O.I of 10 (Figure 7.10a). Out of the five clones tested, only one (Trb1 1535) produced promising results in the rescue of IL-4-mediated repression of IL-1+OSM-induced MMP-13 ($p=0.08$). Whilst this result was not statistically significant, it was felt that the finding warranted further investigation. A second experiment was performed using an M.O.I of 25 (Figure

7.10b). The M.O.I was increased from 10 to 25 in order to try and maximise any effects of the Trb1 shRNA. Unfortunately the first shRNA experiment (Figure 7.10a) used the entire stock of Trb1 1539 and so this clone was not included in the second experiment (Figure 7.10b). Figure 7.10b showed a statistically significant rescue of IL-4-mediated repression of IL-1+OSM-induced MMP-13 by Trb1 1535. Again, none of the other clones were able to rescue IL-4-mediated repression of IL-1+OSM-induced MMP-13. IL-1+OSM-stimulated levels of MMP-13 were reduced following transduction with some shRNA clones. This made the effect of the shRNA clones on IL-1+OSM+IL-4-induced MMP-13 expression difficult to interpret. Despite this, the preliminary work with shRNA identified one commercially available Trb1 shRNA clone that appeared to successfully rescue IL-4-mediated repression of IL-1+OSM-induced MMP-13. Further work would be needed to assess the reproducibility of this finding.

Taken together, the preliminary experiments involving siRNA and shRNA would suggest that effective silencing of Trb1 is much more complex than silencing of Trb3. However, the data suggest that when Trb1 is effectively silenced, this knockdown is able to effectively rescue IL-4-mediated repression of IL-1+OSM-induced MMP-13. Further work is needed to understand the reproducibility issues concerning Trb1 gene silencing.

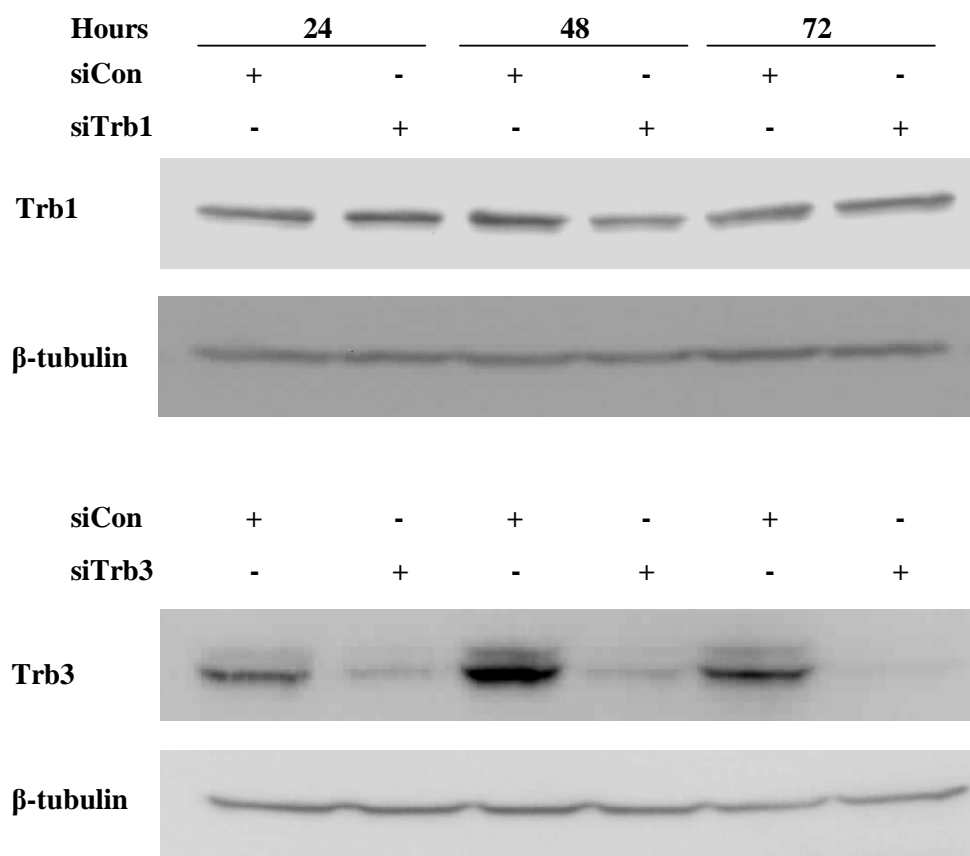


Figure 7.8 Transfection timecourse to determine the efficiency of Trb1 and Trb3 gene silencing in SW1353 cells, as determined by Western blot. Following transfection with siRNA specific to Trb1, Trb3 or siCon (100 nM) for 24, 48 or 72 hours, total cell lysates were prepared and separated by SDS-PAGE on a 10% polyacrylamide gel with a molecular weight marker. Protein fractions were transferred to PVDF membranes. Blots were probed with Trb1, Trb3 and β -tubulin followed by goat anti-rabbit HRP. The blots were visualised using ECL and are representative of two independent experiments.

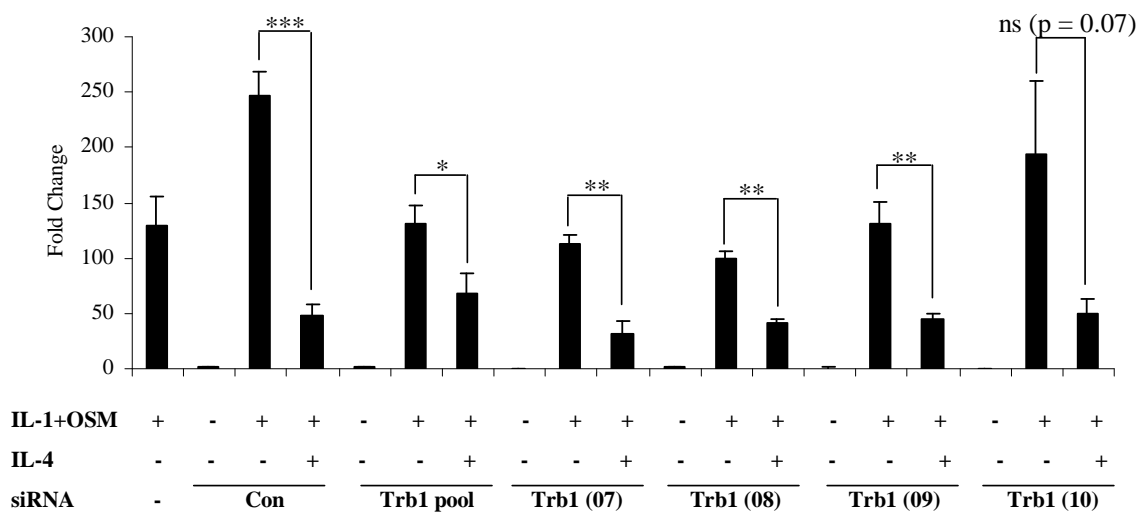


Figure 7.9 The effect of Trb1 gene silencing on MMP-13 expression in SW1353 cells. SW1353 cells were stimulated with control, IL-1+OSM (0.5 and 10 ng/ml, respectively) or IL-1+OSM+IL-4 (0.5, 10 and 20 ng/ml, respectively) for 24 hours following a 28 hour transfection with siRNA specific to Trb1 (Dharmacon SMARTpool), individual Dharmacon Trb1 siRNA (07-10) or siCon (100 nM). Real-time RT-PCR of the isolated RNA was performed for MMP-13 72 hours after the start of transfection. Data are presented as fold induction relative to the basal siCon-transfected expression (mean \pm S.E.M, $n = 4$). *** = $p \leq 0.001$; ** = $p \leq 0.01$; * = $p \leq 0.05$, ns = not significant. Data are from a single experiment only.

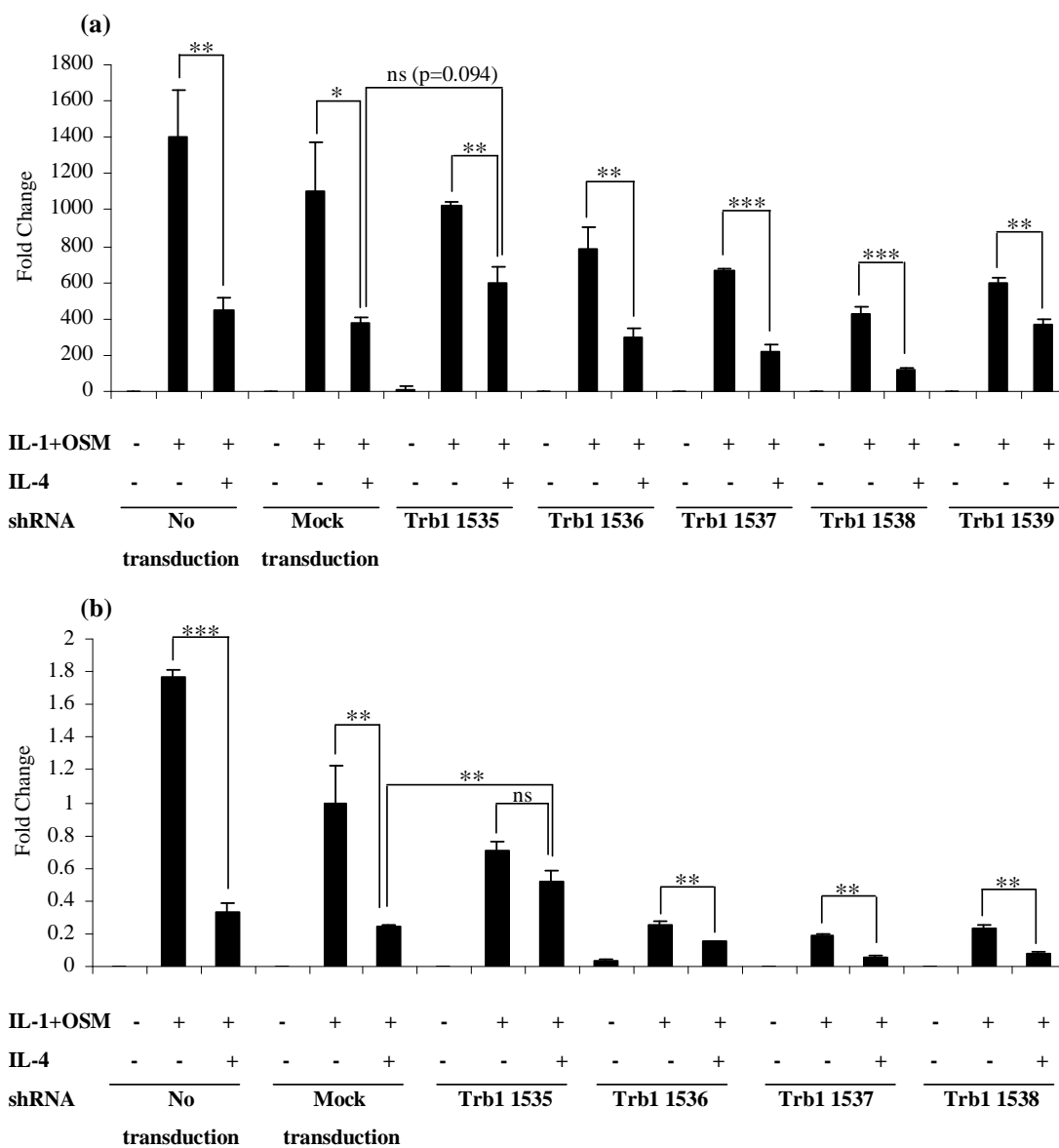


Figure 7.10 The effect of shRNA Trb1 gene silencing on MMP-13 expression in SW1353 cells. SW1353 cells were stimulated with control, IL-1+OSM (0.5 and 10 ng/ml, respectively) or IL-1+OSM+IL-4 (0.5, 10 and 20 ng/ml, respectively) for 24 hours following a 28 hour transduction with various shRNA specific to Trb1 (1535 - 1539) (MOI 10 (a) or 25 (b)). Real-time RT-PCR of the isolated RNA was performed for MMP-13 72 hours after the start of transduction. Data are presented as fold induction relative to the mock-transduced expression (mean \pm S.E.M, $n = 4$). *** = $p \leq 0.001$; ** = $p \leq 0.01$; * = $p \leq 0.05$; ns = not significant.

7.2.9 The effect of over-expression of Trb1, 2 or 3 on MMP-13 expression in SW1353 cells

Gene silencing data presented in this chapter have indicated a potential anti-inflammatory role for Trb1 (rescue of IL-4-mediated repression of IL-1+OSM-induced MMP-13 following Trb1 silencing) and a pro-inflammatory role for Trb3 (inhibition of IL-1+OSM-induced MMP-13 expression following Trb3 silencing). Experiments were performed using over-expression plasmids for the tribbles proteins to assess the effect of over-expression of these proteins on MMP-13 expression. It was hoped that over-expression of tribbles might result in converse effects to siRNA, thereby validating the interpretation. However, over-expression of Trb1 and Trb2 had no significant effect on IL-1+OSM+IL-4-induced MMP-13 expression. Over-expression of Trb3 was shown to enhance IL-1+OSM-induced MMP-13 expression when compared to pcDNA3.1 transfected SW1353 cells (Figure 7.11). The data presented here, along with those presented in Figure 7.6, support a pro-inflammatory role for Trb3 as over-expression resulted in a super-induction of MMP-13 (by IL-1+OSM) and silencing of Trb3 abolished IL-1+OSM-induced MMP-13 expression. Whilst this experiment was repeated three times, over-expression of Trb3 at the protein level (as demonstrated by Western blot) was only demonstrated in a single experiment (data not shown) and so it was assumed the over-expression was ineffective in the other two experiments. For this reason, the data from the other two experiments were not included.

7.2.10 The effect of IL-1+OSM and IL-1+OSM+IL-4 on the subcellular localisation of Trb1 and Trb3

At the time of study, no information existed on the subcellular localisation of tribbles proteins in chondrocytes. These experiments aimed to determine the subcellular localisation of tribbles proteins under basal conditions in SW1353 cells. In addition, they examined the effect of IL-1+OSM and IL-1+OSM+IL-4 treatment on the localisation of tribbles. Only one Trb2 antibody was available commercially at the time of study and this was ineffective in my experiments (data not shown). Various control antibodies were used to assess the purity of each fraction, for example MEK-2 was used as a marker of the cytoplasmic fraction, lamin A/C for the soluble nuclear fraction and histone H3 for the chromatin-bound nuclear fraction. The localisation of Akt was examined in order to provide another control

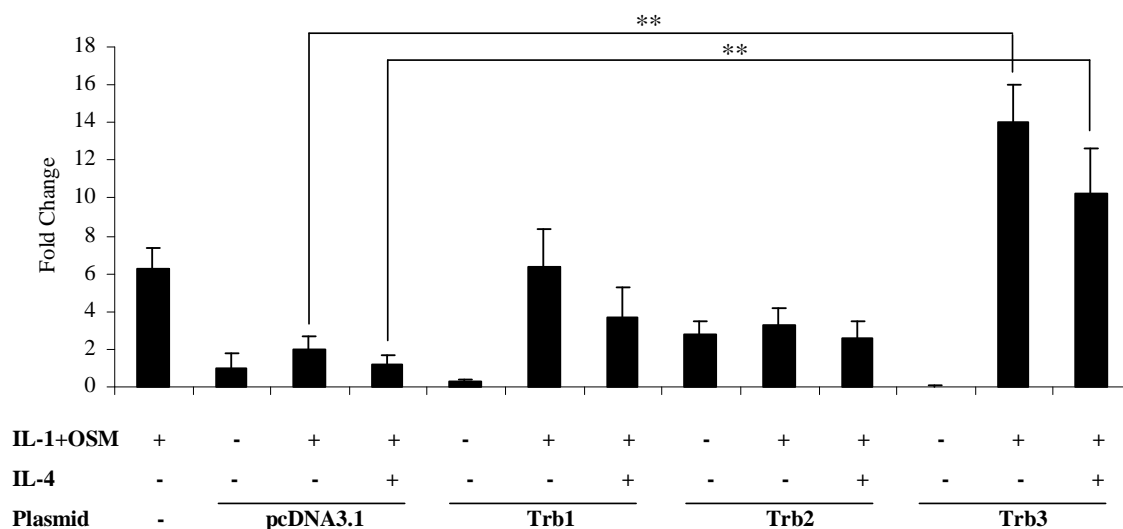


Figure 7.11 The effect of over-expression of Trb1, 2 or 3 on MMP-13 expression in SW1353 cells. SW1353 cells were stimulated with control, IL-1+OSM (0.5 and 10 ng/ml, respectively) or IL-1+OSM+IL-4 (0.5, 10 and 20 ng/ml, respectively) for 24 hours following a 28 hour transfection with over-expression plasmids specific to Trb1, Trb2, Trb3 or pcDNA3.1. Real-time RT-PCR of the isolated RNA was performed for MMP-13 following stimulation. Data are presented as fold induction relative to the pcDNA3.1-transduced basal expression (mean \pm S.E.M, $n = 6$) and are taken from a single experiment. ** = $p \leq 0.01$.

for the experiment. Akt is known to be mainly localised to the cytoplasmic fraction, which is demonstrated in Figure 7.12. In addition, data presented in Chapter 3 of this thesis showed that both OSM and IL-4 increase phosphorylation of Akt when compared to basal. This is also shown in Figure 7.12, indicating that cytokine stimulations worked as expected. Figure 7.12 demonstrates that Trb1 is principally cytoplasmic under basal and stimulated conditions. However, IL-1+OSM was shown to slightly enrich Trb1 in the membrane-bound fraction and IL-1+OSM+IL-4 increased this enrichment even more so. Trb3 was shown to be localised to the soluble-nuclear fraction under all conditions, but was also present in the cytoplasmic fraction under all conditions and to a lesser extent in the membrane-bound fraction. IL-1+OSM+IL-4 also increased Trb3 in the membrane-bound fraction, as was the case with Trb1.

7.2.11 MKK-Trb1 and –Trb3 interactions in SW1353 cells

The tribbles family of proteins has been identified as regulators of MAPK pathways (Kiss-Toth et al. 2006). They have been shown to interact with MAPK activators, MAPKKs and, in turn, modulate the activity of these MAPKKs (Kiss-Toth et al. 2004; Kiss-Toth et al. 2006). To assess any physical interactions between the tribbles and MAPKKs in SW1353 cells, a green fluorescent protein (GFP)-based protein fragment complementation assay (PCA) was used (as described in section 2.2.10.3). Multiple controls (MEK1 V1-pcDNA3.1, MKK4 V1-pcDNA3.1, MKK6 V1-pcDNA3.1, MKK7 V1-pcDNA3.1, Trb1 V2-pcDNA3.1, Trb3 V2-pcDNA3.1 and pcDNA3.1-pcDNA3.1) were included in the experiment to exclude false positive results. All controls were negative, however, for clarity only one example is shown in each figure (Figure 7.13 and 7.14). Data presented in Figure 7.13 demonstrate a physical interaction between Trb1 and MEK1, MKK4, MKK6 and MKK7. These data demonstrated that the MKK6-Trb1 and MKK7-Trb1 complexes are primarily located in the nucleus, whereas the MEK1-Trb1 and MKK4-Trb1 complex are primarily cytoplasmic. Given that subcellular localisation data in Figure 7.12 indicated that Trb1 is primarily cytoplasmic, data in Figure 7.13 suggests that Trb1 relocates to the nucleus when complexed with MKK6 and MKK7. Trb3 was also shown to form complexes with MEK1, MKK4, MKK6 and MKK7 (Figure 7.14). All the MKK-Trb3 complexes appeared to be nuclear, with the exception of MKK6-Trb3, which may be partially cytoplasmic.

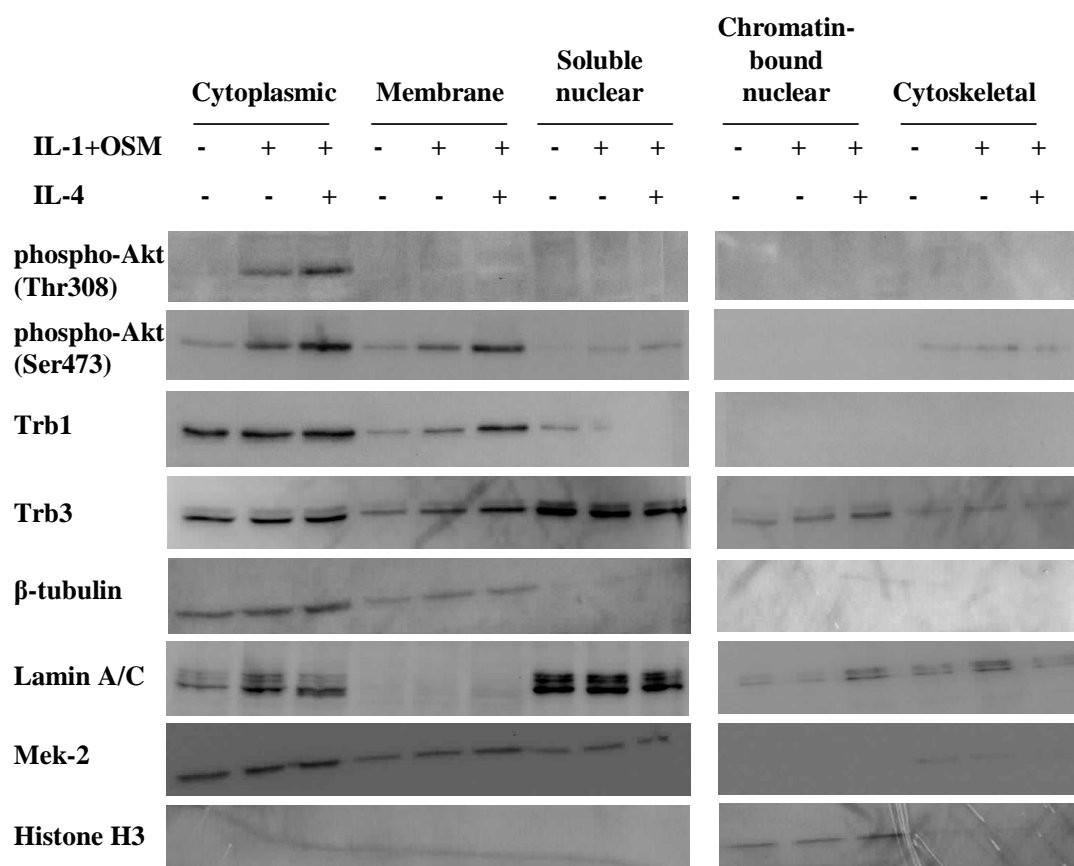


Figure 7.12 The effect of IL-1+OSM and IL-1+OSM+IL-4 on the subcellular localisation of Akt, Trb1 and Trb3, as determined by Western blot. SW1353 cells were stimulated with control, IL-1+OSM (0.5 and 10 ng/ml, respectively) or IL-1+OSM+IL-4 (0.5, 10 and 20 ng/ml, respectively) for 20 minutes. A subcellular protein fractionation kit was used to separate the cytoplasmic, membrane, soluble nuclear, chromatin-bound nuclear and cytoskeletal fractions. These lysates were separated by SDS-PAGE on a 10% polyacrylamide gel with a molecular weight marker. Protein fractions were transferred to PVDF membranes. Blots were probed with phospho-Akt (Thr308), phospho-Akt (Ser473), Trb1, Trb3, β -tubulin, lamin A/C, Mek-2 and histone H3 followed by goat anti-rabbit HRP. The blots were visualised using ECL and are representative of three independent experiments.

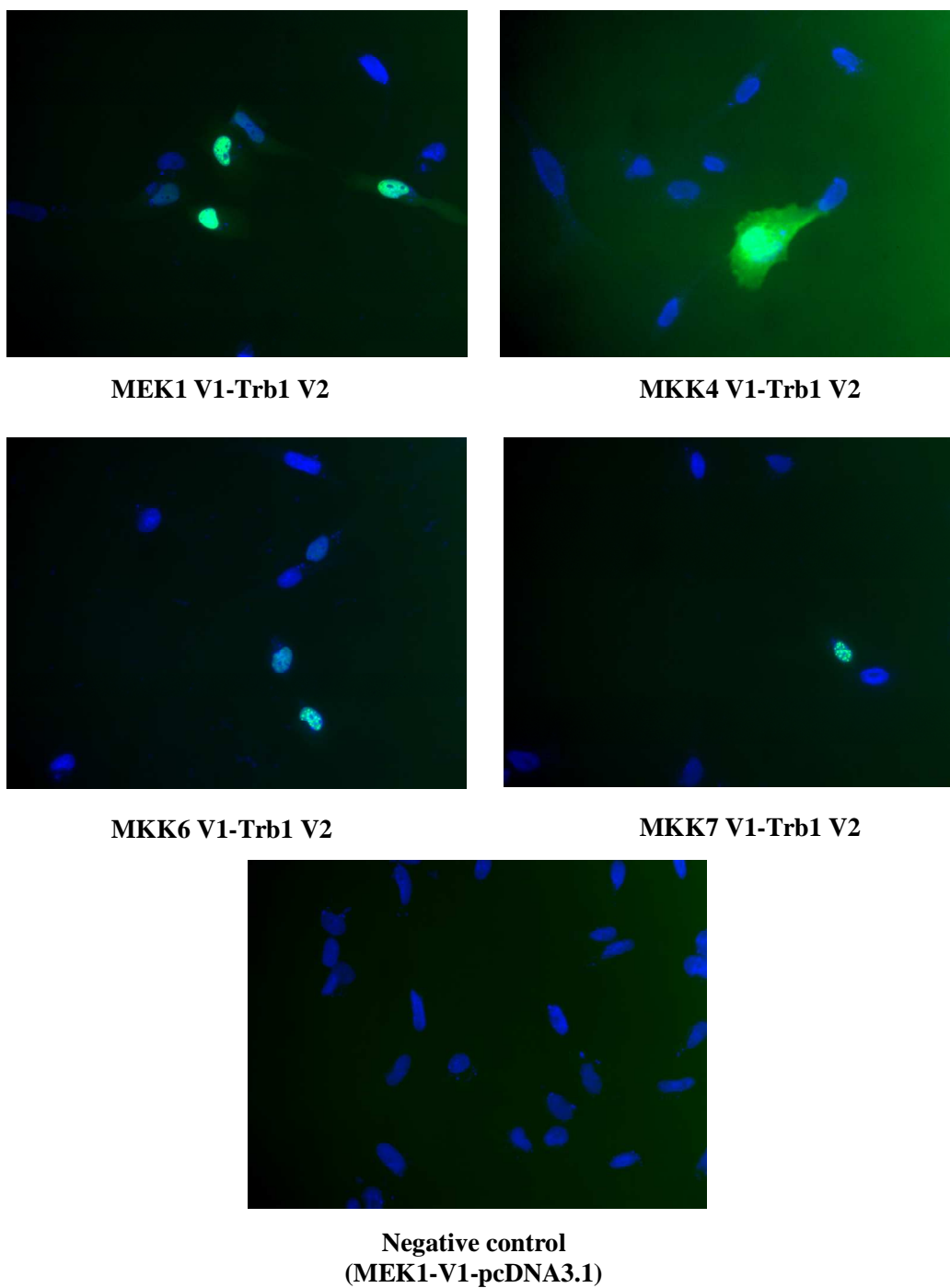


Figure 7.13 MEK1- and MKK-Trb1 interactions in SW1353 cells. Physical interaction between Trb1 and MKKs was investigated by GFP-based protein fragment complementation assay. MEK1, MKK4, MKK6 and MKK7 were fused to the N-terminal fragment of Venus GFP (V1) and Trb1 was fused to the C-terminal fragment of Venus GFP (V2). Various combinations of expression constructs were co-transfected and the GFP signal was visualised by fluorescence microscopy. Representative cells show the interaction between Trb1 and MKKs.

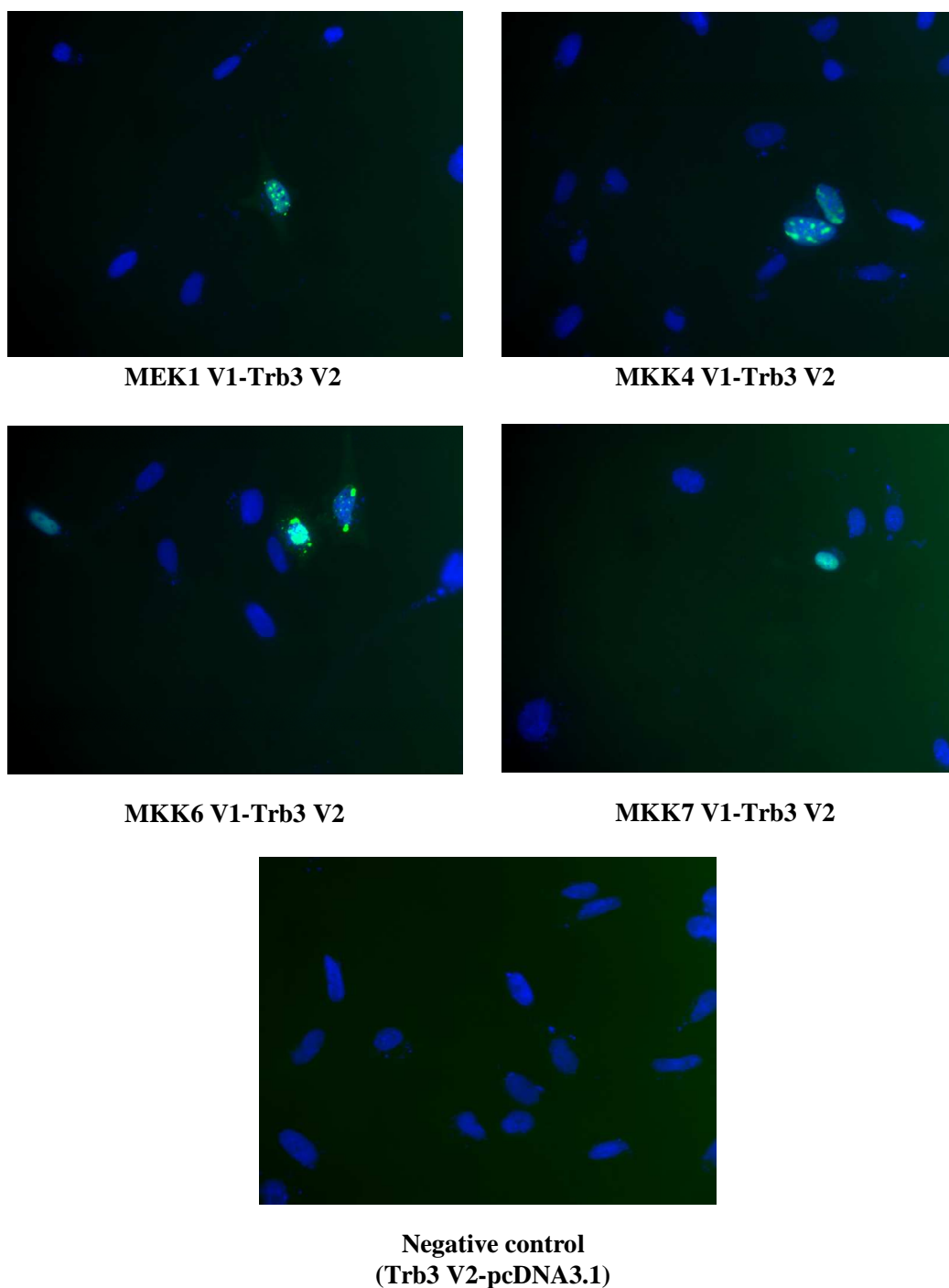


Figure 7.14 MEK1- and MKK-Trb3 interactions in SW1353 cells. Physical interaction between Trb3 and MKKs was investigated by GFP-based protein fragment complementation assay. MEK1, MKK4, MKK6 and MKK7 were fused to the N-terminal fragment of Venus GFP (V1) and Trb3 was fused to the C-terminal fragment of Venus GFP (V2). Various combinations of expression constructs were co-transfected and the GFP signal was visualised by fluorescence microscopy. Representative cells show the interaction between Trb3 and MKKs.

7.3 Discussion

Genome-wide microarrays described in Chapter 6 of this thesis highlighted numerous genes that were differentially expressed in IL-1+OSM+IL-4-treated cells/cartilage compared to IL-1+OSM-treated cells/cartilage, one of which was Trb1. This initial screen demonstrated Trb1 induction following IL-1+OSM stimulation of human chondrocytes and bovine cartilage, and this induction was further augmented following the inclusion of IL-4. This suggested that “anti-inflammatory” agents, such as IL-4, may mediate their repressive effects on MMP gene expression via increased Trb1 expression. Preliminary gene silencing experiments using siRNA specific to Trb1 provided more evidence that Trb1 may indeed be an important protein in mediating the chondroprotective effects of IL-4. Silencing of Trb1 was found to rescue IL-4-mediated repression of IL-1+OSM-induced MMP-13 expression, suggesting an anti-inflammatory role for Trb1. STAT6 is a major IL-4 signalling molecule and further experiments confirmed IL-4-mediated repression of IL-1+OSM-induced MMP-13 was STAT6-dependent. This indicated that STAT6 is upstream of Trb1, with increased Trb1 transcription resulting from STAT6-binding to the Trb1 promoter (bioinformatics confirmed there is a STAT6 binding element within the Trb1 promoter sequence).

In many instances MMP-13 expression following Trb1 silencing was found to be equal to, or greater than, that induced by IL-1+OSM. This phenomenon suggests that alterations in tribbles levels regulate the magnitude of the resultant pro-inflammatory stimulus in terms of MMP expression. This hyper-inducement of MMP expression has been observed previously. The IL-1+OSM+IL-4 stimulus consistently results in increased MMP-1 gene expression when compared to IL-1+OSM-induced MMP-1 expression. This IL-1+OSM-IL-4-induced increase in MMP-1 expression has also been shown to be STAT6-dependent. Previously, the potential mechanism for the observations that suggest pro-inflammatory stimuli are regulated in terms of the magnitude of MMP expression was unknown. The data presented here indicate that alterations in tribbles levels may impact upon this.

A recent study had suggested a role for Trb1 in the control of adipose tissue inflammation (Ostertag et al. 2010). Trb1 was found to be specifically up-regulated during acute and chronic inflammation in the white adipose tissue of mice. In adipocytes, Trb1 was found to

act as a nuclear transcriptional coactivator for the NF κ B subunit RelA, thereby promoting the induction of pro-inflammatory cytokines. It is not without precedent that this reported pro-inflammatory role for Trb1 is in apparent conflict with the anti-inflammatory role of Trb1 in chondrocytes. Indeed, IL-4 itself is known to be both pro- and anti-inflammatory depending on the circumstances and cell-type. Discrepancies in the function of mammalian and *Drosophila* tribbles have been reported (Kiss-Toth et al. 2004). It is thought that tribbles function in *Drosophila* is cell-type specific (Seher and Leptin 2000) and it is speculated that the same applies to the mammalian tribbles (Kiss-Toth et al. 2004).

Trb1 belongs to a family of three tribbles proteins and further gene silencing identified a novel role for Trb3 in IL-1+OSM-induced MMP-13 expression. Knockdown of Trb3 gene expression was shown to reproducibly abolish IL-1+OSM-induced MMP-13 expression, indicating a possible pro-inflammatory role for Trb3. Experiments involving TNF α +OSM, another pro-inflammatory cytokine combination known to synergistically induce cartilage degradation, extended these initial observations by also proving to be Trb3-dependent for MMP-13 induction. This suspected pro-inflammatory role for Trb3 was further confirmed by over-expression experiments, demonstrating that over-expression of Trb3 enhanced IL-1+OSM-induced MMP-13 expression. This apparently pro-inflammatory role for Trb3 is in agreement with the study by Cravero et al. (2009), which demonstrated that a significantly higher level of Trb3 was found in OA chondrocytes when compared to age-matched control chondrocytes. Taken together, these novel findings suggest individual tribbles may have opposing roles in MMP regulation.

The effects of Trb3 gene silencing on IL-1+OSM-induced MMP-13 expression were highly reproducible. However, problems were encountered with Trb1 gene silencing. Data presented in this chapter found that silencing of Trb1 was not always effective, leading to differing results when examining the effects of Trb1 knockdown on MMP-13 expression. Attempts to rationalise this ineffective silencing through the use of several different gene silencing reagents proved unsuccessful. It seems evident that extensive optimisation of the Trb1 silencing protocol is necessary in order to obtain reproducible gene knockdown. Despite problems with reproducibility, preliminary data suggest that when Trb1 gene silencing is effective, IL-4-mediated repression of IL-1+OSM-induced MMP-13 is rescued.

This finding has been replicated in both SW1353 cells and primary human articular chondrocytes, indicating that this is a valid result.

The function(s) of the tribbles proteins is still poorly understood. They have been identified as regulators of MAPK pathways (Kiss-Toth et al. 2006) and are known to interact with MAPK activators and MAPKKs, to modulate the activity of MAPKKs. Tribbles have also been shown to interact with components of the PI3K pathway (including Akt) as well as the transcription factors C/EBP, ATF4 and p65, thus enabling them to regulate the level of activation within these signalling systems (Hegedus et al. 2006). However, many aspects of the molecular basis of tribbles action remain unclear. Previous data revealed that in OA chondrocytes, specific Akt3 silencing repressed cytokine-induced MMP-13 expression but not MMP-1 (Litherland et al. 2008). Furthermore, Trb3 has been shown to bind to Akt and inhibit its phosphorylation in hepatocytes (Du et al. 2003), and Trb3 expression appears elevated in OA chondrocytes when compared to normal chondrocytes (Cravero et al. 2009). These findings, in addition to the data presented here, suggest a definite role for tribbles in MMP regulation. It is possible that the apparent regulation by tribbles of the magnitude of specific MMP induction demonstrated in this chapter may be related to their ability to regulate MAPK cascades. Previous work by the Kiss-Toth group (Kiss-Toth et al. 2004) investigated the physical interactions of Trb1/3 and various members of the MAPK signalling pathway in HeLa cells. This study found that MEK-1 interacts with both Trb1 and Trb3, whereas MKK7 specifically interacted with Trb-3 and MKK4 specifically interacted with Trb1. No interactions between Trb1 or 3 were detected between MEKK-1, MLK-3, ERK-2, JNK-1 or p38. In contrast to the 2004 study by Kiss-Toth et al., data presented in this chapter demonstrated that physical interactions could be detected between both Trb1 and Trb3 and MEK1, MKK4, MKK6 and MKK7 in SW1353 cells. Although not all cells exhibited fluorescence in this assay, punctate nuclear staining was indicative of the predicted localisation of these complexes. Due to time constraints, this assay was completed only once and so repeats are necessary to confirm the findings reported here. However, multiple controls were included in the experiment to exclude false positive results and fluorescence can only occur when two proteins physically interact within the same cell, and so the findings can be viewed with some confidence. The demonstration of these physical interactions in chondrocytes suggests that tribbles impact on pro-inflammatory MMP

regulation by controlling the balance of key signalling pathways through interactions with central components in the MAPK and PI3K pathway (interactions between tribbles and Akt have been previously documented (Cravero et al. 2009)).

Subcellular localisation data presented in this chapter found Trb1 to be mainly cytoplasmic in SW1353 cells, which is in contrast to data presented by other groups. Kiss-Toth et al. (2006) found Trb1 to be localised to the nucleus of HeLa cells. However, it is quite possible that the subcellular localisation of tribbles proteins is cell-type dependent. Trb3 was shown to be predominantly localised to the soluble-nuclear fraction in SW1353 cells, which is in agreement with previous reports (Ord and Ord 2003; Kiss-Toth et al. 2006). Indeed, some tribbles have been shown to possess nuclear localisation sequences (personal communication, Endre Kiss-Toth, Sheffield University). All the studies that have investigated the subcellular localisation of tribbles (to date) have been based upon the use of over-expression plasmids, therefore their conclusions should be regarded with some caution. The majority of signalling molecules act as part of a multiprotein complex, therefore higher than normal levels of a particular protein can lead to non-physiological intracellular localisation (Hegedus et al. 2007). When expressed as GFP fusion proteins, both Trb1 and Trb3 were localised to the nucleus of HeLa cells (Kiss-Toth et al. 2006). Trb3-GFP fusion protein has also been shown to be nuclear in GT1-7, Cos-7 and CHO cells (Ord and Ord 2003). Conversely, studies investigating the cellular localisation of Trb2 have suggested that Trb2 is found mainly in the cytoplasm (Wilkin et al. 1997; Saka and Smith 2004). A more recent paper agreed with these findings (Kiss-Toth et al. 2006).

Data presented in Chapter 5 of this thesis clearly showed the phosphorylation, and hence activation, of Akt by both OSM and IL-4. This finding posed the question of how two cytokines with opposing effects on cartilage (OSM being catabolic and IL-4 being anabolic), can both activate the same signalling molecule. The finding that tribbles proteins appear to play an important role in the regulation of cytokine-induced MMP expression may explain the activation of Akt in both OSM- and IL-4-signalling pathways. The important physiological function of tribbles proteins is now widely accepted; however, the molecular basis of tribbles function is still poorly understood. The presence of a kinase-like domain in tribbles proteins that appears to be catalytically inactive suggests that tribbles are

'kinase-dead' proteins. One hypothesis put forward by a recent review (Hegedus et al. 2007) suggests that tribbles may function as decoy proteins, by competing with active protein kinases for binding partners, thereby affecting the activation of downstream signalling pathways. One hypothesis that may explain the activation of Akt by both OSM and IL-4 could be that following either OSM-mediated Akt activation or IL-4-mediated Akt activation, tribbles proteins act to sequester either activated Akt or signalling molecules downstream of Akt, thereby altering downstream signalling events. This could mean that relatively subtle changes in tribbles expression, as demonstrated for Trb1 in this thesis, may still result in marked alterations in downstream signalling events and resultant MMP expression.

The observation that the magnitude of specific MMP induction appears to be regulated by tribbles suggests that alterations in functional levels of specific tribbles proteins may protect against aberrant MMP gene expression in chondrocytes. Future work should concentrate on identifying how individual tribbles mediate their effects. As tribbles are thought to be pseudo-kinases, protein interactions are likely to be their mechanism of action for regulating MMP-13 expression. In fact, it is likely that tribbles regulate signalling cross-talk, especially within an inflammatory environment. The consequences of specific tribbles over-expression or deletion in animal models of arthritis would need to be examined, in addition to molecular approaches to identify the mechanism by which tribbles regulate MMP-13. The data presented in this chapter represent highly novel data, which could lead to the development of a therapy to specifically target MMP-13, potentially ameliorating joint damage in arthritis.

7.4 Summary

- Individual tribbles may have opposing roles in MMP regulation
 - Data indicate a possible anti-inflammatory role for Trb1 as gene silencing of Trb1 results in the rescue of IL-4-mediated repression of IL-1+OSM-induced MMP-13.

- Data indicate a possible pro-inflammatory role for Trb3 as gene silencing of Trb3 abolishes IL-1+OSM-induced MMP-13 expression and over-expression of Trb3 enhances IL-1+OSM-induced MMP-13 expression.
- Under basal conditions Trb1 appears to be primarily cytoplasmic, whereas Trb3 appears to be predominantly nuclear.
- Both Trb1 and Trb3 interact with MEK1, MKK4, MKK6 and MKK7 in SW1353 cells.

Chapter 8: General discussion

Cartilage degradation in arthritic disease is characterised by irreversible collagenolysis. Of the enzymes capable of hydrolysing native collagen fibrils, MMP-13 is considered the major collagenolytic MMP in OA, whilst MMP-1 is thought to be the major destructive collagenase in RA. Inhibiting the action of these enzymes to prevent cartilage destruction is a highly sought after aim in arthritis research.

OA has historically been considered a ‘wear and tear’ process involving an imbalance between degradation and repair of the articular cartilage and subchondral bone favouring gradual catabolism. OA was originally thought of as a primarily non-inflammatory condition as opposed to RA where both local and systemic inflammation is a central feature. However, this theory is now being reconsidered as inflammatory cytokines and mediators produced by joint tissues are increasingly being shown to play a role in the pathogenesis of OA, perpetuating disease progression and therefore representing potential therapeutic targets (Goldring and Goldring 2007, Abramson and Attur 2009). The destructive process mediated by pro-inflammatory cytokines can be limited by anti-inflammatory mediators such as IL-4. Whilst up-regulation of some anti-inflammatory cytokines and inhibitory mediators does occur in chronic inflammatory conditions such as RA, it occurs at levels insufficient to prevent cartilage degradation. This imbalance between pro and anti-inflammatory cytokines is reflected by an abundance of pro-inflammatory cytokines, but a virtual absence of anti-inflammatory cytokines such as IL-4 in RA synovium. This is despite the presence of high levels of IL-4 in peripheral blood mononuclear cells of RA patients (Miossec et al. 1990). In 1996, Cawston et al. reported that IL-4 acted as a protective factor by specifically blocking the release of collagen from bovine nasal cartilage stimulated to resorb with IL-1+OSM, preventing pro-inflammatory cytokine-induced cartilage breakdown. However, direct administration of IL-4 to treat arthritis would undoubtedly result in potentially disastrous side-effects due to its known pro-inflammatory effects on target cells in other parts of the body. The aim of this PhD was

to further understand the protective mechanism of action of IL-4 in order to identify more specific therapeutic targets.

A bovine nasal cartilage explant model was used to investigate the effect of IL-4 on cartilage degradation and collagenase expression. The addition of the pro-inflammatory combination of IL-1+OSM to bovine nasal cartilage in explant culture induced an increase in the synthesis of procollagenases and a release of collagen fragments. This study corroborated the original findings of Cawston et al (1996), demonstrating that IL-4 was able to prevent IL-1+OSM-mediated cartilage collagen breakdown. Expanding on this original finding, data presented in Chapter 3 demonstrated that IL-4 was equally chondroprotective when addition of IL-4 was delayed until day 7 of the 14 day bovine nasal cartilage timecourse. IL-4 was shown to strongly and reproducibly down-regulate IL-1+OSM-induced MMP-13 expression in both primary chondrocytes and bovine nasal cartilage. For the first time, data presented in Chapter 3 demonstrated that complete repression of IL-1+OSM-induced MMP-13 expression occurred within 24 hours of IL-4 addition to bovine nasal cartilage. It has been suspected for some time that the chondroprotective effect of IL-4 in IL-1+OSM-induced cartilage collagen degradation was due to the strong repression of MMP-13 mRNA expression and/or the inhibition of activation of latent MMPs. Data presented in this thesis strongly suggest that it is the repression of MMP-13 that is responsible for the protective effect of IL-4 on cartilage degradation. The specific repression of MMP-13 by IL-4 is an important finding in relation to possible future therapies. Understanding the mechanism by which MMP-13 is specifically repressed could lead to a therapy with minimal side effects. Also reported in Chapter 3 was the finding that IL-4 differentially regulated MMP-1 and MMP-13 expression in bovine cartilage, primary chondrocytes and the chondrosarcoma cell line SW1353. IL-4 reproducibly inhibited IL-1+OSM-induced MMP-13 in bovine nasal chondrocytes and, albeit to a slightly lesser extent, in human articular chondrocytes and SW1353 cells. In contrast, IL-4 appeared to have no significant effect on IL-1+OSM-induced MMP-1 expression in any of the three cell types. If anything, a pattern of increasing MMP-1 expression in the presence of IL-4 was observed in all three cell types, although these increases were rarely statistically significant. This differential expression had been previously reported after examination of MMP expression by Northern blot (Pyle

2003), however this was the first study to examine MMP expression by real-time RT-PCR. These findings of differential collagenase gene expression in chondrocytes indicate that the signalling that drives collagenase transcriptional activation and subsequent production, especially of MMP-13, represents a therapeutic target that could have significant benefits for OA.

As IL-4 was shown to rapidly repress IL-1+OSM-induced MMP-13 expression, Chapter 4 sought to investigate the possibility that IL-4 induces epigenetic changes in the MMP-13 promoter, thereby leading to reduced gene expression. Epigenetic modifications provide information as to where and when a gene should be expressed as opposed to altering the structure or function of a gene. The predominant epigenetic modification of DNA in mammalian genomes is DNA methylation. Previous work by Roach et al. (2005) suggested that the increase in MMP-13 expression observed in OA cartilage correlated with demethylation at specific sites within the MMP-13 promoter. It was therefore hypothesised that IL-4 (in combination with IL-1+OSM) could decrease IL-1+OSM-induced MMP-13 mRNA expression by increasing MMP-13 promoter methylation. However, examination of the methylation status of the MMP-13 promoter via two different methods (bisulphite sequencing and pyrosequencing) found no evidence of a role for changes in MMP-13 promoter methylation in the regulation of MMP-13 gene expression by IL-1, IL-1+OSM or IL-1+OSM+IL-4 in bovine chondrocytes.

IL-4 is known to signal through IRS2, resulting in the activation of PI3K and its downstream target Akt. However, the role of this pathway in IL-4-induced gene expression is still unclear. Previous work in the group (Litherland et al. 2008) has demonstrated that OSM stimulates Akt phosphorylation in human articular chondrocytes, indicating Akt activation. Studies into PI3K signalling in chondrocytes in Chapter 5 confirmed that both OSM and IL-4 stimulation of chondrocytes resulted in the phosphorylation and hence activation of Akt. Due to the completely opposing effects of these two cytokines on cartilage destruction, this finding posed an interesting question. That is, how do the signalling pathways induced by two cytokines with opposing effects on cartilage degradation, both result in Akt activation? This question was further investigated in Chapter 7 of this thesis. Following the confirmation of PI3K-dependent Akt activation by

IL-4 in chondrocytes, Chapter 5 sought to examine the roles of PI3K p110 isoforms in IL-4-dependent Akt phosphorylation. The study by Litherland et al. (2008) indicated a role for p110 α and Akt1 in MMP-1 gene induction by IL-1+OSM. In addition, involvement of p110 δ and Akt3 were implicated in MMP-13 induction. No particular PI3K p110 isoform was found to have a clear role in IL-4-dependent Akt activation. In fact, data presented in Chapter 5 highlighted possible differences in PI3K p110 isoform involvement in different cell types. The involvement of specific PI3K p110 isoforms was difficult to interpret due to the same molecules (i.e. Akt) apparently being utilised by OSM (pro-inflammatory) and IL-4 (anti-inflammatory). Despite the uncertainty in the involvement of any specific PI3K p110 isoform in IL-4-dependent Akt activation, data presented in Chapter 5 did corroborate the findings of Litherland et al. (2008), indicating that p110 δ is required for MMP-13 induction by IL-1+OSM in chondrocytes. In support of this apparently pro-inflammatory role for PI3K p110 δ in chondrocytes, a 2006 study demonstrated a role for PI3K p110 δ in allergic airway inflammation in a murine asthma model (Lee et al. 2006).

Chapter 6 presented the findings of genome-wide screens following cytokine-treatment of bovine nasal cartilage, human articular chondrocytes and the chondrosarcoma cell line SW1353. The aim of this study was to identify candidate genes involved in the repression of MMP-13 by IL-4, and therefore the chondroprotective action of IL-4. A number of similarities were observed in the gene expression profiles of the three different systems and this, along with an extensive literature search, formed the basis of the selection of genes for further study. The results of this genome-wide study were limited due to the lack of replicates. However, the inclusion of numerous internal controls strengthened the reliability of the results. Indeed, the intention here was to generate new leads for investigations into the mechanism of action of IL-4, rather than generate publishable data.

One of the genes selected for further study following the genome-wide screen was Trb1. Preliminary studies into the role of tribbles in MMP regulation in chondrocytes revealed several novel findings. Gene silencing of Trb1 via siRNA resulted in the rescue of IL-4-mediated repression of IL-1+OSM-induced MMP-13 expression, indicating an anti-inflammatory role for Trb1 in the context of MMP regulation in chondrocytes. As the tribbles family of proteins are a relatively newly discovered family of proteins, there is

currently no literature available on the role of Trb1 in chondrocytes. However, a recent paper identified Trb1 as a tumour suppressor gene in acute myeloid leukaemia, with reduced Trb1 activity resulting in enhanced cell survival, thereby contributing to the pathogenesis of the disease (Gilby et al. 2010). Conversely, Trb1 has been shown to be up-regulated in acute and chronic inflammation in the white adipose tissue of mice (Ostertag et al. 2010). The genome-wide analysis described in Chapter 6 of this thesis reported an up-regulation of Trb1 by the pro-inflammatory cytokines IL-1+OSM, in agreement with the findings of Ostertag et al. (2010). However, the addition of the anti-inflammatory cytokine IL-4 to IL-1+OSM was shown to further increase Trb1 expression, indicating that Trb1 can dictate both pro- and anti-inflammatory responses depending on the functional levels of Trb1 within a cell. Expanding on the initial finding of Trb1 involvement in repression of MMP-13 by IL-4, further gene silencing experiments revealed a completely novel role for Trb3 in the pro-inflammatory induction of MMP-13 by IL-1+OSM. In support of a pro-inflammatory role for Trb3, experiments demonstrated that over-expression of Trb3 enhanced IL-1+OSM-induced MMP-13 expression. Trb3 has been linked to various pathological conditions including insulin resistance, diabetes and cardiovascular disease (Ord et al. 2009) and therefore a potentially pathogenic role for Trb3 in chondrocytes is not unexpected. Moreover, Trb3 is known to be expressed at higher levels in OA chondrocytes than in normal chondrocytes (Cravero et al. 2009), further supporting a pathogenic role for Trb3 in the development of OA.

These novel findings suggest that tribbles family members are integral to MMP regulation in chondrocytes. IL-4-mediated repression of IL-1+OSM-induced MMP-13 was shown to be STAT6-dependent. Previous work indicated that the chondroprotective nature of IL-4 was due to the expression of a STAT6-responsive gene (Pyle 2003). The data presented in Chapter 7 appear to confirm this. The tribbles are a relatively newly discovered family of proteins and so their role in cell signalling and gene regulation in response to inflammatory stimuli has not been well investigated. Therefore, the model proposed in this thesis whereby Trb1 and Trb3 regulate MMP-13 gene expression during pro- and anti-inflammatory signalling is speculative and further work is required to confirm this hypothesis.

As tribbles have been previously implicated in the control of MAPK signalling pathways (Kiss-Toth et al. 2004), further work examined physical interactions between tribbles proteins and MAPKKs. A GFP-based PCA assay demonstrated physical interactions between Trb1/Trb3 and MEK-1, MKK4, MKK6 and MKK7 in chondrocytes. The involvement of MAPKs in MMP signalling is well established, although not clearly understood (Rowan and Young 2007). For example, activation of the JNK and ERK pathways by IL-1 is known to result in the phosphorylation and activation of the activating protein-1 (AP-1) family member c-Jun, which subsequently dimerizes with c-Fos to drive transcription of various MMP genes, including MMP-1 and -13 (Vincenti and Brinckerhoff 2002). For that reason, the demonstration of these interactions between tribbles and MAPKKs is an important finding in relation to MMP regulation in chondrocytes. Following on from these preliminary findings, the suspected involvement of tribbles in the regulation of MAPK signalling pathways would need to be assessed in relation to pro- and anti-inflammatory stimuli. The phosphorylation status of various signalling molecules within the MAPK signalling pathway would be assessed following tribbles gene silencing, to identify any altered phosphorylation events following tribbles interaction. However, it may well be that phosphorylation events are unaltered by tribbles and instead the intracellular sequestration of signalling molecules could be responsible for the alteration of downstream signalling events following Akt activation, resulting in either the enhancement or abolishment of MMP expression. Co-immunoprecipitation experiments using tribbles antibodies, combined with mass spectrometry, could be used to identify tribbles-interacting proteins in stimulated chondrocytes. Following this, the subcellular localisation in which tribbles and identified binding partners are located would be determined under both basal and stimulated conditions.

One of the questions posed by data presented in Chapter 5 of this thesis was how do two cytokines (namely, OSM and IL-4) both activate Akt and yet have completely opposing effects on cartilage degradation and MMP regulation. The finding that the tribbles family of proteins appear to play an important role in MMP regulation in chondrocytes could partly explain this. It has been suggested that tribbles may function as decoy proteins (Hegedus et al. 2007), affecting the outcome of signalling pathways by competing with active protein kinases for binding partners. Trb3 is known to inhibit Akt in chondrocytes (Cravero et al.

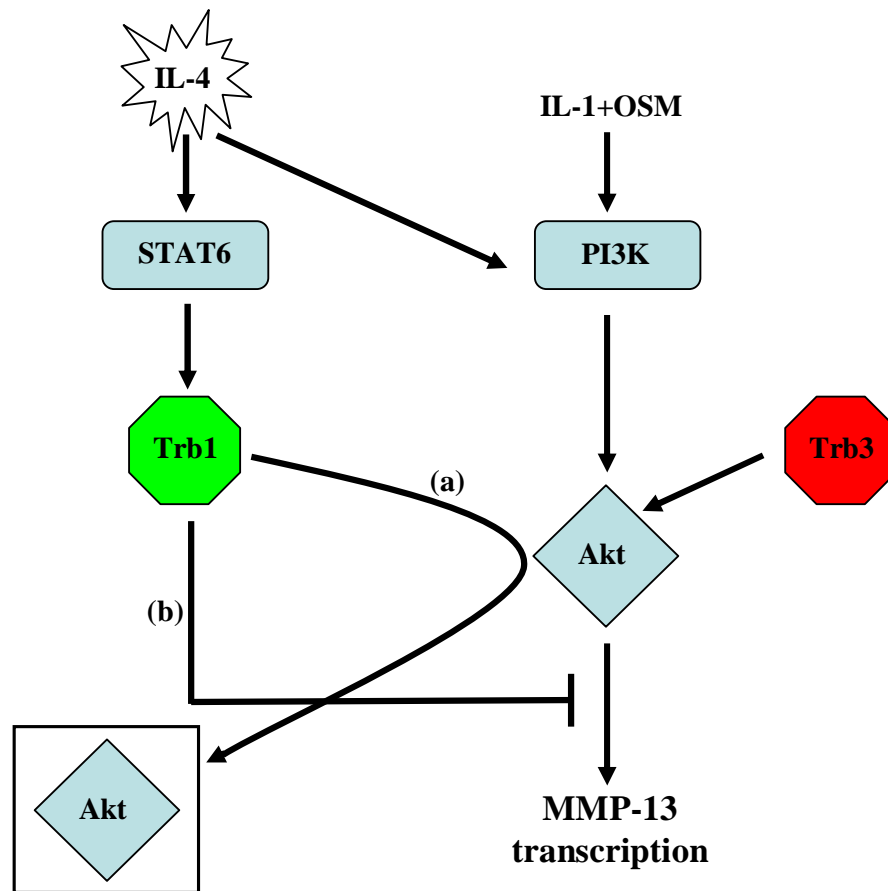


Figure 8.1 Diagram summarising the possible involvement of Trb proteins in MMP-13 expression and repression. Gene-silencing of Trb1 (via siRNA) has been shown to rescue IL-4-mediated repression of IL-1+OSM-induced MMP-13. This repression has been shown to be STAT6-dependent, suggesting STAT6 is upstream of Trb1, with increased Trb1 transcription via STAT6-binding to the Trb1 promoter. Tribbles-regulated MMP expression is further supported in that Trb3 silencing abolishes MMP-13 expression, supporting a pro-inflammatory role for Trb3. OSM and IL-4 signalling are both known to result in Akt activation and Trb proteins are known Akt-binding partners. It is hypothesised that IL-4 functions to repress MMP-13 expression via an upregulation of Trb1. Trb1 is then thought to (a) sequester activated Akt molecules, thereby preventing downstream signalling and inhibiting MMP-13 transcription and/or (b) act as a decoy protein for protein kinases downstream of Akt, again inhibiting MMP-13 transcription.

2009), and previous work within the department has provided compelling evidence that Akt-dependent signalling is critical for MMP expression in chondrocytes (Litherland et al. 2008). As Trb3 appears to play an important role in the pro-inflammatory cytokine induction of MMP-13, it could be hypothesised that following OSM-mediated Akt activation, tribbles proteins act to sequester activated Akt or signalling molecules downstream of Akt, thereby altering downstream signalling events in favour of MMP activation and therefore matrix catabolism. Data presented in Chapters 6 and 7 of this thesis have shown levels of Trb1 to be up-regulated in response to IL-4 in chondrocytes. Therefore, downstream signalling events following IL-4-mediated Akt activation could be hypothesised to be altered by the involvement of Trb1 (as opposed to Trb3), thereby preventing the induction of MMPs and resulting in the inhibition of cartilage degradation observed in the presence of IL-4. Given more time, experiments using a Trb3-deficient mouse model could be used to further examine the role of Trb3 in IL-1+OSM-induced MMP-13 induction in cartilage. The hypothesis described here would predict that Trb3-deficiency would protect against IL-1+OSM-induced arthritis following inter-articular over-expression of IL-1+OSM via adenoviral gene transfer. Previous studies have successfully used adenoviral gene transfer to over-express murine IL-1 and murine OSM intraarticularly in the knees of C57BL/6 mice resulting in increased MMP expression and cartilage destruction (Rowan et al. 2003). In addition, a Trb1 over-expression mouse model could be used to test the hypothesis that cartilage-specific Trb1 over-expression would result in fewer arthritic changes. Both transgenic animals are now available for these studies (A D Rowan and E Kiss-Toth, personal communication). C-myc tagged Trb1 and Trb3 over-expression constructs are available and so the hypothesised modulation of PI3K/Akt signalling pathways by tribbles would be examined using co-immunoprecipitation.

There are currently no treatments for OA that block cartilage destruction, and treatments for RA are expensive and ineffective in some patients. The increasing ageing population is resulting in a mounting disease burden that requires the development of new therapies. The success of current biological therapies indicates that targeting key mediators is a viable and important therapeutic strategy. Data presented in this thesis have demonstrated that IL-4 is able to specifically inhibit MMP-13 expression, a finding which opens up the possibility of

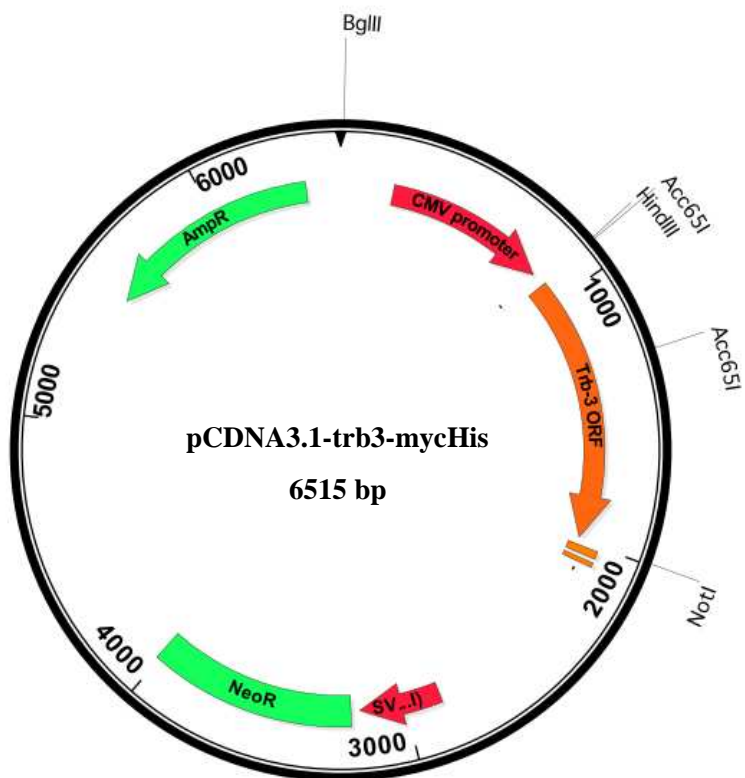
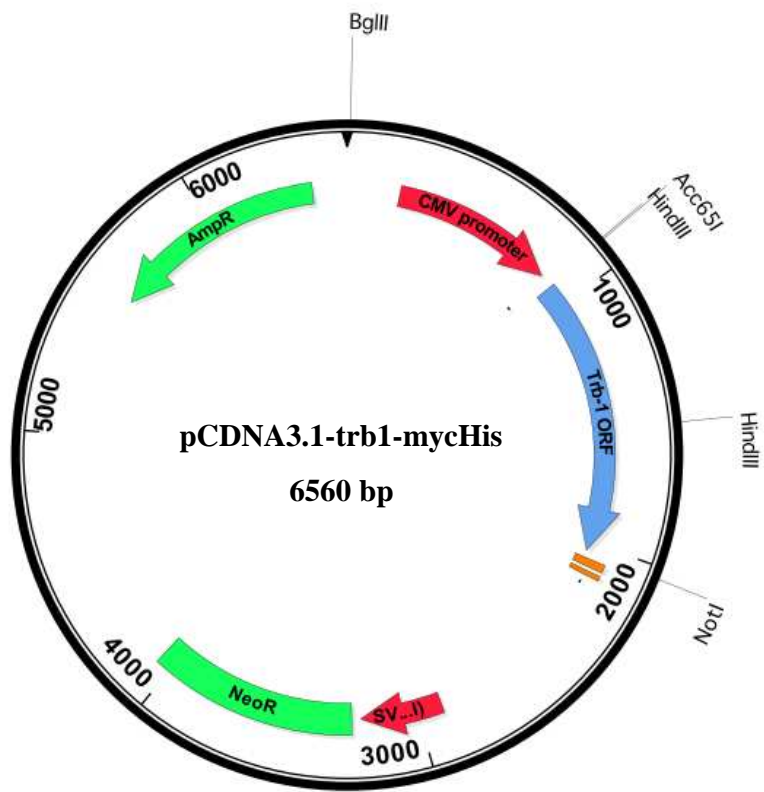
designing a drug to mimic this action. However, a better understanding of the mechanisms by which MMP genes are regulated is required to minimise potential side effects. The highly novel observations presented in this thesis demonstrating the involvement of the tribbles family of proteins in both pro- and anti-inflammatory MMP-13 regulation could provide a detailed understanding of the molecular mechanisms by which a key MMP gene is regulated in disease. Further work to unravel the mechanism of action by which tribbles regulate MMP expression could result in new therapies. Arthritic disease results in severe and prolonged disability and so any new therapy to limit cartilage destruction would dramatically reduce the escalating burden on the health services.

Summary of possible future studies:

- Characterise the impact of Trb1 over-expression and Trb3 deletion in arthritis models.
- Determine what factors regulate tribbles expression and identify their binding partners in chondrocytes.
- Investigate the molecular mechanisms of tribbles-controlled MMP-13 gene expression.
- Determine what other, if any, genes (including MMPs) are also regulated in a similar manner by tribbles.
- Examine which signalling pathways tribbles regulate and, to what extent tribbles impact on these signalling pathways in pro-inflammatory cytokine-stimulated chondrocytes.
- Investigate the binding partners of individual tribbles; and whether re-compartmentalisation of signalling molecules explains tribbles function in regulating MMP expression.

The most significant finding of this thesis is that IL-4 appears to prevent IL-1+OSM-induced cartilage destruction by specifically repressing MMP-13. Genome-wide microarrays identified Trb1 as a potential gene involved in the repression of MMP-13 by IL-4. Gene silencing experiments in chondrocytes confirmed that transfection with Trb1 specific siRNA resulted in the rescue of IL-4 mediated repression of IL-1+OSM-induced

MMP-13 expression, indicating an anti-inflammatory role for Trb1. Trb1 belongs to family of three tribbles proteins and additional studies to investigate the roles of other tribbles family members in MMP regulation identified Trb3 as having a potentially pro-inflammatory role in MMP regulation in chondrocytes. Silencing of Trb3 was reproducibly shown to abolish IL-1+OSM-induced MMP-13 expression. The novel preliminary data presented in this thesis indicate that tribbles proteins act as key regulators of catabolic and anabolic responses in chondrocytes. From these findings it could be hypothesised that alterations in functional levels of specific tribbles proteins may protect against aberrant MMP gene expression in chondrocytes. The identification of this potentially important regulatory mechanism of signalling pathways important in MMP-13 gene expression in chondrocytes could be translated into a tractable therapy for arthritis.



Genome-wide microarray results**Bovine nasal cartilage: IL-1+OSM+IL-4 vs IL-1+OSM**

Affymetrix ID	Fold change	Regulation	Symbol	Gene name
Bt.958.1.A1_at	157.97	up		Transcribed sequence with strong similarity to protein sp:P98066 (H.sapiens) TSG6_HUMAN Tumor necrosis factor-inducible protein TSG-6 precursor
Bt.19204.1.S1_at	44.89	up		Transcribed sequences
Bt.9202.1.S1_at	29.08	up		Transcribed sequence with strong similarity to protein sp:Q14314 (H.sapiens) FGL2_HUMAN Fibrolysin precursor
Bt.5362.1.S1_at	24.17	up	SERPINA3	serine (or cysteine) proteinase inhibitor, clade A (alpha-1 antitrypsin), member 3
Bt.4321.1.S1_at	23.31	up		Transcribed sequence with strong similarity to protein sp:Q9NSE2 (H.sapiens) CISH_HUMAN Cytokine-inducible SH2-containing protein
Bt.13556.2.A1_x_at	18.60	up	HF1	H factor 1 (complement)
Bt.13556.2.A1_at	18.27	up	HF1	H factor 1 (complement)
Bt.3307.1.A1_at	17.83	up		Transcribed sequence with strong similarity to protein pir:A57005 (H.sapiens) A57005 Norrie disease candidate protein - human
Bt.17331.1.A1_at	17.74	up		Transcribed sequence
Bt.13556.1.S1_a_at	16.96	up	HF1	H factor 1 (complement)
Bt.25478.1.A1_at	16.84	up		Transcribed sequence with strong similarity to protein ref:NP_066025.1 (H.sapiens) CEGP1 protein [Homo sapiens]
Bt.25236.1.A1_at	12.06	up		Transcribed sequences
Bt.13892.1.S1_at	11.71	up		Transcribed sequences
Bt.26538.1.S1_at	11.02	up		Transcribed sequence with moderate similarity to protein sp:Q15884 (H.sapiens) X123_HUMAN Putative protein X123
Bt.17780.1.A1_at	10.34	up		Transcribed sequence with weak similarity to protein sp:P14784 (H.sapiens) IL2B_HUMAN Interleukin-2 receptor beta chain precursor
Bt.23514.1.S1_at	9.88	up		Transcribed sequence with moderate similarity to protein sp:P01023 (H.sapiens) A2MG_HUMAN Alpha-2-macroglobulin precursor
Bt.28182.1.A1_at	9.82	up		Transcribed sequences
Bt.22545.2.S1_at	9.72	up		Transcribed sequence with strong similarity to protein pir:B36346 (H.sapiens) B36346 fibulin 1 precursor, splice form B - human
Bt.26803.1.A1_at	9.31	up		Transcribed sequences
Bt.8124.1.S2_at	9.18	up	COL1A2	collagen, type I, alpha 2
Bt.1929.1.S1_at	9.16	up		Transcribed sequences
Bt.9062.1.S1_at	9.13	up		Transcribed sequence with weak similarity to protein ref:NP_071420.1 (H.sapiens) secreted modular calcium-binding protein 1 [Homo sapiens]
Bt.14209.1.A1_at	9.08	up		Transcribed sequences
Bt.15488.1.A1_at	8.77	up		Transcribed sequence
Bt.17517.1.S1_at	8.60	up		Transcribed sequences
Bt.19231.1.S1_at	8.39	up		Transcribed sequence with strong similarity to protein sp:Q99574 (H.sapiens) NEUS_HUMAN Neuroserpin precursor
Bt.4063.1.S1_at	8.12	up	PLA2G7	phospholipase A2, group VII (platelet-activatingfactor acetylhydrolase, plasma)
Bt.7176.1.S1_at	7.84	up	SPON1	spondin 1, (f-spondin) extracellular matrixprotein
Bt.2017.1.S1_at	7.69	up	TFPI2	tissue factor pathway inhibitor 2
Bt.17036.1.A1_s_at	7.69	up		Transcribed sequence with strong similarity to protein pir:A41706 (H.sapiens) A41706 tryptophan--tRNA ligase
Bt.2236.1.S1_at	7.57	up		Transcribed sequences

Bt.19866.1.A1_at	7.44	up		Transcribed sequence with strong similarity to protein sp:Q9P2J9 (H.sapiens) PDP2_HUMAN [Pyruvate dehydrogenase [Lipoamide]]-phosphatase 2, mitochondrial precursor
Bt.8124.1.S1_at	7.23	up	COL1A2	collagen, type I, alpha 2
Bt.13482.1.S1_at	7.03	up		Transcribed sequence with moderate similarity to protein sp:P48745 (H.sapiens) NOV_HUMAN NOV protein homolog precursor
Bt.1736.1.A1_at	6.90	up		Transcribed sequence with strong similarity to protein ref:NP_003736.1 (H.sapiens) JAK binding protein [Homo sapiens]
Bt.2841.1.S1_at	6.77	up	WARS	tryptophanyl-tRNA synthetase
Bt.5530.1.S1_at	6.76	up	SDR1	short-chain dehydrogenase/reductase 1
Bt.4209.2.S1_a_at	6.73	up	C3	component 3
Bt.13526.1.S1_at	6.58	up		Transcribed sequences
Bt.982.1.S1_at	6.46	up	SERPINA1	serine (or cysteine) proteinase inhibitor, cladeA (alpha-1antitrypsin, antitrypsin), member 1
Bt.17881.1.S1_at	6.40	up		Transcribed sequences
Bt.4209.2.S1_at	6.39	up	C3	component 3
Bt.15298.1.A1_at	6.37	up		Transcribed sequences
Bt.3595.1.S1_at	6.27	up	MGP	matrix Gla protein
Bt.12440.1.A1_at	6.13	up		Transcribed sequence
Bt.422.1.S1_at	5.99	up	IGFBP-3	insulin-like growth factor binding protein-3
Bt.9421.1.S1_at	5.99	up	VIT	vitrin
Bt.26813.1.S1_at	5.86	up		Transcribed sequences
Bt.28209.1.S1_at	5.81	up		Transcribed sequences
Bt.3100.1.A1_at	5.77	up		Transcribed sequence
Bt.20745.1.A1_at	5.72	up		Transcribed sequences
Bt.24212.1.S1_at	5.60	up		Transcribed sequences
Bt.3247.1.S1_at	5.56	up		Transcribed sequence with moderate similarity to protein pir:T46488 (H.sapiens) T46488 hypothetical protein DKFZp434J065.1 - human
Bt.16048.1.S1_at	5.32	up		Transcribed sequence with weak similarity to protein sp:P10124 (H.sapiens) PGSG_HUMAN Secretory granule proteoglycan core protein precursor
Bt.22699.2.A1_at	5.26	up		Transcribed sequence with strong similarity to protein sp:Q12857 (H.sapiens) NFIA_HUMAN Nuclear factor 1 A-type
Bt.5598.1.S1_at	5.25	up		Transcribed sequence with strong similarity to protein ref:NP_064515.1 (H.sapiens) chromosome 8 open reading frame 4; C8ORF4 protein [Homo sapiens]
Bt.719.1.A1_at	5.23	up		Transcribed sequences
Bt.27202.1.A1_at	5.21	up		Transcribed sequences
Bt.390.1.S1_at	5.14	up	CALB3	calbindin 3, (vitamin D-dependent calciumbinding protein)
Bt.23864.1.A1_at	5.12	up		Transcribed sequences
Bt.24898.1.S1_at	5.09	up		Transcribed sequence with weak similarity to protein ref:NP_076973.1 (H.sapiens) hypothetical protein MGC2731 [Homo sapiens]
Bt.2638.1.S1_at	5.02	up	SERPINF1	serine (or cysteine) proteinase inhibitor, cladeF (alpha-2 antiplasmin, pigment epithelium derivedfactor), member 1
Bt.4939.1.S1_at	5.02	up		Transcribed sequence with strong similarity to protein pir:JE0174 (H.sapiens) JE0174 frizzled protein-2 - human
Bt.5861.1.S1_at	5.00	up		Transcribed sequence with moderate similarity to protein ref:NP_005935.3 (H.sapiens) OX-2 membrane glycoprotein precursor; MRC OX-2 antigen; antigen identified by monoclonal antibody MRC OX-2
Bt.982.1.S1_a_at	4.99	up	SERPINA1	serine (or cysteine) proteinase inhibitor, cladeA (alpha-1antitrypsin, antitrypsin), member 1
Bt.1855.1.S1_at	4.97	up	CST3	cystatin C (amyloid angiopathy and cerebralhemorrhage)

Bt.17865.1.A1_at	4.90	up		Transcribed sequence with moderate similarity to protein ref:NP_443178.1 (H.sapiens) hypothetical protein MGC20702 [Homo sapiens]
Bt.25733.1.A1_at	4.82	up		Transcribed sequence with moderate similarity to protein ref:NP_000203.1 (H.sapiens) integrin beta chain, beta 3 precursor; platelet glycoprotein IIIa precursor [Homo sapiens]
Bt.23354.1.S1_at	4.77	up		Transcribed sequence with moderate similarity to protein pir:A29939 (H.sapiens) A29939 epoxide hydrolase
Bt.4627.1.S1_at	4.72	up	SLC6A8	solute carrier family 6 (neurotransmitter transporter, creatine), member 8
Bt.4844.1.S1_at	4.71	up	PTN	pleiotrophin [heparin binding growth factor 8, neurite growth-promoting factor 1]
Bt.28162.3.S1_at	4.70	up		Transcribed sequence with strong similarity to protein pir:A40424 (H.sapiens) A40424 phospholamban - human
Bt.5847.1.S1_at	4.66	up		Transcribed sequence
Bt.555.1.S1_at	4.58	up	CA4	carbonic anhydrase IV
Bt.1319.1.S1_at	4.54	up		Transcribed sequences
Bt.21284.2.S1_at	4.53	up		Transcribed sequence with moderate similarity to protein ref:NP_057525.1 (H.sapiens) cysteine-rich motor neuron 1; cysteine-rich repeat-containing protein S52 precursor, [Homo sapiens]
Bt.26774.1.S1_at	4.50	up		Transcribed sequences
Bt.4209.1.S1_a_at	4.47	up	C3	component 3
Bt.6321.1.S1_at	4.44	up		Transcribed sequences
Bt.11679.1.S1_at	4.37	up		Transcribed sequences
Bt.18634.2.S1_at	4.36	up		Transcribed sequences
Bt.12694.1.S1_at	4.24	up		Transcribed sequence with strong similarity to protein ref:NP_055267.1 (H.sapiens) death receptor 6 [Homo sapiens]
Bt.27778.1.A1_at	4.23	up		Transcribed sequences
Bt.272.1.S1_at	4.23	up	PIM1	pim-1 oncogene
Bt.9379.1.S1_at	4.22	up	MAOA	monoamine oxydase A
Bt.25009.1.S1_at	4.21	up		Transcribed sequences
Bt.24211.1.A1_at	4.21	up		Transcribed sequence with strong similarity to protein ref:NP_060150.2 (H.sapiens) asporin
Bt.4627.1.S2_at	4.18	up	SLC6A8	solute carrier family 6 (neurotransmitter transporter, creatine), member 8
Bt.6802.1.S1_at	4.17	up		Transcribed sequences
Bt.28583.1.S1_s_at	4.16	up	LOC404102	similar to pro alpha 1(I) collagen
Bt.27543.1.A1_at	4.15	up		Transcribed sequences
Bt.376.1.S2_at	4.10	up	NPR3	natriuretic peptide receptor C [atrionatriureticpeptide receptor C]
Bt.9412.1.S1_at	4.10	up		Transcribed sequence with moderate similarity to protein pir:S46657 (H.sapiens) S46657 collagen alpha 1
Bt.23575.1.A1_at	4.08	up		Transcribed sequences
Bt.24452.1.S1_at	4.07	up		Transcribed sequence with strong similarity to protein ref:NP_004782.1 (H.sapiens) integrin, beta-like 1
Bt.28651.1.S1_at	4.05	up		Transcribed sequence with strong similarity to protein ref:NP_443083.1 (H.sapiens) similar to RhoGAP [Homo sapiens]
Bt.15939.1.A1_at	4.04	up		Transcribed sequences
Bt.6408.2.A1_at	4.01	up		Transcribed sequences
Bt.24904.1.A1_at	3.97	up		Transcribed sequence with strong similarity to protein sp:Q9H324 (H.sapiens) AT10_HUMAN ADAMTS-10 precursor
Bt.15828.2.S1_at	3.94	up		Transcribed sequence with strong similarity to protein ref:NP_079471.1 (H.sapiens) G-protein-coupled receptor induced protein [Homo sapiens]
Bt.15908.1.S1_at	3.94	up		Transcribed sequence with moderate similarity to protein pir:T08785 (H.sapiens) T08785 hypothetical protein DKFZp586A0522.1 - human
Bt.4394.1.S1_at	3.93	up	GUCY1B3	guanylate cyclase 1, soluble, beta 3

Bt.18264.1.A1_at	3.92	up		Transcribed sequences
Bt.632.1.S1_at	3.90	up	TIMP1	tissue inhibitor of metalloproteinase 1[erythroid potentiating activity, collagenase inhibitor]
Bt.22974.1.S1_at	3.90	up	SYNE1	spectrin repeat containing, nuclear envelope 1
Bt.14369.1.A1_at	3.86	up		Transcribed sequences
Bt.13780.1.A1_at	3.85	up		Transcribed sequence with strong similarity to protein sp:O43609 (H.sapiens) SPY1_HUMAN Sprouty homolog 1
Bt.27990.1.S1_at	3.84	up	5htr2a	5-hydroxytryptamine receptor 2A
Bt.24328.1.S1_at	3.83	up		Transcribed sequences
Bt.8549.1.S2_at	3.83	up	LOC404067	similar to pro alpha 1(I) collagen
Bt.29718.1.A1_a_at	3.83	up		Clone bghrmv3 growth hormone receptor mRNA, variant 5' UTR and partial cds
Bt.23042.1.S1_at	3.81	up	MT-1A	metallothionein-1A
Bt.24881.1.S1_at	3.78	up		Transcribed sequence with moderate similarity to protein ref:NP_036204.1 (H.sapiens) complement component C1q receptor [Homo sapiens]
Bt.16382.1.A1_at	3.78	up		Transcribed sequences
Bt.29718.1.S1_a_at	3.78	up		Clone bghrmv3 growth hormone receptor mRNA, variant 5' UTR and partial cds
Bt.13306.2.S1_at	3.76	up		Transcribed sequences
Bt.17518.1.S1_at	3.75	up		Transcribed sequences
Bt.13290.1.S1_at	3.73	up		Transcribed sequence with moderate similarity to protein pir:I38891 (H.sapiens) I38891 hypothetical protein - human
Bt.12606.1.S1_a_at	3.72	up		Transcribed sequences
Bt.22538.1.A1_at	3.72	up		Transcribed sequence with strong similarity to protein ref:NP_114072.1 (H.sapiens) frizzled homolog 8; frizzled
Bt.6483.1.A1_at	3.66	up		Transcribed sequences
Bt.3964.1.S1_at	3.61	up	SLC2A3	solute carrier family 2 (facilitated glucosetransporter), member 3
Bt.632.1.S1_s_at	3.60	up	TIMP1	tissue inhibitor of metalloproteinase 1[erythroid potentiating activity, collagenase inhibitor]
Bt.8549.1.S1_at	3.59	up	LOC404067	similar to pro alpha 1(I) collagen
Bt.15828.1.S1_at	3.55	up		Transcribed sequence with strong similarity to protein ref:NP_079471.1 (H.sapiens) G-protein-coupled receptor induced protein [Homo sapiens]
Bt.18581.1.A1_at	3.55	up		Transcribed sequence
Bt.8486.1.S1_at	3.50	up		Transcribed sequences
Bt.7393.1.S1_at	3.47	up		Transcribed sequences
Bt.1807.1.A1_at	3.47	up		Transcribed sequences
Bt.20404.1.S1_at	3.46	up		Transcribed sequences
Bt.27976.1.S1_at	3.44	up		MRNA for similar to tissue inhibitor of metalloproteinases, partial cds, clone: ORCS11139
Bt.16381.1.S1_at	3.43	up		Transcribed sequences
Bt.6556.1.S1_at	3.43	up		Transcribed sequence with weak similarity to protein prf:2208449A (H.sapiens) 2208449A eotaxin [Homo sapiens]
Bt.11599.1.S1_at	3.41	up		Transcribed sequences
Bt.4653.1.S2_at	3.41	up	PECAM1	platelet/endothelial cell adhesion molecule [CD31 antigen]
Bt.20979.1.S1_at	3.40	up		Transcribed sequences
Bt.21284.1.A1_at	3.38	up		Transcribed sequence with moderate similarity to protein ref:NP_057525.1 (H.sapiens) cysteine-rich motor neuron 1; cysteine-rich repeat-containing protein S52 precursor, [Homo sapiens]
Bt.13849.1.S1_at	3.38	up		Transcribed sequence with moderate similarity to protein ref:NP_067017.1 (H.sapiens) solute carrier family 30
Bt.13306.1.S1_at	3.37	up		Transcribed sequences
Bt.26053.1.A1_at	3.37	up		Transcribed sequence with moderate similarity to protein pir:A40970 (H.sapiens) A40970 undulin 1 - human
Bt.8948.1.S1_at	3.36	up	LOX	lysyl oxidase

Bt.22735.1.S1_at	3.35	up		Transcribed sequence with strong similarity to protein ref:NP_115755.2 (H.sapiens) synaptotagmin-like 2, isoform b; chromosome 11 synaptotagmin [Homo sapiens]
Bt.28162.1.S1_at	3.34	up		Transcribed sequence with strong similarity to protein pir:A40424 (H.sapiens) A40424 phospholamban - human
Bt.13387.1.S1_at	3.33	up		Transcribed sequence with weak similarity to protein sp:P05156 (H.sapiens) CFAI_HUMAN Complement factor I precursor
Bt.21540.1.S1_at	3.31	up	FGFR2	FGF-receptor
Bt.26971.1.S1_at	3.31	up		Transcribed sequences
Bt.16284.1.A1_at	3.30	up		Transcribed sequences
Bt.3216.1.A1_at	3.29	up		Transcribed sequence with strong similarity to protein ref:NP_057692.1 (H.sapiens) ALEX1 protein [Homo sapiens]
Bt.5075.1.S1_at	3.29	up		Transcribed sequence with moderate similarity to protein ref:NP_066925.1 (H.sapiens) serine protease inhibitor, Kunitz type, 2; placental bikunin
Bt.4552.4.A1_at	3.28	up	PLCB4	phospholipase C beta
Bt.8131.1.S1_at	3.27	up	ALCAM	activated leucocyte cell adhesion molecule
Bt.22063.1.A1_at	3.26	up		Transcribed sequences
Bt.13566.1.A1_at	3.26	up		Transcribed sequence
Bt.6504.1.S1_at	3.26	up		Transcribed sequences
Bt.20373.1.S1_at	3.25	up		Transcribed sequence with strong similarity to protein sp:O14786 (H.sapiens) NRP1_HUMAN Neuropilin-1 precursor
Bt.22974.1.A1_at	3.20	up	SYNE1	spectrin repeat containing, nuclear envelope 1
Bt.23791.1.A1_at	3.20	up		Transcribed sequence
Bt.9724.1.S1_at	3.18	up		Transcribed sequences
Bt.16012.1.S1_at	3.18	up	GHR	growth hormone receptor
Bt.8897.1.S1_at	3.17	up	C20orf114	von Ebner minor salivary gland protein
Bt.29378.1.A1_at	3.16	up		Transcribed sequence
Bt.24997.1.S1_at	3.16	up		Transcribed sequences
Bt.20064.2.S1_at	3.16	up		Transcribed sequence with moderate similarity to protein ref:NP_005777.2 (H.sapiens) serologically defined colon cancer antigen 33 [Homo sapiens]
Bt.24434.1.A1_at	3.16	up		Transcribed sequences
Bt.20064.1.S1_at	3.12	up		Transcribed sequence with moderate similarity to protein ref:NP_005777.2 (H.sapiens) serologically defined colon cancer antigen 33 [Homo sapiens]
Bt.20295.1.A1_at	3.12	up		Transcribed sequences
Bt.12765.1.S1_at	3.11	up	RDH10	retinol dehydrogenase 10 (all-trans)
Bt.29350.1.A1_at	3.11	up		Transcribed sequence with moderate similarity to protein sp:P57059 (H.sapiens) SN1L_HUMAN Probable serine/threonine protein kinase SNF1LK
Bt.20532.1.S1_at	3.10	up		Transcribed sequence with strong similarity to protein pir:S27332 (H.sapiens) S27332 proteasome chain LMP2 - human
Bt.13039.1.A1_at	3.10	up	ITGB3	integrin, beta 3 (platelet glycoprotein IIIa, antigen CD61)
Bt.19508.1.A1_at	3.09	up		Transcribed sequence with weak similarity to protein ref:NP_005699.1 (H.sapiens) glypican 6 precursor [Homo sapiens]
Bt.26426.1.A1_at	3.09	up		Transcribed sequences
Bt.24532.1.A1_at	3.06	up		Transcribed sequence with moderate similarity to protein ref:NP_062529.1 (M.musculus) ecotropic viral integration site 27; IL-17B receptor [Mus musculus]
Bt.26095.1.A1_at	3.05	up		Transcribed sequences
Bt.22076.1.A1_at	3.05	up		Transcribed sequences
Bt.10442.2.S1_a_at	3.05	up	COL12A1	collagen, type XII, alpha 1
Bt.29806.1.A1_at	3.05	up		Clone bghrmv6 growth hormone receptor mRNA, variant 5' UTR and partial cds
Bt.27091.2.S1_at	3.04	up		Transcribed sequences

Bt.4167.1.S1_at	3.04	up		Transcribed sequence with strong similarity to protein pir:S55272 (H.sapiens) S55272 DNA-binding protein NEFA precursor - human
Bt.26328.1.A1_at	3.03	up		Transcribed sequence
Bt.23276.1.S1_at	3.03	up		Transcribed sequence with strong similarity to protein sp:Q9Y4K1 (H.sapiens) AIM1_HUMAN Absent in melanoma 1 protein
Bt.17606.1.A1_at	3.03	up		Transcribed sequence
Bt.28659.1.A1_at	3.02	up		Transcribed sequences
Bt.28162.2.A1_at	3.02	up		Transcribed sequence with strong similarity to protein pir:A40424 (H.sapiens) A40424 phospholamban - human
Bt.4263.1.S1_at	3.01	up	GPRK5	G protein-coupled receptor kinase 5
Bt.21924.1.A1_at	3.00	up		Transcribed sequences
Bt.13482.2.S1_at	3.00	up		Transcribed sequence with moderate similarity to protein sp:P48745 (H.sapiens) NOV_HUMAN NOV protein homolog precursor
Bt.347.1.S1_at	2.97	up	CHAD	chondroadherin
Bt.19834.1.A1_at	2.97	up		Transcribed sequence
Bt.16857.1.A1_at	2.97	up		Transcribed sequence with weak similarity to protein ref:NP_077024.1 (H.sapiens) hypothetical protein FLJ11354 [Homo sapiens]
Bt.10565.1.A1_at	2.95	up		Transcribed sequence with moderate similarity to protein pir:T12520 (H.sapiens) T12520 hypothetical protein DKFZp434G173.1 - human
Bt.4586.1.S1_at	2.95	up	GNG2	guanine nucleotide binding protein (G protein), gamma 2
Bt.20226.1.A1_at	2.95	up		Transcribed sequences
Bt.20490.1.S1_at	2.94	up		Transcribed sequence with moderate similarity to protein ref:NP_036253.2 (H.sapiens) binder of Rho GTPases 4; Cdc42 effector protein 4 [Homo sapiens]
Bt.2519.1.S1_at	2.92	up	PLAU	plasminogen activator, urokinase
Bt.23276.2.S1_at	2.92	up		Transcribed sequence with strong similarity to protein sp:Q9Y4K1 (H.sapiens) AIM1_HUMAN Absent in melanoma 1 protein
Bt.17738.1.A1_at	2.91	up		Transcribed sequences
Bt.6279.1.A1_at	2.91	up		Transcribed sequence with strong similarity to protein ref:NP_004990.1 (H.sapiens) myosin VI [Homo sapiens]
Bt.3732.1.A1_at	2.91	up		Transcribed sequences
Bt.22953.1.S1_at	2.88	up	TYRP2	tyrosinase-related protein-2
Bt.13330.1.S1_at	2.88	up		Transcribed sequences
Bt.13039.1.S1_at	2.88	up	ITGB3	integrin, beta 3 (platelet glycoprotein IIIa, antigen CD61)
Bt.7130.1.S1_at	2.87	up		Transcribed sequence with strong similarity to protein sp:Q9Y5Z0 (H.sapiens) BAE2_HUMAN Beta secretase 2 precursor
Bt.18689.1.S1_at	2.86	up		Transcribed sequences
Bt.1433.1.S1_at	2.86	up		Transcribed sequences
Bt.15939.2.S1_at	2.85	up		Transcribed sequences
Bt.16510.1.A1_at	2.84	up		Transcribed sequences
Bt.11017.1.S1_at	2.83	up		Transcribed sequence with moderate similarity to protein pir:T12520 (H.sapiens) T12520 hypothetical protein DKFZp434G173.1 - human
Bt.28393.1.S1_at	2.81	up		Transcribed sequence with weak similarity to protein sp:P08174 (H.sapiens) DAF_HUMAN Complement decay-accelerating factor precursor
Bt.26445.1.A1_at	2.80	up		Transcribed sequence
Bt.3913.1.S1_at	2.79	up	VEGFC	vascular endothelial growth factor C
Bt.15692.1.A1_at	2.78	up		Transcribed sequence with weak similarity to protein sp:Q9NV58 (H.sapiens) RN19_HUMAN RING finger protein 19
Bt.21924.2.S1_at	2.77	up		Transcribed sequences
Bt.16769.1.A1_at	2.77	up		Transcribed sequence

Bt.17324.1.A1_at	2.76	up		Transcribed sequences
Bt.10150.1.S1_at	2.76	up		Transcribed sequences
Bt.22349.2.S1_at	2.74	up		Transcribed sequences
Bt.10340.1.S1_at	2.74	up		Transcribed sequences
Bt.10442.2.A1_at	2.72	up	COL12A1	collagen, type XII, alpha 1
Bt.4901.1.S1_at	2.72	up		Transcribed sequence with strong similarity to protein pir:B46619 (H.sapiens) B46619 Ca ²⁺ /calmodulin-dependent protein kinase
Bt.20706.1.A1_at	2.71	up		Transcribed sequences
Bt.10222.1.S1_at	2.71	up		Transcribed sequences
Bt.22000.1.A1_at	2.71	up		Transcribed sequences
Bt.19097.2.S1_at	2.70	up		Transcribed sequences
Bt.28780.2.A1_a_at	2.70	up		Transcribed sequence with weak similarity to protein pir:A55380 (H.sapiens) A55380 faciogenital dysplasia-associated protein FGD1 - human
Bt.19355.1.A1_at	2.70	up		Transcribed sequence with moderate similarity to protein pir:S41819 (H.sapiens) S41819 nucleoporin p62 - human
Bt.13553.2.S1_at	2.70	up		Transcribed sequence with strong similarity to protein ref:NP_068747.1 (H.sapiens) hypothetical protein FLJ22649 similar to signal peptidase SPC22/ [Homo sapiens]
Bt.27769.1.A1_at	2.69	up		Transcribed sequence
Bt.19517.1.S1_at	2.69	up		Transcribed sequence with moderate similarity to protein sp:P21860 (H.sapiens) ERB3_HUMAN Receptor protein-tyrosine kinase erbB-3 precursor
Bt.10076.1.S1_at	2.69	up		Transcribed sequences
Bt.11315.1.A1_at	2.68	up		Transcribed sequences
Bt.11324.1.A1_s_at	2.67	up		Transcribed sequence
Bt.23770.1.A1_at	2.66	up		Transcribed sequences
Bt.20393.1.S1_at	2.66	up		Transcribed sequence with strong similarity to protein prf:2121279A (H.sapiens) 2121279A protein disulfide isomerase-related protein [Homo sapiens]
Bt.663.1.S1_at	2.65	up		Transcribed sequences
Bt.5878.1.A1_at	2.65	up		Transcribed sequence with moderate similarity to protein sp:P20132 (H.sapiens) SDHL_HUMAN L-serine dehydratase
Bt.1974.1.S1_at	2.65	up		Transcribed sequences
Bt.8486.2.S1_at	2.65	up		Transcribed sequences
Bt.9594.1.S1_at	2.65	up		Transcribed sequences
Bt.24342.1.A1_at	2.65	up		Transcribed sequence with strong similarity to protein ref:NP_066969.1 (H.sapiens) angiopoietin-like factor [Homo sapiens]
Bt.24941.1.S1_at	2.64	up		Transcribed sequence with weak similarity to protein sp:P08910 (H.sapiens) HPS1_HUMAN Protein PHPS1-2
Bt.6449.1.S1_at	2.64	up		Transcribed sequence with strong similarity to protein sp:Q9UBX5 (H.sapiens) FBL5_HUMAN Fibulin-5 precursor
Bt.21762.2.S1_at	2.62	up		Transcribed sequences
Bt.19217.1.A1_at	2.62	up		Transcribed sequences
Bt.20430.1.A1_at	2.62	up		Transcribed sequence with moderate similarity to protein ref:NP_478144.1 (H.sapiens) HEAT-like repeat-containing protein, isoform 1; MGC4163 protein [Homo sapiens]
Bt.12964.1.A1_at	2.61	up		Transcribed sequence
Bt.25099.1.A1_at	2.60	up		Transcribed sequence with strong similarity to protein ref:NP_004568.1 (H.sapiens) phosphoserine phosphatase [Homo sapiens]
Bt.8803.1.A1_at	2.60	up		Transcribed sequence with moderate similarity to protein sp:P00736 (H.sapiens) C1R_HUMAN Complement C1r component precursor
Bt.3580.1.A1_at	2.59	up		Transcribed sequence with weak similarity to protein sp:Q99538 (H.sapiens) LEGU_HUMAN Legumain precursor
Bt.19295.1.S1_at	2.59	up		Transcribed sequences

Bt.13912.1.S1_at	2.58	up		Transcribed sequences
Bt.21294.1.A1_at	2.57	up		Transcribed sequences
Bt.12912.1.S2_at	2.56	up	COL4A1	collagen, type IV, alpha 1
Bt.3034.1.S1_at	2.56	up	COMP	cartilage oligomeric matrix protein
Bt.29411.2.A1_at	2.56	up		Transcribed sequence with strong similarity to protein pir:T00352 (H.sapiens) T00352 hypothetical protein KIAA0701 - human
Bt.9789.1.S1_at	2.56	up		Transcribed sequence with strong similarity to protein sp:O14640 (H.sapiens) DVL1_HUMAN Segment polarity protein dishevelled homolog DVL-1
Bt.26560.1.A1_at	2.55	up		Transcribed sequences
Bt.3699.1.S1_at	2.55	up		Transcribed sequence with strong similarity to protein ref:NP_004402.1 (H.sapiens) dynein, cytoplasmic, intermediate polypeptide 1 [Homo sapiens]
Bt.448.1.S1_at	2.55	up	PLCB1	phosphoinositide-specific phospholipase C beta1
Bt.624.1.S1_at	2.54	up		Transcribed sequence with strong similarity to protein ref:NP_055398.1 (H.sapiens) LIM and cysteine-rich domains 1; dyxin [Homo sapiens]
Bt.11704.1.S1_at	2.54	up		Transcribed sequences
Bt.23651.1.A1_at	2.54	up		Transcribed sequences
Bt.24928.1.S1_at	2.54	up		Transcribed sequence with strong similarity to protein ref:NP_055705.1 (H.sapiens) downregulated in ovarian cancer 1 [Homo sapiens]
Bt.26204.1.A1_at	2.53	up		Transcribed sequences
Bt.27091.1.S1_at	2.53	up		Transcribed sequences
Bt.19845.1.S1_at	2.53	up		Transcribed sequences
Bt.20569.3.S1_at	2.52	up		Transcribed sequences
Bt.19978.1.A1_at	2.52	up		Transcribed sequences
Bt.9026.1.S1_at	2.51	up	ITPR2	inositol 1,4,5-triphosphate receptor, type 2
Bt.9966.2.S1_a_at	2.51	up		Transcribed sequence with strong similarity to protein pir:CGHU2V (H.sapiens) CGHU2V collagen alpha 2
Bt.13912.2.A1_at	2.50	up		Transcribed sequences
Bt.3797.1.S1_at	2.50	up	FMOD	fibromodulin
Bt.27379.1.A1_at	2.50	up		Transcribed sequences
Bt.725.1.S1_at	2.49	up		Transcribed sequence with moderate similarity to protein ref:NP_006198.1 (H.sapiens) platelet-derived growth factor receptor-like protein; platelet-derived growth factor-beta-like tumor suppressor [Homo sapiens]
Bt.18689.2.A1_at	2.48	up		Transcribed sequences
Bt.13871.1.S1_at	2.48	up		Transcribed sequences
Bt.20596.1.S1_at	2.47	up		Transcribed sequence with moderate similarity to protein ref:NP_005788.1 (H.sapiens) epithelial V-like antigen 1 precursor [Homo sapiens]
Bt.9412.3.S1_at	2.46	up		Transcribed sequence with moderate similarity to protein pir:S46657 (H.sapiens) S46657 collagen alpha 1
Bt.19100.3.A1_at	2.46	up		Transcribed sequences
Bt.29411.1.S1_at	2.46	up		Transcribed sequence with strong similarity to protein pir:T00352 (H.sapiens) T00352 hypothetical protein KIAA0701 - human
Bt.23672.1.A1_at	2.45	up		Transcribed sequences
Bt.8463.1.S1_at	2.44	up		Transcribed sequences
Bt.19541.1.A1_at	2.44	up		Transcribed sequence
Bt.5656.1.S1_at	2.42	up		Transcribed sequence with strong similarity to protein sp:Q99689 (H.sapiens) FEZ1_HUMAN Fasciculation and elongation protein zeta 1
Bt.12455.1.S1_at	2.42	up		Transcribed sequences
Bt.29806.1.S1_at	2.42	up		Clone bghrmv6 growth hormone receptor mRNA, variant 5 UTR and partial cds
Bt.20162.1.S1_at	2.42	up		Transcribed sequences

Bt.17309.2.A1_at	2.42	up		Transcribed sequences
Bt.11081.1.S1_at	2.42	up		Transcribed sequences
Bt.4110.1.S1_at	2.42	up	HRH1	histamine H1 receptor
Bt.4594.1.S1_at	2.42	up	NB25	MHC class II (BoLA-DQB)
Bt.121.1.S1_at	2.41	up	FRZB	frizzled-related protein
				Transcribed sequence with weak similarity to protein ref:NP_060416.1 (H.sapiens) hypothetical protein FLJ20731 [Homo sapiens]
Bt.26885.1.S1_at	2.41	up		Transcribed sequences
Bt.25075.1.A1_at	2.40	up		Transcribed sequences
Bt.22857.1.S1_at	2.39	up	TRB2	TRB-2 protein
Bt.126.1.S2_at	2.39	up	KCNJ2	potassium inwardly-rectifying channel, subfamilyJ, member 2
Bt.24026.1.A1_at	2.39	up		Transcribed sequences
				Transcribed sequence with weak similarity to protein sp:P11369 (M.musculus) POL2_MOUSE Retrovirus-related POL polyprotein [Contains: Reverse transcriptase ; Endonuclease]
Bt.19533.1.A1_at	2.37	up		Transcribed sequence with strong similarity to protein ref:NP_071738.1 (H.sapiens) 17kD fetal brain protein [Homo sapiens]
Bt.5599.1.S1_at	2.37	up		Transcribed sequences
Bt.14249.1.A1_at	2.37	up		Transcribed sequences
				Clone bghrmv8 growth hormone receptor mRNA, variant 5 UTR and partial cds
Bt.29717.1.S1_a_at	2.37	up		Transcribed sequences
Bt.16195.2.A1_at	2.36	up		Transcribed sequences
				Partial mRNA for fibroblast growth factor receptor 2 (FGFR2 gene), isoform IIIc
Bt.29696.1.S1_at	2.35	up		Transcribed sequences
Bt.6778.1.S1_at	2.34	up		Transcribed sequences
				Transcribed sequence with strong similarity to protein pir:CGHU2V (H.sapiens) CGHU2V collagen alpha 2
Bt.9966.1.S1_at	2.34	up		Transcribed sequences
Bt.10861.2.S1_at	2.33	up		Transcribed sequences
Bt.28159.1.S1_at	2.33	up		Transcribed sequences
Bt.22165.1.S1_at	2.32	up		Transcribed sequences
				Transcribed sequence with strong similarity to protein sp:P46934 (H.sapiens) NED4_HUMAN NEDD-4 protein
Bt.19024.1.A1_at	2.32	up		Transcribed sequences
Bt.24255.1.S1_at	2.32	up		Transcribed sequences
				Transcribed sequence with moderate similarity to protein pir:A42926 (H.sapiens) A42926 L6 surface protein - human
Bt.6087.2.S1_a_at	2.31	up		Transcribed sequences
				Transcribed sequence with moderate similarity to protein sp:P08236 (H.sapiens) BGLR_HUMAN Beta-glucuronidase precursor
Bt.15712.1.S1_at	2.31	up		Transcribed sequences
Bt.17195.1.A1_at	2.31	up		Transcribed sequences
				Transcribed sequence with moderate similarity to protein ref:NP_004853.1 (H.sapiens) LPS-induced TNF-alpha factor [Homo sapiens]
Bt.9286.2.S1_at	2.31	up		Transcribed sequences
				Transcribed sequence with moderate similarity to protein ref:NP_003390.2 (H.sapiens) X-prolyl aminopeptidase 2, membrane-bound; aminoacylproline aminopeptidase; aminopeptidase P; X-prolyl aminopeptidase 2
Bt.13651.2.A1_at	2.31	up		Transcribed sequences
Bt.16555.1.A1_at	2.31	up		Transcribed sequences
				Transcribed sequence with moderate similarity to protein ref:NP_064629.1 (H.sapiens) choline phosphotransferase 1; cholinephosphotransferase 1; cholinephosphotransferase 1 alpha [Homo sapiens]
Bt.22082.1.S1_at	2.30	up		Transcribed sequences
				Transcribed sequence with moderate similarity to protein pir:S46657 (H.sapiens) S46657 collagen alpha 1
Bt.9412.2.S1_at	2.30	up		phospholipase C
Bt.4552.1.S1_a_at	2.30	up		Transcribed sequences
Bt.19167.1.A1_at	2.30	up		Transcribed sequences
				Transcribed sequence with strong similarity to protein sp:P80095 (H.sapiens) PHS_HUMAN Pterin-4-alpha-carbinolamine dehydratase
Bt.23171.2.S1_at	2.29	up		Transcribed sequences

Bt.23351.1.S1_at	2.29	up		Transcribed sequence with strong similarity to protein prf:2117157A (H.sapiens) 2117157A oligosaccharyltransferase [Homo sapiens]
Bt.10341.1.S1_at	2.29	up		Transcribed sequences
Bt.19390.1.S1_at	2.29	up		Transcribed sequences
Bt.2505.2.S1_at	2.29	up		Transcribed sequence with strong similarity to protein ref:NP_079434.1 (H.sapiens) hypothetical protein FLJ22251 [Homo sapiens]
Bt.9289.1.S1_at	2.28	up		Transcribed sequences
Bt.7310.1.S1_at	2.28	up		Transcribed sequences
Bt.20803.1.A1_at	2.28	up		Transcribed sequences
Bt.11599.2.S1_at	2.28	up		Transcribed sequences
Bt.1998.1.S1_at	2.27	up		Transcribed sequence with strong similarity to protein pir:C35826 (H.sapiens) C35826 hypothetical 13K protein A - human
Bt.13906.1.S1_at	2.26	up		Transcribed sequences
Bt.21164.1.S1_at	2.26	up		Transcribed sequence with moderate similarity to protein prf:1001205A (H.sapiens) 1001205A c-myc gene [Homo sapiens]
Bt.15540.1.A1_at	2.26	up		Transcribed sequences
Bt.10077.1.S2_at	2.26	up	IRF1	interferon responsive factor 1
Bt.20226.2.A1_at	2.25	up		Transcribed sequences
Bt.19329.1.A1_at	2.25	up		Transcribed sequences
Bt.20327.1.S1_a_at	2.25	up		Transcribed sequence with weak similarity to protein pir:JC4343 (H.sapiens) JC4343 uridine phosphorylase
Bt.6127.2.S1_at	2.25	up		Transcribed sequence with moderate similarity to protein pir:B32688 (H.sapiens) B32688 beta-galactosidase-related protein - human
Bt.6592.1.S1_at	2.25	up		Transcribed sequence with strong similarity to protein sp:P55290 (H.sapiens) CADD_HUMAN Cadherin-13 precursor
Bt.4105.2.A1_at	2.24	up		Transcribed sequence with moderate similarity to protein ref:NP_112230.1 (H.sapiens) G protein coupled receptor interacting protein, complement-c1q tumor necrosis factor-related [Homo sapiens]
Bt.9124.1.A1_at	2.24	up		Transcribed sequences
Bt.9286.1.S1_at	2.24	up		Transcribed sequence with moderate similarity to protein ref:NP_004853.1 (H.sapiens) LPS-induced TNF-alpha factor [Homo sapiens]
Bt.702.1.S1_at	2.23	up		Transcribed sequences
Bt.4275.2.S1_at	2.23	up		Transcribed sequences
Bt.20428.2.S1_a_at	2.23	up		Transcribed sequence with moderate similarity to protein ref:NP_003972.1 (H.sapiens) protein regulator of cytokinesis 1; protein regulating cytokinesis 1 [Homo sapiens]
Bt.22390.2.S1_at	2.23	up		Transcribed sequence with moderate similarity to protein pir:KUHU (H.sapiens) KUHU ferroxidase
Bt.13336.2.S1_at	2.22	up		Transcribed sequence with strong similarity to protein pir:T46486 (H.sapiens) T46486 chromosomal protein CAPC homolog DKFZp434F205.1 [similarity] - human
Bt.27081.1.S1_at	2.22	up		Transcribed sequences
Bt.12285.3.S1_a_at	2.22	up		Transcribed sequence with moderate similarity to protein sp:Q13287 (H.sapiens) NMI_HUMAN N-myc-interactor
Bt.2726.1.S1_at	2.22	up		Transcribed sequences
Bt.19811.1.A1_at	2.21	up		Transcribed sequences
Bt.14370.1.A1_at	2.21	up		Transcribed sequences
Bt.10043.1.S1_at	2.21	up		Transcribed sequences
Bt.12728.3.S1_at	2.21	up		Transcribed sequences
Bt.5576.1.S1_at	2.20	up		Transcribed sequences

Bt.13506.1.A1_at	2.20	up		Transcribed sequence with weak similarity to protein ref:NP_490719.1 (C.elegans) Y48G1A.3.p [Caenorhabditis elegans]
Bt.20846.1.A1_a_at	2.20	up		Transcribed sequence with strong similarity to protein sp:O15194 (H.sapiens) NIF1_HUMAN Nuclear LIM interactor-interacting factor 1
Bt.10816.1.S1_s_at	2.19	up		Transcribed sequences
Bt.22664.1.A1_at	2.19	up		Transcribed sequences
Bt.12285.2.S1_a_at	2.19	up		Transcribed sequence with moderate similarity to protein sp:Q13287 (H.sapiens) NMI_HUMAN N-myc-interactor
Bt.4095.1.A1_at	2.18	up		Transcribed sequences
Bt.7804.1.S1_at	2.18	up	GYG	glycogenin
Bt.2388.1.S1_at	2.18	up		Transcribed sequences
Bt.18325.2.A1_at	2.18	up		Transcribed sequence with moderate similarity to protein pir:I37356 (H.sapiens) I37356 epithelial microtubule-associated protein, 115K - human
Bt.8894.1.S1_at	2.18	up		Transcribed sequences
Bt.21482.3.A1_at	2.17	up		Transcribed sequence with moderate similarity to protein ref:NP_001189.1 (H.sapiens) B-lymphocyte-induced maturation protein 1; positive regulatory domain I-binding factor 1 [Homo sapiens]
Bt.2220.2.A1_a_at	2.17	up	selP	selenoprotein P
Bt.17792.1.S1_at	2.17	up		Transcribed sequence with weak similarity to protein ref:NP_065984.1 (H.sapiens) zinc finger protein 317; KRAB-containing zinc finger protein 317 [Homo sapiens]
Bt.24405.1.S1_at	2.16	up		Transcribed sequence with strong similarity to protein ref:NP_570139.1 (H.sapiens) similar to uroplakin 1B; tetraspan [Homo sapiens]
Bt.10398.1.S1_at	2.16	up		Transcribed sequence with strong similarity to protein pir:A44323 (H.sapiens) A44323 pentaxin PTX3 precursor - human
Bt.23394.1.S1_at	2.16	up		Transcribed sequences
Bt.198.1.S1_at	2.16	up	ASPH	aspartate beta-hydroxylase
Bt.1976.1.S1_at	2.16	up		Transcribed sequence with strong similarity to protein pir:A49013 (H.sapiens) A49013 tumor cell suppression protein HTS1 [imported] - human
Bt.4275.1.S1_at	2.16	up		Transcribed sequences
Bt.3125.1.S1_at	2.16	up		Transcribed sequence with strong similarity to protein ref:NP_036395.1 (H.sapiens) tubulin tyrosine ligase-like 1; tubulin-tyrosine ligase; chromosome 22 open reading frame 7 [Homo sapiens]
Bt.27811.1.S1_at	2.16	up		Transcribed sequence with strong similarity to protein pir:I37904 (H.sapiens) I37904 c-myc promoter-binding protein ir1B - human
Bt.10111.1.S1_at	2.16	up		Transcribed sequences
Bt.3580.2.S1_at	2.15	up		Transcribed sequence with weak similarity to protein sp:Q99538 (H.sapiens) LEGU_HUMAN Legumain precursor
Bt.22270.1.S1_at	2.14	up		Transcribed sequences
Bt.29696.1.A1_at	2.14	up		Partial mRNA for fibroblast growth factor receptor 2 (FGFR2 gene), isoform IIIc
Bt.25101.1.S1_at	2.14	up		Transcribed sequences
Bt.6302.1.S1_at	2.14	up		Transcribed sequence with moderate similarity to protein ref:NP_003795.1 (H.sapiens) receptor
Bt.27971.1.S1_at	2.14	up	CB11	cyanogen bromide
Bt.3198.2.S1_at	2.14	up		Transcribed sequence with strong similarity to protein sp:Q01082 (H.sapiens) SPCO_HUMAN Spectrin beta chain, brain 1
Bt.20654.1.A1_a_at	2.14	up		Transcribed sequences
Bt.28614.1.A1_at	2.13	up		Transcribed sequences
Bt.22869.1.S1_at	2.13	up	FABP5	fatty acid binding protein 5

Bt.1286.1.S1_a_at	2.13	up		Transcribed sequence with moderate similarity to protein ref:NP_002880.1 (H.sapiens) retinoic acid receptor responder
Bt.2129.1.S1_at	2.13	up		Transcribed sequence with weak similarity to protein pir:T31613 (C.elegans) T31613 hypothetical protein Y50E8A.i - Caenorhabditis elegans
Bt.22204.1.A1_at	2.12	up		Transcribed sequence with weak similarity to protein ref:NP_055164.1 (H.sapiens) apolipoprotein L, 3; TNF-inducible protein CG12-1 [Homo sapiens]
Bt.22139.1.S1_at	2.11	up		Transcribed sequences
Bt.21390.1.S1_at	2.11	up	LOC404065	pro-alpha 1(II) mRNA
Bt.18642.1.A1_at	2.11	up		Transcribed sequences
Bt.24687.1.A1_at	2.11	up		Transcribed sequence with weak similarity to protein ref:NP_112203.1 (H.sapiens) exonuclease NEF-sp [Homo sapiens]
Bt.17883.1.S1_at	2.11	up		Transcribed sequences
Bt.23586.1.S1_at	2.10	up		Transcribed sequence with strong similarity to protein ref:NP_002950.3 (H.sapiens) sortilin 1 preproprotein; neurotensin receptor 3; neurotensin receptor, 100-kD; 100 kDa NT receptor; glycoprotein 95 [Homo sapiens]
Bt.12714.1.A1_at	2.10	up		Transcribed sequence with moderate similarity to protein sp:Q92561 (H.sapiens) Y273_HUMAN Hypothetical protein KIAA0273
Bt.979.1.A1_at	2.10	up		Transcribed sequence with weak similarity to protein sp:Q9UBC5 (H.sapiens) MYHL_HUMAN Brush border myosin I
Bt.25052.1.S1_at	2.09	up		Transcribed sequence with strong similarity to protein ref:NP_055104.2 (H.sapiens) calpain 6; calpain-like protease; calpamodulin [Homo sapiens]
Bt.27957.1.A1_at	2.09	up		Transcribed sequence with moderate similarity to protein pir:T34522 (H.sapiens) T34522 hypothetical protein DKFZp566D244.1 - human
Bt.18080.2.S1_at	2.08	up		Transcribed sequence with strong similarity to protein ref:NP_060369.1 (H.sapiens) hypothetical protein FLJ20607; tescalcin; likely ortholog of mouse tescalcin [Homo sapiens]
Bt.355.1.S1_at	2.08	up	CALD1	caldesmon, smooth muscle
Bt.4565.1.S1_at	2.08	up		Transcribed sequence with strong similarity to protein sp:O43623 (H.sapiens) SLUG_HUMAN Zinc finger protein SLUG
Bt.15839.1.S1_at	2.08	up		Transcribed sequences
Bt.7156.1.S1_at	2.08	up	SLC4A4	solute carrier family 4, sodium bicarbonatecotransporter, member 4
Bt.21956.2.A1_at	2.08	up		Transcribed sequences
Bt.21150.1.A1_at	2.08	up		Transcribed sequence with weak similarity to protein sp:Q92889 (H.sapiens) XPF_HUMAN DNA-repair protein complementing XP-F cell
Bt.28702.1.S1_at	2.07	up		Transcribed sequences
Bt.1552.1.S1_at	2.07	up	SARS	seryl-tRNA synthetase
Bt.21085.1.S1_at	2.07	up		Transcribed sequences
Bt.28530.1.A1_at	2.07	up		Transcribed sequence with moderate similarity to protein pdb:1DVM (H.sapiens) A Chain A, Active Form Of Human Pai-1
Bt.26317.1.A1_at	2.06	up		Transcribed sequence with weak similarity to protein ref:NP_079268.1 (H.sapiens) hypothetical protein FLJ12547 [Homo sapiens]
Bt.18094.1.A1_at	2.06	up		Transcribed sequences
Bt.27884.1.S1_at	2.06	up		Transcribed sequence with weak similarity to protein sp:Q99536 (H.sapiens) VAT1_HUMAN Synaptic vesicle membrane protein VAT-1 homolog
Bt.22822.1.S1_at	2.06	up		Transcribed sequence with strong similarity to protein sp:P00722 (E. coli) BGAL_ECOLI Beta-galactosidase
Bt.16891.1.A1_at	2.06	up		Transcribed sequence with strong similarity to protein sp:O00141 (H.sapiens) SGK_HUMAN Serine/threonine-protein kinase Sgk

Bt.19583.1.A1_at	2.06	up		Transcribed sequences
Bt.19845.2.A1_at	2.06	up		Transcribed sequences
Bt.6374.1.S1_at	2.06	up		Transcribed sequences
Bt.5120.1.S1_at	2.05	up	NNT	nicotinamide nucleotide transhydrogenase
Bt.4818.1.S1_at	2.05	up		Transcribed sequence with moderate similarity to protein ref:NP_116010.1 (H.sapiens) X-linked protein [Homo sapiens]
Bt.3278.1.A1_at	2.05	up		Transcribed sequences
Bt.20479.1.S1_at	2.05	up		Transcribed sequence with moderate similarity to protein ref:NP_057314.1 (H.sapiens) flavohemoprotein b5+b5R [Homo sapiens]
Bt.23000.2.S1_a_at	2.05	up		Transcribed sequence with weak similarity to protein pir:T48686 (H.sapiens) T48686 hypothetical protein DKFZp761D1823.1 - human
Bt.28566.1.S1_at	2.05	up		Transcribed sequences
Bt.727.2.S1_at	2.05	up		Transcribed sequence with strong similarity to protein sp:Q9Y3C0 (H.sapiens) AD16_HUMAN Protein AD-016
Bt.17212.1.A1_at	2.05	up		Transcribed sequences
Bt.23127.1.S1_at	2.05	up		Transcribed sequence with moderate similarity to protein sp:P42785 (H.sapiens) PCP_HUMAN Lysosomal Pro-X carboxypeptidase precursor
Bt.5203.1.S1_at	2.05	up	PRDX4	peroxiredoxin 4
Bt.6377.1.S1_at	2.04	up		Transcribed sequence with weak similarity to protein ref:NP_005813.1 (H.sapiens) Down syndrome critical region gene 1- like 1 protein; thyroid hormone-responsive
Bt.2765.1.S1_at	2.03	up		Transcribed sequences
Bt.9325.1.A1_at	2.03	up		Transcribed sequences
Bt.23779.1.A1_at	2.03	up		Transcribed sequence
Bt.29306.1.A1_at	2.03	up		Transcribed sequences
Bt.426.1.S1_at	2.03	up	DBT	component of branched chain keto aciddehydrogenase complex; maple syrup urine disease]
Bt.10543.1.S1_at	2.03	up		Transcribed sequences
Bt.26444.1.A1_at	2.02	up		Transcribed sequence
Bt.24228.1.S1_at	2.02	up		Transcribed sequences
Bt.21800.1.S1_at	2.02	up		Transcribed sequence with strong similarity to protein sp:O94855 (H.sapiens) S24D_HUMAN Protein transport protein Sec24D
Bt.1422.1.S1_at	2.02	up		Transcribed sequences
Bt.19548.1.A1_at	2.02	up		Transcribed sequence
Bt.10077.1.S3_at	2.02	up	IRF1	interferon responsive factor 1
Bt.16514.1.S1_at	2.02	up		Transcribed sequence with weak similarity to protein ref:NP_076433.1 (H.sapiens) cytochrome P450 isoform 4F12 [Homo sapiens]
Bt.21543.2.S1_at	2.02	up		Transcribed sequences
Bt.4855.1.S1_a_at	2.02	up	SLC6A9	solute carrier family 6 (neurotransmittertransporter, glycine), member 9
Bt.11832.2.A1_at	2.02	up		Transcribed sequences
Bt.22251.1.A1_at	2.01	up		Transcribed sequence
Bt.9667.2.S1_at	2.01	up		Transcribed sequences
Bt.2600.1.A1_at	2.01	up		Transcribed sequences
Bt.29686.1.S1_at	2.01	up		Partial mRNA for fibroblast growth factor receptor 2 (FGFR2 gene), isoform IIIb
Bt.231.1.S1_at	2.01	up	TXN	thioredoxin
Bt.2052.2.S1_at	2.01	up		Transcribed sequences
Bt.9004.1.S1_at	2.01	up		Transcribed sequence with moderate similarity to protein ref:NP_001181.1 (H.sapiens) branched chain aminotransferase 2, mitochondrial [Homo sapiens]
Bt.24778.1.S1_at	2.00	up		Transcribed sequences
Bt.2046.1.S1_at	2.00	up	ext1	sushi repeat-containing protein
Bt.16142.3.A1_at	2.00	up		Transcribed sequences

Bt.22265.1.S1_at	2.00	up		Transcribed sequence with strong similarity to protein sp:P18146 (H.sapiens) EGR1_HUMAN Early growth response protein 1
Bt.20934.1.S1_at	2.00	up		Transcribed sequences
Bt.29794.1.A1_at	2.00	down		Glucose induced gene {clone 2C} [cattle, thoracic aorta smooth muscle cells, mRNA Partial, 162 nt]
Bt.16538.2.A1_at	2.00	down		Transcribed sequences
Bt.24678.1.A1_at	2.00	down		Transcribed sequence with weak similarity to protein ref:NP_008994.1 (H.sapiens) vascular Rab-GAP/TBC-containing [Homo sapiens]
Bt.29423.1.A1_at	2.00	down		Transcribed sequence with weak similarity to protein sp:P01876 (H.sapiens) ALC1_HUMAN Ig alpha-1 chain C region
Bt.7912.1.A1_at	2.00	down		Transcribed sequences
Bt.16018.1.S2_at	2.00	down	CASP4	caspase 4, apoptosis-related cysteine protease
Bt.21944.1.S1_at	2.01	down		Transcribed sequence with moderate similarity to protein sp:P18827 (H.sapiens) SDC1_HUMAN Syndecan-1 precursor
Bt.4544.1.S1_at	2.01	down		Transcribed sequence with moderate similarity to protein pir:B36429 (H.sapiens) B36429 integrin alpha-6 chain form A precursor - human
Bt.13278.1.S1_at	2.01	down		Transcribed sequences
Bt.11276.2.A1_at	2.01	down		Transcribed sequence with weak similarity to protein ref:NP_079345.1 (H.sapiens) hypothetical protein FLJ14299 [Homo sapiens]
Bt.28644.1.A1_at	2.01	down		Transcribed sequences
Bt.28208.1.S1_at	2.02	down		Transcribed sequence with strong similarity to protein sp:O00757 (H.sapiens) F16Q_HUMAN Fructose-1,6-bisphosphatase isozyme 2
Bt.23786.1.A1_at	2.02	down		Transcribed sequences
Bt.24424.1.S1_at	2.02	down		Transcribed sequence with weak similarity to protein prf:2124399A (H.sapiens) 2124399A transposase-like protein [Homo sapiens]
Bt.18203.1.A1_at	2.02	down		Transcribed sequence with strong similarity to protein sp:P57087 (H.sapiens) JAM2_HUMAN Junctional adhesion molecule 2 precursor
Bt.5301.2.S1_a_at	2.02	down	THBS	thrombospondin
Bt.8335.1.S1_at	2.03	down		Transcribed sequences
Bt.15732.1.S1_at	2.03	down		Transcribed sequences
Bt.20692.1.A1_at	2.03	down		Transcribed sequences
Bt.27591.1.S1_at	2.04	down		Transcribed sequence with moderate similarity to protein ref:NP_079230.1 (H.sapiens) hypothetical protein FLJ11807 [Homo sapiens]
Bt.16340.1.A1_at	2.04	down		Transcribed sequence with weak similarity to protein ref:NP_055886.1 (H.sapiens) GTPase regulator associated with the focal adhesion kinase pp125 [Homo sapiens]
Bt.26901.1.S1_at	2.05	down		Transcribed sequence with moderate similarity to protein ref:NP_067541.1 (M.musculus) junctophilin 2 [Mus musculus]
Bt.9193.1.S1_at	2.05	down		Transcribed sequences
Bt.28558.1.S1_at	2.05	down		Transcribed sequences
Bt.25112.1.S1_at	2.05	down		Transcribed sequence with strong similarity to protein ref:NP_057192.1 (H.sapiens) androgen induced protein; CGI-103 protein [Homo sapiens]
Bt.28382.1.S1_at	2.06	down		Transcribed sequences
Bt.7236.1.S1_at	2.06	down	PIK3R1	phosphoinositide-3-kinase, regulatory subunit, polypeptide 1 (p85 alpha)
Bt.303.1.S1_at	2.06	down	P2RY1	purinergic receptor P2Y1
Bt.13608.1.A1_at	2.07	down		Transcribed sequence
Bt.22010.1.S1_at	2.07	down		Transcribed sequences
Bt.546.3.S1_a_at	2.07	down	KCNMA1	potassium large conductance calcium-activated channel, subfamily M, alpha member 1
Bt.86.1.S1_at	2.08	down	SERPINF2	alpha-2-plasmin inhibitor

Bt.27433.2.A1_at	2.08	down		Transcribed sequence with strong similarity to protein ref:NP_071732.1 (H.sapiens) RAB38; Rab-related GTP-binding protein [Homo sapiens]
Bt.4375.1.S1_at	2.09	down		Transcribed sequence with strong similarity to protein ref:NP_003770.1 (H.sapiens) UDP-Gal:betaGlcNAc beta 1,4-galactosyltransferase 3
Bt.17939.1.S1_at	2.09	down		Transcribed sequence with strong similarity to protein sp:P20700 (H.sapiens) LAM1_HUMAN Lamin B1
Bt.20880.1.S1_at	2.09	down		Transcribed sequence with weak similarity to protein ref:NP_003719.2 (H.sapiens) unc5
Bt.1969.1.S1_at	2.10	down		Transcribed sequence with weak similarity to protein ref:NP_066921.1 (H.sapiens) calcium channel, voltage-dependent, alpha 1H subunit [Homo sapiens]
Bt.16521.2.A1_at	2.10	down		Transcribed sequence with weak similarity to protein ref:NP_476946.1 (D.melanogaster) lio-P1; pigeon [Drosophila melanogaster]
Bt.27425.1.A1_a_at	2.10	down		Transcribed sequences
Bt.8328.1.S1_at	2.10	down		Transcribed sequences
Bt.17230.1.A1_at	2.11	down		Transcribed sequences
Bt.18631.1.A1_at	2.11	down		Transcribed sequences
Bt.5789.1.S1_at	2.11	down		Transcribed sequence with strong similarity to protein ref:NP_076201.1 (M.musculus) spinster-like protein [Mus musculus]
Bt.5301.2.A1_at	2.11	down	THBS	thrombospondin
Bt.11276.1.A1_at	2.11	down		Transcribed sequence with weak similarity to protein ref:NP_079345.1 (H.sapiens) hypothetical protein FLJ14299 [Homo sapiens]
Bt.5432.3.S1_at	2.11	down		Transcribed sequence with weak similarity to protein ref:NP_005436.1 (H.sapiens) chondroitin sulfate proteoglycan 6
Bt.514.1.S1_at	2.12	down	DNAJC6	DnaJ (Hsp40) homolog, subfamily C, member 6
Bt.7901.3.S1_at	2.12	down		Transcribed sequences
Bt.25294.1.A1_at	2.12	down		Transcribed sequence
Bt.5038.1.S1_at	2.12	down	FGF1	fibroblast growth factor, acidic [endothelial growth factor]
Bt.22747.1.S1_at	2.12	down		Transcribed sequences
Bt.15970.1.A1_at	2.13	down		Transcribed sequence with moderate similarity to protein ref:NP_006527.1 (H.sapiens) calcium activated chloride channel 2 precursor [Homo sapiens]
Bt.19462.1.A1_at	2.14	down		Transcribed sequence
Bt.6963.1.A1_at	2.14	down		Transcribed sequence with moderate similarity to protein pir:A38445 (H.sapiens) A38445 EV12B protein precursor - human
Bt.236.1.S1_at	2.14	down	BTC	betacellulin
Bt.11061.1.S1_at	2.14	down		Transcribed sequence with moderate similarity to protein pir:A32160 (H.sapiens) A32160 tenascin-C - human
Bt.4763.1.S1_at	2.15	down	CD3Z	antigen CD3Z, zeta polypeptide
Bt.16521.1.S1_at	2.15	down		Transcribed sequence with weak similarity to protein ref:NP_476946.1 (D.melanogaster) lio-P1; pigeon [Drosophila melanogaster]
Bt.18444.2.A1_at	2.16	down		Transcribed sequences
Bt.29880.1.A1_at	2.16	down		Epidermal growth factor receptor precursor (EGFR) mRNA, partial cds
Bt.5110.1.A1_at	2.17	down		Transcribed sequences
Bt.3405.1.S1_at	2.17	down		Transcribed sequences
Bt.10922.1.A1_at	2.17	down		Transcribed sequences
Bt.19482.1.A1_at	2.18	down		Transcribed sequence with moderate similarity to protein sp:P02786 (H.sapiens) TFR1_HUMAN Transferrin receptor protein 1
Bt.2318.1.A1_at	2.18	down		Transcribed sequences

Bt.11030.1.S1_at	2.19	down		Transcribed sequence with weak similarity to protein sp:Q9NLA6 (D.melanogaster) OAF_DROME Out at first protein [Contains: Out at first short protein]
Bt.7641.1.S1_at	2.19	down		Transcribed sequence with moderate similarity to protein sp:O00764 (H.sapiens) PDXX_HUMAN Pyridoxine kinase
Bt.7468.1.S1_at	2.19	down		Transcribed sequences
Bt.18843.1.A1_at	2.20	down		Transcribed sequences
Bt.16311.1.A1_at	2.20	down		Transcribed sequences
Bt.2304.1.A1_at	2.20	down		Transcribed sequences
Bt.22475.1.S1_at	2.21	down		Transcribed sequence with strong similarity to protein ref:NP_005867.1 (H.sapiens) nuclear protein, marker for differentiated aortic smooth muscle [Homo sapiens]
Bt.3532.1.A1_at	2.22	down		Transcribed sequences
Bt.3891.1.S1_at	2.22	down		Transcribed sequences
Bt.24157.1.A1_at	2.22	down		Transcribed sequence with weak similarity to protein pir:T12458 (H.sapiens) T12458 hypothetical protein DKFZp564O0823.1 - human
Bt.18083.1.S1_at	2.23	down		Transcribed sequence with weak similarity to protein ref:NP_057479.1 (H.sapiens) butyrate-induced transcript 1; hypothetical protein; butyrate-induced transcript 1 [Homo sapiens]
Bt.22339.2.S1_at	2.23	down		Transcribed sequences
Bt.6771.1.S1_at	2.23	down		Transcribed sequence with weak similarity to protein ref:NP_116256.1 (H.sapiens) hypothetical protein FLJ14966 [Homo sapiens]
Bt.9832.1.S1_at	2.24	down		Transcribed sequences
Bt.9542.1.S1_at	2.24	down		Transcribed sequence with strong similarity to protein sp:P18031 (H.sapiens) PTN1_HUMAN Protein-tyrosine phosphatase, non-receptor type 1
Bt.7784.1.S1_at	2.24	down		Transcribed sequences
Bt.5943.2.S1_at	2.24	down		Transcribed sequences
Bt.18130.1.A1_at	2.24	down		Transcribed sequences
Bt.10604.1.A1_at	2.24	down		Transcribed sequence
Bt.19213.1.A1_at	2.25	down		Transcribed sequences
Bt.13546.1.A1_at	2.25	down		Transcribed sequences
Bt.18820.1.S1_at	2.26	down		Transcribed sequences
Bt.11462.1.S1_at	2.26	down		Transcribed sequence with moderate similarity to protein pir:A33880 (H.sapiens) A33880 syndecan 2 - human
Bt.21319.1.A1_at	2.26	down		Transcribed sequences
Bt.546.2.S1_at	2.27	down		BK potassium ion channel isoform B
Bt.5432.2.S1_at	2.27	down		Transcribed sequence with weak similarity to protein ref:NP_005436.1 (H.sapiens) chondroitin sulfate proteoglycan 6
Bt.12936.1.S1_at	2.27	down	CATHL5	cathelicidin 5
Bt.4053.1.S1_at	2.28	down	TBXA2R	thromboxane A2 receptor
Bt.3533.1.S1_at	2.28	down		Transcribed sequence with strong similarity to protein sp:P43268 (H.sapiens) ETV4_HUMAN ADENOVIRUS E1A ENHANCER BINDING PROTEIN
Bt.9925.1.S1_at	2.28	down		Transcribed sequences
Bt.9833.1.S1_a_at	2.28	down		Transcribed sequence with moderate similarity to protein ref:NP_077276.1 (H.sapiens) hypothetical protein MGC2217 [Homo sapiens]
Bt.352.5.S1_a_at	2.28	down	FP	prostaglandin F2alpha receptor isoform-epsilon
Bt.13026.1.A1_at	2.28	down	DAX-1	orphan nuclear receptor DAX-1
Bt.5336.1.A1_a_at	2.28	down	TF	transferrin
Bt.29724.1.S1_at	2.29	down		6-phosphofructo-2-kinase [cattle, brain, mRNA Partial, 1428 nt]
Bt.25403.1.A1_at	2.29	down		Transcribed sequence
Bt.26316.1.A1_at	2.29	down		Transcribed sequences
Bt.5432.1.S1_at	2.30	down		Transcribed sequence with weak similarity to protein ref:NP_005436.1 (H.sapiens) chondroitin sulfate proteoglycan 6

Bt.546.1.S1_at	2.30	down	KCNMA1	potassium large conductance calcium-activated channel, subfamily M, alpha member 1
Bt.16311.2.S1_at	2.31	down		Transcribed sequences
Bt.8031.2.S1_a_at	2.31	down		Transcribed sequence with strong similarity to protein sp:Q99687 (H.sapiens) MEI3_HUMAN Homeobox protein Meis3
Bt.10124.1.S1_at	2.32	down		Transcribed sequence with moderate similarity to protein pir:T46910 (H.sapiens) T46910 hypothetical protein DKFZp761L0424.1 - human
Bt.1546.1.S1_at	2.32	down		Transcribed sequences
Bt.15905.1.S1_at	2.32	down		Transcribed sequences
Bt.13466.1.S1_at	2.32	down		Transcribed sequence with strong similarity to protein ref:NP_115912.1 (H.sapiens) oxysterol-binding protein-like protein 6; OSBP-related protein 6 [Homo sapiens]
Bt.18444.1.A1_at	2.33	down		Transcribed sequences
Bt.5313.1.S1_at	2.34	down	MMP2	matrix metalloproteinase 2 (72 KDa type IV collagenase)
Bt.26440.1.A1_at	2.34	down		Transcribed sequences
Bt.26969.1.A1_at	2.34	down		Transcribed sequences
Bt.18251.2.A1_at	2.36	down		Transcribed sequence with moderate similarity to protein pir:T46364 (H.sapiens) T46364 hypothetical protein DKFZp434P0116.1 - human
Bt.18845.1.A1_at	2.36	down		Transcribed sequence
Bt.21981.2.S1_at	2.36	down		Transcribed sequences
Bt.13071.4.S1_at	2.36	down	CACNA1A	calcium channel, voltage-dependent, P/Q type, alpha 1A subunit
Bt.26284.1.A1_at	2.36	down		Transcribed sequence
Bt.10921.1.S1_at	2.37	down		Transcribed sequences
Bt.22987.1.A1_at	2.37	down	PRG4	proteoglycan 4, (megakaryocyte stimulating factor, articular superficial zone protein, camptodactyly, arthropathy, coxa vara, pericarditis syndrome)
Bt.3996.1.S1_at	2.37	down		Transcribed sequences
Bt.2903.1.S1_at	2.38	down	CXADR	coxsackie virus and adenovirus receptor
Bt.17654.1.A1_at	2.38	down		Transcribed sequence
Bt.21252.2.S1_at	2.39	down		Transcribed sequence with moderate similarity to protein sp:Q02846 (H.sapiens) CYGD_HUMAN Retinal guanylyl cyclase 1 precursor
Bt.15958.3.S1_at	2.40	down		Transcribed sequence with strong similarity to protein sp:P21439 (H.sapiens) MDR3_HUMAN Multidrug resistance protein 3
Bt.17330.1.A1_at	2.40	down		Transcribed sequence
Bt.27573.1.A1_at	2.41	down		Transcribed sequence
Bt.25850.1.S1_at	2.42	down		Transcribed sequences
Bt.18623.1.A1_at	2.43	down		Transcribed sequences
Bt.27228.1.A1_at	2.43	down		Transcribed sequence with weak similarity to protein ref:NP_056982.1 (H.sapiens) HIV-1 inducer of short transcripts binding protein [Homo sapiens]
Bt.1087.1.S1_at	2.44	down	MYO10	Transcribed sequence with strong similarity to protein ref:NP_004661.1 (H.sapiens) 3-prime-phosphoadenosine 5-prime-phosphosulfate synthase 2 [Homo sapiens]
Bt.4506.1.S1_at	2.44	down		myosin X
Bt.2494.2.S1_a_at	2.44	down		Transcribed sequences
Bt.29129.1.S1_at	2.45	down		Transcribed sequence with strong similarity to protein ref:NP_006399.1 (H.sapiens) anterior gradient 2 homolog
Bt.16740.1.A1_at	2.46	down	ST3GAL-V	Transcribed sequence with moderate similarity to protein sp:Q13751 (H.sapiens) LMB3_HUMAN Laminin beta-3 chain precursor
Bt.17585.1.S1_at	2.46	down		alpha2,3-sialyltransferase
Bt.16088.1.A1_at	2.47	down		Transcribed sequence with strong similarity to protein sp:Q9NQX4 (H.sapiens) MY5C_HUMAN Myosin Vc
Bt.5078.1.S1_at	2.48	down		Transcribed sequence with moderate similarity to protein sp:Q9UNF1 (H.sapiens) MGD2_HUMAN Melanoma-associated antigen D2

Bt.26198.1.A1_at	2.48	down		Transcribed sequences
Bt.3857.1.S1_at	2.48	down	ENDOG	endonuclease G
Bt.13570.1.S1_at	2.48	down	PRKRA	protein kinase, interferon-inducible double stranded RNA dependent activator
Bt.6838.1.A1_at	2.48	down		Transcribed sequence
Bt.22637.1.S1_at	2.49	down		Transcribed sequences
Bt.7641.2.S1_a_at	2.49	down		Transcribed sequence with moderate similarity to protein sp:O00764 (H.sapiens) PDXK_HUMAN Pyridoxine kinase
Bt.18009.1.A1_at	2.49	down		Transcribed sequences
Bt.7012.1.S1_at	2.49	down		Transcribed sequence with moderate similarity to protein sp:O75363 (H.sapiens) BCAS_HUMAN Breast carcinoma amplified sequence 1
Bt.2359.1.A1_at	2.51	down		Transcribed sequence with moderate similarity to protein sp:P06241 (H.sapiens) FYN_HUMAN Proto-oncogene tyrosine-protein kinase FYN
Bt.16567.1.A1_at	2.51	down		Transcribed sequences
Bt.28773.1.A1_at	2.52	down		Transcribed sequences
Bt.24477.1.S1_a_at	2.53	down		Transcribed sequence with strong similarity to protein sp:O60704 (H.sapiens) TPS2_HUMAN Protein-tyrosine sulfotransferase 2
Bt.13071.3.S1_at	2.53	down	CACNA1A	calcium channel, voltage-dependent, P/Q type, alpha 1A subunit
Bt.13570.1.A1_at	2.54	down	PRKRA	protein kinase, interferon-inducible double stranded RNA dependent activator
Bt.13071.1.S1_at	2.55	down	CACNA1A	calcium channel, voltage-dependent, P/Q type, alpha 1A subunit
Bt.5011.1.S2_at	2.56	down	LTBP2	latent transforming growth factor beta binding protein 2 (NOTE:redefinition of symbol)
Bt.7346.1.S1_at	2.57	down		Transcribed sequence with moderate similarity to protein sp:P19012 (H.sapiens) K1CO_HUMAN Keratin, type I cytoskeletal 15
Bt.22854.1.S1_at	2.57	down	CA2	carbonic anhydrase II
Bt.6879.1.S1_at	2.58	down		Transcribed sequences
Bt.21685.1.A1_at	2.60	down		Transcribed sequences
Bt.14098.1.S1_at	2.61	down		Transcribed sequence with strong similarity to protein ref:NP_055083.1 (H.sapiens) microtubule-associated protein, RP/EB family, member 2; T-cell activation protein, EB1 family; APC-binding protein EB1 [Homo sapiens]
Bt.27441.1.S1_at	2.62	down		Transcribed sequences
Bt.26735.1.S1_at	2.63	down		Transcribed sequences
Bt.13878.1.S1_at	2.64	down	GCH1	GTP cyclohydrolase 1 (dopa-responsive dystonia)
Bt.21224.1.S1_at	2.66	down		Transcribed sequence with weak similarity to protein ref:NP_083061.1 (M.musculus) RIKEN cDNA 1200017A24 [Mus musculus]
Bt.28708.1.S1_at	2.67	down		Transcribed sequences
Bt.22987.2.S1_at	2.68	down	PRG4	proteoglycan 4, (megakaryocyte stimulating factor, articular superficial zone protein, camptodactyly, arthropathy, coxa vara, pericarditis syndrome)
Bt.28728.1.A1_at	2.68	down		Transcribed sequence with strong similarity to protein ref:NP_116179.1 (H.sapiens) hypothetical protein FLJ14466 [Homo sapiens]
Bt.4802.1.S1_at	2.69	down	LTF	lactoferrin [lactotransferrin]
Bt.18073.1.A1_at	2.69	down		Transcribed sequences
Bt.19072.1.A1_at	2.70	down		Transcribed sequences
Bt.13027.1.A1_at	2.70	down		11 beta-hydroxysteroid dehydrogenase type 1
Bt.15675.1.S1_at	2.70	down	ADAMTS4	a disintegrin-like and metalloprotease(reprolysin type) with thrombospondin type 1 motif, 4
Bt.8667.1.S1_at	2.75	down		Transcribed sequence with weak similarity to protein ref:NP_569999.1 (D.melanogaster) EG:BACH48C10.2 gene product [Drosophila melanogaster]
Bt.22050.1.S1_at	2.76	down		Transcribed sequence with strong similarity to protein pir:TVHUHC (H.sapiens) TVHUHC protein-tyrosine kinase

Bt.21102.1.S1_at	2.76	down		Transcribed sequences
Bt.20748.1.A1_at	2.77	down		Transcribed sequences
Bt.13071.2.S1_at	2.77	down	CACNA1A	calcium channel, voltage-dependent, P/Q type, alpha 1A subunit
Bt.3513.1.A1_at	2.78	down		Transcribed sequences
Bt.15554.1.A1_at	2.78	down		Transcribed sequences
Bt.4199.1.S1_at	2.79	down	IL1RN	interleukin 1 receptor antagonist
Bt.13125.1.S1_s_at	2.79	down	BNBD-5	neutrophil beta-defensin 5
Bt.29066.1.A1_at	2.80	down		Transcribed sequence
Bt.26926.1.S1_at	2.80	down		Transcribed sequences
Bt.13071.3.A1_at	2.80	down	CACNA1A	calcium channel, voltage-dependent, P/Q type, alpha 1A subunit
Bt.13159.1.A1_at	2.80	down	PTPRZ1	protein tyrosine phosphatase, receptor-type, Z polypeptide 1
Bt.15188.1.S1_at	2.81	down		Transcribed sequences
Bt.15808.1.S1_at	2.81	down		Transcribed sequences
Bt.20512.1.S1_at	2.84	down		Transcribed sequence with moderate similarity to protein pir:A53317 (H.sapiens) A53317 collagen alpha 1
Bt.28195.1.S1_at	2.84	down		Transcribed sequences
Bt.18298.1.A1_at	2.85	down		Transcribed sequences
Bt.2318.2.S1_at	2.87	down		Transcribed sequences
Bt.15037.1.S1_at	2.90	down		Transcribed sequences
Bt.18618.1.A1_at	2.90	down		Transcribed sequences
Bt.20512.2.S1_at	2.92	down		Transcribed sequence with moderate similarity to protein pir:A53317 (H.sapiens) A53317 collagen alpha 1
Bt.12757.1.S1_at	2.93	down	NGFB	nerve growth factor, beta polypeptide
Bt.20942.1.S1_at	2.93	down		Transcribed sequences
Bt.546.3.A1_at	2.93	down	KCNMA1	potassium large conductance calcium-activated channel, subfamily M, alpha member 1
Bt.26040.1.A1_at	2.94	down		Transcribed sequence
Bt.16049.1.S1_at	2.95	down		Transcribed sequence with moderate similarity to protein sp:Q13571 (H.sapiens) LAM5_HUMAN Lysosomal-associated multitransmembrane protein
Bt.24592.1.S1_at	3.01	down		Transcribed sequence with moderate similarity to protein pir:A32160 (H.sapiens) A32160 tenascin-C - human
Bt.24231.2.S1_at	3.01	down		Transcribed sequence with weak similarity to protein ref:NP_068509.1 (R.norvegicus) IP63 protein [Rattus norvegicus]
Bt.4137.1.A1_at	3.02	down		Transcribed sequence with weak similarity to protein sp:P27469 (H.sapiens) G0S2_HUMAN Putative lymphocyte G0/G1 switch protein 2
Bt.20636.1.A1_at	3.04	down		Transcribed sequence with weak similarity to protein ref:NP_493307.1 (C.elegans) F22G12.5.p [Caenorhabditis elegans]
Bt.11570.1.A1_at	3.04	down		Transcribed sequences
Bt.155.1.S1_at	3.05	down	IL8	interleukin 8 [neutrophil activating peptide 1]
Bt.24231.1.A1_at	3.06	down		Transcribed sequence with weak similarity to protein ref:NP_068509.1 (R.norvegicus) IP63 protein [Rattus norvegicus]
Bt.22322.1.S1_at	3.06	down		Transcribed sequence with moderate similarity to protein sp:P02735 (H.sapiens) SAA_HUMAN Serum amyloid A protein precursor
Bt.26110.1.A1_at	3.06	down		Transcribed sequence
Bt.5403.1.S1_at	3.07	down	XDH	xanthine dehydrogenase
Bt.8790.1.S1_at	3.08	down		Transcribed sequences
Bt.23325.1.A1_at	3.09	down		Transcribed sequences
Bt.21962.1.S1_at	3.09	down		Transcribed sequences
Bt.15579.1.A1_at	3.11	down		Transcribed sequences
Bt.352.2.S1_at	3.11	down	FP	prostaglandin F2alpha receptor isoform-aplpha
Bt.29152.1.S1_at	3.11	down		Transcribed sequences
Bt.26365.1.A1_at	3.12	down		Transcribed sequences
Bt.29208.1.S1_at	3.12	down		Transcribed sequences

Bt.19095.1.S1_at	3.14	down		Transcribed sequences
Bt.23809.1.A1_s_at	3.16	down		Transcribed sequences
Bt.4013.1.S1_at	3.18	down		platelet-activating factor acetylhydrolase 2
				Transcribed sequence with moderate similarity to protein ref:NP_003380.2 (H.sapiens) coronin, actin-binding protein, 2A; coronin 2A; coronin-like protein B; WD-repeat protein 2; WD protein IR10 [Homo sapiens]
Bt.17910.2.S1_at	3.19	down		Transcribed sequences
Bt.4688.1.S1_a_at	3.20	down		Transcribed sequences
Bt.11515.1.A1_at	3.21	down		Transcribed sequence
Bt.5011.1.S1_at	3.22	down	LTBP2	latent transforming growth factor beta bindingprotein 2 (NOTE:redefinition of symbol)
Bt.26847.1.S1_at	3.23	down		Transcribed sequence with weak similarity to protein sp:O43561 (H.sapiens) LAT_HUMAN Linker for activation of T cells
Bt.27339.1.A1_at	3.25	down		Transcribed sequence with strong similarity to protein sp:P08473 (H.sapiens) NEP_HUMAN Neprilysin
Bt.23776.1.A1_at	3.26	down		Transcribed sequences
Bt.10865.1.S1_at	3.30	down		Transcribed sequences
Bt.24124.1.A1_at	3.32	down		Transcribed sequences
Bt.28243.1.S1_a_at	3.34	down		Transcribed sequence with moderate similarity to protein sp:O95497 (H.sapiens) VNN1_HUMAN Pantetheinase precursor
Bt.22339.1.A1_at	3.36	down		Transcribed sequences
Bt.25307.1.A1_at	3.37	down		Transcribed sequence
Bt.21798.1.S1_at	3.37	down		Transcribed sequence with weak similarity to protein ref:NP_570115.1 (H.sapiens) immunity associated protein 1; ortholog of mouse imap38 [Homo sapiens]
Bt.22080.1.S1_at	3.40	down		Transcribed sequences
Bt.27240.1.A1_at	3.42	down		Transcribed sequence with moderate similarity to protein ref:NP_057438.1 (H.sapiens) organic anion transporter OATP-E [Homo sapiens]
Bt.22987.2.A1_at	3.43	down	PRG4	proteoglycan 4, (megakaryocyte stimulating factor, articular superficial zone protein, camptodactyly, arthropathy, coxa vara, pericarditis syndrome)
Bt.23664.1.S1_at	3.45	down		Transcribed sequence with strong similarity to protein pir:T47142 (H.sapiens) T47142 hypothetical protein DKFZp761P0724.1 - human
Bt.1756.1.S1_at	3.46	down		Transcribed sequence with strong similarity to protein pir:BMHU7 (H.sapiens) BMHU7 bone morphogenetic protein 7 precursor - human
Bt.352.1.S1_at	3.48	down	PTGFR	prostaglandin F receptor
Bt.26847.2.S1_at	3.50	down		Transcribed sequence with weak similarity to protein sp:O43561 (H.sapiens) LAT_HUMAN Linker for activation of T cells
Bt.19423.2.S1_at	3.51	down		Transcribed sequences
Bt.13071.2.A1_at	3.59	down	CACNA1A	calcium channel, voltage-dependent, P/Q type, alpha 1A subunit
Bt.611.1.S2_at	3.65	down	CXCL1	chemokine (C-X-C motif) ligand 1
Bt.16201.1.S1_at	3.68	down		Transcribed sequence with weak similarity to protein sp:P06702 (H.sapiens) S109_HUMAN Calgranulin B
Bt.20148.1.S1_at	3.69	down		Transcribed sequence with weak similarity to protein ref:NP_114424.1 (H.sapiens) MSTP031 protein [Homo sapiens]
Bt.3681.1.S1_at	3.72	down		Transcribed sequence with moderate similarity to protein sp:Q99542 (H.sapiens) MM19_HUMAN Matrix metalloproteinase-19 precursor
Bt.132.1.S1_at	3.73	down	DEFB1	defensin, beta 1 (enteric)
Bt.28243.2.S1_at	3.73	down		Transcribed sequence with moderate similarity to protein sp:O95497 (H.sapiens) VNN1_HUMAN Pantetheinase precursor
Bt.1647.1.S1_at	3.76	down	CRYGS	crystallin, gamma polypeptide 8 [crystallin,gamma S]
Bt.3590.1.A1_at	3.79	down		Transcribed sequence with weak similarity to protein pir:B34087 (H.sapiens) B34087 hypothetical protein
Bt.17766.1.S1_at	3.79	down		Transcribed sequences
Bt.24919.1.S1_at	3.84	down		Transcribed sequences

Bt.26847.1.S1_a_at	3.84	down		Transcribed sequence with weak similarity to protein sp:O43561 (H.sapiens) LAT_HUMAN Linker for activation of T cells
Bt.19423.1.S1_at	3.86	down		Transcribed sequences
Bt.2452.1.S1_at	3.88	down	LUM	lumican
Bt.20649.2.S1_at	3.88	down		Transcribed sequences
Bt.8031.1.S1_at	3.97	down		Transcribed sequence with strong similarity to protein sp:Q99687 (H.sapiens) MEI3_HUMAN Homeobox protein Meis3
Bt.18111.1.A1_at	3.98	down		Transcribed sequence with moderate similarity to protein pir:B34087 (H.sapiens) B34087 hypothetical protein
Bt.8031.3.S1_a_at	3.99	down		Transcribed sequence with strong similarity to protein sp:Q99687 (H.sapiens) MEI3_HUMAN Homeobox protein Meis3
Bt.27339.2.S1_at	4.00	down		Transcribed sequence with strong similarity to protein sp:P08473 (H.sapiens) NEP_HUMAN Neprilysin
Bt.28752.1.A1_at	4.02	down		Transcribed sequence with weak similarity to protein ref:NP_077816.1 (H.sapiens) ATPase, Class V, type 10C; ATPase type IV, phospholipid transporting
Bt.23093.1.S1_at	4.04	down		Transcribed sequence with moderate similarity to protein sp:P19875 (H.sapiens) MI2A_HUMAN Macrophage inflammatory protein-2-alpha precursor
Bt.23126.1.S1_at	4.06	down	NOS2A	nitric oxide synthase 2A (inducible, hepatocytes)
Bt.16058.2.S1_at	4.07	down		Transcribed sequences
Bt.643.1.S1_at	4.07	down		Transcribed sequence with weak similarity to protein sp:P55773 (H.sapiens) SY23_HUMAN Small inducible cytokine A23 precursor
Bt.16058.1.A1_at	4.11	down		Transcribed sequences
Bt.16201.2.A1_at	4.11	down		Transcribed sequence with weak similarity to protein sp:P06702 (H.sapiens) S109_HUMAN Calgranulin B
Bt.4374.1.S1_at	4.13	down		Transcribed sequences
Bt.3540.1.S1_at	4.20	down		Transcribed sequence with strong similarity to protein ref:NP_003005.1 (H.sapiens) secreted frizzled-related protein 4; secreted frizzled-related protein 4 [Homo sapiens]
Bt.13744.1.A1_at	4.20	down		Transcribed sequences
Bt.9774.1.S1_a_at	4.24	down		Transcribed sequence with moderate similarity to protein ref:NP_115789.1 (H.sapiens) normal mucosa of esophagus specific 1 [Homo sapiens]
Bt.17752.1.A1_at	4.28	down		Transcribed sequence with weak similarity to protein pir:B34087 (H.sapiens) B34087 hypothetical protein
Bt.15731.1.A1_at	4.30	down		Transcribed sequence with moderate similarity to protein ref:NP_009199.1 (H.sapiens) Ig superfamily protein [Homo sapiens]
Bt.8945.1.S1_at	4.35	down	TLR2	toll-like receptor 2
Bt.357.1.S1_at	4.35	down	S100A12	S100 calcium binding protein A12 (calgranulinC)
Bt.15802.2.S1_at	4.41	down		Transcribed sequence with strong similarity to protein sp:Q13887 (H.sapiens) KLF5_HUMAN Krueppel-like factor 5
Bt.3774.1.A1_at	4.55	down		Transcribed sequences
Bt.19272.1.A1_at	4.57	down		Transcribed sequence
Bt.15802.1.S1_at	4.73	down		Transcribed sequence with strong similarity to protein sp:Q13887 (H.sapiens) KLF5_HUMAN Krueppel-like factor 5
Bt.13108.1.S1_at	4.79	down	ADAMTS5	a disintegrin-like and metalloprotease (reprolysin type) with thrombospondin type 1 motif, 5 (aggrecanase-2)
Bt.9633.1.S1_at	4.83	down		Transcribed sequence with weak similarity to protein ref:NP_113630.1 (H.sapiens) brain cell membrane protein 1 [Homo sapiens]
Bt.1756.2.S1_at	4.95	down		Transcribed sequence with strong similarity to protein pir:BMHU7 (H.sapiens) BMHU7 bone morphogenetic protein 7 precursor - human
Bt.6261.1.S1_at	4.97	down		Transcribed sequences
Bt.13108.1.A1_at	5.07	down	ADAMTS5	a disintegrin-like and metalloprotease (reprolysin type) with thrombospondin type 1 motif, 5 (aggrecanase-2)

Bt.310.1.S1_at	5.10	down	CATHL1	cathelicidin 1
Bt.366.2.S2_a_at	5.75	down	M-CSF alpha	macrophage-colony stimulating factor alpha
Bt.4714.1.S1_at	5.85	down	MMP9	matrix metalloproteinase 9 (gelatinase B, 92kDa) matrix metalloproteinase 9 (gelatinase B, 92kDa) gelatinase, 92kDa type IV collagenase)
Bt.27605.1.A1_at	6.08	down		Transcribed sequence with weak similarity to protein pir:A55119 (H.sapiens) A55119 potassium channel protein romk-1 - human
Bt.562.1.S1_at	6.35	down	PFKFB1	6-phosphofructo-2 kinase/fructose-2,6-biphosphatase 1
Bt.11904.1.S1_at	6.36	down		Transcribed sequence with strong similarity to protein sp:Q9UKU0 (H.sapiens) LCFF_HUMAN Long-chain-fatty-acid--CoA ligase 6
Bt.14191.1.A1_at	6.65	down		Transcribed sequence
Bt.493.1.S1_at	6.79	down	LIF	leukemia inhibitory factor [cholinergic differentiation factor]
Bt.29580.1.S1_at	7.07	down		Transcribed sequences
Bt.26268.1.A1_at	7.80	down		Transcribed sequences
Bt.16077.1.S1_at	7.94	down		Transcribed sequence with weak similarity to protein sp:O60896 (H.sapiens) RMP3_HUMAN Receptor activity-modifying protein 3 precursor
Bt.8479.1.A1_at	8.04	down		Transcribed sequence with moderate similarity to protein prf:2019232A (H.sapiens) 2019232A NO synthase [Homo sapiens]
Bt.5136.1.S1_at	8.61	down	TIMP3	tissue inhibitor of metalloproteinase 3 (Sorsbyfundus dystrophy, pseudo-inflammatory)
Bt.4417.1.S1_at	9.58	down	CDH2	cadherin 2 [N-cadherin] [N-cadherin 1]
Bt.10870.1.S1_at	9.80	down		Transcribed sequences
Bt.13046.1.A1_at	9.95	down	AHR	aryl hydrocarbon receptor
Bt.12283.1.A1_at	10.25	down		Transcribed sequence with weak similarity to protein sp:O95661 (H.sapiens) RHO1_HUMAN Rho-related GTP-binding protein Rho1
Bt.21197.1.A1_at	10.31	down		Transcribed sequences
Bt.39.1.S1_at	10.53	down	MMP13	matrix metalloproteinase 13 (collagenase 3)
Bt.23126.2.S1_at	10.63	down	NOS2A	nitric oxide synthase 2A (inducible, hepatocytes)
Bt.2537.2.S1_at	10.93	down	CHRNA3	cholinergic receptor, nicotinic, alpha polypeptide 3
Bt.23126.2.A1_at	11.04	down	NOS2A	nitric oxide synthase 2A (inducible, hepatocytes)
Bt.26231.1.S1_at	12.02	down		Transcribed sequences
Bt.13046.1.S1_at	14.36	down	AHR	aryl hydrocarbon receptor
Bt.26157.1.A1_at	15.09	down		Transcribed sequences
Bt.3686.1.S1_at	20.08	down	IL6	interleukin 6 [interferon, beta 2]
Bt.262.1.S1_at	21.19	down	TKDP3	trophoblast Kunitz domain protein 3
Bt.27152.1.A1_at	27.60	down		Transcribed sequences
Bt.9560.1.S1_at	66.77	down	CCL20	chemokine (C-C motif) ligand 20

Genome-wide microarray results**Human articular chondrocytes: IL-1+OSM+IL-4 vs IL-1+OSM**

Symbol	Fold Change	Gene name
CCL26	88.98	Homo sapiens chemokine (C-C motif) ligand 26 (CCL26), mRNA.
SNFT	15.27	Homo sapiens Jun dimerization protein p21SNFT (SNFT), mRNA.
ANPEP	10.07	Homo sapiens alanyl (membrane) aminopeptidase (aminopeptidase N, aminopeptidase M, microsomal aminopeptidase, CD13, p150) (ANPEP), mRNA.
RGS4	8.64	Homo sapiens regulator of G-protein signalling 4 (RGS4), mRNA.
SELP	6.83	Homo sapiens selectin P (granule membrane protein 140kDa, antigen CD62) (SELP), mRNA.
	5.95	Homo sapiens clone 25194 mRNA sequence
IL1RL1	5.57	Homo sapiens interleukin 1 receptor-like 1 (IL1RL1), transcript variant 2, mRNA.
CSN1S1	5.51	Homo sapiens casein alpha s1 (CSN1S1), transcript variant 2, mRNA.
POSTN	5.03	Homo sapiens periostin, osteoblast specific factor (POSTN), mRNA.
NPPB	5.03	Homo sapiens natriuretic peptide precursor B (NPPB), mRNA.
ISLR	4.95	Homo sapiens immunoglobulin superfamily containing leucine-rich repeat (ISLR), transcript variant 1, mRNA.
ISLR	4.70	Homo sapiens immunoglobulin superfamily containing leucine-rich repeat (ISLR), transcript variant 2, mRNA.
SOCS1	4.56	Homo sapiens suppressor of cytokine signaling 1 (SOCS1), mRNA.
CCL13	4.54	Homo sapiens chemokine (C-C motif) ligand 13 (CCL13), mRNA.
IGFBP5	4.54	Homo sapiens insulin-like growth factor binding protein 5 (IGFBP5), mRNA.
IL13RA2	4.53	Homo sapiens interleukin 13 receptor, alpha 2 (IL13RA2), mRNA.
POSTN	4.45	Homo sapiens periostin, osteoblast specific factor (POSTN), mRNA.
LPL	4.25	Homo sapiens lipoprotein lipase (LPL), mRNA.
IGFBP5	3.98	Homo sapiens insulin-like growth factor binding protein 5 (IGFBP5), mRNA.
FGL2	3.65	Homo sapiens fibrinogen-like 2 (FGL2), mRNA.
MAOA	3.54	Homo sapiens monoamine oxidase A (MAOA), nuclear gene encoding mitochondrial protein, mRNA.
SPON1	3.53	Homo sapiens spondin 1, extracellular matrix protein (SPON1), mRNA.
C1QTNF1	3.39	Homo sapiens C1q and tumor necrosis factor related protein 1 (C1QTNF1), mRNA.
PCDH18	3.36	Homo sapiens protocadherin 18 (PCDH18), mRNA.
CH25H	3.33	Homo sapiens cholesterol 25-hydroxylase (CH25H), mRNA.
CCL11	3.26	Homo sapiens chemokine (C-C motif) ligand 11 (CCL11), mRNA.
IL1RL1	3.21	Homo sapiens interleukin 1 receptor-like 1 (IL1RL1), transcript variant 2, mRNA.
ISG20	3.05	Homo sapiens interferon stimulated exonuclease gene 20kDa (ISG20), mRNA.
RRS1	3.04	Homo sapiens RRS1 ribosome biogenesis regulator homolog (S. cerevisiae) (RRS1), mRNA.
HAPLN1	2.95	Homo sapiens hyaluronan and proteoglycan link protein 1 (HAPLN1), mRNA.
CHST7	2.82	Homo sapiens carbohydrate (N-acetylglucosamine 6-O) sulfotransferase 7 (CHST7), mRNA.
SPINT2	2.77	Homo sapiens serine peptidase inhibitor, Kunitz type, 2 (SPINT2), mRNA.
TFPI	2.75	Homo sapiens tissue factor pathway inhibitor (lipoprotein-associated coagulation inhibitor) (TFPI), transcript variant 1, mRNA.
ST8SIA1	2.73	Homo sapiens ST8 alpha-N-acetyl-neuraminide alpha-2,8-sialyltransferase 1 (ST8SIA1), mRNA.
LOC648517	2.71	PREDICTED: Homo sapiens similar to Aldo-keto reductase family 1 member C1 (20-alpha-hydroxysteroid dehydrogenase) (20-alpha-HSD) (Trans-1,2-dihydrobenzene-1,2-diol dehydrogenase) (High-affinity hepatic bile acid-binding protein) (HBAB) (Chlordecone reductase homolog HAKRC..., transcript variant 1 (LOC648517), mRNA.
IFI27	2.68	Homo sapiens interferon, alpha-inducible protein 27 (IFI27), mRNA.
ATF3	2.67	Homo sapiens activating transcription factor 3 (ATF3), transcript variant 4, mRNA.
GUCY1A3	2.65	Homo sapiens guanylate cyclase 1, soluble, alpha 3 (GUCY1A3), mRNA.
NET1	2.63	Homo sapiens neuroepithelial cell transforming gene 1 (NET1), mRNA.
FLJ90166	2.59	Homo sapiens adenomatous polyposis coli down-regulated 1-like (APCDD1L), mRNA.
PIM1	2.57	Homo sapiens pim-1 oncogene (PIM1), mRNA.
CSN1S1	2.57	Homo sapiens casein alpha s1 (CSN1S1), transcript variant 1, mRNA.

IL24	2.57	Homo sapiens interleukin 24 (IL24), transcript variant 2, mRNA.
PPFIBP2	2.55	Homo sapiens PTPRF interacting protein, binding protein 2 (liprin beta 2) (PPFIBP2), mRNA.
TFPI	2.53	Homo sapiens tissue factor pathway inhibitor (lipoprotein-associated coagulation inhibitor) (TFPI), transcript variant 2, mRNA.
ATP1A1	2.50	Homo sapiens ATPase, Na ⁺ /K ⁺ transporting, alpha 1 polypeptide (ATP1A1), transcript variant 1, mRNA.
PCDH18	2.44	Homo sapiens protocadherin 18 (PCDH18), mRNA.
TNC	2.44	Homo sapiens tenascin C (hexabrachion) (TNC), mRNA.
C1QTNF1	2.43	Homo sapiens C1q and tumor necrosis factor related protein 1 (C1QTNF1), transcript variant 1, mRNA.
HAPLN1	2.40	Homo sapiens hyaluronan and proteoglycan link protein 1 (HAPLN1), mRNA.
IL18BP	2.39	Homo sapiens interleukin 18 binding protein (IL18BP), transcript variant A, mRNA.
DBC1	2.37	Homo sapiens deleted in bladder cancer 1 (DBC1), mRNA.
HIST2H2AA3	2.36	Homo sapiens histone cluster 2, H2aa3 (HIST2H2AA3), mRNA.
SLIT2	2.36	Homo sapiens slit homolog 2 (Drosophila) (SLIT2), mRNA.
GADD45G	2.36	Homo sapiens growth arrest and DNA-damage-inducible, gamma (GADD45G), mRNA.
MEOX1	2.35	Homo sapiens mesenchyme homeo box 1 (MEOX1), transcript variant 1, mRNA.
FKBP1A	2.33	Homo sapiens FK506 binding protein 1A, 12kDa (FKBP1A), transcript variant 12B, mRNA.
OXTR	2.32	Homo sapiens oxytocin receptor (OXTR), mRNA.
LRRC17	2.30	Homo sapiens leucine rich repeat containing 17 (LRRC17), transcript variant 1, mRNA.
GRP	2.29	Homo sapiens gastrin-releasing peptide (GRP), transcript variant 3, mRNA.
AKR1C2	2.29	Homo sapiens aldo-keto reductase family 1, member C2 (dihydrodiol dehydrogenase 2; bile acid binding protein; 3-alpha hydroxysteroid dehydrogenase, type III) (AKR1C2), transcript variant 1, mRNA. XM_943424 XM_943425 XM_943427
HIST2H2AA3	2.28	Homo sapiens histone cluster 2, H2aa3 (HIST2H2AA3), mRNA.
TDG	2.25	Homo sapiens thymine-DNA glycosylase (TDG), mRNA.
CTSC	2.25	Homo sapiens cathepsin C (CTSC), transcript variant 1, mRNA.
PRP2	2.23	Homo sapiens proline-rich protein PRP2 (PRP2), mRNA.
SERPINB4	2.23	Homo sapiens serpin peptidase inhibitor, clade B (ovalbumin), member 4 (SERPINB4), mRNA.
NET1	2.21	Homo sapiens neuroepithelial cell transforming gene 1 (NET1), mRNA.
CISH	2.20	Homo sapiens cytokine inducible SH2-containing protein (CISH), mRNA.
UGP2	2.20	Homo sapiens UDP-glucose pyrophosphorylase 2 (UGP2), transcript variant 1, mRNA.
MSX1	2.20	Homo sapiens msh homeo box homolog 1 (Drosophila) (MSX1), mRNA.
IFITM1	2.20	Homo sapiens interferon induced transmembrane protein 1 (9-27) (IFITM1), mRNA.
COL8A1	2.19	Homo sapiens collagen, type VIII, alpha 1 (COL8A1), transcript variant 1, mRNA.
BHLHB5	2.18	Homo sapiens basic helix-loop-helix domain containing, class B, 5 (BHLHB5), mRNA.
IL18R1	2.18	Homo sapiens interleukin 18 receptor 1 (IL18R1), mRNA.
LOC642489	2.18	PREDICTED: Homo sapiens similar to FK506-binding protein 1A (LOC642489), mRNA.
IGSF4	2.17	Homo sapiens cell adhesion molecule 1 (CADM1), mRNA.
PDGFRL	2.16	Homo sapiens platelet-derived growth factor receptor-like (PDGFRL), mRNA.
MX1	2.15	Homo sapiens myxovirus (influenza virus) resistance 1, interferon-inducible protein p78 (mouse) (MX1), mRNA.
ISLR	2.15	Homo sapiens immunoglobulin superfamily containing leucine-rich repeat (ISLR), transcript variant 1, mRNA.
SLC2A6	2.15	Homo sapiens solute carrier family 2 (facilitated glucose transporter), member 6 (SLC2A6), mRNA.
FKBP1A	2.14	Homo sapiens FK506 binding protein 1A, 12kDa (FKBP1A), transcript variant 12A, mRNA.
FLJ13391	2.13	Homo sapiens transmembrane protein 166 (TMEM166), mRNA.
TWISTNB	2.13	Homo sapiens TWIST neighbor (TWISTNB), mRNA.
CFI	2.11	Homo sapiens complement factor I (CFI), mRNA.
C15orf48	2.10	Homo sapiens chromosome 15 open reading frame 48 (C15orf48), transcript variant 2, mRNA.
ATP1A1	2.09	Homo sapiens ATPase, Na ⁺ /K ⁺ transporting, alpha 1 polypeptide (ATP1A1), transcript variant 1, mRNA.
CDC45L	2.08	Homo sapiens CDC45 cell division cycle 45-like (<i>S. cerevisiae</i>) (CDC45L), mRNA.

CKLF	2.08	Homo sapiens chemokine-like factor (CKLF), transcript variant 3, mRNA.
CYB5A	2.08	Homo sapiens cytochrome b5 type A (microsomal) (CYB5A), transcript variant 2, mRNA.
MYB	2.04	Homo sapiens v-myb myeloblastosis viral oncogene homolog (avian) (MYB), mRNA.
FKBP1A	2.04	Homo sapiens FK506 binding protein 1A, 12kDa (FKBP1A), transcript variant 12A, mRNA.
GUCY1A3	2.04	Homo sapiens guanylate cyclase 1, soluble, alpha 3 (GUCY1A3), mRNA.
PTGIS	2.02	Homo sapiens prostaglandin I2 (prostacyclin) synthase (PTGIS), mRNA.
CDC42EP2	2.02	Homo sapiens CDC42 effector protein (Rho GTPase binding) 2 (CDC42EP2), mRNA.
C10orf81	2.01	Homo sapiens chromosome 10 open reading frame 81 (C10orf81), mRNA.
PRKCZ	2.01	Homo sapiens protein kinase C, zeta (PRKCZ), transcript variant 1, mRNA.
CYB5A	2.01	Homo sapiens cytochrome b5 type A (microsomal) (CYB5A), transcript variant 1, mRNA.
HIST2H2AC	2.00	Homo sapiens histone cluster 2, H2ac (HIST2H2AC), mRNA.
VAMP5	1.99	Homo sapiens vesicle-associated membrane protein 5 (myobrevin) (VAMP5), mRNA.
LOXL3	1.99	Homo sapiens lysyl oxidase-like 3 (LOXL3), mRNA.
ARL4	1.98	Homo sapiens ADP-ribosylation factor-like 4 (ARL4), transcript variant 1, mRNA.
MEIS1	1.98	Homo sapiens Meis homeobox 1 (MEIS1), mRNA.
MRPS6	1.96	Homo sapiens mitochondrial ribosomal protein S6 (MRPS6), nuclear gene encoding mitochondrial protein, mRNA.
ARRDC4	1.96	Homo sapiens arrestin domain containing 4 (ARRDC4), mRNA.
TRPV2	1.96	Homo sapiens transient receptor potential cation channel, subfamily V, member 2 (TRPV2), mRNA.
CDK5RAP2	1.96	Homo sapiens CDK5 regulatory subunit associated protein 2 (CDK5RAP2), transcript variant 2, mRNA.
PRRX2	1.95	Homo sapiens paired related homeobox 2 (PRRX2), mRNA.
PSMB9	1.94	Homo sapiens proteasome (prosome, macropain) subunit, beta type, 9 (large multifunctional peptidase 2) (PSMB9), transcript variant 1, mRNA.
C11orf70	1.94	Homo sapiens chromosome 11 open reading frame 70 (C11orf70), mRNA.
EPSTI1	1.94	Homo sapiens epithelial stromal interaction 1 (breast) (EPSTI1), transcript variant 2, mRNA.
GNE	1.92	Homo sapiens glucosamine (UDP-N-acetyl)-2-epimerase/N-acetylmannosamine kinase (GNE), mRNA.
MS4A6A	1.92	Homo sapiens membrane-spanning 4-domains, subfamily A, member 6A (MS4A6A), transcript variant 3, mRNA.
C11orf70	1.91	Homo sapiens chromosome 11 open reading frame 70 (C11orf70), mRNA.
ATP1A1	1.91	Homo sapiens ATPase, Na ⁺ /K ⁺ transporting, alpha 1 polypeptide (ATP1A1), transcript variant 2, mRNA.
EIF1B	1.91	Homo sapiens eukaryotic translation initiation factor 1B (EIF1B), mRNA.
IFI35	1.91	Homo sapiens interferon-induced protein 35 (IFI35), mRNA.
RHBDD2	1.91	Homo sapiens rhomboid domain containing 2 (RHBDD2), transcript variant 1, mRNA.
C10orf116	1.90	Homo sapiens chromosome 10 open reading frame 116 (C10orf116), mRNA.
COL6A1	1.90	Homo sapiens collagen, type VI, alpha 1 (COL6A1), mRNA.
EPHA3	1.90	Homo sapiens EPH receptor A3 (EPHA3), transcript variant 1, mRNA.
COL24A1	1.89	Homo sapiens collagen, type XXIV, alpha 1 (COL24A1), mRNA.
MYL9	1.89	Homo sapiens myosin, light chain 9, regulatory (MYL9), transcript variant 1, mRNA.
GHR	1.89	Homo sapiens growth hormone receptor (GHR), mRNA.
OAS2	1.88	Homo sapiens 2'-5'-oligoadenylate synthetase 2, 69/71kDa (OAS2), transcript variant 1, mRNA.
SFRP2	1.88	Homo sapiens secreted frizzled-related protein 2 (SFRP2), mRNA.
SLC16A4	1.87	Homo sapiens solute carrier family 16, member 4 (monocarboxylic acid transporter 5) (SLC16A4), mRNA.
KRTCAP2	1.87	Homo sapiens keratinocyte associated protein 2 (KRTCAP2), mRNA.
COL6A3	1.87	Homo sapiens collagen, type VI, alpha 3 (COL6A3), transcript variant 1, mRNA.
CDC42EP5	1.86	Homo sapiens CDC42 effector protein (Rho GTPase binding) 5 (CDC42EP5), mRNA.
FLJ39155	1.86	Homo sapiens EGF-like, fibronectin type III and laminin G domains (EGFLAM), transcript variant 1, mRNA.
SLC25A25	1.85	Homo sapiens solute carrier family 25 (mitochondrial carrier; phosphate carrier), member 25 (SLC25A25), nuclear gene encoding mitochondrial protein, transcript variant 1, mRNA.
RHBDD2	1.85	Homo sapiens rhomboid domain containing 2 (RHBDD2), mRNA.
C6orf129	1.85	Homo sapiens chromosome 6 open reading frame 129 (C6orf129), mRNA.

PDZK1IP1	1.85	Homo sapiens PDZK1 interacting protein 1 (PDZK1IP1), mRNA.
ARRDC4	1.85	Homo sapiens arrestin domain containing 4 (ARRDC4), mRNA.
LOC646786	1.85	PREDICTED: Homo sapiens similar to Afadin (AF-6 protein) (LOC646786), mRNA.
	1.84	AGENCOURT_10229596 NIH_MGC_141 Homo sapiens cDNA clone IMAGE:6563923 5, mRNA sequence
PRKCZ	1.84	Homo sapiens protein kinase C, zeta (PRKCZ), transcript variant 1, mRNA.
C19orf10	1.84	Homo sapiens chromosome 19 open reading frame 10 (C19orf10), mRNA.
AK2	1.83	Homo sapiens adenylate kinase 2 (AK2), transcript variant AK2A, mRNA.
		Homo sapiens solute carrier organic anion transporter family, member 2A1 (SLCO2A1), mRNA.
SLCO2A1	1.83	
LOC441019	1.83	PREDICTED: Homo sapiens hypothetical LOC441019 (LOC441019), mRNA.
ANG	1.82	Homo sapiens angiogenin, ribonuclease, RNase A family, 5 (ANG), mRNA.
ARMET	1.82	Homo sapiens arginine-rich, mutated in early stage tumors (ARMET), mRNA.
		Homo sapiens glucosaminyl (N-acetyl) transferase 2, I-branching enzyme (I blood group) (GCNT2), transcript variant 2, mRNA.
GCNT2	1.81	
IGSF3	1.81	Homo sapiens immunoglobulin superfamily, member 3 (IGSF3), transcript variant 1, mRNA.
	1.80	zx42c01.r1 Soares_total_fetus_Nb2HF8_9w Homo sapiens cDNA clone IMAGE:789120 5, mRNA sequence
		Homo sapiens DNA segment, Chr 15, Wayne State University 75, expressed (D15Wsu75e), mRNA.
D15Wsu75e	1.80	
VAMP8	1.80	Homo sapiens vesicle-associated membrane protein 8 (endobrevin) (VAMP8), mRNA.
S100A4	1.80	Homo sapiens S100 calcium binding protein A4 (S100A4), transcript variant 1, mRNA.
AHNAK	1.80	Homo sapiens AHNAK nucleoprotein (AHNAK), transcript variant 2, mRNA.
DLX5	1.79	Homo sapiens distal-less homeo box 5 (DLX5), mRNA.
S100A11	1.79	Homo sapiens S100 calcium binding protein A11 (S100A11), mRNA.
UST	1.79	Homo sapiens uronyl-2-sulfotransferase (UST), mRNA.
		Homo sapiens endothelial differentiation, sphingolipid G-protein-coupled receptor, 3 (EDG3), mRNA.
EDG3	1.79	
RASL11A	1.78	Homo sapiens RAS-like, family 11, member A (RASL11A), mRNA.
DIXDC1	1.78	Homo sapiens DIX domain containing 1 (DIXDC1), transcript variant 1, mRNA.
FKBP2	1.77	Homo sapiens FK506 binding protein 2, 13kDa (FKBP2), transcript variant 1, mRNA.
		Homo sapiens aldo-keto reductase family 1, member C3 (3-alpha hydroxysteroid dehydrogenase, type II) (AKR1C3), mRNA.
AKR1C3	1.77	
PTGFRN	1.77	Homo sapiens prostaglandin F2 receptor negative regulator (PTGFRN), mRNA.
SLA	1.77	Homo sapiens Src-like-adaptor (SLA), mRNA.
OSR2	1.77	Homo sapiens odd-skipped related 2 (Drosophila) (OSR2), mRNA.
RAG1API	1.77	Homo sapiens recombination activating gene 1 activating protein 1 (RAG1API), mRNA.
		Homo sapiens PR domain containing 1, with ZNF domain (PRDM1), transcript variant 1, mRNA.
PRDM1	1.77	
NDP	1.76	Homo sapiens Norrie disease (pseudoglioma) (NDP), mRNA.
SATB2	1.76	Homo sapiens SATB homeobox 2 (SATB2), mRNA.
TMEM93	1.76	Homo sapiens transmembrane protein 93 (TMEM93), transcript variant 2, mRNA.
DUSP5	1.75	Homo sapiens dual specificity phosphatase 5 (DUSP5), mRNA.
TRAFD1	1.75	Homo sapiens TRAF-type zinc finger domain containing 1 (TRAFD1), mRNA.
BAD	1.75	Homo sapiens BCL2-antagonist of cell death (BAD), transcript variant 1, mRNA.
KLF2	1.75	Homo sapiens Kruppel-like factor 2 (lung) (KLF2), mRNA.
S100A4	1.75	Homo sapiens S100 calcium binding protein A4 (S100A4), transcript variant 1, mRNA.
INSIG1	1.74	Homo sapiens insulin induced gene 1 (INSIG1), transcript variant 2, mRNA.
FCRLM2	1.74	Homo sapiens Fc receptor-like B (FCRLB), mRNA.
MSC	1.74	Homo sapiens musculin (activated B-cell factor-1) (MSC), mRNA.
AHNAK	1.74	Homo sapiens AHNAK nucleoprotein (AHNAK), transcript variant 2, mRNA.
COPZ2	1.74	Homo sapiens coatomer protein complex, subunit zeta 2 (COPZ2), mRNA.
		Homo sapiens interferon-induced protein with tetratricopeptide repeats 1 (IFIT1), transcript variant 2, mRNA.
IFIT1	1.74	
CGGBP1	1.74	Homo sapiens CGG triplet repeat binding protein 1 (CGGBP1), transcript variant 2, mRNA.
ZCSL2	1.73	Homo sapiens DPH3, KTI11 homolog (S. cerevisiae) (DPH3), transcript variant 1, mRNA.
ZNHIT1	1.73	Homo sapiens zinc finger, HIT type 1 (ZNHIT1), mRNA.
HIST1H2AC	1.73	Homo sapiens histone cluster 1, H2ac (HIST1H2AC), mRNA.

PSME2	1.73	Homo sapiens proteasome (prosome, macropain) activator subunit 2 (PA28 beta) (PSME2), mRNA.
LOC728489	1.73	Homo sapiens similar to CG12379-PA (LOC728489), mRNA.
LOC255783	1.73	PREDICTED: Homo sapiens hypothetical protein LOC255783, transcript variant 2 (LOC255783), misc RNA.
MATN2	1.73	Homo sapiens matrilin 2 (MATN2), transcript variant 2, mRNA.
LHFP	1.73	Homo sapiens lipoma HMGIC fusion partner (LHFP), mRNA.
DSCR1L1	1.72	Homo sapiens regulator of calcineurin 2 (RCAN2), mRNA.
PTPLA	1.72	Homo sapiens protein tyrosine phosphatase-like (proline instead of catalytic arginine), member a (PTPLA), mRNA.
MRPS18C	1.71	Homo sapiens mitochondrial ribosomal protein S18C (MRPS18C), nuclear gene encoding mitochondrial protein, mRNA.
KCNK1	1.71	Homo sapiens potassium channel, subfamily K, member 1 (KCNK1), mRNA.
APH1B	1.70	Homo sapiens anterior pharynx defective 1 homolog B (<i>C. elegans</i>) (APH1B), mRNA.
ISG15	1.70	Homo sapiens ISG15 ubiquitin-like modifier (ISG15), mRNA.
TNFSF12	1.70	Homo sapiens tumor necrosis factor (ligand) superfamily, member 12 (TNFSF12), mRNA.
AHI1	1.70	Homo sapiens Abelson helper integration site 1 (AHI1), mRNA.
FABP3	1.70	Homo sapiens fatty acid binding protein 3, muscle and heart (mammary-derived growth inhibitor) (FABP3), mRNA.
PCBD1	1.70	Homo sapiens 6-pyruvoyl-tetrahydropterin synthase/dimerization cofactor of hepatocyte nuclear factor 1 alpha (TCF1) (PCBD1), transcript variant 2, mRNA.
MGC33212	1.70	Homo sapiens hypothetical protein MGC33212 (MGC33212), mRNA.
MAPRE2	1.69	Homo sapiens microtubule-associated protein, RP/EB family, member 2 (MAPRE2), mRNA.
EGFL6	1.69	Homo sapiens EGF-like-domain, multiple 6 (EGFL6), mRNA.
AK2	1.69	Homo sapiens adenylate kinase 2 (AK2), transcript variant AK2A, mRNA.
FLJ20186	1.69	Homo sapiens hypothetical protein FLJ20186 (FLJ20186), transcript variant 2, mRNA.
CLTB	1.69	Homo sapiens clathrin, light chain (Lcb) (CLTB), transcript variant 1, mRNA.
CKLF	1.69	Homo sapiens chemokine-like factor (CKLF), transcript variant 6, mRNA.
C6orf79	1.69	Homo sapiens chromosome 6 open reading frame 79 (C6orf79), transcript variant 2, mRNA.
TGFBR3	1.68	Homo sapiens transforming growth factor, beta receptor III (TGFBR3), mRNA.
ORF1-FL49	1.68	Homo sapiens putative nuclear protein ORF1-FL49 (ORF1-FL49), mRNA.
AYP1p1	1.68	PREDICTED: Homo sapiens AYP1 pseudogene 1 (AYP1p1), misc RNA.
SLC5A3	1.68	Homo sapiens solute carrier family 5 (inositol transporters), member 3 (SLC5A3), mRNA.
HIST1H2BD	1.68	Homo sapiens cDNA FLJ40058 fis, clone TCOLN1000180
HSPC023	1.67	Homo sapiens histone cluster 1, H2bd (HIST1H2BD), transcript variant 2, mRNA.
TDO2	1.67	Homo sapiens HSPC023 protein (HSPC023), mRNA.
TFPI	1.67	Homo sapiens tryptophan 2,3-dioxygenase (TDO2), mRNA.
TPD52L1	1.67	Homo sapiens tissue factor pathway inhibitor (lipoprotein-associated coagulation inhibitor) (TFPI), transcript variant 2, mRNA.
SRGN	1.67	Homo sapiens tumor protein D52-like 1 (TPD52L1), transcript variant 3, mRNA.
NDUFC1	1.66	Homo sapiens serglycin (SRGN), mRNA.
TIMP4	1.66	Homo sapiens NADH dehydrogenase (ubiquinone) 1, subcomplex unknown, 1, 6kDa (NDUFC1), mRNA.
SSBP2	1.66	Homo sapiens TIMP metalloproteinase inhibitor 4 (TIMP4), mRNA.
KLF6	1.66	Homo sapiens single-stranded DNA binding protein 2 (SSBP2), mRNA.
PTMS	1.66	Homo sapiens Kruppel-like factor 6 (KLF6), transcript variant 2, mRNA.
DPH3	1.66	Homo sapiens parathyroid hormone-related protein (PTMS), mRNA.
RBMS1	1.66	Homo sapiens DPH3, KTI11 homolog (<i>S. cerevisiae</i>) (DPH3), transcript variant 2, mRNA.
LOC388642	1.65	Homo sapiens RNA binding motif, single stranded interacting protein 1 (RBMS1), transcript variant 3, mRNA.
MGC17839	1.65	PREDICTED: Homo sapiens similar to Triosephosphate isomerase (TIM) (Triose-phosphate isomerase), transcript variant 3 (LOC388642), mRNA.
NOD1	1.65	Homo sapiens transmembrane protein 136 (TMEM136), mRNA.
SUCNR1	1.65	Homo sapiens nucleotide-binding oligomerization domain containing 1 (NOD1), mRNA.
EIF4E2	1.65	Homo sapiens succinate receptor 1 (SUCNR1), mRNA.
	1.65	Homo sapiens eukaryotic translation initiation factor 4E family member 2 (EIF4E2), mRNA.

ITGB8	1.65	Homo sapiens integrin, beta 8 (ITGB8), mRNA.
TSPO	1.65	Homo sapiens translocator protein (18kDa) (TSPO), transcript variant PBR-S, mRNA.
STRA13	1.65	Homo sapiens stimulated by retinoic acid 13 homolog (mouse) (STRA13), mRNA.
CLEC4A	1.65	Homo sapiens C-type lectin domain family 4, member A (CLEC4A), transcript variant 4, mRNA.
C17orf58	1.65	PREDICTED: Homo sapiens chromosome 17 open reading frame 58, transcript variant 3 (C17orf58), mRNA.
BOLA3	1.65	Homo sapiens bolA homolog 3 (E. coli) (BOLA3), transcript variant 1, mRNA.
ARID5A	1.65	Homo sapiens AT rich interactive domain 5A (MRF1-like) (ARID5A), mRNA.
DBI	1.64	Homo sapiens diazepam binding inhibitor (GABA receptor modulator, acyl-Coenzyme A binding protein) (DBI), transcript variant 2, mRNA.
SDF2L1	1.64	Homo sapiens stromal cell-derived factor 2-like 1 (SDF2L1), mRNA.
MAPK1	1.64	Homo sapiens mitogen-activated protein kinase 1 (MAPK1), transcript variant 2, mRNA.
IFI6	1.64	Homo sapiens interferon, alpha-inducible protein 6 (IFI6), transcript variant 2, mRNA.
PMCH	1.64	Homo sapiens pro-melanin-concentrating hormone (PMCH), mRNA.
TDG	1.64	Homo sapiens thymine-DNA glycosylase (TDG), mRNA.
DRAP1	1.64	Homo sapiens DR1-associated protein 1 (negative cofactor 2 alpha) (DRAP1), mRNA.
NET1	1.64	Homo sapiens neuroepithelial cell transforming gene 1 (NET1), mRNA.
PLAUR	1.64	Homo sapiens plasminogen activator, urokinase receptor (PLAUR), transcript variant 2, mRNA.
OSBPL8	1.64	Homo sapiens oxysterol binding protein-like 8 (OSBPL8), transcript variant 1, mRNA.
C22orf16	1.63	Homo sapiens chromosome 22 open reading frame 16 (C22orf16), mRNA.
CA12	1.63	Homo sapiens carbonic anhydrase XII (CA12), transcript variant 1, mRNA.
CRIP1	1.63	Homo sapiens cysteine-rich protein 1 (intestinal) (CRIP1), mRNA.
OAS1	1.63	Homo sapiens 2',5'-oligoadenylate synthetase 1, 40/46kDa (OAS1), transcript variant 2, mRNA.
COX7A1	1.63	Homo sapiens cytochrome c oxidase subunit VIIa polypeptide 1 (muscle) (COX7A1), mRNA.
PDCD5	1.63	Homo sapiens programmed cell death 5 (PDCD5), mRNA.
FLJ20186	1.63	Homo sapiens hypothetical protein FLJ20186 (FLJ20186), transcript variant 2, mRNA.
GPM6B	1.62	Homo sapiens glycoprotein M6B (GPM6B), transcript variant 1, mRNA.
CUTA	1.62	Homo sapiens cutA divalent cation tolerance homolog (E. coli) (CUTA), transcript variant 1, mRNA.
MRPS24	1.62	Homo sapiens mitochondrial ribosomal protein S24 (MRPS24), nuclear gene encoding mitochondrial protein, mRNA.
PCBD1	1.62	Homo sapiens pterin-4 alpha-carbinolamine dehydratase/dimerization cofactor of hepatocyte nuclear factor 1 alpha (TCF1) (PCBD1), mRNA.
PLEKHH2	1.62	Homo sapiens pleckstrin homology domain containing, family H (with MyTH4 domain) member 2 (PLEKHH2), mRNA.
SNRPB2	1.62	Homo sapiens small nuclear ribonucleoprotein polypeptide B" (SNRPB2), transcript variant 1, mRNA.
SH3BGL3	1.62	Homo sapiens SH3 domain binding glutamic acid-rich protein like 3 (SH3BGL3), mRNA.
APOL2	1.62	Homo sapiens apolipoprotein L, 2 (APOL2), transcript variant beta, mRNA.
FLJ21986	1.62	Homo sapiens hypothetical protein FLJ21986 (FLJ21986), mRNA.
WFDC3	1.62	Homo sapiens WAP four-disulfide core domain 3 (WFDC3), transcript variant 4, mRNA.
IL1RN	1.62	Homo sapiens interleukin 1 receptor antagonist (IL1RN), transcript variant 1, mRNA.
WFDC3	1.62	Homo sapiens WAP four-disulfide core domain 3 (WFDC3), transcript variant 2, mRNA.
PI3	1.61	Homo sapiens peptidase inhibitor 3, skin-derived (SKALP) (PI3), mRNA.
LOC51334	1.61	Homo sapiens proline rich 16 (PRR16), mRNA.
KCNK6	1.61	Homo sapiens potassium channel, subfamily K, member 6 (KCNK6), mRNA.
FAIM3	1.61	Homo sapiens Fas apoptotic inhibitory molecule 3 (FAIM3), mRNA.
CDK5RAP2	1.61	Homo sapiens CDK5 regulatory subunit associated protein 2 (CDK5RAP2), transcript variant 2, mRNA.
RIPK2	1.61	Homo sapiens receptor-interacting serine-threonine kinase 2 (RIPK2), mRNA.
METRNL	1.61	Homo sapiens meteorin, glial cell differentiation regulator-like (METRNL), mRNA.
SLC38A6	1.61	Homo sapiens solute carrier family 38, member 6 (SLC38A6), mRNA.
PDK3	1.61	Homo sapiens pyruvate dehydrogenase kinase, isozyme 3 (PDK3), mRNA.
BATF	1.60	Homo sapiens basic leucine zipper transcription factor, ATF-like (BATF), mRNA.
PPIC	1.60	Homo sapiens peptidylprolyl isomerase C (cyclophilin C) (PPIC), mRNA.

TKT	1.60	Homo sapiens transketolase (Wernicke-Korsakoff syndrome) (TKT), mRNA.
C17orf58	1.60	Homo sapiens chromosome 17 open reading frame 58 (C17orf58), transcript variant 2, mRNA.
BAIAP2L2	1.60	Homo sapiens BAI1-associated protein 2-like 2 (BAIAP2L2), mRNA.
ID2	1.60	Homo sapiens inhibitor of DNA binding 2, dominant negative helix-loop-helix protein (ID2), mRNA.
CIDEA	1.60	Homo sapiens cell death-inducing DFFA-like effector a (CIDEA), transcript variant 2, mRNA.
BOLA3	1.60	Homo sapiens bolA-like 3 (E. coli) (BOLA3), mRNA.
C7orf24	1.60	Homo sapiens chromosome 7 open reading frame 24 (C7orf24), mRNA.
SLC16A4	1.59	Homo sapiens solute carrier family 16, member 4 (monocarboxylic acid transporter 5) (SLC16A4), mRNA.
MRPL14	1.59	Homo sapiens mitochondrial ribosomal protein L14 (MRPL14), nuclear gene encoding mitochondrial protein, mRNA.
MGC40579	1.59	Homo sapiens hypothetical protein MGC40579 (MGC40579), mRNA.
DYNC2LI1	1.59	Homo sapiens dynein, cytoplasmic 2, light intermediate chain 1 (DYNC2LI1), transcript variant 2, mRNA.
IRF8	1.59	Homo sapiens interferon regulatory factor 8 (IRF8), mRNA.
C1orf41	1.59	Homo sapiens chromosome 1 open reading frame 41 (C1orf41), mRNA.
PPAP2B	1.59	Homo sapiens phosphatidic acid phosphatase type 2B (PPAP2B), transcript variant 2, mRNA.
CIB1	1.59	Homo sapiens calcium and integrin binding 1 (calmyrin) (CIB1), mRNA.
NRN1	1.59	Homo sapiens neuritin 1 (NRN1), mRNA.
RNASE4	1.59	Homo sapiens ribonuclease, RNase A family, 4 (RNASE4), transcript variant 1, mRNA.
TMOD1	1.59	Homo sapiens tropomodulin 1 (TMOD1), mRNA.
RPP21	1.59	Homo sapiens ribonuclease P/MRP 21kDa subunit (RPP21), mRNA.
RPL36AL	1.59	Homo sapiens ribosomal protein L36a-like (RPL36AL), mRNA.
SERTAD3	1.59	Homo sapiens SERTA domain containing 3 (SERTAD3), transcript variant 2, mRNA.
FLJ39155	1.59	Homo sapiens EGF-like, fibronectin type III and laminin G domains (EGFLAM), transcript variant 4, mRNA.
RARRES3	1.58	Homo sapiens retinoic acid receptor responder (tazarotene induced) 3 (RARRES3), mRNA.
COX17	1.58	Homo sapiens COX17 cytochrome c oxidase assembly homolog (S. cerevisiae) (COX17), nuclear gene encoding mitochondrial protein, mRNA.
FAM14A	1.58	Homo sapiens family with sequence similarity 14, member A (FAM14A), mRNA.
SEC14L1	1.58	Homo sapiens SEC14-like 1 (S. cerevisiae) (SEC14L1), transcript variant 1, mRNA.
HSCB	1.58	Homo sapiens HscB iron-sulfur cluster co-chaperone homolog (E. coli) (HSCB), mRNA.
TSPO	1.58	Homo sapiens translocator protein (18kDa) (TSPO), transcript variant PBR, mRNA.
TUBB2C	1.58	Homo sapiens tubulin, beta 2C (TUBB2C), mRNA.
RWDD1	1.58	Homo sapiens RWD domain containing 1 (RWDD1), transcript variant 3, mRNA.
IL17R	1.58	Homo sapiens interleukin 17 receptor (IL17R), mRNA.
SEMA4B	1.58	Homo sapiens sema domain, immunoglobulin domain (Ig), transmembrane domain (TM) and short cytoplasmic domain, (semaphorin) 4B (SEMA4B), transcript variant 1, mRNA.
RRAS	1.58	Homo sapiens related RAS viral (r-ras) oncogene homolog (RRAS), mRNA.
RAB11FIP1	1.58	Homo sapiens RAB11 family interacting protein 1 (class I) (RAB11FIP1), transcript variant 3, mRNA.
LOC56901	1.58	Homo sapiens NADH dehydrogenase (ubiquinone) 1 alpha subcomplex, 4-like 2 (NDUFA4L2), mRNA.
MRPL54	1.58	Homo sapiens mitochondrial ribosomal protein L54 (MRPL54), nuclear gene encoding mitochondrial protein, mRNA.
C1GALT1C1	1.57	Homo sapiens C1GALT1-specific chaperone 1 (C1GALT1C1), transcript variant 2, mRNA.
KIAA1434	1.57	Homo sapiens hypothetical protein KIAA1434 (KIAA1434), mRNA.
LOC653610	1.57	PREDICTED: Homo sapiens similar to Histone H2A.o (H2A/o) (H2A.2) (H2a-615) (LOC653610), mRNA.
NFE2	1.57	Homo sapiens nuclear factor (erythroid-derived 2), 45kDa (NFE2), mRNA.
MYL9	1.57	Homo sapiens myosin, light chain 9, regulatory (MYL9), transcript variant 1, mRNA.
OBFC2A	1.57	Homo sapiens oligonucleotide/oligosaccharide-binding fold containing 2A (OBFC2A), transcript variant 2, mRNA.
PLP2	1.57	Homo sapiens proteolipid protein 2 (colonic epithelium-enriched) (PLP2), mRNA.
UXT	1.57	Homo sapiens ubiquitously-expressed transcript (UXT), transcript variant 1, mRNA.

NUDT14	1.57	Homo sapiens nudix (nucleoside diphosphate linked moiety X)-type motif 14 (NUDT14), mRNA.
DCI	1.57	Homo sapiens dodecenoyl-Coenzyme A delta isomerase (3,2 trans-enoyl-Coenzyme A isomerase) (DCI), nuclear gene encoding mitochondrial protein, mRNA.
LOC650298	1.57	PREDICTED: Homo sapiens similar to 40S ribosomal protein S26 (LOC650298), mRNA.
SCO2	1.57	Homo sapiens SCO cytochrome oxidase deficient homolog 2 (yeast) (SCO2), nuclear gene encoding mitochondrial protein, mRNA.
GPM6B	1.57	Homo sapiens glycoprotein M6B (GPM6B), transcript variant 4, mRNA.
BLVRB	1.57	Homo sapiens biliverdin reductase B (flavin reductase (NADPH)) (BLVRB), mRNA.
EMP3	1.56	Homo sapiens epithelial membrane protein 3 (EMP3), mRNA.
C1orf50	1.56	Homo sapiens chromosome 1 open reading frame 50 (C1orf50), mRNA.
C16orf61	1.56	Homo sapiens chromosome 16 open reading frame 61 (C16orf61), mRNA.
COL8A1	1.56	Homo sapiens collagen, type VIII, alpha 1 (COL8A1), transcript variant 2, mRNA.
GLRX2	1.56	Homo sapiens glutaredoxin 2 (GLRX2), transcript variant 2, mRNA.
RP11-529I10.4	1.56	Homo sapiens deleted in a mouse model of primary ciliary dyskinesia (RP11-529I10.4), mRNA.
BST2	1.56	Homo sapiens bone marrow stromal cell antigen 2 (BST2), mRNA.
FST	1.56	Homo sapiens follistatin (FST), transcript variant FST344, mRNA.
GTF2IRD2	1.56	Homo sapiens GTF2I repeat domain containing 2 (GTF2IRD2), mRNA.
DNAL1	1.56	AV762101 MDS Homo sapiens cDNA clone MDSEOA03 5, mRNA sequence
LOX	1.55	Homo sapiens dynein, axonemal, light chain 1 (DNAL1), mRNA.
ATOX1	1.55	Homo sapiens lysyl oxidase (LOX), mRNA.
APIP	1.55	Homo sapiens ATX1 antioxidant protein 1 homolog (yeast) (ATOX1), mRNA.
RPL34	1.55	Homo sapiens APAF1 interacting protein (APIP), mRNA.
LARP6	1.55	Homo sapiens ribosomal protein L34 (RPL34), transcript variant 2, mRNA.
RNASE4	1.55	Homo sapiens La ribonucleoprotein domain family, member 6 (LARP6), transcript variant 2, mRNA.
FCGR2B	1.55	Homo sapiens ribonuclease, RNase A family, 4 (RNASE4), transcript variant 1, mRNA.
MRPL27	1.55	Homo sapiens Fc fragment of IgG, low affinity IIb, receptor (CD32) (FCGR2B), transcript variant 1, mRNA.
SNRPF	1.55	Homo sapiens mitochondrial ribosomal protein L27 (MRPL27), nuclear gene encoding mitochondrial protein, transcript variant 1, mRNA.
SLA	1.55	Homo sapiens small nuclear ribonucleoprotein polypeptide F (SNRPF), mRNA.
ZNF593	1.55	Homo sapiens Src-like-adaptor (SLA), transcript variant 2, mRNA.
LOC400948	1.55	Homo sapiens zinc finger protein 593 (ZNF593), mRNA.
PSMB10	1.55	PREDICTED: Homo sapiens similar to CG33774-PA (LOC400948), mRNA.
MS4A6A	1.55	Homo sapiens proteasome (prosome, macropain) subunit, beta type, 10 (PSMB10), mRNA.
C9orf89	1.55	Homo sapiens membrane-spanning 4-domains, subfamily A, member 6A (MS4A6A), transcript variant 2, mRNA.
SCNM1	1.55	Homo sapiens chromosome 9 open reading frame 89 (C9orf89), mRNA.
BOLA2	1.55	Homo sapiens sodium channel modifier 1 (SCNM1), mRNA.
NDUFA11	1.54	Homo sapiens bolA homolog 2 (E. coli) (BOLA2), mRNA.
MGC71993	1.54	Homo sapiens NADH dehydrogenase (ubiquinone) 1 alpha subcomplex, 11, 14.7kDa (NDUFA11), mRNA.
C17orf58	1.54	Homo sapiens similar to DNA segment, Chr 11, Brigham & Womens Genetics 0434 expressed (MGC71993), mRNA.
FKBP1A	1.54	Homo sapiens chromosome 17 open reading frame 58 (C17orf58), transcript variant 2, mRNA.
DCXR	1.54	Homo sapiens FK506 binding protein 1A, 12kDa (FKBP1A), transcript variant 12A, mRNA.
HCFC1R1	1.54	Homo sapiens dicarbonyl/L-xylulose reductase (DCXR), mRNA.
TUBB6	1.54	Homo sapiens host cell factor C1 regulator 1 (XPO1 dependent) (HCFC1R1), transcript variant 2, mRNA.
ZCD1	1.54	PREDICTED: Homo sapiens tubulin, beta 6 (TUBB6), mRNA.
ATPIF1	1.54	Homo sapiens zinc finger, CDGSH-type domain 1 (ZCD1), mRNA.
NDUFB8	1.54	Homo sapiens ATPase inhibitory factor 1 (ATPIF1), nuclear gene encoding mitochondrial protein, transcript variant 1, mRNA.
		Homo sapiens NADH dehydrogenase (ubiquinone) 1 beta subcomplex, 8, 19kDa (NDUFB8), mRNA.

ATP5I	1.54	Homo sapiens ATP synthase, H ⁺ transporting, mitochondrial F0 complex, subunit E (ATP5I), nuclear gene encoding mitochondrial protein, mRNA.
EBPL	1.54	Homo sapiens emopamil binding protein-like (EBPL), mRNA.
	1.54	Homo sapiens cDNA clone IMAGE:30530513
PSMB6	1.54	Homo sapiens proteasome (prosome, macropain) subunit, beta type, 6 (PSMB6), mRNA.
NDUFB6	1.54	Homo sapiens NADH dehydrogenase (ubiquinone) 1 beta subcomplex, 6, 17kDa (NDUFB6), nuclear gene encoding mitochondrial protein, transcript variant 1, mRNA.
	1.54	Homo sapiens mRNA; cDNA DKFZp686F09166 (from clone DKFZp686F09166)
SNAPC2	1.54	Homo sapiens small nuclear RNA activating complex, polypeptide 2, 45kDa (SNAPC2), mRNA.
RRBP1	1.53	Homo sapiens ribosome binding protein 1 homolog 180kDa (dog) (RRBP1), transcript variant 1, mRNA.
SNRPC	1.53	Homo sapiens small nuclear ribonucleoprotein polypeptide C (SNRPC), mRNA.
LOC205251	1.53	Homo sapiens hypothetical protein LOC205251 (LOC205251), mRNA.
		Homo sapiens Yip1 interacting factor homolog B (<i>S. cerevisiae</i>) (YIF1B), transcript variant 4, mRNA.
YIF1B	1.53	
PSMB2	1.53	Homo sapiens proteasome (prosome, macropain) subunit, beta type, 2 (PSMB2), mRNA.
PMAIP1	1.53	Homo sapiens phorbol-12-myristate-13-acetate-induced protein 1 (PMAIP1), mRNA.
ATP5D	1.53	Homo sapiens ATP synthase, H ⁺ transporting, mitochondrial F1 complex, delta subunit (ATP5D), nuclear gene encoding mitochondrial protein, transcript variant 2, mRNA.
NHP2L1	1.53	Homo sapiens NHP2 non-histone chromosome protein 2-like 1 (<i>S. cerevisiae</i>) (NHP2L1), transcript variant 1, mRNA.
UGP2	1.53	Homo sapiens UDP-glucose pyrophosphorylase 2 (UGP2), transcript variant 1, mRNA.
C20orf35	1.53	Homo sapiens chromosome 20 open reading frame 35 (C20orf35), transcript variant 1, mRNA.
KHSRP	1.53	Homo sapiens KH-type splicing regulatory protein (FUSE binding protein 2) (KHSRP), mRNA.
DDIT3	1.53	Homo sapiens DNA-damage-inducible transcript 3 (DDIT3), mRNA.
RIT1	1.53	Homo sapiens Ras-like without CAAX 1 (RIT1), mRNA.
LOC285016	1.53	Homo sapiens hypothetical protein LOC285016 (LOC285016), mRNA.
CTSC	1.53	Homo sapiens cathepsin C (CTSC), transcript variant 1, mRNA.
MGC2574	1.53	Homo sapiens coiled-coil domain containing 86 (CCDC86), mRNA.
MRPL55	1.53	Homo sapiens mitochondrial ribosomal protein L55 (MRPL55), nuclear gene encoding mitochondrial protein, transcript variant 6, mRNA.
GAS2L3	1.53	Homo sapiens growth arrest-specific 2 like 3 (GAS2L3), mRNA.
LOC440928	1.53	PREDICTED: Homo sapiens hypothetical LOC440928 (LOC440928), mRNA.
C20orf24	1.53	Homo sapiens chromosome 20 open reading frame 24 (C20orf24), transcript variant 4, mRNA.
C9orf21	1.53	Homo sapiens chromosome 9 open reading frame 21 (C9orf21), mRNA.
RAB38	1.53	Homo sapiens RAB38, member RAS oncogene family (RAB38), mRNA.
HRAS	1.53	Homo sapiens v-Ha-ras Harvey rat sarcoma viral oncogene homolog (HRAS), transcript variant 2, mRNA.
LOC652545	1.53	PREDICTED: Homo sapiens similar to Protein C21orf70 homolog (LOC652545), mRNA.
USMG5	1.52	Homo sapiens upregulated during skeletal muscle growth 5 homolog (mouse) (USMG5), mRNA.
PRKCA	1.52	Homo sapiens protein kinase C, alpha (PRKCA), mRNA.
LOC650832	1.52	PREDICTED: Homo sapiens similar to mitogen-activated protein kinase kinase 3 isoform A (LOC650832), mRNA.
C17orf61	1.52	Homo sapiens chromosome 17 open reading frame 61 (C17orf61), mRNA.
QP-C	1.52	Homo sapiens low molecular mass ubiquinone-binding protein (9.5kD) (QP-C), nuclear gene encoding mitochondrial protein, mRNA.
EGFLAM	1.52	Homo sapiens EGF-like, fibronectin type III and laminin G domains (EGFLAM), transcript variant 3, mRNA.
COX8A	1.52	Homo sapiens cytochrome c oxidase subunit 8A (ubiquitous) (COX8A), mRNA.
LOC650982	1.52	PREDICTED: Homo sapiens similar to DC2 protein (LOC650982), mRNA.
PCBD1	1.52	Homo sapiens 6-pyruvoyl-tetrahydropterin synthase/dimerization cofactor of hepatocyte nuclear factor 1 alpha (TCF1) (PCBD1), transcript variant 2, mRNA.
C1orf53	1.52	Homo sapiens chromosome 1 open reading frame 53 (C1orf53), mRNA.
IBRDC3	1.52	Homo sapiens IBR domain containing 3 (IBRDC3), mRNA.

MRPL36	1.52	Homo sapiens mitochondrial ribosomal protein L36 (MRPL36), nuclear gene encoding mitochondrial protein, mRNA.
LRIG1	1.52	Homo sapiens leucine-rich repeats and immunoglobulin-like domains 1 (LRIG1), mRNA.
RRAD	1.52	Homo sapiens Ras-related associated with diabetes (RRAD), mRNA.
MAGOH	1.52	Homo sapiens mago-nashi homolog, proliferation-associated (Drosophila) (MAGOH), mRNA.
CLEC4A	1.52	Homo sapiens C-type lectin domain family 4, member A (CLEC4A), transcript variant 4, mRNA.
AHNAK	1.52	Homo sapiens AHNAK nucleoprotein (AHNAK), transcript variant 1, mRNA.
QIL1	1.52	Homo sapiens hypothetical protein P117 (P117), mRNA.
HSPC176	1.52	Homo sapiens trafficking protein particle complex 2-like (TRAPPC2L), mRNA.
ANXA2	1.52	Homo sapiens annexin A2 (ANXA2), transcript variant 2, mRNA.
C15orf48	1.52	Homo sapiens chromosome 15 open reading frame 48 (C15orf48), transcript variant 2, mRNA.
LOC286016	1.52	Homo sapiens hypothetical protein LOC286016 (LOC286016) on chromosome 7.
METRNL	1.51	PREDICTED: Homo sapiens meteorin, glial cell differentiation regulator-like (METRNL), mRNA.
GALNAC4S-6ST	1.51	Homo sapiens B cell RAG associated protein (GALNAC4S-6ST), mRNA.
NDUFB2	1.51	Homo sapiens NADH dehydrogenase (ubiquinone) 1 beta subcomplex, 2, 8kDa (NDUFB2), nuclear gene encoding mitochondrial protein, mRNA.
MGC3731	1.51	Homo sapiens hypothetical protein MGC3731 (MGC3731), mRNA.
CDC25B	1.51	Homo sapiens cell division cycle 25 homolog B (S. pombe) (CDC25B), transcript variant 2, mRNA.
BCYRN1	1.51	Homo sapiens brain cytoplasmic RNA 1, Bc1 analog (mouse) (BCYRN1) on chromosome 2.
SERPINH1	1.51	Homo sapiens serpin peptidase inhibitor, clade H (heat shock protein 47), member 1, (collagen binding protein 1) (SERPINH1), mRNA.
DUSP6	1.51	Homo sapiens dual specificity phosphatase 6 (DUSP6), transcript variant 2, mRNA.
DPM3	1.51	Homo sapiens dolichyl-phosphate mannosyltransferase polypeptide 3 (DPM3), transcript variant 2, mRNA.
LOC51255	1.51	Homo sapiens ring finger protein 181 (RNF181), mRNA.
H2BFS	1.51	Homo sapiens H2B histone family, member S (H2BFS), mRNA.
C10orf72	1.51	Homo sapiens chromosome 10 open reading frame 72 (C10orf72), transcript variant 1, mRNA.
DCTN3	1.51	Homo sapiens dynactin 3 (p22) (DCTN3), transcript variant 2, mRNA.
C21orf34	1.51	Homo sapiens chromosome 21 open reading frame 34 (C21orf34), transcript variant 1, mRNA.
FAM96B	1.51	BX093329 Soares_parathyroid_tumor_NbHPA Homo sapiens cDNA clone IMAGp998A124183 ; IMAGE:1648403, mRNA sequence
ECGF1	1.51	Homo sapiens family with sequence similarity 96, member B (FAM96B), mRNA.
TIMP2	1.51	Homo sapiens endothelial cell growth factor 1 (platelet-derived) (ECGF1), mRNA.
ALG13	1.51	Homo sapiens TIMP metallopeptidase inhibitor 2 (TIMP2), mRNA.
SHFM1	1.51	Homo sapiens asparagine-linked glycosylation 13 homolog (S. cerevisiae) (ALG13), mRNA.
NPEPL1	1.51	Homo sapiens split hand/foot malformation (ectrodactyly) type 1 (SHFM1), mRNA.
MRPS12	1.51	Homo sapiens aminopeptidase-like 1 (NPEPL1), mRNA.
LOC653566	1.51	Homo sapiens mitochondrial ribosomal protein S12 (MRPS12), nuclear gene encoding mitochondrial protein, transcript variant 3, mRNA.
GPR64	1.51	Homo sapiens similar to Signal peptidase complex subunit 2 (Microsomal signal peptidase 25 kDa subunit) (SPase 25 kDa subunit) (LOC653566), mRNA.
TMPT	1.50	Homo sapiens G protein-coupled receptor 64 (GPR64), mRNA.
CCBE1	1.50	Homo sapiens transmembrane protein 120A (TMEM120A), mRNA.
S100A13	1.50	Homo sapiens collagen and calcium binding EGF domains 1 (CCBE1), mRNA.
LOC84661	1.50	Homo sapiens S100 calcium binding protein A13 (S100A13), transcript variant 3, mRNA.
SSNA1	1.50	Homo sapiens dpy-30-like protein (HDPY-30), mRNA.
CCDC68	1.50	Homo sapiens Sjogren's syndrome nuclear autoantigen 1 (SSNA1), mRNA.
FKBP11	1.50	Homo sapiens cDNA clone IMAGE:5277162
HBXIP	1.50	Homo sapiens coiled-coil domain containing 68 (CCDC68), mRNA.
TRG20	1.50	Homo sapiens FK506 binding protein 11, 19 kDa (FKBP11), mRNA.
	1.50	Homo sapiens hepatitis B virus x interacting protein (HBXIP), mRNA.
	1.50	Homo sapiens mediator complex subunit 10 (MED10), mRNA.

COBLL1	1.50	Homo sapiens COBL-like 1 (COBLL1), mRNA.
ZMYND11	-1.50	Homo sapiens zinc finger, MYND domain containing 11 (ZMYND11), transcript variant 1, mRNA.
BACE2	-1.50	Homo sapiens beta-site APP-cleaving enzyme 2 (BACE2), transcript variant c, mRNA.
AGL	-1.50	Homo sapiens amylo-1, 6-glucosidase, 4-alpha-glucanotransferase (glycogen debranching enzyme, glycogen storage disease type III) (AGL), transcript variant 5, mRNA.
CACHD1	-1.50	Homo sapiens cache domain containing 1 (CACHD1), mRNA.
WSB2	-1.50	Homo sapiens WD repeat and SOCS box-containing 2 (WSB2), mRNA.
NXT2	-1.50	Homo sapiens nuclear transport factor 2-like export factor 2 (NXT2), mRNA.
ARHGEF3	-1.50	Homo sapiens Rho guanine nucleotide exchange factor (GEF) 3 (ARHGEF3), mRNA.
TOM1	-1.50	Homo sapiens target of myb1 (chicken) (TOM1), mRNA.
CHES1	-1.50	Homo sapiens checkpoint suppressor 1 (CHES1), mRNA.
NTN4	-1.51	Homo sapiens netrin 4 (NTN4), mRNA.
TMEM154	-1.51	Homo sapiens transmembrane protein 154 (TMEM154), mRNA.
C8orf52	-1.51	Homo sapiens integrator complex subunit 8 (INTS8), mRNA.
HDGFRP3	-1.51	Homo sapiens hepatoma-derived growth factor, related protein 3 (HDGFRP3), mRNA.
LOC648695	-1.51	PREDICTED: Homo sapiens similar to retinoblastoma binding protein 4, transcript variant 4 (LOC648695), mRNA.
HNMT	-1.51	Homo sapiens histamine N-methyltransferase (HNMT), transcript variant 2, mRNA.
ZNF148	-1.51	Homo sapiens zinc finger protein 148 (ZNF148), mRNA.
KIAA1754	-1.51	Homo sapiens KIAA1754 (KIAA1754), mRNA.
ZNF503	-1.51	Homo sapiens zinc finger protein 503 (ZNF503), mRNA.
DUSP10	-1.51	Homo sapiens dual specificity phosphatase 10 (DUSP10), transcript variant 3, mRNA.
IRF2BP2	-1.51	Homo sapiens interferon regulatory factor 2 binding protein 2 (IRF2BP2), mRNA.
ZNF265	-1.51	Homo sapiens zinc finger, RAN-binding domain containing 2 (ZNRANB2), transcript variant 2, mRNA.
SLC4A7	-1.51	Homo sapiens solute carrier family 4, sodium bicarbonate cotransporter, member 7 (SLC4A7), mRNA.
GPR177	-1.51	Homo sapiens G protein-coupled receptor 177 (GPR177), transcript variant 2, mRNA.
SRPX2	-1.51	Homo sapiens sushi-repeat-containing protein, X-linked 2 (SRPX2), mRNA.
GPR177	-1.52	Homo sapiens G protein-coupled receptor 177 (GPR177), transcript variant 2, mRNA.
RBM25	-1.52	Homo sapiens RNA binding motif protein 25 (RBM25), mRNA.
TCF12	-1.52	Homo sapiens transcription factor 12 (HTF4, helix-loop-helix transcription factors 4) (TCF12), transcript variant 2, mRNA.
CROP	-1.52	Homo sapiens cisplatin resistance-associated overexpressed protein (CROP), transcript variant 1, mRNA.
VPS41	-1.52	Homo sapiens vacuolar protein sorting 41 homolog (S. cerevisiae) (VPS41), transcript variant 1, mRNA.
SNAPC1	-1.52	Homo sapiens small nuclear RNA activating complex, polypeptide 1, 43kDa (SNAPC1), mRNA.
RAB23	-1.52	Homo sapiens RAB23, member RAS oncogene family (RAB23), transcript variant 1, mRNA.
SESN3	-1.52	Homo sapiens sestrin 3 (SESN3), mRNA.
PDE1A	-1.52	Homo sapiens phosphodiesterase 1A, calmodulin-dependent (PDE1A), transcript variant 2, mRNA.
CERK	-1.52	Homo sapiens ceramide kinase (CERK), transcript variant 2, mRNA.
ITPR3	-1.52	Homo sapiens inositol 1,4,5-triphosphate receptor, type 3 (ITPR3), mRNA.
PPP3CA	-1.52	Homo sapiens protein phosphatase 3 (formerly 2B), catalytic subunit, alpha isoform (PPP3CA), mRNA.
PCM1	-1.52	Homo sapiens pericentriolar material 1 (PCM1), mRNA.
SLC35F2	-1.53	Homo sapiens solute carrier family 35, member F2 (SLC35F2), mRNA.
SLC25A37	-1.53	Homo sapiens solute carrier family 25, member 37 (SLC25A37), transcript variant 1, mRNA.
VLDLR	-1.53	Homo sapiens very low density lipoprotein receptor (VLDLR), transcript variant 2, mRNA.
CXCL5	-1.53	Homo sapiens chemokine (C-X-C motif) ligand 5 (CXCL5), mRNA.
PLD1	-1.53	Homo sapiens phospholipase D1, phosphatidylcholine-specific (PLD1), mRNA.
YTHDF3	-1.53	Homo sapiens YTH domain family, member 3 (YTHDF3), mRNA.
ADFP	-1.53	Homo sapiens adipose differentiation-related protein (ADFP), mRNA.

C4orf18	-1.53	Homo sapiens chromosome 4 open reading frame 18 (C4orf18), transcript variant 2, mRNA.
CBX1	-1.53	Homo sapiens chromobox homolog 1 (HP1 beta homolog Drosophila) (CBX1), mRNA.
MYH9	-1.53	Homo sapiens myosin, heavy polypeptide 9, non-muscle (MYH9), mRNA.
ZMPSTE24	-1.53	Homo sapiens zinc metallopeptidase (STE24 homolog, yeast) (ZMPSTE24), mRNA.
GALNT10	-1.53	Homo sapiens UDP-N-acetyl-alpha-D-galactosamine:polypeptide N-acetylgalactosaminyltransferase 10 (GalNAc-T10) (GALNT10), transcript variant 1, mRNA.
NAT13	-1.53	Homo sapiens N-acetyltransferase 13 (NAT13), mRNA.
TMEM38B	-1.53	Homo sapiens transmembrane protein 38B (TMEM38B), mRNA.
PXDN	-1.53	Homo sapiens peroxidasin homolog (Drosophila) (PXDN), mRNA. XM_935184 XM_936786 XM_942966 XM_942982 XM_942986 XM_942994 XM_943000
DEK	-1.53	Homo sapiens DEK oncogene (DNA binding) (DEK), mRNA.
POFUT1	-1.54	Homo sapiens protein O-fucosyltransferase 1 (POFUT1), transcript variant 1, mRNA.
TMEM106B	-1.54	Homo sapiens transmembrane protein 106B (TMEM106B), mRNA.
FAT	-1.54	Homo sapiens FAT tumor suppressor homolog 1 (Drosophila) (FAT), mRNA.
XPO4	-1.54	Homo sapiens exportin 4 (XPO4), mRNA.
TMEM106B	-1.54	Homo sapiens transmembrane protein 106B (TMEM106B), mRNA. -1.54 AV737943 CB Homo sapiens cDNA clone CBDAEG06 5, mRNA sequence
FLJ12649	-1.54	PREDICTED: Homo sapiens hypothetical protein FLJ12649, transcript variant 1 (FLJ12649), mRNA.
SNAPC4	-1.54	Homo sapiens small nuclear RNA activating complex, polypeptide 4, 190kDa (SNAPC4), mRNA.
C1orf24	-1.54	Homo sapiens chromosome 1 open reading frame 24 (C1orf24), transcript variant 1, mRNA.
PABPC1	-1.54	Homo sapiens poly(A) binding protein, cytoplasmic 1 (PABPC1), mRNA.
CTSO	-1.55	Homo sapiens cathepsin O (CTSO), mRNA.
TIMP3	-1.55	Homo sapiens TIMP metallopeptidase inhibitor 3 (Sorsby fundus dystrophy, pseudoinflammatory) (TIMP3), mRNA.
MTDH	-1.55	Homo sapiens metadherin (MTDH), mRNA.
ALS2CR13	-1.55	Homo sapiens amyotrophic lateral sclerosis 2 (juvenile) chromosome region, candidate 13 (ALS2CR13), mRNA.
MAP4K4	-1.55	Homo sapiens mitogen-activated protein kinase kinase kinase kinase 4 (MAP4K4), transcript variant 3, mRNA.
ITGB5	-1.55	PREDICTED: Homo sapiens integrin, beta 5, transcript variant 8 (ITGB5), mRNA.
FZD2	-1.55	Homo sapiens frizzled homolog 2 (Drosophila) (FZD2), mRNA.
ALDH1B1	-1.55	Homo sapiens aldehyde dehydrogenase 1 family, member B1 (ALDH1B1), nuclear gene encoding mitochondrial protein, mRNA.
NBPF11	-1.55	Homo sapiens neuroblastoma breakpoint family, member 11 (NBPF11), mRNA.
CTNNB1	-1.55	PREDICTED: Homo sapiens catenin (cadherin-associated protein), beta 1, 88kDa, transcript variant 4 (CTNNB1), mRNA.
BBX	-1.55	Homo sapiens bobby sox homolog (Drosophila) (BBX), mRNA.
CRTAC1	-1.55	Homo sapiens cartilage acidic protein 1 (CRTAC1), mRNA.
BHLHB3	-1.56	Homo sapiens basic helix-loop-helix domain containing, class B, 3 (BHLHB3), mRNA.
SIPA1L2	-1.56	Homo sapiens signal-induced proliferation-associated 1 like 2 (SIPA1L2), mRNA.
PDXK	-1.56	Homo sapiens pyridoxal (pyridoxine, vitamin B6) kinase (PDXK), mRNA.
NAV2	-1.56	Homo sapiens neuron navigator 2 (NAV2), transcript variant 2, mRNA.
ZNF302	-1.56	Homo sapiens zinc finger protein 302 (ZNF302), transcript variant 1, mRNA.
GAS6	-1.56	Homo sapiens growth arrest-specific 6 (GAS6), mRNA.
TNS3	-1.56	Homo sapiens tensin 3 (TNS3), mRNA.
LPP	-1.56	Homo sapiens LIM domain containing preferred translocation partner in lipoma (LPP), mRNA.
ABCC4	-1.56	Homo sapiens ATP-binding cassette, sub-family C (CFTR/MRP), member 4 (ABCC4), mRNA.
COL16A1	-1.56	Homo sapiens collagen, type XVI, alpha 1 (COL16A1), mRNA.
LOC642934	-1.56	PREDICTED: Homo sapiens hypothetical protein LOC642934 (LOC642934), mRNA.
DHFRL1	-1.56	Homo sapiens dihydrofolate reductase-like 1 (DHFRL1), mRNA.
NMD3	-1.56	Homo sapiens NMD3 homolog (S. cerevisiae) (NMD3), mRNA.
SMAD4	-1.57	Homo sapiens SMAD family member 4 (SMAD4), mRNA.

NOL8	-1.57	Homo sapiens nucleolar protein 8 (NOL8), mRNA.
ABCA1	-1.57	Homo sapiens ATP-binding cassette, sub-family A (ABC1), member 1 (ABCA1), mRNA.
DDEFL1	-1.57	Homo sapiens development and differentiation enhancing factor-like 1 (DDEFL1), mRNA.
FMO4	-1.57	Homo sapiens flavin containing monooxygenase 4 (FMO4), mRNA.
WDFY1	-1.57	Homo sapiens WD repeat and FYVE domain containing 1 (WDFY1), mRNA.
NISCH	-1.57	Homo sapiens nischarin (NISCH), mRNA.
GAS6	-1.57	PREDICTED: Homo sapiens growth arrest-specific 6, transcript variant 2 (GAS6), mRNA.
TCEA1	-1.57	Homo sapiens transcription elongation factor A (SID), 1 (TCEA1), transcript variant 2, mRNA.
JMJD1C	-1.57	Homo sapiens jumonji domain containing 1C (JMJD1C), mRNA.
MUM1	-1.57	Homo sapiens melanoma associated antigen (mutated) 1 (MUM1), mRNA.
EFEMP1	-1.57	Homo sapiens EGF-containing fibulin-like extracellular matrix protein 1 (EFEMP1), transcript variant 1, mRNA.
FHL2	-1.57	Homo sapiens four and a half LIM domains 2 (FHL2), transcript variant 2, mRNA.
FNDC3A	-1.57	Homo sapiens fibronectin type III domain containing 3A (FNDC3A), transcript variant 1, mRNA.
CYFIP2	-1.58	Homo sapiens cytoplasmic FMR1 interacting protein 2 (CYFIP2), mRNA.
MCM4	-1.58	Homo sapiens MCM4 minichromosome maintenance deficient 4 (<i>S. cerevisiae</i>) (MCM4), transcript variant 1, mRNA.
MMP11	-1.58	Homo sapiens matrix metalloproteinase 11 (stromelysin 3) (MMP11), mRNA.
GPNMB	-1.58	Homo sapiens glycoprotein (transmembrane) nmb (GPNMB), transcript variant 1, mRNA.
TNFRSF10B	-1.58	Homo sapiens tumor necrosis factor receptor superfamily, member 10b (TNFRSF10B), transcript variant 1, mRNA.
LUM	-1.58	Homo sapiens lumican (LUM), mRNA.
PPM2C	-1.58	Homo sapiens protein phosphatase 2C, magnesium-dependent, catalytic subunit (PPM2C), nuclear gene encoding mitochondrial protein, mRNA.
CD14	-1.58	Homo sapiens CD14 molecule (CD14), transcript variant 2, mRNA.
ZNF91	-1.58	Homo sapiens zinc finger protein 91 (HPF7, HTF10) (ZNF91), mRNA.
LANCL1	-1.58	Homo sapiens LanC lantibiotic synthetase component C-like 1 (bacterial) (LANCL1), mRNA.
ZBTB33	-1.58	Homo sapiens zinc finger and BTB domain containing 33 (ZBTB33), mRNA.
SP3	-1.58	Homo sapiens Sp3 transcription factor (SP3), transcript variant 2, mRNA.
DACT1	-1.59	Homo sapiens dapper, antagonist of beta-catenin, homolog 1 (<i>Xenopus laevis</i>) (DACT1), mRNA.
	-1.59	BX099724 Soares_fetal_liver_spleen_1NFLS_S1 Homo sapiens cDNA clone
	-1.59	IMAGp998F201004, mRNA sequence
C5orf13	-1.59	Homo sapiens chromosome 5 open reading frame 13 (C5orf13), mRNA.
C1orf71	-1.59	Homo sapiens chromosome 1 open reading frame 71 (C1orf71), mRNA.
C1orf24	-1.59	Homo sapiens chromosome 1 open reading frame 24 (C1orf24), transcript variant 2, mRNA.
DPP4	-1.59	Homo sapiens dipeptidyl-peptidase 4 (CD26, adenosine deaminase complexing protein 2) (DPP4), mRNA.
IRX3	-1.59	Homo sapiens iroquois homeobox 3 (IRX3), mRNA.
THBS2	-1.59	Homo sapiens thrombospondin 2 (THBS2), mRNA.
NGFB	-1.60	Homo sapiens nerve growth factor, beta polypeptide (NGFB), mRNA.
ZNF295	-1.60	Homo sapiens zinc finger protein 295 (ZNF295), mRNA.
CD24	-1.60	Homo sapiens CD24 molecule (CD24), mRNA.
DKFZP686A01247	-1.60	Homo sapiens LIM and calponin homology domains 1 (LIMCH1), mRNA.
RPA1	-1.60	Homo sapiens replication protein A1, 70kDa (RPA1), mRNA.
APP	-1.60	Homo sapiens amyloid beta (A4) precursor protein (peptidase nexin-II, Alzheimer disease) (APP), transcript variant 3, mRNA.
PLAU	-1.60	Homo sapiens plasminogen activator, urokinase (PLAU), mRNA.
ITGB1	-1.60	Homo sapiens integrin, beta 1 (fibronectin receptor, beta polypeptide, antigen CD29 includes MDF2, MSK12) (ITGB1), transcript variant 1E, mRNA.
COLEC12	-1.60	Homo sapiens collectin sub-family member 12 (COLEC12), mRNA.
ITGB2	-1.60	Homo sapiens integrin, beta 2 (antigen CD18 (p95), lymphocyte function-associated antigen 1; macrophage antigen 1 (mac-1) beta subunit) (ITGB2), mRNA.
COL5A1	-1.60	Homo sapiens collagen, type V, alpha 1 (COL5A1), mRNA.

CTNNB1	-1.60	Homo sapiens catenin (cadherin-associated protein), beta 1, 88kDa (CTNNB1), mRNA. XM_945653 XM_945654 XM_945655 XM_945657
ZNF195	-1.60	Homo sapiens zinc finger protein 195 (ZNF195), mRNA.
CTSK	-1.60	Homo sapiens cathepsin K (CTSK), mRNA.
PRKAA1	-1.60	Homo sapiens protein kinase, AMP-activated, alpha 1 catalytic subunit (PRKAA1), transcript variant 2, mRNA.
PCNA	-1.60	Homo sapiens proliferating cell nuclear antigen (PCNA), transcript variant 2, mRNA.
ADAMTS5	-1.61	Homo sapiens ADAM metalloproteinase with thrombospondin type 1 motif, 5 (aggrecanase-2) (ADAMTS5), mRNA.
SPOCK	-1.61	Homo sapiens sparc/osteonectin, cwcv and kazal-like domains proteoglycan (testican) (SPOCK), mRNA.
RECK	-1.61	Homo sapiens reversion-inducing-cysteine-rich protein with kazal motifs (RECK), mRNA.
FUT8	-1.61	Homo sapiens fucosyltransferase 8 (alpha (1,6) fucosyltransferase) (FUT8), transcript variant 2, mRNA.
TPM1	-1.61	Homo sapiens tropomyosin 1 (alpha) (TPM1), transcript variant 3, mRNA.
SGCD	-1.61	Homo sapiens sarcoglycan, delta (35kDa dystrophin-associated glycoprotein) (SGCD), transcript variant 1, mRNA.
KIAA0194	-1.61	PREDICTED: Homo sapiens KIAA0194 protein (KIAA0194), mRNA.
NBPF20	-1.61	Homo sapiens neuroblastoma breakpoint family, member 20 (NBPF20), mRNA.
PDLIM3	-1.61	Homo sapiens PDZ and LIM domain 3 (PDLIM3), mRNA.
ENAH	-1.62	Homo sapiens enabled homolog (Drosophila) (ENAH), transcript variant 2, mRNA.
SEMA3C	-1.62	Homo sapiens sema domain, immunoglobulin domain (Ig), short basic domain, secreted, (semaphorin) 3C (SEMA3C), mRNA.
F13A1	-1.62	Homo sapiens coagulation factor XIII, A1 polypeptide (F13A1), mRNA.
CD55	-1.62	Homo sapiens CD55 molecule, decay accelerating factor for complement (Cromer blood group) (CD55), mRNA.
C17orf70	-1.62	Homo sapiens chromosome 17 open reading frame 70 (C17orf70), mRNA.
ENAH	-1.62	Homo sapiens enabled homolog (Drosophila) (ENAH), transcript variant 2, mRNA.
FLJ12716	-1.62	Homo sapiens FLJ12716 protein (FLJ12716), transcript variant 2, mRNA.
LAMA1	-1.62	Homo sapiens laminin, alpha 1 (LAMA1), mRNA.
VGLL4	-1.62	Homo sapiens vestigial like 4 (Drosophila) (VGLL4), mRNA.
TCF12	-1.62	Homo sapiens transcription factor 12 (HTF4, helix-loop-helix transcription factors 4) (TCF12), transcript variant 1, mRNA.
ITGB5	-1.62	Homo sapiens integrin, beta 5 (ITGB5), mRNA. XM_944688 XM_944693
TNPO1	-1.62	Homo sapiens transportin 1 (TNPO1), transcript variant 1, mRNA.
UBQLN2	-1.63	Homo sapiens ubiquilin 2 (UBQLN2), mRNA.
OSR1	-1.63	Homo sapiens odd-skipped related 1 (Drosophila) (OSR1), mRNA.
ALOX5	-1.63	Homo sapiens arachidonate 5-lipoxygenase (ALOX5), mRNA.
VAV3	-1.63	Homo sapiens vav 3 guanine nucleotide exchange factor (VAV3), transcript variant 1, mRNA.
PAWR	-1.63	Homo sapiens PRKC, apoptosis, WT1, regulator (PAWR), mRNA.
ATP2B1	-1.64	Homo sapiens ATPase, Ca ⁺⁺ transporting, plasma membrane 1 (ATP2B1), transcript variant 1, mRNA.
SH3BP4	-1.64	Homo sapiens SH3-domain binding protein 4 (SH3BP4), mRNA.
NT5E	-1.64	Homo sapiens 5'-nucleotidase, ecto (CD73) (NT5E), mRNA.

		Homo sapiens neuroblastoma breakpoint family, member 10 (NBPF10), mRNA. XM_930727 XM_930739 XM_930751 XM_930759 XM_930766 XM_930776 XM_930785 XM_930797 XM_930808 XM_930830 XM_930841 XM_930850 XM_930862 XM_930872 XM_930880 XM_930889 XM_930897 XM_930903 XM_930910 XM_930917 XM_930926 XM_930936 XM_930943 XM_930951 XM_930954 XM_930961 XM_930967 XM_930975 XM_930985 XM_930993 XM_931003 XM_931009 XM_931015 XM_931021 XM_931027 XM_931033 XM_931038 XM_931044 XM_931049 XM_931055 XM_931060 XM_931066 XM_931069 XM_931072 XM_931076 XM_931080 XM_931084 XM_931090 XM_931096 XM_931102 XM_931110 XM_931119 XM_931125 XM_931131 XM_931137 XM_931138 XM_931145 XM_931149 XM_931157 XM_931161 XM_931164 XM_931169 XM_931174 XM_931178 XM_931183 XM_931188 XM_931191 XM_931196 XM_931202 XM_931208 XM_931213 XM_931221 XM_931229 XM_931234 XM_931240 XM_931245 XM_931251 XM_931255 XM_931259 XM_931264 XM_931269 XM_931277 XM_931282 XM_931291 XM_931299 XM_931308 XM_931317 XM_931322 XM_931328 XM_931335
NBPF10	-1.64	
GAS6	-1.64	Homo sapiens growth arrest-specific 6 (GAS6), mRNA.
ARHGAP1	-1.64	Homo sapiens Rho GTPase activating protein 1 (ARHGAP1), mRNA.
PAPLN	-1.64	Homo sapiens papilin, proteoglycan-like sulfated glycoprotein (PAPLN), mRNA.
VPS26	-1.64	Homo sapiens vacuolar protein sorting 26 (yeast) (VPS26), mRNA.
FLJ11259	-1.65	Homo sapiens hypothetical protein FLJ11259 (FLJ11259), mRNA.
SLC24A3	-1.65	Homo sapiens solute carrier family 24 (sodium/potassium/calcium exchanger), member 3 (SLC24A3), mRNA.
ABI3BP	-1.65	Homo sapiens ABI gene family, member 3 (NESH) binding protein (ABI3BP), mRNA.
SRGAP1	-1.65	Homo sapiens SLIT-ROBO Rho GTPase activating protein 1 (SRGAP1), mRNA.
PDGFC	-1.65	Homo sapiens platelet derived growth factor C (PDGFC), mRNA.
HOM-TES-103	-1.65	Homo sapiens hypothetical protein LOC25900 (HOM-TES-103), transcript variant 2, mRNA.
BMP4	-1.66	Homo sapiens bone morphogenetic protein 4 (BMP4), transcript variant 1, mRNA.
PIGQ	-1.66	Homo sapiens phosphatidylinositol glycan anchor biosynthesis, class Q (PIGQ), transcript variant 2, mRNA.
DYRK2	-1.66	Homo sapiens dual-specificity tyrosine-(Y)-phosphorylation regulated kinase 2 (DYRK2), transcript variant 1, mRNA.
TMEPAI	-1.66	Homo sapiens transmembrane, prostate androgen induced RNA (TMEPAI), transcript variant 2, mRNA.
SPP1	-1.66	Homo sapiens secreted phosphoprotein 1 (osteopontin, bone sialoprotein I, early T-lymphocyte activation 1) (SPP1), transcript variant 1, mRNA.
SLC27A1	-1.66	Homo sapiens solute carrier family 27 (fatty acid transporter), member 1 (SLC27A1), mRNA.
TPM1	-1.66	Homo sapiens tropomyosin 1 (alpha) (TPM1), transcript variant 6, mRNA.
CABC1	-1.66	Homo sapiens chaperone, ABC1 activity of bc1 complex like (S. pombe) (CABC1), mRNA.
AOX1	-1.67	Homo sapiens aldehyde oxidase 1 (AOX1), mRNA.
TBL1XR1	-1.67	Homo sapiens transducin (beta)-like 1X-linked receptor 1 (TBL1XR1), mRNA.
CMAH	-1.67	Homo sapiens cytidine monophosphate-N-acetylneuraminic acid hydroxylase (CMP-N-acetylneuraminate monooxygenase) (CMAH) on chromosome 6.
CLCN7	-1.67	Homo sapiens chloride channel 7 (CLCN7), mRNA.
NMB	-1.68	Homo sapiens neuromedin B (NMB), transcript variant 1, mRNA.
C21orf66	-1.68	Homo sapiens chromosome 21 open reading frame 66 (C21orf66), transcript variant 1, mRNA.
DPYSL3	-1.68	Homo sapiens dihydropyrimidinase-like 3 (DPYSL3), mRNA.
RAB23	-1.68	Homo sapiens RAB23, member RAS oncogene family (RAB23), transcript variant 1, mRNA.
Sep-11	-1.69	Homo sapiens septin 11 (SEPT11), mRNA.
LASS6	-1.69	Homo sapiens LAG1 homolog, ceramide synthase 6 (LASS6), mRNA.
IRXL1	-1.69	Homo sapiens mohawk homeobox (MKX), mRNA.
RPS6KA2	-1.69	Homo sapiens ribosomal protein S6 kinase, 90kDa, polypeptide 2 (RPS6KA2), transcript variant 1, mRNA.
CXorf6	-1.69	Homo sapiens chromosome X open reading frame 6 (CXorf6), mRNA.
DFNA5	-1.69	Homo sapiens deafness, autosomal dominant 5 (DFNA5), mRNA.

A2M	-1.70	Homo sapiens alpha-2-macroglobulin (A2M), mRNA.
PLS3	-1.70	Homo sapiens plastin 3 (T isoform) (PLS3), mRNA.
SLC43A3	-1.70	Homo sapiens solute carrier family 43, member 3 (SLC43A3), mRNA.
GREM1	-1.71	Homo sapiens gremlin 1, cysteine knot superfamily, homolog (Xenopus laevis) (GREM1), mRNA.
CCL3L3	-1.71	Homo sapiens chemokine (C-C motif) ligand 3-like 3 (CCL3L3), mRNA.
ZSCAN2	-1.71	Homo sapiens zinc finger and SCAN domain containing 2 (ZSCAN2), transcript variant 1, mRNA.
PAQR3	-1.71	Homo sapiens progesterin and adipoQ receptor family member III (PAQR3), mRNA.
PSD3	-1.71	Homo sapiens pleckstrin and Sec7 domain containing 3 (PSD3), transcript variant 2, mRNA.
ARNT2	-1.71	Homo sapiens aryl-hydrocarbon receptor nuclear translocator 2 (ARNT2), mRNA.
DBN1	-1.72	Homo sapiens drebrin 1 (DBN1), transcript variant 2, mRNA.
CMAH	-1.72	Homo sapiens cytidine monophosphate-N-acetylneuraminic acid hydroxylase (CMP-N-acetylneuraminate monooxygenase) (CMAH) on chromosome 6.
HIF1A	-1.72	Homo sapiens hypoxia-inducible factor 1, alpha subunit (basic helix-loop-helix transcription factor) (HIF1A), transcript variant 1, mRNA.
C20orf82	-1.72	PREDICTED: Homo sapiens chromosome 20 open reading frame 82 (C20orf82), mRNA.
SVEP1	-1.72	Homo sapiens sushi, von Willebrand factor type A, EGF and pentraxin domain containing 1 (SVEP1), mRNA.
ZSWIM4	-1.73	Homo sapiens mRNA; cDNA DKFZp779O0231 (from clone DKFZp779O0231)
BCAT1	-1.73	Homo sapiens zinc finger, SWIM-type containing 4 (ZSWIM4), mRNA.
SPP1	-1.73	Homo sapiens branched chain aminotransferase 1, cytosolic (BCAT1), mRNA.
BNIP3L	-1.73	Homo sapiens secreted phosphoprotein 1 (osteopontin, bone sialoprotein I, early T-lymphocyte activation 1) (SPP1), transcript variant 2, mRNA.
PDZRN3	-1.74	Homo sapiens BCL2/adenovirus E1B 19kDa interacting protein 3-like (BNIP3L), mRNA.
OGN	-1.75	PREDICTED: Homo sapiens PDZ domain containing RING finger 3, transcript variant 3 (PDZRN3), mRNA.
GJA1	-1.75	Homo sapiens osteoglycin (osteoinductive factor, mimecan) (OGN), transcript variant 2, mRNA.
TPM1	-1.75	Homo sapiens gap junction protein, alpha 1, 43kDa (connexin 43) (GJA1), mRNA.
PLS3	-1.75	Homo sapiens tropomyosin 1 (alpha) (TPM1), transcript variant 6, mRNA.
CLIC4	-1.75	Homo sapiens plastin 3 (T isoform) (PLS3), mRNA.
HIF1A	-1.76	Homo sapiens chloride intracellular channel 4 (CLIC4), mRNA.
GPR177	-1.76	Homo sapiens hypoxia-inducible factor 1, alpha subunit (basic helix-loop-helix transcription factor) (HIF1A), transcript variant 2, mRNA.
C4orf18	-1.76	Homo sapiens G protein-coupled receptor 177 (GPR177), transcript variant 1, mRNA.
GNPTAB	-1.76	Homo sapiens chromosome 4 open reading frame 18 (C4orf18), transcript variant 2, mRNA.
PTX3	-1.76	Homo sapiens N-acetylglucosamine-1-phosphate transferase, alpha and beta subunits (GNPTAB), mRNA.
COL11A1	-1.76	Homo sapiens pentraxin-related gene, rapidly induced by IL-1 beta (PTX3), mRNA.
KCNMA1	-1.76	Homo sapiens collagen, type XI, alpha 1 (COL11A1), transcript variant B, mRNA.
LANCL1	-1.76	Homo sapiens potassium large conductance calcium-activated channel, subfamily M, alpha member 1 (KCNMA1), transcript variant 2, mRNA.
C6orf69	-1.77	Homo sapiens LanC lantibiotic synthetase component C-like 1 (bacterial) (LANCL1), mRNA.
HTRA4	-1.79	Homo sapiens potassium channel tetramerisation domain containing 20 (KCTD20), mRNA.
BDKRB1	-1.79	AV737317 CB Homo sapiens cDNA clone CBCAQH03 5, mRNA sequence
GAS7	-1.79	Homo sapiens HtrA serine peptidase 4 (HTRA4), mRNA.
SLC43A3	-1.80	Homo sapiens bradykinin receptor B1 (BDKRB1), mRNA.
PABPC4	-1.80	Homo sapiens growth arrest-specific 7 (GAS7), transcript variant b, mRNA.
TMEPAI	-1.80	Homo sapiens cDNA clone IMAGE:5261213
SSPN	-1.81	Homo sapiens solute carrier family 43, member 3 (SLC43A3), mRNA.
ADCY4	-1.81	Homo sapiens poly(A) binding protein, cytoplasmic 4 (inducible form) (PABPC4), mRNA.
		Homo sapiens transmembrane, prostate androgen induced RNA (TMEPAI), transcript variant 2, mRNA.
		Homo sapiens sarcospan (Kras oncogene-associated gene) (SSPN), mRNA.
		Homo sapiens adenylate cyclase 4 (ADCY4), mRNA.

RHOBTB3	-1.82	Homo sapiens Rho-related BTB domain containing 3 (RHOBTB3), mRNA.
MTSS1	-1.82	Homo sapiens metastasis suppressor 1 (MTSS1), mRNA.
RECK	-1.83	Homo sapiens reversion-inducing-cysteine-rich protein with kazal motifs (RECK), mRNA.
DACT1	-1.83	Homo sapiens dapper, antagonist of beta-catenin, homolog 1 (Xenopus laevis) (DACT1), transcript variant 1, mRNA.
PLTP	-1.83	Homo sapiens phospholipid transfer protein (PLTP), transcript variant 1, mRNA.
ZCCHC14	-1.83	Homo sapiens zinc finger, CCHC domain containing 14 (ZCCHC14), mRNA.
ARHGAP22	-1.84	Homo sapiens Rho GTPase activating protein 22 (ARHGAP22), mRNA.
VGLL3	-1.84	Homo sapiens vestigial like 3 (Drosophila) (VGLL3), mRNA.
RASD1	-1.84	Homo sapiens RAS, dexamethasone-induced 1 (RASD1), mRNA.
ZMAT3	-1.84	Homo sapiens zinc finger, matrin type 3 (ZMAT3), transcript variant 2, mRNA.
ANKRD10	-1.84	Homo sapiens ankyrin repeat domain 10 (ANKRD10), mRNA.
SLITRK4	-1.84	Homo sapiens SLIT and NTRK-like family, member 4 (SLITRK4), mRNA.
ANGPTL7	-1.85	Homo sapiens angiopoietin-like 7 (ANGPTL7), mRNA.
BMP2	-1.85	Homo sapiens bone morphogenetic protein 2 (BMP2), mRNA.
CCND1	-1.85	Homo sapiens cyclin D1 (PRAD1: parathyroid adenomatosis 1) (CCND1), mRNA.
MCM7	-1.86	Homo sapiens minichromosome maintenance complex component 7 (MCM7), transcript variant 2, mRNA.
KLHL24	-1.86	Homo sapiens kelch-like 24 (Drosophila) (KLHL24), mRNA.
CRISPLD2	-1.86	Homo sapiens cysteine-rich secretory protein LCCL domain containing 2 (CRISPLD2), mRNA.
LPXN	-1.86	Homo sapiens leupaxin (LPXN), mRNA.
FAM107B	-1.86	Homo sapiens family with sequence similarity 107, member B (FAM107B), mRNA.
HNMT	-1.87	Homo sapiens histamine N-methyltransferase (HNMT), transcript variant 1, mRNA.
PLXDC2	-1.87	Homo sapiens plexin domain containing 2 (PLXDC2), mRNA.
LRRC20	-1.88	Homo sapiens leucine rich repeat containing 20 (LRRC20), transcript variant 1, mRNA.
SPOCD1	-1.89	Homo sapiens SPOC domain containing 1 (SPOCD1), mRNA.
LAMB1	-1.90	Homo sapiens laminin, beta 1 (LAMB1), mRNA.
CDH11	-1.90	Homo sapiens cadherin 11, type 2, OB-cadherin (osteoblast) (CDH11), mRNA.
	-1.92	Homo sapiens mRNA; cDNA DKFZp564O0862 (from clone DKFZp564O0862)
CXCL12	-1.92	Homo sapiens chemokine (C-X-C motif) ligand 12 (stromal cell-derived factor 1) (CXCL12), transcript variant 1, mRNA.
FRMD6	-1.94	Homo sapiens FERM domain containing 6 (FRMD6), mRNA.
EVI2A	-1.94	Homo sapiens ecotropic viral integration site 2A (EVI2A), transcript variant 2, mRNA.
TMEM119	-1.94	Homo sapiens transmembrane protein 119 (TMEM119), mRNA.
IL33	-1.95	Homo sapiens interleukin 33 (IL33), mRNA.
LOC654103	-1.95	PREDICTED: Homo sapiens similar to solute carrier family 25, member 37 (LOC654103), mRNA.
CCDC14	-1.95	Homo sapiens coiled-coil domain containing 14 (CCDC14), mRNA.
CXCL12	-1.96	Homo sapiens chemokine (C-X-C motif) ligand 12 (stromal cell-derived factor 1) (CXCL12), transcript variant 2, mRNA.
CYP27A1	-1.97	Homo sapiens cytochrome P450, family 27, subfamily A, polypeptide 1 (CYP27A1), nuclear gene encoding mitochondrial protein, mRNA.
LOXL4	-1.99	Homo sapiens lysyl oxidase-like 4 (LOXL4), mRNA.
FLJ14054	-2.01	Homo sapiens hypothetical protein FLJ14054 (FLJ14054), mRNA.
GREM1	-2.02	Homo sapiens gremlin 1, cysteine knot superfamily, homolog (Xenopus laevis) (GREM1), mRNA.
MYLK	-2.02	Homo sapiens myosin, light polypeptide kinase (MYLK), transcript variant 6, mRNA.
PDE5A	-2.06	Homo sapiens phosphodiesterase 5A, cGMP-specific (PDE5A), transcript variant 3, mRNA.
HNMT	-2.06	Homo sapiens histamine N-methyltransferase (HNMT), transcript variant 1, mRNA.
LOC653778	-2.08	PREDICTED: Homo sapiens similar to solute carrier family 25, member 37 (LOC653778), mRNA.
SOX4	-2.08	Homo sapiens SRY (sex determining region Y)-box 4 (SOX4), mRNA.
GALNT1	-2.08	Homo sapiens UDP-N-acetyl-alpha-D-galactosamine:polypeptide N-acetylgalactosaminyltransferase 1 (GalNAc-T1) (GALNT1), mRNA.
HIF1A	-2.09	Homo sapiens hypoxia-inducible factor 1, alpha subunit (basic helix-loop-helix transcription factor) (HIF1A), transcript variant 2, mRNA.
LAMB1	-2.09	Homo sapiens laminin, beta 1 (LAMB1), mRNA.
MMP13	-2.10	Homo sapiens matrix metalloproteinase 13 (collagenase 3) (MMP13), mRNA.

ANTXR1	-2.12	Homo sapiens anthrax toxin receptor 1 (ANTXR1), transcript variant 1, mRNA.
SLC38A2	-2.14	Homo sapiens solute carrier family 38, member 2 (SLC38A2), mRNA.
ENPP2	-2.15	Homo sapiens ectonucleotide pyrophosphatase/phosphodiesterase 2 (autotaxin) (ENPP2), mRNA.
FBXO32	-2.15	Homo sapiens F-box protein 32 (FBXO32), transcript variant 1, mRNA.
SFRP4	-2.16	Homo sapiens secreted frizzled-related protein 4 (SFRP4), mRNA.
THBS1	-2.16	Homo sapiens thrombospondin 1 (THBS1), mRNA.
IL26	-2.19	Homo sapiens interleukin 26 (IL26), mRNA.
GDF15	-2.19	Homo sapiens growth differentiation factor 15 (GDF15), mRNA.
CXCL12	-2.21	Homo sapiens chemokine (C-X-C motif) ligand 12 (stromal cell-derived factor 1) (CXCL12), transcript variant 3, mRNA.
ENPP2	-2.21	Homo sapiens ectonucleotide pyrophosphatase/phosphodiesterase 2 (autotaxin) (ENPP2), transcript variant 2, mRNA.
KIAA0564	-2.24	Homo sapiens KIAA0564 protein (KIAA0564), transcript variant 1, mRNA.
ANKRD1	-2.31	Homo sapiens ankyrin repeat domain 1 (cardiac muscle) (ANKRD1), mRNA.
MYLK	-2.32	Homo sapiens myosin, light chain kinase (MYLK), transcript variant 2, mRNA.
ALPL	-2.32	Homo sapiens alkaline phosphatase, liver/bone/kidney (ALPL), mRNA.
SCG5	-2.34	Homo sapiens secretogranin V (7B2 protein) (SCG5), mRNA.
EVI2A	-2.35	Homo sapiens ecotropic viral integration site 2A (EVI2A), transcript variant 2, mRNA.
ADAMTS1	-2.52	Homo sapiens ADAM metalloproteinase with thrombospondin type 1 motif, 1 (ADAMTS1), mRNA.
SDC1	-2.57	Homo sapiens syndecan 1 (SDC1), transcript variant 2, mRNA.
FBXO32	-2.58	Homo sapiens F-box protein 32 (FBXO32), transcript variant 2, mRNA.
GEM	-2.72	Homo sapiens GTP binding protein overexpressed in skeletal muscle (GEM), transcript variant 1, mRNA.
GEM	-2.85	Homo sapiens GTP binding protein overexpressed in skeletal muscle (GEM), transcript variant 2, mRNA.
GAS1	-3.06	Homo sapiens growth arrest-specific 1 (GAS1), mRNA.
GAS1	-4.13	Homo sapiens growth arrest-specific 1 (GAS1), mRNA.

Genome-wide microarray results**SW1353 cells: IL-1+OSM+IL-4 vs IL-1+OSM**

Symbol	Fold change	Gene name
CCL26	21.07	Homo sapiens chemokine (C-C motif) ligand 26 (CCL26), mRNA.
FST	5.13	Homo sapiens follistatin (FST), transcript variant FST344, mRNA.
RGS4	4.77	Homo sapiens regulator of G-protein signalling 4 (RGS4), mRNA.
SNFT	4.67	Homo sapiens Jun dimerization protein p21SNFT (SNFT), mRNA.
FST	4.30	Homo sapiens follistatin (FST), transcript variant FST317, mRNA.
VCAM1	4.09	Homo sapiens vascular cell adhesion molecule 1 (VCAM1), transcript variant 1, mRNA.
PPFIBP2	4.08	Homo sapiens PTPRF interacting protein, binding protein 2 (liprin beta 2) (PPFIBP2), mRNA.
LOC653671	4.08	PREDICTED: Homo sapiens similar to Beta-defensin 103A precursor (Beta-defensin 3) (DEFB-3) (BD-3) (hBD-3) (HBD3) (Defensin-like protein) (LOC653671), mRNA.
TNC	3.99	Homo sapiens tenascin C (hexabrachion) (TNC), mRNA.
DEFB103A	3.75	Homo sapiens defensin, beta 103A (DEFB103A), mRNA.
SERPINB4	3.59	Homo sapiens serpin peptidase inhibitor, clade B (ovalbumin), member 4 (SERPINB4), mRNA.
SERPINB3	3.36	Homo sapiens serpin peptidase inhibitor, clade B (ovalbumin), member 3 (SERPINB3), mRNA.
ADCY8	3.08	Homo sapiens adenylate cyclase 8 (brain) (ADCY8), mRNA.
INHBE	2.96	Homo sapiens inhibin, beta E (INHBE), mRNA.
CISH	2.86	Homo sapiens cytokine inducible SH2-containing protein (CISH), mRNA.
CDKN1A	2.84	Homo sapiens cyclin-dependent kinase inhibitor 1A (p21, Cip1) (CDKN1A), transcript variant 2, mRNA.
ARRDC4	2.76	Homo sapiens arrestin domain containing 4 (ARRDC4), mRNA.
DCBLD2	2.67	Homo sapiens discoidin, CUB and LCCL domain containing 2 (DCBLD2), mRNA.
IL13RA2	2.66	Homo sapiens interleukin 13 receptor, alpha 2 (IL13RA2), mRNA.
FAM101A	2.65	Homo sapiens family with sequence similarity 101, member A (FAM101A), mRNA.
IL1F5	2.62	Homo sapiens interleukin 1 family, member 5 (delta) (IL1F5), transcript variant 2, mRNA.
PMP22	2.60	Homo sapiens peripheral myelin protein 22 (PMP22), transcript variant 3, mRNA.
GADD45A	2.59	Homo sapiens growth arrest and DNA-damage-inducible, alpha (GADD45A), mRNA.
SOCS1	2.59	Homo sapiens suppressor of cytokine signaling 1 (SOCS1), mRNA.
SERPINB3	2.57	Homo sapiens serpin peptidase inhibitor, clade B (ovalbumin), member 3 (SERPINB3), mRNA.
CENTA1	2.53	Homo sapiens centaurin, alpha 1 (CENTA1), mRNA.
NIPA1	2.45	Homo sapiens non imprinted in Prader-Willi/Angelman syndrome 1 (NIPA1), mRNA.
DCUN1D3	2.44	Homo sapiens DCN1, defective in cullin neddylation 1, domain containing 3 (S. cerevisiae) (DCUN1D3), mRNA.
HAS2	2.42	Homo sapiens hyaluronan synthase 2 (HAS2), mRNA.
DEFB103A	2.41	Homo sapiens defensin, beta 103A (DEFB103A), mRNA.
KITLG	2.38	Homo sapiens KIT ligand (KITLG), transcript variant b, mRNA.
KAL1	2.34	Homo sapiens Kallmann syndrome 1 sequence (KAL1), mRNA.
LBH	2.34	Homo sapiens limb bud and heart development homolog (mouse) (LBH), mRNA.
PMP22	2.30	Homo sapiens peripheral myelin protein 22 (PMP22), transcript variant 2, mRNA.
GADD45A	2.29	Homo sapiens growth arrest and DNA-damage-inducible, alpha (GADD45A), mRNA.
IGFBP3	2.28	Homo sapiens insulin-like growth factor binding protein 3 (IGFBP3), transcript variant 1, mRNA.
CCL5	2.27	Homo sapiens chemokine (C-C motif) ligand 5 (CCL5), mRNA.
LOX	2.27	Homo sapiens lysyl oxidase (LOX), mRNA.
LOXL3	2.21	Homo sapiens lysyl oxidase-like 3 (LOXL3), mRNA.
TNC	2.20	Homo sapiens tenascin C (hexabrachion) (TNC), mRNA.
KITLG	2.17	Homo sapiens KIT ligand (KITLG), transcript variant b, mRNA.
NPPB	2.11	Homo sapiens natriuretic peptide precursor B (NPPB), mRNA.
MESP1	2.11	Homo sapiens mesoderm posterior 1 homolog (mouse) (MESP1), mRNA.
KLF2	2.11	Homo sapiens Kruppel-like factor 2 (lung) (KLF2), mRNA.

MAPKAPK3	2.07	Homo sapiens mitogen-activated protein kinase-activated protein kinase 3 (MAPKAPK3), mRNA.
ITGAX	2.06	Homo sapiens integrin, alpha X (complement component 3 receptor 4 subunit) (ITGAX), mRNA.
LOC652481	2.05	PREDICTED: Homo sapiens similar to Mitochondrial import inner membrane translocase subunit Tim23 (LOC652481), mRNA.
TRIB3	1.98	Homo sapiens tribbles homolog 3 (Drosophila) (TRIB3), mRNA.
ANXA8	1.98	Homo sapiens annexin A8-like 2 (ANXA8L2), mRNA.
SLC3A2	1.97	Homo sapiens solute carrier family 3 (activators of dibasic and neutral amino acid transport), member 2 (SLC3A2), transcript variant 6, mRNA.
HAS2	1.94	Homo sapiens hyaluronan synthase 2 (HAS2), mRNA.
SUSD2	1.94	Homo sapiens sushi domain containing 2 (SUSD2), mRNA.
SERPINB13	1.94	Homo sapiens serpin peptidase inhibitor, clade B (ovalbumin), member 13 (SERPINB13), mRNA.
KLF6	1.92	Homo sapiens Kruppel-like factor 6 (KLF6), transcript variant 1, mRNA. Homo sapiens SHC (Src homology 2 domain containing) family, member 4 (SHC4), mRNA.
SHC4	1.92	
C1QTNF1	1.91	Homo sapiens C1q and tumor necrosis factor related protein 1 (C1QTNF1), mRNA.
PMAIP1	1.90	Homo sapiens phorbol-12-myristate-13-acetate-induced protein 1 (PMAIP1), mRNA.
ORF1-FL49	1.90	Homo sapiens putative nuclear protein ORF1-FL49 (ORF1-FL49), mRNA.
ITGB3	1.89	Homo sapiens integrin, beta 3 (platelet glycoprotein IIIa, antigen CD61) (ITGB3), mRNA.
PDCD1LG2	1.88	Homo sapiens programmed cell death 1 ligand 2 (PDCD1LG2), mRNA.
CCL5	1.88	Homo sapiens chemokine (C-C motif) ligand 5 (CCL5), mRNA.
ARL4C	1.88	Homo sapiens ADP-ribosylation factor-like 4C (ARL4C), mRNA.
CHST7	1.87	Homo sapiens carbohydrate (N-acetylglucosamine 6-O) sulfotransferase 7 (CHST7), mRNA.
CTSL	1.87	Homo sapiens cathepsin L (CTSL), transcript variant 1, mRNA.
C1orf24	1.86	Homo sapiens chromosome 1 open reading frame 24 (C1orf24), transcript variant 2, mRNA.
DEFB104A	1.85	Homo sapiens defensin, beta 104A (DEFB104A), mRNA.
ENC1	1.85	Homo sapiens ectodermal-neural cortex (with BTB-like domain) (ENC1), mRNA.
FLJ40504	1.85	Homo sapiens hypothetical protein FLJ40504 (FLJ40504), mRNA.
IL17R	1.83	Homo sapiens interleukin 17 receptor (IL17R), mRNA.
FLNB	1.82	Homo sapiens filamin B, beta (actin binding protein 278) (FLNB), mRNA.
SGPL1	1.82	Homo sapiens sphingosine-1-phosphate lyase 1 (SGPL1), mRNA.
SLC35D2	1.82	Homo sapiens solute carrier family 35, member D2 (SLC35D2), mRNA.
GAS2L3	1.82	Homo sapiens growth arrest-specific 2 like 3 (GAS2L3), mRNA.
ACN9	1.81	Homo sapiens ACN9 homolog (S. cerevisiae) (ACN9), mRNA.
GNE	1.81	Homo sapiens glucosamine (UDP-N-acetyl)-2-epimerase/N-acetylmannosamine kinase (GNE), mRNA.
PGM2	1.80	Homo sapiens phosphoglucomutase 2 (PGM2), mRNA.
SBDSP	1.80	Homo sapiens Shwachman-Bodian-Diamond syndrome pseudogene (SBDSP) on chromosome 7.
SERPINB7	1.79	Homo sapiens serpin peptidase inhibitor, clade B (ovalbumin), member 7 (SERPINB7), mRNA.
WNT5B	1.79	Homo sapiens wingless-type MMTV integration site family, member 5B (WNT5B), transcript variant 1, mRNA.
PRRX1	1.78	Homo sapiens paired related homeobox 1 (PRRX1), transcript variant pmx-1b, mRNA.
PRKDC	1.78	Homo sapiens protein kinase, DNA-activated, catalytic polypeptide (PRKDC), transcript variant 1, mRNA.
SERPINB2	1.78	Homo sapiens serpin peptidase inhibitor, clade B (ovalbumin), member 2 (SERPINB2), mRNA.
GLIPR1	1.77	Homo sapiens GLI pathogenesis-related 1 (glioma) (GLIPR1), mRNA.
TXNRD1	1.77	Homo sapiens thioredoxin reductase 1 (TXNRD1), transcript variant 1, mRNA.
COL6A1	1.77	Homo sapiens collagen, type VI, alpha 1 (COL6A1), mRNA.
PAPPA	1.76	Homo sapiens pregnancy-associated plasma protein A, pappalysin 1 (PAPPA), mRNA.
CAMTA1	1.76	Homo sapiens calmodulin binding transcription activator 1 (CAMTA1), mRNA.
KIAA1913	1.74	Homo sapiens KIAA1913 (KIAA1913), mRNA.

MRPS6	1.74	Homo sapiens mitochondrial ribosomal protein S6 (MRPS6), nuclear gene encoding mitochondrial protein, mRNA.
EGR1	1.73	Homo sapiens early growth response 1 (EGR1), mRNA.
TXNRD1	1.72	Homo sapiens thioredoxin reductase 1 (TXNRD1), transcript variant 4, mRNA.
LMNA	1.72	Homo sapiens lamin A/C (LMNA), transcript variant 2, mRNA.
ANXA2	1.72	Homo sapiens annexin A2 (ANXA2), transcript variant 2, mRNA.
LOC651348	1.72	PREDICTED: Homo sapiens similar to tropomyosin 3, gamma isoform 2, transcript variant 2 (LOC651348), mRNA.
CDC45L	1.72	Homo sapiens CDC45 cell division cycle 45-like (<i>S. cerevisiae</i>) (CDC45L), mRNA.
TRIB1	1.71	Homo sapiens tribbles homolog 1 (<i>Drosophila</i>) (TRIB1), mRNA.
MAP3K8	1.71	Homo sapiens mitogen-activated protein kinase kinase kinase 8 (MAP3K8), mRNA.
AK5	1.71	Homo sapiens adenylate kinase 5 (AK5), transcript variant 2, mRNA.
DLX5	1.71	Homo sapiens distal-less homeo box 5 (DLX5), mRNA.
DEFB104B	1.70	Homo sapiens defensin, beta 104B (DEFB104B), mRNA.
IL18R1	1.70	Homo sapiens interleukin 18 receptor 1 (IL18R1), mRNA.
TUBB	1.70	Homo sapiens tubulin, beta (TUBB), mRNA.
TPM3	1.69	Homo sapiens tropomyosin 3 (TPM3), transcript variant 2, mRNA.
CTNS	1.69	Homo sapiens cystinosis, nephropathic (CTNS), transcript variant 2, mRNA.
LOC57149	1.69	Homo sapiens hypothetical protein A-211C6.1 (LOC57149), mRNA.
TWISTNB	1.68	Homo sapiens TWIST neighbor (TWISTNB), mRNA.
MAP1B	1.68	Homo sapiens microtubule-associated protein 1B (MAP1B), transcript variant 2, mRNA.
FER1L3	1.68	Homo sapiens fer-1-like 3, myoferlin (<i>C. elegans</i>) (FER1L3), transcript variant 1, mRNA.
RRAS2	1.67	Homo sapiens related RAS viral (r-ras) oncogene homolog 2 (RRAS2), mRNA.
IGFBP3	1.67	Homo sapiens insulin-like growth factor binding protein 3 (IGFBP3), transcript variant 1, mRNA.
PTPN4	1.67	Homo sapiens protein tyrosine phosphatase, non-receptor type 4 (megakaryocyte) (PTPN4), mRNA.
PGRMC2	1.66	Homo sapiens progesterone receptor membrane component 2 (PGRMC2), mRNA.
DCBLD2	1.66	Homo sapiens discoidin, CUB and LCCL domain containing 2 (DCBLD2), mRNA.
DCI	1.66	Homo sapiens dodecenoyl-Coenzyme A delta isomerase (3,2 trans-enoyl-Coenzyme A isomerase) (DCI), nuclear gene encoding mitochondrial protein, mRNA.
UFD1L	1.66	Homo sapiens ubiquitin fusion degradation 1-like (UFD1L), mRNA.
PPFIBP1	1.66	Homo sapiens PTPRF interacting protein, binding protein 1 (liprin beta 1) (PPFIBP1), transcript variant 1, mRNA.
FNDC1	1.66	Homo sapiens fibronectin type III domain containing 1 (FNDC1), mRNA.
SPANXB1	1.65	Homo sapiens SPANX family, member B1 (SPANXB1), mRNA.
SLC25A4	1.65	Homo sapiens solute carrier family 25 (mitochondrial carrier; adenine nucleotide translocator), member 4 (SLC25A4), nuclear gene encoding mitochondrial protein, mRNA.
HERPUD1	1.65	Homo sapiens homocysteine-inducible, endoplasmic reticulum stress-inducible, ubiquitin-like domain member 1 (HERPUD1), transcript variant 3, mRNA.
NRP1	1.65	Homo sapiens neuropilin 1 (NRP1), transcript variant 1, mRNA.
RHBDD2	1.65	Homo sapiens rhomboid domain containing 2 (RHBDD2), mRNA.
PLOD2	1.64	Homo sapiens procollagen-lysine, 2-oxoglutarate 5-dioxygenase 2 (PLOD2), transcript variant 1, mRNA.
WDRPUH	1.64	Homo sapiens WD40-repeat protein upregulated in HCC (WDRPUH), mRNA.
LOC389286	1.64	Homo sapiens similar to FKSG62 (LOC389286), mRNA.
CANT1	1.63	Homo sapiens calcium activated nucleotidase 1 (CANT1), mRNA.
SERPINB8	1.63	Homo sapiens serpin peptidase inhibitor, clade B (ovalbumin), member 8 (SERPINB8), transcript variant 1, mRNA.
ATP2B4	1.63	Homo sapiens ATPase, Ca ⁺⁺ transporting, plasma membrane 4 (ATP2B4), transcript variant 2, mRNA.
AXL	1.63	Homo sapiens AXL receptor tyrosine kinase (AXL), transcript variant 2, mRNA.
SBDSP	1.63	Homo sapiens Shwachman-Bodian-Diamond syndrome pseudogene (SBDSP) on chromosome 7.
LOC644743	1.63	PREDICTED: Homo sapiens hypothetical protein LOC644743 (LOC644743), mRNA.
CAT	1.62	Homo sapiens catalase (CAT), mRNA.

COMT	1.62	Homo sapiens catechol-O-methyltransferase (COMT), transcript variant MB-COMT, mRNA.
AIM1	1.62	Homo sapiens absent in melanoma 1 (AIM1), mRNA.
LOC399942	1.62	PREDICTED: Homo sapiens similar to Tubulin alpha-2 chain (Alpha-tubulin 2), transcript variant 5 (LOC399942), mRNA.
DUSP5	1.62	Homo sapiens dual specificity phosphatase 5 (DUSP5), mRNA.
C3orf58	1.62	Homo sapiens chromosome 3 open reading frame 58 (C3orf58), mRNA.
LOC162073	1.62	PREDICTED: Homo sapiens hypothetical protein LOC162073, transcript variant 4 (LOC162073), mRNA.
FGG	1.61	Homo sapiens fibrinogen gamma chain (FGG), transcript variant gamma-A, mRNA.
MED8	1.61	Homo sapiens mediator of RNA polymerase II transcription, subunit 8 homolog (S. cerevisiae) (MED8), transcript variant 3, mRNA.
CTNS	1.61	Homo sapiens cystinosis, nephropathic (CTNS), transcript variant 2, mRNA.
	1.61	Homo sapiens mRNA; cDNA DKFZp686F1546 (from clone DKFZp686F1546)
PLEKHF1	1.61	Homo sapiens pleckstrin homology domain containing, family F (with FYVE domain) member 1 (PLEKHF1), mRNA.
KLF6	1.61	Homo sapiens Kruppel-like factor 6 (KLF6), transcript variant 2, mRNA.
RGS3	1.61	Homo sapiens regulator of G-protein signalling 3 (RGS3), transcript variant 5, mRNA.
		Homo sapiens serpin peptidase inhibitor, clade B (ovalbumin), member 7
SERPINB7	1.61	(SERPINB7), mRNA.
		Homo sapiens PALM2-AKAP2 protein (PALM2-AKAP2), transcript variant 2, mRNA.
PALM2-AKAP2	1.61	
STRN3	1.60	Homo sapiens striatin, calmodulin binding protein 3 (STRN3), mRNA.
NFE2	1.60	Homo sapiens nuclear factor (erythroid-derived 2), 45kDa (NFE2), mRNA.
FLJ13391	1.60	Homo sapiens transmembrane protein 166 (TMEM166), mRNA.
DTX3L	1.60	Homo sapiens deltex 3-like (Drosophila) (DTX3L), mRNA.
C18orf55	1.60	Homo sapiens chromosome 18 open reading frame 55 (C18orf55), mRNA.
		Homo sapiens fer-1-like 3, myoferlin (C. elegans) (FER1L3), transcript variant 1, mRNA.
FER1L3	1.59	
		Homo sapiens solute carrier family 7, (cationic amino acid transporter, y+ system) member 11 (SLC7A11), mRNA.
SLC7A11	1.59	
		PREDICTED: Homo sapiens meteorin, glial cell differentiation regulator-like
METRNL	1.59	(METRNL), mRNA.
PITRM1	1.59	Homo sapiens pitrilysin metallopeptidase 1 (PITRM1), mRNA.
MGLL	1.58	Homo sapiens monoglyceride lipase (MGLL), transcript variant 1, mRNA.
		Homo sapiens annexin A8 (ANXA8), mRNA. XM_931361 XM_931369 XM_931374 XM_931375 XM_931378 XM_931383 XM_931388 XM_931391 XM_931399 XM_931404 XM_931411
ANXA8L1	1.58	
DDIT3	1.58	Homo sapiens DNA-damage-inducible transcript 3 (DDIT3), mRNA.
CSF2	1.58	Homo sapiens colony stimulating factor 2 (granulocyte-macrophage) (CSF2), mRNA.
PFKP	1.58	Homo sapiens phosphofructokinase, platelet (PFKP), mRNA.
	1.58	Homo sapiens HGC.6.3 mRNA, complete cds
		Homo sapiens mitochondrial ribosomal protein S18A (MRPS18A), nuclear gene encoding mitochondrial protein, mRNA.
MRPS18A	1.57	
TUBB4Q	1.57	Homo sapiens tubulin, beta polypeptide 4, member Q (TUBB4Q), mRNA.
		Homo sapiens membrane metallo-endopeptidase (neutral endopeptidase, enkephalinase, CALLA, CD10) (MME), transcript variant 2a, mRNA.
MME	1.57	
		Homo sapiens transglutaminase 2 (C polypeptide, protein-glutamine-gamma-glutamyltransferase) (TGM2), transcript variant 1, mRNA.
TGM2	1.57	
PDZK1IP1	1.57	Homo sapiens PDZK1 interacting protein 1 (PDZK1IP1), mRNA.
		Homo sapiens actin related protein 2/3 complex, subunit 1B, 41kDa (ARPC1B), mRNA.
ARPC1B	1.57	
TUBB	1.57	Homo sapiens tubulin, beta polypeptide (TUBB), mRNA.
UXT	1.57	Homo sapiens ubiquitously-expressed transcript (UXT), transcript variant 1, mRNA.
WARS	1.57	Homo sapiens tryptophanyl-tRNA synthetase (WARS), transcript variant 4, mRNA.
ASNS	1.57	Homo sapiens asparagine synthetase (ASNS), transcript variant 1, mRNA.
CAV2	1.57	Homo sapiens caveolin 2 (CAV2), transcript variant 1, mRNA.
		Homo sapiens sperm protein associated with the nucleus, X-linked, family member A1
SPANXA1	1.56	(SPANXA1), mRNA.
HSPA1B	1.56	Homo sapiens heat shock 70kDa protein 1B (HSPA1B), mRNA.

FOXD1	1.56	Homo sapiens forkhead box D1 (FOXD1), mRNA.
ATP2B4	1.56	Homo sapiens ATPase, Ca ⁺⁺ transporting, plasma membrane 4 (ATP2B4), transcript variant 2, mRNA.
ATF3	1.56	Homo sapiens activating transcription factor 3 (ATF3), transcript variant 4, mRNA.
RHBDD2	1.56	Homo sapiens rhomboid domain containing 2 (RHBDD2), transcript variant 1, mRNA.
THBS1	1.56	Homo sapiens thrombospondin 1 (THBS1), mRNA.
C2orf18	1.56	Homo sapiens chromosome 2 open reading frame 18 (C2orf18), mRNA.
LOC653506	1.56	PREDICTED: Homo sapiens similar to meteorin, glial cell differentiation regulator-like (LOC653506), mRNA.
CARS	1.56	Homo sapiens cysteinyl-tRNA synthetase (CARS), transcript variant 4, mRNA.
LOC652846	1.55	PREDICTED: Homo sapiens similar to Annexin A8 (Annexin VIII) (Vascular anticoagulant-beta) (VAC-beta) (LOC652846), mRNA.
KRT18	1.55	Homo sapiens keratin 18 (KRT18), transcript variant 2, mRNA.
KRT16	1.55	Homo sapiens keratin 16 (focal non-epidermolytic palmoplantar keratoderma) (KRT16), mRNA.
LOC650611	1.55	PREDICTED: Homo sapiens similar to Keratin, type I cytoskeletal 16 (Cytokeratin-16) (CK-16) (Keratin-16) (K16), transcript variant 1 (LOC650611), mRNA.
PLOD2	1.55	Homo sapiens procollagen-lysine, 2-oxoglutarate 5-dioxygenase 2 (PLOD2), transcript variant 1, mRNA.
IER3	1.55	Homo sapiens immediate early response 3 (IER3), transcript variant long, mRNA.
LOC653743	1.55	PREDICTED: Homo sapiens similar to hypothetical protein DKFZp566J091 (LOC653743), mRNA.
PPID	1.55	Homo sapiens peptidylprolyl isomerase D (cyclophilin D) (PPID), mRNA.
SLC26A6	1.55	Homo sapiens solute carrier family 26, member 6 (SLC26A6), transcript variant 3, mRNA.
FLJ20366	1.55	Homo sapiens hypothetical protein FLJ20366 (FLJ20366), mRNA.
BST2	1.54	Homo sapiens bone marrow stromal cell antigen 2 (BST2), mRNA.
LRRFIP2	1.54	Homo sapiens leucine rich repeat (in FLII) interacting protein 2 (LRRFIP2), transcript variant 1, mRNA.
TMEM16K	1.54	Homo sapiens transmembrane protein 16K (TMEM16K), mRNA.
UFD1L	1.54	Homo sapiens ubiquitin fusion degradation 1 like (yeast) (UFD1L), transcript variant 2, mRNA.
SLC25A25	1.54	Homo sapiens solute carrier family 25 (mitochondrial carrier; phosphate carrier), member 25 (SLC25A25), nuclear gene encoding mitochondrial protein, transcript variant 1, mRNA.
C1orf24	1.54	Homo sapiens chromosome 1 open reading frame 24 (C1orf24), transcript variant 1, mRNA.
CAPN2	1.54	Homo sapiens calpain 2, (m/II) large subunit (CAPN2), mRNA.
ATP5G1	1.54	Homo sapiens ATP synthase, H ⁺ transporting, mitochondrial F0 complex, subunit C1 (subunit 9) (ATP5G1), nuclear gene encoding mitochondrial protein, transcript variant 1, mRNA.
LOC644330	1.54	PREDICTED: Homo sapiens similar to tropomyosin 3 isoform 2, transcript variant 2 (LOC644330), mRNA.
SAMD4A	1.53	Homo sapiens sterile alpha motif domain containing 4A (SAMD4A), mRNA.
MYO1C	1.53	Homo sapiens myosin IC (MYO1C), mRNA.
LOC51334	1.53	Homo sapiens proline rich 16 (PRR16), mRNA.
CDKN2A	1.53	Homo sapiens cyclin-dependent kinase inhibitor 2A (melanoma, p16, inhibits CDK4) (CDKN2A), transcript variant 3, mRNA.
CTTN	1.53	Homo sapiens cortactin (CTTN), transcript variant 2, mRNA.
HSD3B1	1.53	Homo sapiens hydroxy-delta-5-steroid dehydrogenase, 3 beta- and steroid delta-isomerase 1 (HSD3B1), mRNA.
RUVBL1	1.53	PREDICTED: Homo sapiens RuvB-like 1 (E. coli) (RUVBL1), mRNA.
SERPINB8	1.53	Homo sapiens serpin peptidase inhibitor, clade B (ovalbumin), member 8 (SERPINB8), transcript variant 3, mRNA.
HAPLN1	1.53	Homo sapiens hyaluronan and proteoglycan link protein 1 (HAPLN1), mRNA.
TUBB6	1.53	Homo sapiens tubulin, beta 6 (TUBB6), mRNA.
RAP1GDS1	1.52	Homo sapiens RAP1, GTP-GDP dissociation stimulator 1 (RAP1GDS1), mRNA.
SH3PXD2A	1.52	Homo sapiens SH3 and PX domains 2A (SH3PXD2A), mRNA.
SPHK1	1.52	Homo sapiens sphingosine kinase 1 (SPHK1), transcript variant 1, mRNA.

LOC650034	1.52	PREDICTED: Homo sapiens similar to uncharacterized protein family UPF0227 member RGD1359682 (LOC650034), mRNA.
ARL4	1.52	Homo sapiens ADP-ribosylation factor-like 4 (ARL4), transcript variant 1, mRNA.
DNAJB6	1.52	Homo sapiens DnaJ (Hsp40) homolog, subfamily B, member 6 (DNAJB6), transcript variant 2, mRNA.
MAP1B	1.52	Homo sapiens microtubule-associated protein 1B (MAP1B), transcript variant 1, mRNA.
PCK2	1.52	Homo sapiens phosphoenolpyruvate carboxykinase 2 (mitochondrial) (PCK2), nuclear gene encoding mitochondrial protein, transcript variant 2, mRNA.
UPP1	1.52	Homo sapiens uridine phosphorylase 1 (UPP1), transcript variant 2, mRNA.
SARS	1.51	Homo sapiens seryl-tRNA synthetase (SARS), mRNA.
MFHAS1	1.51	Homo sapiens malignant fibrous histiocytoma amplified sequence 1 (MFHAS1), mRNA.
TUBB2A	1.51	Homo sapiens tubulin, beta 2A (TUBB2A), mRNA.
KTN1	1.51	Homo sapiens kinesin 1 (kinesin receptor) (KTN1), transcript variant 4, mRNA.
MMD	1.51	Homo sapiens monocyte to macrophage differentiation-associated (MMD), mRNA.
SPRY2	1.51	Homo sapiens sprouty homolog 2 (Drosophila) (SPRY2), mRNA.
CSPG4	1.51	Homo sapiens chondroitin sulfate proteoglycan 4 (melanoma-associated) (CSPG4), mRNA.
TUBA1A	1.51	Homo sapiens tubulin, alpha 1a (TUBA1A), mRNA.
NFIL3	1.51	Homo sapiens nuclear factor, interleukin 3 regulated (NFIL3), mRNA.
LMCD1	1.51	Homo sapiens LIM and cysteine-rich domains 1 (LMCD1), mRNA.
ISG20	1.51	Homo sapiens interferon stimulated exonuclease gene 20kDa (ISG20), mRNA.
EXT1	1.51	Homo sapiens exostoses (multiple) 1 (EXT1), mRNA.
HNRPA3	1.50	Homo sapiens heterogeneous nuclear ribonucleoprotein A3 (HNRPA3), mRNA.
NBPF20	1.50	Homo sapiens neuroblastoma breakpoint family, member 20 (NBPF20), mRNA.
PLK2	1.50	Homo sapiens polo-like kinase 2 (Drosophila) (PLK2), mRNA.
LSM12	1.50	Homo sapiens LSM12 homolog (S. cerevisiae) (LSM12), mRNA.
NFS1	1.50	Homo sapiens NFS1 nitrogen fixation 1 (S. cerevisiae) (NFS1), nuclear gene encoding mitochondrial protein, transcript variant 2, mRNA.
LOC645074	1.50	PREDICTED: Homo sapiens similar to Keratin, type I cytoskeletal 16 (Cytokeratin-16) (CK-16) (Keratin-16) (K16) (LOC645074), mRNA.
IL1F8	1.50	Homo sapiens interleukin 1 family, member 8 (eta) (IL1F8), transcript variant 2, mRNA.
TRADD	1.50	Homo sapiens TNFRSF1A-associated via death domain (TRADD), transcript variant 1, mRNA.
UQCRH	-1.50	Homo sapiens ubiquinol-cytochrome c reductase hinge protein (UQCRH), mRNA.
HCG2P7	-1.50	Homo sapiens HLA complex group 2 pseudogene 7 (HCG2P7) on chromosome 6.
	-1.50	full-length cDNA clone CS0DI004YB08 of Placenta Cot 25-normalized of Homo sapiens (human)
LSM5	-1.50	Homo sapiens LSM5 homolog, U6 small nuclear RNA associated (S. cerevisiae) (LSM5), mRNA.
SAA4	-1.50	Homo sapiens serum amyloid A4, constitutive (SAA4), mRNA.
PTTG3	-1.50	Homo sapiens pituitary tumor-transforming 3 (PTTG3) on chromosome 8.
PPP3CA	-1.50	Homo sapiens protein phosphatase 3 (formerly 2B), catalytic subunit, alpha isoform (PPP3CA), mRNA.
SHROOM4	-1.50	Homo sapiens shroom family member 4 (SHROOM4), mRNA.
ASCIZ	-1.50	Homo sapiens ATM/ATR-Substrate Chk2-Interacting Zn ²⁺ -finger protein (ASCIZ), mRNA.
FEZ1	-1.50	Homo sapiens fasciculation and elongation protein zeta 1 (zygin I) (FEZ1), transcript variant 1, mRNA.
CAMK2N1	-1.51	Homo sapiens calcium/calmodulin-dependent protein kinase II inhibitor 1 (CAMK2N1), mRNA.
KIAA0391	-1.51	Homo sapiens KIAA0391 (KIAA0391), mRNA.
C14orf106	-1.51	Homo sapiens chromosome 14 open reading frame 106 (C14orf106), mRNA.
C20orf108	-1.51	Homo sapiens chromosome 20 open reading frame 108 (C20orf108), mRNA.
GNAI1	-1.51	Homo sapiens guanine nucleotide binding protein (G protein), alpha inhibiting activity polypeptide 1 (GNAI1), mRNA.
APPBP1	-1.51	Homo sapiens amyloid beta precursor protein binding protein 1 (APPBP1), transcript variant 3, mRNA.

LOC653226	-1.51	PREDICTED: Homo sapiens similar to Signal recognition particle 9 kDa protein (SRP9) (LOC653226), mRNA.
CAST1	-1.51	Homo sapiens ELKS/RAB6-interacting/CAST family member 2 (ERC2), mRNA.
MCM7	-1.51	Homo sapiens minichromosome maintenance complex component 7 (MCM7), transcript variant 2, mRNA.
OIP5	-1.51	Homo sapiens Opa interacting protein 5 (OIP5), mRNA.
LOC375449	-1.51	Homo sapiens similar to microtubule associated testis specific serine/threonine protein kinase (LOC375449), mRNA.
CDKN3	-1.51	Homo sapiens cyclin-dependent kinase inhibitor 3 (CDK2-associated dual specificity phosphatase) (CDKN3), mRNA.
CPE	-1.51	Homo sapiens carboxypeptidase E (CPE), mRNA.
DUSP19	-1.52	Homo sapiens dual specificity phosphatase 19 (DUSP19), mRNA.
SDCBP	-1.52	Homo sapiens syndecan binding protein (syntenin) (SDCBP), transcript variant 2, mRNA.
RGS17	-1.52	Homo sapiens regulator of G-protein signalling 17 (RGS17), mRNA.
CTDSP1	-1.52	Homo sapiens CTD (carboxy-terminal domain, RNA polymerase II, polypeptide A) small phosphatase 1 (CTDSP1), transcript variant 1, mRNA.
ZNF69	-1.52	Homo sapiens zinc finger protein 69 (ZNF69), mRNA.
LRP10	-1.52	Homo sapiens low density lipoprotein receptor-related protein 10 (LRP10), mRNA.
LOC399900	-1.52	Homo sapiens hypothetical gene supported by AK093779 (LOC399900), mRNA.
	-1.52	xj89b12.x1 Soares_NFL_T_GBC_S1 Homo sapiens cDNA clone IMAGE:2664383 3, mRNA sequence
NINJ1	-1.52	Homo sapiens ninjurin 1 (NINJ1), mRNA.
MBTD1	-1.52	Homo sapiens mbt domain containing 1 (MBTD1), mRNA.
MARCKS	-1.52	Homo sapiens myristoylated alanine-rich protein kinase C substrate (MARCKS), mRNA.
FAS	-1.52	Homo sapiens Fas (TNF receptor superfamily, member 6) (FAS), transcript variant 7, mRNA.
C14orf153	-1.52	Homo sapiens chromosome 14 open reading frame 153 (C14orf153), mRNA.
ATP1B3	-1.52	Homo sapiens ATPase, Na ⁺ /K ⁺ transporting, beta 3 polypeptide (ATP1B3), mRNA. XM_945518
NFKBIZ	-1.52	Homo sapiens nuclear factor of kappa light polypeptide gene enhancer in B-cells inhibitor, zeta (NFKBIZ), transcript variant 2, mRNA.
ARHGEF3	-1.53	Homo sapiens Rho guanine nucleotide exchange factor (GEF) 3 (ARHGEF3), mRNA.
THBS2	-1.53	Homo sapiens thrombospondin 2 (THBS2), mRNA.
C6orf160	-1.53	PREDICTED: Homo sapiens chromosome 6 open reading frame 160, transcript variant 4 (C6orf160), mRNA.
TBC1D9	-1.53	Homo sapiens TBC1 domain family, member 9 (with GRAM domain) (TBC1D9), mRNA.
C14orf143	-1.53	Homo sapiens chromosome 14 open reading frame 143 (C14orf143), mRNA.
FLJ21062	-1.53	Homo sapiens hypothetical protein FLJ21062 (FLJ21062), mRNA.
SSTR2	-1.53	Homo sapiens somatostatin receptor 2 (SSTR2), mRNA.
MAN1A1	-1.53	Homo sapiens mannosidase, alpha, class 1A, member 1 (MAN1A1), mRNA.
SDFR1	-1.53	Homo sapiens stromal cell derived factor receptor 1 (SDFR1), transcript variant beta, mRNA.
FUT8	-1.53	Homo sapiens fucosyltransferase 8 (alpha (1,6) fucosyltransferase) (FUT8), transcript variant 2, mRNA.
LOC642989	-1.54	PREDICTED: Homo sapiens similar to 40S ribosomal protein S25 (LOC642989), mRNA.
TRIM13	-1.54	Homo sapiens tripartite motif-containing 13 (TRIM13), transcript variant 4, mRNA.
LMO4	-1.54	Homo sapiens LIM domain only 4 (LMO4), mRNA.
APBB3	-1.54	Homo sapiens amyloid beta (A4) precursor protein-binding, family B, member 3 (APBB3), transcript variant 2, mRNA.
SMC4	-1.54	Homo sapiens structural maintenance of chromosomes 4 (SMC4), transcript variant 2, mRNA.
C2orf33	-1.54	Homo sapiens chromosome 2 open reading frame 33 (C2orf33), mRNA.
ITGB3BP	-1.54	Homo sapiens integrin beta 3 binding protein (beta3-endonexin) (ITGB3BP), mRNA.
PTGS2	-1.54	Homo sapiens prostaglandin-endoperoxide synthase 2 (prostaglandin G/H synthase and cyclooxygenase) (PTGS2), mRNA.
KIAA0564	-1.54	Homo sapiens KIAA0564 protein (KIAA0564), transcript variant 1, mRNA.

HIF1A	-1.54	Homo sapiens hypoxia-inducible factor 1, alpha subunit (basic helix-loop-helix transcription factor) (HIF1A), transcript variant 2, mRNA.
SMC2	-1.54	Homo sapiens structural maintenance of chromosomes 2 (SMC2), transcript variant 1, mRNA.
LOC441087	-1.54	Homo sapiens cDNA clone IMAGE:5277415, partial cds
RGS2	-1.55	Homo sapiens regulator of G-protein signalling 2, 24kDa (RGS2), mRNA.
YIPF5	-1.55	Homo sapiens Yip1 domain family, member 5 (YIPF5), transcript variant 2, mRNA.
MAD2L1	-1.55	Homo sapiens MAD2 mitotic arrest deficient-like 1 (yeast) (MAD2L1), mRNA. Homo sapiens proteasome (prosome, macropain) subunit, alpha type, 2 (PSMA2), mRNA.
PSMA2	-1.55	
HYPK	-1.55	Homo sapiens Huntingtin interacting protein K (HYPK), mRNA.
PNN	-1.55	Homo sapiens pinin, desmosome associated protein (PNN), mRNA.
WSB1	-1.55	Homo sapiens cDNA: FLJ21027 fis, clone CAE07110 Homo sapiens WD repeat and SOCS box-containing 1 (WSB1), transcript variant 3, mRNA.
CREB1	-1.55	Homo sapiens cAMP responsive element binding protein 1 (CREB1), transcript variant A, mRNA.
RPA3	-1.56	Homo sapiens replication protein A3, 14kDa (RPA3), mRNA.
PDPR	-1.56	Homo sapiens pyruvate dehydrogenase phosphatase regulatory subunit (PDPR), mRNA.
EID2B	-1.56	Homo sapiens EP300 interacting inhibitor of differentiation 2B (EID2B), mRNA.
PILRB	-1.56	Homo sapiens paired immunoglobulin-like type 2 receptor beta (PILRB), transcript variant 2, mRNA.
MTSS1	-1.57	Homo sapiens metastasis suppressor 1 (MTSS1), mRNA.
GIMAP8	-1.57	Homo sapiens GTPase, IMAP family member 8 (GIMAP8), mRNA.
PRICKLE1	-1.57	Homo sapiens prickle homolog 1 (Drosophila) (PRICKLE1), mRNA.
DEFB4	-1.57	Homo sapiens defensin, beta 4 (DEFB4), mRNA.
HAT1	-1.57	Homo sapiens histone acetyltransferase 1 (HAT1), transcript variant 1, mRNA.
KIAA0672	-1.57	Homo sapiens KIAA0672 gene product (KIAA0672), mRNA.
GRK5	-1.57	Homo sapiens G protein-coupled receptor kinase 5 (GRK5), mRNA.
MBD4	-1.57	Homo sapiens methyl-CpG binding domain protein 4 (MBD4), mRNA.
GYPC	-1.57	PREDICTED: Homo sapiens glycoporphin C (Gerbich blood group) (GYPC), mRNA.
SLC43A3	-1.57	Homo sapiens solute carrier family 43, member 3 (SLC43A3), mRNA.
CTSO	-1.57	Homo sapiens cathepsin O (CTSO), mRNA.
LPXN	-1.57	Homo sapiens leupaxin (LPXN), mRNA.
LOC389787	-1.57	PREDICTED: Homo sapiens similar to Translationally-controlled tumor protein (TCTP) (p23) (Histamine-releasing factor) (HRF) (Fortilin) (LOC389787), mRNA.
ALG5	-1.57	Homo sapiens asparagine-linked glycosylation 5 homolog (S. cerevisiae, dolichyl-phosphate beta-glucosyltransferase) (ALG5), mRNA.
TMED7	-1.57	Homo sapiens transmembrane emp24 protein transport domain containing 7 (TMED7), mRNA.
IL7R	-1.57	PREDICTED: Homo sapiens interleukin 7 receptor (IL7R), mRNA.
LOC654194	-1.58	PREDICTED: Homo sapiens similar to ribosomal protein S27 (LOC654194), mRNA.
KNTC2	-1.58	we85a04.x1 Soares_NFL_T_GBC_S1 Homo sapiens cDNA clone IMAGE:2347854 3, mRNA sequence Homo sapiens NDC80 homolog, kinetochore complex component (S. cerevisiae) (NDC80), mRNA.
KIAA1794	-1.59	Homo sapiens KIAA1794 (KIAA1794), mRNA.
TNIP3	-1.59	Homo sapiens TNFAIP3 interacting protein 3 (TNIP3), mRNA.
LRAP	-1.59	Homo sapiens leukocyte-derived arginine aminopeptidase (LRAP), mRNA.
PLCL2	-1.59	Homo sapiens phospholipase C-like 2 (PLCL2), mRNA.
C7orf11	-1.60	Homo sapiens chromosome 7 open reading frame 11 (C7orf11), mRNA.
CCL7	-1.60	Homo sapiens chemokine (C-C motif) ligand 7 (CCL7), mRNA.
CKAP2	-1.60	Homo sapiens cytoskeleton associated protein 2 (CKAP2), mRNA.
LOC130355	-1.60	Homo sapiens hypothetical protein LOC130355 (LOC130355), mRNA.
TGFBI	-1.60	Homo sapiens transforming growth factor, beta-induced, 68kDa (TGFBI), mRNA.
HMMR	-1.61	Homo sapiens hyaluronan-mediated motility receptor (RHAMM) (HMMR), transcript variant 1, mRNA.
GAS1	-1.61	Homo sapiens growth arrest-specific 1 (GAS1), mRNA.

CHRNA5	-1.61	Homo sapiens cholinergic receptor, nicotinic, alpha 5 (CHRNA5), mRNA.
LRRFIP1	-1.61	Homo sapiens leucine rich repeat (in FLII) interacting protein 1 (LRRFIP1), mRNA.
FLJ38451	-1.61	Homo sapiens FLJ38451 protein (FLJ38451), mRNA.
CCNB1	-1.61	Homo sapiens cyclin B1 (CCNB1), mRNA.
NEK2	-1.62	Homo sapiens NIMA (never in mitosis gene a)-related kinase 2 (NEK2), mRNA.
SUB1	-1.62	Homo sapiens SUB1 homolog (<i>S. cerevisiae</i>) (SUB1), mRNA.
LUM	-1.62	Homo sapiens lumican (LUM), mRNA.
GMNN	-1.62	Homo sapiens geminin, DNA replication inhibitor (GMNN), mRNA.
CCDC14	-1.62	Homo sapiens coiled-coil domain containing 14 (CCDC14), mRNA.
HIGD1A	-1.62	Homo sapiens HIG1 domain family, member 1A (HIGD1A), mRNA.
FAM113A	-1.62	Homo sapiens family with sequence similarity 113, member A (FAM113A), mRNA. PREDICTED: Homo sapiens similar to 40S ribosomal protein S26 (LOC649518), mRNA.
LOC649518	-1.62	mRNA.
BMP2	-1.63	Homo sapiens bone morphogenetic protein 2 (BMP2), mRNA.
GIMAP4	-1.63	Homo sapiens GTPase, IMAP family member 4 (GIMAP4), mRNA.
CXCL5	-1.63	Homo sapiens chemokine (C-X-C motif) ligand 5 (CXCL5), mRNA.
GBP2	-1.63	Homo sapiens guanylate binding protein 2, interferon-inducible (GBP2), mRNA.
DDX17	-1.64	Homo sapiens DEAD (Asp-Glu-Ala-Asp) box polypeptide 17 (DDX17), transcript variant 2, mRNA.
HRSP12	-1.64	Homo sapiens heat-responsive protein 12 (HRSP12), mRNA.
EPAS1	-1.64	Homo sapiens endothelial PAS domain protein 1 (EPAS1), mRNA.
BMP6	-1.65	Homo sapiens bone morphogenetic protein 6 (BMP6), mRNA.
GGH	-1.65	Homo sapiens gamma-glutamyl hydrolase (conjugase, folylpolyglutamate hydrolase) (GGH), mRNA.
APBB3	-1.65	Homo sapiens amyloid beta (A4) precursor protein-binding, family B, member 3 (APBB3), transcript variant 4, mRNA.
C10orf80	-1.65	Homo sapiens chromosome 10 open reading frame 80 (C10orf80), mRNA.
SLC27A1	-1.65	Homo sapiens solute carrier family 27 (fatty acid transporter), member 1 (SLC27A1), mRNA.
MCM10	-1.65	Homo sapiens minichromosome maintenance complex component 10 (MCM10), transcript variant 2, mRNA.
LIMK2	-1.65	Homo sapiens LIM domain kinase 2 (LIMK2), transcript variant 1, mRNA.
SMARCC2	-1.65	Homo sapiens SWI/SNF related, matrix associated, actin dependent regulator of chromatin, subfamily c, member 2 (SMARCC2), transcript variant 1, mRNA.
MTE	-1.65	Homo sapiens metallothionein E (MTE), mRNA.
C1orf176	-1.66	Homo sapiens chromosome 1 open reading frame 176 (C1orf176), mRNA.
FLJ23657	-1.66	Homo sapiens chromosome 4 open reading frame 26 (C4orf26), mRNA.
CD163	-1.66	Homo sapiens CD163 molecule (CD163), transcript variant 2, mRNA.
LYN	-1.66	Homo sapiens v-yes-1 Yamaguchi sarcoma viral related oncogene homolog (LYN), mRNA.
C12orf35	-1.66	Homo sapiens chromosome 12 open reading frame 35 (C12orf35), mRNA.
TP53TG3	-1.66	Homo sapiens TP53TG3 protein (TP53TG3), transcript variant 2, mRNA.
GGH	-1.66	Homo sapiens gamma-glutamyl hydrolase (conjugase, folylpolyglutamate hydrolase) (GGH), mRNA.
ZNF549	-1.66	Homo sapiens zinc finger protein 549 (ZNF549), mRNA.
HCAP-G	-1.67	Homo sapiens non-SMC condensin I complex, subunit G (NCAPG), mRNA.
PFKFB3	-1.67	Homo sapiens 6-phosphofructo-2-kinase/fructose-2,6-bisphosphatase 3 (PFKFB3), mRNA.
RAB27A	-1.67	Homo sapiens RAB27A, member RAS oncogene family (RAB27A), transcript variant 1, mRNA.
PTMA	-1.67	Homo sapiens prothymosin, alpha (gene sequence 28) (PTMA), mRNA.
NUSAP1	-1.67	Homo sapiens nucleolar and spindle associated protein 1 (NUSAP1), transcript variant 1, mRNA.
SAA1	-1.67	Homo sapiens serum amyloid A1 (SAA1), transcript variant 1, mRNA.
GLT8D2	-1.67	Homo sapiens glycosyltransferase 8 domain containing 2 (GLT8D2), mRNA.
PPM2C	-1.67	Homo sapiens protein phosphatase 2C, magnesium-dependent, catalytic subunit (PPM2C), nuclear gene encoding mitochondrial protein, mRNA.
FAM119A	-1.68	Homo sapiens family with sequence similarity 119, member A (FAM119A), mRNA.
MMP9	-1.68	Homo sapiens matrix metalloproteinase 9 (gelatinase B, 92kDa gelatinase, 92kDa type IV collagenase) (MMP9), mRNA.

SBSN	-1.68	Homo sapiens suprabasin (SBSN), mRNA.
MMP12	-1.69	Homo sapiens matrix metalloproteinase 12 (macrophage elastase) (MMP12), mRNA.
	-1.69	MR1-GN0172-061100-005-h03 GN0172 Homo sapiens cDNA, mRNA sequence
STC1	-1.69	Homo sapiens stanniocalcin 1 (STC1), mRNA.
		Homo sapiens tumor necrosis factor receptor superfamily, member 1B (TNFRSF1B), mRNA.
TNFRSF1B	-1.69	
HRSP12	-1.69	Homo sapiens heat-responsive protein 12 (HRSP12), mRNA.
MYLK	-1.70	Homo sapiens myosin, light chain kinase (MYLK), transcript variant 2, mRNA.
OLFML3	-1.70	Homo sapiens olfactomedin-like 3 (OLFML3), mRNA.
TNFAIP6	-1.70	Homo sapiens tumor necrosis factor, alpha-induced protein 6 (TNFAIP6), mRNA.
MYLIP	-1.71	Homo sapiens myosin regulatory light chain interacting protein (MYLIP), mRNA.
ST3GAL6	-1.71	Homo sapiens ST3 beta-galactoside alpha-2,3-sialyltransferase 6 (ST3GAL6), mRNA.
		Homo sapiens GTP cyclohydrolase 1 (dopa-responsive dystonia) (GCH1), transcript variant 2, mRNA.
GCH1	-1.71	
		Homo sapiens endothelial differentiation, lysophosphatidic acid G-protein-coupled receptor, 2 (EDG2), transcript variant 1, mRNA.
EDG2	-1.71	
KLHL24	-1.71	Homo sapiens kelch-like 24 (Drosophila) (KLHL24), mRNA.
KIF11	-1.71	Homo sapiens kinesin family member 11 (KIF11), mRNA.
HMGB2	-1.71	Homo sapiens high-mobility group box 2 (HMGB2), mRNA.
FKBP14	-1.72	Homo sapiens FK506 binding protein 14, 22 kDa (FKBP14), mRNA.
		Homo sapiens synovial sarcoma translocation, chromosome 18 (SS18), transcript variant 2, mRNA.
SS18	-1.72	
RAD51AP1	-1.72	Homo sapiens RAD51 associated protein 1 (RAD51AP1), mRNA.
		Homo sapiens oculocutaneous albinism II (pink-eye dilution homolog, mouse) (OCA2), mRNA.
OCA2	-1.72	
GRIPAP1	-1.73	Homo sapiens GRIP1 associated protein 1 (GRIPAP1), transcript variant 2, mRNA.
ORM2	-1.73	Homo sapiens orosomucoid 2 (ORM2), mRNA.
SAA1	-1.73	Homo sapiens serum amyloid A1 (SAA1), transcript variant 2, mRNA.
		Homo sapiens protein tyrosine phosphatase-like (proline instead of catalytic arginine), member b (PTPLB), mRNA.
PTPLB	-1.74	
KCNK1	-1.74	Homo sapiens potassium channel, subfamily K, member 1 (KCNK1), mRNA.
FAM20C	-1.74	Homo sapiens family with sequence similarity 20, member C (FAM20C), mRNA.
FLJ11259	-1.74	Homo sapiens hypothetical protein FLJ11259 (FLJ11259), mRNA.
		Homo sapiens solute carrier family 30 (zinc transporter), member 3 (SLC30A3), mRNA.
SLC30A3	-1.74	
		Homo sapiens asp (abnormal spindle)-like, microcephaly associated (Drosophila) (ASPM), mRNA.
ASPM	-1.75	
		Homo sapiens chromosome 4 open reading frame 18 (C4orf18), transcript variant 2, mRNA.
C4orf18	-1.75	
CD82	-1.76	Homo sapiens CD82 molecule (CD82), transcript variant 2, mRNA.
TNFAIP3	-1.76	Homo sapiens tumor necrosis factor, alpha-induced protein 3 (TNFAIP3), mRNA.
C12orf35	-1.76	Homo sapiens chromosome 12 open reading frame 35 (C12orf35), mRNA.
		Homo sapiens signal transducer and activator of transcription 1, 91kDa (STAT1), transcript variant beta, mRNA.
STAT1	-1.76	
		Homo sapiens TSC22 domain family, member 1 (TSC22D1), transcript variant 1, mRNA.
TSC22D1	-1.76	
RPLP1	-1.77	Homo sapiens ribosomal protein, large, P1 (RPLP1), transcript variant 1, mRNA.
		Homo sapiens LSM3 homolog, U6 small nuclear RNA associated (S. cerevisiae) (LSM3), mRNA.
LSM3	-1.77	
MMP12	-1.77	Homo sapiens matrix metalloproteinase 12 (macrophage elastase) (MMP12), mRNA.
ZNF503	-1.77	Homo sapiens zinc finger protein 503 (ZNF503), mRNA.
		Homo sapiens solute carrier family 25, member 37 (SLC25A37), transcript variant 1, mRNA.
SLC25A37	-1.78	
		Homo sapiens solute carrier family 39 (zinc transporter), member 8 (SLC39A8), mRNA.
SLC39A8	-1.78	
FLJ20701	-1.79	Homo sapiens phosphotyrosine interaction domain containing 1 (PID1), mRNA.
		Homo sapiens paroxysmal nonkinesigenic dyskinesia (PNKD), transcript variant 2, mRNA.
PNKD	-1.79	
GABARAPL2	-1.80	Homo sapiens GABA(A) receptor-associated protein-like 2 (GABARAPL2), mRNA.
FAM9C	-1.80	Homo sapiens family with sequence similarity 9, member C (FAM9C), mRNA.

STOM	-1.81	Homo sapiens stomatin (STOM), transcript variant 1, mRNA.
VGF	-1.82	Homo sapiens VGF nerve growth factor inducible (VGF), mRNA.
DSCR1L1	-1.82	Homo sapiens regulator of calcineurin 2 (RCAN2), mRNA.
ADD3	-1.82	Homo sapiens adducin 3 (gamma) (ADD3), transcript variant 1, mRNA.
MGC17330	-1.83	Homo sapiens phosphoinositide-3-kinase interacting protein 1 (PIK3IP1), mRNA.
TDP1	-1.83	Homo sapiens tyrosyl-DNA phosphodiesterase 1 (TDP1), transcript variant 1, mRNA.
PABPC1	-1.83	Homo sapiens poly(A) binding protein, cytoplasmic 1 (PABPC1), mRNA.
		Homo sapiens chemokine (C-X-C motif) ligand 13 (B-cell chemoattractant) (CXCL13), mRNA.
CXCL13	-1.84	
GJA1	-1.85	Homo sapiens gap junction protein, alpha 1, 43kDa (connexin 43) (GJA1), mRNA.
PDGFC	-1.86	Homo sapiens platelet derived growth factor C (PDGFC), mRNA.
VNN2	-1.86	Homo sapiens vanin 2 (VNN2), transcript variant 1, mRNA.
GDF15	-1.87	Homo sapiens growth differentiation factor 15 (GDF15), mRNA.
ANTXR1	-1.87	Homo sapiens anthrax toxin receptor 1 (ANTXR1), transcript variant 1, mRNA.
		xr14b10.x1 NCI_CGAP_Lu28 Homo sapiens cDNA clone IMAGE:2760091 3, mRNA sequence
	-1.88	
GAS1	-1.88	Homo sapiens growth arrest-specific 1 (GAS1), mRNA.
ANGPTL2	-1.91	Homo sapiens angiopoietin-like 2 (ANGPTL2), mRNA.
HCK	-1.91	Homo sapiens hemopoietic cell kinase (HCK), mRNA.
		Homo sapiens solute carrier family 1 (glial high affinity glutamate transporter), member 3 (SLC1A3), mRNA.
SLC1A3	-1.92	
C3orf34	-1.93	Homo sapiens chromosome 3 open reading frame 34 (C3orf34), mRNA.
ZNF91	-1.94	Homo sapiens zinc finger protein 91 (HPF7, HTF10) (ZNF91), mRNA.
		Homo sapiens hydroxysteroid (11-beta) dehydrogenase 1 (HSD11B1), transcript variant 2, mRNA.
HSD11B1	-1.94	
FCAR	-1.95	Homo sapiens Fc fragment of IgA, receptor for (FCAR), transcript variant 9, mRNA.
CA2	-1.96	Homo sapiens carbonic anhydrase II (CA2), mRNA.
MT1E	-1.96	Homo sapiens metallothionein 1E (MT1E), mRNA.
SLPI	-1.97	Homo sapiens secretory leukocyte peptidase inhibitor (SLPI), mRNA.
EFNA1	-1.97	Homo sapiens ephrin-A1 (EFNA1), transcript variant 1, mRNA.
		Homo sapiens sema domain, immunoglobulin domain (Ig), short basic domain, secreted, (semaphorin) 3E (SEMA3E), mRNA.
SEMA3E	-2.00	
		Homo sapiens v-maf musculoaponeurotic fibrosarcoma oncogene homolog B (avian) (MAFB), mRNA.
MAFB	-2.00	
HEY1	-2.00	Homo sapiens hairy/enhancer-of-split related with YRPW motif 1 (HEY1), mRNA.
CMKOR1	-2.01	Homo sapiens chemokine orphan receptor 1 (CMKOR1), mRNA.
LAMB1	-2.01	Homo sapiens laminin, beta 1 (LAMB1), mRNA.
		Homo sapiens phosphatidic acid phosphatase type 2B (PPAP2B), transcript variant 1, mRNA.
PPAP2B	-2.02	
DUSP23	-2.06	Homo sapiens dual specificity phosphatase 23 (DUSP23), mRNA.
KIAA1754	-2.07	Homo sapiens KIAA1754 (KIAA1754), mRNA.
MRGPRX3	-2.08	Homo sapiens MAS-related GPR, member X3 (MRGPRX3), mRNA.
		Homo sapiens nuclear factor I/X (CCAAT-binding transcription factor) (NFIX), mRNA.
NFIX	-2.09	
		Homo sapiens WNT1 inducible signaling pathway protein 1 (WISP1), transcript variant 1, mRNA.
WISP1	-2.13	
		Homo sapiens B-cell CLL/lymphoma 6 (zinc finger protein 51) (BCL6), transcript variant 1, mRNA.
BCL6	-2.13	
SNX10	-2.13	Homo sapiens sorting nexin 10 (SNX10), mRNA.
MMP8	-2.13	Homo sapiens matrix metalloproteinase 8 (neutrophil collagenase) (MMP8), mRNA.
		Homo sapiens hydroxysteroid (11-beta) dehydrogenase 1 (HSD11B1), transcript variant 1, mRNA.
HSD11B1	-2.17	
CD163	-2.20	Homo sapiens CD163 molecule (CD163), transcript variant 2, mRNA.
MT1G	-2.20	Homo sapiens metallothionein 1G (MT1G), mRNA.
		Homo sapiens acyl-CoA synthetase long-chain family member 4 (ACSL4), transcript variant 1, mRNA.
ACSL4	-2.23	
LOC441019	-2.23	PREDICTED: Homo sapiens hypothetical LOC441019 (LOC441019), mRNA.
OLFM1	-2.26	Homo sapiens olfactomedin 1 (OLFM1), transcript variant 1, mRNA.
MT1H	-2.26	Homo sapiens metallothionein 1H (MT1H), mRNA.

KCNMB4	-2.29	Homo sapiens potassium large conductance calcium-activated channel, subfamily M, beta member 4 (KCNMB4), mRNA.
SAA2	-2.40	Homo sapiens serum amyloid A2 (SAA2), mRNA.
PI3	-2.40	Homo sapiens peptidase inhibitor 3, skin-derived (SKALP) (PI3), mRNA.
MT1F	-2.40	Homo sapiens metallothionein 1F (MT1F), mRNA.
DNER	-2.44	Homo sapiens delta-notch-like EGF repeat-containing transmembrane (DNER), mRNA.
CA2	-2.44	Homo sapiens carbonic anhydrase II (CA2), mRNA.
HSD11B1	-2.60	Homo sapiens hydroxysteroid (11-beta) dehydrogenase 1 (HSD11B1), transcript variant 2, mRNA.
MMP13	-2.63	Homo sapiens matrix metalloproteinase 13 (collagenase 3) (MMP13), mRNA.
CXCL5	-2.82	Homo sapiens chemokine (C-X-C motif) ligand 5 (CXCL5), mRNA.
LOC654103	-2.85	PREDICTED: Homo sapiens similar to solute carrier family 25, member 37 (LOC654103), mRNA.
LOC653778	-2.97	PREDICTED: Homo sapiens similar to solute carrier family 25, member 37 (LOC653778), mRNA.
MT1B	-3.15	Homo sapiens metallothionein 1B (MT1B), mRNA.
COL10A1	-3.25	Homo sapiens collagen, type X, alpha 1 (Schmid metaphyseal chondrodysplasia) (COL10A1), mRNA.
S100A8	-3.80	Homo sapiens S100 calcium binding protein A8 (S100A8), mRNA.
LBP	-3.93	Homo sapiens lipopolysaccharide binding protein (LBP), mRNA.
CCL20	-4.17	Homo sapiens chemokine (C-C motif) ligand 20 (CCL20), mRNA.
ORM1	-4.43	Homo sapiens orosomucoid 1 (ORM1), mRNA.
S100A9	-4.82	Homo sapiens S100 calcium binding protein A9 (calgranulin B) (S100A9), mRNA.
CRP	-8.97	Homo sapiens C-reactive protein, pentraxin-related (CRP), mRNA.

- Abramson, S.B. and A. Amin. 2002. Blocking the effects of IL-1 in rheumatoid arthritis protects bone and cartilage. *Rheumatology* **41**: 972-980.
- Abramson, S.B. and M. Attur. 2009. Developments in the scientific understanding of osteoarthritis. *Arthritis Res Ther* **11**: 227.
- Akhtar, N., Z. Rasheed, S. Ramamurthy, A.N. Anbazhagan, F.R. Voss and T.M. Haqqi. MicroRNA-27b regulates the expression of matrix metalloproteinase 13 in human osteoarthritis chondrocytes. 2010. *Arthritis Rheum* **62**: 1361-71.
- Aigner, T. and J. Dudhia. 1997. Phenotypic modulation of chondrocytes as a potential therapeutic target in osteoarthritis: a hypothesis. *Ann Rheum Dis* **56**: 287-91.
- Aigner, T., K. Fundel, J. Saas, P.M. Gebhard, J. Haag, T. Weiss, A. Zien, F. Obermayr, R. Zimmer, and E. Bartnik. 2006. Large-scale gene expression profiling reveals major pathogenetic pathways of cartilage degeneration in osteoarthritis. *Arthritis Rheum* **54**: 3533-44.
- Aman, M.J., T.D. Lamkin, H. Okada, T. Kurosaki, and K.S. Ravichandran. 1998. The inositol phosphatase SHIP inhibits Akt/PKB activation in B cells. *J Biol Chem* **273**: 33922-8.
- Andersson, A.K., C. Li, and F.M. Brennan. 2008. Recent developments in the immunobiology of rheumatoid arthritis. *Arthritis Res Ther* **10**: 204.
- Appleton, C.T., V. Pitelka, J. Henry, and F. Beier. 2007. Global analyses of gene expression in early experimental osteoarthritis. *Arthritis Rheum* **56**: 1854-68.
- Arend, W.P. and J.M. Dayer. 1990. Cytokines and cytokine inhibitors or antagonists in rheumatoid arthritis. *Arthritis Rheum* **33**: 305-15.
- Arend, W.P., M. Malyak, M.F. Smith, Jr., T.D. Whisenand, J.L. Slack, J.E. Sims, J.G. Giri, and S.K. Dower. 1994. Binding of IL-1 alpha, IL-1 beta, and IL-1 receptor antagonist by soluble IL-1 receptors and levels of soluble IL-1 receptors in synovial fluids. *J Immunol* **153**: 4766-74.
- Arthritis Research Campaign. 2002. *Arthritis Statistics*. Available at: <http://www.arc.org.uk/arthritisinfo/astats.asp> last accessed: 24 May 2007.
- Backer, J.M., M.G. Myers, Jr., S.E. Shoelson, D.J. Chin, X.J. Sun, M. Miralpeix, P. Hu, B. Margolis, E.Y. Skolnik, J. Schlessinger, and et al. 1992. Phosphatidylinositol 3'-kinase is activated by association with IRS-1 during insulin stimulation. *Embo J* **11**: 3469-79.
- Bansal, G., K.M. Druey, Z. Zie. 2007. R4 RGS proteins: regulation of G-protein signaling and beyond. *Pharmacol Ther* **116**: 473-95.
- Barksby, H.E., W. Hui, and I. Wappler. 2006. Interleukin-1 in combination with oncostatin M up-regulates multiple genes in chondrocytes *Arthritis and Rheumatism* **54**: 540-550.
- Barre, P.E., F. Redini, K. Boumediene, C. Vielpeau, and J.P. Pujol. 2000. Semiquantitative reverse transcription-polymerase chain reaction analysis of syndecan-1 and -4 messages in cartilage and cultured chondrocytes from osteoarthritic joints. *Osteoarthritis Cartilage* **8**: 34-43.
- Barrett, A.J. 1980. The many forms and functions of cellular proteinases. *Fed Proc* **39**: 9-14.
- Bigg, H. and A.D. Rowan. 2001. The inhibition of metalloproteinases as a therapeutic target in rheumatoid arthritis and osteoarthritis *Curr Opin Pharmacol* **1**: 314-20.
- Black, R.A., S.R. Kronheim, M. Cantrell, M.C. Deeley, C.J. March, K.S. Prickett, J. Wignall, P.J. Conlon, D. Cosman, T.P. Hopp, and et al. 1988. Generation of

- biologically active interleukin-1 beta by proteolytic cleavage of the inactive precursor. *J Biol Chem* **263**: 9437-42.
- Blanchard, C., S. Durual, M. Estienne, S. Emami, S. Vasseur, and J.C. Cuber. 2005. Eotaxin-3/CCL26 gene expression in intestinal epithelial cells is up-regulated by interleukin-4 and interleukin-13 via the signal transducer and activator of transcription 6. *Int J Biochem Cell Biol* **37**: 2559-73.
- Bogdan, C., Y. Vodovotz, J. Paik, Q. Xie, and C. Nathan. 1994. Mechanism of suppression of nitric oxide synthase expression by interleukin-4 in primay mouse macrophages. *Journal of Leukocyte Biology* **55**: 227-233.
- Bonder, C.S., H.L. Dickensheets, J.J. Finlay-Jones, R.P. Donnelly, and P.H. Hart. 1998. Involvement of the IL-2 receptor gamma-chain (gammac) in the control by IL-4 of human monocyte and macrophage proinflammatory mediator production. *J Immunol* **160**: 4048-56.
- Borden, P., D. Solymar, A. Sucharczuk, B. Lindman, P. Cannon, and R.A. Heller. 1996. Cytokine control of interstitial collagenase and collagenase-3 gene expression in human chondrocytes. *J Biol Chem* **271**: 23577-81.
- Bower, K.E., J.M. Fritz, and K.L. McGuire. 2004. Transcriptional repression of MMP-1 by p21SNFT and reduced in vitro invasiveness of hepatocarcinoma cells. *Oncogene* **23**: 8805-14.
- Boyd, J.H., B. Kan, H. Roberts, Y. Wang, and K.R. Walley. 2008. S100A8 and S100A9 mediate endotoxin-induced cardiomyocyte dysfunction via the receptor for advanced glycation end products. *Circ Res* **102**: 1239-46.
- Brew, K., D. Dinakarpanian, and H. Nagase. 2000. Tissue inhibitors of metalloproteinases: evolution, structure and function. *Biochim Biophys Acta* **1477**: 267-83.
- Brew, K. and H. Nagase. 2010. The tissue inhibitors of metalloproteinases (TIMPs): an ancient family with structural and functional diversity. *Biochim Biophys Acta* **1803**: 55-71.
- Brinckerhoff, C.E., J.L. Rutter, and U. Benbow. 2000. Interstitial collagenases as markers of tumor progression. *Clin Cancer Res* **6**: 4823-30.
- British Medical Association and Royal Pharmaceutical Society of Great Britain. 2005. *British National Formulary*. BMJ Publishing Group Ltd.
- Burrage, P.S., K.S. Mix, and C.E. Brinckerhoff. 2006. Matrix metalloproteinases: role in arthritis. *Front Biosci* **11**: 529-43.
- Bush, K.A., J.S. Walker, C.S. Lee, and B.W. Kirkham. 2001. Cytokine expression and synovial pathology in the initiation and spontaneous resolution phases of adjuvant arthritis: interleukin-17 expression is upregulated in early disease. *Clin Exp Immunol* **123**: 487-95.
- Camps, M., T. Ruckle, H. Ji, V. Ardisson, F. Rintelen, J. Shaw, C. Ferrandi, C. Chabert, C. Gillieron, B. Francon, T. Martin, D. Gretener, D. Perrin, D. Leroy, P.A. Vitte, E. Hirsch, M.P. Wymann, R. Cirillo, M.K. Schwarz, and C. Rommel. 2005. Blockade of PI3Kgamma suppresses joint inflammation and damage in mouse models of rheumatoid arthritis. *Nat Med* **11**: 936-43.
- Carey, G.B., E. Semenova, X. Qi, and A.D. Keegan. 2007. IL-4 protects the B-cell lymphoma cell line CH31 from anti-IgM-induced growth arrest and apoptosis: contribution of the PI-3 kinase/AKT pathway. *Cell Res* **17**: 942-55.
- Carnero, A. 2010. The PKB/AKT pathway in cancer. *Curr Pharm Des* **16**: 34-44.

- Cawston, T.E. 1998. Matrix metalloproteinases and TIMPs: properties and implications for the rheumatic diseases. *Molecular Medicine Today* **4**: 130-137.
- Cawston, T.E., V.A. Curry, and C.A. Summers. 1998. The role of oncostatin M in animal and human connective tissue collagen turnover and its localisation within the rheumatoid joint *Arthritis and Rheumatism* **41**: 1760-1771.
- Cawston, T.E., A.J. Ellis, H. Bigg, and V. Curry. 1996. Interleukin-4 blocks the release of collagen fragments from bovine cartilage treated with cytokines. *Biochim Biophys Acta* **1314**: 226-32.
- Cawston, T.E., A.J. Ellis, G. Humin, and E. Lean. 1995. Interleukin-1 and oncostatin M in combination promote the release of collagen fragments from bovine cartilage treated with cytokines. *Biochim Biophys Res Commun* **215**: 377-85.
- Cawston, T.E. and D.A. Young. 2010. Proteinases involved in matrix turnover during cartilage and bone breakdown. *Cell Tissue Res* **339**: 221-35.
- Chae, S.C., Y.R. Park, S.C. Shim, I.K. Lee, and H.T. Chung. 2005. Eotaxin-3 gene polymorphisms are associated with rheumatoid arthritis in a Korean population. *Hum Immunol* **66**: 314-20.
- Chen, W., M.O. Daines, and G.K. Hershey. 2004. Methylation of STAT6 modulates STAT6 phosphorylation, nuclear translocation, and DNA-binding activity. *J Immunol* **172**: 6744-50.
- Chen, X.H., B.K. Patel, L.M. Wang, M. Frankel, N. Ellmore, R.A. Flavell, W.J. LaRochelle, and J.H. Pierce. 1997. Jak1 expression is required for mediating interleukin-4-induced tyrosine phosphorylation of insulin receptor substrate and Stat6 signaling molecules. *J Biol Chem* **272**: 6556-60.
- Cheung, K.S., K. Hashimoto, N. Yamada, and H.I. Roach. 2008. Expression of ADAMTS-4 by chondrocytes in the surface zone of human osteoarthritic cartilage is regulated by epigenetic DNA de-methylation. *Rheumatol Int* **29**: 525-34.
- Chicoine, E., P.O. Esteve, O. Robledo, C. Van Themsche, E.F. Potworowski, and Y. St-Pierre. 2002. Evidence for the role of promoter methylation in the regulation of MMP-9 gene expression. *Biochem Biophys Res Commun* **297**: 765-72.
- Chizzolini, C., R. Rezzonico, C. De Luca, D. Burger, and J.M. Dayer. 2000. Th2 cell membrane factors in association with IL-4 enhance matrix metalloproteinase-1 (MMP-1) while decreasing MMP-9 production by granulocyte-macrophage colony-stimulating factor-differentiated human monocytes. *J Immunol* **164**: 5952-60.
- Chomczynski, P. and N. Sacchi. 2006. The single-step method of RNA isolation by acid guanidinium thiocyanate-phenol-chloroform extraction: twenty-something years on. *Nat Protoc* **1**: 581-5.
- Chu, C.Q., M. Field, M. Feldmann, and R.N. Maini. 1991. Localization of tumor necrosis factor alpha in synovial tissues and at the cartilage-pannus junction in patients with rheumatoid arthritis. *Arthritis Rheum* **34**: 1125-32.
- Chung, L., D. Dinakarpanian, N. Yoshida, J.L. Lauer-Fields, G.B. Fields, R. Visse, and H. Nagase. 2004. Collagenase unwinds triple-helical collagen prior to peptide bond hydrolysis. *Embo J* **23**: 3020-30.
- Clark, I.M. and A.E. Parker. 2003. Metalloproteinases: their role in arthritis and potential as therapeutic targets. *Expert Opin. Ther. Targets* **7**: 19-34.
- Cleaver, C.S. 2000. The role of interleukin-4 and interleukin-13 in the prevention of cartilage breakdown. In *Musculoskeletal Research Group*. Newcastle University, Newcastle-upon-Tyne.

- Cleaver, C.S., A.D. Rowan, and T.E. Cawston. 2001. Interleukin 13 blocks the release of collagen from bovine nasal cartilage treated with proinflammatory cytokines. *Ann Rheum Dis* **60**: 150-157.
- Colotta, F., S.K. Dower, J.E. Sims, and A. Mantovani. 1994. The type II 'decoy' receptor: a novel regulatory pathway for interleukin 1. *Immunol Today* **15**: 562-6.
- Colotta, F., F. Re, M. Muzio, R. Bertini, N. Polentarutti, M. Sironi, J.G. Giri, S.K. Dower, J.E. Sims, and A. Mantovani. 1993. Interleukin-1 type II receptor: a decoy target for IL-1 that is regulated by IL-4. *Science* **261**: 472-5.
- Cope, A.P., D.L. Gibbons, D. Aderka, B.M. Foxwell, D. Wallach, R.N. Maini, M. Feldmann, and F.M. Brennan. 1993. Differential regulation of tumour necrosis factor receptors (TNF-R) by IL-4; upregulation of P55 and P75 TNF-R on synovial joint mononuclear cells. *Cytokine* **5**: 205-12.
- Cravero, J.D., C.S. Carlson, H.J. Im, R.R. Yammani, D. Long, and R.F. Loeser. 2009. Increased expression of the Akt/PKB inhibitor TRB3 in osteoarthritic chondrocytes inhibits insulin-like growth factor 1-mediated cell survival and proteoglycan synthesis. *Arthritis Rheum* **60**: 492-500.
- Cremer, M.A., E.F. Rosloniec, and A.H. Kang. 1998. The cartilage collagens: a review of their structure, organization, and role in the pathogenesis of experimental arthritis in animals and in human rheumatic disease. *J Mol Med* **76**: 275-88.
- Cush, J.J., J.B. Splawski, R. Thomas, J.E. McFarlin, H. Schulze-Koops, L.S. Davis, K. Fujita, and P.E. Lipsky. 1995. Elevated interleukin-10 levels in patients with rheumatoid arthritis. *Arthritis Rheum* **38**: 96-104.
- Dahl, C. and P. Guldberg. 2003. DNA methylation analysis techniques. *Biogerontology* **4**: 233-50.
- Dayer, J.M., B. Beutler, and A. Cerami. 1985. Cachectin/tumor necrosis factor stimulates collagenase and prostaglandin E2 production by human synovial cells and dermal fibroblasts. *J Exp Med* **162**: 2163-8.
- de Waal Malefyt, R., J. Abrams, B. Bennett, C.G. Figdor, and J.E. de Vries. 1991. Interleukin 10(IL-10) inhibits cytokine synthesis by human monocytes: an autoregulatory role of IL-10 produced by monocytes. *J Exp Med* **174**: 1209-20.
- Decock, J., R. Paridaens, and S. Ye. 2008. Genetic polymorphisms of matrix metalloproteinases in lung, breast and colorectal cancer. *Clin Genet* **73**: 197-211.
- DeKruyff, R.H., Y. Fang, S.F. Wolf, and D.T. Umetsu. 1995. IL-12 inhibits IL-4 synthesis in keyhole limpet hemocyanin-primed CD4+ T cells through an effect on antigen-presenting cells. *J Immunol* **154**: 2578-87.
- Deng, J., C.H. James, L. Patel, A. Smith, K.G. Burnand, H. Rahmoune, J.R. Lamb, and B. Davis. 2009. Human tribbles homologue 2 is expressed in unstable regions of carotid plaques and regulates macrophage IL-10 in vitro. *Clin Sci (Lond)* **116**: 241-8.
- Dingle, J.T., D.P. Page Thomas, and B. Hazleman. 1987. The role of cytokines in arthritic diseases: in vitro and in vivo measurements of cartilage degradation. *Int J Tissue React* **9**: 349-54.
- Doble, B.W. and J.R. Woodgett. 2003. GSK-3: tricks of the trade for a multi-tasking kinase. *J Cell Sci* **116**: 1175-86.
- Doi, H., K. Nishida, M. Yorimitsu, T. Komiyama, Y. Kadota, T. Tetsunaga, A. Yoshida, S. Kubota, M. Takigawa, and T. Ozaki. 2008. Interleukin-4 downregulates the cyclic tensile stress-induced matrix metalloproteinases-13 and cathepsin B expression by rat normal chondrocytes. *Acta Med Okayama* **62**: 119-26.

- Du, K., S. Herzig, R.N. Kulkarni, and M. Montminy. 2003. TRB3: a tribbles homolog that inhibits Akt/PKB activation by insulin in liver. *Science* **300**: 1574-7.
- Du, P., W.A. Kibbe, and S.M. Lin. 2008. lumi: a pipeline for processing Illumina microarray. *Bioinformatics* **24**: 1547-8.
- Eder, K., H. Guan, H.Y. Sung, J. Ward, A. Angyal, M. Janas, G. Sarmay, E. Duda, M. Turner, S.K. Dower, S.E. Francis, D.C. Crossman, and E. Kiss-Toth. 2008. Tribbles-2 is a novel regulator of inflammatory activation of monocytes. *Int Immunol* **20**: 1543-50.
- El Mabrouk, M., H.Y. Qureshi, W.Q. Li, J. Sylvester, and M. Zafarullah. 2008. Interleukin-4 antagonizes oncostatin M and transforming growth factor beta-induced responses in articular chondrocytes. *J Cell Biochem* **103**: 588-97.
- Eleswarapu, S.V., N.D. Leipzig, and K.A. Athanasiou. 2007. Gene expression of single articular chondrocytes. *Cell Tissue Res* **327**: 43-54.
- Ellis, A.J., V.A. Curry, E.K. Powell, and T.E. Cawston. 1994. The prevention of collagen breakdown in bovine nasal cartilage by TIMP, TIMP-2 and a low molecular weight synthetic inhibitor. *Biochem Biophys Res Commun* **201**: 94-101.
- English, W.R., B. Holtz, G. Vogt, V. Knauper, and G. Murphy. 2001. Characterization of the role of the "MT-loop": an eight-amino acid insertion specific to progelatinase A (MMP2) activating membrane-type matrix metalloproteinases. *J Biol Chem* **276**: 42018-26.
- Felson, D.T. 2006. Clinical practice. Osteoarthritis of the knee. *N Engl J Med* **354**: 841-8.
- Felson, D.T., R.C. Lawrence, P.A. Dieppe, R. Hirsch, C.G. Helmick, J.M. Jordan, R.S. Kington, N.E. Lane, M.C. Nevitt, Y. Zhang, M. Sowers, T. McAlindon, T.D. Spector, A.R. Poole, S.Z. Yanovski, G. Ateshian, L. Sharma, J.A. Buckwalter, K.D. Brandt, and J.F. Fries. 2000. Osteoarthritis: new insights. Part 1: the disease and its risk factors. *Ann Intern Med* **133**: 635-46.
- Fontana, A., H. Hengartner, E. Weber, K. Fehr, P.J. Grob, and G. Cohen. 1982. Interleukin 1 activity in the synovial fluid of patients with rheumatoid arthritis. *Rheumatol Int* **2**: 49-53.
- Franke, T.F. 2008. PI3K/Akt: getting it right matters. *Oncogene* **27**: 6473-88.
- Freije, J.M., I. Diez-Itza, M. Balbin, L.M. Sanchez, R. Blasco, J. Tolivia, and C. Lopez-Otin. 1994. Molecular cloning and expression of collagenase-3, a novel human matrix metalloproteinase produced by breast carcinomas. *J Biol Chem* **269**: 16766-73.
- Fridman, R., M. Toth, D. Pena, and S. Mobashery. 1995. Activation of progelatinase B (MMP-9) by gelatinase A (MMP-2). *Cancer Res* **55**: 2548-55.
- Frommer, M., L.E. McDonald, D.S. Millar, C.M. Collis, F. Watt, G.W. Grigg, P.L. Molloy, and C.L. Paul. 1992. A genomic sequencing protocol that yields a positive display of 5-methylcytosine residues in individual DNA strands. *Proc Natl Acad Sci U S A* **89**: 1827-31.
- Fujita, T., Y. Azuma, R. Fukuyama, Y. Hattori, C. Yoshida, M. Koida, K. Ogita, and T. Komori. 2004. Runx2 induces osteoblast and chondrocyte differentiation and enhances their migration by coupling with PI3K-Akt signaling. *J Cell Biol* **166**: 85-95.
- Fukui, N., Y. Miyamoto, M. Nakajima, Y. Ikeda, A. Hikita, H. Furukawa, H. Mitomi, N. Tanaka, Y. Katsuragawa, S. Yamamoto, M. Sawabe, T. Juji, T. Mori, R. Suzuki, and S. Ikegawa. 2008. Zonal gene expression of chondrocytes in osteoarthritic cartilage. *Arthritis Rheum* **58**: 3843-53.

- Gebauer, M., J. Saas, F. Sohler, J. Haag, S. Soder, M. Pieper, E. Bartnik, J. Beninga, R. Zimmer, and T. Aigner. 2005. Comparison of the chondrosarcoma cell line SW1353 with primary human adult articular chondrocytes with regard to their gene expression profile and reactivity to IL-1beta. *Osteoarthritis Cartilage* **13**: 697-708.
- GeneGo Inc. 2010. *Oncostatin M signaling via JAK/STAT in human cells and Oncostatin M signaling via MAPK in human cells*. Available at: <http://www.genego.com> last accessed: 9 September 2010.
- Geng, Y., L. Zhou, W.J. Thompson, and M. Lotz. 1998. Cyclic GMP and cGMP-binding phosphodiesterase are required for interleukin-1-induced nitric oxide synthesis in human articular chondrocytes. *J Biol Chem* **273**: 27484-91.
- Geyer, M., S. Grassel, R.H. Straub, G. Schett, R. Dinser, J. Grifka, S. Gay, E. Neumann, and U. Muller-Ladner. 2009. Differential transcriptome analysis of intraarticular lesional vs intact cartilage reveals new candidate genes in osteoarthritis pathophysiology. *Osteoarthritis Cartilage* **17**: 328-35.
- Gilby, D.C., H.Y. Sung, P.R. Winship, A.C. Goodeve, J.T. Reilly, E. Kiss-Toth. 2010. Tribbles-1 and -2 are tumour suppressors, down-regulated in human acute myeloid leukaemia. *Immunol Lett* **130**: 115-24.
- Goenka, S., S.H. Cho, and M. Boothby. 2007. Collaborator of Stat6 (CoaSt6)-associated poly(ADP-ribose) polymerase activity modulates Stat6-dependent gene transcription. *J Biol Chem* **282**: 18732-9.
- Goldring, M.B. and S.R. Goldring. 2007. Osteoarthritis. *J Cell Physiol* **213**: 626-34.
- Goldring, S.R. and M.B. Goldring. 2004. The role of cytokines in cartilage matrix degeneration in osteoarthritis. *Clinical Orthopaedics and Related Research*: S27-36.
- Goldring, S.R. and M.B. Goldring. 2006. Clinical aspects, pathology and pathophysiology of osteoarthritis. *J Musculoskelet Neuronal Interact* **6**: 376-8.
- Gomez-Lechon, M.J. 1999. Oncostatin M: signal transduction and biological activity. *Life Sci* **65**: 2019-30.
- Gonzalez, E. and T.E. McGraw. 2009. The Akt kinases: isoform specificity in metabolism and cancer. *Cell Cycle* **8**: 2502-8.
- Greene, J., M. Wang, Y.E. Liu, L.A. Raymond, C. Rosen, and Y.E. Shi. 1996. Molecular cloning and characterization of human tissue inhibitor of metalloproteinase 4. *J Biol Chem* **271**: 30375-80.
- Greenfeder, S.A., P. Nunes, L. Kwee, M. Labow, R.A. Chizzonite, and G. Ju. 1995. Molecular cloning and characterization of a second subunit of the interleukin 1 receptor complex. *J Biol Chem* **270**: 13757-65.
- Gregerson, P. 1997. *Genetic analysis of rheumatic diseases*, Philadelphia.
- Gupta, S., M. Jiang, A. Anthony, and A.B. Pernis. 1999. Lineage-specific modulation of interleukin 4 signaling by interferon regulatory factor 4. *J Exp Med* **190**: 1837-48.
- Hardingham, T.E. and A.J. Fosang. 1992. Proteoglycans: many forms and many functions. *Faseb J* **6**: 861-70.
- Hardingham, T.E. and A.J. Fosang. 1995. The structure of aggrecan and its turnover in cartilage. *J Rheumatol Suppl* **43**: 86-90.
- Hart, P., G. Vitti, and D. Burgess. 1989. Potential anti-inflammatory effects of interleukin-4: suppression of human monocyte tumor necrosis factor alpha, interleukin-1 and prostaglandin E2. *Proc Natl Acad Sci U S A*. **86**: 3803-3807.
- Hascall, V.C., C.J. Handley, D.J. McQuillan, G.K. Hascall, H.C. Robinson, and D.A. Lowther. 1983. The effect of serum on biosynthesis of proteoglycans by bovine articular cartilage in culture. *Arch Biochem Biophys* **224**: 206-23.

- Hashimoto, S., T. Gon, I. Takeshita, S. Maruoka, and T. Horie. 2001. IL-4 and IL-13 induce myofibroblastic phenotype of human lung fibroblasts through c-Jun NH2-terminal kinase-dependent pathway. *J Allergy Clin Immunol* **107**: 1001-1008.
- Hasty, K.A., J.J. Jeffrey, M.S. Hibbs, and H.G. Welgus. 1987. The collagen substrate specificity of human neutrophil collagenase. *J Biol Chem* **262**: 10048-52.
- Hawkins, P.T., K.E. Anderson, K. Davidson, and L.R. Stephens. 2006. Signalling through Class I PI3Ks in mammalian cells. *Biochem Soc Trans* **34**: 647-62.
- He, L., F.A. Simmen, H.M. Mehendale, M.J. Ronis, and T.M. Badger. 2006. Chronic ethanol intake impairs insulin signaling in rats by disrupting Akt association with the cell membrane. Role of TRB3 in inhibition of Akt/protein kinase B activation. *J Biol Chem* **281**: 11126-34.
- Hebenstreit, D., G. Wirnsberger, J. Horejs-Hoeck, and A. Duschl. 2006. Signaling mechanisms, interaction partners and target genes of STAT6. *Cytokine & Growth Factor Reviews* **17**: 173-188.
- Hedbom, E. and D. Heinegard. 1993. Binding of fibromodulin and decorin to separate sites on fibrillar collagens. *J Biol Chem* **268**: 27307-12.
- Hegedus, Z., A. Czibula, and E. Kiss-Toth. 2007. Tribbles: a family of kinase-like proteins with potent signalling regulatory function. *Cell Signal* **19**: 238-50.
- Heinrich, P.C., I. Behrmann, S. Haan, H.M. Hermanns, G. Muller-Newen, and F. Schaper. 2003. Principles of interleukin (IL)-6-type cytokine signalling and its regulation. *Biochem J* **374**: 1-20.
- Hembry, R.M., M.R. Bagga, J.J. Reynolds, and D.L. Hamblen. 1995. Immunolocalisation studies on six matrix metalloproteinases and their inhibitors, TIMP-1 and TIMP-2, in synovia from patients with osteo- and rheumatoid arthritis. *Ann Rheum Dis* **54**: 25-32.
- Henderson, B. and E.R. Pettipher. 1989. Arthritogenic actions of recombinant IL-1 and tumour necrosis factor alpha in the rabbit: evidence for synergistic interactions between cytokines in vivo. *Clin Exp Immunol* **75**: 306-10.
- Hirayama, T., S. Dai, S. Abbas, Y. Yamanaka, and Y. Abu-Amer. 2005. Inhibition of inflammatory bone erosion by constitutively active STAT-6 through blockade of JNK and NF-kappaB activation. *Arthritis Rheum* **52**: 2719-29.
- Hockberg, M.C., A.J. Silman, J.S. Smolen, M.E. Weinblatt and M.H. Weisman. 2003. *Rheumatology*. Mosby.
- Hocking, A.M., T. Shinomura, and D.J. McQuillan. 1998. Leucine-rich repeat glycoproteins of the extracellular matrix. *Matrix Biol* **17**: 1-19.
- Hou, J., U. Schindler, W.J. Henzel, T.C. Ho, M. Brasseur, and S.L. McKnight. 1994. An interleukin-4-induced transcription factor: IL-4 Stat. *Science* **265**: 1701-6.
- Huber, M., S. Trattnig, and F. Lintner. 2000. Anatomy, biochemistry, and physiology of articular cartilage. *Invest Radiol* **35**: 573-80.
- Hui, W., H.E. Barksby, and D.A. Young. 2005. Oncostatin M in combination with tumour necrosis factor alpha induces a chondrocyte membrane associated aggrecanase that is distinct from ADAMTS aggrecanase-1 or -2. *Ann Rheum Dis* **64**: 1624-1632.
- Hui, W., M. Bell, and G. Carroll. 1996. Oncostatin M (OSM) stimulates resorption and inhibits synthesis of proteoglycan in porcine articular cartilage explants. *Cytokine* **8**: 495-500.
- Hui, W., A.D. Rowan, C.D. Richards, and T.E. Cawston. 2003. Oncostatin M in combination with tumor necrosis factor alpha induces cartilage damage and matrix metalloproteinase expression in vitro and in vivo. *Arthritis Rheum* **48**: 3404-18.

- Hussain, S., J.W. Assender, M. Bond, L.F. Wong, D. Murphy, and A.C. Newby. 2002. Activation of protein kinase C ζ is essential for cytokine-induced metalloproteinase-1, -3, and -9 secretion from rabbit smooth muscle cells and inhibits proliferation. *J Biol Chem* **277**: 27345-52.
- Iliopoulos, D., K.N. Malizos, and A. Tsezou. 2007. Epigenetic regulation of leptin affects MMP-13 expression in osteoarthritic chondrocytes: possible molecular target for osteoarthritis therapeutic intervention. *Ann Rheum Dis* **66**: 1616-21.
- Imani, F., K.J. Rager, B. Catipovic, and D.G. Marsh. 1997. Interleukin-4 (IL-4) induces phosphatidylinositol 3-kinase (p85) dephosphorylation. Implications for the role of SHP-1 in the IL-4-induced signals in human B cells. *J Biol Chem* **272**: 7927-31.
- Ishii, M., H. Wen, C.A. Corsa, T. Liu, A.L. Coelho, R.M. Allen, W.F.t. Carson, K.A. Cavassani, X. Li, N.W. Lukacs, C.M. Hogaboam, Y. Dou, and S.L. Kunkel. 2009. Epigenetic regulation of the alternatively activated macrophage phenotype. *Blood* **114**: 3244-54.
- Iynedjian, P.B. 2005. Lack of evidence for a role of TRB3/NIPK as an inhibitor of PKB-mediated insulin signalling in primary hepatocytes. *Biochem J* **386**: 113-8.
- Jaenisch, R. and A. Bird. 2003. Epigenetic regulation of gene expression: how the genome integrates intrinsic and environmental signals. *Nat Genet* **33 Suppl**: 245-54.
- Jiang, Y.H., J. Bressler, and A.L. Beaudet. 2004. Epigenetics and human disease. *Annu Rev Genomics Hum Genet* **5**: 479-510.
- Jirholt, J., A.K.B. Lindqvist, and R. Holmdahl. 2001. The genetics of rheumatoid arthritis and the need for animal models to find and understand the underlying genes. *Arthritis Research* **3**: 87-97.
- Johnson, A.R., A.G. Pavlovsky, D.F. Ortwine, F. Prior, C.F. Man, D.A. Bornemeier, C.A. Banotai, W.T. Mueller, P. McConnell, C. Yan, V. Baragi, C. Lesch, W.H. Roark, M. Wilson, K. Datta, R. Guzman, H.K. Han, and R.D. Dyer. 2007. Discovery and characterization of a novel inhibitor of matrix metalloprotease-13 that reduces cartilage damage in vivo without joint fibroplasia side effects. *J Biol Chem* **282**: 27781-91.
- Johnson, K.R., K.Y. Johnson, K.P. Becker, J. Bielawski, C. Mao, and L.M. Obeid. 2003. Role of human sphingosine-1-phosphate phosphatase 1 in the regulation of intra- and extracellular sphingosine-1-phosphate levels and cell viability. *J Biol Chem* **278**: 34541-7.
- Jones, P.A. and S.B. Baylin. 2002. The fundamental role of epigenetic events in cancer. *Nat Rev Genet* **3**: 415-28.
- Joosten, L.A., E. Lubberts, P. Durez, M.M. Helsen, M.J. Jacobs, M. Goldman, and W.B. van den Berg. 1997. Role of interleukin-4 and interleukin-10 in murine collagen-induced arthritis. Protective effect of interleukin-4 and interleukin-10 treatment on cartilage destruction. *Arthritis Rheum* **40**: 249-60.
- Joosten, L.A.B., E. Lubberts, M.M.A. Helsen, and et al. 1999. Protection against cartilage and bone destruction by systemic interleukin-4 treatment in established murine type II collagen-induced arthritis. *Arthritis Res* **1**: 81-91.
- Jubb, R.W. and H.B. Fell. 1980. The breakdown of collagen by chondrocytes. *J Pathol* **130**: 159-162.
- Jungel, A., C. Ospelt, M. Lesch, M. Thiel, T. Sunyer, O. Schorr, B.A. Michel, R.E. Gay, C. Kolling, C. Flory, S. Gay, and M. Neidhart. 2010. Effect of the oral application of a highly selective MMP-13 inhibitor in three different animal models of rheumatoid arthritis. *Ann Rheum Dis* **69**: 898-902.

- Kaminski, A., H.J. Welters, E.R. Kaminski, and N.G. Morgan. 2010. Human and rodent pancreatic beta-cells express IL-4 receptors and IL-4 protects against beta-cell apoptosis by activation of the PI3K and JAK/STAT pathways. *Biosci Rep* **30**: 169-75.
- Karlsson, C., T. Dehne, A. Lindahl, M. Brittberg, A. Pruss, M. Sittinger, and J. Ringe. 2010. Genome-wide expression profiling reveals new candidate genes associated with osteoarthritis. *Osteoarthritis Cartilage* **18**: 581-92.
- Karouzakis, E., R.E. Gay, B.A. Michel, S. Gay, and M. Neidhart. 2009. DNA hypomethylation in rheumatoid arthritis synovial fibroblasts. *Arthritis Rheum* **60**: 3613-22.
- Keeshan, K., Y. He, B.J. Wouters, O. Shestova, L. Xu, H. Sai, C.G. Rodriguez, I. Maillard, J.W. Tobias, P. Valk, M. Carroll, J.C. Aster, R. Delwel, and W.S. Pear. 2006. Tribbles homolog 2 inactivates C/EBPalpha and causes acute myelogenous leukemia. *Cancer Cell* **10**: 401-11.
- Kehlen, A., R. Lauterbach, A.N. Santos, K. Thiele, U. Kabisch, E. Weber, D. Riemann, and J. Langner. 2001. IL-1 beta- and IL-4-induced down-regulation of autotaxin mRNA and PC-1 in fibroblast-like synoviocytes of patients with rheumatoid arthritis (RA). *Clin Exp Immunol* **123**: 147-54.
- Kelly-Welch, A.E., E.M. Hanson, M.R. Boothby, and A.D. Keegan. 2003. Interleukin-4 and interleukin-13 signaling connection maps *Science* **300**: 1527-29.
- Kim, E.K. and E.J. Choi. 2010. Pathological roles of MAPK signaling pathways in human diseases. *Biochim Biophys Acta* **1802**: 396-405.
- Kiss-Toth, E., S.M. Bagstaff, H.Y. Sung, V. Jozsa, C. Dempsey, J.C. Caunt, K.M. Oxley, D.H. Wyllie, T. Polgar, M. Harte, A. O'Neill, E.E. Qwarnstrom, and S.K. Dower. 2004. Human tribbles, a protein family controlling mitogen-activated protein kinase cascades. *J Biol Chem* **279**: 42703-8.
- Kiss-Toth, E., D.H. Wyllie, K. Holland, L. Marsden, V. Jozsa, K.M. Oxley, T. Polgar, E.E. Qwarnstrom, and S.K. Dower. 2006. Functional mapping and identification of novel regulators for the Toll/Interleukin-1 signalling network by transcription expression cloning. *Cell Signal* **18**: 202-14.
- Klingenspor, M., P. Xu, R.D. Cohen, C. Welch, and K. Reue. 1999. Altered gene expression pattern in the fatty liver dystrophy mouse reveals impaired insulin-mediated cytoskeleton dynamics. *J Biol Chem* **274**: 23078-84.
- Knauper, V., C. Lopez-Otin, B. Smith, G. Knight, and G. Murphy. 1996a. Biochemical characterization of human collagenase-3. *J Biol Chem* **271**: 1544-50.
- Knauper, V., G. Murphy, and H. Tschesche. 1996b. Activation of human neutrophil procollagenase by stromelysin 2. *Eur J Biochem* **235**: 187-91.
- Knauper, V., H. Will, C. Lopez-Otin, B. Smith, S.J. Atkinson, H. Stanton, R.M. Hembry, and G. Murphy. 1996c. Cellular mechanisms for human procollagenase-3 (MMP-13) activation. Evidence that MT1-MMP (MMP-14) and gelatinase a (MMP-2) are able to generate active enzyme. *J Biol Chem* **271**: 17124-31.
- Koshy, P.J., N. Henderson, C. Logan, P.F. Life, T.E. Cawston, and A.D. Rowan. 2002a. Interleukin 17 induces cartilage collagen breakdown: novel synergistic effects in combination with proinflammatory cytokines. *Ann Rheum Dis* **61**: 704-13.
- Koshy, P.J.T., C.J. Lundy, A.D. Rowan, S. Porter, D.R. Edwards, A. Hogan, I.M. Clark, and T.E. Cawston. 2002b. The modulation of matrix metalloproteinase and ADAM gene expression in human chondrocytes by interleukin-1 and oncostatin M. *Arthritis and Rheumatism* **46**: 961-967.

- Koshy, P.J.T., A.D. Rowan, P.F. Life, and T.E. Cawston. 1999. 96-well plate assays for measuring collagenase activity using 3H-acetylated collagen. *Anal Biochem* **275**: 202-207.
- Kuettner, K.E. 1992. Biochemistry of articular cartilage in health and disease. *Clin Biochem* **25**: 155-63.
- Kuhn, R., K. Rajewsky, and W. Muller. 1991. Generation and analysis of interleukin-4 deficient mice. *Science* **254**: 707-10.
- Kumar, P. and M. Clark. 2005. *Kumar and Clark Clinical Medicine*. Saunders.
- Kwan, J.A., C.J. Schulze, W. Wang, H. Leon, M. Sariahmetoglu, M. Sung, J. Sawicka, D.E. Sims, G. Sawicki, and R. Schulz. 2004. Matrix metalloproteinase-2 (MMP-2) is present in the nucleus of cardiac myocytes and is capable of cleaving poly (ADP-ribose) polymerase (PARP) in vitro. *Faseb J* **18**: 690-2.
- Laemmli, U.K. 1970. Cleavage of structural proteins during the assembly of the head of bacteriophage T4. *Nature* **227**: 680-5.
- Lauer-Fields, J.L., M.J. Chalmers, S.A. Busby, D. Minond, P.R. Griffin, and G.B. Fields. 2009. Identification of specific hemopexin-like domain residues that facilitate matrix metalloproteinase collagenolytic activity. *J Biol Chem* **284**: 24017-24.
- Lee, K.K., A.K. Leung, M.K. Tang, D.Q. Cai, C. Schneider, C. Brancolini, and P.H. Chow. 2001. Functions of the growth arrest specific 1 gene in the development of the mouse embryo. *Dev Biol* **234**: 188-203.
- Lee, K.S., H.K. Lee, J.S. Hayflick, Y.C. Lee, and K.D. Puri. 2006. Inhibition of phosphoinositide 3-kinase delta attenuates allergic airway inflammation and hyperresponsiveness in murine asthma model. *Faseb J* **20**: 455-65.
- Lee, Y.W. and A.A. Hirani. 2006. Role of interleukin-4 in atherosclerosis. *Arch Pharm Res* **29**: 1-15.
- Leonard, W.J. and J.J. O'Shea. 1998. Jaks and STATs: biological implications. *Annu Rev Immunol* **16**: 293-322.
- Leonhardt, H., A.W. Page, H.U. Weier, and T.H. Bestor. 1992. A targeting sequence directs DNA methyltransferase to sites of DNA replication in mammalian nuclei. *Cell* **71**: 865-73.
- Li, L.C. and R. Dahiya. 2002. MethPrimer: designing primers for methylation PCRs. *Bioinformatics* **18**: 1427-31.
- Liang, J. and J.M. Slingerland. 2003. Multiple roles of the PI3K/PKB (Akt) pathway in cell cycle progression. *Cell Cycle* **2**: 339-45.
- Limb, G.A., K. Matter, G. Murphy, A.D. Cambrey, P.N. Bishop, G.E. Morris, and P.T. Khaw. 2005. Matrix metalloproteinase-1 associates with intracellular organelles and confers resistance to lamin A/C degradation during apoptosis. *Am J Pathol* **166**: 1555-63.
- Lin, K.R., S.F. Lee, C.M. Hung, C.L. Li, H.F. Yang-Yen, and J.J. Yen. 2007. Survival factor withdrawal-induced apoptosis of TF-1 cells involves a TRB2-Mcl-1 axis-dependent pathway. *J Biol Chem* **282**: 21962-72.
- Lin, S.M., P. Du, W. Huber, and W.A. Kibbe. 2008. Model-based variance-stabilizing transformation for Illumina microarray data. *Nucleic Acids Res* **36**: e11.
- Ling, H. and A.D. Recklies. 2004. The chitinase 3-like protein human cartilage glycoprotein 39 inhibits cellular responses to the inflammatory cytokines interleukin-1 and tumour necrosis factor-alpha. *Biochem J* **380**: 651-9.
- Litherland, G.J., N.J. Morris, M. Walker, S.J. Yeaman. 2007. Role of glycogen content in insulin resistance in human muscle cells. *J Cell Physiol* **211**: 344-52.

- Litherland, G.J., C. Dixon, R.L. Lakey, T. Robson, D. Jones, D.A. Young, T.E. Cawston, and A.D. Rowan. 2008. Synergistic collagenase expression and cartilage collagenolysis are phosphatidylinositol 3-kinase/Akt signaling-dependent. *J Biol Chem* **283**: 14221-9.
- Litherland G.J., M.S. Elias, W. Hui, C.D. Macdonald, J.B. Catterall, M.J. Barter, M.J. Farren, M. Jefferson, A.D. Rowan. 2010. Protein kinase C isoforms zeta and iota mediate collagenase expression and cartilage destruction via STAT3- and ERK-dependent c-fos induction. *J Biol Chem* **285**:22414.
- Liu, B., J. Liao, X. Rao, S.A. Kushner, C.D. Chung, D.D. Chang, and K. Shuai. 1998. Inhibition of Stat1-mediated gene activation by PIAS1. *Proc Natl Acad Sci U S A* **95**: 10626-31.
- Liu, Q., T. Sasaki, I. Kozieradzki, A. Wakeham, A. Itie, D.J. Dumont, and J.M. Penninger. 1999. SHIP is a negative regulator of growth factor receptor-mediated PKB/Akt activation and myeloid cell survival. *Genes Dev* **13**: 786-91.
- Loeuille, D., I. Chary-Valckenaere, J. Champigneulle, A.C. Rat, F. Toussaint, A. Pinzano-Watrin, J.C. Goebel, D. Mainard, A. Blum, J. Pourel, P. Netter, and P. Gillet. 2005. Macroscopic and microscopic features of synovial membrane inflammation in the osteoarthritic knee: correlating magnetic resonance imaging findings with disease severity. *Arthritis Rheum* **52**: 3492-501.
- Losman, J.A., X.P. Chen, D. Hilton, and P. Rothman. 1999. Cutting edge: SOCS-1 is a potent inhibitor of IL-4 signal transduction. *J Immunol* **162**: 3770-4.
- Lubberts, E., L.A. Joosten, M. Chabaud, L. van Den Bersselaar, B. Oppers, C.J. Coenen-De Roo, C.D. Richards, P. Miossec, and W.B. van Den Berg. 2000. IL-4 gene therapy for collagen arthritis suppresses synovial IL-17 and osteoprotegerin ligand and prevents bone erosion. *J Clin Invest* **105**: 1697-710.
- Lubberts, E., L.A. Joosten, B. Oppers, L. van den Bersselaar, C.J. Coenen-de Roo, J.K. Kolls, P. Schwarzenberger, F.A. van de Loo, and W.B. van den Berg. 2001. IL-1-independent role of IL-17 in synovial inflammation and joint destruction during collagen-induced arthritis. *J Immunol* **167**: 1004-13.
- Lubberts, E., L.A. Joosten, F.A. van de Loo, P. Schwarzenberger, J. Kolls, and W.B. van den Berg. 2002. Overexpression of IL-17 in the knee joint of collagen type II immunized mice promotes collagen arthritis and aggravates joint destruction. *Inflamm Res* **51**: 102-4.
- Luo, D., B. Mari, I. Stoll, and P. Anglard. 2002. Alternative splicing and promoter usage generates an intracellular stromelysin 3 isoform directly translated as an active matrix metalloproteinase. *J Biol Chem* **277**: 25527-36.
- Macias, M.J., S. Wiesner, and M. Sudol. 2002. WW and SH3 domains, two different scaffolds to recognize proline-rich ligands. *FEBS Lett* **513**: 30-7.
- MacNaul, K.L., N. Chartrain, M. Lark, M.J. Tocci, and N.I. Hutchinson. 1990. Discoordinate expression of stromelysin, collagenase, and tissue inhibitor of metalloproteinases-1 in rheumatoid human synovial fibroblasts. Synergistic effects of interleukin-1 and tumor necrosis factor-alpha on stromelysin expression. *J Biol Chem* **265**: 17238-45.
- Mangashetti, L.S., S.M. Khapli, and M.R. Wani. 2005. IL-4 inhibits bone-resorbing activity of mature osteoclasts by affecting NF-kappa B and Ca²⁺ signaling. *J Immunol* **175**: 917-25.
- Manicourt, D.H., P. Poilvache, E.A. Van, J.P. Devogelaer, M.E. Lenz, and E.J. Thornar. 2000. Synovial fluid levels of tumour necrosis factor alpha and oncostatin M

- correlate with levels of markers of the degradation of crosslinked collagen and cartilage aggrecan in rheumatoid arthritis but not in osteoarthritis. *Arthritis and Rheumatism* **43**: 281-288.
- Mata, J., S. Curado, A. Ephrussi, and P. Rorth. 2000. Tribbles coordinates mitosis and morphogenesis in *Drosophila* by regulating string/CDC25 proteolysis. *Cell* **101**: 511-22.
- Matrisian, L.M. 1992. The matrix-degrading metalloproteinases. *Bioessays* **14**: 455-63.
- Matsumoto, M., S. Han, T. Kitamura, and D. Accili. 2006. Dual role of transcription factor FoxO1 in controlling hepatic insulin sensitivity and lipid metabolism. *J Clin Invest* **116**: 2464-72.
- Mayumi-Matsuda, K., S. Kojima, H. Suzuki, and T. Sakata. 1999. Identification of a novel kinase-like gene induced during neuronal cell death. *Biochem Biophys Res Commun* **258**: 260-4.
- McClelland, M. and R. Ivarie. 1982. Asymmetrical distribution of CpG in an 'average' mammalian gene. *Nucleic Acids Res* **10**: 7865-77.
- Mengshol, J.A., M.P. Vincenti, C.I. Coon, A. Barchowsky, and C.E. Brinckerhoff. 2000. Interleukin-1 induction of collagenase 3 (matrix metalloproteinase 13) gene expression in chondrocytes requires p38, c-Jun N-terminal kinase, and nuclear factor kappaB: differential regulation of collagenase 1 and collagenase 3. *Arthritis Rheum* **43**: 801-11.
- Mikita, T., M. Kurama, and U. Schindler. 1998. Synergistic activation of the germline epsilon promoter mediated by Stat6 and C/EBP beta. *J Immunol* **161**: 1822-8.
- Miller, E.J., E.D. Harris, E. Chung, J.E. Finch, P. McCroskery, and W.T. Butler. 1976. Cleavage of type II and III collagens with mammalian collagenase: site of cleavage and primary structure of NH₂-terminal portion of the smaller fragment released from both collagens. *Biochemistry* **15**: 787-92.
- Millward-Sadler, S.J., M.O. Wright, L.W. Davies, G. Nuki, and D.M. Salter. 2000. Mechanotransduction via integrins and interleukin-4 results in altered aggrecan and matrix metalloproteinase 3 gene expression in normal, but not osteoarthritic, human articular chondrocytes. *Arthritis Rheum* **43**: 2091-9.
- Millward-Sadler, S.J., M.O. Wright, H. Lee, K. Nishida, H. Caldwell, G. Nuki, and D.M. Salter. 1999. Integrin-regulated secretion of interleukin 4: A novel pathway of mechanotransduction in human articular chondrocytes. *J Cell Biol* **145**: 183-9.
- Milner, J.M., S.F. Elliott, and T.E. Cawston. 2001. Activation of procollagenases is a key control point in cartilage collagen degradation. *Arthritis and Rheumatism* **44**: 2084-2096.
- Milner, J.M., A.D. Rowan, T.E. Cawston, and D.A. Young. 2006. Metalloproteinase and inhibitor expression profiling of resorbing cartilage reveals pro-collagenase activation as a crucial step for collagenolysis. *Arthritis Research and Therapy* **8**.
- Minty, A., P. Chalon, J.M. Derocq, X. Dumont, J.C. Guillemot, M. Kaghad, C. Labit, P. Leplatois, P. Liauzun, B. Miloux, and et al. 1993. Interleukin-13 is a new human lymphokine regulating inflammatory and immune responses. *Nature* **362**: 248-50.
- Miossec, P., M. Naviliat, A. Dupuy d'Angeac, J. Sany, and J. Banchereau. 1990. Low levels of interleukin-4 and high levels of transforming growth factor beta in rheumatoid synovitis. *Arthritis Rheum* **33**: 1180-7.
- Mitchell, P.G., H.A. Magna, L.M. Reeves, L.L. Lopresti-Morrow, S.A. Yocum, P.J. Rosner, K.F. Geoghegan, and J.E. Hambor. 1996. Cloning, expression, and type II

- collagenolytic activity of matrix metalloproteinase-13 from human osteoarthritic cartilage. *J Clin Invest* **97**: 761-8.
- Moore, K. and A. Dalley. 1999. *Clinically orientated anatomy*. Lippincott Williams & Wilkins.
- Muir, H. 1995. The chondrocyte, architect of cartilage. Biomechanics, structure, function and molecular biology of cartilage matrix macromolecules. *Bioessays* **17**: 1039-48.
- Murphy, G., M.I. Cockett, P.E. Stephens, B.J. Smith, and A.J. Docherty. 1987. Stromelysin is an activator of procollagenase. A study with natural and recombinant enzymes. *Biochem J* **248**: 265-8.
- Murphy, G. and H. Nagase. 2008. Progress in matrix metalloproteinase research. *Mol Aspects Med* **29**: 290-308.
- Nagase, H., R. Visse, and G. Murphy. 2006. Structure and function of matrix metalloproteinases and TIMPs. *Cardiovasc Res* **69**: 562-73.
- Nagase, H. and J.F. Woessner, Jr. 1999. Matrix metalloproteinases. *J Biol Chem* **274**: 21491-4.
- Naiki, T., E. Saijou, Y. Miyaoka, K. Sekine, and A. Miyajima. 2007. TRB2, a mouse Tribbles ortholog, suppresses adipocyte differentiation by inhibiting AKT and C/EBPbeta. *J Biol Chem* **282**: 24075-82.
- Nelms, K., A.L. Snow, J. Hu-Li, and W.E. Paul. 1998. FRIP, a hematopoietic cell-specific rasGAP-interacting protein phosphorylated in response to cytokine stimulation. *Immunity* **9**: 13-24.
- Nemoto, O., H. Yamada, T. Kikuchi, M. Shinmei, K. Obata, H. Sato, and M. Seiki. 1997. Suppression of matrix metalloproteinase-3 synthesis by interleukin-4 in human articular chondrocytes. *J Rheumatol* **24**: 1774-9.
- Nochi, H., H. Tomura, M. Tobo, N. Tanaka, K. Sato, T. Shinozaki, T. Kobayashi, K. Takagishi, H. Ohta, F. Okajima, and K. Tamoto. 2008. Stimulatory role of lysophosphatidic acid in cyclooxygenase-2 induction by synovial fluid of patients with rheumatoid arthritis in fibroblast-like synovial cells. *J Immunol* **181**: 5111-9.
- Noffz, G., Z. Qin, M. Kopf, and T. Blankenstein. 1998. Neutrophils but not eosinophils are involved in growth suppression of IL-4-secreting tumors. *J Immunol* **160**: 345-50.
- Ogryzko, V.V., R.L. Schiltz, V. Russanova, B.H. Howard, and Y. Nakatani. 1996. The transcriptional coactivators p300 and CBP are histone acetyltransferases. *Cell* **87**: 953-9.
- Ohuchi, E., K. Imai, Y. Fujii, H. Sato, M. Seiki, and Y. Okada. 1997. Membrane type 1 matrix metalloproteinase digests interstitial collagens and other extracellular matrix macromolecules. *J Biol Chem* **272**: 2446-51.
- Okamura, N., M. Hasegawa, Y. Nakoshi, T. Iino, A. Sudo, K. Imanaka-Yoshida, T. Yoshida, and A. Uchida. 2009. Deficiency of tenascin-C delays articular cartilage repair in mice. *Osteoarthritis Cartilage*.
- Okumura, Y., H. Sato, M. Seiki, and H. Kido. 1997. Proteolytic activation of the precursor of membrane type 1 matrix metalloproteinase by human plasmin. A possible cell surface activator. *FEBS Lett* **402**: 181-4.
- Olver, S., S. Apte, A. Baz, and N. Kienzle. 2007. The duplicitous effects of interleukin 4 on tumour immunity: how can the same cytokine improve or impair control of tumour growth? *Tissue Antigens* **69**: 293-8.
- Ooi, S.K. and T.H. Bestor. 2008. The colorful history of active DNA demethylation. *Cell* **133**: 1145-8.

- Ord, D. and T. Ord. 2003. Mouse NIPK interacts with ATF4 and affects its transcriptional activity. *Exp Cell Res* **286**: 308-20.
- Ord, T., D. Ord, M. Koivomagi, K. Juhkam, T. Ord. 2009. Human TRB3 is upregulated in stressed cells by the induction of translationally efficient mRNA containing a truncated 5'-UTR. *Gene* **444**: 24-32.
- Ostertag, A., A. Jones, A.J. Rose, M. Liebert, S. Kleinsorg, A. Reimann, A. Vegiopoulos, M.B. Diaz, D. Strzoda, M. Yamamoto, T. Satoh, S. Akira, and S. Herzig. 2010. Control of adipose tissue inflammation through TRB1. *Diabetes* **59**: 1991-2000.
- Otero, M. and M.B. Goldring. 2007. Cells of the synovium in rheumatoid arthritis. Chondrocytes. *Arthritis Res Ther* **9**: 220.
- Overgaard, M.T., H.B. Boldt, L.S. Laursen, L. Sottrup-Jensen, C.A. Conover, and C. Oxvig. 2001. Pregnancy-associated plasma protein-A2 (PAPP-A2), a novel insulin-like growth factor-binding protein-5 proteinase. *J Biol Chem* **276**: 21849-53.
- Patterson, M.L., S.J. Atkinson, V. Knauper, and G. Murphy. 2001. Specific collagenolysis by gelatinase A, MMP-2, is determined by the hemopexin domain and not the fibronectin-like domain. *FEBS Lett* **503**: 158-62.
- Paul, W.E. 1991. Interleukin-4: a prototypic immunoregulatory lymphokine. *Blood* **77**: 1859-70.
- Pavloff, N., P.W. Staskus, N.S. Kishnani, and S.P. Hawkes. 1992. A new inhibitor of metalloproteinases from chicken: ChIMP-3. A third member of the TIMP family. *J Biol Chem* **267**: 17321-6.
- Pei, D. and S.J. Weiss. 1995. Furin-dependent intracellular activation of the human stromelysin-3 zymogen. *Nature* **375**: 244-7.
- Pelletier, J.P., J.A. DiBattista, P. Roughley, R. McCollum, and J. Martel-Pelletier. 1993. Cytokines and inflammation in cartilage degradation. *Rheum Dis Clin North Am* **19**: 545-68.
- Pelletier, J.P., J. Martel-Pelletier, and S.B. Abramson. 2001. Osteoarthritis, an inflammatory disease: potential implication for the selection of new therapeutic targets. *Arthritis Rheum* **44**: 1237-47.
- Perez, G.M., M. Melo, A.D. Keegan, and J. Zamorano. 2002. Aspirin and salicylates inhibit the IL-4- and IL-13-induced activation of STAT6. *J Immunol* **168**: 1428-34.
- Pernis, A., B. Witthuhn, A.D. Keegan, K. Nelms, E. Garfein, J.N. Ihle, W.E. Paul, J.H. Pierce, and P. Rothman. 1995. Interleukin 4 signals through two related pathways. *Proc Natl Acad Sci U S A* **92**: 7971-5.
- Pesu, M., S. Aittomaki, T. Valineva, and O. Silvennoinen. 2003. PU.1 is required for transcriptional activation of the Stat6 response element in the Igepsilon promoter. *Eur J Immunol* **33**: 1727-35.
- Pesu, M., K. Takaluoma, S. Aittomaki, A. Lagerstedt, K. Saksela, P.E. Kovanen, and O. Silvennoinen. 2000. Interleukin-4-induced transcriptional activation by stat6 involves multiple serine/threonine kinase pathways and serine phosphorylation of stat6. *Blood* **95**: 494-502.
- Pettipher, E.R., G.A. Higgs, and B. Henderson. 1986. Arthritogenic activity of interleukin 1. *Agents Actions* **19**: 337-8.
- Piecha, D., J. Weik, H. Kheil, G. Becher, A. Timmermann, A. Jaworski, M. Burger, and M.W. Hofmann. 2010. Novel selective MMP-13 inhibitors reduce collagen degradation in bovine articular and human osteoarthritis cartilage explants. *Inflamm Res* **59**: 379-89.

- Plater-Zyberk, C., J. Buckton, S. Thompson, J. Spaul, E. Zanders, J. Papworth, and P.F. Life. 2001. Amelioration of arthritis in two murine models using antibodies to oncostatin M. *Arthritis Rheum* **44**: 2697-702.
- Pradhan, S. and P.O. Esteve. 2003. Mammalian DNA (cytosine-5) methyltransferases and their expression. *Clin Immunol* **109**: 6-16.
- Pyle, A. 2003. The mechanism of interleukin-4 inhibition of collagen release from cartilage: implications for arthritis. In *Musculoskeletal Research Group*. Newcastle University, Newcastle upon Tyne.
- Rajasekhar, L., L.B. Liou, C.Y. Chan, W.P. Tsai, and C.Y. Cheng. 2004. Matrix metalloproteinase-8 in sera and from polymorphonuclear leucocytes in rheumatoid arthritis: in vitro characterization and correlation with disease activity. *Clin Exp Rheumatol* **22**: 597-602.
- Ramaswamy, S., N. Nakamura, F. Vazquez, D.B. Batt, S. Perera, T.M. Roberts, and W.R. Sellers. 1999. Regulation of G1 progression by the PTEN tumor suppressor protein is linked to inhibition of the phosphatidylinositol 3-kinase/Akt pathway. *Proc Natl Acad Sci U S A* **96**: 2110-5.
- Rayasam, G.V., V.K. Tulasi, R. Sodhi, J.A. Davis, and A. Ray. 2009. Glycogen synthase kinase 3: more than a namesake. *Br J Pharmacol* **156**: 885-98.
- Razin, A. and H. Cedar. 1977. Distribution of 5-methylcytosine in chromatin. *Proc Natl Acad Sci U S A* **74**: 2725-8.
- Reboul, P., J.P. Pelletier, G. Tardif, J.M. Cloutier, and J. Martel-Pelletier. 1996. The new collagenase, collagenase-3, is expressed and synthesized by human chondrocytes but not by synoviocytes. A role in osteoarthritis. *J Clin Invest* **97**: 2011-9.
- Rechsteiner, M. and S.W. Rogers. 1996. PEST sequences and regulation by proteolysis. *Trends Biochem Sci* **21**: 267-71.
- Reed, K., M.L. Poulin, L. Yan, and A.M. Parissenti. 2009. Comparison of bisulfite sequencing PCR with pyrosequencing for measuring differences in DNA methylation. *Anal Biochem*.
- Rengel, Y., C. Ospelt, and S. Gay. 2007. Proteinases in the joint: clinical relevance of proteinases in joint destruction. *Arthritis Res Ther* **9**: 221.
- Reunanen, N. and V. Kähäri. 2005. Eureka Bioscience Collection: Matrix Metalloproteinases in Cancer Cell Invasion. In: Landes Bioscience.
- Richardson, B. 2003. Impact of aging on DNA methylation. *Ageing Res Rev* **2**: 245-61.
- Richardson, B.C. 2002. Role of DNA methylation in the regulation of cell function: autoimmunity, aging and cancer. *J Nutr* **132**: 2401S-2405S.
- Rico, M.C., J.M. Manns, J.B. Driban, A.B. Uknis, S.P. Kunapuli, and R.A. Dela Cadena. 2008. Thrombospondin-1 and transforming growth factor beta are pro-inflammatory molecules in rheumatoid arthritis. *Transl Res* **152**: 95-8.
- Roach, H.I. and T. Aigner. 2007. DNA methylation in osteoarthritic chondrocytes: a new molecular target. *Osteoarthritis Cartilage* **15**: 128-37.
- Roach, H.I., N. Yamada, K.S. Cheung, S. Tilley, N.M. Clarke, R.O. Oreffo, S. Kokubun, and F. Bronner. 2005. Association between the abnormal expression of matrix-degrading enzymes by human osteoarthritic chondrocytes and demethylation of specific CpG sites in the promoter regions. *Arthritis Rheum* **52**: 3110-24.
- Rogers, S., R. Wells, and M. Rechsteiner. 1986. Amino acid sequences common to rapidly degraded proteins: the PEST hypothesis. *Science* **234**: 364-8.
- Rommel, C., M. Camps, and H. Ji. 2007. PI3K delta and PI3K gamma: partners in crime in inflammation in rheumatoid arthritis and beyond? *Nat Rev Immunol* **7**: 191-201.

- Rosenberg, K., H. Olsson, M. Morgelin, and D. Heinegard. 1998. Cartilage oligomeric matrix protein shows high affinity zinc-dependent interaction with triple helical collagen. *J Biol Chem* **273**: 20397-403.
- Roughley, P.J. 2006. The structure and function of cartilage proteoglycans. *Eur Cell Mater* **12**: 92-101.
- Rowan, A.D., W. Hui, T.E. Cawston, and C.D. Richards. 2003. Adenoviral gene transfer of interleukin-1 in combination with oncostatin-M induces significant joint damage in a murine model. *American Journal of Pathology* **162**: 1975-1984.
- Rowan, A.D., and D.A. Young. 2007. Collagenase gene regulation by pro-inflammatory cytokines in cartilage. *Front Biosci* **12**: 536-550.
- Ryan, J.J., L.J. McReynolds, H. Huang, K. Nelms, and W.E. Paul. 1998. Characterization of a mobile Stat6 activation motif in the human IL-4 receptor. *J Immunol* **161**: 1811-21.
- Sah, R.L., A.C. Chen, A.J. Grodzinsky, and S.B. Trippel. 1994. Differential effects of bFGF and IGF-I on matrix metabolism in calf and adult bovine cartilage explants. *Arch Biochem Biophys* **308**: 137-47.
- Saka, Y. and J.C. Smith. 2004. A *Xenopus* tribbles orthologue is required for the progression of mitosis and for development of the nervous system. *Dev Biol* **273**: 210-25.
- Saklatvala, J. 1986. Tumour necrosis factor alpha stimulates resorption and inhibits synthesis of proteoglycan in cartilage. *Nature* **322**: 547-9.
- Salminen-Mankonen, H., A.M. Saamanen, M. Jalkanen, E. Vuorio, and L. Pirila. 2005. Syndecan-1 expression is upregulated in degenerating articular cartilage in a transgenic mouse model for osteoarthritis. *Scand J Rheumatol* **34**: 469-74.
- Salter, D.M., S.J. Millward-Sadler, G. Nuki, and M.O. Wright. 2001. Integrin-interleukin-4 mechanotransduction pathways in human chondrocytes. *Clin Orthop Relat Res*: S49-60.
- Sandell, L.J. and T. Aigner. 2001. Articular cartilage and changes in arthritis. An introduction: cell biology of osteoarthritis. *Arthritis Res* **3**: 107-13.
- Sato, N., N. Maehara, G.H. Su, and M. Goggins. 2003. Effects of 5-aza-2'-deoxycytidine on matrix metalloproteinase expression and pancreatic cancer cell invasiveness. *J Natl Cancer Inst* **95**: 327-30.
- Sato, T., K. Konomi, S. Yamasaki, S. Aratani, K. Tsuchimochi, M. Yokouchi, K. Masuko-Hongo, N. Yagishita, H. Nakamura, S. Komiya, M. Beppu, H. Aoki, K. Nishioka, and T. Nakajima. 2006. Comparative analysis of gene expression profiles in intact and damaged regions of human osteoarthritic cartilage. *Arthritis Rheum* **54**: 808-17.
- Schwarzer, R., S. Dames, D. Tondera, A. Klippel, and J. Kaufmann. 2006. TRB3 is a PI 3-kinase dependent indicator for nutrient starvation. *Cell Signal* **18**: 899-909.
- Seher, T.C. and M. Leptin. 2000. Tribbles, a cell-cycle brake that coordinates proliferation and morphogenesis during *Drosophila* gastrulation. *Curr Biol* **10**: 623-9.
- Sfikakis, P.P. The first decade of biologic TNF antagonists in clinical practice: lessons learned, unresolved issues and future directions. *Curr Dir Autoimmun* **11**: 180-210.
- Shaw, N., M. Zhao, C. Cheng, H. Xu, J. Saarikettu, Y. Li, Y. Da, Z. Yao, O. Silvennoinen, J. Yang, Z.J. Liu, B.C. Wang, and Z. Rao. 2007. The multifunctional human p100 protein 'hooks' methylated ligands. *Nat Struct Mol Biol* **14**: 779-84.
- Shingleton, W.D., D.J. Hodges, P. Brick, and T.E. Cawston. 1996. Collagenase: a key enzyme in collagen turnover. *Biochem Cell Biol* **74** 759-775: 759-775.

- Sims, J.E. and D.E. Smith. 2010. The IL-1 family: regulators of immunity. *Nat Rev Immunol* **10**: 89-102.
- Singer-Sam, J., J.M. LeBon, R.L. Tanguay, and A.D. Riggs. 1990. A quantitative HpaII-PCR assay to measure methylation of DNA from a small number of cells. *Nucleic Acids Res* **18**: 687.
- Skolnik, E.Y., C.H. Lee, A. Batzer, L.M. Vicentini, M. Zhou, R. Daly, M.J. Myers, Jr., J.M. Backer, A. Ullrich, M.F. White, and et al. 1993. The SH2/SH3 domain-containing protein GRB2 interacts with tyrosine-phosphorylated IRS1 and Shc: implications for insulin control of ras signalling. *Embo J* **12**: 1929-36.
- Smith, M.D., S. Triantafyllou, A. Parker, P.P. Youssef, and M. Coleman. 1997. Synovial membrane inflammation and cytokine production in patients with early osteoarthritis. *J Rheumatol* **24**: 365-71.
- Sofat, N. 2009. Analysing the role of endogenous matrix molecules in the development of osteoarthritis. *Int J Exp Pathol* **90**: 463-79.
- Spector, T.D. and A.J. MacGregor. 2004. Risk factors for osteoarthritis: genetics. *Osteoarthritis Cartilage* **12 Suppl A**: S39-44.
- Springman, E.B., E.L. Angleton, H. Birkedal-Hansen, and H.E. Van Wart. 1990. Multiple modes of activation of latent human fibroblast collagenase: evidence for the role of a Cys73 active-site zinc complex in latency and a "cysteine switch" mechanism for activation. *Proc Natl Acad Sci U S A* **87**: 364-8.
- Starkman, B.G., J.D. Cravero, M. Delcarlo, and R.F. Loeser. 2005. IGF-I stimulation of proteoglycan synthesis by chondrocytes requires activation of the PI 3-kinase pathway but not ERK MAPK. *Biochem J* **389**: 723-9.
- Steffensen, B., U.M. Wallon, and C.M. Overall. 1995. Extracellular matrix binding properties of recombinant fibronectin type II-like modules of human 72-kDa gelatinase/type IV collagenase. High affinity binding to native type I collagen but not native type IV collagen. *J Biol Chem* **270**: 11555-66.
- Stetler-Stevenson, W.G., H.C. Krutzsch, and L.A. Liotta. 1989. Tissue inhibitor of metalloproteinase (TIMP-2). A new member of the metalloproteinase inhibitor family. *J Biol Chem* **264**: 17374-8.
- Stremme, S., S. Duerr, B. Bau, E. Schmid, and T. Aigner. 2003. MMP-8 is only a minor gene product of human adult articular chondrocytes of the knee. *Clin Exp Rheumatol* **21**: 205-9.
- Strickland, D.K., J.D. Ashcom, S. Williams, W.H. Burgess, M. Migliorini, and W.S. Argraves. 1990. Sequence identity between the alpha 2-macroglobulin receptor and low density lipoprotein receptor-related protein suggests that this molecule is a multifunctional receptor. *J Biol Chem* **265**: 17401-4.
- Stutz, A.M. and M. Woisetschlager. 1999. Functional synergism of STAT6 with either NF-kappa B or PU.1 to mediate IL-4-induced activation of IgE germline gene transcription. *J Immunol* **163**: 4383-91.
- Stylianou, E. and J. Saklatvala. 1998. Interleukin-1. *Int J Biochem Cell Biol* **30**: 1075-9.
- Stylianou, E. and J. Saklatvala. 1998. Interleukin 1. *The International Journal of Biochemistry & Cell Biology* **30**: 1075-79.
- Sun, X.J., L.M. Wang, Y. Zhang, L. Yenush, M.G. Myers, Jr., E. Glasheen, W.S. Lane, J.H. Pierce, and M.F. White. 1995. Role of IRS-2 in insulin and cytokine signalling. *Nature* **377**: 173-7.
- Sung, H.Y., H. Guan, A. Czibula, A.R. King, K. Eder, E. Heath, S.K. Suvarna, S.K. Dower, A.G. Wilson, S.E. Francis, D.C. Crossman, and E. Kiss-Toth. 2007. Human

- tribbles-1 controls proliferation and chemotaxis of smooth muscle cells via MAPK signaling pathways. *J Biol Chem* **282**: 18379-87.
- Sweeney, S.E. and G.S. Firestein. 2004. Rheumatoid arthritis: regulation of synovial inflammation. *Int J Biochem Cell Biol* **36**: 372-8.
- Takai, D. and P.A. Jones. 2002. Comprehensive analysis of CpG islands in human chromosomes 21 and 22. *Proc Natl Acad Sci U S A* **99**: 3740-5.
- Takaishi, H., T. Kimura, S. Dalal, Y. Okada, and J. D'Armiento. 2008. Joint diseases and matrix metalloproteinases: a role for MMP-13. *Curr Pharm Biotechnol* **9**: 47-54.
- Tang, K., R.L. Finley, Jr., D. Nie, and K.V. Honn. 2000. Identification of 12-lipoxygenase interaction with cellular proteins by yeast two-hybrid screening. *Biochemistry* **39**: 3185-91.
- Tardif, G., D. Hum, J.P. Pelletier, N. Duval, J. Martel-Pelletier. 2009. Regulation of the IGFBP-5 and MMP-13 genes by the microRNAs miR-140 and miR-27a in human osteoarthritic chondrocytes. *BMC Musculoskelet Disord* **10**:148.
- te Velde, A.A., R.J. Huijbens, K. Heije, J.E. de Vries, and C.G. Figdor. 1990. Interleukin-4 (IL-4) inhibits secretion of IL-1 beta, tumor necrosis factor alpha, and IL-6 by human monocytes. *Blood* **76**: 1392-7.
- Temenoff, J.S. and A.G. Mikos. 2000. Review: tissue engineering for regeneration of articular cartilage. *Biomaterials* **21**: 431-40.
- Tepper, R.I., R.L. Coffman, and P. Leder. 1992. An eosinophil-dependent mechanism for the antitumor effect of interleukin-4. *Science* **257**: 548-51.
- Tepper, R.I., P.K. Pattengale, and P. Leder. 1989. Murine interleukin-4 displays potent anti-tumor activity in vivo. *Cell* **57**: 503-12.
- Tetlow, L.C., D.J. Adlam, and D.E. Woolley. 2001. Matrix metalloproteinase and proinflammatory cytokine production by chondrocytes of human osteoarthritic cartilage: associations with degenerative changes. *Arthritis Rheum* **44**: 585-94.
- Tetta, C., G. Camussi, V. Modena, C. Di Vittorio, and C. Baglioni. 1990. Tumour necrosis factor in serum and synovial fluid of patients with active and severe rheumatoid arthritis. *Ann Rheum Dis* **49**: 665-7.
- Thienes, C.P., L. De Monte, S. Monticelli, M. Busslinger, H.J. Gould, and D. Vercelli. 1997. The transcription factor B cell-specific activator protein (BSAP) enhances both IL-4- and CD40-mediated activation of the human epsilon germline promoter. *J Immunol* **158**: 5874-82.
- Tost, J. and I.G. Gut. 2007. DNA methylation analysis by pyrosequencing. *Nat Protoc* **2**: 2265-75.
- Towbin, H., T. Staehelin, and J. Gordon. 1979. Electrophoretic transfer of proteins from polyacrylamide gels to nitrocellulose sheets: procedure and some applications. *Proc Natl Acad Sci U S A* **76**: 4350-4.
- Toyoda, H., S. Tanaka, T. Miyagawa, Y. Honda, K. Tokunaga, and M. Honda. 2010. Anti-Tribbles homolog 2 autoantibodies in Japanese patients with narcolepsy. *Sleep* **33**: 875-8.
- Valineva, T., J. Yang, R. Palovuori, and O. Silvennoinen. 2005. The transcriptional co-activator protein p100 recruits histone acetyltransferase activity to STAT6 and mediates interaction between the CREB-binding protein and STAT6. *J Biol Chem* **280**: 14989-96.
- Valineva, T., J. Yang, and O. Silvennoinen. 2006. Characterization of RNA helicase A as component of STAT6-dependent enhanceosome. *Nucleic Acids Res* **34**: 3938-46.

- van de Loo, A.A. and W.B. van den Berg. 1990. Effects of murine recombinant interleukin 1 on synovial joints in mice: measurement of patellar cartilage metabolism and joint inflammation. *Ann Rheum Dis* **49**: 238-45.
- van den Berg, W.B. 1998. Joint inflammation and cartilage destruction may occur uncoupled. *Springer Semin Immunopathol* **20**: 149-164.
- van den Berg, W.B. and P.L. van Riel. 2005. Uncoupling of inflammation and destruction in rheumatoid arthritis: myth or reality? *Arthritis Rheum* **52**: 995-9.
- van Lent, P.L., L.C. Grevers, A.B. Blom, O.J. Arntz, F.A. van de Loo, P. van der Kraan, S. Abdollahi-Roodsaz, G. Srikrishna, H. Freeze, A. Sloetjes, W. Nacken, T. Vogl, J. Roth, and W.B. van den Berg. 2008. Stimulation of chondrocyte-mediated cartilage destruction by S100A8 in experimental murine arthritis. *Arthritis Rheum* **58**: 3776-87.
- Van Lint, P. and C. Libert. 2006. Matrix metalloproteinase-8: cleavage can be decisive. *Cytokine Growth Factor Rev* **17**: 217-23.
- van Roon, J.A., J.L. van Roy, F.H. Gmelig-Meyling, F.P. Lafeber, and J.W. Bijlsma. 1996. Prevention and reversal of cartilage degradation in rheumatoid arthritis by interleukin-10 and interleukin-4. *Arthritis Rheum* **39**: 829-35.
- Van Wart, H.E. and H. Birkedal-Hansen. 1990. The cysteine switch: a principle of regulation of metalloproteinase activity with potential applicability to the entire matrix metalloproteinase gene family. *Proc Natl Acad Sci U S A* **87**: 5578-82.
- Vannier, E., L.C. Miller, and C.A. Dinarello. 1992. Coordinated antiinflammatory effects of interleukin 4: interleukin 4 suppresses interleukin 1 production but up-regulates gene expression and synthesis of interleukin 1 receptor antagonist. *Proc Natl Acad Sci U S A* **89**: 4076-80.
- Verhoef, C.M., J.A. van Roon, M.E. Vianen, J.W. Bijlsma, and F.P. Lafeber. 2001. Interleukin 10 (IL-10), not IL-4 or interferon-gamma production, correlates with progression of joint destruction in rheumatoid arthritis. *J Rheumatol* **28**: 1960-6.
- Vilimek, D. and V. Duronio. 2006. Cytokine-stimulated phosphorylation of GSK-3 is primarily dependent upon PKCs, not PKB. *Biochem Cell Biol* **84**: 20-9.
- Vincenti, M.P. and C.E. Brinckerhoff. 2002. Transcriptional regulation of collagenase (MMP-1, MMP-13) genes in arthritis: integration of complex signaling pathways for the recruitment of gene-specific transcription factors. *Arthritis Res* **4**: 157-64.
- Walmsley, M., P.D. Katsikis, E. Abney, S. Parry, R.O. Williams, R.N. Maini, and M. Feldmann. 1996. Interleukin-10 inhibition of the progression of established collagen-induced arthritis. *Arthritis Rheum* **39**: 495-503.
- Wang, H.Y., W.E. Paul, and A.D. Keegan. 1996. IL-4 function can be transferred to the IL-2 receptor by tyrosine containing sequences found in the IL-4 receptor alpha chain. *Immunity* **4**: 113-21.
- Wang, L.M., M.G. Myers, Jr., X.J. Sun, S.A. Aaronson, M. White, and J.H. Pierce. 1993. IRS-1: essential for insulin- and IL-4-stimulated mitogenesis in hematopoietic cells. *Science* **261**: 1591-4.
- Watanabe, K., Y. Tanaka, I. Morimoto, K. Yahata, K. Zeki, T. Fujihira, U. Yamashita, and S. Eto. 1990. Interleukin-4 as a potent inhibitor of bone resorption. *Biochem Biophys Res Commun* **172**: 1035-41.
- Welgus, H.G., J.J. Jeffrey, and A.Z. Eisen. 1981. The collagen substrate specificity of human skin fibroblast collagenase. *J Biol Chem* **256**: 9511-5.

- Welgus, H.G., G.P. Stricklin, A.Z. Eisen, E.A. Bauer, R.V. Cooney, and J.J. Jeffrey. 1979. A specific inhibitor of vertebrate collagenase produced by human skin fibroblasts. *J Biol Chem* **254**: 1938-43.
- White, M.F. 2006. Regulating insulin signaling and beta-cell function through IRS proteins. *Can J Physiol Pharmacol* **84**: 725-37.
- Wilkin, F., N. Suarez-Huerta, B. Robaye, J. Peetermans, F. Libert, J.E. Dumont, and C. Maenhaut. 1997. Characterization of a phosphoprotein whose mRNA is regulated by the mitogenic pathways in dog thyroid cells. *Eur J Biochem* **248**: 660-8.
- Wong, M., P. Wuethrich, P. Egli, and E. Hunziker. 1996. Zone-specific cell biosynthetic activity in mature bovine articular cartilage: a new method using confocal microscopic stereology and quantitative autoradiography. *J Orthop Res* **14**: 424-32.
- Yammani, R.R., C.S. Carlson, A.R. Bresnick, and R.F. Loeser. 2006. Increase in production of matrix metalloproteinase 13 by human articular chondrocytes due to stimulation with S100A4: Role of the receptor for advanced glycation end products. *Arthritis Rheum* **54**: 2901-11.
- Yang, J., S. Aittomaki, M. Pesu, K. Carter, J. Saarinen, N. Kalkkinen, E. Kieff, and O. Silvennoinen. 2002. Identification of p100 as a coactivator for STAT6 that bridges STAT6 with RNA polymerase II. *Embo J* **21**: 4950-8.
- Yang, J., T. Valineva, J. Hong, T. Bu, Z. Yao, O.N. Jensen, M.J. Frilander, and O. Silvennoinen. 2007a. Transcriptional co-activator protein p100 interacts with snRNP proteins and facilitates the assembly of the spliceosome. *Nucleic Acids Res* **35**: 4485-94.
- Yang, L., D. McBurney, S.C. Tang, S.G. Carlson, and W.E. Horton, Jr. 2007b. A novel role for Bcl-2 associated-athanogene-1 (Bag-1) in regulation of the endoplasmic reticulum stress response in mammalian chondrocytes. *J Cell Biochem* **102**: 786-800.
- Yang, X.J., V.V. Ogryzko, J. Nishikawa, B.H. Howard, and Y. Nakatani. 1996. A p300/CBP-associated factor that competes with the adenoviral oncoprotein E1A. *Nature* **382**: 319-24.
- Ye, S. 2000. Polymorphism in matrix metalloproteinase gene promoters: implication in regulation of gene expression and susceptibility of various diseases. *Matrix Biol* **19**: 623-9.
- Zamorano, J. and A.D. Keegan. 1998. Regulation of apoptosis by tyrosine-containing domains of IL-4R alpha: Y497 and Y713, but not the STAT6-docking tyrosines, signal protection from apoptosis. *J Immunol* **161**: 859-67.
- Zaragoza, C., E. Lopez-Rivera, C. Garcia-Rama, M. Saura, A. Martinez-Ruiz, T.R. Lizarbe, F. Martin-de-Lara, and S. Lamas. 2006. Cbfa-1 mediates nitric oxide regulation of MMP-13 in osteoblasts. *J Cell Sci* **119**: 1896-902.
- Zaragoza, C., E. Soria, E. Lopez, D. Browning, M. Balbin, C. Lopez-Otin, and S. Lamas. 2002. Activation of the mitogen activated protein kinase extracellular signal-regulated kinase 1 and 2 by the nitric oxide-cGMP-cGMP-dependent protein kinase axis regulates the expression of matrix metalloproteinase 13 in vascular endothelial cells. *Mol Pharmacol* **62**: 927-35.
- Zhang, Y., J.L. Davis, and W. Li. 2005. Identification of tribbles homolog 2 as an autoantigen in autoimmune uveitis by phage display. *Mol Immunol* **42**: 1275-81.